

**Assessment of Hydrodynamic and Water Quality Impacts for
Channel Deepening in the Thimble Shoals, Norfolk Harbor,
And Elizabeth River Channels**

Final Report

Submitted to

Virginia Port Authority
101 W Main Street, Suite 600
Norfolk, VA 23510

by

Jian Shen, Rico Wang, and Mac Sisson

Special Report No. 454
In Applied Marine Science and Ocean Engineering

doi:10.21220/V5R41Z

Virginia Institute of Marine Science
School of Marine Science
College of William and Mary
Gloucester Point, Virginia 23062

September 2017

Table of Contents

1. Introduction	1
2. Approach	1
2.1 Hydrodynamic and water quality models	2
Figure 2-1: A diagram of the modeling approach for the James River	3
Figure 2-2: The current HEM3D model grid for the James River	4
Figure 2-3: A diagram of kinetic processes of the eutrophication model	5
Figure 2-4: A map showing the linkage of the watershed and James River models.....	10
2.3 Transport Time	10
Figure 2-5: A diagram illustrating freshwater age and residence time in an estuary.....	11
2.4 Scenarios: Existing Condition, Future Condition, and Scenarios	12
Table 2-1: Description of the scenarios	13
Table 2-2: Description of Channel Configurations.....	14
3. Model Calibration and Verification	15
Figure 3-1: Tidal and surface elevation monitoring stations	16
Figure 3-2: Water quality monitoring stations.....	17
Figure 3-3: Comparison of surface elevation between model predictions and observations	18
Figure 3-4: Comparison of surface elevation between model predictions and observations (each panel shows a comparison of one month)	18
Figure 3-5: Taylor diagram representing model-data comparisons at 6 tidal stations in the James River. Three axes represent correlation coefficients (blue lines), the centered root-mean-square error (green lines), and normalized standard deviation (black lines) (Station location: 1=JMS043.78, 2= JMS073.37, 3=APP001.83, 4= JMS018.23, 5= JMS002.55, 6= Sewells Point).	19
Figure 3-6: Comparison of salinity (surface, middle, and bottom layers) between model predictions and observations. (Red points signify observations and blue lines are model simulations).	20
Figure 3-7: Comparison of salinity (surface, middle, and bottom layers) between model predictions and observations. (Red points signify observations and blue lines are model simulations).	21
Figure 3-8: Comparison of vertical mean salinity intrusion long the James in January to March period (solid line is modeled mean salinity and dashed lines are modeled minimum and maximum salinity, and the vertical bar shows the variation of observations).	22
Figure 3-9: Comparison of vertical mean salinity intrusion along the James in the April-to-June period (solid line is modeled mean salinity and dashed lines are modeled minimum and maximum salinity, and the vertical bar shows the variation of observations).	22
Figure 3-10: Comparison of vertical mean salinity intrusion along the James in the July-to-September period (solid line is modeled mean salinity and dashed lines are modeled minimum and maximum salinity, and the vertical bar shows the variation of observations).....	23
Figure 3-11: Comparison of vertical mean salinity intrusion along the James in the October-to-December period (solid line is modeled mean salinity and dashed lines are modeled minimum and maximum salinity, and the vertical bar shows the variation of observations).....	23
Figure 3-12: Model verification results at Station LE5-4 (red and black lines are daily averaged model results at surface and the bottom, respectively. Blue and green lines are daily maximum and minimum concentrations in the water column, respectively. Statistics are computed using both data at the surface and bottom layers. Downward-pointing triangle symbols are observations at the surface, and upward-pointing triangle symbols are observations at the bottom).....	26

Figure 3-15: Model verification results at Station LFA01 (see caption of Fig. 3-12 for descriptions of lines and symbols)	29
.....	30
Figure 3-16: Model verification results at Station RET5-2 (see caption of Fig. 3-12 for descriptions of lines and symbols)	30
Figure 3-18: Model verification results at Station LE5-2 (see caption of Fig. 3-12 for descriptions of lines and symbols)	32
Figure 3-19: Model verification results at Station LE5-3 (see caption of Fig. 3-12 for descriptions of lines and symbols)	34
Figure 3-20: Model verification results at Station LE5-6 (see caption of Fig. 3-12 for descriptions of lines and symbols)	34
Figure 3-21: Model verification results at Station EBE1 (see caption of Fig. 3-12 for descriptions of lines and symbols)	35
4. Model Results of DO	35
4.1 Existing Condition and Future Condition	36
Table 4-1-1: Comparison of Baseline 1 and Baseline 2 DO results in spring.....	36
Table 4-1-2: Comparison of Baseline 1 and Baseline 2 DO results in summer.....	37
Figure 4-1-1: Model Grid of Baseline Condition 1.....	38
Figure 4-1-2: Model Grid of Baseline Condition 2.....	39
Figure 4-1-3: Comparison of Baseline 1 and Baseline 2 results at Station LE5-4.....	40
Figure 4-1-4: Comparison of Baseline 1 and Baseline 2 results at Station ELI2 (last panel shows the difference of bottom DO)	41
Figure 4-1-5: Comparison of Baseline 1 and Baseline 2 results at Station SBE5.....	42
4.2 Model Scenarios 3-1 and 3-2	43
Table 4-2-1: Comparison of Scenario 3-1 to Baseline 1 for DO results during spring.....	44
Table 4-2-2: Comparison of Scenario 3-1 to Baseline 1 for DO results during summer	44
Table 4-2-3: Comparison of Scenario 3-2 to Baseline 2 for DO results during spring.....	45
Table 4-2-4: Comparison of Scenario 3-2 to Baseline 2 for DO results during summer	45
Figure 4-2-1: Model Grid of Scenario 3-1 (Deepening NH Channel)	46
Figure 4-2-2: Model Grid of Scenario 3-2 (Deepening NH Channel)	47
Figure 4-2-3: Comparison of Scenario 3-1 to Baseline 1 results at Station LE5-4.....	48
Figure 4-2-4: Comparison of Scenario 3-1 to Baseline 1 results at Station ELI2.....	49
Figure 4-2-5: Comparison of Scenario 3-1 to Baseline 1 results at Station SBE5.....	50
Figure 4-2-6: Comparison of Scenario 3-2 to Baseline 2 results at Station LE5-4.....	51
Figure 4-2-7: Comparison of Scenario 3-2 to Baseline 2 results at Station ELI2.....	52
Figure 4-2-8: Comparison of Scenario 3-2 to Baseline 2 results at Station SBE5.....	53
4.3 Model Scenarios 4-1 and 4-2	53
Table 4-3-1: Comparison of Scenario 4-1 to Baseline 1 for DO results during spring.....	54
Table 4-3-2: Comparison of Scenario 4-1 to Baseline 1 for DO results during summer	55
Table 4-3-3: Comparison of Scenario 4-2 to Baseline 2 for DO results during spring.....	56
Table 4-3-4: Comparison of Scenario 4-2 to Baseline 2 for DO results during summer	56

Figure 4-3-1: Model Grid of Scenario 4-1 (Deepening SB Channel)	57
Figure 4-3-2: Model Grid of Scenario 4-2 (Deepening SB Channel)	58
Figure 4-3-3: Comparison of Scenario 4-1 to Baseline 1 results at Station LE5-4 (last panel shows the difference of bottom DO (scenario-baseline)	59
Figure 4-3-4: Comparison of Scenario 4-1 to Baseline 1 results at Station ELI2.....	60
Figure 4-3-5: Comparison of Scenario 4-1 to Baseline 1 results at Station SBE5.....	61
Figure 4-3-6: Comparison of Scenario 4-2 to Baseline 2 results at Station LE5-4.....	62
Figure 4-3-7: Comparison of Scenario 4-2 to Baseline 2 results at Station ELI2.....	63
Figure 4-3-8: Comparison of Scenario 4-2 to Baseline 2 results at Station SBE5.....	64
4.4 Model Scenarios 5-1 and 5-2.....	65
Table 4-4-1: Comparison of Scenario 5-1 to Baseline 1 DO results during spring	66
Table 4-4-2: Comparison of Scenario 5-1 to Baseline 1 DO results during summer	66
Table 4-4-3: Comparison of Scenario 5-2 to Baseline 2 DO results during spring	67
Table 4-4-4: Comparison of Scenario 5-2 to Baseline 2 DO results during summer	67
Figure 4-4-1: Model Grid of Scenario 5-1 (Deepening NH & SB Channels).....	68
Figure 4-4-2: Model Grid of Scenario 5-2 (Deepening NH & SB Channels).....	69
Figure 4-4-3: Comparison of Scenario 5-1 to Baseline 1 results at Station LE5-4.....	70
Figure 4-4-4: Comparison of Scenario 5-1 to Baseline 1 results at Station ELI2.....	71
Figure 4-4-5: Comparison of Scenario 5-1 to Baseline 1 results at Station SBE5.....	72
Figure 4-4-6: Comparison of Scenario 5-2 to Baseline 2 results at Station LE5-4.....	73
Figure 4-4-7: Comparison of Scenario 5-2 to Baseline 2 results at Station ELI2.....	74
Figure 4-4-8: Comparison of Scenario 5-2 to Baseline 2 results at Station SBE5.....	75
5 Transport Time	76
5.1. Existing Condition and Future Condition	76
Figure 5-1-1: Distribution of mean difference of daily vertical averaged freshwater age (days) (Baseline 2 minus Baseline 1, mean difference).....	77
Figure 5-1-2: Distribution of difference of saltwater age (days)	78
(Baseline 2 minus Baseline 1, mean difference).....	78
Figure 5-1-3: Distribution of difference of renewal time (days).....	79
(Baseline 2 minus Baseline 1, mean difference).....	79
5.2. Scenarios 3-1 and 3-2	79
Figure 5-2-1: Distribution of difference of freshwater age (days)	80
(Scenario 3-1 minus Baseline 1, mean difference)	80
Figure 5-2-2: Distribution of difference of saltwater age (days)	81
(Scenario 3-1 minus Baseline 1, mean difference)	81
Figure 5-2-3: Distribution of difference of renewal time (days).....	82
(Scenario 3-1 minus Baseline 1, mean difference)	82
Figure 5-2-4: Distribution of difference of freshwater age (days)	83
(Scenario 3-2 minus Baseline 2, mean difference)	83
Figure 5-2-5: Distribution of difference of saltwater age (days)	84

(Scenario 3-2 minus Baseline 2, mean difference)	84
Figure 5-2-6: Distribution of difference of renewal time (days).....	85
(Scenario 3-2 minus Baseline 2, mean difference)	85
5.3. Scenarios 4-1 and 4-2	86
Figure 5-3-1: Distribution of difference of freshwater age (days)	87
(Scenario 4-1 minus Baseline 1, mean difference)	87
Figure 5-3-2: Distribution of difference of saltwater age (days)	88
(Scenario 4-1 minus Baseline 1, mean difference)	88
Figure 5-3-3: Distribution of difference of renewal time (days).....	89
(Scenario 4-1 minus Baseline 1, mean difference)	89
Figure 5-3-4: Distribution of difference of freshwater age (days)	90
(Scenario 4-2 minus Baseline 2, mean difference)	90
Figure 5-3-5: Distribution of difference of saltwater age (days)	91
(Scenario 4-2 minus Baseline 2, mean difference)	91
Figure 5-3-6: Distribution of difference of renewal time (days).....	92
(Scenario 4-2 minus Baseline 2, mean difference)	92
5.4. Scenarios 5-1 and 5-2	93
Figure 5-4-1: Distribution of difference of freshwater age (days)	94
(Scenario 5-1 minus Baseline 1, mean difference)	94
Figure 5-4-2: Distribution of difference of saltwater age (days)	95
(Scenario 5-1 minus Baseline 1, mean difference)	95
Figure 5-4-3: Distribution of difference of renewal time (days).....	96
(Scenario 5-1 minus Baseline 1, mean difference)	96
Figure 5-4-4: Distribution of difference of freshwater age (days)	97
(Scenario 5-2 minus Baseline 2, mean difference)	97
Figure 5-4-5: Distribution of difference of saltwater age (days)	98
(Scenario 5-2 minus Baseline 2, mean difference)	98
Figure 5-4-6: Distribution of difference of renewal time (days).....	99
(Scenario 5-2 minus Baseline 2, mean difference)	99
6. Summary.....	100
7. References	100
Appendix A.	A1
<u>Appendix B.</u>	<u>B1</u>
<u>Appendix C.</u>	<u>C1</u>
<u>Appendix D.</u>	<u>D1</u>
<u>Appendix E.</u>	<u>E1</u>

1. Introduction

To investigate the feasibility for Norfolk Harbor channel deepening in the lower James and Elizabeth Rivers, one of the key services of the project is to evaluate the impacts of deepening the Atlantic Ocean Channel to 55 feet (from 50 feet), Thimble Shoal Channel to 55 feet (from 50 feet), Elizabeth River (north of Lambert Point) to 50 feet (from 45 feet) and the Southern Branch (north of the I64 Bridge) to 50/45/45 feet. In general, the shipping channel dredging will result in enhancement of estuarine gravitational circulation, accentuate the tidal and wind wave influence upstream, and affect the ecosystem dynamics in the lower Bay, particularly, dissolved oxygen (DO) in the James River and Elizabeth River. The real question is how much is that impact? Can it be quantitatively evaluated? Can the impact be measured temporally and spatially? VIMS scientists are working with engineers of Moffatt and Nichol and the Norfolk District of the U. S. Army Corps of Engineers to evaluate the impact of channel deepening on the hydrodynamics and dissolved oxygen (DO), and the flushing capabilities of the Lower James and Elizabeth Rivers, and to provide statistical measures to assess the impact resulting from channel deepening both locally and globally.

This report documents hydrodynamic and water quality model simulations for this study and key findings of the water quality model results related to environment assessment, particularly, changes of dissolved oxygen and flushing capacity.

2. Approach

The James River is a very unique estuary. Although it receives the largest discharge of nutrients among all Virginia tributaries, the DO conditions are generally good due to its strong gravitational circulation (Kuo and Neilson, 1987), which transports a large amount of high DO water from the Chesapeake Bay into the James River. The horizontal eddy system associated with the frontal system near Newport News Point is the important feature for the transport and retention of larvae inside the estuary (Shen et al., 1999). The Elizabeth River is a sub-estuary of the Lower James River, and these water bodies influence each other through their connection. The pollutant transport in and out of the Elizabeth River is strongly influenced by the James River. On the other hand, the recently observed harmful algae bloom (HAB) in the Elizabeth River and lower James River during the summer starts from the Lafayette River, a tributary of the Elizabeth River and is then transported to the James due to this unique eddy system (Morse et al., 2011). The long residence time of the Lafayette plus the nutrient input from stormwater is a possible trigger of the initiation of the HAB. Because of this unique geometry and estuary and subestuary configuration, any change of dynamics field and alteration of the estuary circulation could alter the transport processes of nutrients and pollutants. Gravitational circulation is the key mechanism of the estuarine transport processes that transports freshwater and pollutants out of the estuary near the surface and transports Bay waters from the outside to the bottom waters of the James. The strength of the circulation depends on the water depth. Increase of water depth will result in an increased gravitational circulation. With an increase of gravitational circulation, the estuarine stratification will increase. If the estuary becomes too stratified, the surface aeration will be reduced; consequently, the DO condition will decline (Shen et al., 2013).

The change of gravitational circulation could result in the change of estuarine residence time and transport time. The residence time is one of the important indexes for the dynamics condition for the ecosystem. The retention and transport of pollutants highly depend on the transport time (Nixon et al., 1996). The study of Chesapeake Bay (Shen and Wang, 2007) shows that the residence time will increase with an increase of stratification. Although an increase of stratification can result in an increase of transport of dissolved substances out of the Bay, it can decrease the vertical exchange of DO and degrade bottom DO. The vertical stratification strongly depends on the depth. The increase of channel depth due to dredging could cause changes of estuarine circulation and stratification. Consequently, both material transport and residence time can be altered. However, in the previous studies, the impact of channel deepening on DO has not been well-understood.

To evaluate the change of dynamics and its impact of DO, we not only need to examine the change of surface elevation, current, and salinity, but more importantly, we need to evaluate both the change of hydrodynamic conditions and the change of water quality conditions. Although there are many water quality parameters that need to be considered, two key water quality indicators are DO and algae. These two parameters are used by VA-DEQ to determine the existence of impaired conditions of a waterbody.

2.1 Hydrodynamic and water quality models

Currently VIMS is assisting Virginia DEQ to develop a James River water quality model using the HEM-3D modeling system to address water quality impairments in the James River based on DO and Chl-a criteria. The HEM-3D model was developed at the Virginia Institute of Marine Science (Park et al., 1995). The transports of state variables are driven by the EFDC model. The eutrophication model simulates the spatial and temporal distributions of water quality parameters including dissolved oxygen, phytoplankton (3 groups), and various species of carbon, nitrogen, phosphorus, and silica. The model is linked to the watershed model. Flow and loadings of nutrients from upstream and adjacent watersheds discharge to the water column to drive transport of water and water quality state variables. A sediment process model with twenty-seven state variables (DiToro and Fitzpatrick, 1993) has also been developed. The sediment process model, upon receiving the particulate organic matter deposited from the overlying water column, simulates their diagenesis and the resulting fluxes of inorganic substances (ammonium, nitrate, phosphate, and silica) and sediment oxygen demand back to the water column. The coupling of the sediment process model enables the model to simulate the long-term changes in water quality conditions in response to changes in nutrient loadings. A diagram of the modeling system is shown in Figure 2-1.

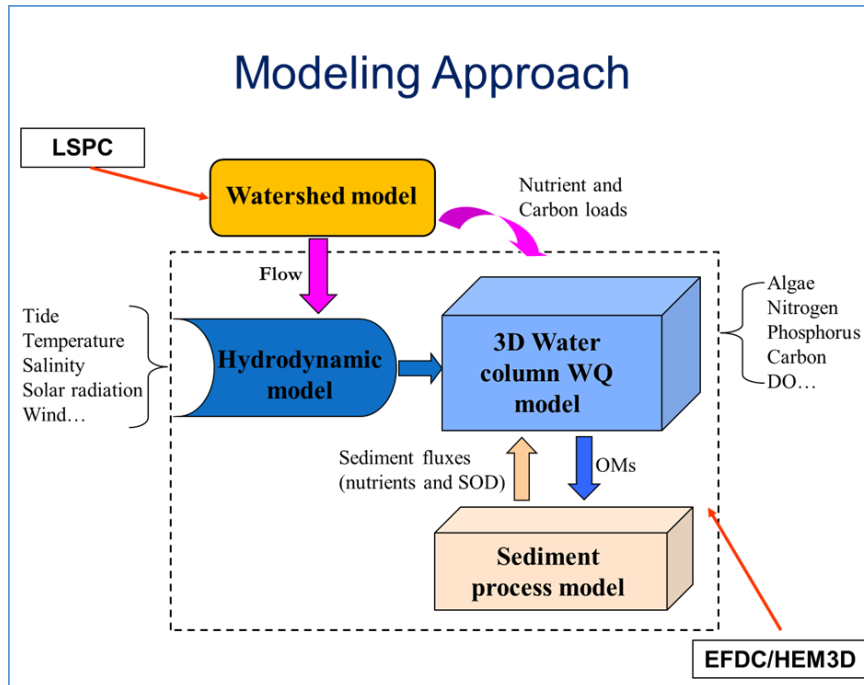


Figure 2-1: A diagram of the modeling approach for the James River

Hydrodynamic model

The hydrodynamic model of HEM3D modeling system is the Environmental Fluid Dynamics Code (EFDC). The EFDC model is an EPA-approved modeling tool (<http://www.epa.gov/athens/wwqtsc/html/efdc.html>). It is a general-purpose modeling package for simulating 1D, 2D, or 3D flow, transport, and bio-geochemical processes in surface water systems, including rivers, lakes, estuaries, reservoirs, wetlands, and coastal regions. EFDC was originally developed by Hamrick (1992; 1997) at the Virginia Institute of Marine Science for estuarine and coastal applications and is a public domain software. The EFDC model uses curvilinear, orthogonal horizontal coordinates and sigma vertical coordinates to represent the physical characteristics of a water body. The vertical mixing is parameterized using the Mellor and Yamada (1982) level 2.5 turbulence closure scheme as modified by Galperin et al. (1988). A high-order transport with anti-numerical diffusion scheme is implemented in the model that provides accurate transport for salinity and pollutants. In addition to the simulation of hydrodynamics, salinity, and temperature, EFDC is capable of simulating cohesive and non-cohesive sediment transport, near-field and far-field discharge dilution from multiple sources, eutrophication processes, the transport and fate of toxic contaminants in the water, and sediment phases (Shen et al., 2012), and the transport and fate of various life stages of finfish and shellfish. The model has been applied successfully to study James River transport processes (Shen and Lin, 2006, Shen et al., 2016), impact of dynamics on HAB in the lower James (Morse et al., 2011), and Chesapeake Bay (Hong and Shen, 2013).

For the present study, the model grid developed by VIMS for DEQ (Shen et al., 2016) was refined for a better representation of the channels. The model grid near the James River mouth is shown in (Figure 2-2). The James River hydrodynamic model has been set up, which is driven by

surface elevation specification along the James River mouth, freshwater discharge from the USGS gauge at Richmond and the lateral watershed runoff. Lateral inflows below the fall line are provided by the DEQ watershed model, which outputs daily flow. The open boundary conditions of tide, salinity, and temperature are driven by hourly outputs from a large Chesapeake Bay model of the SCHISM (Zhang et al., 2017). For details of SCHISM model simulations, reader is referred to Zhang et al. (2017).

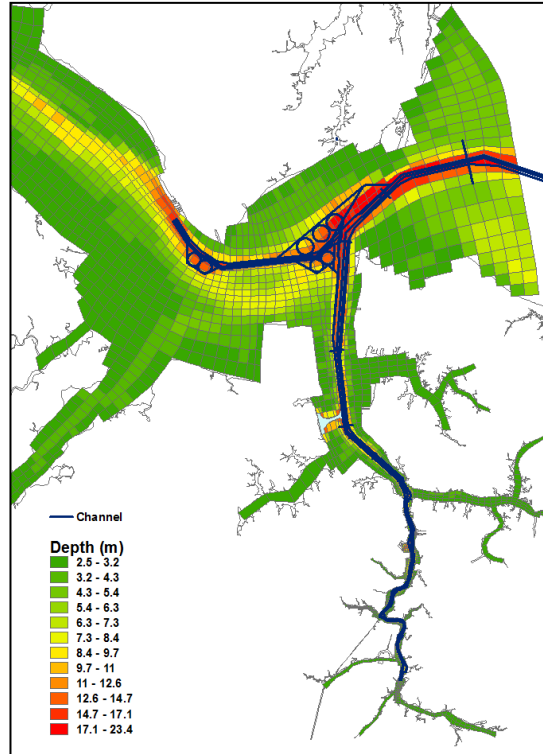


Figure 2-2: The current HEM3D model grid for the James River

Water Quality Model

The water quality model is a eutrophication model, which was developed at the Virginia Institute of Marine Science (Park et al., 1995). The eutrophication model is based on the original CE-QUAL-ICM water quality model developed by the Chesapeake Bay Program (Cercio and Cole, 1994; Cercio et al., 2010). The eutrophication model is a sub-model and is linked to the Environmental Fluid Dynamics Computer Code (EFDC; Hamrick, 1992). The transports of state variables are driven by the EFDC model. The eutrophication model simulates the spatial and temporal distributions of water quality parameters including dissolved oxygen, phytoplankton (3 groups), and various species of carbon, nitrogen, phosphorus, and silica. The kinetic processes is shown in Figure 2-3. The eutrophication model is capable of simulating 19 state variables for the eutrophication processes, which are:

- 1) cyanobacteria (blue-green algae)
- 2) diatoms
- 3) green algae (others)
- 4) refractory particulate organic carbon (RPOC)
- 5) labile particulate organic carbon (LPOC)
- 6) dissolved organic carbon (DOC)
- 7) refractory particulate organic phosphorus (RPOP)
- 8) labile particulate organic phosphorus (LPOP)
- 9) dissolved organic phosphorus (DOP)
- 10) total phosphate (PO_4)
- 11) refractory particulate organic nitrogen (RPON)
- 12) labile particulate organic nitrogen (LPON)
- 13) dissolved organic nitrogen (DON)
- 14) ammonium nitrogen (NH_4)
- 15) nitrate nitrogen (NO_{23})
- 16) particulate biogenic silica (PU)
- 17) available silica (SA)
- 18) chemical oxygen demand (COD)

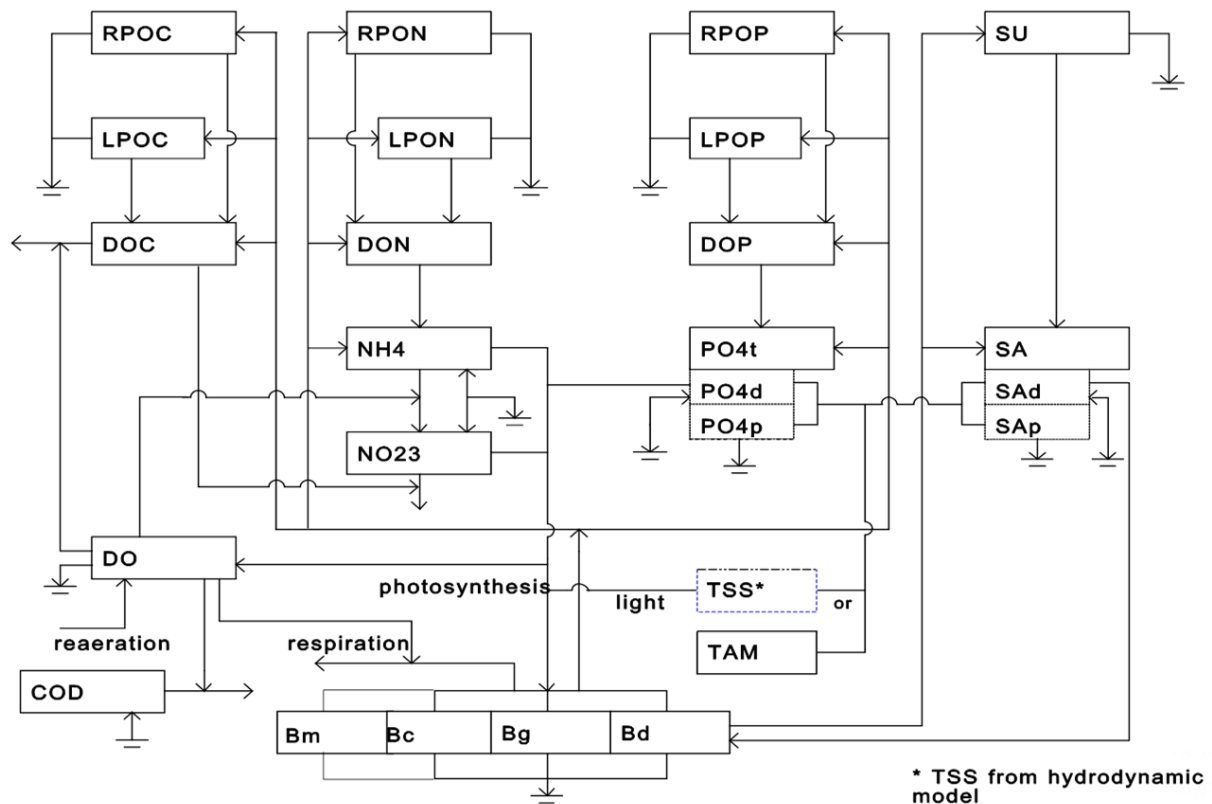


Figure 2-3: A diagram of kinetic processes of the eutrophication model

The governing mass-balance equation for water quality state variables consists of physical transport, advective and diffusive, and kinetic processes, which can be expressed as follows:

$$\frac{\partial C}{\partial t} + \frac{\partial(uC)}{\partial x} + \frac{\partial(vC)}{\partial y} + \frac{\partial(wC)}{\partial z} = \frac{\partial}{\partial x} K_x \frac{\partial(C)}{\partial x} + \frac{\partial}{\partial y} K_y \frac{\partial(C)}{\partial y} + \frac{\partial}{\partial z} K_z + \text{reaction} + \text{source} + \text{sink}$$

Where u , v , and w are velocities in the x-, y-, and z- directions, which are computed from the EFDC model. K_x , K_y , and K_z are horizontal diffusion coefficients in the x- and y- directions and the vertical diffusion coefficient in the z-direction, respectively. For the 3D model, K_x and K_y are sub-grid scales diffusion that are computed using the Smagorinsky scheme. K_z values are computed based on calculations by the Mellor-Yamada level 2.5 turbulence closure scheme (Mellor and Yamada, 1982; Galperin et al., 1988). The reaction term includes all biochemical processes, which will be presented below. Source and sink terms are external sources including point and non-point sources, atmospheric deposition, and other sources. The method to solve the transport equation is identical to that for the transport of salinity and thus readers are referred to Hamrick (1992) and Park et al. (1995).

The key state variable used in this project to assess water quality condition of the estuary is dissolved oxygen (DO). The simulation of DO is based on the following process:

(1) Effects of algae on dissolved oxygen in the water column

Algae produce oxygen during photosynthesis and consume oxygen through respiration. The quantity produced during photosynthesis depends on the form of nitrogen taken up. Since oxygen is released in the reduction of nitrate (NO_3), more oxygen is produced, per unit of carbon fixed, when NO_3 is the algal nitrogen source rather than when ammonia NH_4 is the source. When NH_4 is the nitrogen source, one mole of oxygen is produced per mole of carbon dioxide fixed. When NO_3 is the nitrogen source, 1.3 moles of oxygen are produced per mole of carbon dioxide fixed. The equation that describes the effect of algae photosynthesis on DO in the model is:

$$\frac{\partial DO}{\partial t} = \sum_x ((1.3 - 0.3 PN_x) P_x) \text{AOCR} \cdot B_x \quad (2-1)$$

where:

PN_x = algal group x preference for ammonium in which

P_x = production rate of algal group x (day^{-1})

AOCR = DO-to-carbon ratio in respiration (2.67 g O_2 per g C)

B_x = algal biomass (g C m^{-3})

As employed here, basal metabolism is the sum of all internal processes that decrease algal biomass. A portion of the metabolism is respiration and may be viewed as a reversal of production. In respiration, carbon and nutrients are returned to the environment accompanied by the consumption of DO. Respiration cannot proceed in the absence of DO. Basal metabolism decreases in proportion to the decrease of oxygen availability.

The formulation of this process can be described as:

$$\frac{\partial DO}{\partial t} = \sum_x \left(-\frac{DO}{KHR_x + DO} BM_x \right) AOCR \cdot B_x \quad (2-2)$$

where:

KHR_x = half-saturation constant of DO for algal DOC exudation ($g O_2 m^{-3}$)

BM_x = basal metabolism rates for algal group x (day^{-1})

(2) Effects of nitrification on dissolved oxygen

Nitrification is a process mediated by specialized groups of autotrophic bacteria that obtain energy through the oxidation of ammonia to nitrite and the oxidation of nitrite to nitrate. A simplified expression for complete nitrification is:



The equation indicates that two moles of oxygen are required to nitrify one mole of ammonia into nitrate. The simplified equation is not strictly true, however. Cell synthesis by nitrifying bacteria is accomplished by the fixation of carbon dioxide so that less than two moles of oxygen are consumed per mole of ammonium utilized (Wezernak and Gannon, 1968). In this study, nitrification is modeled as a function of available ammonium, dissolved oxygen, and temperature:

$$NT = \frac{DO}{KHONT + DO} \frac{NH_4}{KHNNT + NH_4} f(T) \cdot NTM \quad (2-4)$$

where:

NT = nitrification rate ($gm N m^{-3} day^{-1}$)

NTM = maximum nitrification rate at optimal temperature ($gm N m^{-3} day^{-1}$)

$KHONT$ = half-saturation constant of DO required for nitrification ($gm DO m^{-3}$)

$KHNNT$ = half-saturation constant of NH_4 required for nitrification ($gm N m^{-3}$)

Therefore, the effect of nitrification on DO is described as follows:

$$\frac{\partial DO}{\partial t} = -AONT \cdot NT \quad (2-5)$$

where:

$AONT$ = mass DO consumed per mass ammonia nitrified ($4.33 gm DO gm^{-1} N$)

(3) Effects of surface reaeration on dissolved oxygen

Reaeration occurs only in the model surface cells. The effect of reaeration is:

$$\frac{\partial DO}{\partial t} = \frac{K_R}{\Delta z_s} (DO_s - DO) \quad (2-6)$$

where:

K_R = reaeration coefficient (m day⁻¹)

Δz_s = model layer thickness (m)

DO_s = dissolved oxygen saturation concentration (gm DO m⁻³)

Saturation dissolved oxygen concentration DO_s is computed (Genet et al., 1974):

$$DO_s = 14.5532 - 0.38217 \cdot T + 0.0054258 \cdot T^2 - \frac{CL}{1.80655} (0.1665 - 5.866 \cdot 10^{-3} \cdot T + 9.796 \cdot 10^{-5} \cdot T^2) \quad (2-7)$$

where:

CL = chloride concentration (= salinity/1.80655)

The reaeration coefficient includes the effect of turbulence generated by bottom friction (O'Connor and Dobbins, 1958) and that by surface wind stress (Banks and Herrera, 1977):

$$K_r = \left(K_{r0} \sqrt{\frac{u_{eq}}{h_{eq}}} + W_{rea} \right) \frac{1}{\Delta Z} K T_r^{T-20}$$

u_{eq} = weighted velocity over cross-section (m/s)

h_{eq} = weighted depth over cross-section (m)

W_{rea} = wind-induced reaeration (m/day) = $0.728\sqrt{U_w} - 0.317U_w + 0.0372U_w^2$

U_w is wind velocity (m/s) at the 10-m height

$K T_r$ is constant for temperature correction.

(4) Effects of chemical oxygen demand on dissolved oxygen

In the present model, chemical oxygen demand (COD) represents the reduced materials that can be oxidized through inorganic means. The source of COD is bottom sediment demand. The kinetic equation showing the effect of chemical oxygen demand, including bottom sediment demand (bottom cells only) is:

$$\frac{\partial \text{DO}}{\partial t} = - \frac{\text{DO}}{\text{KHO}_{\text{COD}} + \text{DO}} \text{K}_{\text{COD}} \cdot \text{COD} \quad (2-8)$$

here:

COD = chemical oxygen demand concentrations (g O₂-equivalents m⁻³)
 KHO_{COD} = half-saturation constant of DO for oxidation of COD (g O₂ m⁻³)
 K_{COD} = oxidation rate of COD (day⁻¹)
 BF_{COD} = sediment flux of COD (g O₂-equivalents m⁻² day⁻¹).

$$\text{K}_{\text{COD}} = \text{K}_{\text{CD}} \cdot \exp(\text{KT}_{\text{COD}}[\text{T} - \text{TR}_{\text{COD}}]) \quad (2-9)$$

where:

K_{CD} = oxidation rate of COD at reference temperature TR_{COD} (day⁻¹)
 KT_{COD} = effect of temperature on oxidation of COD (°C⁻¹)
 TR_{COD} = reference temperature for oxidation of COD (°C).

Overall, the internal sources and sinks of dissolved oxygen include algal photosynthesis and respiration, atmospheric reaeration (surface cells only), heterotrophic respiration, nitrification, and oxidation of COD. The complete kinetic equation showing sediment oxygen demand is:

$$\begin{aligned} \frac{\partial \text{DO}}{\partial t} = & \sum_x \left((1.3 - 0.3 \cdot \text{PN}_x) \text{P}_x - \frac{\text{DO}}{\text{KHR}_x + \text{DO}} \text{BM}_x \right) \text{AOCR} \cdot \text{B}_x \\ & + \lambda_1 \frac{\text{K}_R}{\Delta z_s} (\text{DO}_s - \text{DO}) - \frac{\text{DO}}{\text{KHO}_{\text{DOC}} + \text{DO}} \text{AOCR} \cdot \text{K}_{\text{DOC}} \cdot \text{DOC} \\ & - \text{AONT} \cdot \text{NIT} - \frac{\text{DO}}{\text{KHO}_{\text{COD}} + \text{DO}} \text{K}_{\text{COD}} \cdot \text{COD} + \lambda_2 \frac{\text{SOD}}{\Delta z} \end{aligned} \quad (2-10)$$

A sediment process model with twenty-seven state variables (DiToro and Fitzpatrick, 1993) has also been developed. The sediment process model, upon receiving the particulate organic matter deposited from the overlying water column, simulates their diagenesis and the resulting fluxes of inorganic substances (ammonium, nitrate, phosphate, and silica) and sediment oxygen demand back to the water column. The coupling of the sediment process model enables the model to simulate the long-term changes in water quality conditions in response to changes in nutrient loadings.

The model is linked to the DEQ watershed model. Loading of organic carbon, nitrogen (particulate, dissolved, inorganic), and phosphorus (particulate, dissolved, inorganic) are

discharged to the water column from 87 watersheds adjacent to the James and Elizabeth Rivers. Figure 2-4 illustrates the linkage between the James River and the watershed models.

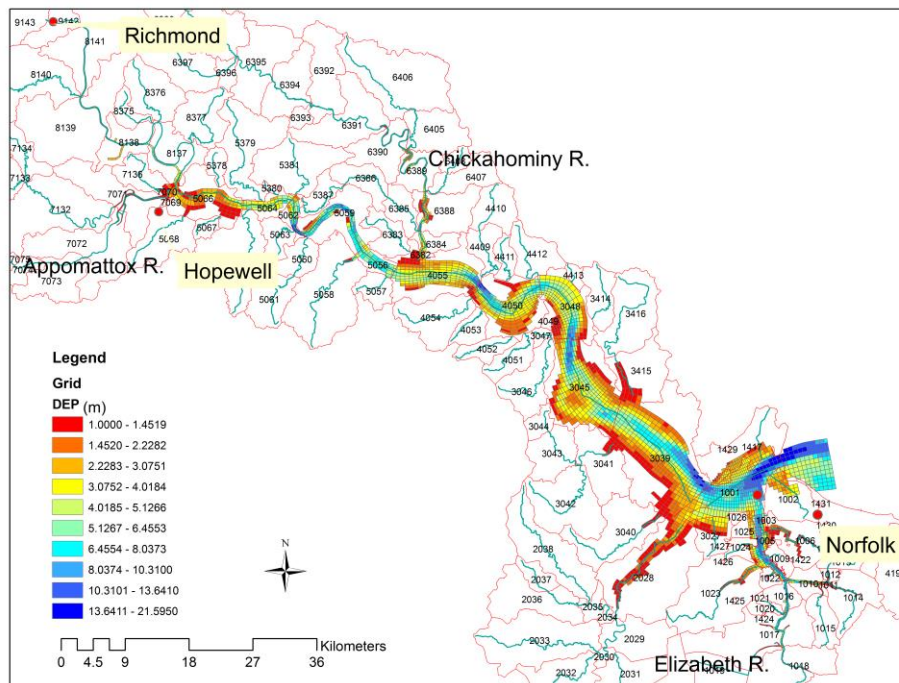


Figure 2-4: A map showing the linkage of the watershed and James River models.

2.3 Transport Time

Any change of hydrodynamic conditions will result in a change of transport processes, which is more important for transporting nutrients and phytoplankton and consequently affecting DO. Because it is difficult to evaluate the change of dynamic conditions (e.g. change of velocity, surface elevation) and their impact of DO, we can use a transport timescale to evaluate the impact of dynamics on water quality as it shows a cumulative effect. Transport timescales, such as residence time and renewal time, are the first-order representatives of the dynamics condition in the estuary, whereas the vertical transport time is directly related to DO exchange (Shen et al., 2013). The transport timescales are applied in this project to evaluate the change of dynamics conditions.

The timescales can be computed using the concept of water age (Delhez et al., 1999; Deleersnijder et al, 2001; Liu et al., 2012; Shen et al., 2013). Freshwater age is the elapsed time since a water parcel leaves the head of a tributary, where it has a continual freshwater input. The age at location x is the mean time required for a parcel to be transported from the head of a river to location x , regardless of its pathway. A diagram of the water age is shown in Figure 2-5. The age clock will be reset to zero if the water parcel travels back to the head, which usually doesn't occur.

Delhez et al. (1999) provided a way to use a numerical model to compute the water age. Assuming there is only one tracer released to a system without internal sources and sinks, the transport equation for computing the tracer concentration $C(t, \vec{x})$ and the age concentration $\alpha(t, \vec{x})$ can be expressed as (Deleersnijder et al., 2001):

$$\frac{\partial C(t, \vec{x})}{\partial t} + \nabla[\vec{u}C(t, \vec{x}) - K\nabla C(t, \vec{x})] = 0 \quad (2-11)$$

$$\frac{\partial \alpha(t, \vec{x})}{\partial t} + \nabla[u(t, \vec{x})\alpha(t, \vec{x}) - K\nabla\alpha(t, \vec{x})] = C(t, \vec{x}) \quad (2-12)$$

The mean age can be calculated as follows:

$$\tau_v(t, \vec{x}) = \frac{\alpha(t, \vec{x})}{C(t, \vec{x})} \quad (2-13)$$

where $\nabla = \vec{i} \frac{\partial}{\partial x} + \vec{j} \frac{\partial}{\partial y} + \vec{k} \frac{\partial}{\partial z}$, and K is the diffusivity tensor.

The advantage of this approach is that it does not depend on the release time, and both temporal and spatial variations can be computed, which is much more convenient compared to the approach using particle tracking. For this study, three timescales are evaluated, which are freshwater age, saltwater age, and renewal time.

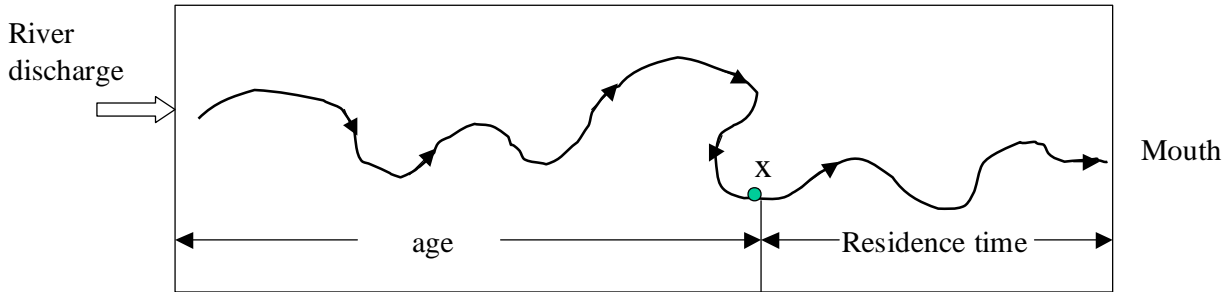


Figure 2-5: A diagram illustrating freshwater age and residence time in an estuary.

Freshwater age

Freshwater age can be used to evaluate the movement of freshwater. If the freshwater age decreases, it indicates that the freshwater moves out of the estuary with significant speed. It also suggests the pollutants discharged from river or runoff will be rapidly transported out. For this study, we look for the overall change of freshwater movement instead of each river. To calculate the freshwater age, tracer concentration $C(t, \vec{x})$ is forced to be 1 at all freshwater discharge locations including the lateral inflow, and the age concentration $\alpha(t, \vec{x})$ is forced to be 0 at the

corresponding discharge location. The initial condition for tracer and age concentrations will be set to zero inside the estuary. The radiation condition is applied to both the tracer and age concentrations, which allows a portion of the tracer to be transported out of the estuary during the ebb tide and to be transported back to the estuary during flood tide (Shen and Haas, 2004).

Saltwater age

Saltwater age can be used to measure the movement of saltwater. The age at a certain location indicates the time elapsed since it enters the mouth of the James. An increase of saltwater age at a certain location indicates that it will take a longer time for saltwater to be moved to that location. The saltwater age is a good indication of the change of gravitational circulation. A strong gravitational circulation will result in a short saltwater age. To calculate the saltwater age, tracer concentration $C(t, \vec{x})$ is forced to be 1 at the James River mouth and age concentration $\alpha(t, \vec{x})$ is also forced to be 0 at the mouth location. The initial condition for tracer and age concentration will be set to zero inside the estuary. Once the tracer has been transported out of the estuary, the age will be set to zero.

Renewal Time

Renewal time is used to evaluate the overall flushing capability of the estuary. And water mass inside the estuary can be replaced by either new freshwater or saltwater from the outside of the Bay. The time required for the water inside the estuary to be replaced by the new water indicates the flushing capability of the estuary. A decrease of the renewal time indicates that the estuary water will be renewed in a short period and pollutants can be diluted and moved out of the estuary much faster. To compute renewal time, tracer concentration $C(t, \vec{x})$ is forced to be 1 at the James River mouth and at the freshwater discharge location, and age concentration $\alpha(t, \vec{x})$ is forced to be 0 at the mouth and the corresponding discharge location. The initial condition for the tracer is set to 1 and age concentration will be set to zero inside the estuary. Because the computation does not depend on an initial condition, the impact of the initial condition will disappear after a short period. For the James River, the residence time is approximately a couple of months. The model was executed for more than 3 years. The result for the first half year was discarded. The age concentration was set to zero as soon as the water parcels moved out of the estuary.

In order to compute timescales, the hydrodynamic model was forced by the same boundary condition as the water quality model. The model simulations were conducted from October 2009 until the end of 2013. The average value of the last three years were examined spatially. Besides, temporal variations at selected stations were examined.

2.4 Scenarios: Existing Condition, Future Condition, and Scenarios

There are eight scenarios that were evaluated based on design, which were used to assess the change of water quality conditions in the James and Elizabeth River. These scenarios included both the existing and future conditions. A description of each scenarios is listed in Table 2-1.

Baseline 1 is the existing condition (Scenario 1), which was used for model calibration. The 2nd Scenario (Baseline 2) is referred to as “future without project.” This baseline scenario included CIEE and NIT Piers as the future condition. According to the previous and current studies of the impact of the 3rd Crossing on the James and Elizabeth River, the impact of the 3rd Crossing was observed to be very local and both minor changes of velocity and salinity occurred only near bridge piers within a couple of hundred meters. It will affect neither vertical stratification nor DO, nor gravitational circulation. Therefore, the impact of the 3rd Crossing is not included in this study. For the local impact of the 3rd Crossing, readers are referred to Appendix A. A detailed description for each scenario is listed in Table 2-1. Channel configuration are listed in Table 2-2. There are three design cases for channel deepening, which are referred to as the deepened NH channel, the deepened SB channel, and the deepened NH & SB channels. Each scenario case was evaluated against existing condition Baseline 1 and future condition Baseline 2. For simulation of each scenario, the bathymetry of the model was changed according to the scenarios and channel configuration (Table 2-2). The depth of deep channel will be altered based on design. For each simulation, the boundary conditions and loadings for water quality parameters were identical.

Table 2-1: Description of the scenarios

Runs	Scenario	Description	Norfolk Harbor Deepened	So Branch Deepened
1	1- Baseline – Existing Conditions	<p>Current Without-project conditions/Baseline Includes:</p> <ul style="list-style-type: none"> CIEE with the 2 cross dikes (as is conditions)– no fill between the dikes, or any dredging of the access channel 	No	No
2	2 -Baseline - Future Without Project Conditions	<p>Future without-project Includes consideration of:</p> <ul style="list-style-type: none"> CBBT – TSC parallel tunnel HRBT – parallel tunnel 3rd Crossing/ Patriots Crossing NIT Piers 1 and 2 removed, with dredged area to -50' CIEE full build out <p>Note: VIMS will provide memo/input detailing how above is being taken into consideration.</p>	No	No
3	3-1	<p>Existing Conditions with deepened NH channel <i>With Project Scenario</i> that includes a deepening of the Norfolk Harbor and Channels <u>without</u> the So Branch of the Elizabeth River, using existing conditions in Run 1.</p>	Yes	No
4	3-2	<p>Future Conditions with deepened NH channel <i>With Project Scenario</i> that includes a deepening of the Norfolk Harbor and Channels <u>without</u> the So Branch of the Elizabeth River deepened, using future conditions noted in Run 2.</p>	Yes	No
5	4-1	<p>Existing Conditions with deepened SB channel <i>With Project Scenario</i> that includes a deepening of the So Branch of the Elizabeth River <u>without</u> the Norfolk Harbor and Channels using existing conditions in Run 1.</p>	No	Yes

6	4-2	Future Conditions with deepened SB Channel With Project Scenario that includes a deepening of the So Branch of the Elizabeth River <u>without</u> the Norfolk Harbor deepened, using future conditions noted in Run 2.	No	Yes
7	5-1	Existing Conditions with deepened NH & SB channels With Project Scenario that includes a deepening of <u>both</u> the Norfolk Harbor and Channels <u>and</u> the So Branch of the Elizabeth River using existing conditions in Run 1.	Yes	Yes
8	5-2	Future Conditions with deepened NH & SB Channel With Project Scenario that includes a deepening of <u>both</u> the So Branch of the Elizabeth River <u>and</u> the Norfolk Harbor, using future conditions noted in Run 2.	Yes	Yes

Table 2-2: Description of Channel Configurations

Norfolk Harbor			
	Channel	<i>Assumed Depth</i>	<i>Comments</i>
A	Atlantic Ocean Channel	-61 feet	57' Req'd + 4' Allowable Overdepth
B	Thimble Shoal Channel	-58 feet	55' Req'd +3' Allowable Overdepth
C	Norfolk Harbor Sewells Point to Lamberts Bend (Norfolk Harbor Entrance Reach, Norfolk Harbor Reach and Craney Island Reach)	-58 feet	55' Req'd +3' Allowable Overdepth
D	Channel to Newport News	-58 feet	55' Req'd +3' Allowable Overdepth
E	Anchorage F	-58 feet	55' Req'd +3' Allowable Overdepth
Elizabeth River, Southern Branch			
		<i>Assumed Depth</i>	<i>Comments</i>
A	Elizabeth River Reach	-47 feet	45' Req'd +2' Allowable Overdepth (note navy deepened to 47' in 2011, 600' wide)
B	Lower Reach	-47 feet	45' Req'd +2' Allowable Overdepth (note navy deepened to 47' in 2011, 600' wide)
C	Middle Reach	-47 feet	45' Req'd +2' Allowable Overdepth
D	Upper Channel, Reach A Nor-So Bridge to Gilmerton With St Julian Turning Basin	-42 feet	40' Req'd +2' Allowable Overdepth
E	Upper Channel, Reach B With Newton Cr Turning Basin	-37 feet	35' Req'd +2' Allowable Overdepth
F	Upper Channel Reach C	-37 feet	35' Req'd +2' Allowable Overdepth

3. Model Calibration and Verification

Both hydrodynamic and water quality models have undergone model calibration and verification. The hydrodynamics model was calibrated against observations of tide, temperature, and salinity. NOAA tidal data are available at Sewells Point. Surface elevation observations are also available at several stations of the Virginia Estuarine and Coastal Observing System (VECOS <http://web2.vims.edu/vecos/Default.aspx>) from 2006-2008. The locations of the observed tide and water quality stations are shown in Figures 3-1 and 3-2. The model calibration of tide is from 2006-2008. The model was forced by surface elevation, salinity, and temperature at the open boundary and the open boundary condition was generated by the Chesapeake Bay large domain model (Zhang et al., 2017). During this calibration period, the Norfolk Harbor Channel was not dredged. An example of model calibration of surface elevation during 2006 is shown in Figures 3-3 and 3-4. Model calibration was for existing (Baseline 1) conditions. The statistics are summarized in the Taylor diagram (Figure 3-5). We used the Taylor diagram to summarize the model performance in a single diagram, which provides a concise statistical summary of how well patterns match each other in terms of their correlation, their root-mean-square error and the ratio of their variance (Taylor, 2001). There are three axes shown in the diagram that represent correlation coefficients, the centered root-mean-square error, and standard deviation. All data (both model and observations) are normalized by the standard deviation at a reference station. The correlation axis shows the correlation between model results and observations. The standard deviation axis indicates the deviation of model results from measurements measured by the standard deviations. For a small value, it indicates that the variation of simulations close to the observation. The root-mean-square shows that root-mean-square error. The errors are within 0.5 root-mean-square error at the reference station. Examples of salinity calibration are shown in Figures 3-6 and 3-7.

The salinity intrusion along the James River is verified by comparing monthly seasonal averaged salinity from 2007-2009 at each station and its corresponding minimum and maximum against the observations. It can be seen that modeled mean salinity are located within the variation of observations along the deep channel of the James River. This suggests that predictions of salt intrusion distance agree with observations. Both maximum and minimum salinity are also plotted, which shows variation of the salt intrusion. The variation is within the range variation of salinity in general. Comparisons are shown in Figures 3-8 to 3-11. Detailed model results of time series plots of tide, salinity, and temperature at selected stations and simulation years are included in Appendices B, C, and D, respectively. Overall, the model results are satisfactory. Although the Chesapeake Bay large domain model and this James River model are calibrated for salinity, we recommend to use large domain model as primary sources to analyze salinity and current because it has a much finer grid resolution for consistency.

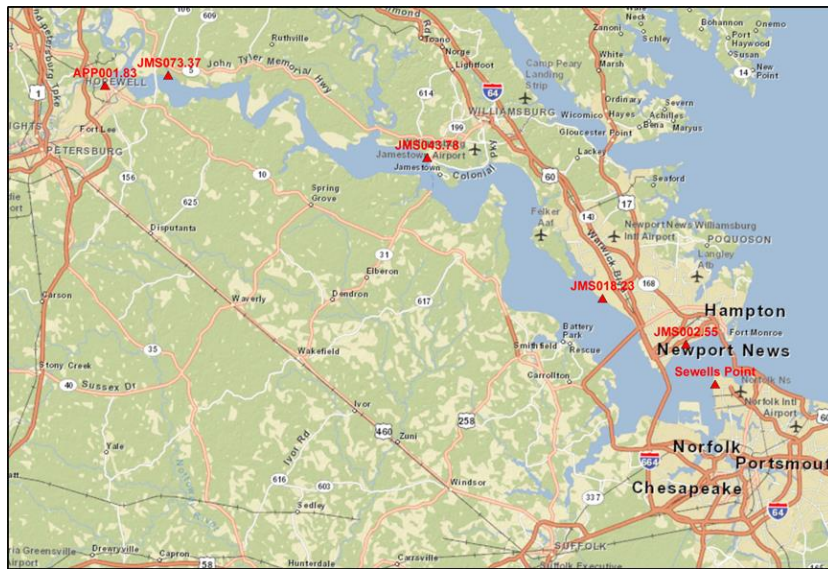


Figure 3-1: Tidal and surface elevation monitoring stations

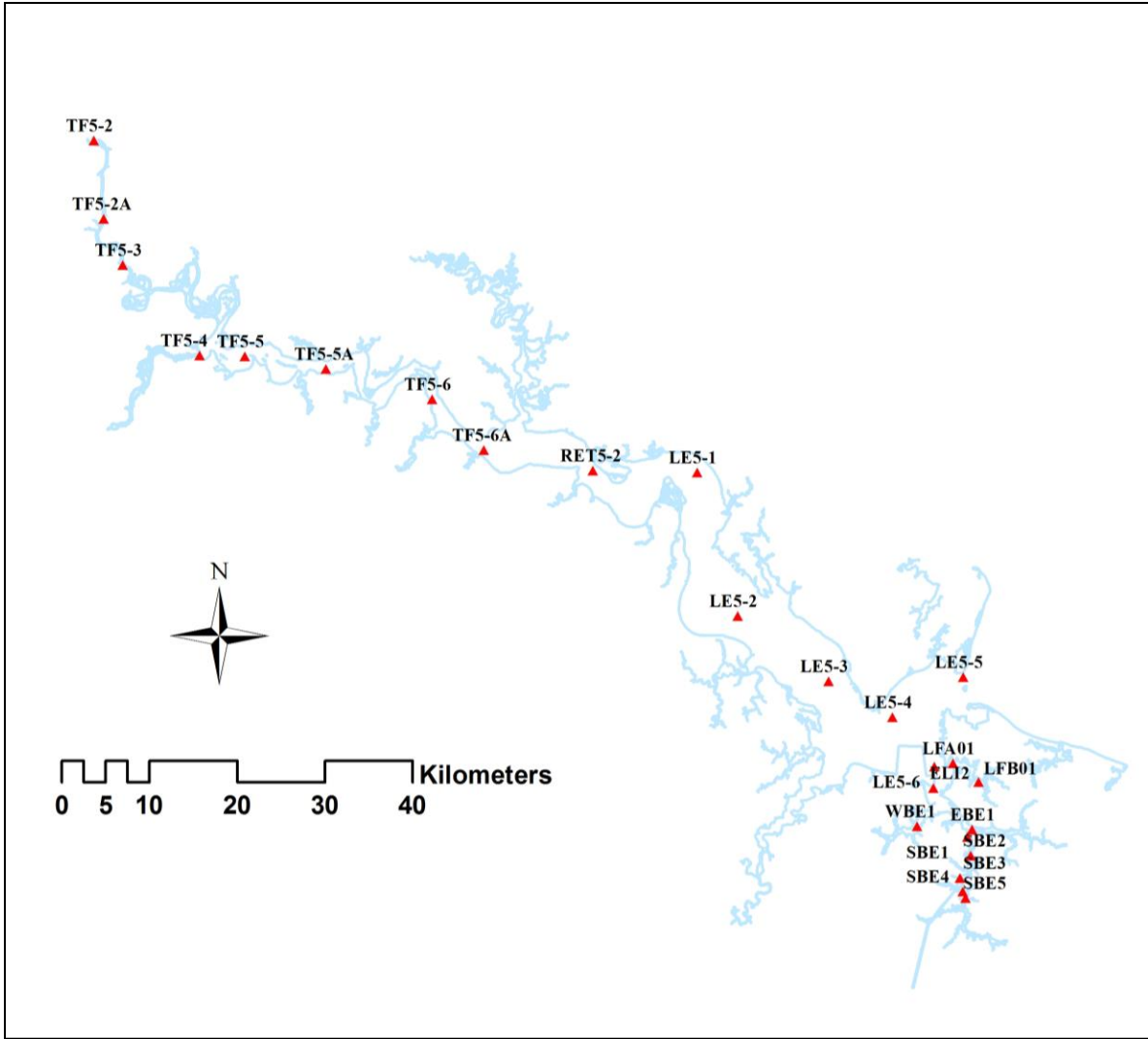


Figure 3-2: Water quality monitoring stations

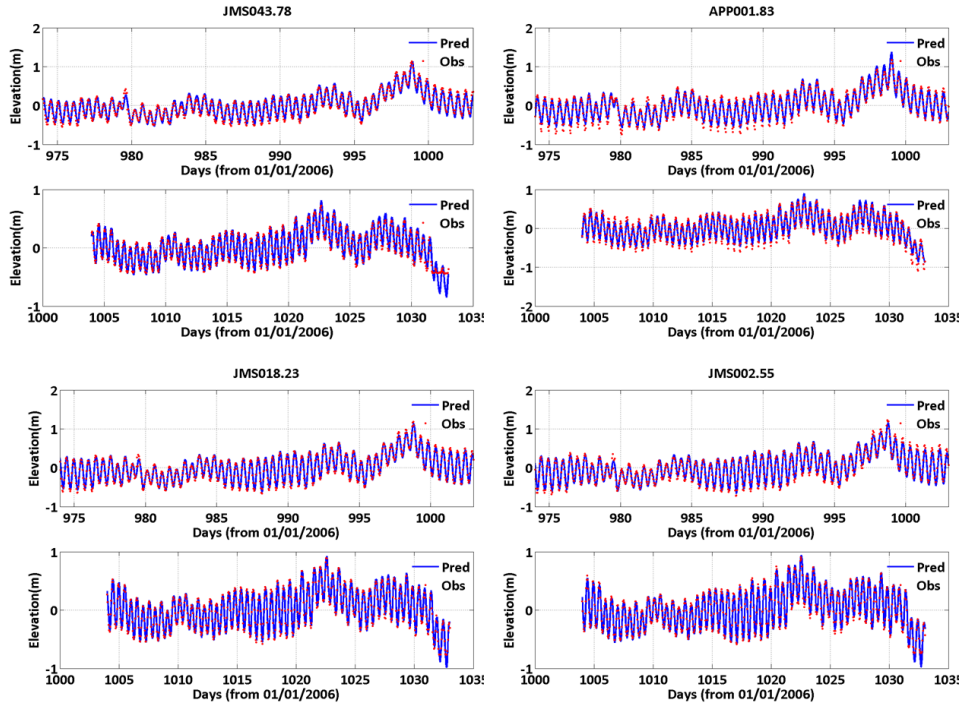


Figure 3-3: Comparison of surface elevation between model predictions and observations

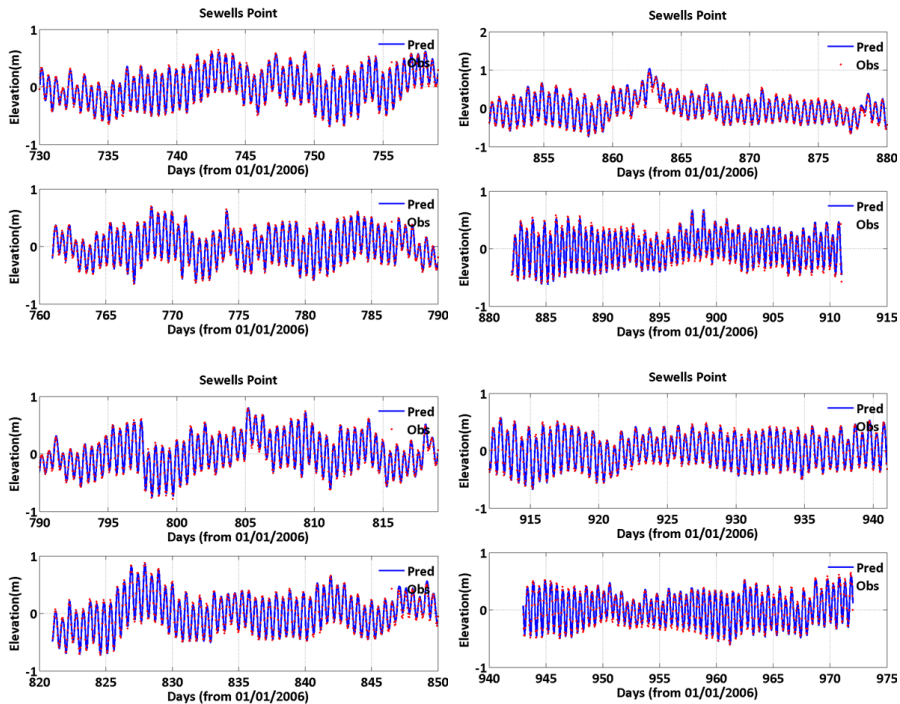


Figure 3-4: Comparison of surface elevation between model predictions and observations (each panel shows a comparison of one month)

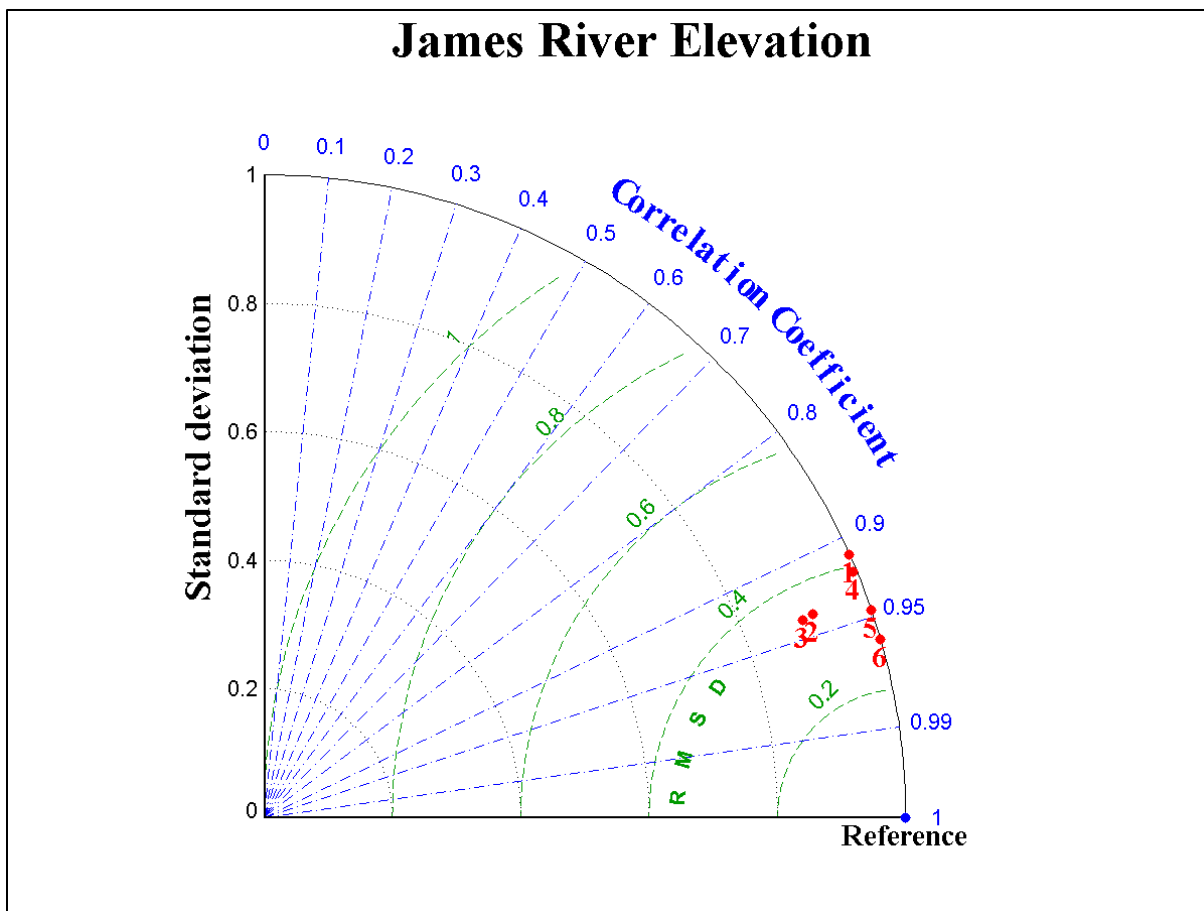


Figure 3-5: Taylor diagram representing model-data comparisons at 6 tidal stations in the James River. Three axes represent correlation coefficients (blue lines), the centered root-mean-square error (green lines), and normalized standard deviation (black lines) (Station location: 1=JMS043.78, 2= JMS073.37, 3=APP001.83, 4= JMS018.23, 5= JMS002.55, 6= Sewells Point).

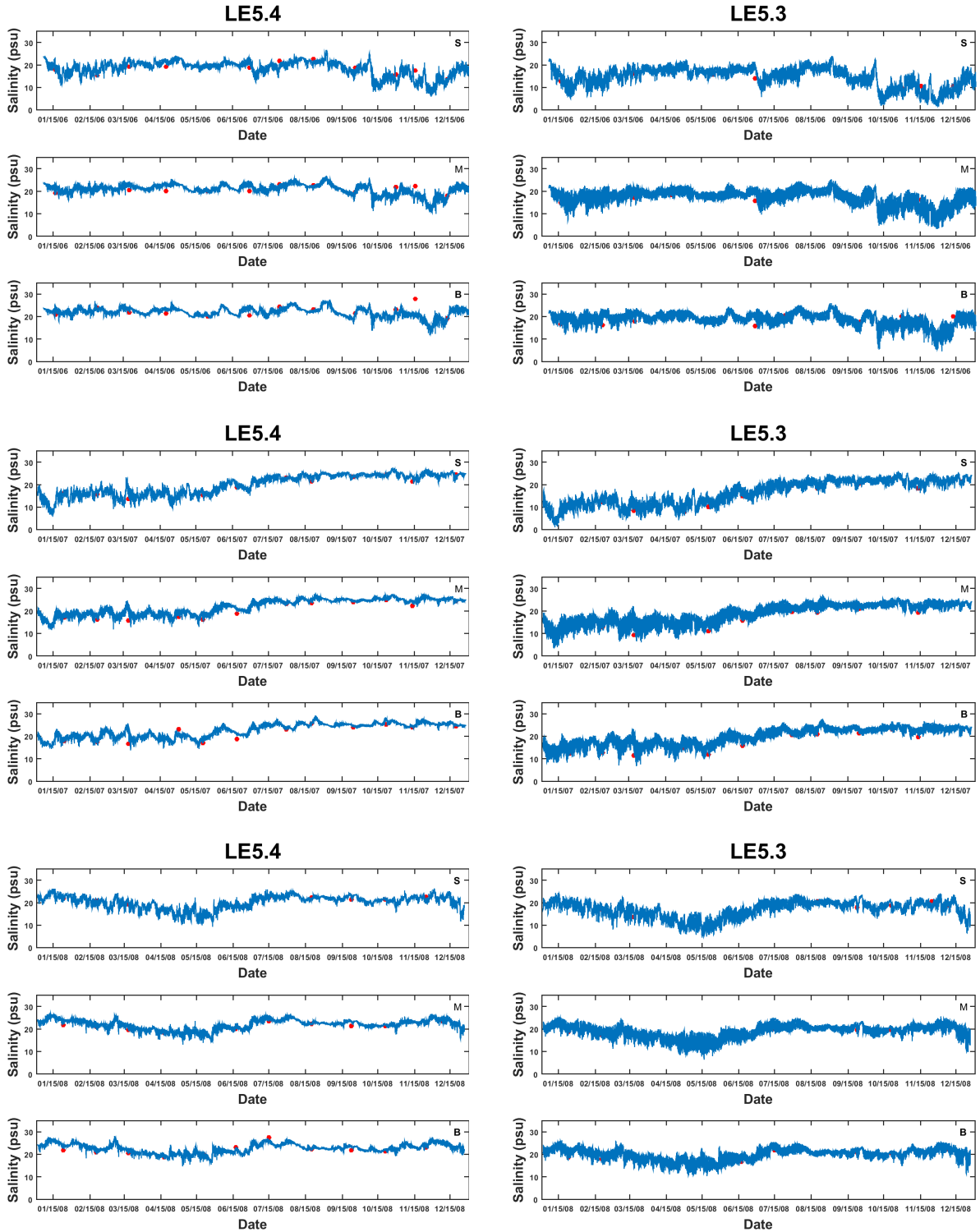


Figure 3-6: Comparison of salinity (surface, middle, and bottom layers) between model predictions and observations. (Red points signify observations and blue lines are model simulations).

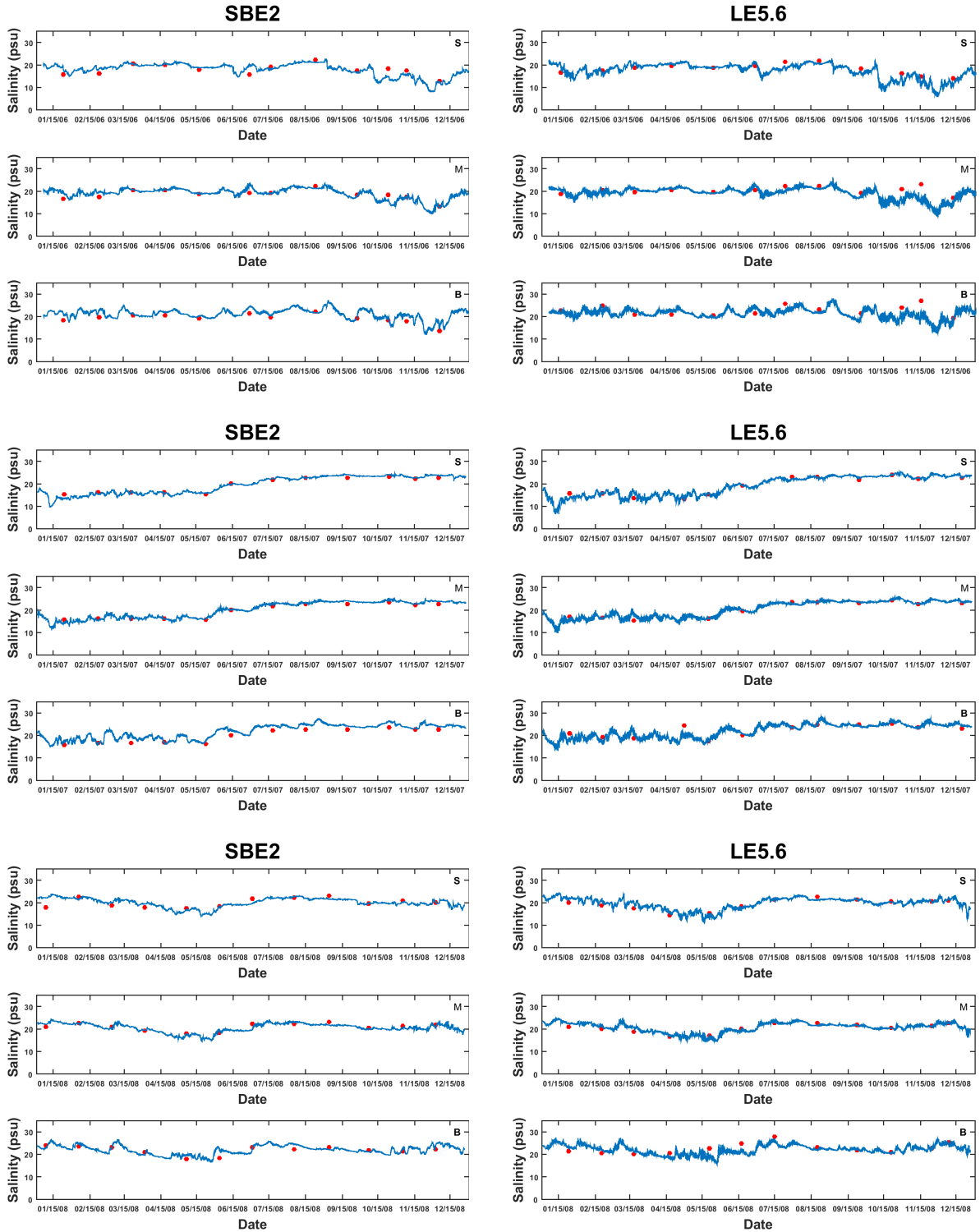


Figure 3-7: Comparison of salinity (surface, middle, and bottom layers) between model predictions and observations. (Red points signify observations and blue lines are model simulations).

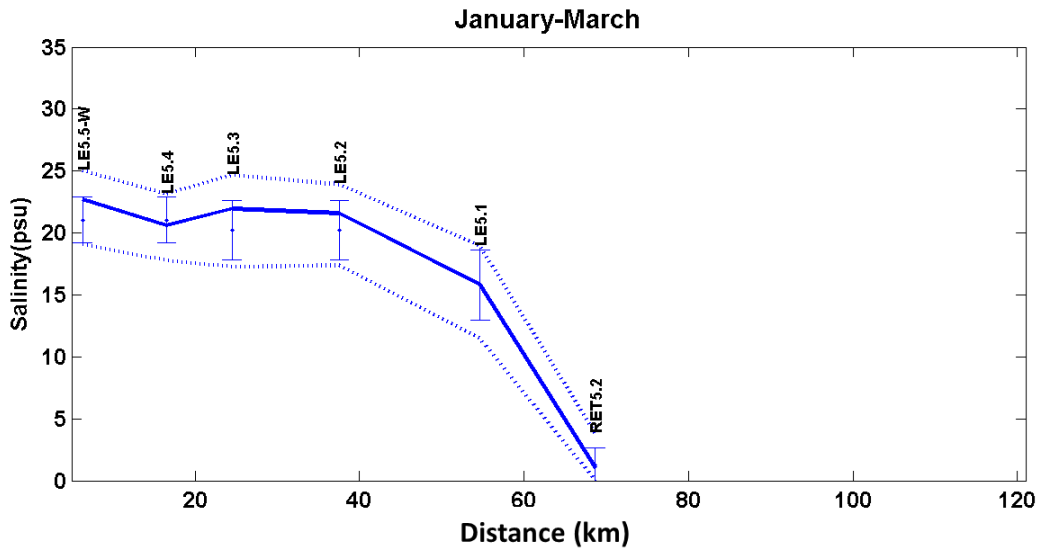


Figure 3-8: Comparison of vertical mean salinity intrusion long the James in January to March period (solid line is modeled mean salinity and dashed lines are modeled minimum and maximum salinity, and the vertical bar shows the variation of observations).

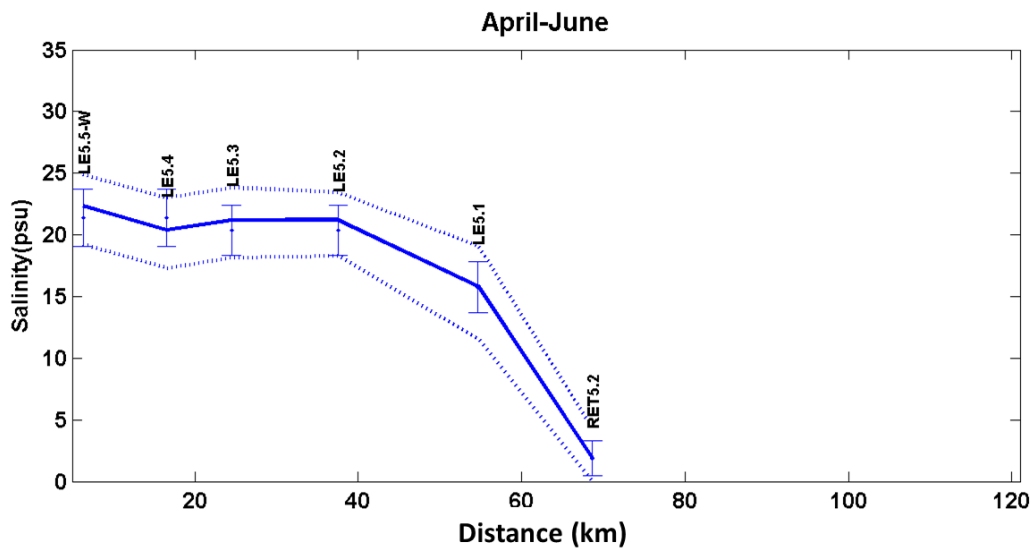


Figure 3-9: Comparison of vertical mean salinity intrusion along the James in the April-to-June period (solid line is modeled mean salinity and dashed lines are modeled minimum and maximum salinity, and the vertical bar shows the variation of observations).

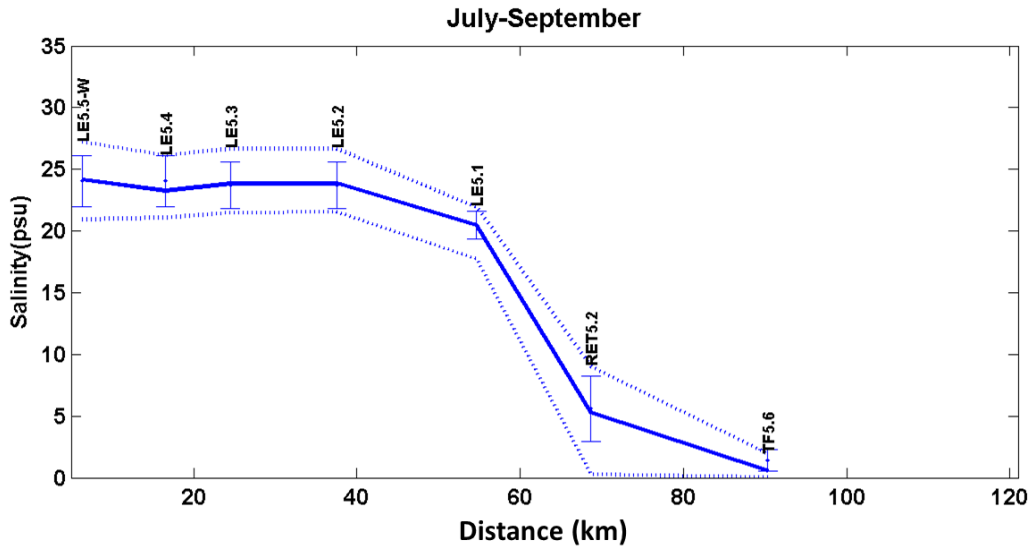


Figure 3-10: Comparison of vertical mean salinity intrusion along the James in the July-to-September period (solid line is modeled mean salinity and dashed lines are modeled minimum and maximum salinity, and the vertical bar shows the variation of observations).

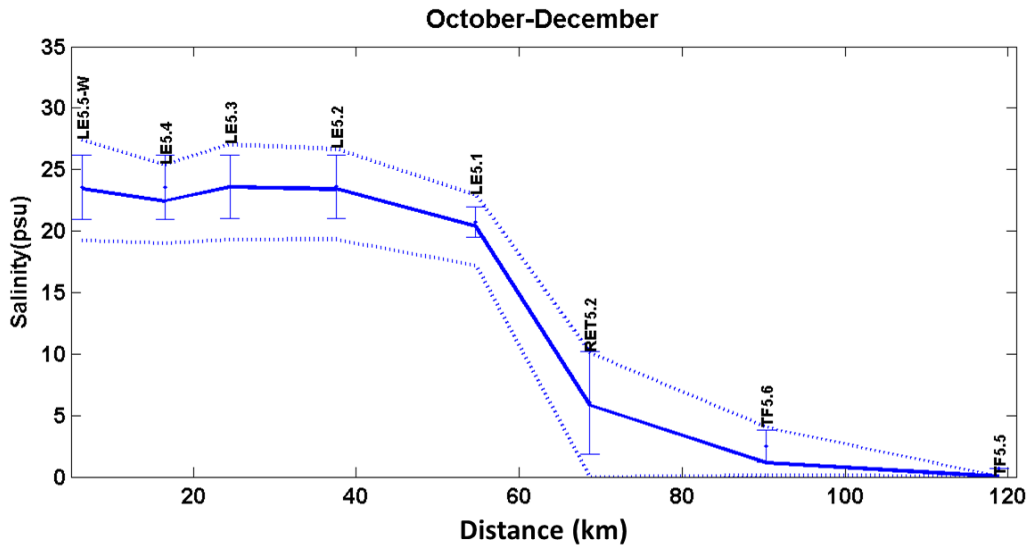


Figure 3-11: Comparison of vertical mean salinity intrusion along the James in the October-to-December period (solid line is modeled mean salinity and dashed lines are modeled minimum and maximum salinity, and the vertical bar shows the variation of observations).

The water quality calibration was conducted during the 2007-2008 period. Model performance was evaluated using multiple quantitative metrics, which are defined as follows:

Mean error: $MER = \sum_{k=1}^n (P_k - O_k)/N$

Absolute error: $AER = \sum_{k=1}^n |P_k - O_k|/N$

Relative error: $REER = \frac{\sum_{k=1}^n |P_k - O_k|}{\sum_{k=1}^n O_k} \times 100\%$

Root-mean-square error: $RMSE = \sqrt{\frac{\sum_{k=1}^n (P_k - O_k)^2}{n}}$

Correlation Coefficient: $R = \frac{\sum (P_k - \bar{P}_k)(O_k - \bar{O}_k)}{\sqrt{\sum (P_k - \bar{P}_k)^2} \sqrt{\sum (O_k - \bar{O}_k)^2}}$

Model Skill: $WS = 1 - \frac{\sum_{k=1}^n (P_k - O_k)^2}{\sum_{k=1}^n (P_k - \bar{P}_k)^2}$

Akaike information criterion $AIC = n \ln(Cgm) + 2 \times k \times (n/(n-k-1))$

where Cgm is mean residual sum of square and k is number of estimated parameters of the linear model (k=2)

$$Cgm = \frac{\sum_{k=1}^n (P_k - O_k)^2}{n}$$

Where P_k are model predicted values, O_k are observed values, and n is the total number of samples.

Comparisons of observations versus model predictions of algae, DIN, DIP, and DO from 2011-2013 at selected stations are shown in Figures 3-12 to 3-20. The model-data-comparison statistics are shown along the tops of these plots. Statistics are computed from the 2007-2013 period. Figures show comparisons of modeled and observed state variables at each station. (Red and black lines are daily averaged model results at surface and bottom, respectively. Blue and green lines are daily maximum and minimum concentrations in the water column, respectively. Statistics are computed using both data at the surface and bottom layers. Downward-pointing triangle symbols are observations at the surface, and upward-pointing triangle symbols are observations at the bottom).

We only plotted results from the last three year here. Comparing model predictions and station observations shows that the model simulates well for algae, DIN, DIP, and DO. The DO simulation has a high accuracy and the root-mean-square error ranges from 0.66 to 1.67 mg/L. The model shows that nitrogen is under-predicted, while algae is over-predicted at Station SBE5. Because the watershed model only includes a portion of the upstream watershed, the watershed upstream of the spillway is not included. Therefore, nitrogen loading seems under-estimated. It can be seen that algal is not limited by the nitrogen. The over-prediction of algae could be due to the light function. The model did not simulate TSS, but rather used the interpolation method to estimate spatial and temporal variations of TSS, which may not represent the temporal variation at this station. In general, DO is well-simulated from a model skill perspective. As all models have tuncertainty, the RMSE error of DO should be taken into consideration when using model results to estimate absolute change of DO when assessing DO variation for different scenarios. The Chesapeake Bay Program introduced a method for correction of model error when conducting DO assessment (Keisman and Shenk, 2013), which can be applied.

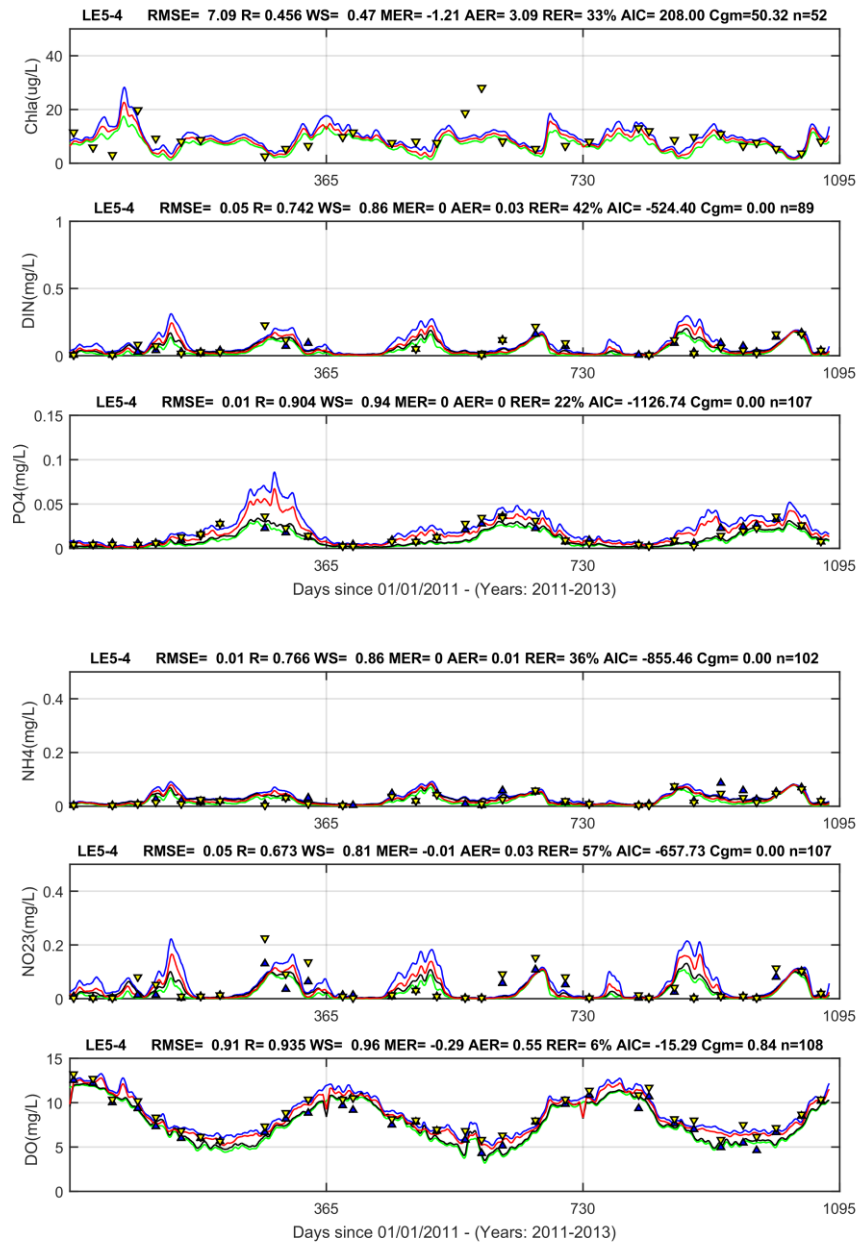


Figure 3-12: Model verification results at Station LE5-4 (red and black lines are daily averaged model results at surface and the bottom, respectively. Blue and green lines are daily maximum and minimum concentrations in the water column, respectively. Statistics are computed using both data at the surface and bottom layers. Downward-pointing triangle symbols are observations at the surface, and upward-pointing triangle symbols are observations at the bottom).

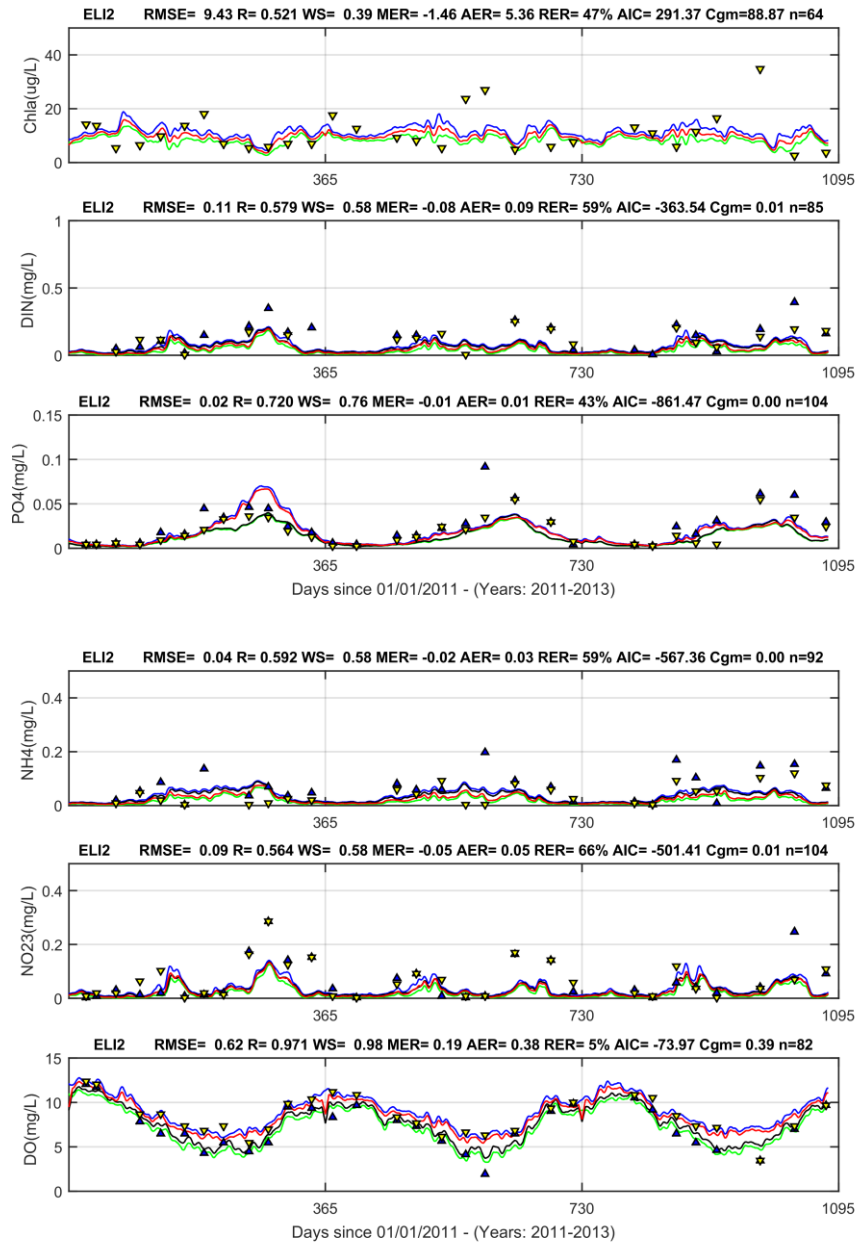


Figure 3-13: Model verification results at Station ELI2 (see caption of Fig. 3-12 for descriptions of lines and symbols)

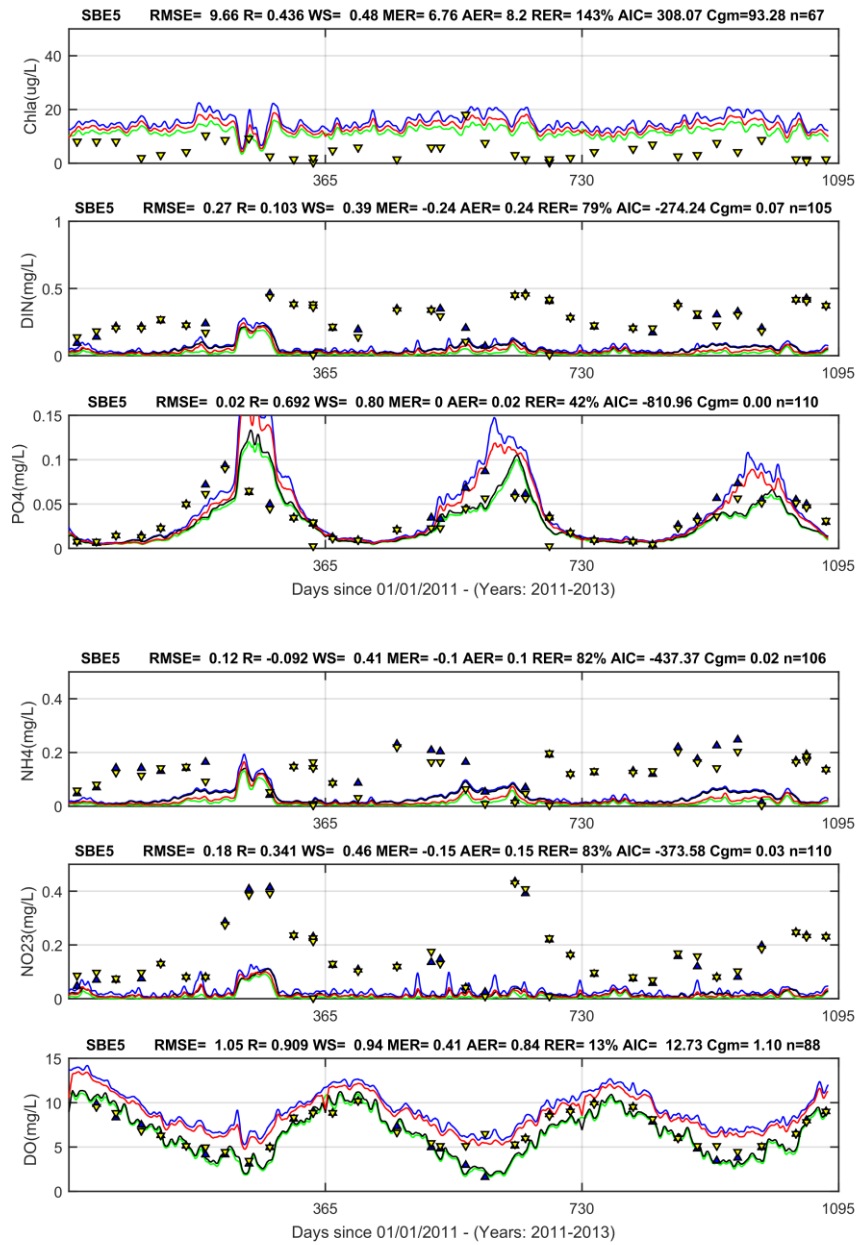


Figure 3-14: Model verification results at Station SBE5 (see caption of Fig. 3-12 for descriptions of lines and symbols)

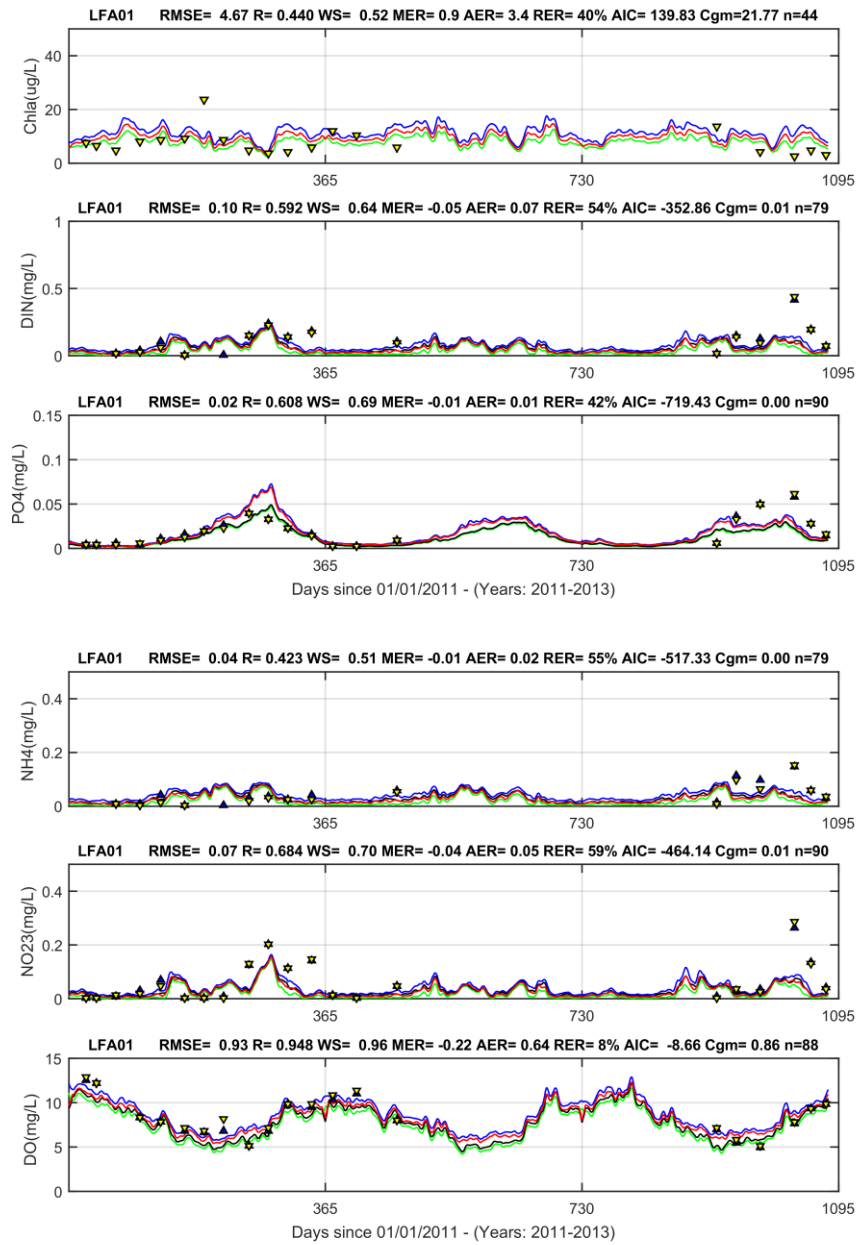


Figure 3-15: Model verification results at Station LFA01 (see caption of Fig. 3-12 for descriptions of lines and symbols)

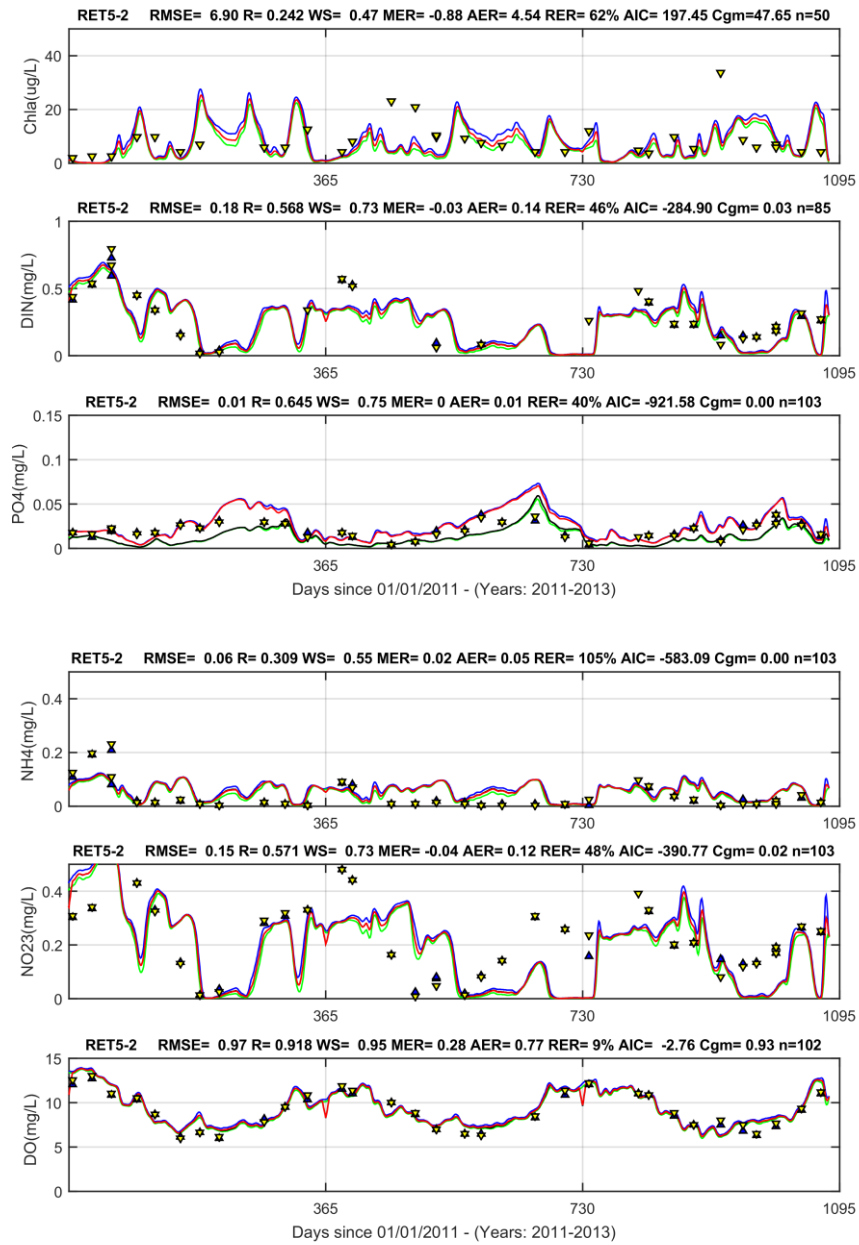


Figure 3-16: Model verification results at Station RET5-2 (see caption of Fig. 3-12 for descriptions of lines and symbols)

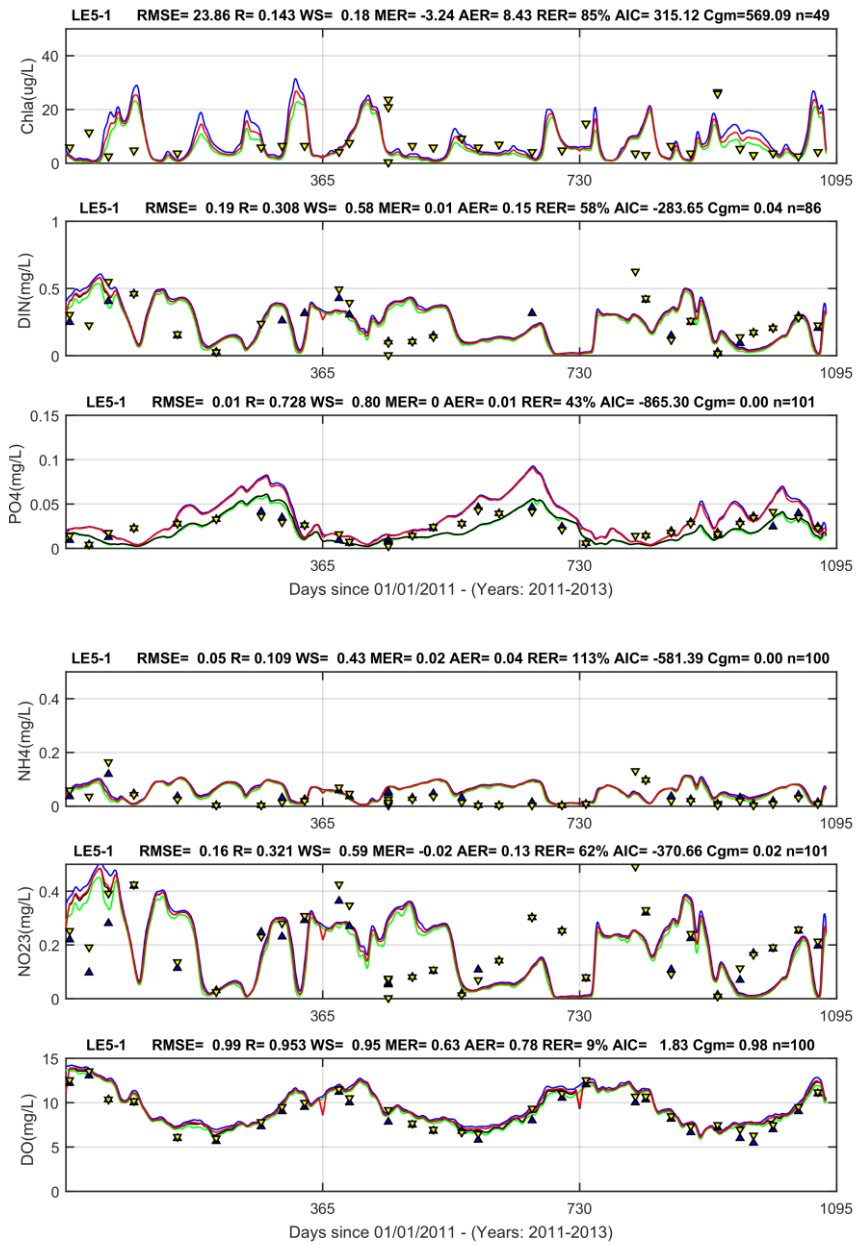


Figure 3-17: Model verification results at Station LE5-1(see caption of Fig. 3-12 for descriptions of lines and symbols)

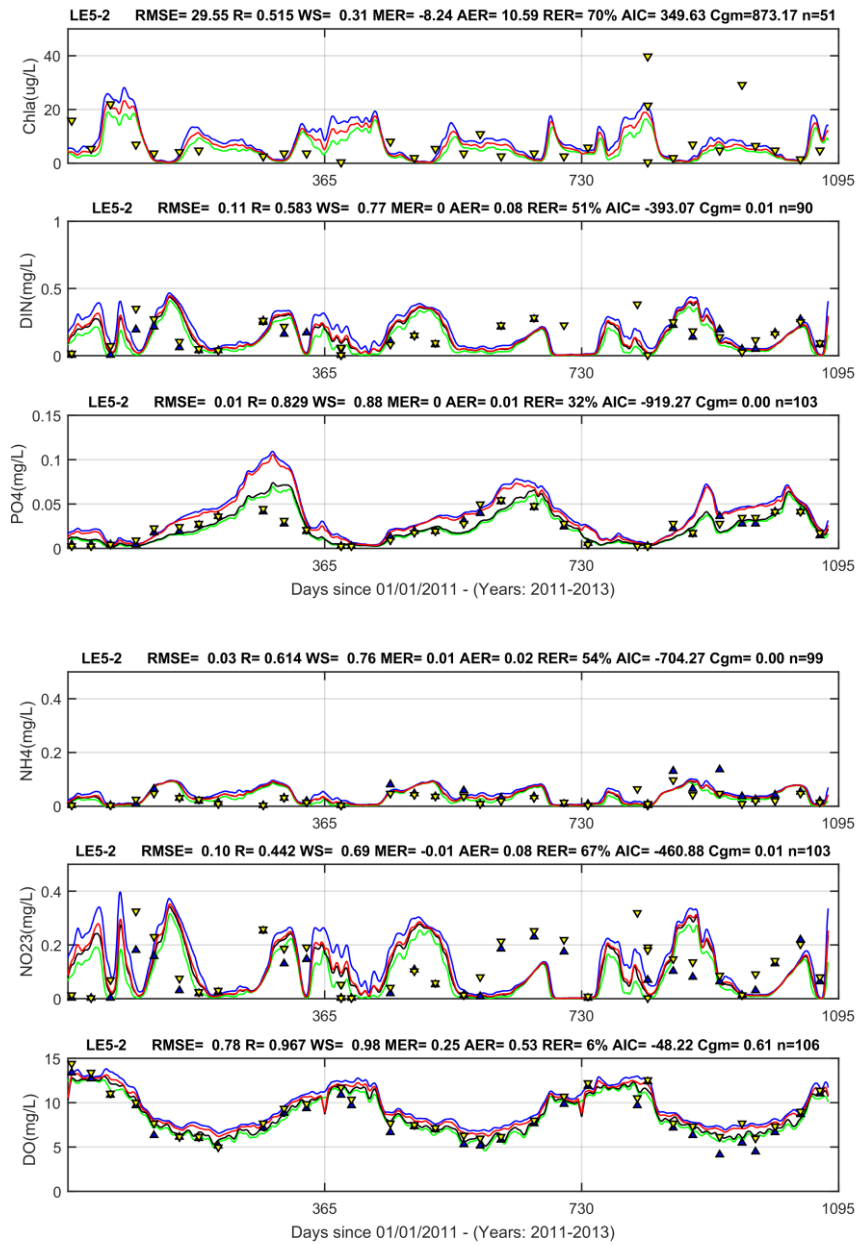


Figure 3-18: Model verification results at Station LE5-2 (see caption of Fig. 3-12 for descriptions of lines and symbols)

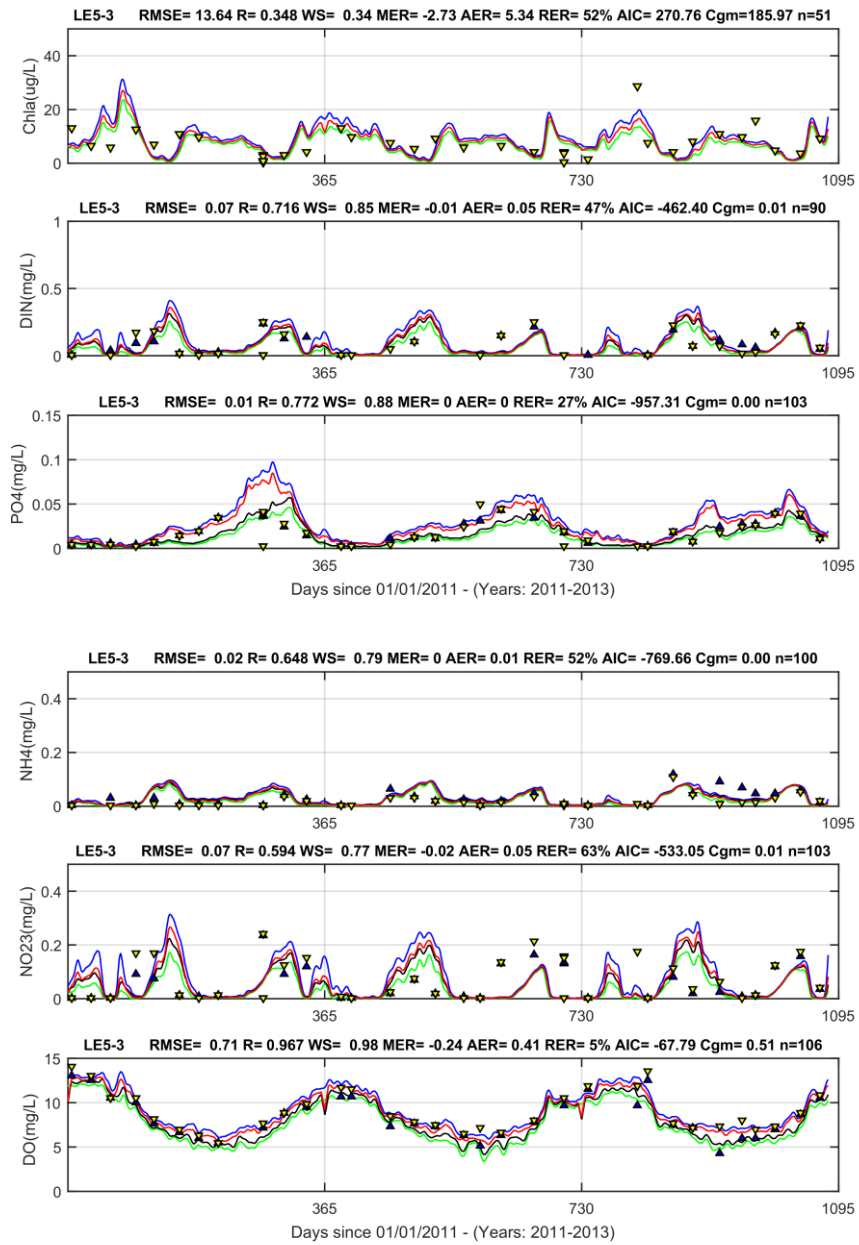


Figure 3-19: Model verification results at Station LE5-3 (see caption of Fig. 3-12 for descriptions of lines and symbols)

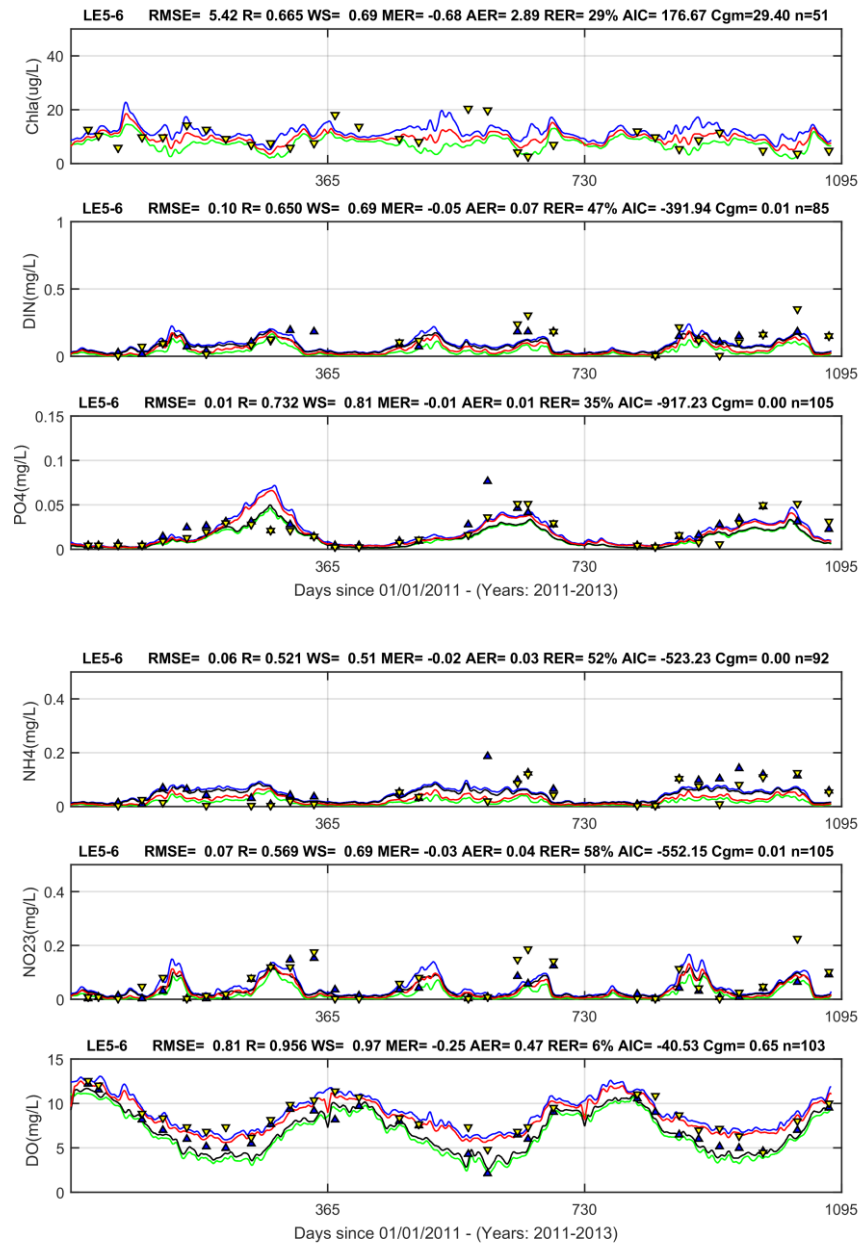


Figure 3-20: Model verification results at Station LE5-6 (see caption of Fig. 3-12 for descriptions of lines and symbols)

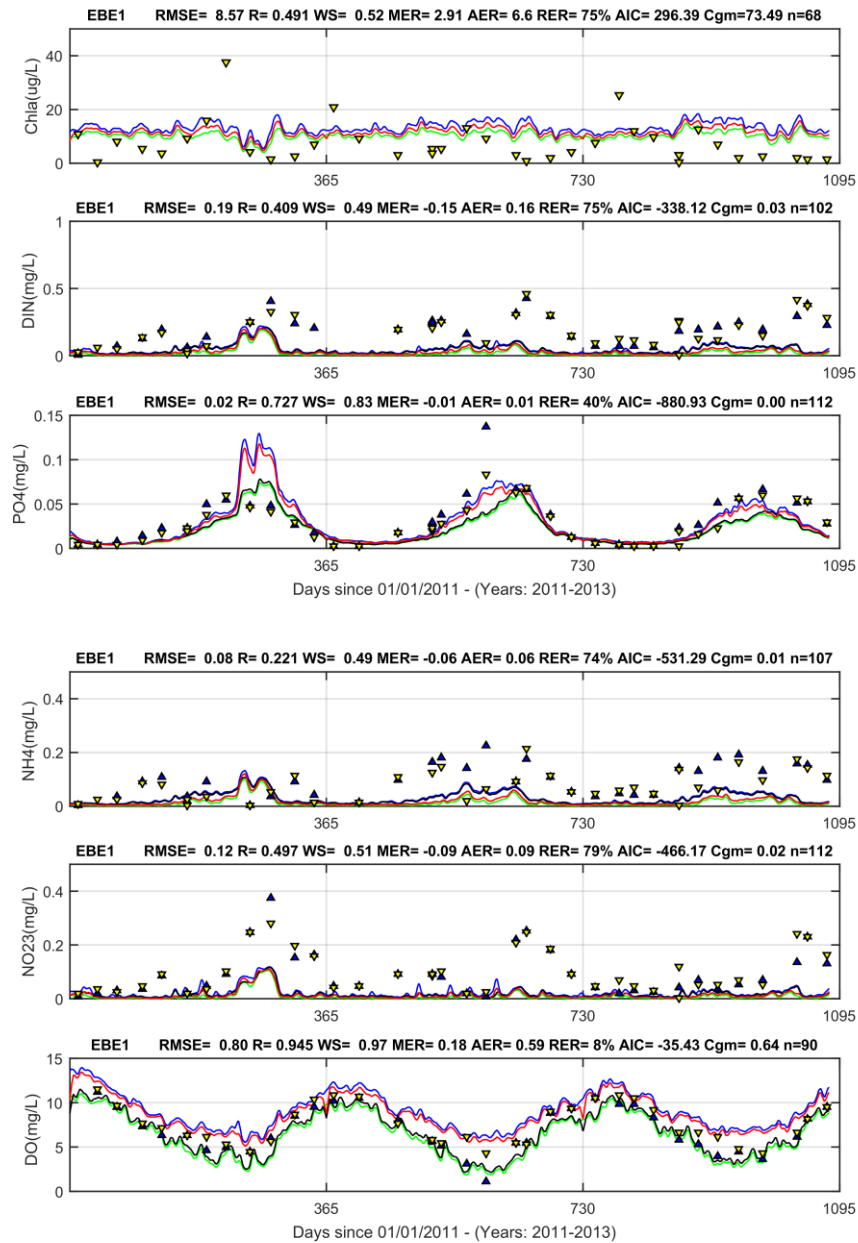


Figure 3-21: Model verification results at Station EBE1 (see caption of Fig. 3-12 for descriptions of lines and symbols)

4. Model Results of DO

Model simulation results will be presented based on scenario. We compare the difference between each scenario and the baseline condition. Statistics in spring (March-May) and summer (July-September) are presented as comparison. Comparisons of the model result for each scenario and baseline condition are conducted at selected EPA monitoring stations. As all

changes of bathymetry are located in the lower James and the Elizabeth Rivers, the impact will be expected to only occur in the lower James and Elizabeth Rivers. Therefore, we only compare the difference in the lower James and the Elizabeth Rivers. The locations of observation stations are shown in Figure 3-2.

4.1 Existing Condition and Future Condition

The model simulations of the existing condition and the future condition are conducted. The simulations are referred to as Baseline 1 (existing condition) and Baseline 2 (future condition) (Table 1). The future condition includes NIT Piers 1 and 2 removed, with an area dredged to -50', and the CIEE fully built out, and 3rd Crossing. Because the 3rd Crossing has only very localized impact and does not affect any far-field circulation and stratification as described in Appendix A, it will not be implicitly simulated. The access channel is dredged to the same depth as the channel. The designing is to ensure the cross-section near the Elizabeth River mouth maintains the same area before and after modification. The reduced portion of the area near the shore is added to the channel. Model grids are shown in Figures 4-1-1 and 4-1-2, respectively.

Summaries of DO statistics for the mean and bottom layer for spring (March to May) and summer (July-September), respectively, are listed in Tables 4-1-1 and 4-1-2. There is very little change in the James River (LE5-4). Relatively larger changes of DO occurred at Stations LE5-6, ELI-2, and SBE-5. It can be seen that the maximum reductions of DO are about 0.34 and 0.48 mg/L at Station LE5-6 during spring and summer, respectively. Changes are less than 11.3% at the bottom. The DO has a slight increase at Station LF01 located inside the Lafayette River.

Comparisons of the two baseline conditions are shown in Figures 4-1-3 to 4-1-5 for selected sections at LE5-4, ELI-2, and SBE-5. The plots for other stations are shown in the full modeling report. There is very little change in the James River (LE5-4). Relatively larger changes of DO occurred at Stations ELI-2 and SBE-5. The averaged change is less than 2.3% and the DO change is less than 0.5 mg/L during summer. The change during summer is even smaller compared to spring when runoff is higher. Note that a large change occurred during the spring period at Station SBE5. Because of changes of channel depth, the gravitational circulation increases during spring when freshwater discharge is high. However, DO is high during the spring period. There are no obvious changes for algae, DIN, and DIP.

Table 4-1-1: Comparison of Baseline 1 and Baseline 2 DO results in spring

Station	Baseline 1		Baseline 2		Difference		% difference	
	Mean (mg/L)	Bottom (mg/L)	Mean (mg/L)	Bottom (mg/L)	Mean (mg/L)	Bottom (mg/L)	Mean	Bottom
LE5-3	7.37	7.16	7.36	7.14	-0.01	-0.01	-0.11	-0.15
LE5-4	7.10	6.95	7.08	6.92	-0.02	-0.02	-0.34	-0.34

LE5-6	7.21	6.35	6.90	6.01	-0.31	-0.34	-4.29	-5.30
ELI2	7.99	7.40	8.18	7.60	0.19	0.20	2.37	2.69
SBE2	6.62	5.45	6.48	5.37	-0.14	-0.08	-2.16	-1.51
SBE5	6.69	5.70	6.35	5.38	-0.35	-0.32	-5.18	-5.58
LFA01	7.68	7.52	8.14	7.98	0.46	0.45	5.94	5.99
WBE1	7.97	7.51	7.70	7.30	-0.26	-0.22	-3.32	-2.86
EBE1	6.68	5.66	6.62	5.61	-0.07	-0.05	-1.00	-0.90

Table 4-1-2: Comparison of Baseline 1 and Baseline 2 DO results in summer

Station	Baseline 1		Baseline 2		Difference		% difference	
	Mean (mg/L)	Bottom (mg/L)	Mean (mg/L)	Bottom (mg/L)	Mean (mg/L)	Bottom (mg/L)	Mean	Bottom
LE5-3	5.83	5.56	5.83	5.55	-0.01	-0.00	-0.09	-0.08
LE5-4	5.34	5.10	5.32	5.08	-0.02	-0.02	-0.43	-0.39
LE5-6	5.28	4.28	4.81	3.80	-0.46	-0.48	-8.77	-11.28
ELI2	5.99	5.16	6.12	5.28	0.13	0.12	2.13	2.28
SBE2	4.41	3.08	4.29	3.02	-0.11	-0.06	-2.53	-1.98
SBE5	4.38	3.20	4.12	2.99	-0.27	-0.21	-6.06	-6.46
LFA01	6.02	5.73	6.37	6.07	0.35	0.34	5.89	5.88
WBE1	6.30	5.66	6.12	5.54	-0.18	-0.12	-2.86	-2.06
EBE1	4.45	3.28	4.39	3.22	-0.06	-0.05	-1.39	-1.63

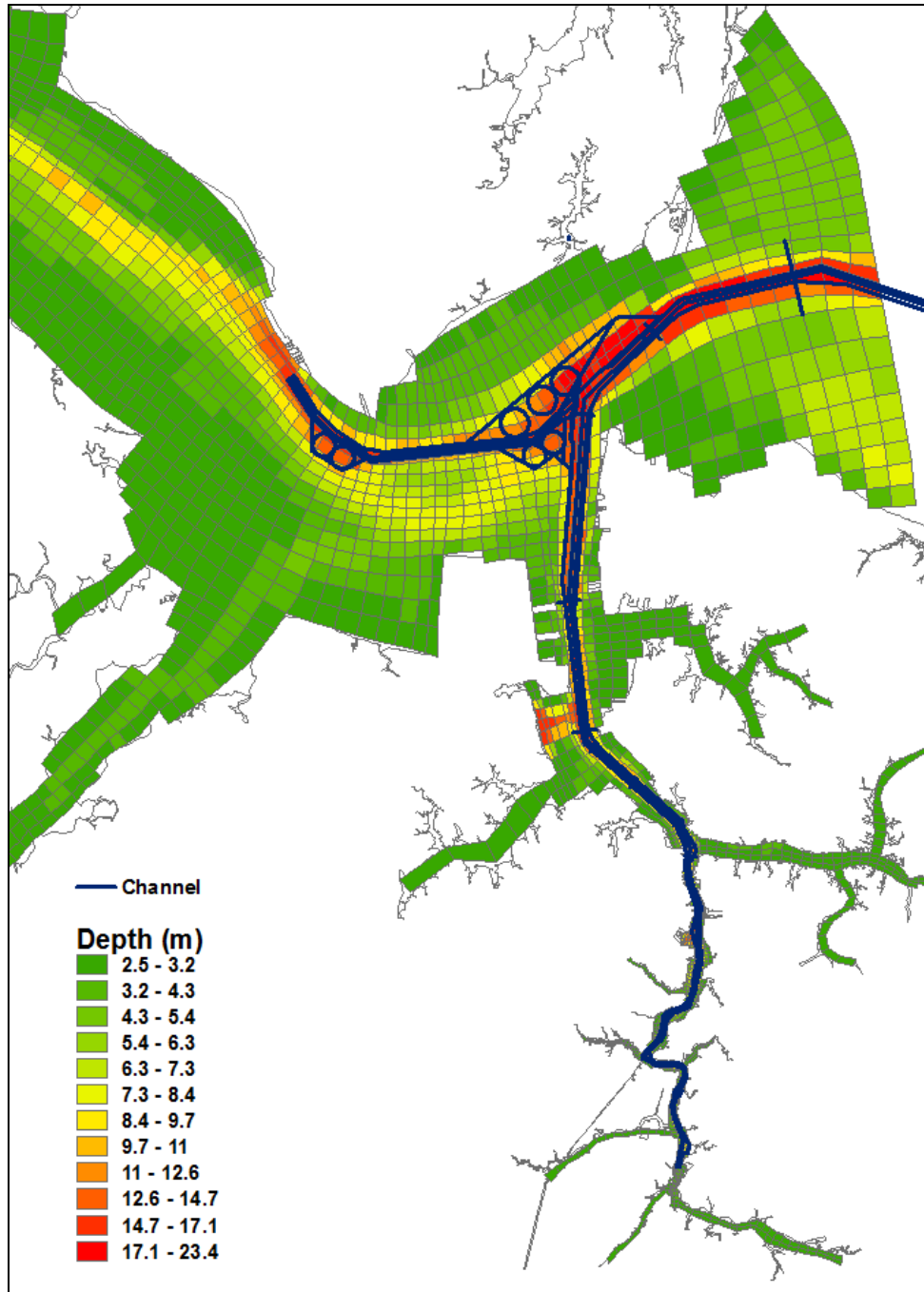


Figure 4-1-1: Model Grid of Baseline Condition 1

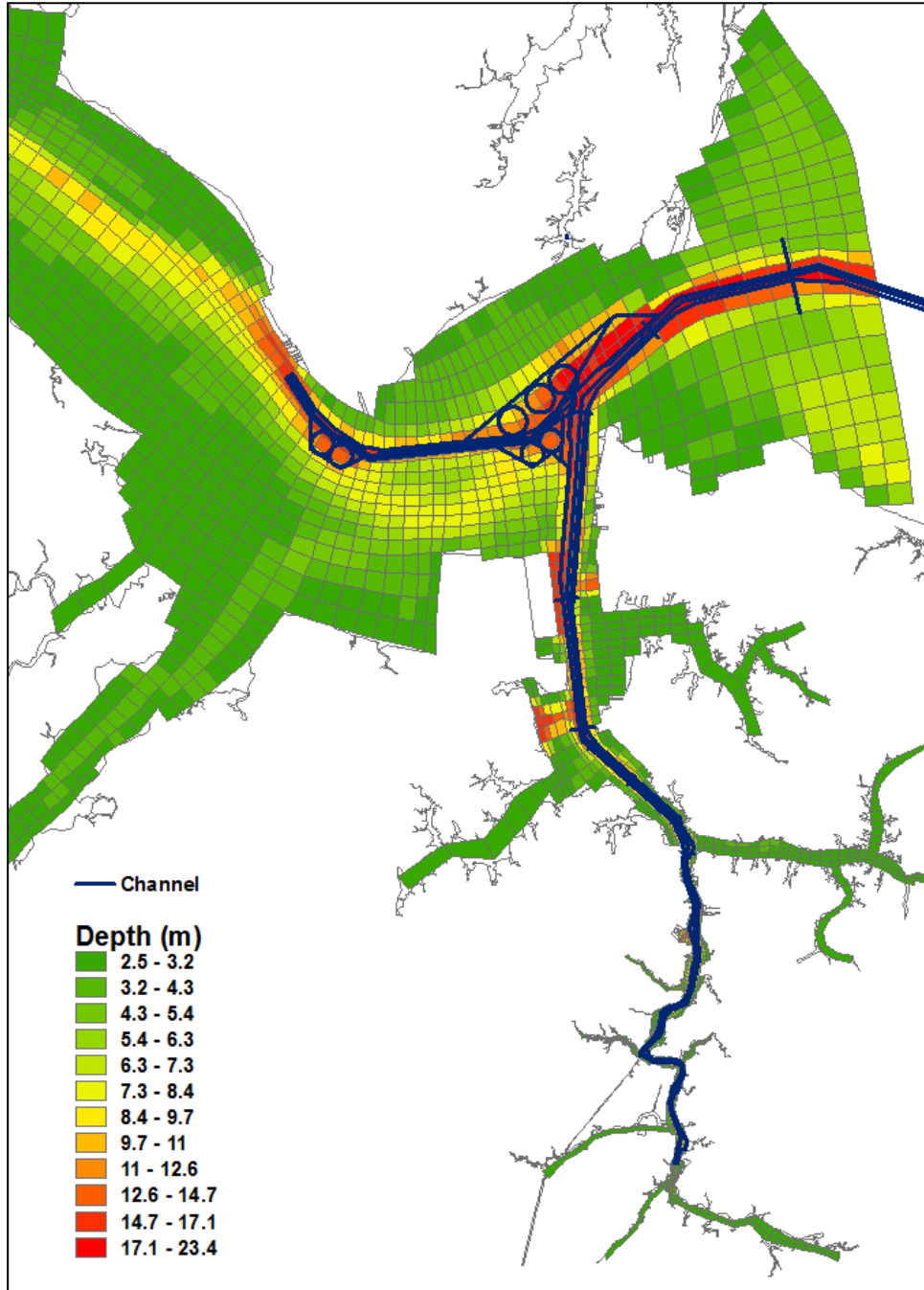


Figure 4-1-2: Model Grid of Baseline Condition 2

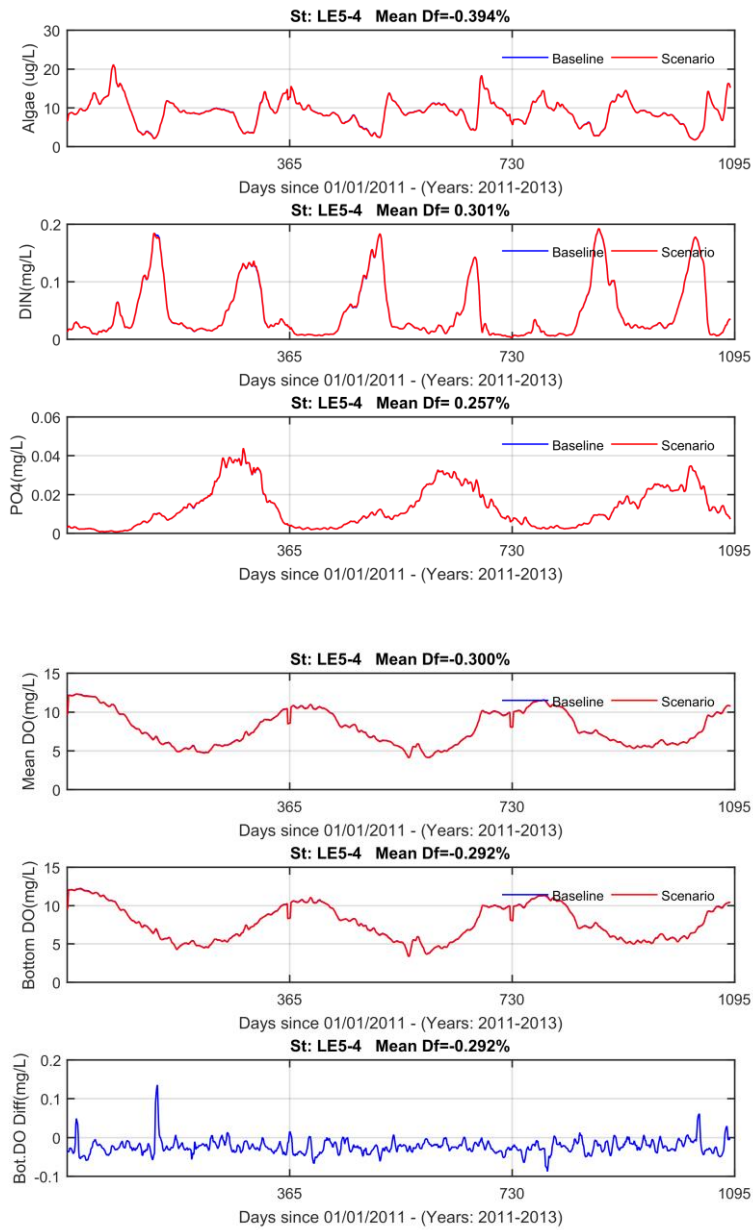


Figure 4-1-3: Comparison of Baseline 1 and Baseline 2 results at Station LE5-4

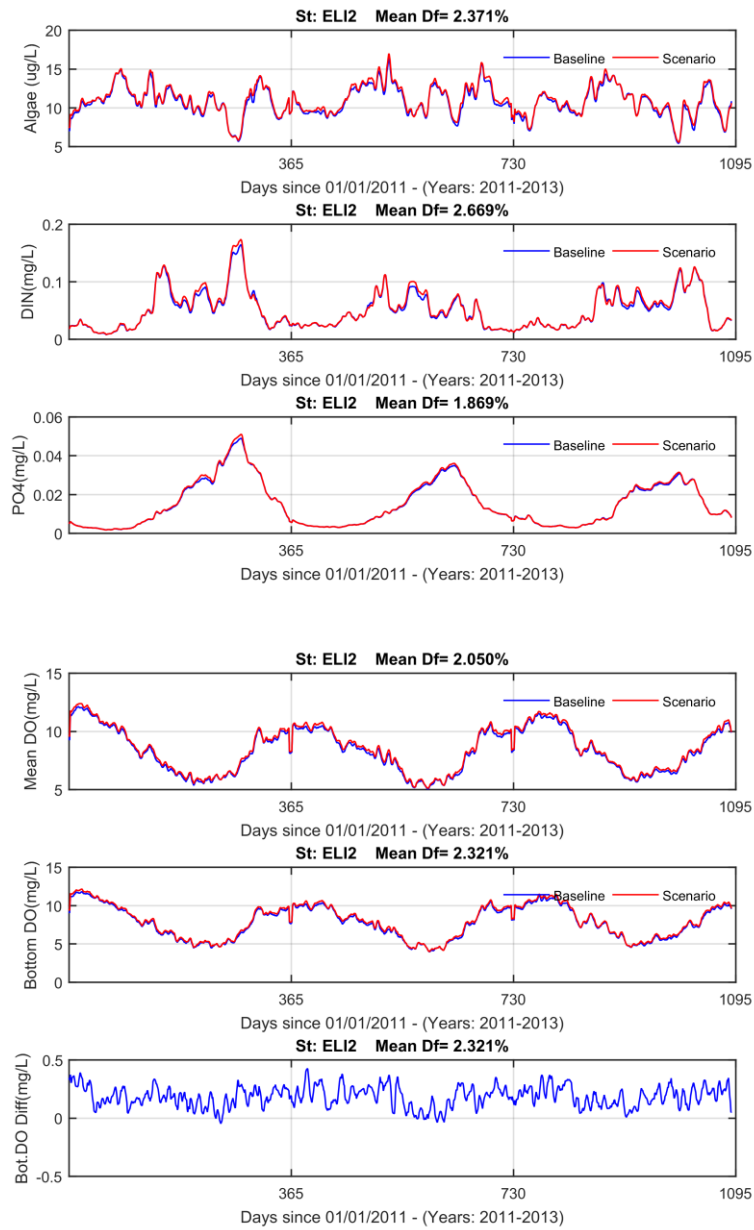


Figure 4-1-4: Comparison of Baseline 1 and Baseline 2 results at Station ELI2 (last panel shows the difference of bottom DO)

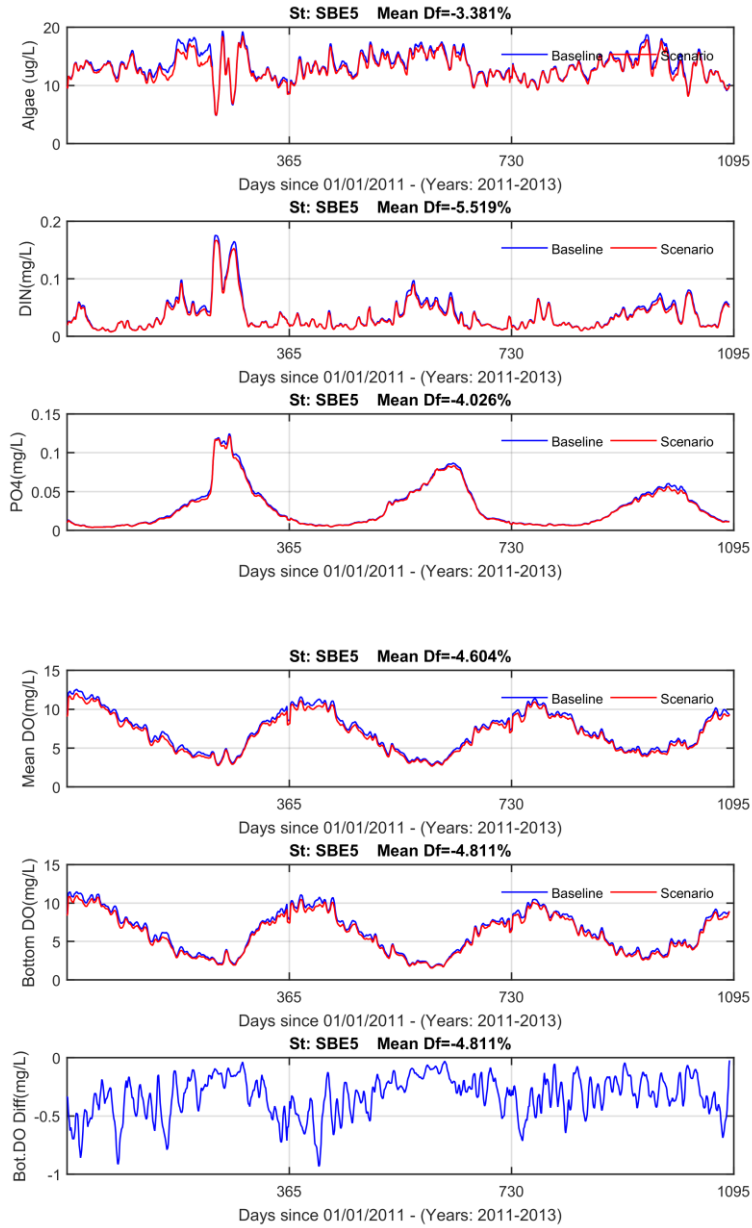


Figure 4-1-5: Comparison of Baseline 1 and Baseline 2 results at Station SBE5

4.2 Model Scenarios 3-1 and 3-2

These scenarios are used to examine the change due to channel deepening of NH channel and compare to the existing condition (Baseline 1) and the future condition (Baseline 2) (see Table 2-1). The model grids with channel deepening of the NH channel for existing and future conditions are shown in Figures 4-2-1 and 4-2-2, respectively.

Summaries of DO statistics for Scenario 3-1 for the mean and at the bottom layer for spring (March to May) and summer (July-September), respectively, are listed in Tables 4-2-1 and 4-2-2 for comparison of Scenario 3-1 to Baseline 1. There is very little change in the James River (LE5-4). A slight decrease of DO occurred at Stations LE5-6 and SBE-5. It can be seen that the maximum reduction of DO is less than 0.15 mg/L at Station LE5-6 during summer. Changes are less than 3.5% at the bottom. The DO has a slight increase at Station LF01 located inside the Lafayette River.

Comparisons of Scenario 3-1 to the existing condition (Baseline 1) are shown in Figures 4-2-3 to 4-2-5 for selected sections at LE5-4, ELI-2, and SBE-5. The plots for other stations are shown in the full modeling report. There is very little change in the James River (LE5-4). Relatively larger changes of DO occurred at Stations ELI-2 and SBE-5. The DO change is less than 0.5 mg/L. The average change is less than 3%. There are no obvious changes for algae, DIN, and DIP.

Summaries of DO statistics for Scenario 3-2 for the mean and at the bottom layer for spring (March to May) and summer (July-September), respectively, are listed in Tables 4-2-3 and 4-2-4 for comparison of Scenario 3-2 to Baseline 2. There is very little change in the James River (LE5-4). A slight decrease of DO occurred at Stations LE5-6 and SBE-5. It can be seen that the maximum reduction of DO is less than 0.17 mg/L at Station LE5-6 during summer. Change is less than 4.4% at the bottom. The DO has a slight increase at Station LF01 located inside the Lafayette River.

Comparisons of the Scenario 3-2 to the future condition (Baseline 2) are shown in Figures 4-2-6 to 4-2-8 for selected sections at LE5-4, ELI-2, and SBE-5. The plots for other stations are shown in the full modeling report. There is very little change in the James River (LE5-4). Relatively larger changes of DO occurred at Stations ELI-2 and SBE-5. The DO change is less than 0.5 mg/L during summer. The average change is less than 2%. There are no obvious changes for algae, DIN, and DIP.

Table 4-2-1: Comparison of Scenario 3-1 to Baseline 1 for DO results during spring

Station	Baseline 1		Scenario 3-1		Difference		% difference	
	Mean (mg/L)	Bottom (mg/L)	Mean (mg/L)	Bottom (mg/L)	Mean (mg/L)	Bottom (mg/L)	Mean	Bottom
LE5-3	7.37	7.16	7.34	7.12	-0.03	-0.03	-0.38	-0.47
LE5-4	7.10	6.95	7.06	6.90	-0.04	-0.04	-0.60	-0.64
LE5-6	7.21	6.35	7.20	6.30	0.00	-0.05	-0.06	-0.83
ELI2	7.99	7.40	8.06	7.46	0.07	0.06	0.93	0.85
SBE2	6.62	5.45	6.53	5.40	-0.09	-0.05	-1.37	-0.92
SBE5	6.69	5.70	6.49	5.53	-0.20	-0.17	-2.98	-3.03
LFA01	7.68	7.52	7.90	7.76	0.22	0.23	2.90	3.10
WBE1	7.97	7.51	7.78	7.36	-0.18	-0.15	-2.29	-2.05
EBE1	6.68	5.66	6.63	5.62	-0.05	-0.03	-0.78	-0.61

Table 4-2-2: Comparison of Scenario 3-1 to Baseline 1 for DO results during summer

Station	Baseline 1		Scenario 3-1		Difference		% difference	
	Mean (mg/L)	Bottom (mg/L)	Mean (mg/L)	Bottom (mg/L)	Mean (mg/L)	Bottom (mg/L)	Mean	Bottom
LE5-3	5.83	5.56	5.80	5.53	-0.03	-0.03	-0.50	-0.56
LE5-4	5.34	5.10	5.28	5.02	-0.06	-0.08	-1.15	-1.48
LE5-6	5.28	4.28	5.21	4.14	-0.06	-0.15	-1.23	-3.41
ELI2	5.99	5.16	6.02	5.16	0.03	-0.00	0.57	-0.05
SBE2	4.41	3.08	4.33	3.03	-0.08	-0.05	-1.82	-1.72
SBE5	4.38	3.20	4.23	3.09	-0.15	-0.11	-3.47	-3.48
LFA01	6.02	5.73	6.19	5.91	0.17	0.18	2.84	3.14
WBE1	6.30	5.66	6.16	5.56	-0.14	-0.10	-2.20	-1.79
EBE1	4.45	3.28	4.39	3.22	-0.06	-0.06	-1.38	-1.83

Table 4-2-3: Comparison of Scenario 3-2 to Baseline 2 for DO results during spring

Station	Baseline 2		Scenario 3-2		Difference		% difference	
	Mean (mg/L)	Bottom (mg/L)	Mean (mg/L)	Bottom (mg/L)	Mean (mg/L)	Bottom (mg/L)	Mean	Bottom
LE5-3	7.36	7.14	7.35	7.16	-0.01	0.01	-0.13	0.18
LE5-4	7.08	6.92	7.05	6.91	-0.03	-0.02	-0.43	-0.26
LE5-6	6.90	6.01	6.90	5.99	0.00	-0.02	0.04	-0.37
ELI2	8.18	7.60	8.25	7.69	0.07	0.09	0.85	1.24
SBE2	6.48	5.37	6.40	5.38	-0.08	0.01	-1.21	0.20
SBE5	6.35	5.38	6.14	5.25	-0.20	-0.13	-3.20	-2.47
LFA01	8.14	7.98	8.42	8.28	0.29	0.30	3.52	3.76
WBE1	7.70	7.30	7.58	7.21	-0.12	-0.09	-1.58	-1.20
EBE1	6.62	5.61	6.59	5.64	-0.03	0.04	-0.45	0.68

Table 4-2-4: Comparison of Scenario 3-2 to Baseline 2 for DO results during summer

Station	Baseline 2		Scenario 3-2		Difference		% difference	
	Mean (mg/L)	Bottom (mg/L)	Mean (mg/L)	Bottom (mg/L)	Mean (mg/L)	Bottom (mg/L)	Mean	Bottom
LE5-3	5.83	5.55	5.80	5.53	-0.03	-0.02	-0.48	-0.38
LE5-4	5.32	5.08	5.26	5.01	-0.06	-0.06	-1.07	-1.22
LE5-6	4.81	3.80	4.76	3.64	-0.06	-0.17	-1.21	-4.35
ELI2	6.12	5.28	6.17	5.32	0.05	0.04	0.82	0.75
SBE2	4.29	3.02	4.26	3.04	-0.03	0.02	-0.77	0.73
SBE5	4.12	2.99	3.98	2.93	-0.14	-0.07	-3.32	-2.32
LFA01	6.37	6.07	6.58	6.28	0.21	0.21	3.25	3.48
WBE1	6.12	5.54	5.99	5.45	-0.13	-0.09	-2.07	-1.61
EBE1	4.39	3.22	4.38	3.24	-0.00	0.02	-0.10	0.61

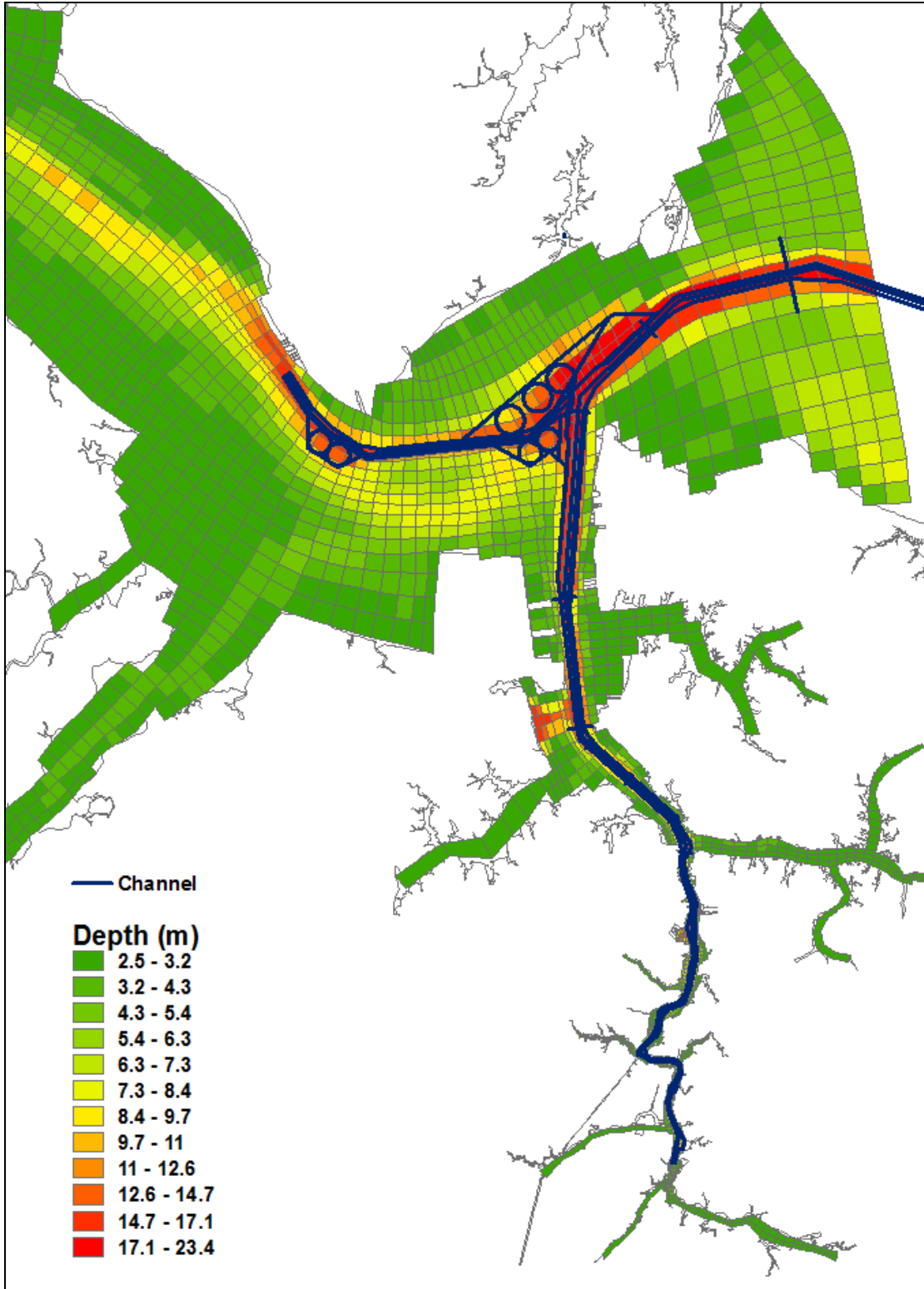


Figure 4-2-1: Model Grid of Scenario 3-1 (Deepening NH Channel)

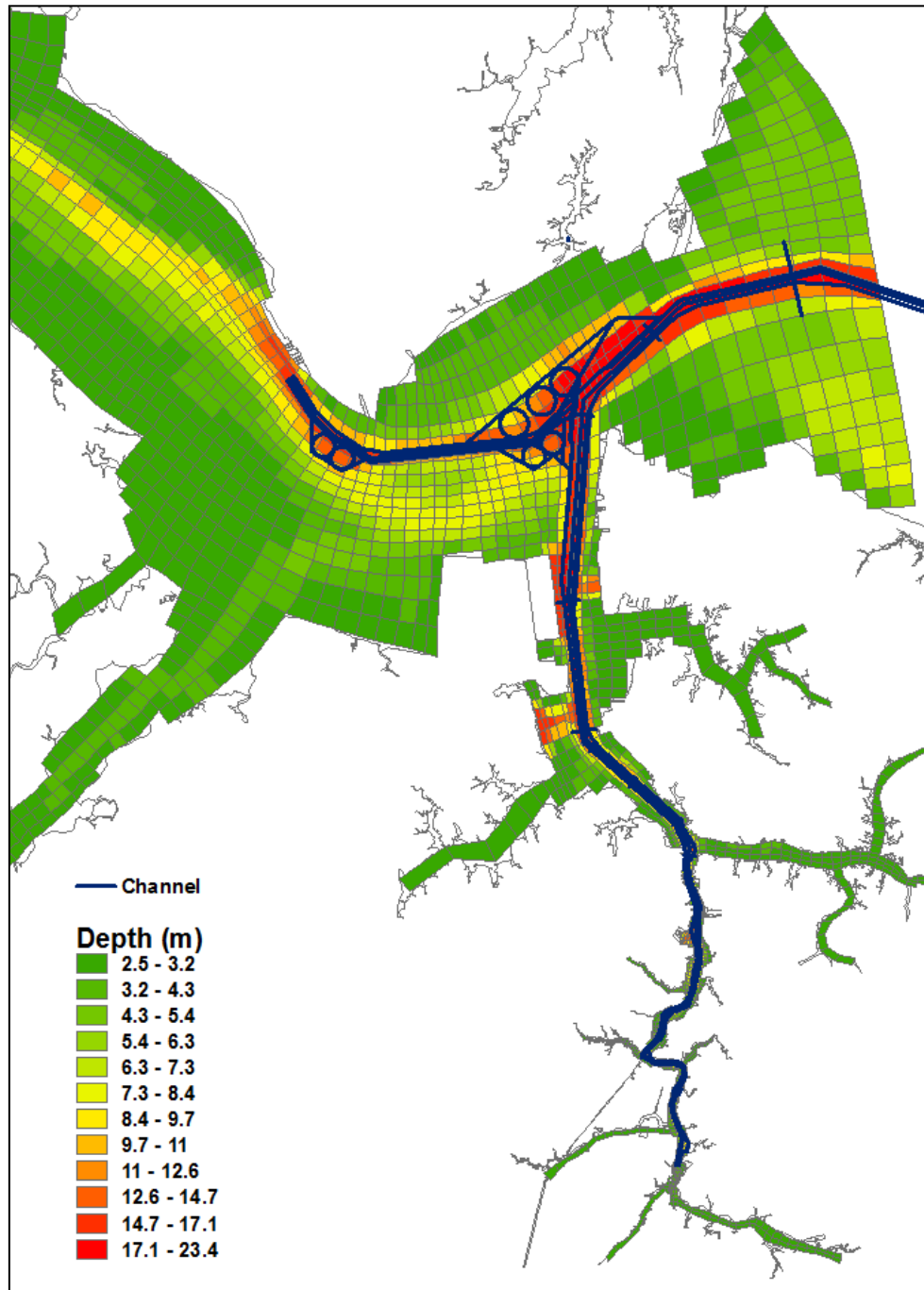


Figure 4-2-2: Model Grid of Scenario 3-2 (Deepening NH Channel)

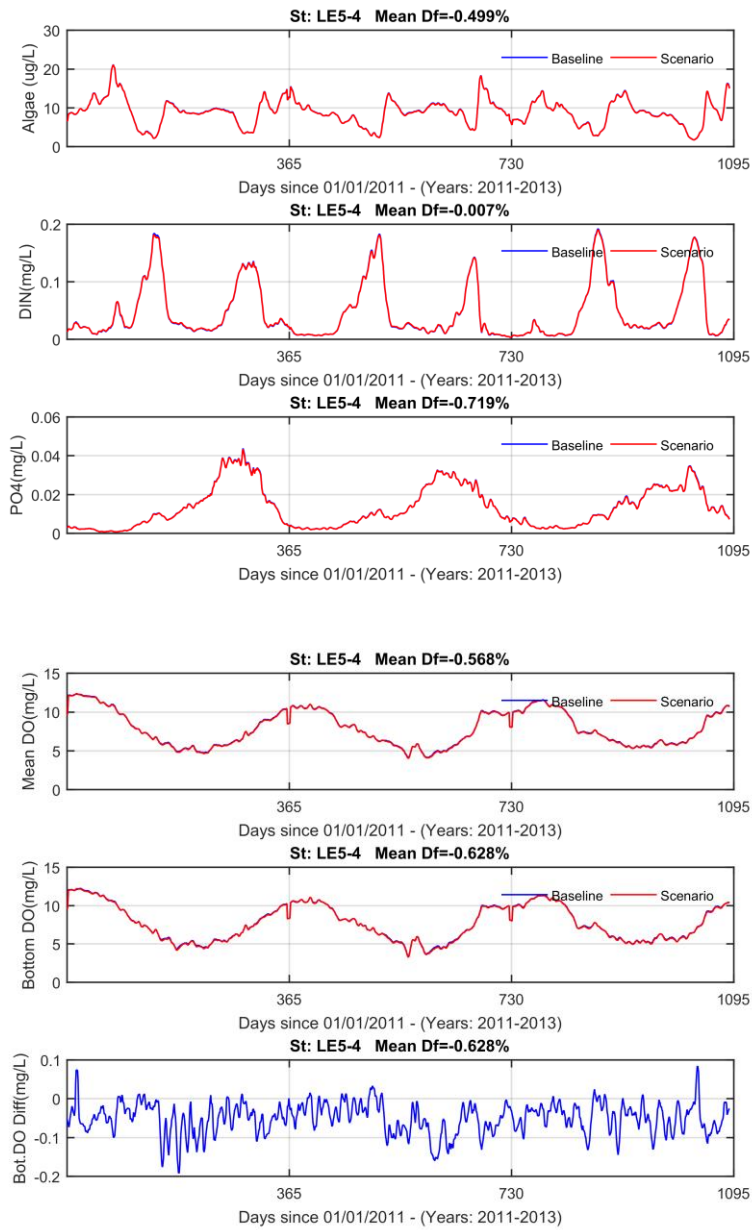


Figure 4-2-3: Comparison of Scenario 3-1 to Baseline 1 results at Station LE5-4

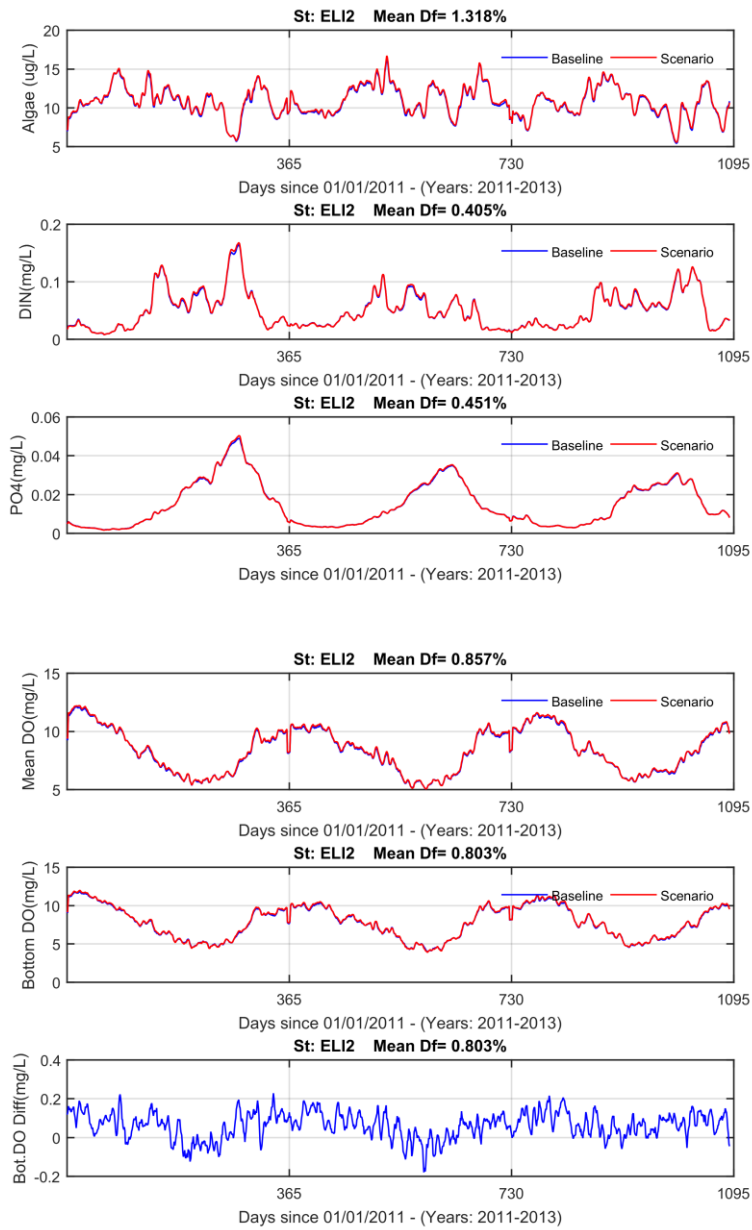


Figure 4-2-4: Comparison of Scenario 3-1 to Baseline 1 results at Station ELI2

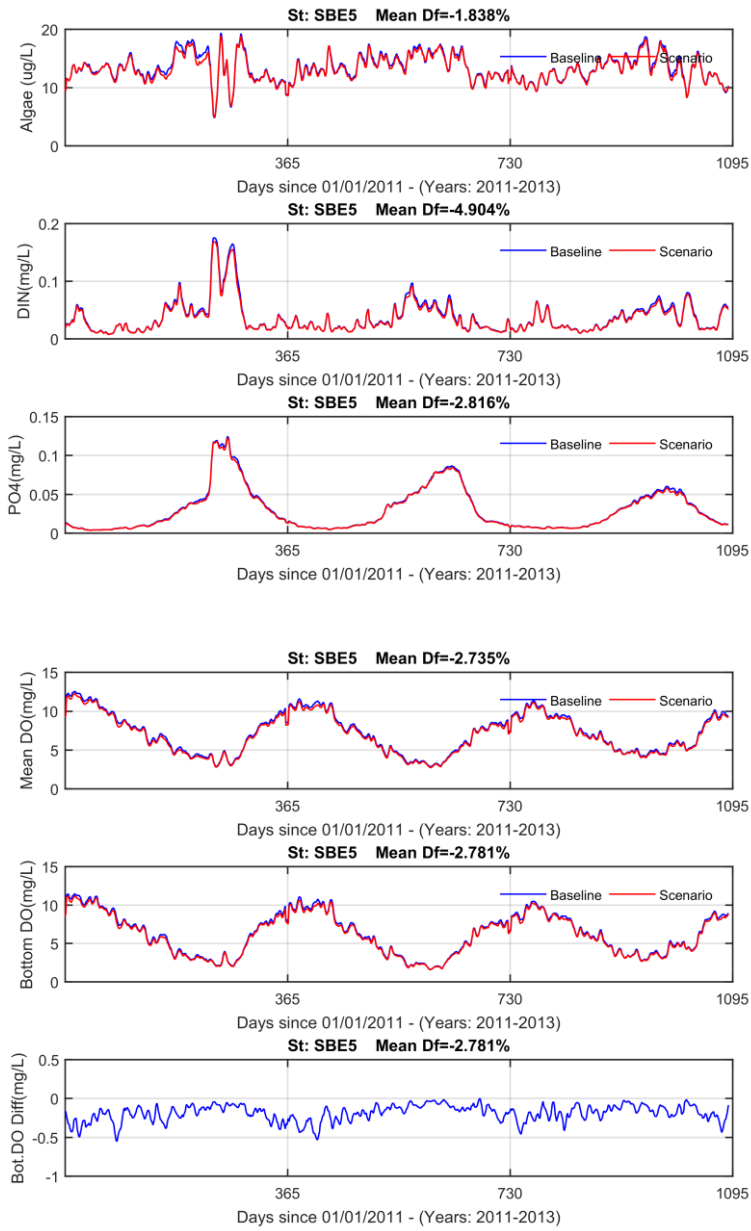


Figure 4-2-5: Comparison of Scenario 3-1 to Baseline 1 results at Station SBE5

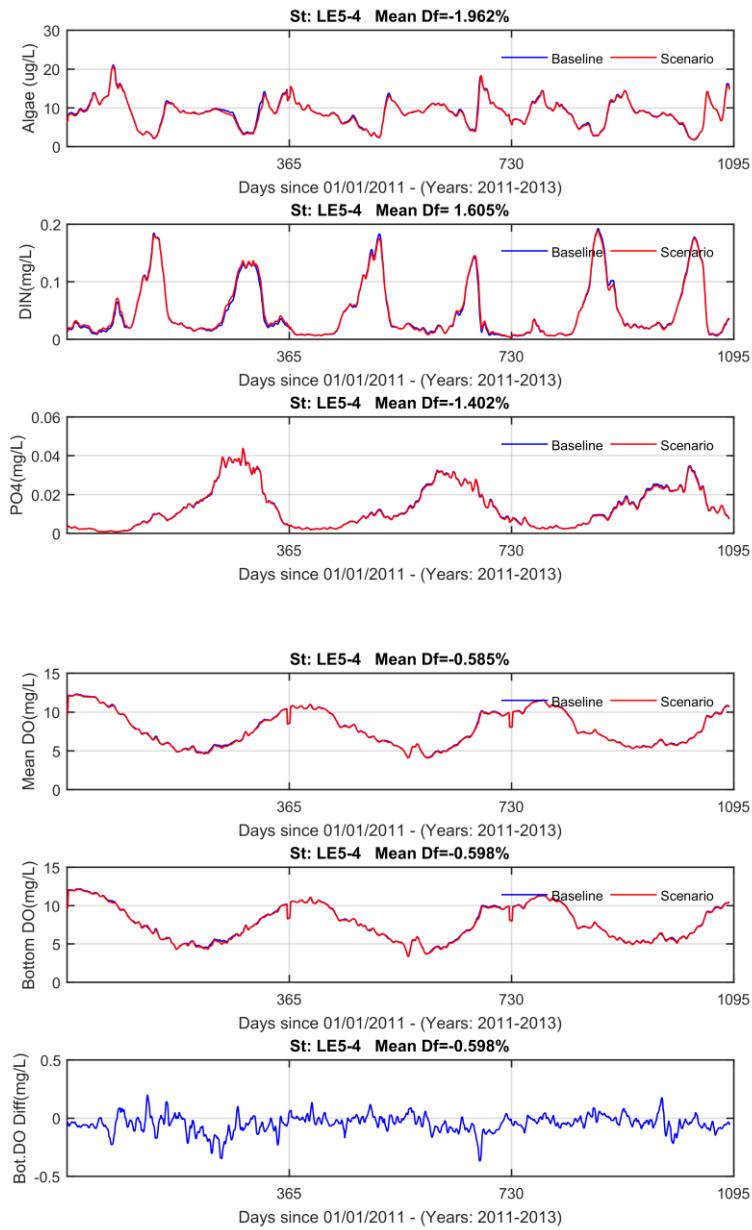


Figure 4-2-6: Comparison of Scenario 3-2 to Baseline 2 results at Station LE5-4

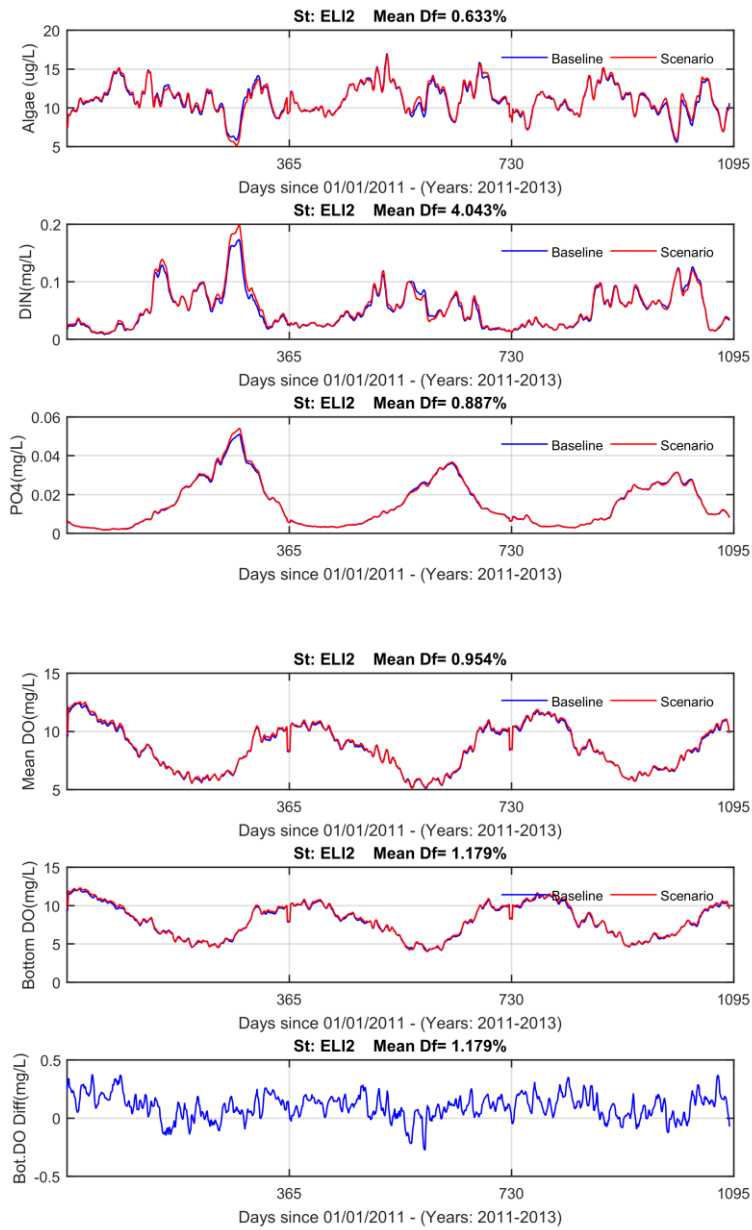


Figure 4-2-7: Comparison of Scenario 3-2 to Baseline 2 results at Station ELI2

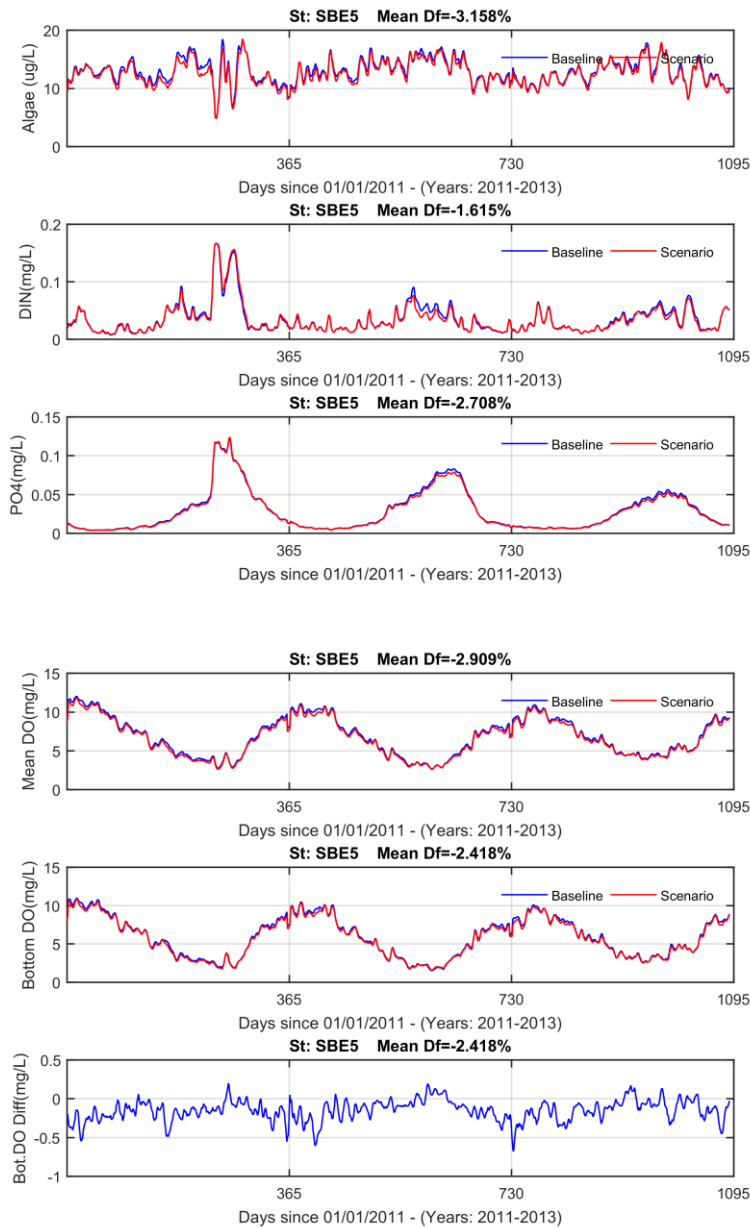


Figure 4-2-8: Comparison of Scenario 3-2 to Baseline 2 results at Station SBE5

4.3 Model Scenarios 4-1 and 4-2

These scenarios are simulated to examine the change due to channel deepening of Elizabeth SB channel and to compare to the existing condition (Baseline 1) and the future condition (Baseline 2) (see Table 2-1). The model grids with channel deepening of the ERSB channel for existing and future conditions are shown in Figures 4-3-1 and 4-3-2, respectively.

Summaries of DO statistics for Scenario 4-1 for both the mean and at the bottom layer for spring (March to May) and summer (July-September), respectively, are listed in Tables 4-3-1 and 4-3-2 for comparison of Scenario 4-1 to Baseline 1. There is very little change in the James River (LE5-4). A slight decrease of DO occurred at Stations SBE-2 and SBE-5, located in the SW channel. It can be seen that the maximum reduction of DO is less than 0.58 mg/L at Station SBE-5 during summer. Changes are about 18% at the bottom.

Comparisons of Scenario 4-1 to the existing condition (Baseline 1) are shown in Figures 4-3-3 to 4-3-5 for selected sections at LE5-4, ELI2, and SBE-5. The plots for other stations are shown in the full modeling report. There is very little change in the James River (LE5-4). A relatively larger change of DO occurred at Station SBE-5. DO changes less than 1.0 mg/L at the bottom during summer. The average change is less than 8%. A large change occurred during spring. As the channel becomes deeper, the stratification increases during spring when runoff is higher. However, bottom DO values are all larger than 5 mg/L and there is no problem meeting the DO criterion during the spring season. There are no obvious changes for algae, DIN, and DIP.

Summaries of DO statistics for Scenario 4-2 for the mean and at the bottom layer for spring (March to May) and summer (July-September), respectively, are listed in Tables 4-3-3 and 4-3-4 for comparison to the DO statistics of Baseline 2. There is very little change in the James River (LE5-4). A slight decrease of DO occurred at Stations SBE-2 and SBE-5, located in the SW channel. It can be seen that the maximum reduction of DO is less than 0.54 mg/L at Station SBE-5 during summer. Changes are about 18% at the bottom.

Comparisons of Scenario 4-2 to the existing condition (Baseline 2) are shown in Figures 4-3-6 to 4-3-8 for selected sections at LE5-4, ELI2, and SBE-5. The plots for other stations are shown in the full modeling report. There is very little change in the James River (LE5-4). A relatively large change of DO occurred at Station SBE-5. The DO change is less than 1.0 mg/L at the bottom during summer. The average change is less than 8%. A large change occurred during spring. As the channel deepens, the stratification increases during spring when runoff is higher. However, bottom DO values are all larger than 5 mg/L and there is no problem meeting the DO criterion during the spring season. Results are similar to those of Scenario 4-1. There are no obvious changes for algae, DIN, and DIP.

Table 4-3-1: Comparison of Scenario 4-1 to Baseline 1 for DO results during spring

Station	Baseline 1		Scenario 4-1		Difference		% difference	
	Mean (mg/L)	Bottom (mg/L)	Mean (mg/L)	Bottom (mg/L)	Mean (mg/L)	Bottom (mg/L)	Mean	Bottom
LE5-3	7.37	7.16	7.39	7.20	0.02	0.05	0.28	0.65
LE5-4	7.10	6.95	7.11	6.98	0.01	0.03	0.17	0.43

LE5-6	7.21	6.35	7.21	6.42	0.01	0.07	0.09	1.18
ELI2	7.99	7.40	7.98	7.44	-0.01	0.04	-0.14	0.55
SBE2	6.62	5.45	6.39	5.25	-0.23	-0.21	-3.53	-3.81
SBE5	6.69	5.70	6.26	5.14	-0.44	-0.56	-6.53	-9.82
LFA01	7.68	7.52	7.83	7.67	0.15	0.15	1.90	1.97
WBE1	7.97	7.51	7.99	7.56	0.02	0.05	0.25	0.65
EBE1	6.68	5.66	6.56	5.58	-0.12	-0.08	-1.80	-1.38

Table 4-3-2: Comparison of Scenario 4-1 to Baseline 1 for DO results during summer

Station	Baseline 1		Scenario 4-1		Difference		% difference	
	Mean (mg/L)	Bottom (mg/L)	Mean (mg/L)	Bottom (mg/L)	Mean (mg/L)	Bottom (mg/L)	Mean	Bottom
LE5-3	5.83	5.56	5.84	5.58	0.00	0.02	0.08	0.34
LE5-4	5.34	5.10	5.34	5.11	0.00	0.01	0.06	0.26
LE5-6	5.28	4.28	5.31	4.36	0.04	0.07	0.73	1.70
ELI2	5.99	5.16	6.03	5.24	0.04	0.08	0.61	1.53
SBE2	4.41	3.08	4.16	2.87	-0.24	-0.21	-5.50	-6.76
SBE5	4.38	3.20	3.93	2.62	-0.45	-0.58	-10.24	-18.14
LFA01	6.02	5.73	6.14	5.86	0.12	0.13	1.95	2.27
WBE1	6.30	5.66	6.27	5.65	-0.03	-0.01	-0.49	-0.12
EBE1	4.45	3.28	4.35	3.21	-0.10	-0.07	-2.15	-2.14

Table 4-3-3: Comparison of Scenario 4-2 to Baseline 2 for DO results during spring

Station	Baseline 2		Scenario 4-2		Difference		% difference	
	Mean (mg/L)	Bottom (mg/L)	Mean (mg/L)	Bottom (mg/L)	Mean (mg/L)	Bottom (mg/L)	Mean	Bottom
LE5-3	7.36	7.14	7.38	7.19	0.02	0.04	0.27	0.61
LE5-4	7.08	6.92	7.09	6.95	0.01	0.03	0.15	0.39
LE5-6	6.90	6.01	6.91	6.07	0.01	0.05	0.21	0.91
ELI2	8.18	7.60	8.17	7.63	-0.01	0.04	-0.11	0.46
SBE2	6.48	5.37	6.25	5.16	-0.23	-0.21	-3.53	-3.96
SBE5	6.35	5.38	5.91	4.83	-0.44	-0.55	-6.88	-10.20
LFA01	8.14	7.98	8.29	8.14	0.15	0.16	1.84	2.03
WBE1	7.70	7.30	7.73	7.36	0.03	0.06	0.42	0.80
EBE1	6.62	5.61	6.50	5.53	-0.12	-0.08	-1.83	-1.41

Table 4-3-4: Comparison of Scenario 4-2 to Baseline 2 for DO results during summer

Station	Baseline 2		Scenario 4-2		Difference		% difference	
	Mean (mg/L)	Bottom (mg/L)	Mean (mg/L)	Bottom (mg/L)	Mean (mg/L)	Bottom (mg/L)	Mean	Bottom
LE5-3	5.83	5.55	5.83	5.57	0.00	0.01	0.05	0.26
LE5-4	5.32	5.08	5.32	5.09	0.00	0.01	0.08	0.28
LE5-6	4.81	3.80	4.85	3.82	0.03	0.02	0.73	0.52
ELI2	6.12	5.28	6.14	5.34	0.02	0.05	0.32	1.02
SBE2	4.29	3.02	4.06	2.81	-0.23	-0.21	-5.39	-6.92
SBE5	4.12	2.99	3.71	2.46	-0.41	-0.54	-9.85	-17.96
LFA01	6.37	6.07	6.48	6.19	0.11	0.12	1.70	1.98
WBE1	6.12	5.54	6.12	5.55	-0.00	0.01	-0.00	0.27
EBE1	4.39	3.22	4.30	3.15	-0.09	-0.07	-2.03	-2.31

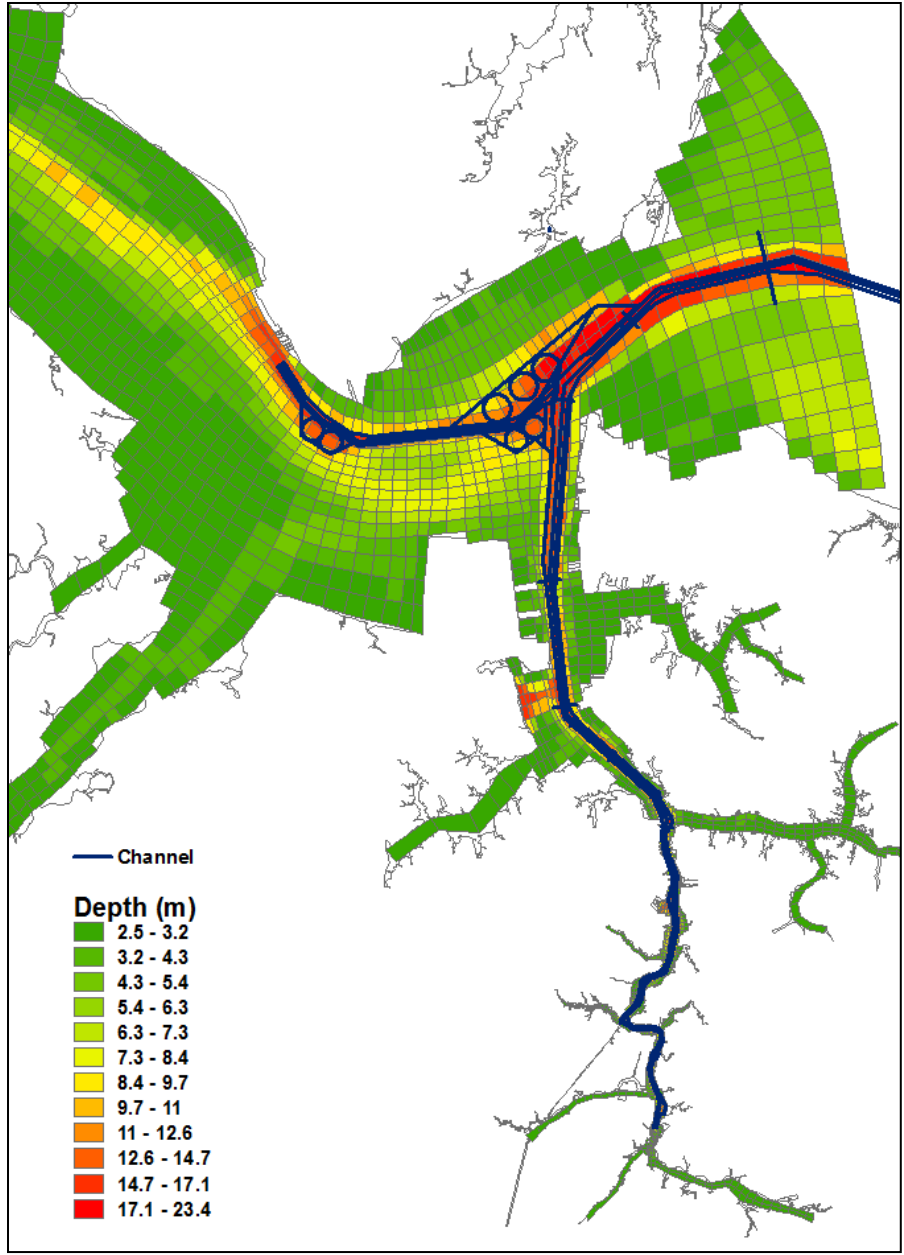


Figure 4-3-1: Model Grid of Scenario 4-1 (Deepening SB Channel)

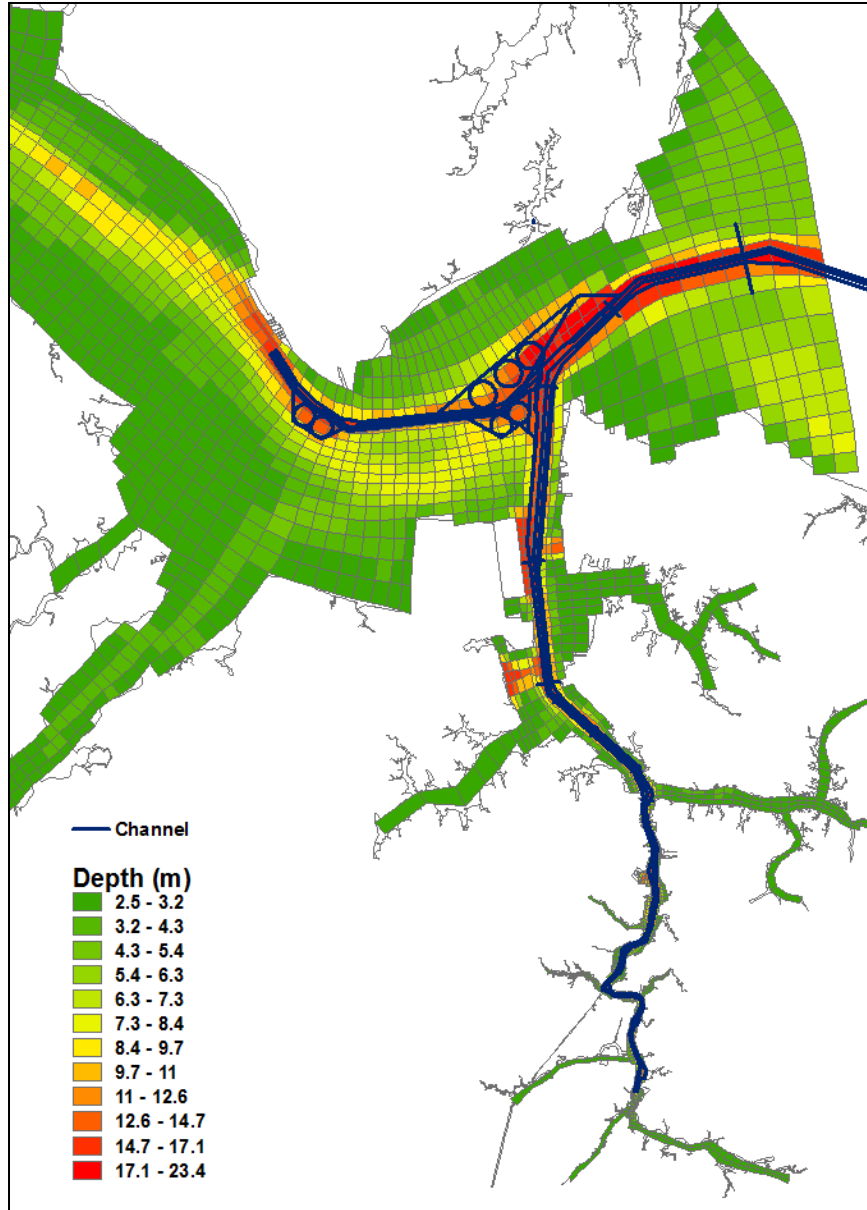


Figure 4-3-2: Model Grid of Scenario 4-2 (Deepening SB Channel)

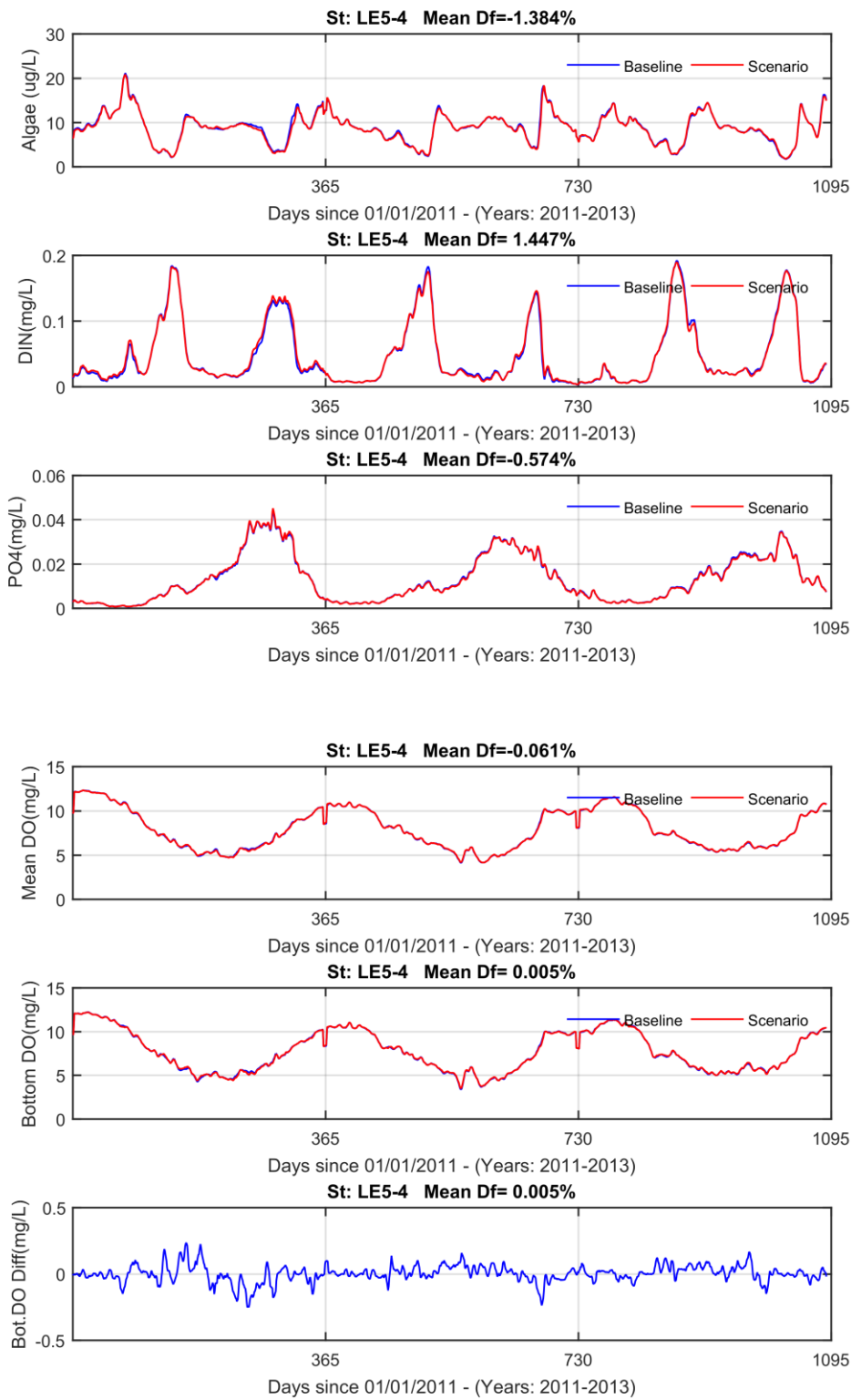


Figure 4-3-3: Comparison of Scenario 4-1 to Baseline 1 results at Station LE5-4 (last panel shows the difference of bottom DO (scenario-baseline))

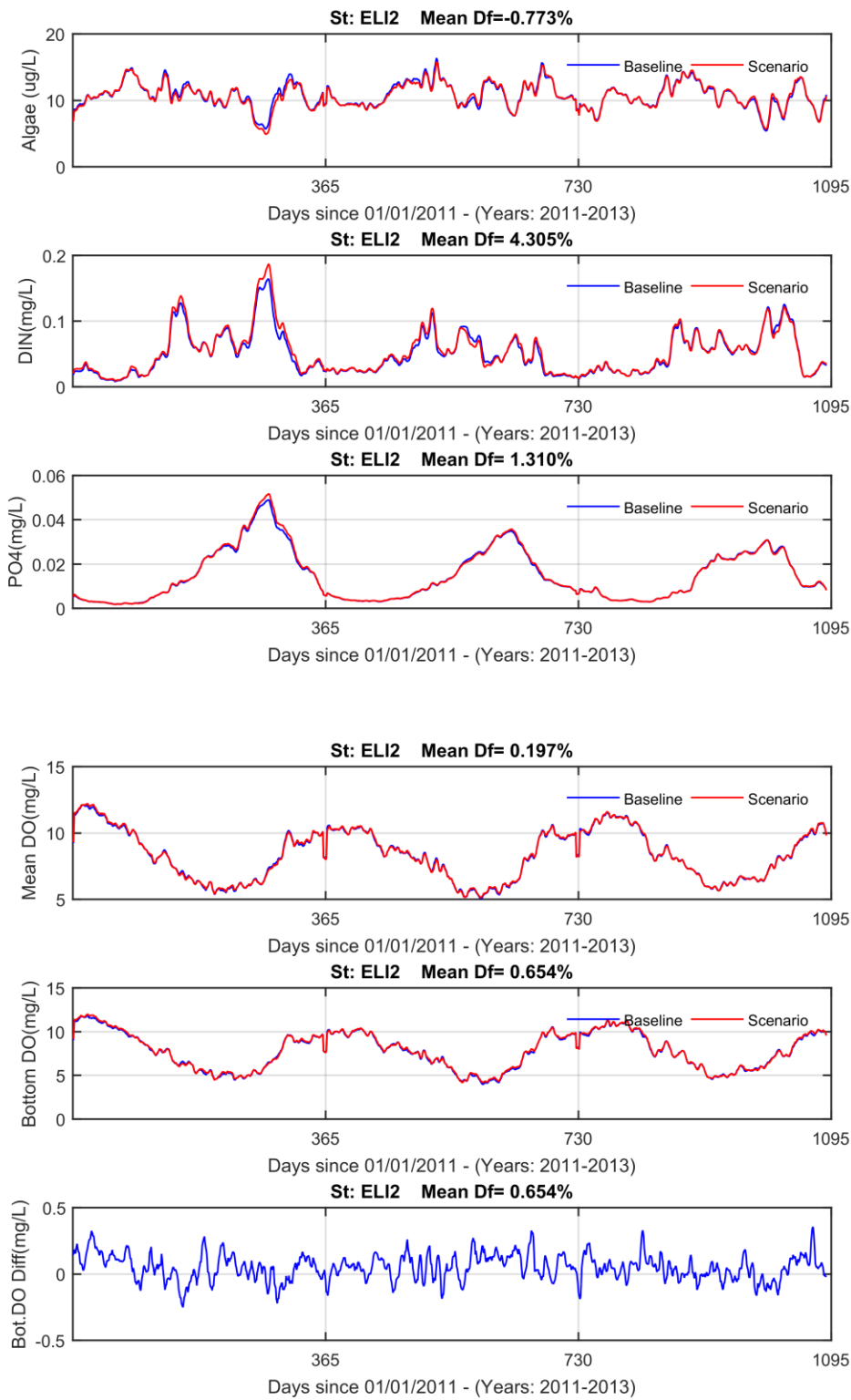


Figure 4-3-4: Comparison of Scenario 4-1 to Baseline 1 results at Station ELI2

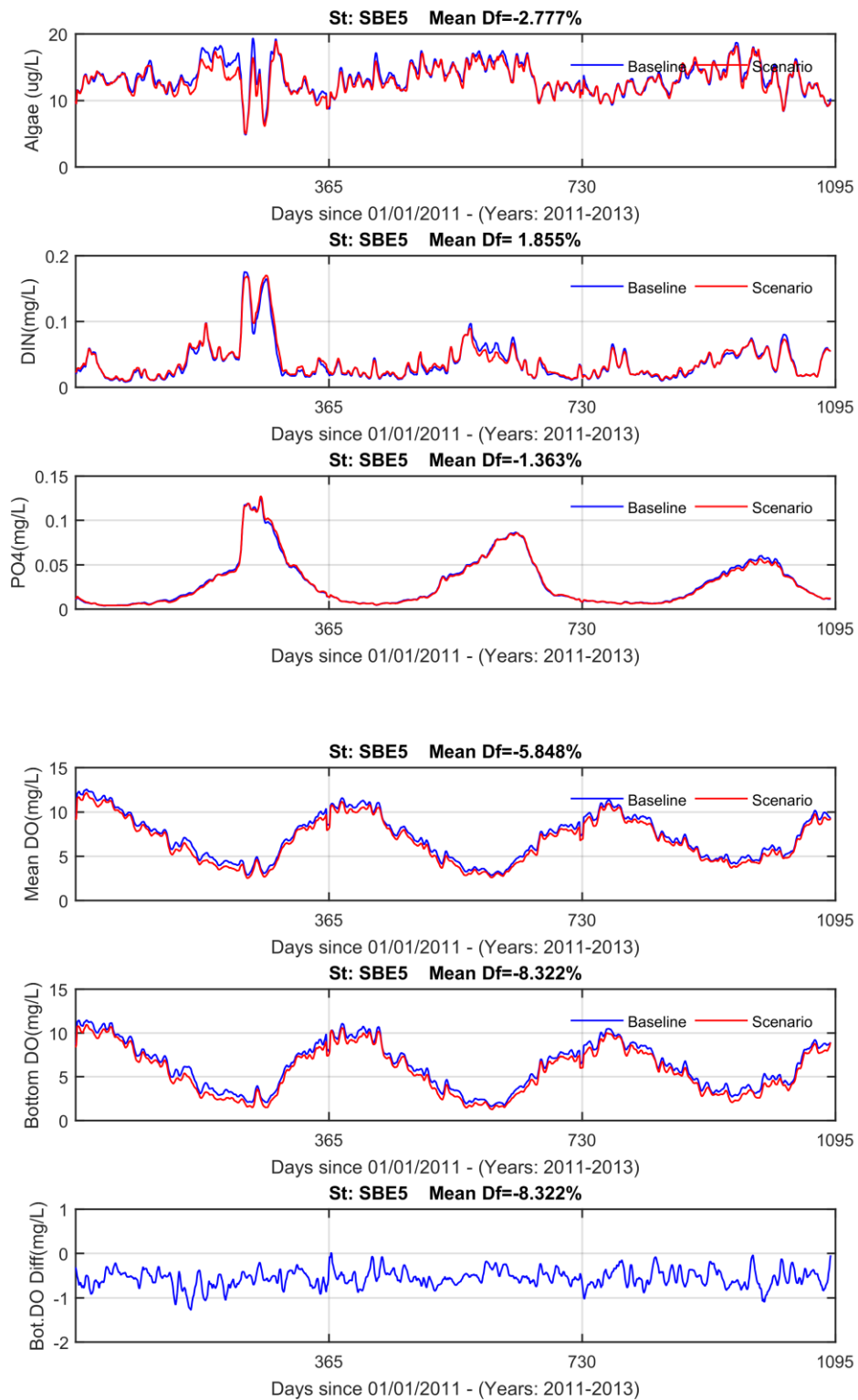


Figure 4-3-5: Comparison of Scenario 4-1 to Baseline 1 results at Station SBE5

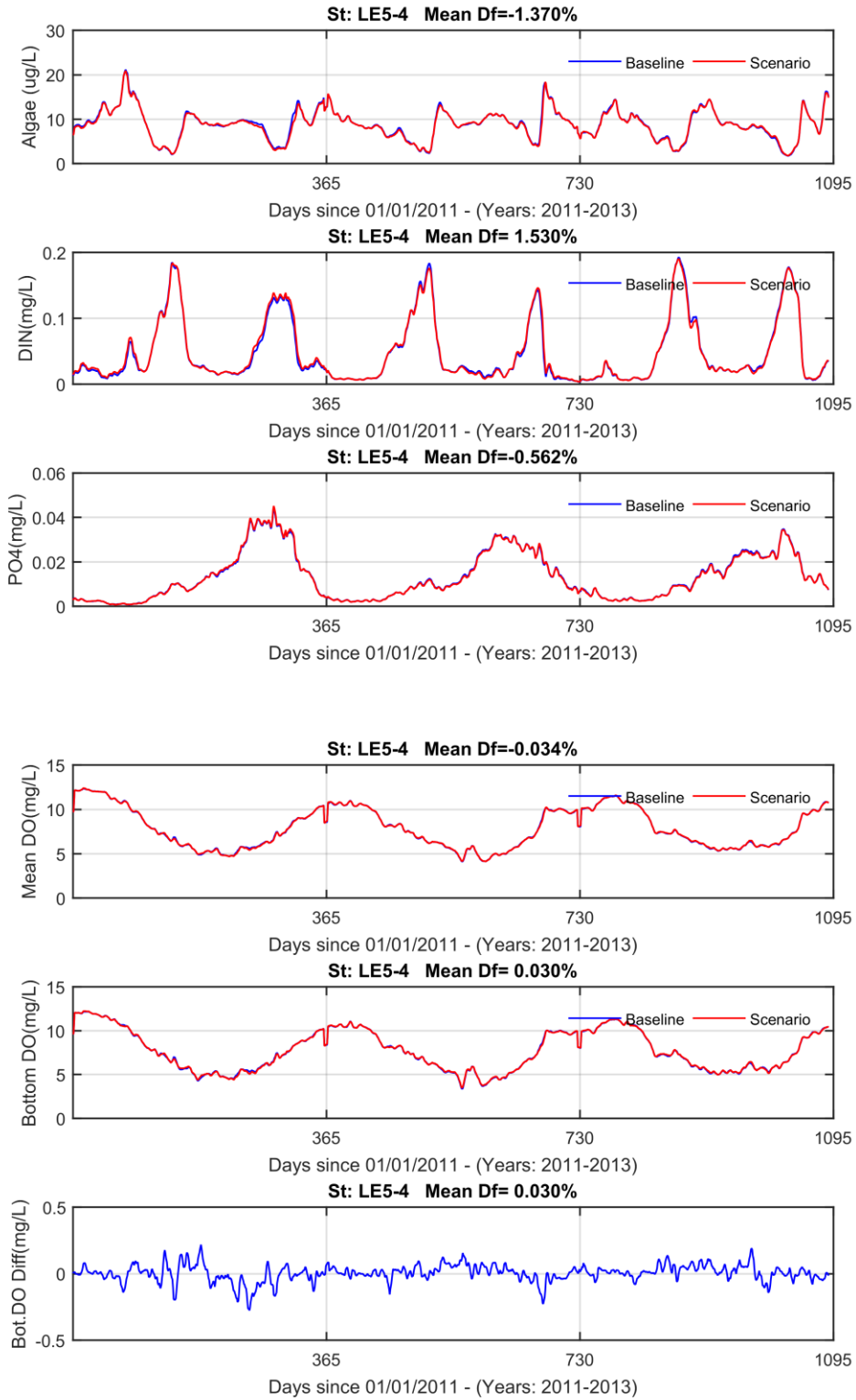


Figure 4-3-6: Comparison of Scenario 4-2 to Baseline 2 results at Station LE5-4

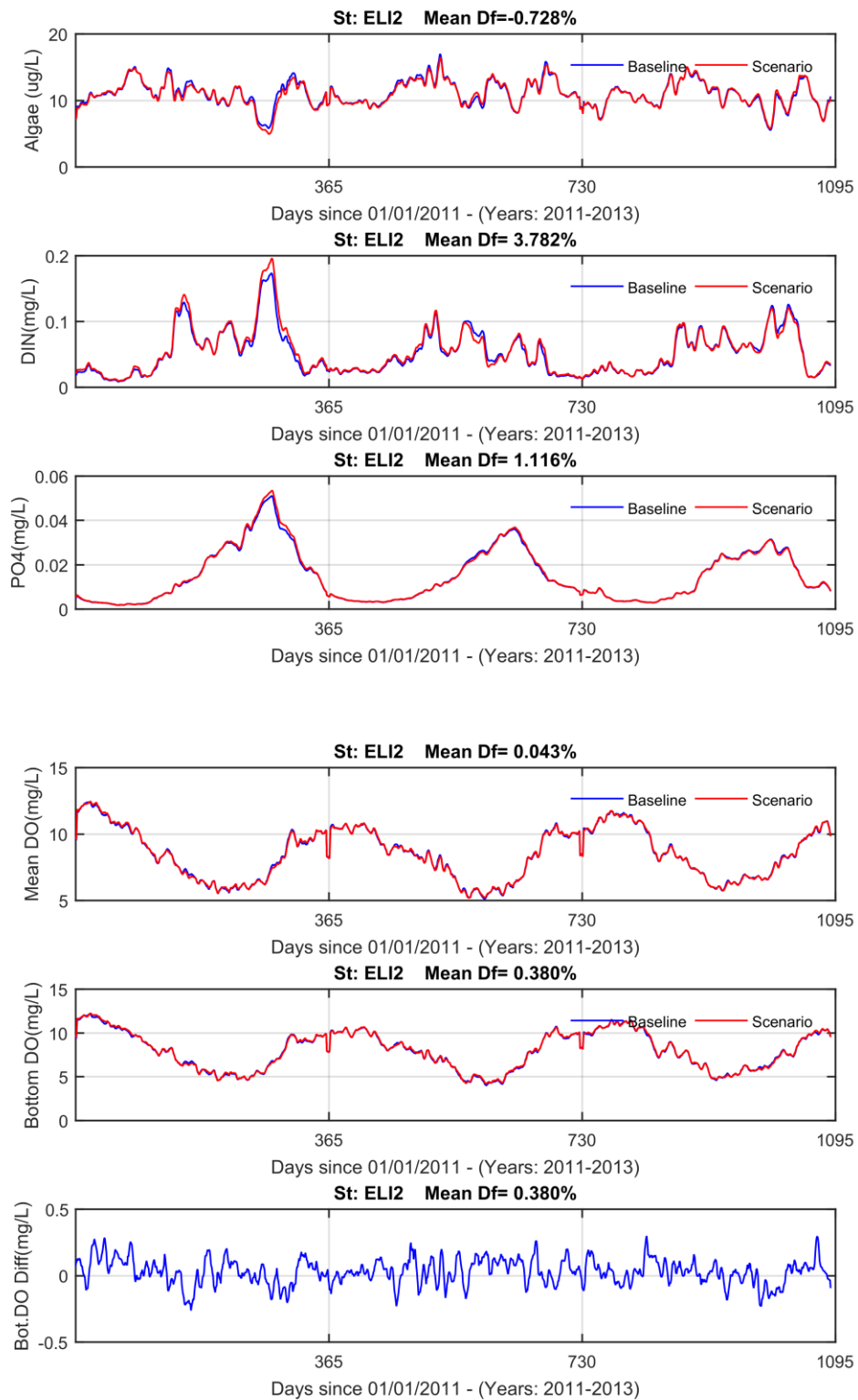


Figure 4-3-7: Comparison of Scenario 4-2 to Baseline 2 results at Station ELI2

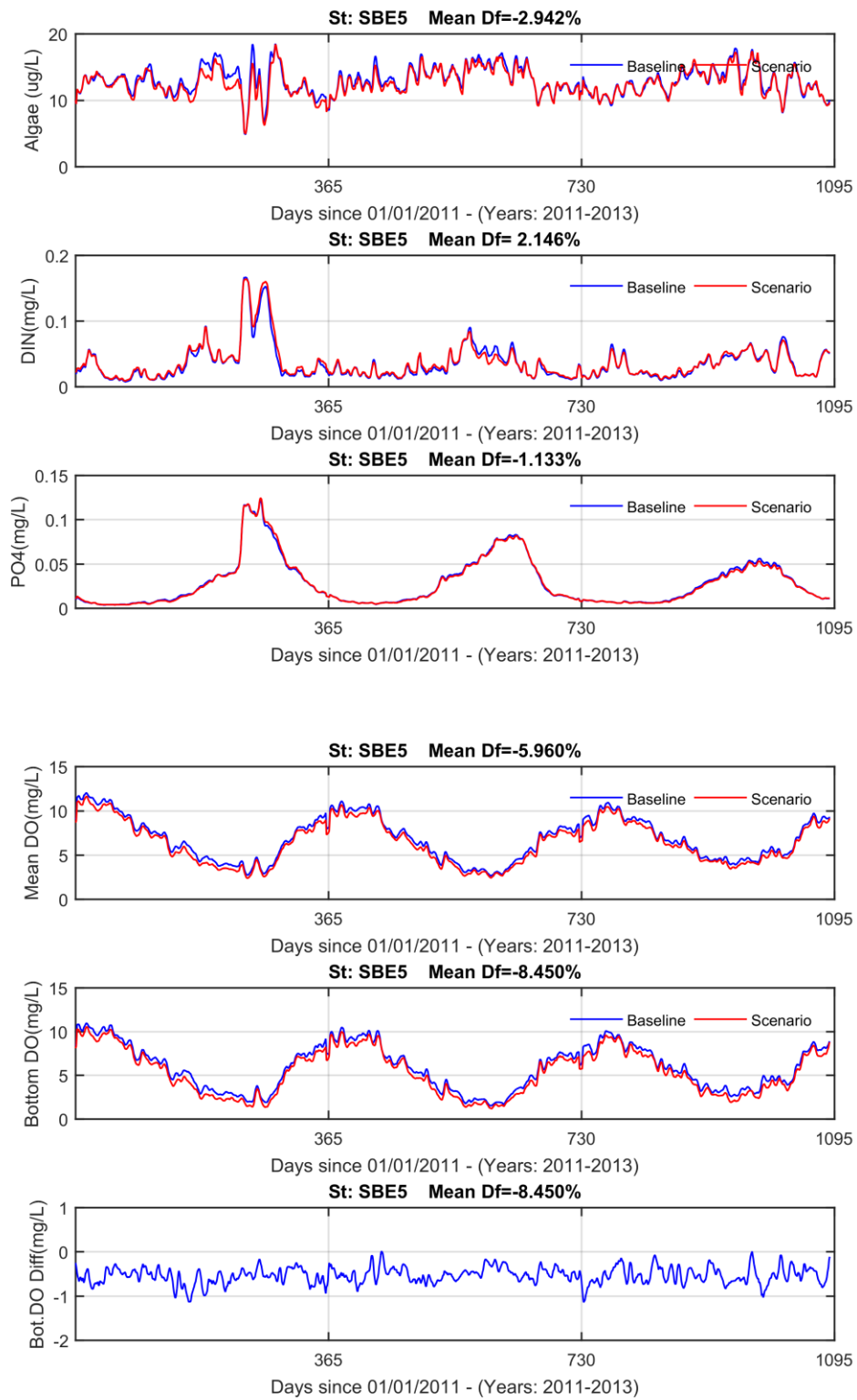


Figure 4-3-8: Comparison of Scenario 4-2 to Baseline 2 results at Station SBE5

4.4 Model Scenarios 5-1 and 5-2

These scenarios are simulated to examine the changes due to channel deepening of James River and Elizabeth River with NHC channels and SB Channel, and to compare to the existing condition (Baseline 1) and the future condition (Baseline 2) (see Table 2-1). The model grids with channel deepening of the NH channel for existing and future conditions are shown in Figures 4-4-1 and 4-4-2, respectively.

Summaries of DO statistics for Scenario 5-1 for both the mean and at the bottom layer for spring (March to May) and summer (July-September), respectively, are listed in Tables 4-4-1 and 4-4-2 for comparison of the scenario to Baseline 1. There is very little change in the James River (LE5-4). A slight decrease of DO occurred at Stations SBE-2 and SBE-5, located in the SW channel. It can be seen that the maximum reduction of DO is less than 0.73 mg/L at Station SBE-5 during summer. Changes are about 13% at the bottom.

Comparisons of the Scenario 5-1 to the existing condition (Baseline 1) are shown in Figures 4-4-3 to 4-4-5 for selected sections at LE5-4, ELI2, and SBE-5. The plots for other stations are shown in the full modeling report. There is very little change in the James River (LE5-4). A relatively large change of DO occurred at Station SBE-5. The DO change is less than 1.0 mg/L at the bottom during summer. The average change is less than 10%. A large change occurred during spring. As the channel deepens, the stratification increases during spring when runoff is higher. However, bottom DO values are all larger than 4.86 mg/L and there is no problem meeting the DO criterion during the spring season. There are no obvious changes for algae, DIN, and DIP.

Summaries of DO statistics for Scenario 5-2 for the mean and at the bottom layer for spring (March to May) and summer (July-September), respectively, are listed in Tables 4-4-3 and 4-4-4 for comparison of Scenario 5-2 to Baseline 2. There is very little change in the James River (LE5-4). A slight decrease of DO occurred at Stations SBE-2 and SBE-5, located in the SW channel. It can be seen that the maximum reduction of DO is less than 0.61 mg/L at Station SBE-5 during summer. Changes are about 20.25% at the bottom.

Comparisons of the Scenario 5-2 to the existing condition (Baseline 2) are shown in Figures 4-4-6 to 4-4-8 for selected sections at LE5-4, ELI-2, and SBE-5. The plots for other stations are shown in the full modeling report. There is very little change in the James River (LE5-4). A relatively large change of DO occurred at Station SBE-5. DO changes less than 1.0 mg/L at the bottom during summer. The average change is less than 11%. A large change occurred during spring. As the channel deepens, the stratification increases during spring when runoff is higher. However, bottom DO values are all larger than 4.6 mg/L and there is no problem meeting the DO criterion during the spring season. Results are similar to those of Scenario 5-1. There are no obvious changes for algae, DIN, and DIP.

Table 4-4-1: Comparison of Scenario 5-1 to Baseline 1 DO results during spring

Station	Baseline 1		Scenario 5-1		Difference		% difference	
	Mean (mg/L)	Bottom (mg/L)	Mean (mg/L)	Bottom (mg/L)	Mean (mg/L)	Bottom (mg/L)	Mean	Bottom
LE5-3	7.37	7.16	7.36	7.17	-0.01	0.01	-0.13	0.15
LE5-4	7.10	6.95	7.07	6.93	-0.03	-0.02	-0.44	-0.26
LE5-6	7.21	6.35	7.21	6.37	-0.00	0.02	-0.01	0.28
ELI2	7.99	7.40	8.05	7.49	0.06	0.10	0.80	1.30
SBE2	6.62	5.45	6.30	5.18	-0.33	-0.27	-4.92	-4.98
SBE5	6.69	5.70	6.06	4.97	-0.64	-0.73	-9.51	-12.82
LFA01	7.68	7.52	8.06	7.92	0.38	0.39	4.91	5.24
WBE1	7.97	7.51	7.81	7.41	-0.15	-0.11	-1.91	-1.40
EBE1	6.68	5.66	6.44	5.47	-0.24	-0.19	-3.63	-3.27

Table 4-4-2: Comparison of Scenario 5-1 to Baseline 1 DO results during summer

Station	Baseline 1		Scenario 5-1		Difference		% difference	
	Mean (mg/L)	Bottom (mg/L)	Mean (mg/L)	Bottom (mg/L)	Mean (mg/L)	Bottom (mg/L)	Mean	Bottom
LE5-3	5.83	5.56	5.81	5.54	-0.03	-0.02	-0.44	-0.29
LE5-4	5.34	5.10	5.28	5.03	-0.06	-0.06	-1.12	-1.24
LE5-6	5.28	4.28	5.25	4.21	-0.02	-0.07	-0.42	-1.72
ELI2	5.99	5.16	6.06	5.24	0.07	0.07	1.11	1.41
SBE2	4.41	3.08	4.08	2.81	-0.32	-0.27	-7.35	-8.88
SBE5	4.38	3.20	3.80	2.53	-0.58	-0.68	-13.34	-21.09
LFA01	6.02	5.73	6.32	6.05	0.30	0.31	4.90	5.47
WBE1	6.30	5.66	6.15	5.57	-0.15	-0.09	-2.40	-1.61
EBE1	4.45	3.28	4.21	3.07	-0.24	-0.21	-5.33	-6.26

Table 4-4-3: Comparison of Scenario 5-2 to Baseline 2 DO results during spring

Station	Baseline 2		Scenario 5-2		Difference		% difference	
	Mean (mg/L)	Bottom (mg/L)	Mean (mg/L)	Bottom (mg/L)	Mean (mg/L)	Bottom (mg/L)	Mean	Bottom
LE5-3	7.36	7.14	7.35	7.16	-0.01	0.01	-0.10	0.20
LE5-4	7.08	6.92	7.05	6.91	-0.03	-0.01	-0.38	-0.18
LE5-6	6.90	6.01	6.91	6.01	0.01	-0.00	0.11	-0.06
ELI2	8.18	7.60	8.24	7.69	0.06	0.09	0.73	1.21
SBE2	6.48	5.37	6.19	5.12	-0.29	-0.26	-4.43	-4.79
SBE5	6.35	5.38	5.75	4.70	-0.59	-0.68	-9.36	-12.60
LFA01	8.14	7.98	8.49	8.35	0.36	0.37	4.37	4.67
WBE1	7.70	7.30	7.60	7.24	-0.10	-0.06	-1.32	-0.86
EBE1	6.62	5.61	6.40	5.44	-0.21	-0.17	-3.20	-2.94

Table 4-4-4: Comparison of Scenario 5-2 to Baseline 2 DO results during summer

Station	Baseline 2		Scenario 5-2		Difference		% difference	
	Mean (mg/L)	Bottom (mg/L)	Mean (mg/L)	Bottom (mg/L)	Mean (mg/L)	Bottom (mg/L)	Mean	Bottom
LE5-3	5.83	5.55	5.80	5.53	-0.03	-0.02	-0.46	-0.39
LE5-4	5.32	5.08	5.26	5.01	-0.06	-0.06	-1.06	-1.21
LE5-6	4.81	3.80	4.77	3.67	-0.04	-0.13	-0.84	-3.38
ELI2	6.12	5.28	6.16	5.33	0.04	0.05	0.68	0.94
SBE2	4.29	3.02	4.01	2.76	-0.28	-0.26	-6.61	-8.47
SBE5	4.12	2.99	3.61	2.39	-0.51	-0.61	-12.29	-20.25
LFA01	6.37	6.07	6.63	6.33	0.26	0.26	4.03	4.37
WBE1	6.12	5.54	6.03	5.50	-0.08	-0.04	-1.36	-0.76
EBE1	4.39	3.22	4.18	3.03	-0.21	-0.19	-4.71	-5.88

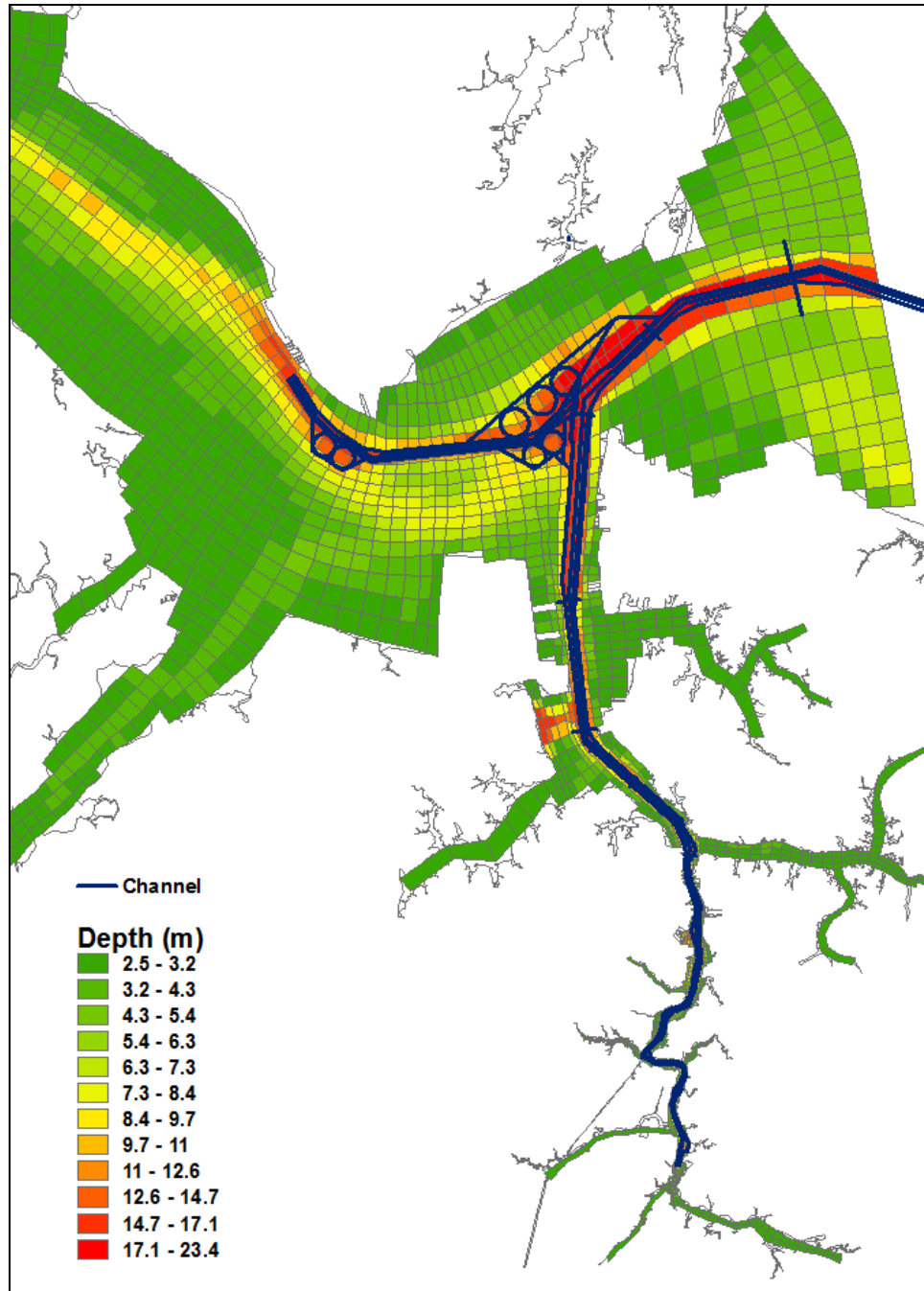


Figure 4-4-1: Model Grid of Scenario 5-1 (Deepening NH & SB Channels)

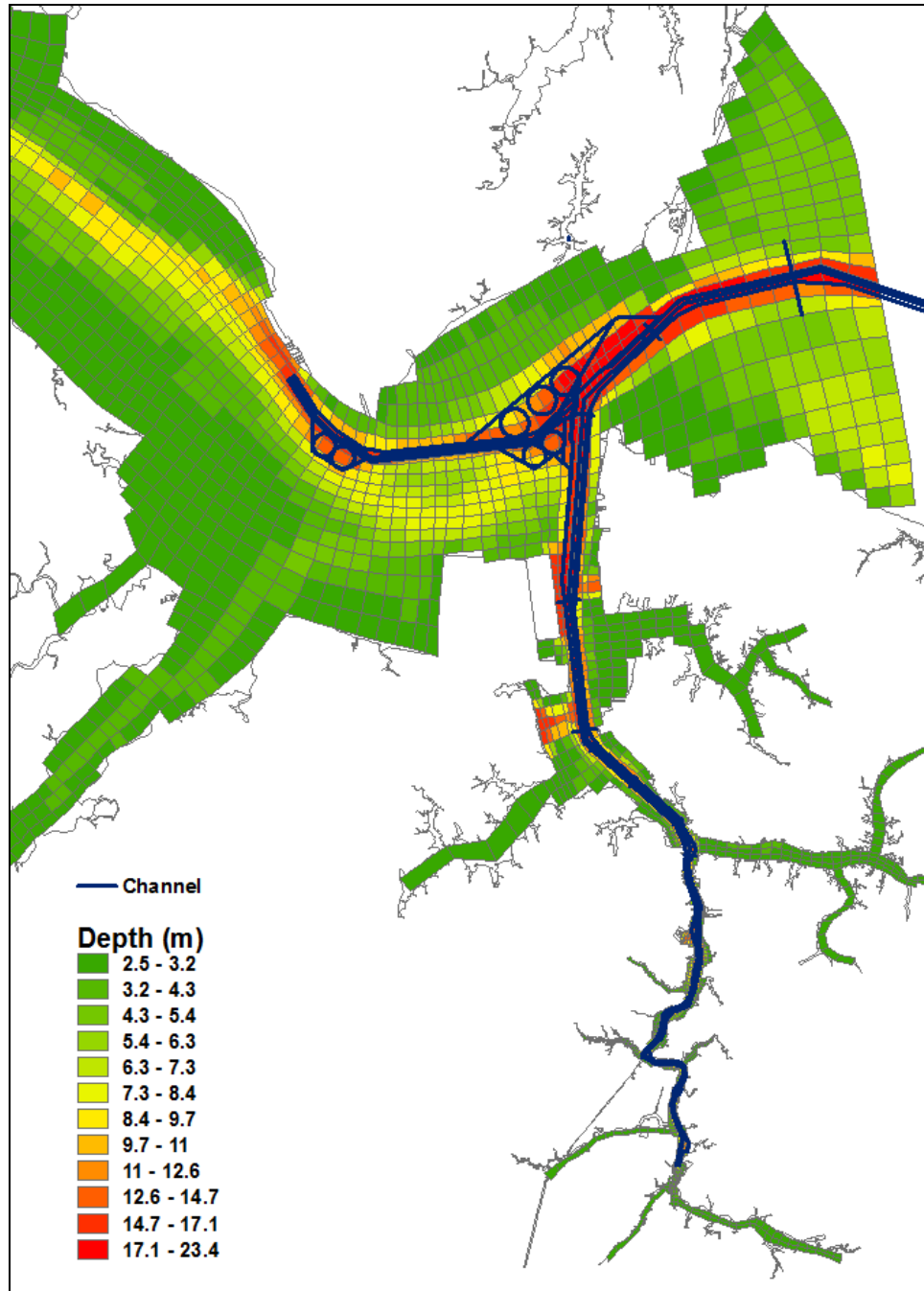


Figure 4-4-2: Model Grid of Scenario 5-2 (Deepening NH & SB Channels)

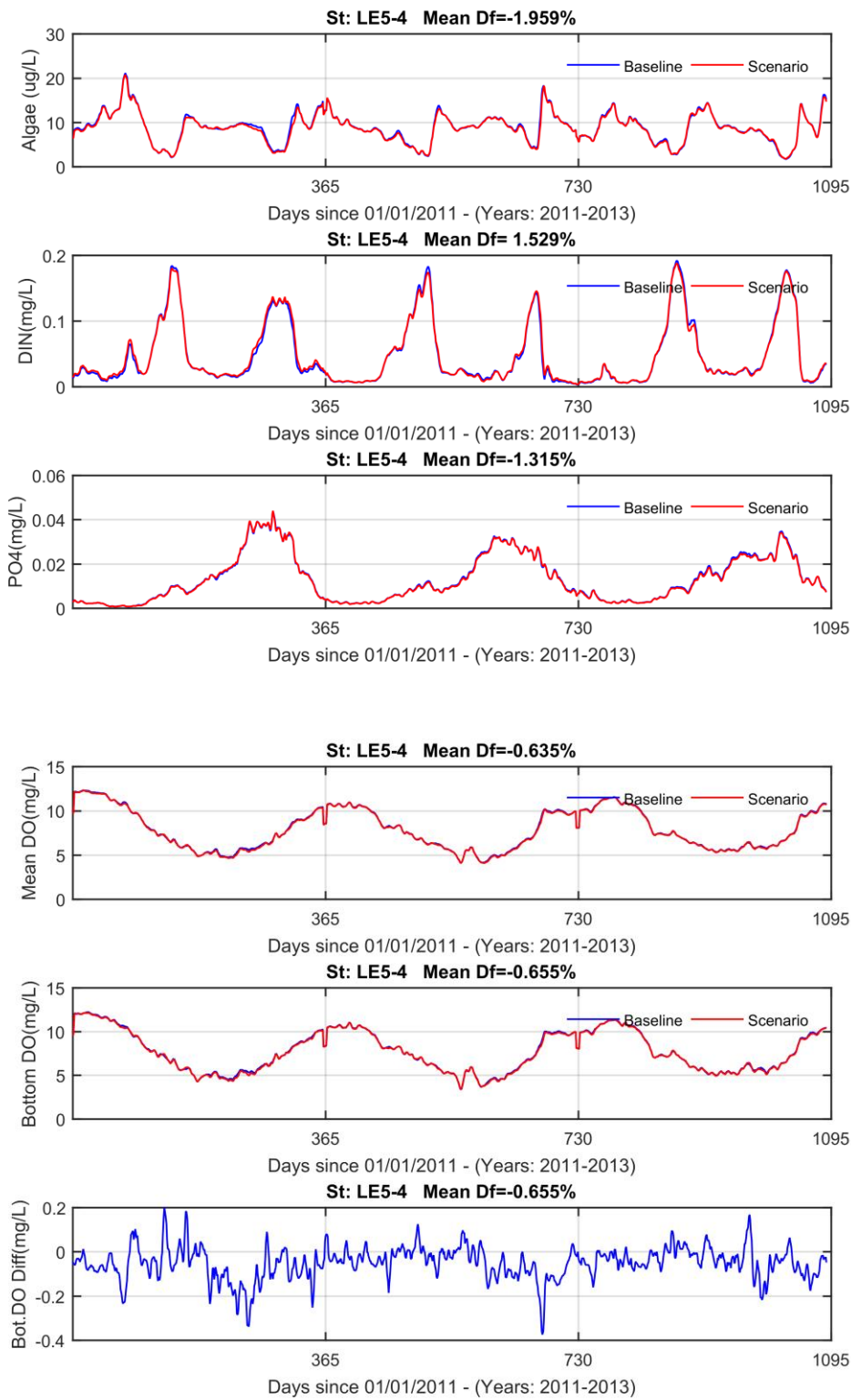


Figure 4-4-3: Comparison of Scenario 5-1 to Baseline 1 results at Station LE5-4

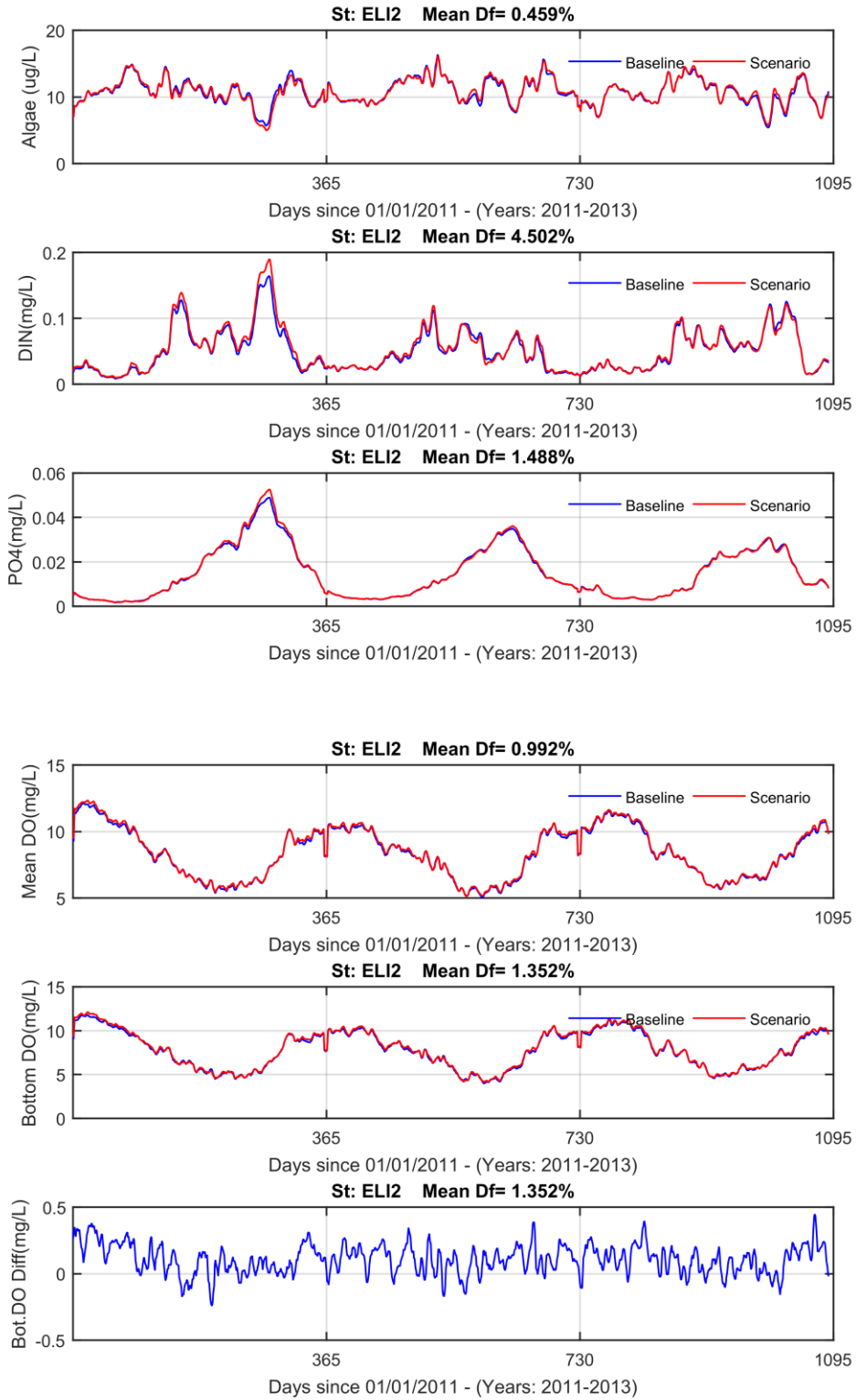


Figure 4-4-4: Comparison of Scenario 5-1 to Baseline 1 results at Station ELI2

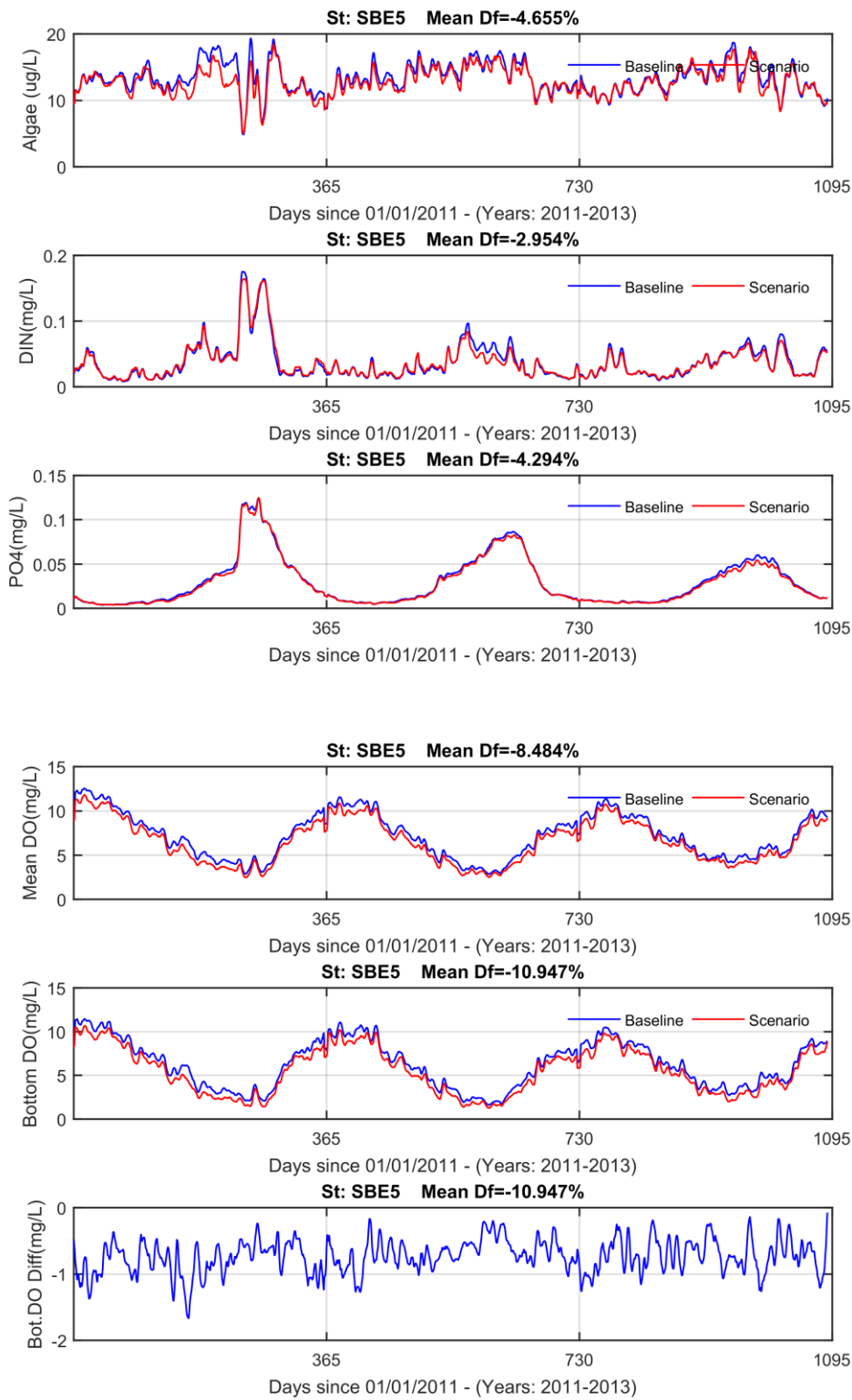


Figure 4-4-5: Comparison of Scenario 5-1 to Baseline 1 results at Station SBE5

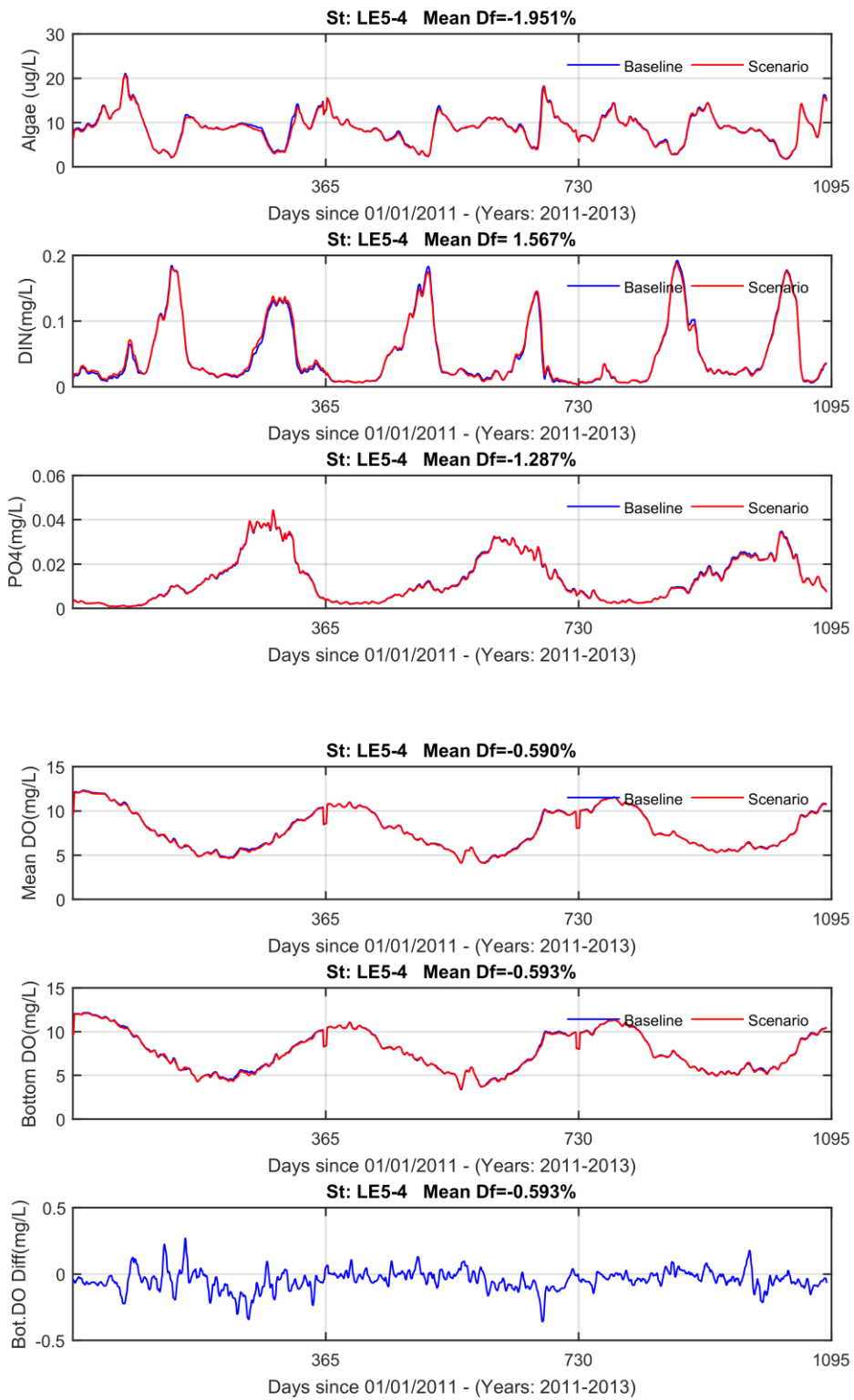


Figure 4-4-6: Comparison of Scenario 5-2 to Baseline 2 results at Station LE5-4

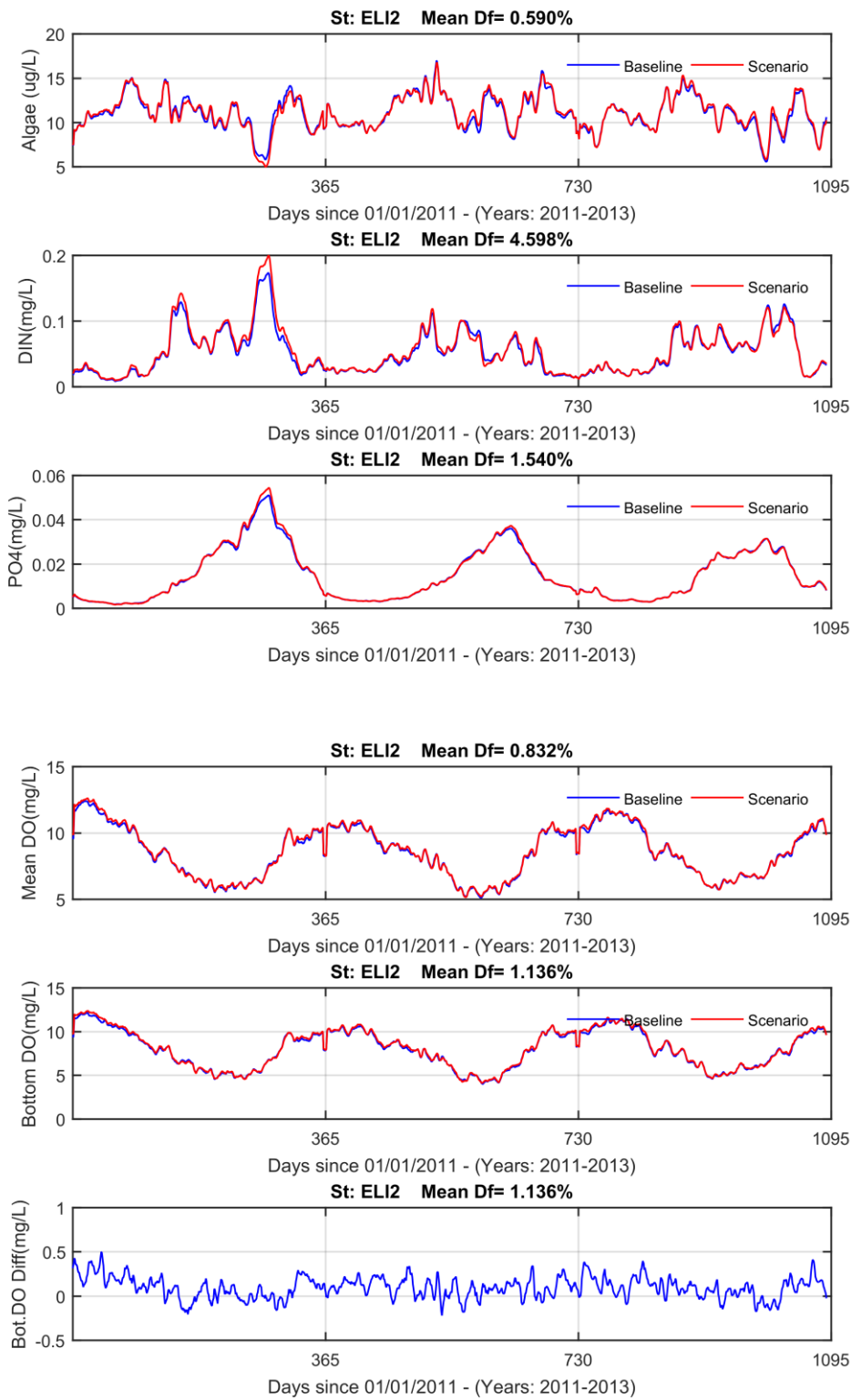


Figure 4-4-7: Comparison of Scenario 5-2 to Baseline 2 results at Station ELI2

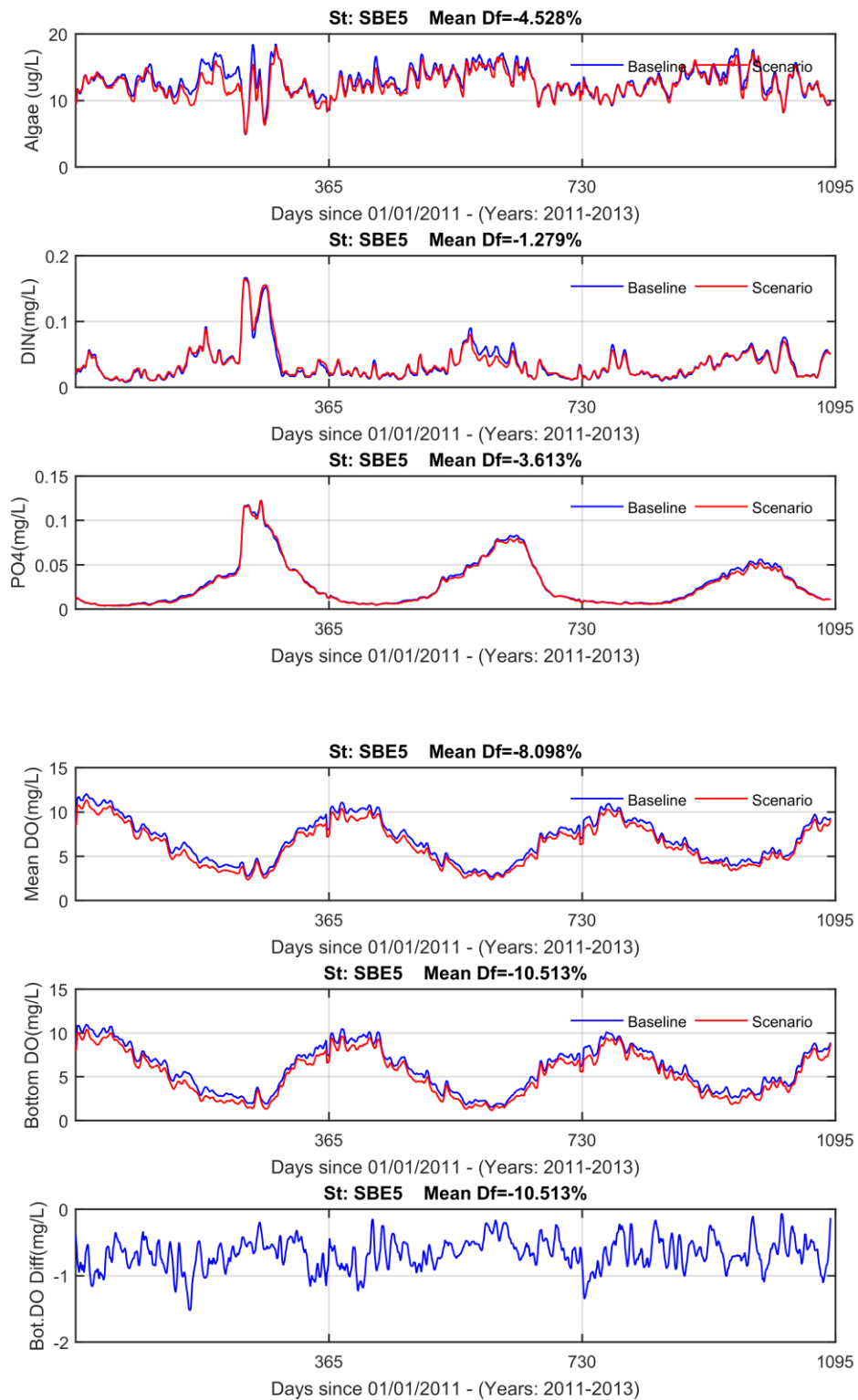


Figure 4-4-8: Comparison of Scenario 5-2 to Baseline 2 results at Station SBE5

5 Transport Time

5.1. Existing Condition and Future Condition

Three timescales, namely freshwater age, saltwater age, and renewal time, are examined and their differences are compared. We compared difference of daily vertical mean age for each timescale at each location for a period of three years. The spatial distribution between the existing condition (Baseline 1) and the future condition (Baseline 2) are compared. Spatial plots for mean for the difference of each timescale are shown in Figures 5-1-1 for freshwater age, in Figure 5-1-2 for saltwater age, and in Figure 5-1-3 for renewal time.

The freshwater age indicates the change of freshwater movement. A decrease of freshwater age indicates that pollutants discharged into the estuary can be more quickly transported out of the estuary. It can be seen that the age decreases slightly in the lower James and Elizabeth River. A large decrease occurs in the Lafayette River.

The saltwater age indicates the change of saltwater movement. When saltwater age decreases, it shows the clean water from outside of estuary can be quickly transported to the estuary. It also indicates that it has less time for oxygen near the bottom layer to be consumed. It can be seen that the age increased lightly in the mesohaline region of the James River and decreases in the Elizabeth River.

The renewal time measures overall flushing of the estuary. Renewal time is a scale to measure the overall pollutant transport time. A short renewal time suggests pollutants discharged into the estuary will be more quickly transported out of the estuary. The renewal time decreases slightly in the lower James River and Elizabeth River. Overall change is less than 0.5 day, except in the Lafayette River. Renewal time decreases more in the Lafayette River.

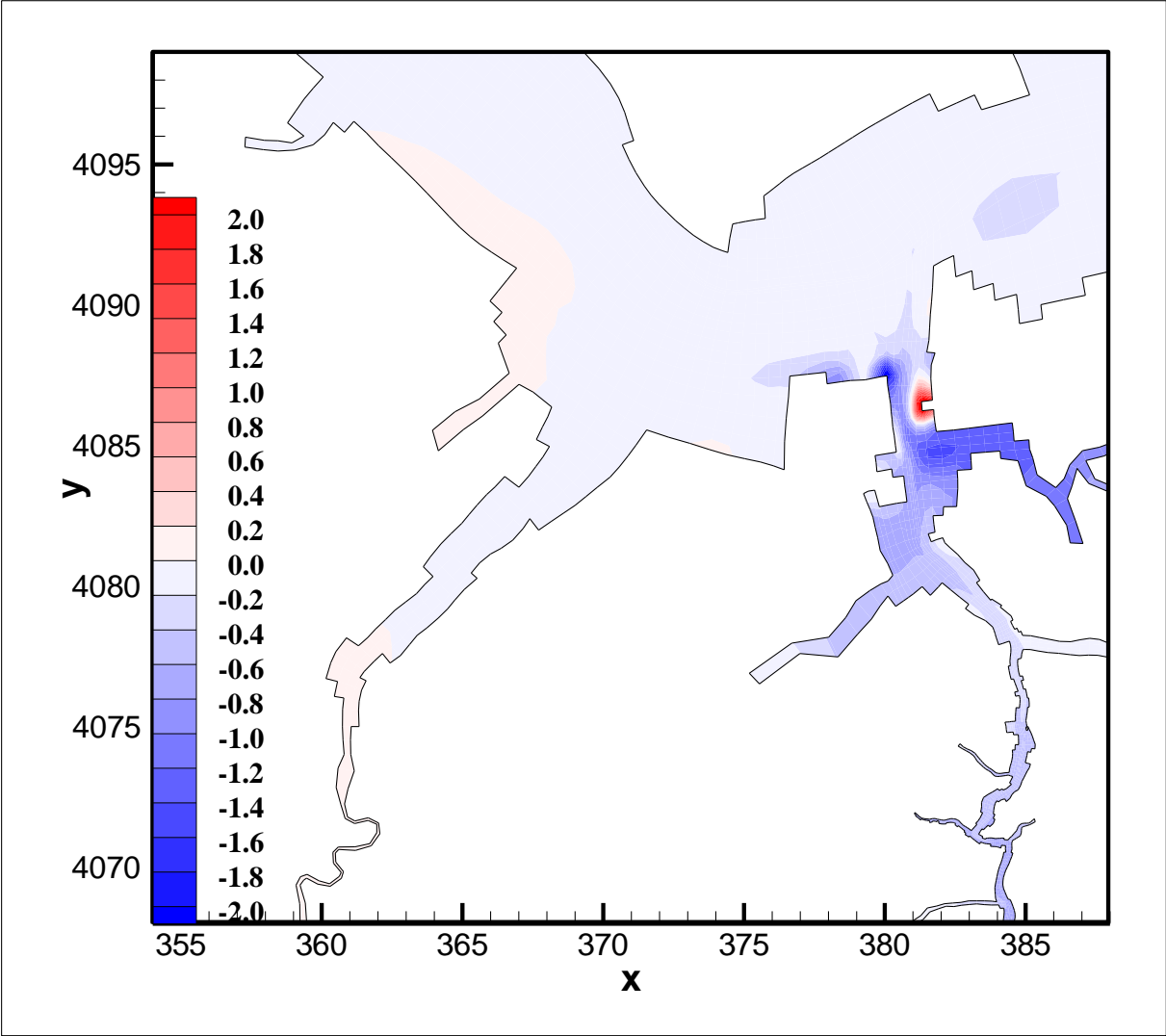
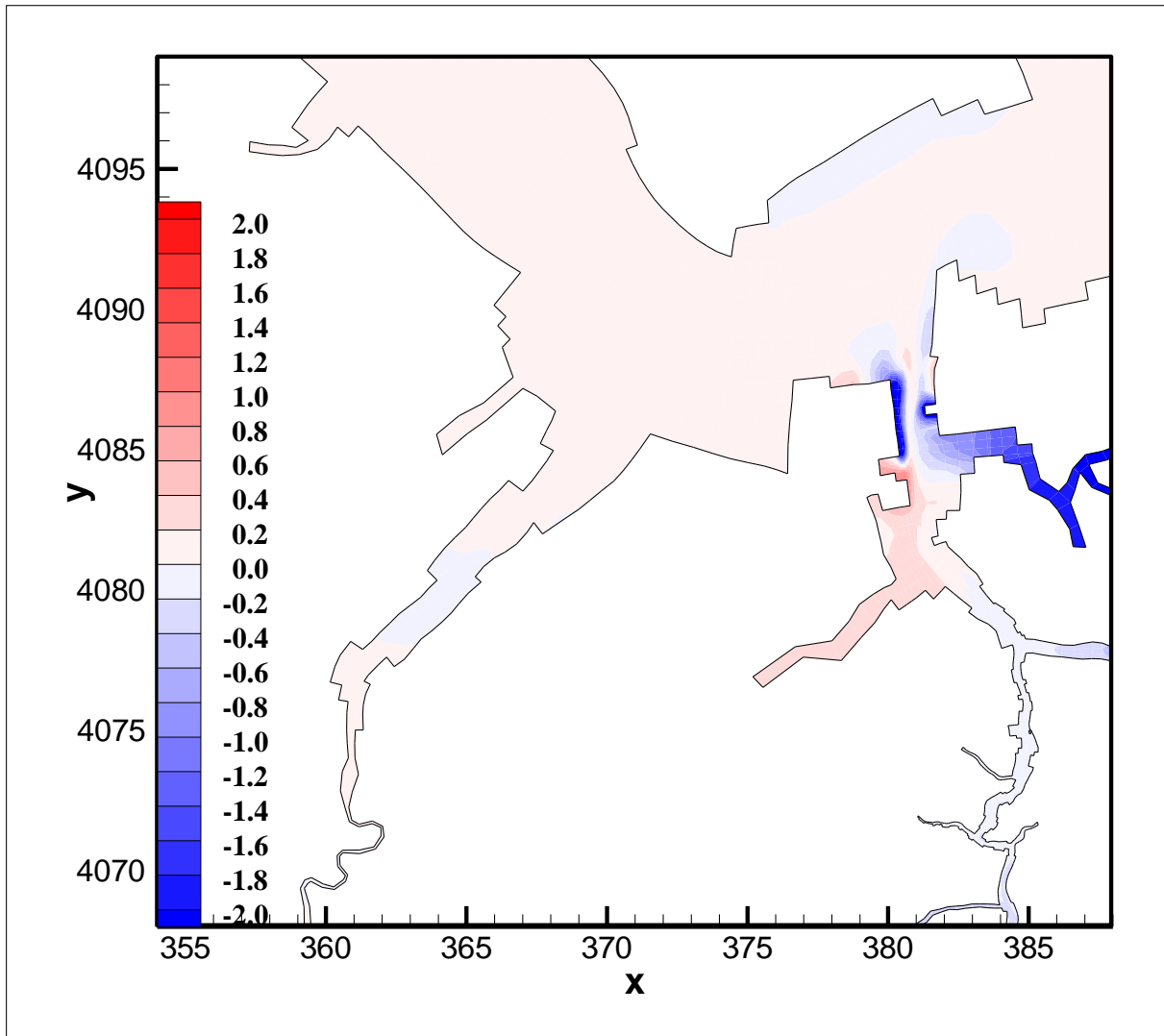
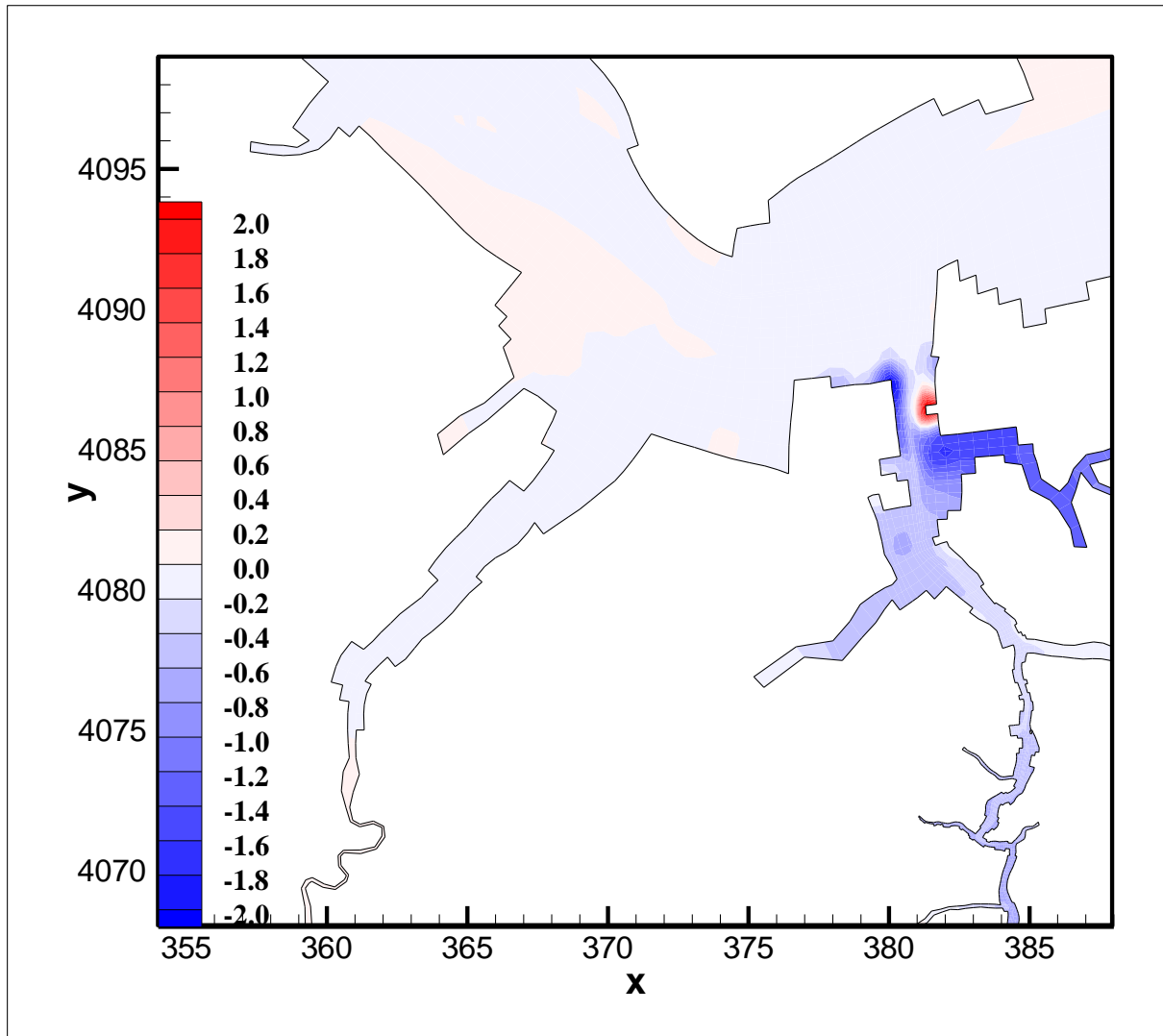


Figure 5-1-1: Distribution of mean difference of daily vertical averaged freshwater age (days) (Baseline 2 minus Baseline 1, mean difference)



**Figure 5-1-2: Distribution of difference of saltwater age (days)
(Baseline 2 minus Baseline 1, mean difference)**



**Figure 5-1-3: Distribution of difference of renewal time (days)
(Baseline 2 minus Baseline 1, mean difference)**

5.2. Scenarios 3-1 and 3-2

Three timescales, namely freshwater age, saltwater age, and renewal time, are examined and their differences are compared. We compared mean difference at each location for a period of three years. The spatial distributions between Scenario 3-1 and Baseline 1 (and between Scenario 3-2 and Baseline 2) are compared. Spatial plots for the mean and standard deviation for the difference of each timescale for Scenario 3-1 from Baseline 1 are shown in Figure 5-2-1 for freshwater age, in Figure 5-2-2 for saltwater age, and in Figure 5-2-3 for renewal time. Spatial plots for the mean for the difference of each timescale for Scenario 3-2 from Baseline 2 are shown in Figure 5-2-4 for freshwater age, in Figure 5-2-5 for saltwater age, and in Figure 5-2-6 for renewal time.

The freshwater age indicates the change of freshwater movement. It can be seen that the age increases slightly in the lower James. The age decreases in the mesohaline region of the James and decreases in tributaries of the Elizabeth River.

The saltwater age indicates the change of saltwater movement. It can be seen that the age decreases in the mesohaline region of the James River and lower Elizabeth River. The age increases slightly in upper James.

The renewal time decreases in the lower James and Elizabeth River.

For Scenario 3-2, the distributions of all three timescales are very similar to those of Scenario 3-1.

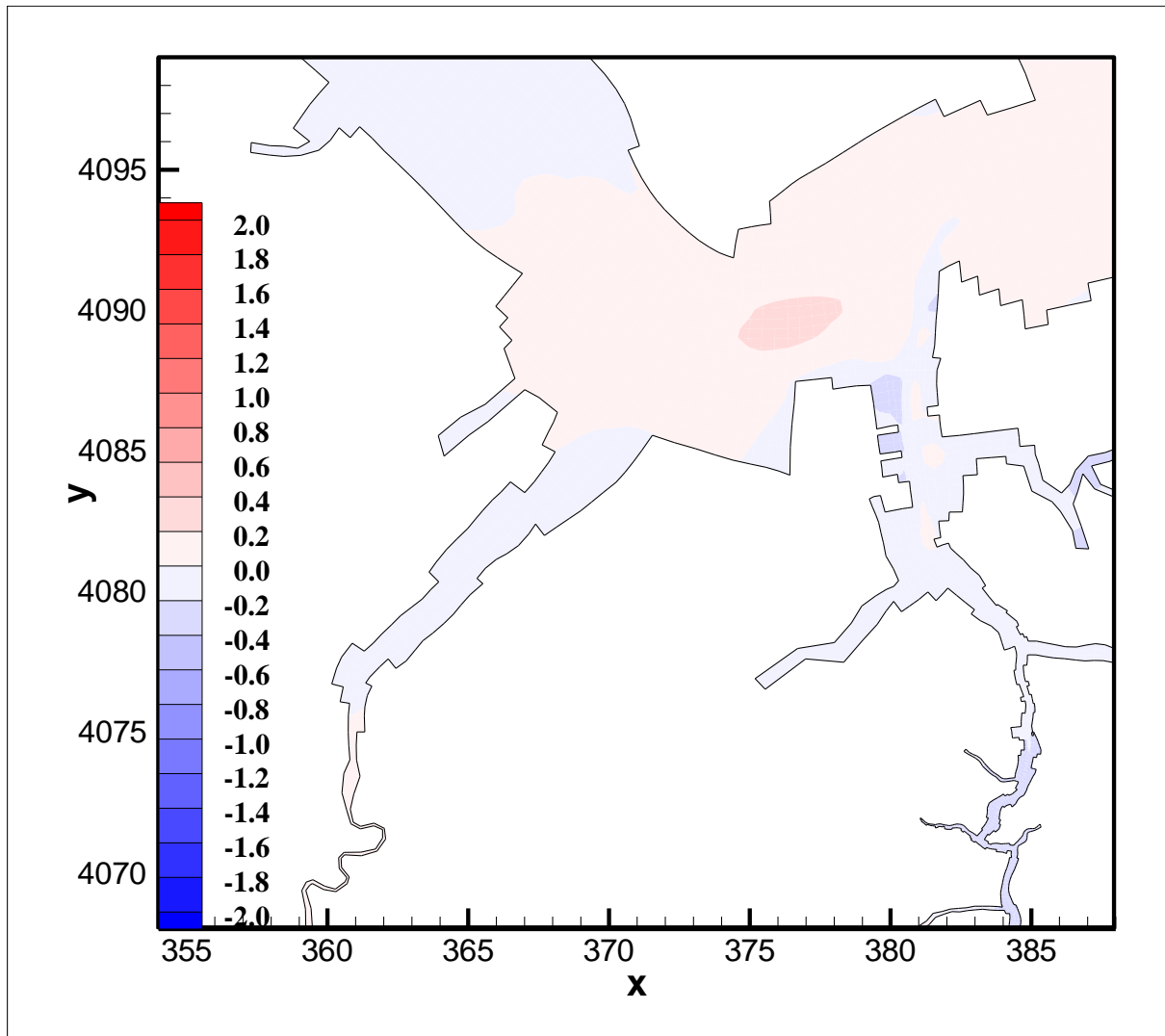


**Figure 5-2-1: Distribution of difference of freshwater age (days)
(Scenario 3-1 minus Baseline 1, mean difference)**

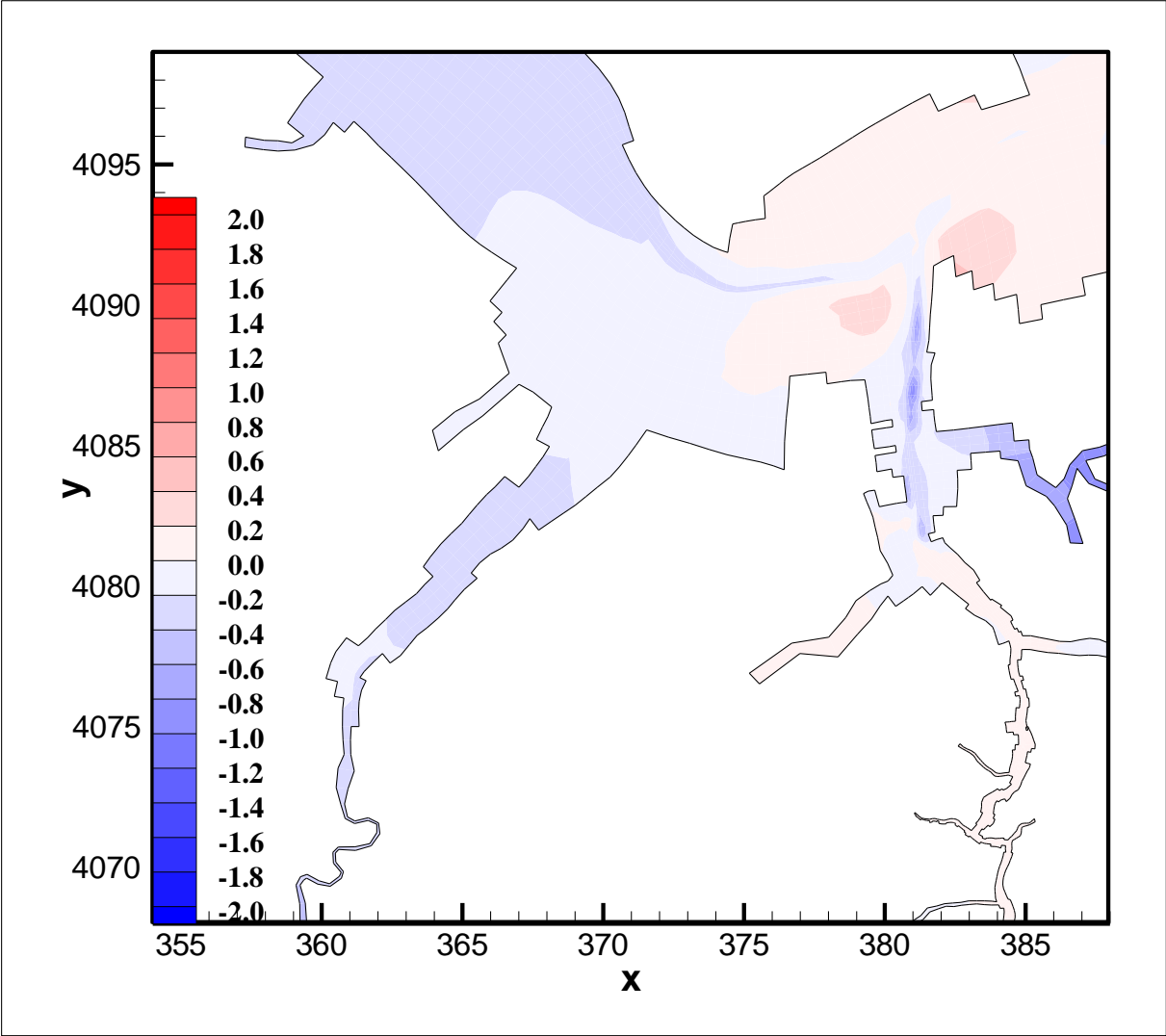


**Figure 5-2-2: Distribution of difference of saltwater age (days)
(Scenario 3-1 minus Baseline 1, mean difference)**

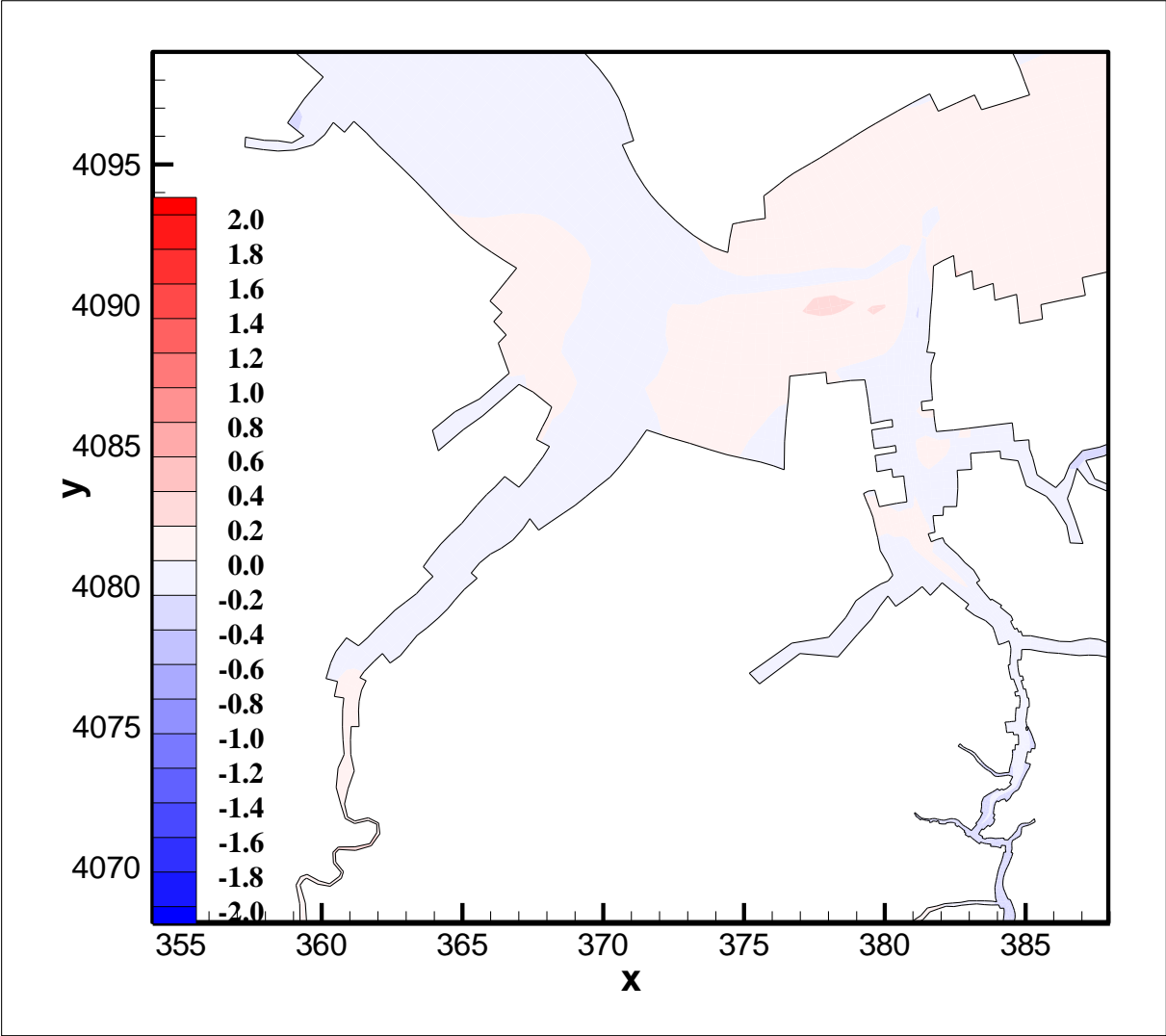


**Figure 5-2-3: Distribution of difference of renewal time (days)
(Scenario 3-1 minus Baseline 1, mean difference)**

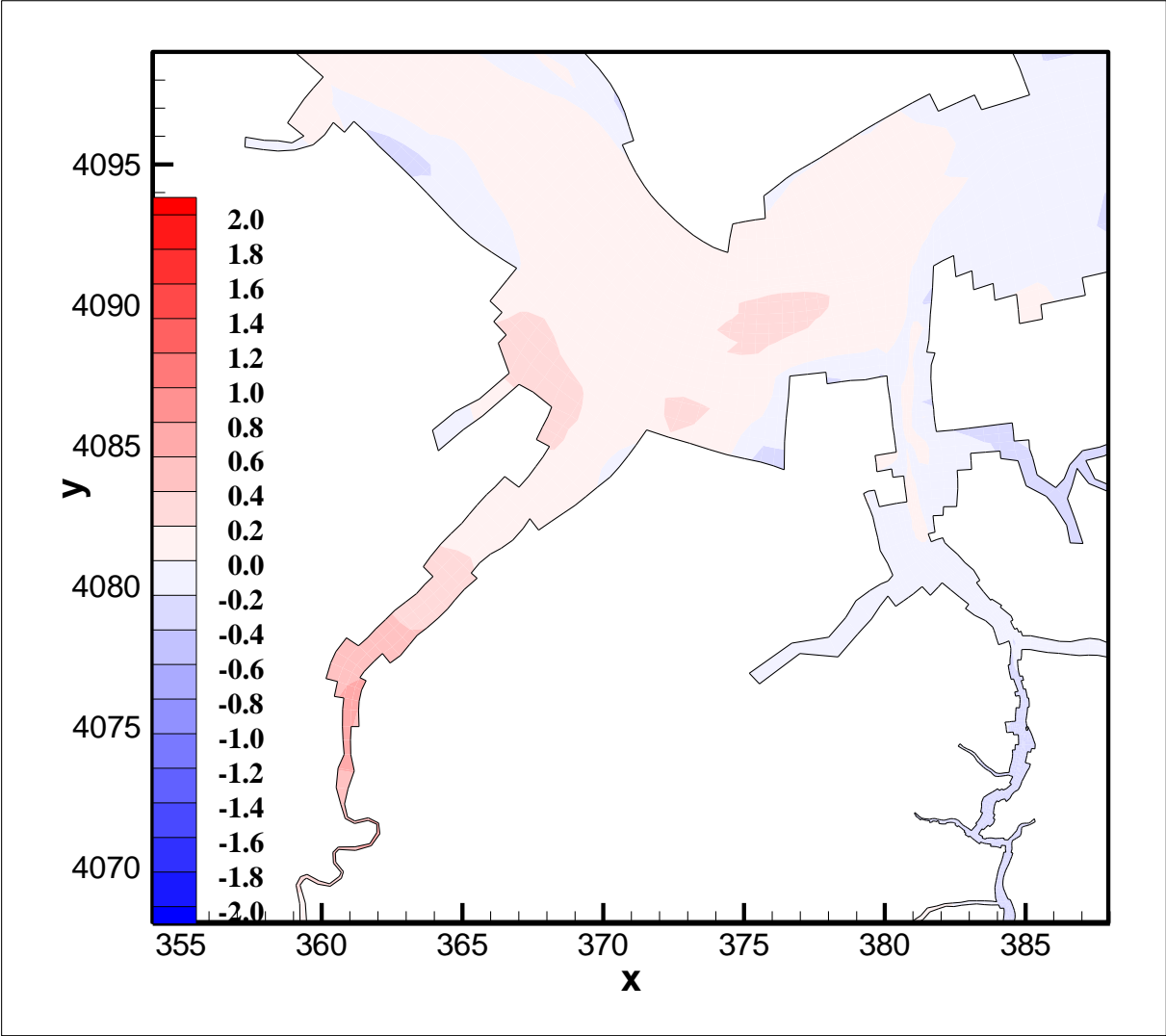


**Figure 5-2-4: Distribution of difference of freshwater age (days)
(Scenario 3-2 minus Baseline 2, mean difference)**

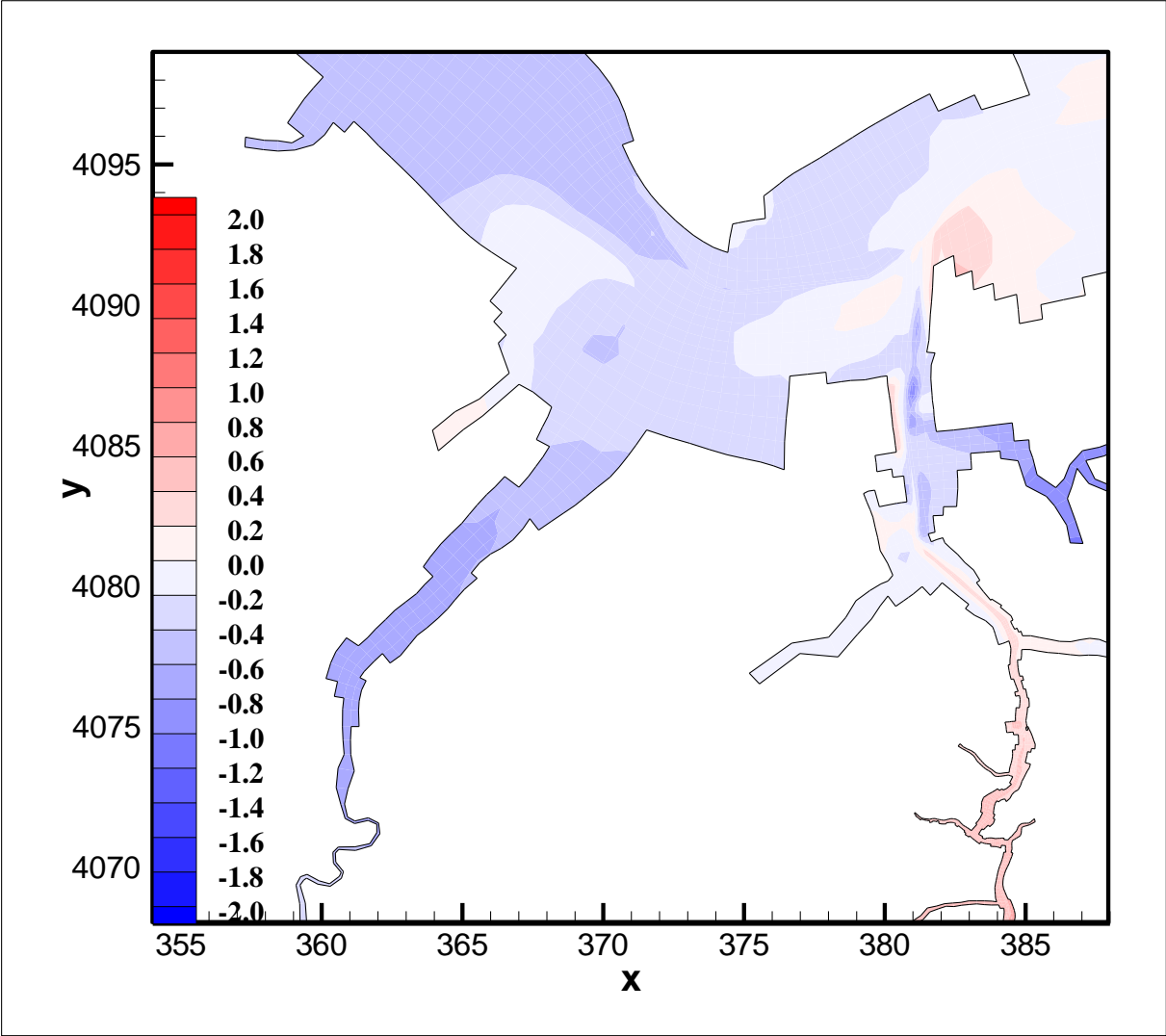


**Figure 5-2-5: Distribution of difference of saltwater age (days)
(Scenario 3-2 minus Baseline 2, mean difference)**

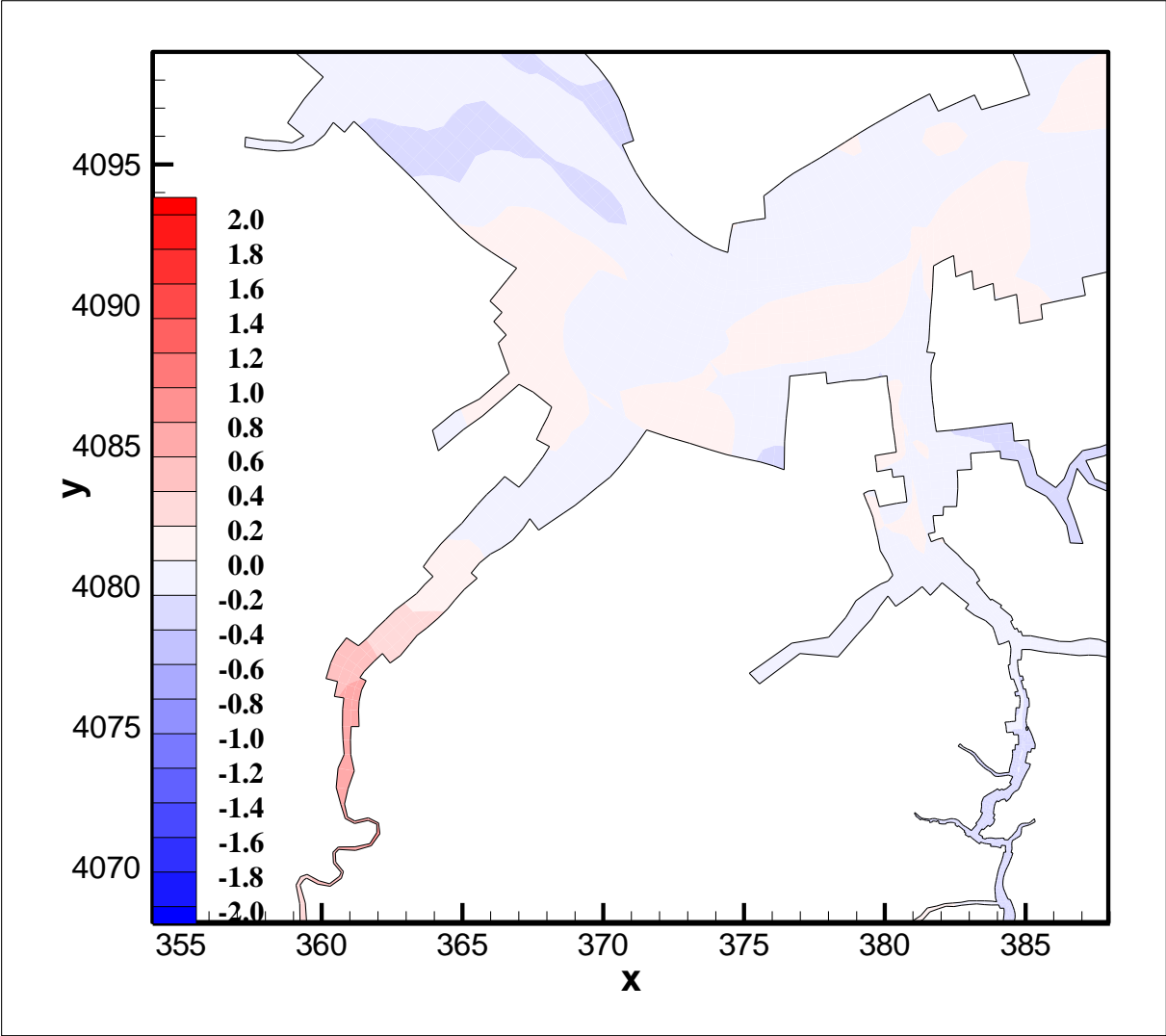


**Figure 5-2-6: Distribution of difference of renewal time (days)
(Scenario 3-2 minus Baseline 2, mean difference)**

5.3. Scenarios 4-1 and 4-2

Three timescales, namely freshwater age, saltwater age, and renewal time, are examined and their differences are compared. For each timescale, we compared the mean difference at each location for a period of three years. The spatial distributions between Scenario 4-1 and Baseline 1 (and between Scenario 4-2 and Baseline 2) are compared. Spatial plots for the mean and standard deviation for the difference of each timescale for Scenario 4-1 from Baseline 1 are shown in Figure 5-3-1 for freshwater age, in Figure 5-3-2 for saltwater age, and in Figure 5-3-3 for renewal time. Spatial plots for the mean for the difference of each timescale for Scenario 4-2 from Baseline 2 are shown in Figure 5-3-4 for freshwater age, in Figure 5-3-5 for saltwater age, and in Figure 5-3-6 for renewal time.

The freshwater age indicates the change of freshwater movement. It can be seen that the age increases slightly in the lower James. The age decreases in tributaries in the Elizabeth River. Changes are very minor.

The saltwater age indicates the change of saltwater movement. It can be seen that the age decreases in the lower James River and Elizabeth River slightly. In general, there is no significant change.

The renewal time is the measure of the overall change of flushing time. The renewal time shows a slight decrease in the lower James. There is not much change overall.

For Scenario 4-2, the distributions of all three timescales are very similar to those of Scenario 4-1.

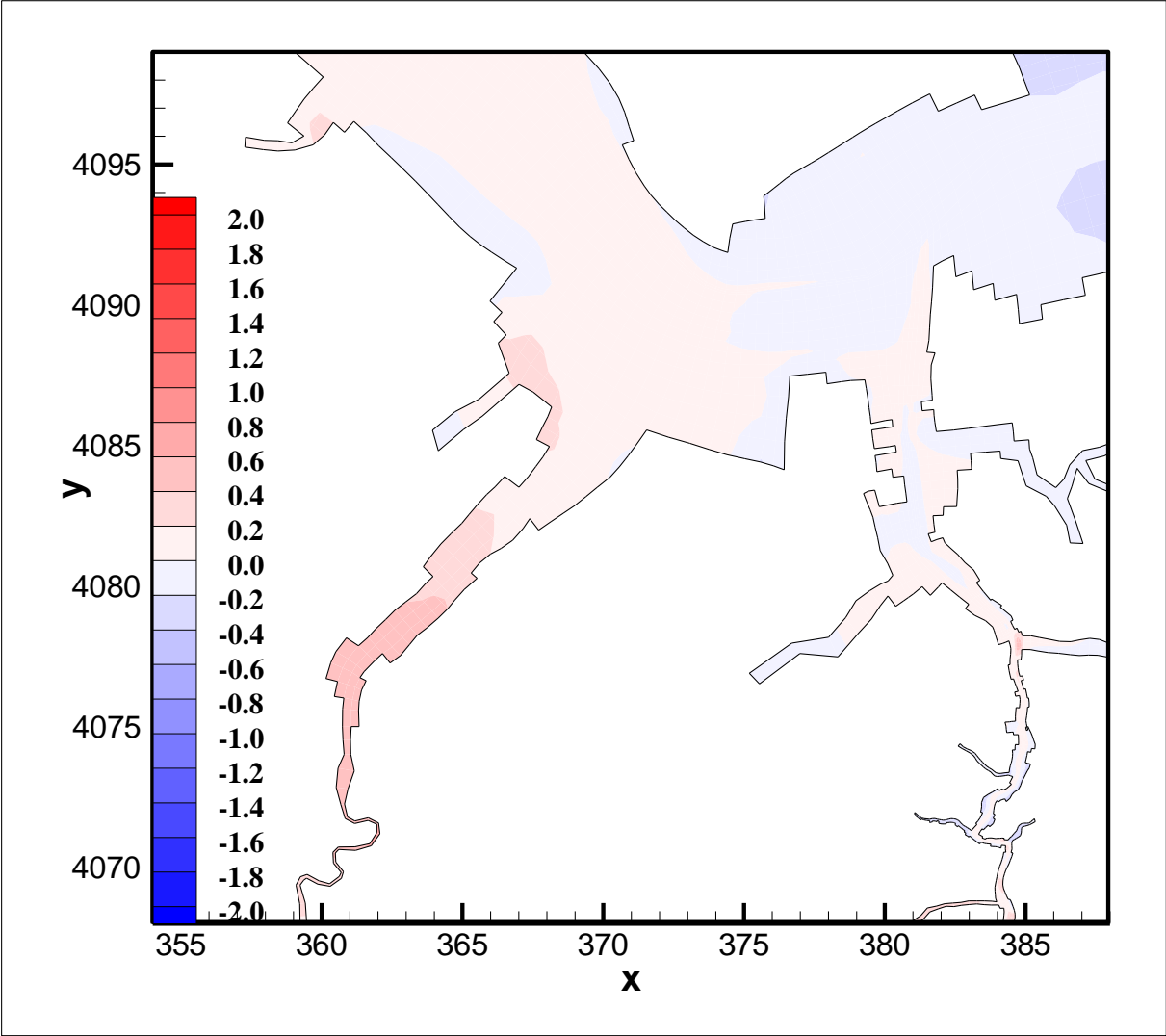


**Figure 5-3-1: Distribution of difference of freshwater age (days)
(Scenario 4-1 minus Baseline 1, mean difference)**

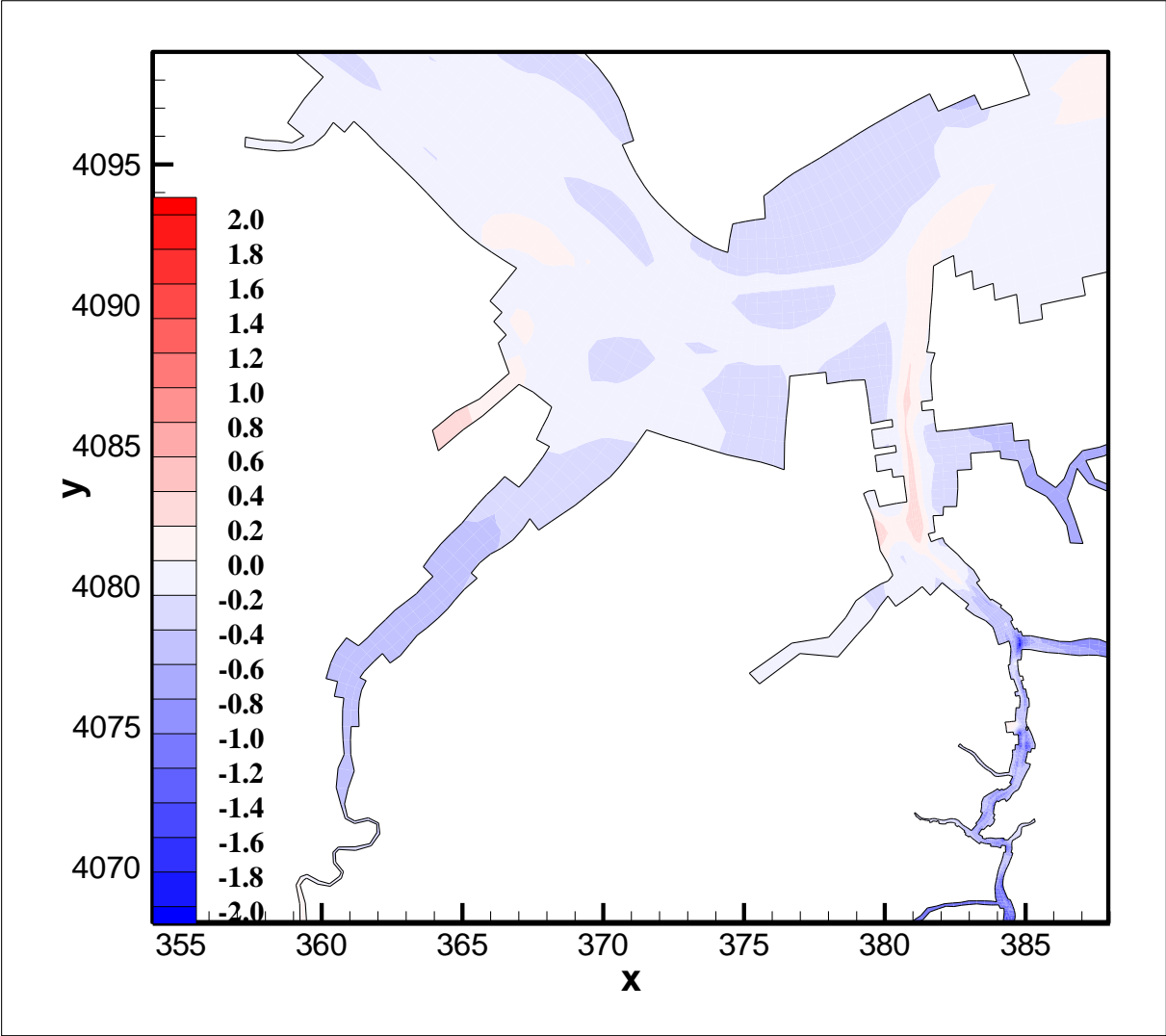


**Figure 5-3-2: Distribution of difference of saltwater age (days)
(Scenario 4-1 minus Baseline 1, mean difference)**

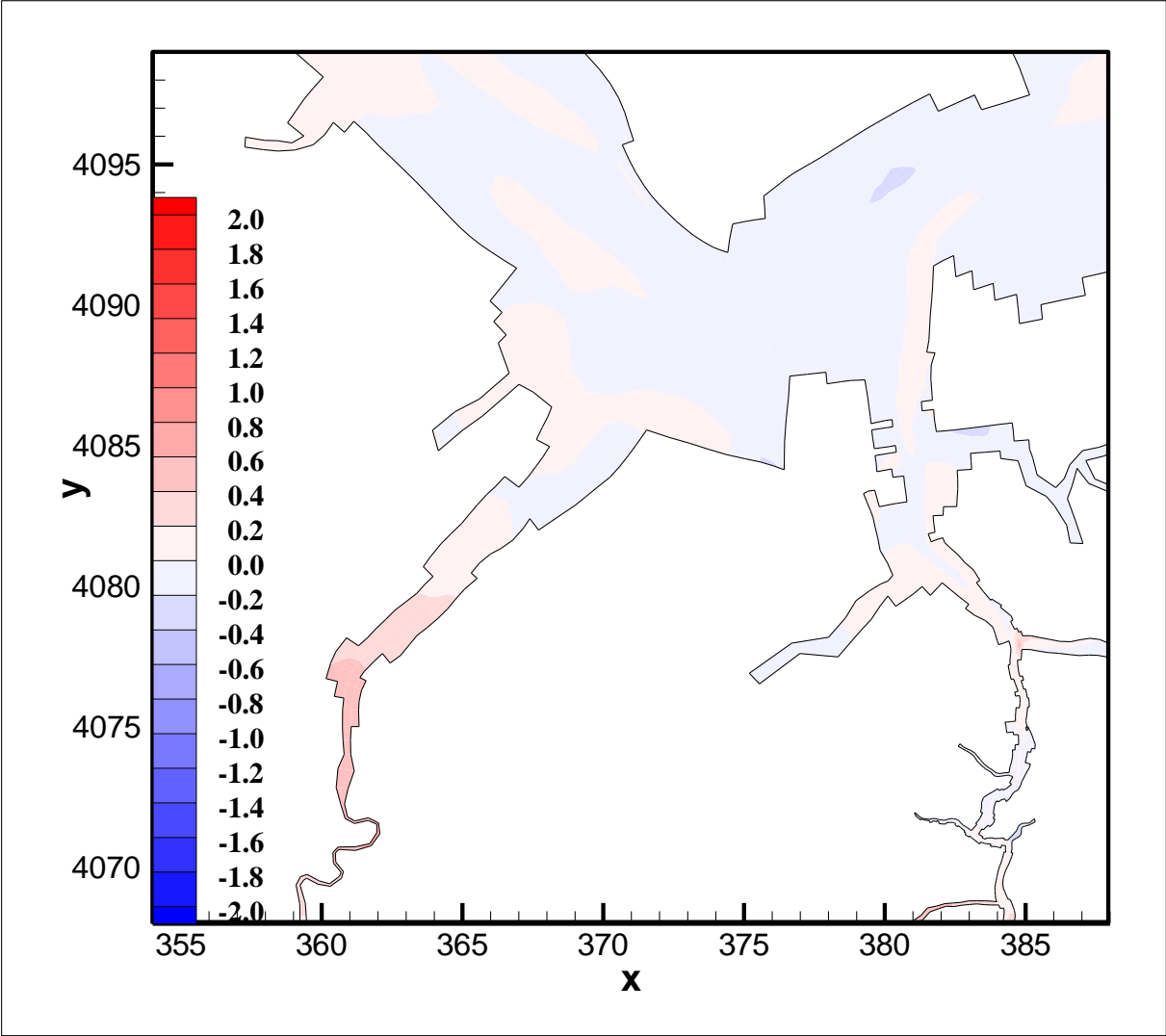


**Figure 5-3-3: Distribution of difference of renewal time (days)
(Scenario 4-1 minus Baseline 1, mean difference)**

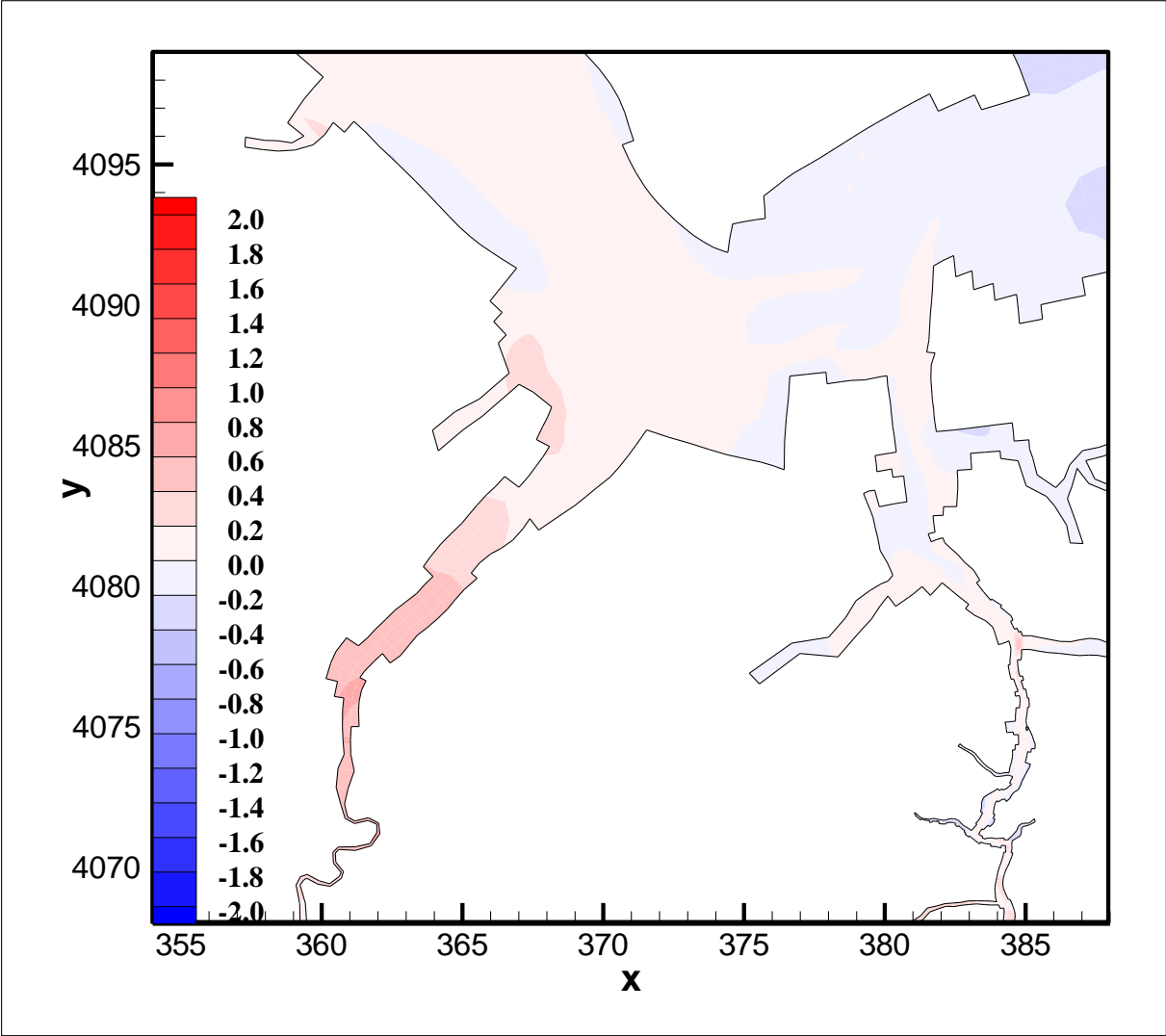


**Figure 5-3-4: Distribution of difference of freshwater age (days)
(Scenario 4-2 minus Baseline 2, mean difference)**

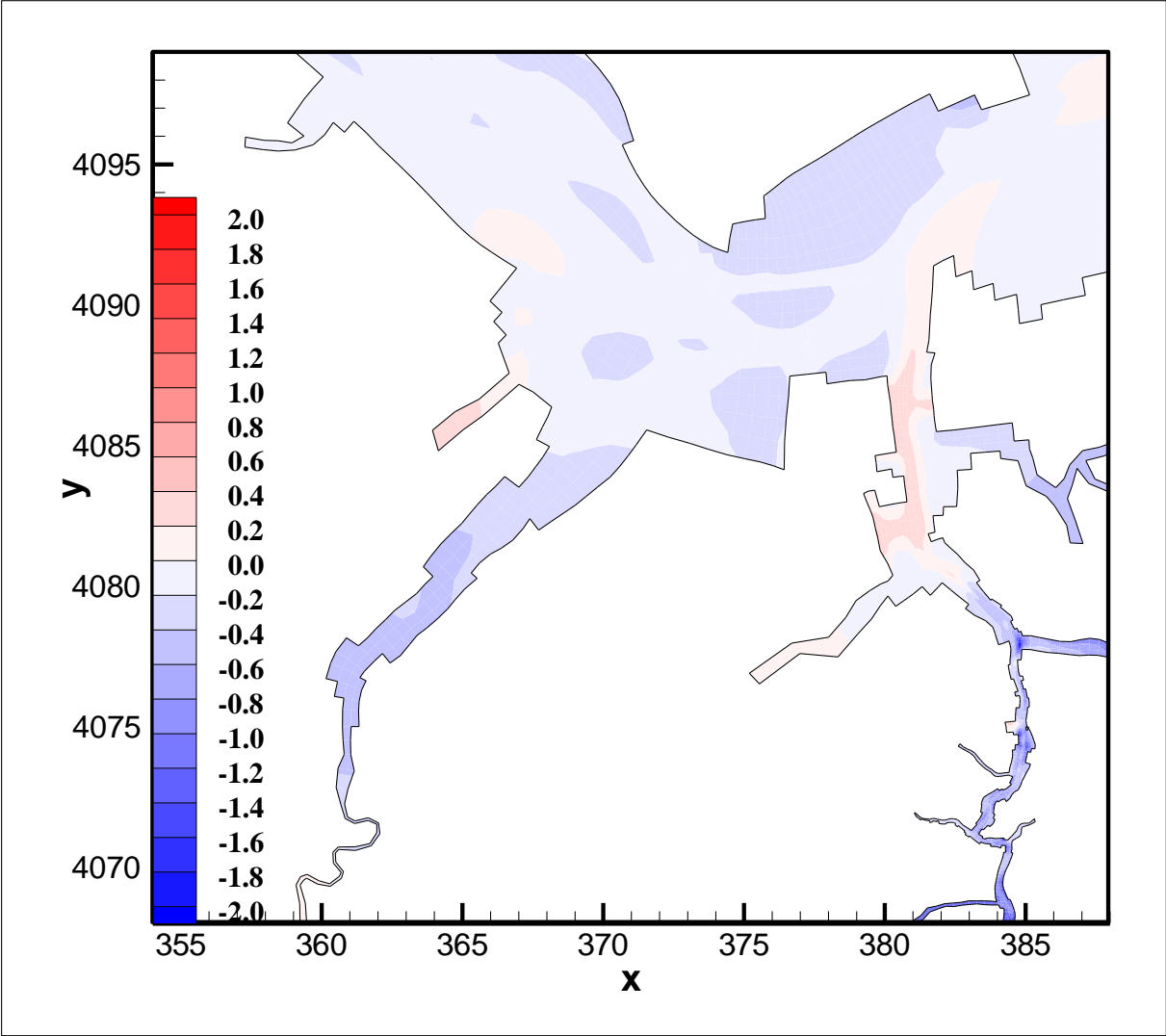


**Figure 5-3-5: Distribution of difference of saltwater age (days)
(Scenario 4-2 minus Baseline 2, mean difference)**

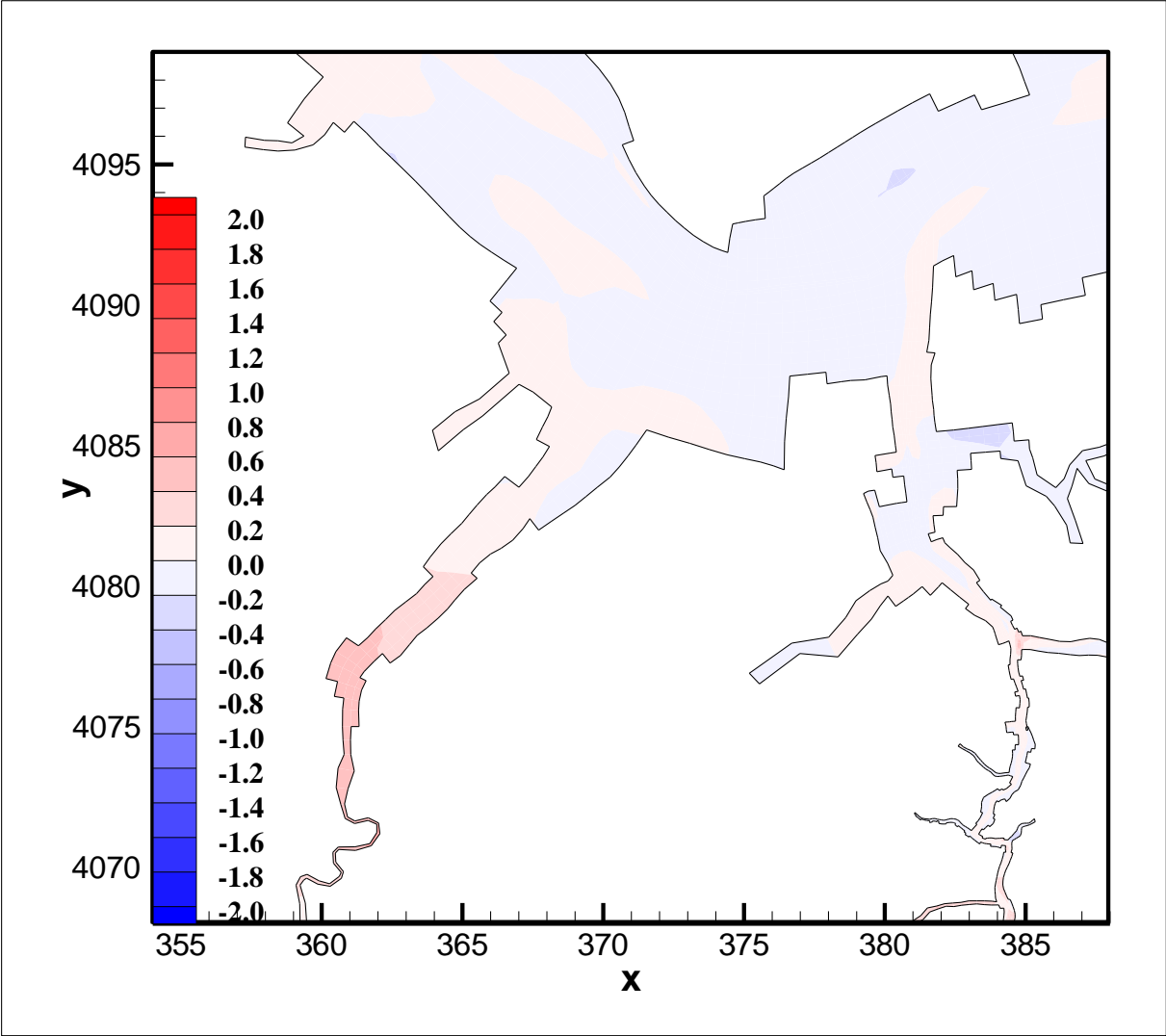


**Figure 5-3-6: Distribution of difference of renewal time (days)
(Scenario 4-2 minus Baseline 2, mean difference)**

5.4. Scenarios 5-1 and 5-2

Three timescales, namely freshwater age, saltwater age, and renewal time, are examined and their differences are compared. We compared the mean difference at each location for a period of three years. The spatial distributions between Scenario 5-1 and Baseline 1 (and between Scenario 5-2 and Baseline 2) are compared. Spatial plots for the mean and standard deviation for the difference of each timescale for Scenario 5-1 from Baseline 1 are shown in Figure 5-4-1 for freshwater age, in Figure 5-4-3 for saltwater age, and in Figure 5-4-5 for renewal time. Spatial plots for the mean for the difference of each timescale for Scenario 5-2 from Baseline 2 are shown in Figure 5-4-4 for freshwater age, in Figure 5-4-5 for saltwater age, and in Figure 5-4-6 for renewal time.

The freshwater age indicates the change of freshwater movement. It can be seen that the age decreases in the upper Elizabeth River and tributaries of the Elizabeth River slightly. The age in the lower James River does not change much.

The saltwater age indicates the change of saltwater movement. It can be seen that the age decreases in the lower James River and lower Elizabeth River slightly. Large changes occurred in the deep channel of the James River. This suggests that the stratification will likely increase in the lower James River.

The renewal time is the measure of the overall change of flushing time. The distribution of renewal time is similar to freshwater age, except renewal time decreases more in the mesohaline portion of the lower James. The renewal time decreases in the upper Elizabeth River and tributaries of the Elizabeth River slightly. Overall, not significant change of flushing is observed.

For Scenario 5-2, the distributions of the three timescales are very similar to those of Scenario 5-1. It can be seen that there is a slight decrease of saltwater age and freshwater age in the upper portion of Elizabeth River. The decrease of saltwater age is slightly more than freshwater age, which indicates an increase of stratification. There is a notable drop in bottom DO in spring and summer at SBE5 (e.g., at SBE5 there is 0.61 mg/L average decrease in summer bottom DO for Scenario 5-2. Although there is a decrease of bottom saltwater age, the effect of bottom water to renew DO will decrease if the downstream station has relatively low DO. The change of bottom DO at Station SEB5 is mainly caused by the decrease of reaeration of DO due to increased stratification.

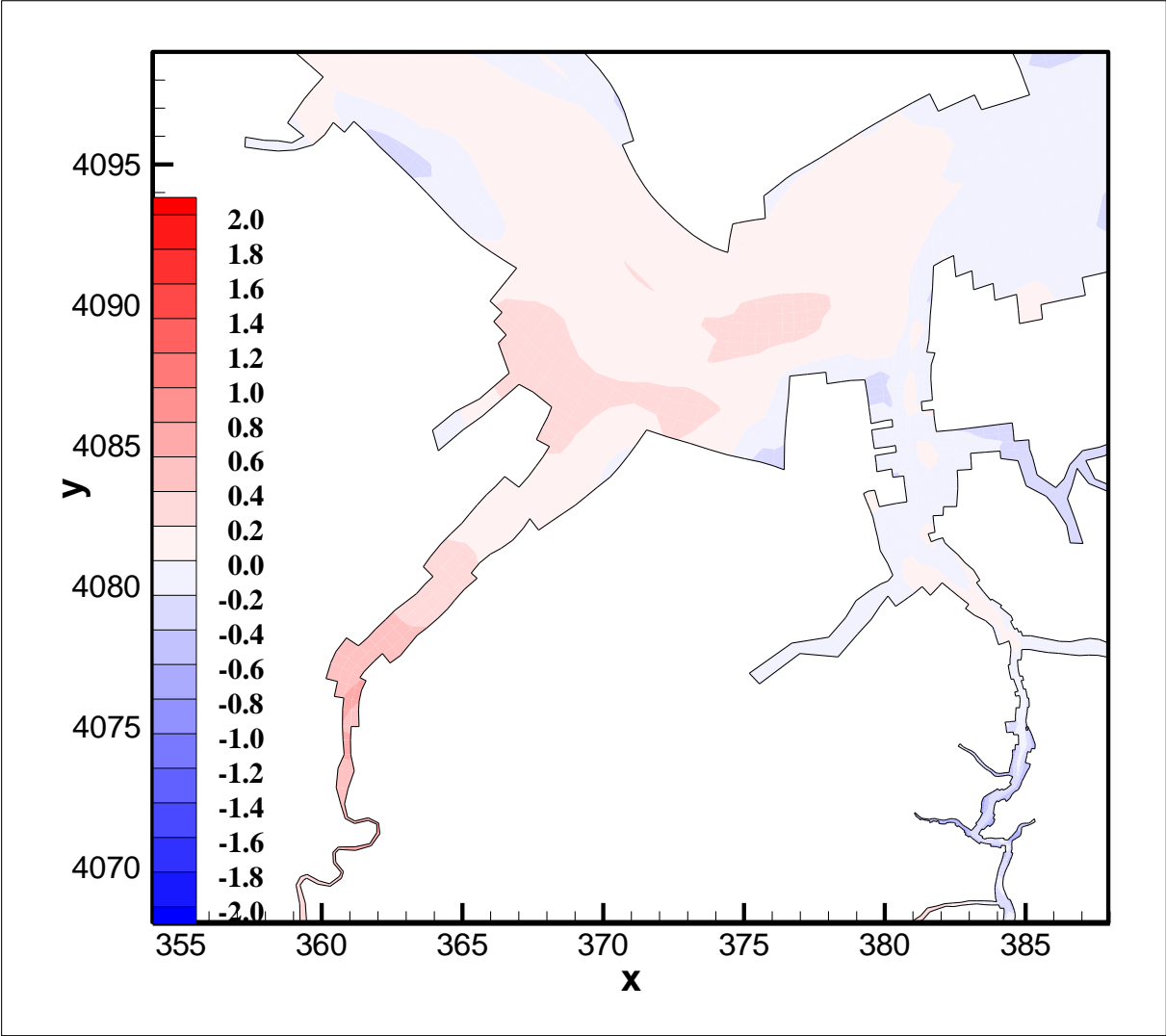


**Figure 5-4-1: Distribution of difference of freshwater age (days)
(Scenario 5-1 minus Baseline 1, mean difference)**

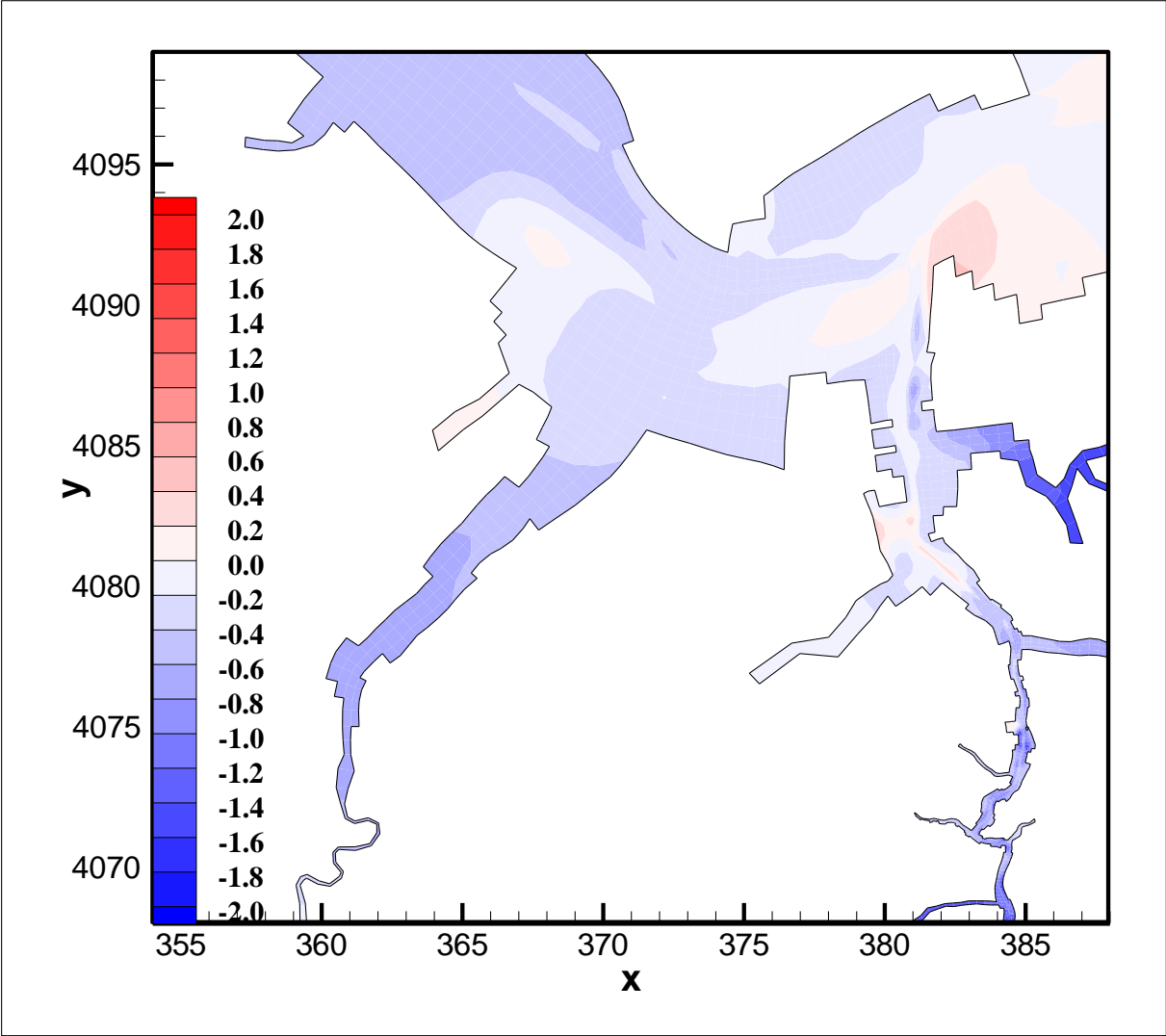


**Figure 5-4-2: Distribution of difference of saltwater age (days)
(Scenario 5-1 minus Baseline 1, mean difference)**

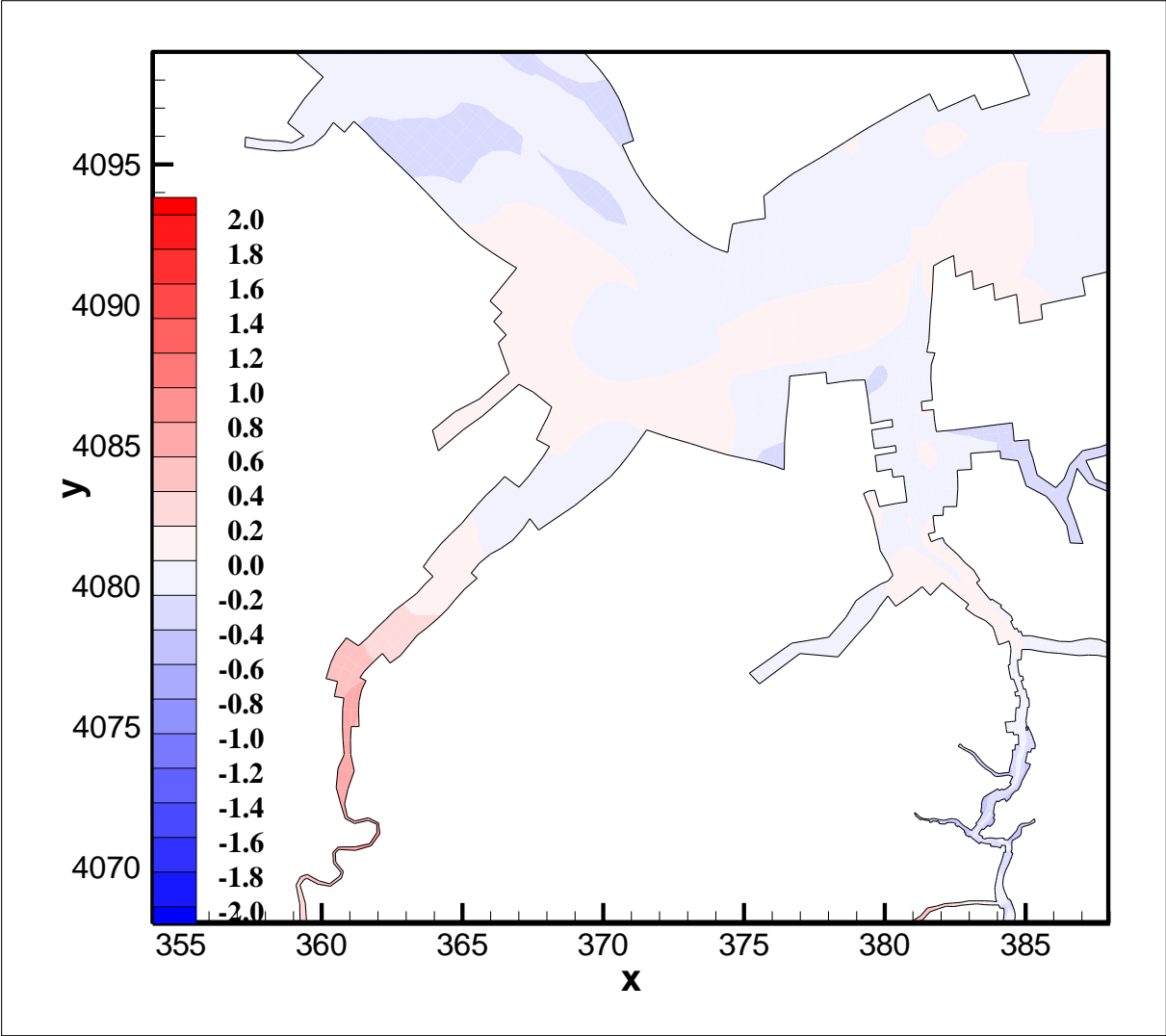


**Figure 5-4-3: Distribution of difference of renewal time (days)
(Scenario 5-1 minus Baseline 1, mean difference)**

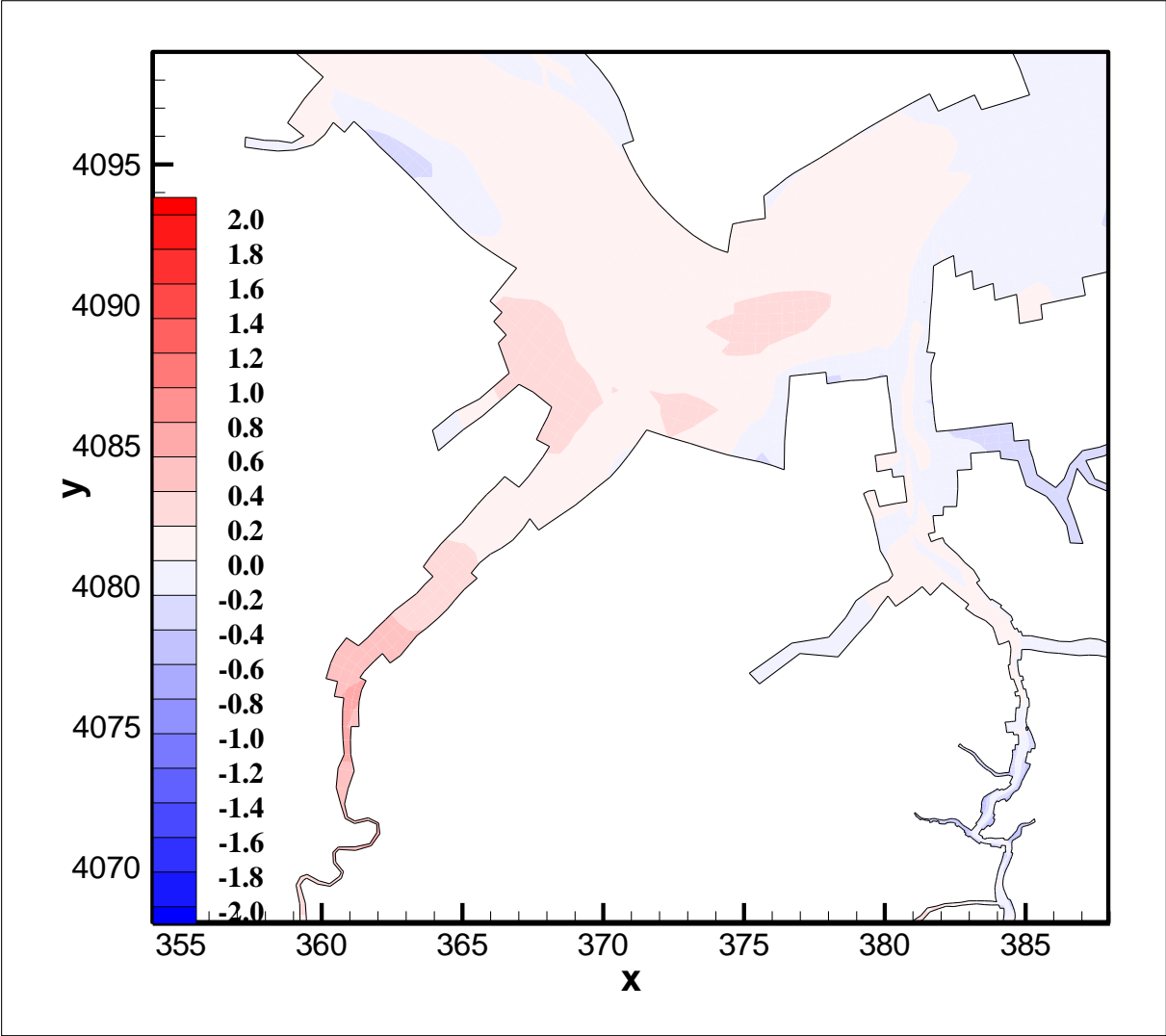


**Figure 5-4-4: Distribution of difference of freshwater age (days)
(Scenario 5-2 minus Baseline 2, mean difference)**

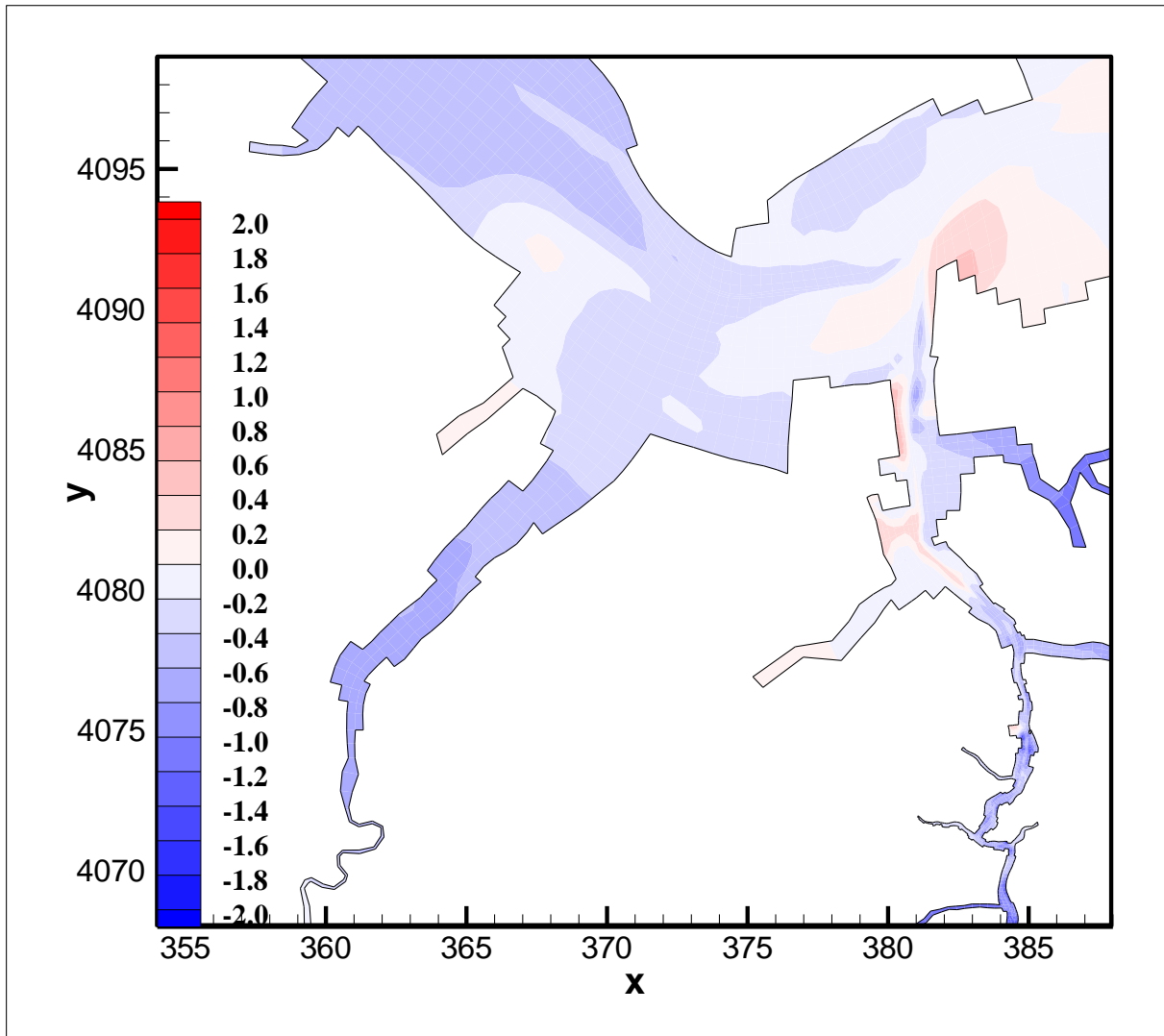


**Figure 5-4-5: Distribution of difference of saltwater age (days)
(Scenario 5-2 minus Baseline 2, mean difference)**

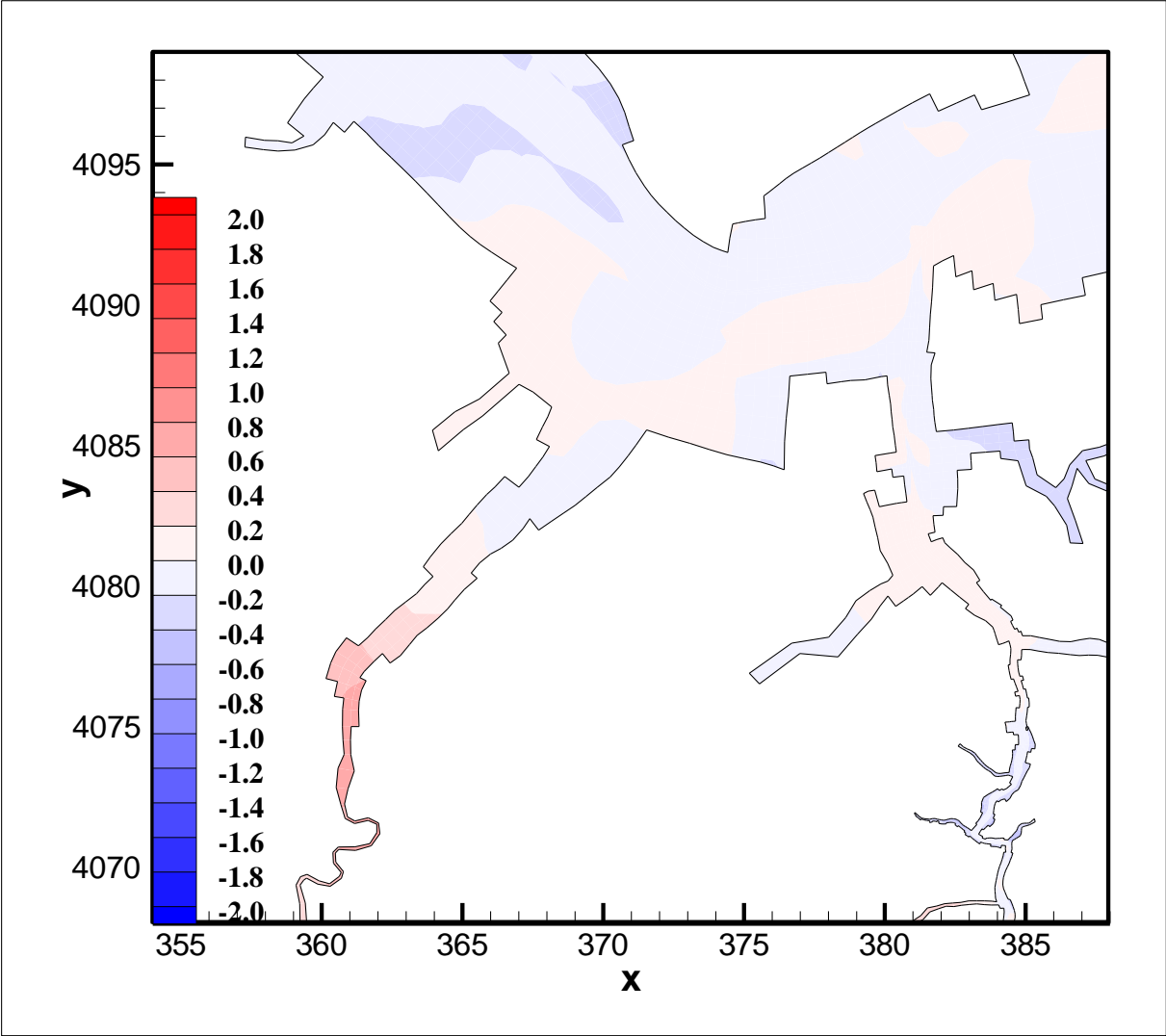


**Figure 5-4-6: Distribution of difference of renewal time (days)
(Scenario 5-2 minus Baseline 2, mean difference)**

6. Summary

The water quality model applied to the James and Elizabeth Rivers has been calibrated against observations. The model has been applied to simulate different scenarios for channel deepening. Five model scenarios have been conducted for multiple dredging design in the lower James River and Elizabeth River (Table 2-1). The results show that DO would not be changed much in the James River. DO decreases slightly in the Elizabeth River. The changes vary from scenario to scenario. The largest change of mean DO concentration is about 0.6 mg/L during the summer period for the Scenario 5-2 at Station SBE5. Note that Station SBE5 has low DO (<5 mg/L) under existing conditions. This station causes the greatest bottom DO depression of all the stations shown, thus, this area is the most problematic. With channel deepening in both James and Elizabeth Rivers, the renewal time is decreased slightly in the mesohaline region of the lower James River and tributaries in the Elizabeth River. There is no obvious change of transport time in general.

7. References

- Banks, R. B. and F. F. Herrera. 1977. Effects of wind and rain on surface reaeration. *J. Environ. Eng. Div., Amer. Soc. Civil Eng.*, 103, 489-504.
- Cerco, C.F. and T. Cole. 1994. Three-Dimensional Eutrophication Model of Chesapeake Bay. *Technical Report EL-94-4*, U.S. Army Engineer Waterways Experiment Station, Vicksburg, MS, 658.
- Cerco, C.F., Kim, S., and M.R. Nole. 2010. The 2010 Chesapeake Bay eutrophication model, a report to the US Environmental Protection Agency Chesapeake Bay Program and to the US Army Engineer Baltimore District. US Army Engineer Research and Development Center, Vicksburg, MS.
- Deleersnijder, E., J. M. Campin, and E. J. M. Delhez. 2001, The concept of age in marine modeling, I. Theory and preliminary model results, *J. Mar. Syst.*, 28, 229–267, doi: 10.1016/S0924-7963(01)00026-4.
- Delhez, E. J. M., J. M. Campin, A. C. Hirst, and E. Deleersnijder. 1999. Toward a general theory of the age in ocean modeling. *Ocean Modelling*, 1: 17-27.
- DiToro, D. M. and J. J. Fitzpatrick. 1993. *Chesapeake Bay sediment flux model*, Contract Report EL-93-2, U. S. Army Engineer Waterways Experiment Station, Vicksburg, MS.
- Galperin, B., L. H. Kantha, S. Hassid, and A. Rosati. 1988. A quasi-equilibrium turbulent energy model for geophysical flows. *J. Atmos. Sci.*, 45, 55-62.
- Genet, L., Smith, D., and M. Sonnen. 1974. Computer program documentation for the dynamic estuary model. U.S. Environmental Protection Agency, Systems Development Branch, Washington, DC.

- Haider, S. 2015. The Third Set of Locks Project.
http://www.americanthinker.com/blog/2015/the_third_set_of_locks_project.html
- Hamrick, J.M. 1992. A Three-Dimensional Environmental Fluid Dynamics Code: Theoretical and Computational Aspects VIMS SRAMSOE # 317, 63 pp.
- Hamrick, J.M. and T.S. Wu, 1997. Computational design and optimization of the EFDC/HEM3D surface water hydrodynamic and eutrophication models. In: Delich, G., Wheeler, M.F., (Eds.),
- Hong, B. and J. Shen, 2013. Linking dynamics of transport timescale and variations of hypoxia in the Chesapeake Bay. *J. Geophys. Res.*, 118, 1-13
- Ison, J. 2015. Panama Canal expansion shipping jobs to Ohio.
<http://www.bucyrustelegraphforum.com/story/news/local/indepth/2015/02/14/panama-canal-expansion-shipping-jobs-to-Ohio.html>
- Keisman, J. and G. Shenk, 2013. Total Maximum Daily Load Criteria Assessment Using Monitoring and Modeling Data. *Journal of the American Water Resources Association (JAWRA)* 1-16. DOI: 10.1111/jawr.12111
- Kuo, A.Y. and B. J. Neilson. 1987. Hypoxia and salinity in Virginia estuaries. *Estuaries* 10, 277-283.
- Liu, H., He, Q., Wang, Y., Chen, J., 2012. Process of suspended sediment mixture in the Yangtze River Estuary. *Acta Geographica Sinica* 67(9), 1269-1281 (In Chinese with English Abstract).
- Mellor, G. L. and T. Yamada. 1982. Development of a turbulence closure model for geophysical fluid problems. *Rev. Geophys. Space Phys.*, 20, 851-875.
- Morse, R. E., J. Shen, J. L. Blanco-Garcia, W. S. Hunley, S. Fentress, M. Wiggins, and M. R. Mulholland. 2011. Environmental and physical controls on the formation and transport of blooms of the dinoflagellate *Cochlodinium polykrikoides* Margalef in lower Chesapeake Bay and its tributaries. *Estuaries and Coasts*, doi:10.1007/s12237-011-9398-2.
- Nixon, S. W., J. W. Ammerman, L. P. Atkinson, V. M. Berounsky, G. Billen, W. C. Boicourt, W. R. Boynton, T.M. Church, D. M. Ditoro, R. Elmgren, J. H. Garber, A. E. Giblin, R. A. Jahnke, N. J. P. Owens, M. E. Q. Pilson, and S. P. Seitzinger. 1996. The fate of nitrogen and phosphorus at the land-sea margin of the North Atlantic Ocean, *Biogeochemistry*, 35(1), 141–180, doi:10.1007/BF02179826
- O'Connor, D.J. and W.E. Dobbins. 1958. Mechanisms of reaeration in natural streams. *Trans. Am. Soc. Civ. Eng.*, 123, 641-684.
- Park, K., A. Y. Kuo, J. Shen, and J. M. Hamrick. 1995. A three-dimensional hydrodynamic eutrophication model (HEM-3D): description of water quality and sediment process submodels. Special Report in Applied Marine Science and Ocean Engineering. No. 327. Virginia Institute of Marine Science, Gloucester Point, VA 23062, 102 pp.

- Shen, J., Boon, J., and A. Y. Kuo. 1999. A numerical study of a tidal intrusion front and its impact on larval dispersion in the James River estuary, Virginia, *Estuary*, 22(3), 681-692.
- Shen, J. and L. Haas. 2004. Calculating age and residence time in the tidal York River using three-dimensional model experiments. *Estuarine, Coastal and Shelf Science* 61(3), 449-461.
- Shen, J. and J. Lin. 2006. Modeling Study of the Influences of tide and stratification on age of water in the tidal James River. *Estuarine, Coastal and Shelf Science*, 68 (1-2): 101-112.
- Shen, J., and H. V. Wang. 2007. Determining the age of water and long-term transport timescale of the Chesapeake Bay, *Estuar. Coast. Shelf Sci.*, 74(4), 750–763, doi:10.1016/j.ecss.2007.05.017.
- Shen, J., B. Hong, and A. Kuo. 2013. Using timescales to interpret dissolved oxygen distributions in the bottom waters of Chesapeake Bay. *Limnology and Oceanography*, 58(6), 2237-2248 (doi:10.4319/lo.2013.58.6.2237)
- Shen, J., Wang, Y., Sisson, M. 2016. Development of the hydrodynamic model for long-term Simulation of water quality processes of the tidal James River, Virginia. *Journal of Marine Science and Engineering*.
- Taylor, K. E. 2001. Summarizing multiple aspects of model performance in a single diagram, *J. Geophys. Res.*, 106(D7), 7183–7192.
- Wezernak, C. T. and J.J. Gannon. 1968. Evaluation of nitrification in streams. *Journal of the Sanitary Engineering Division, ASCE*, 94(SA5): 883-895.
- Zhang, J., H. Wang, F. Ye, and Z. Wang. 2017. Assessment of Hydrodynamic and Water Quality Impacts for Channel Deepening in the Thimble Shoals, Norfolk Harbor, and Elizabeth River Channels. Project report submitted to Moffatt and Nichol and U.S Army Corps of Engineers, Fort Norfolk Office. Special Report in Applied Marine Science and Ocean Engineering No. 455. Virginia Institute of Marine Science, Gloucester Point, VA. 55 pp., doi:10.21220/V5MF0F

VDOT 3rd Crossing Hydrodynamic Modeling Study Progress Report

Project Title: Evaluation of potential impact of the Third Crossing on flow and transport characteristics in the lower James River

Institution: Virginia Institute of Marine Science

PI: Joseph Zhang

Date: April 4, 2016

Status

During the period, the VIMS team has made steady progress in assessing the impact of proposed James River crossings. As of this writing, we have constructed multiple grids for Alternatives A-D, and calibrated the 'Base' (existing condition) against observation. We have adjusted the domain extent a few times in order to optimize the computational cost, and at the moment we are able to restore the original domain that comprises the entire Chesapeake Bay and part of the continental shelf. We have just obtained preliminary results for the 4 Alternatives and are in the process of analyzing the results.

Some preliminary findings are summarized below.

1. Base scenario:
 - a. At the beginning of the project, substantial amount of effort was devoted to sensitivity studies to the grid resolution, choices of boundary conditions, in order to understand the model behavior under very high grid resolution.
 - b. After finishing the calibration on a reduced-domain grid (for the sake of efficiency), we are now able to restore the original domain extent that includes the entire Chesapeake Bay. The boundary conditions at the shelf boundary are provided by a larger-domain SCHISM simulation database and the computational time is optimal for finishing 18 months simulation for each of the scenario run. We have re-calibrated the 3D hydrodynamic variables for elevation, velocity, salinity and temperature against NOAA and EPA observations in the lower Chesapeake Bay with promising results.
2. Alternative A: this scenario calls for expansion of the existing I-64 bridge crossing across James River. The grid uses locally high resolution to resolve the added bridge pilings. We have finished 10 months of simulation and the preliminary results suggest small increase of averaged surface and bottom salinity on the order of ~ 0.3 PSU in the vicinity of the added pilings, due to the decreased flushing there. The salt intrusion along the main channels of James and Elizabeth Rivers is not significantly affected though;
3. Alternative B: this scenario adds a new crossing across the Elizabeth River on top of Alternative A. The changes associated with Alternative A in the James River remain, and in addition there is a modest increase in surface salinity near the Craney Island, likely due to increased turbulence mixing there. The intrusion along the main channels of James and Elizabeth Rivers is not significantly affected;

4. Alternative C: this scenario expands the I-664 bridge and adds a new Elizabeth River crossing (as in Alternative B). The impact on bathymetry is larger and more wide-spread especially in the shallows. As a result, the increase in the turbulence mixing and retention time seems to have led to larger increase in the surface salinity (up to 1PSU) near the project sites. On the other hand, the increase in the bottom salinity is less as the bottom salt intrusion is more channelized;
5. Alternative D: this scenario combines all of the alterations in the other 3 Alternatives, and therefore the changes in the surface and bottom salinity also resemble the combination of those from the other 3 Alternatives, i.e., there are increases in the salinity near the added I-64, I-664, and Elizabeth River pilings, with the bottom salinity being less affected;

All alternatives are found to increase the surface and bottom salinity but at a different rate. In particular, the increase in the surface salinity is on the order of 0.3 PSU with bottom salinity less affected, resulting in less vertical stratification. This is consistent with the fact that the added new bridge pilings partially block the surface flow from upstream and enhance local turbulence mixing.

Future plan:

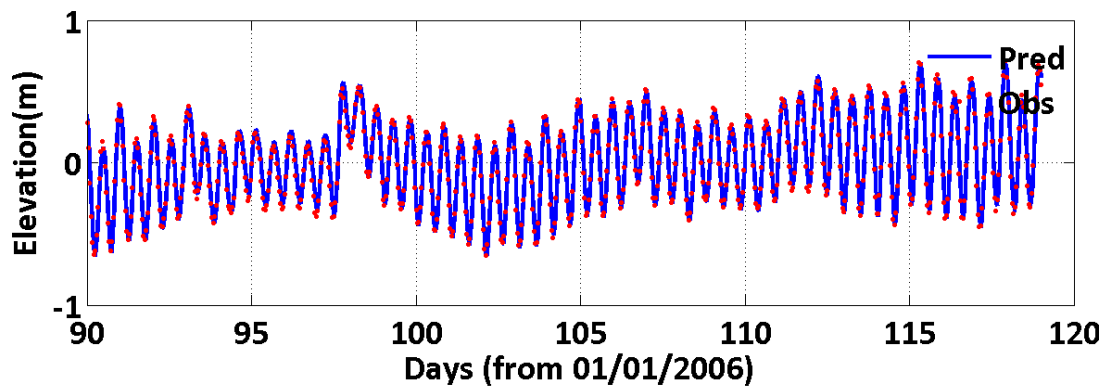
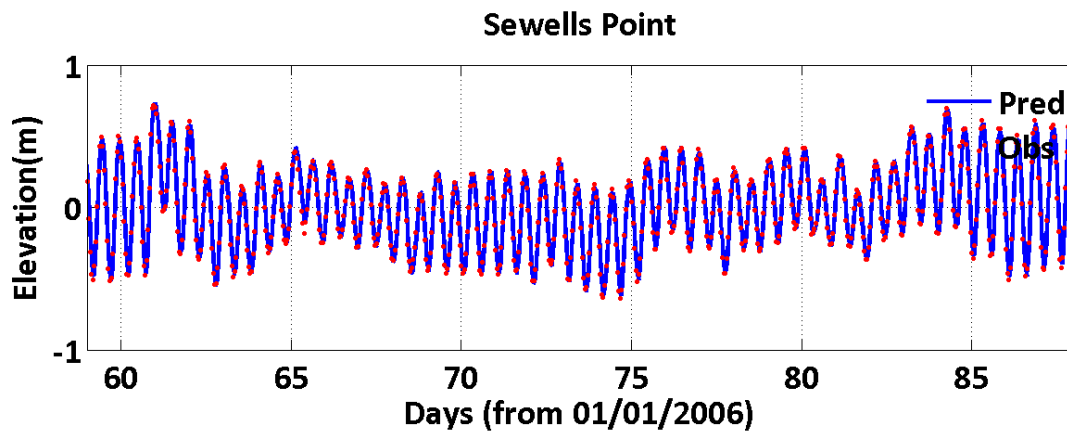
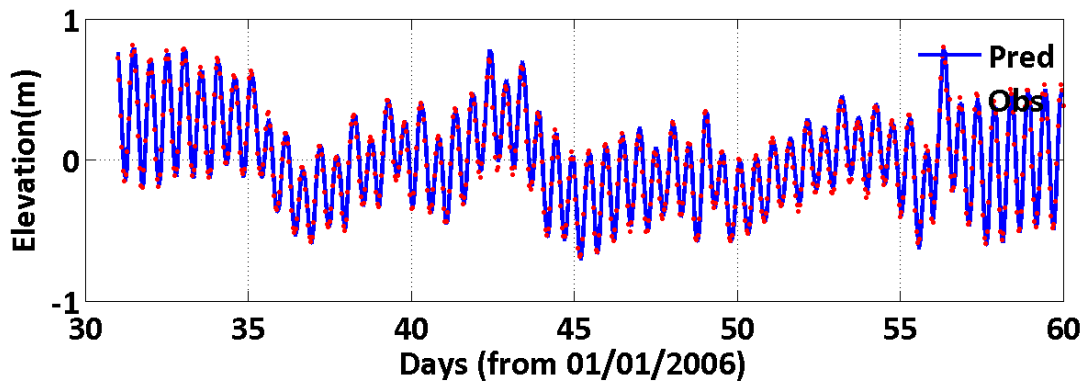
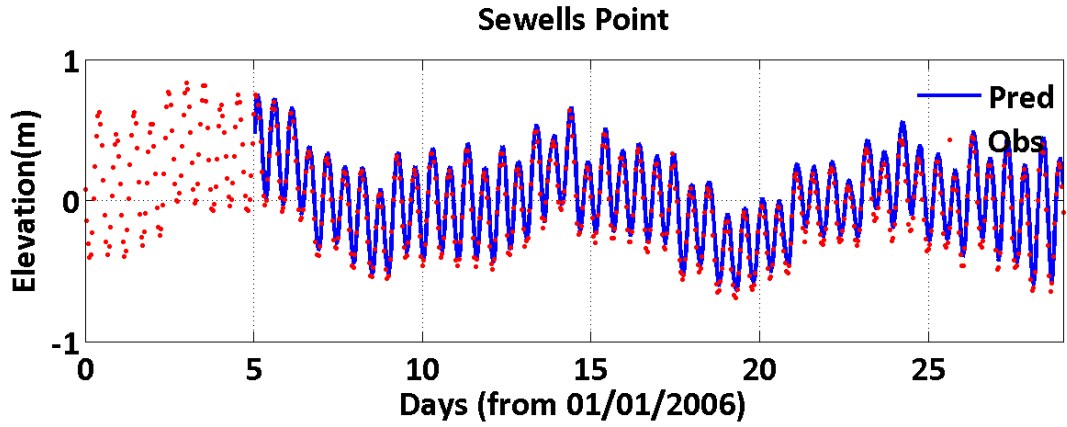
In the following 4 months we will complete the 18-month simulations for all alternatives and conduct more detailed analysis for the potential impact on flushing time and sediment erosion potential.

1. Appendix B

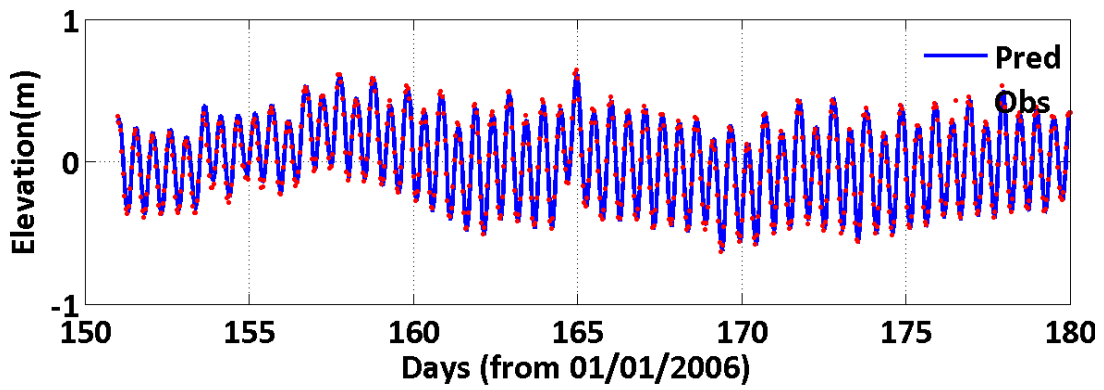
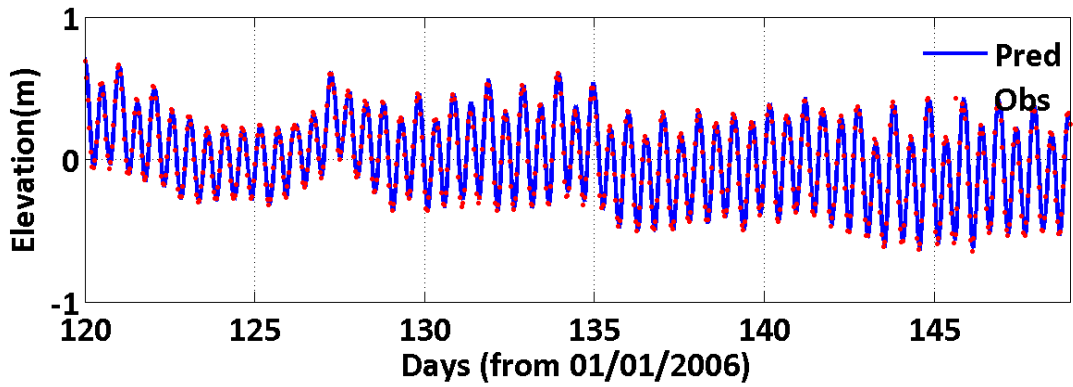
Surface elevations

The model calibration of surface elevation was conducted from 2006-2008. Only the Sewells Point location uses a NOAA tidal gauge station. Five other stations are shallow water monitoring stations, which have depth variational data. The mean sea-level was removed from measurements at each station to compare tidal fluctuation. Data were not collected every day at the shallow water stations. The locations for measurement of observations are shown in Figure 2-1. Time series comparisons between model predictions and observations are shown in subsequent plots. Blue lines in the figures represent model results and red dots represent observations.

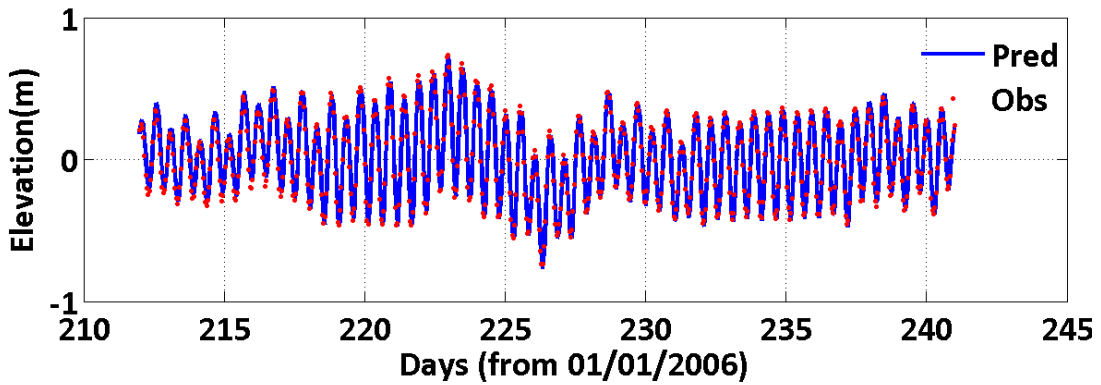
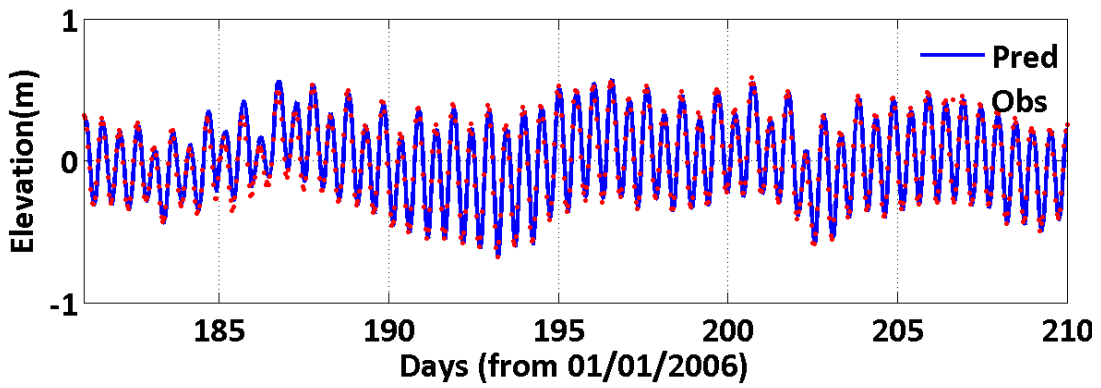
<u>Station</u>	<u>Pages</u>
Sewells Point	B2-B10
JMS002.55	B11-B19
JMS018.23	B20-B28
APP001.83	B29-B37
JMS073.37	B38-B46
JMS043.78	B47-B55



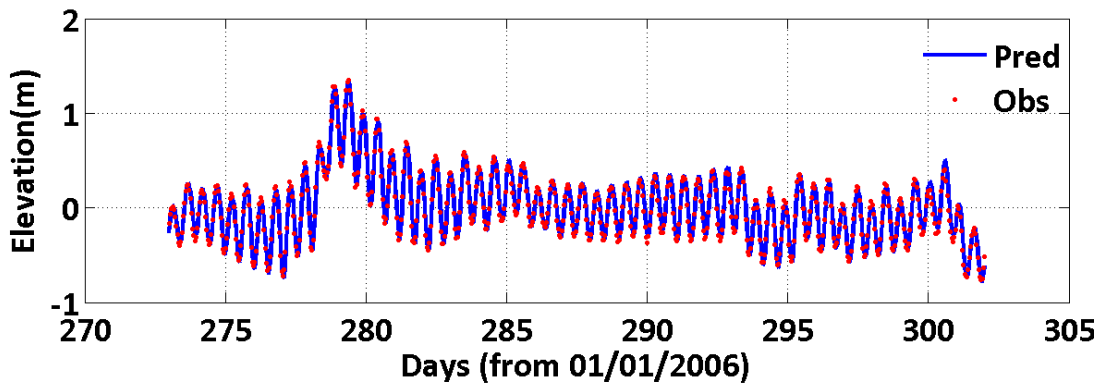
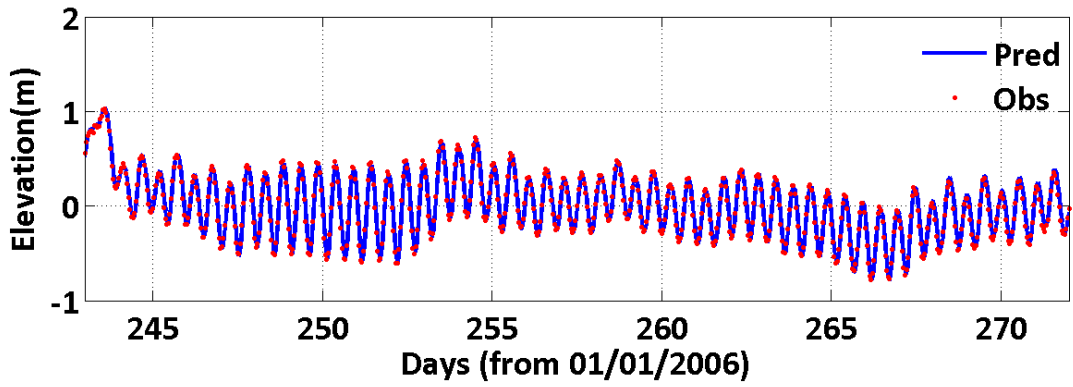
Sewells Point



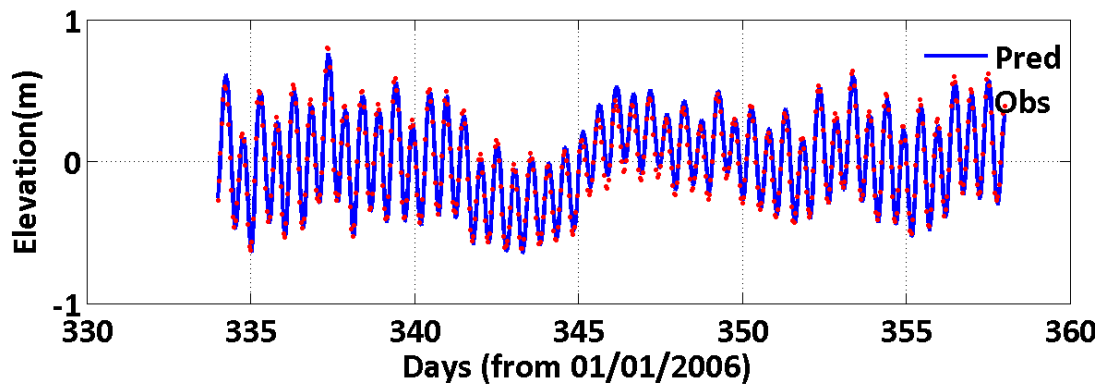
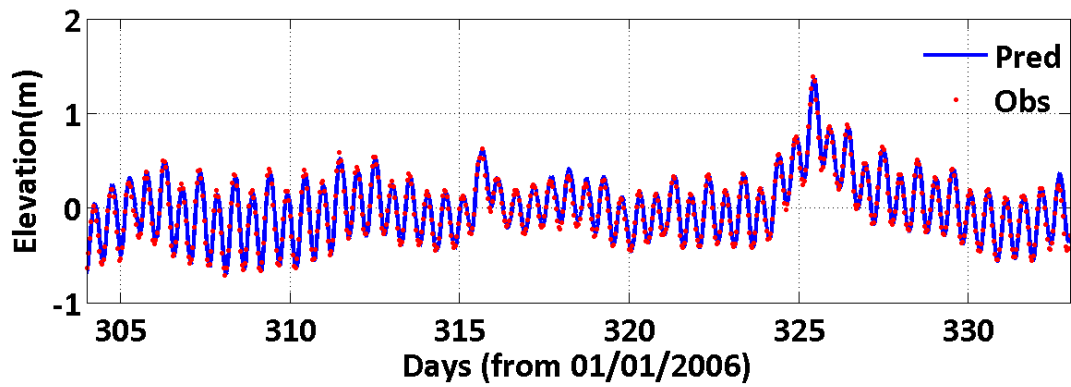
Sewells Point



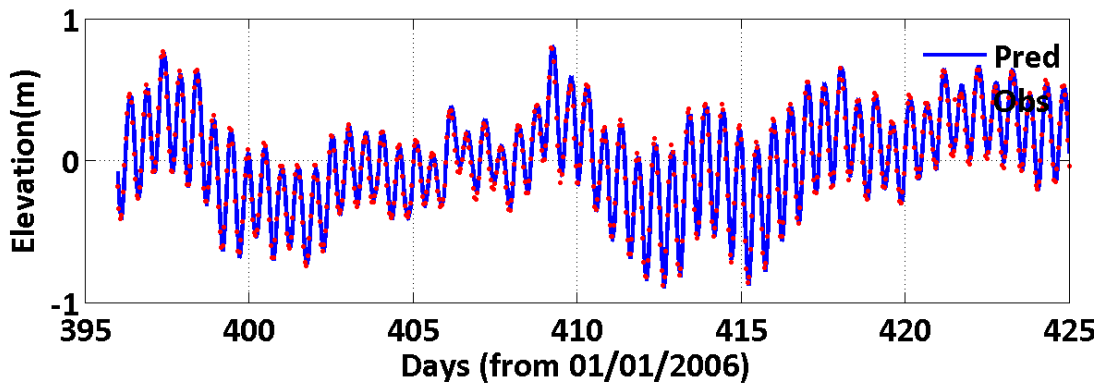
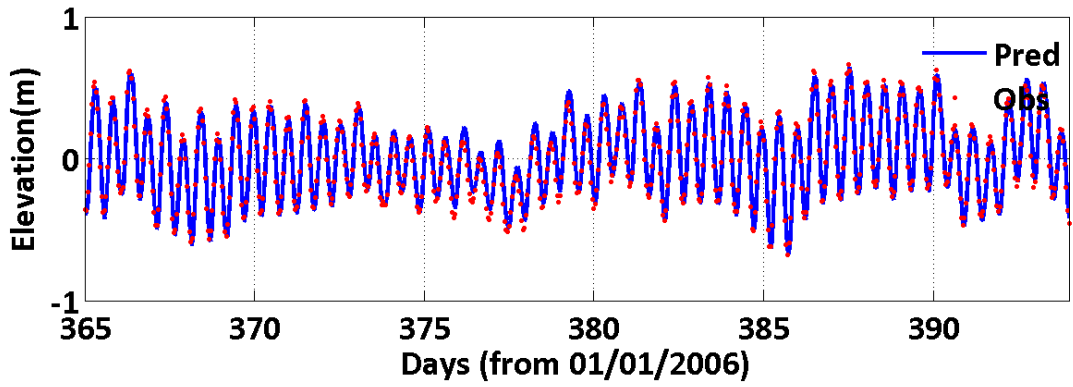
Sewells Point



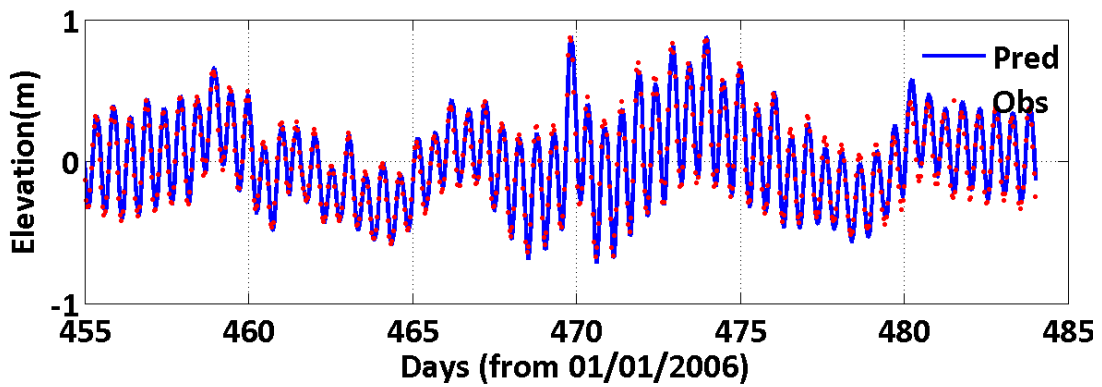
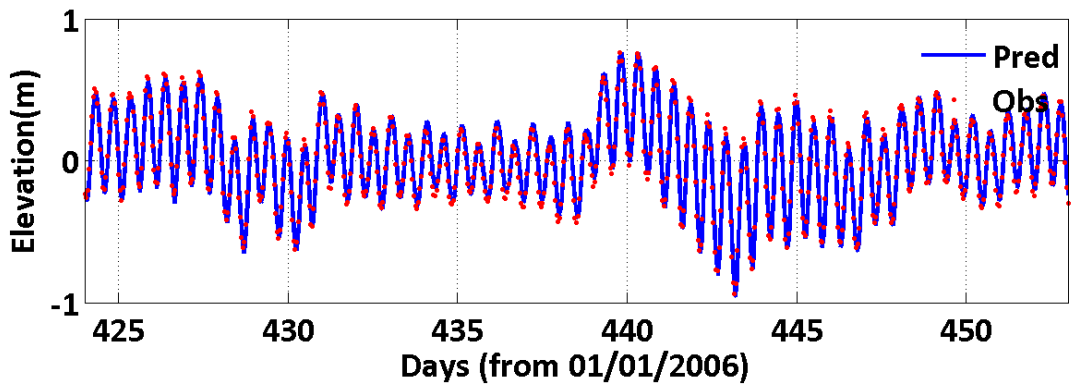
Sewells Point

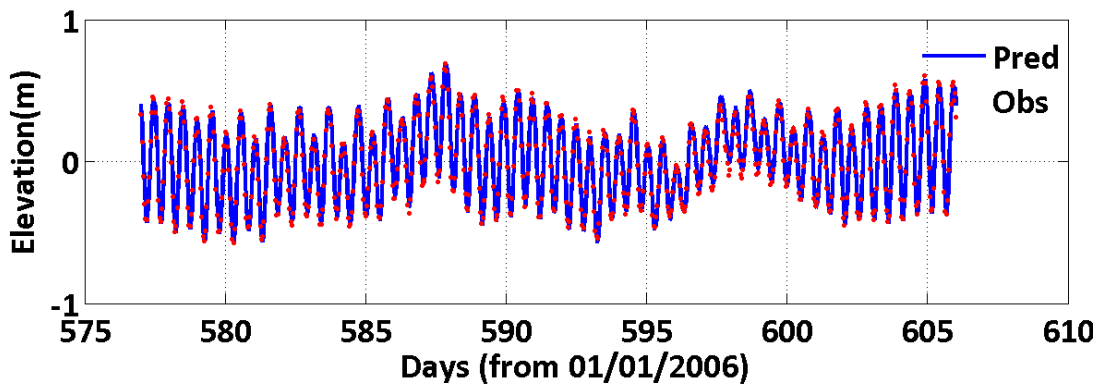
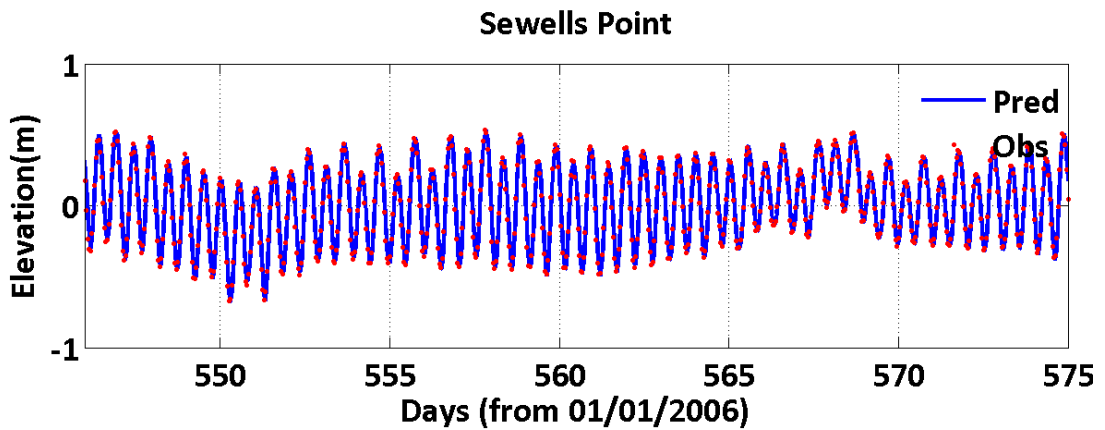
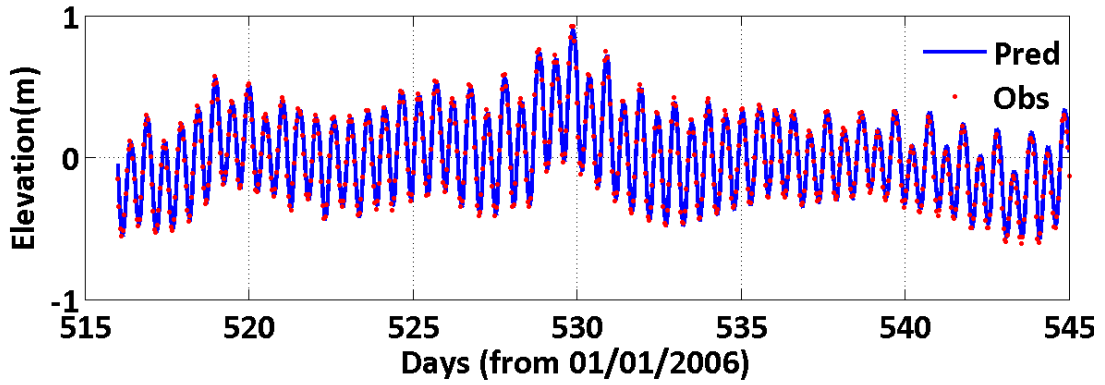
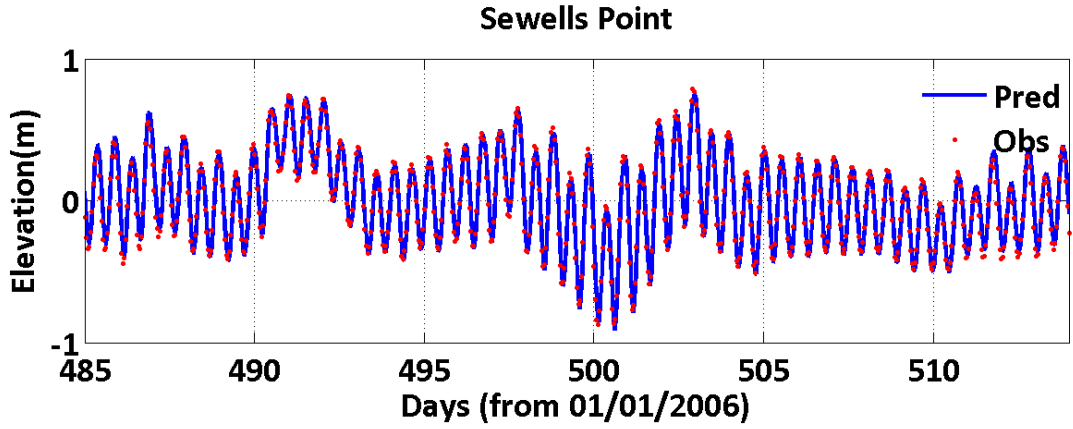


Sewells Point

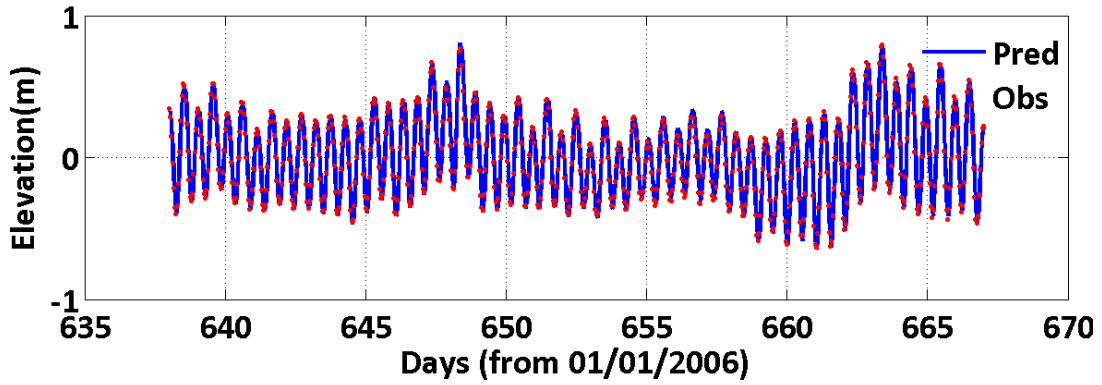
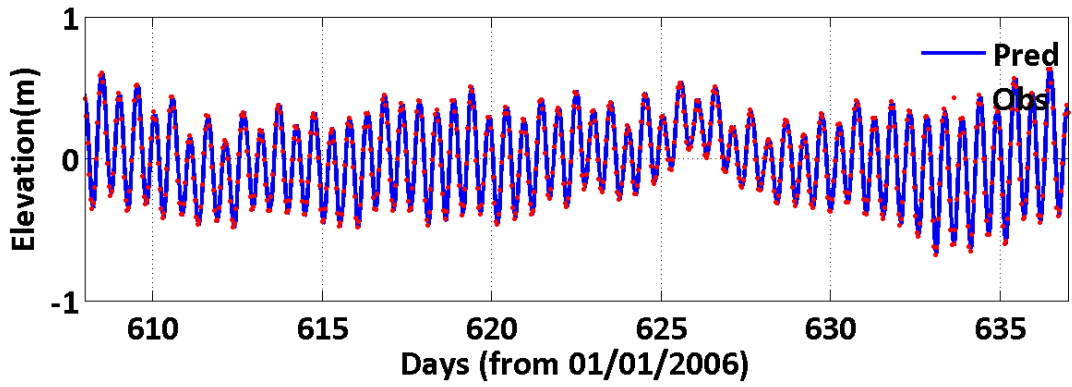


Sewells Point

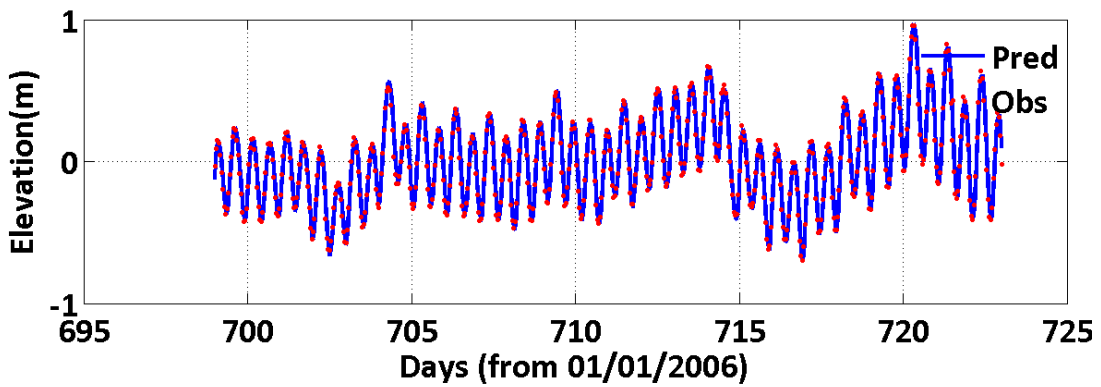
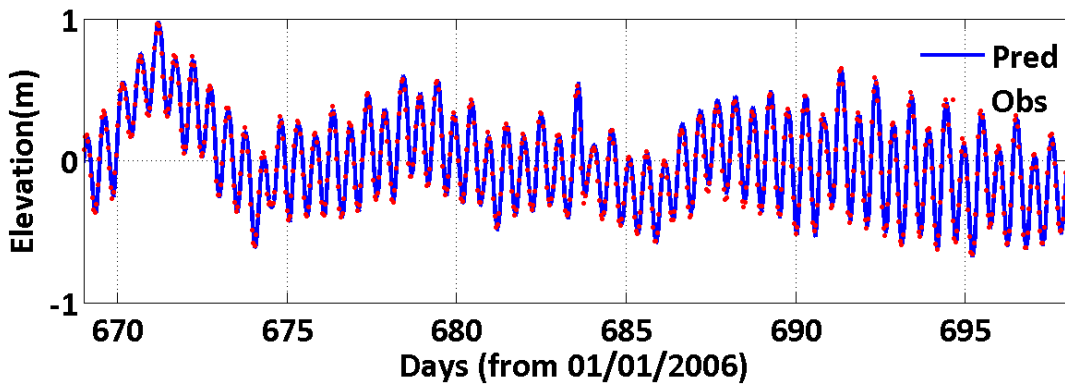




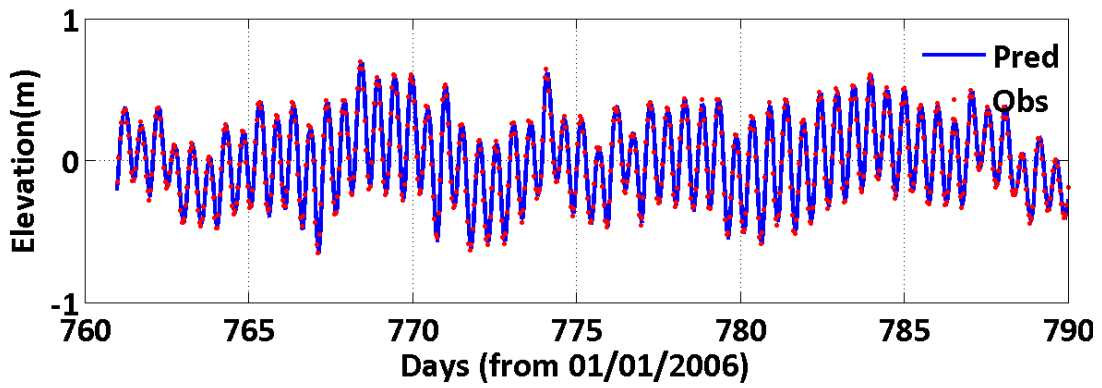
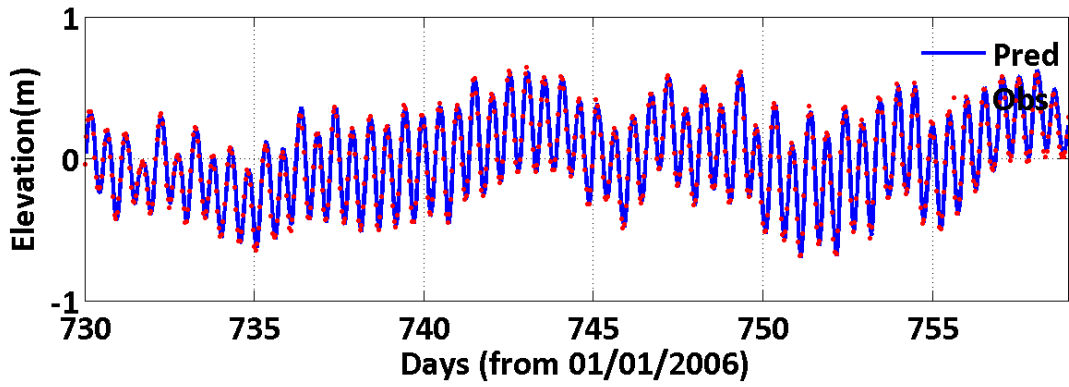
Sewells Point



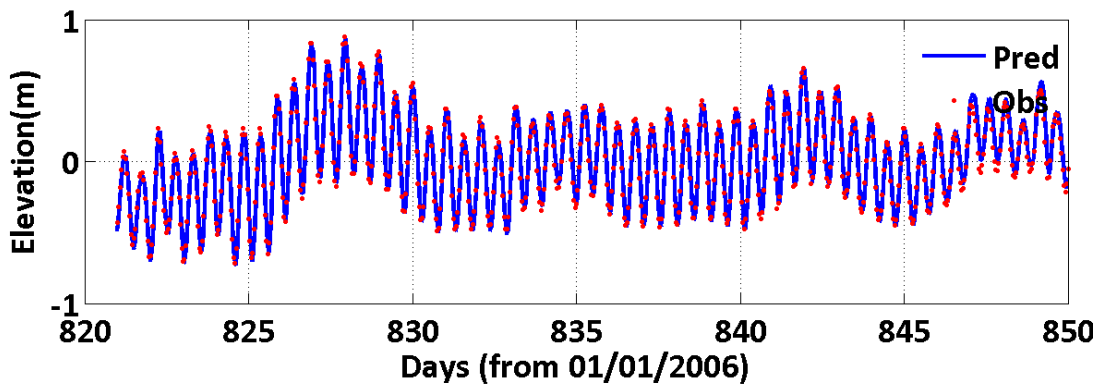
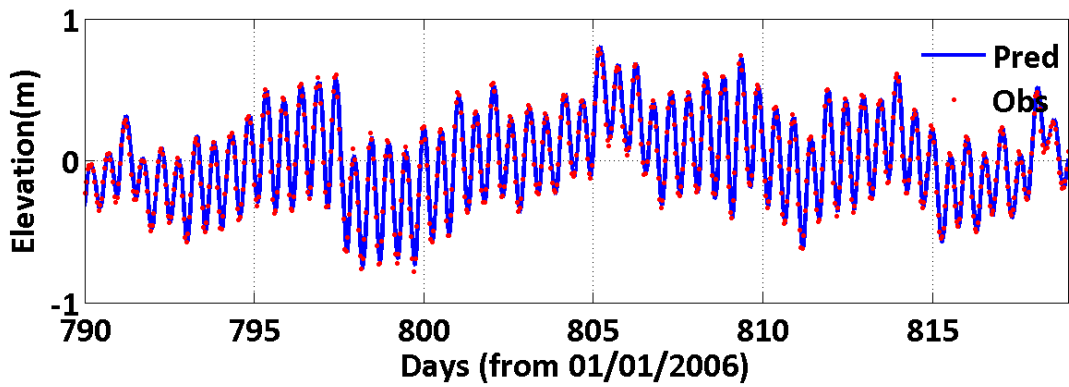
Sewells Point

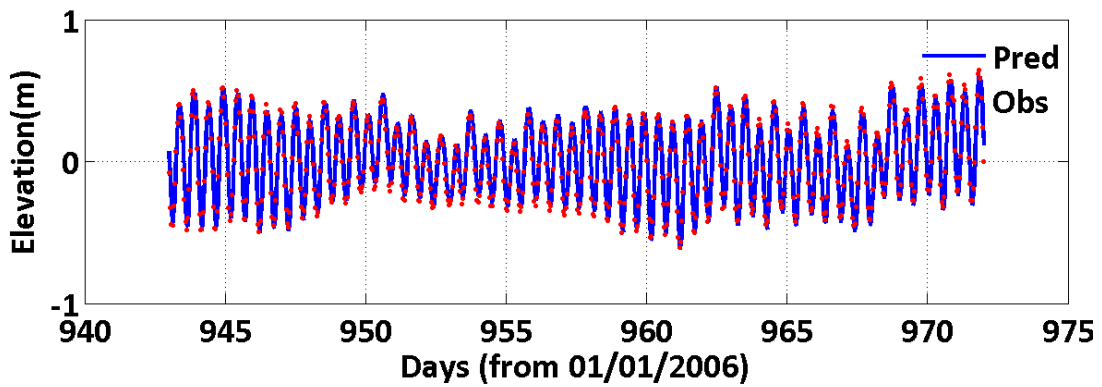
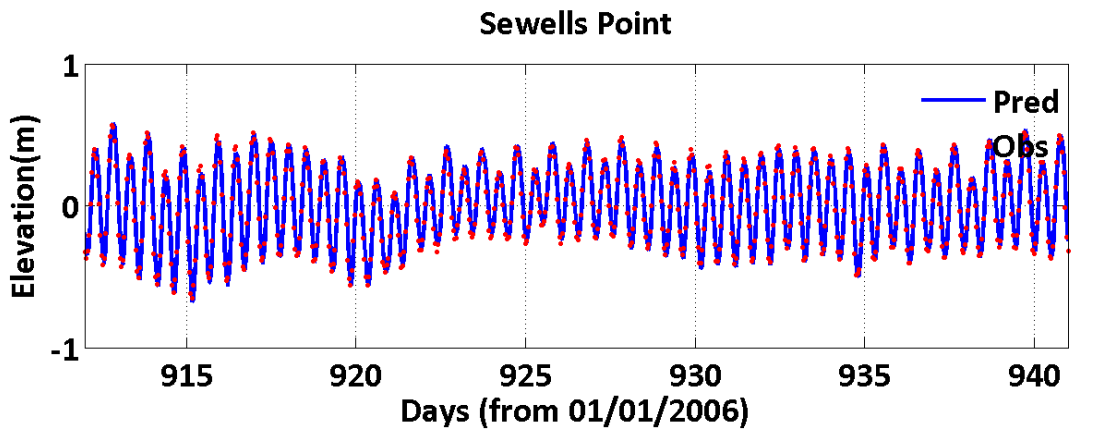
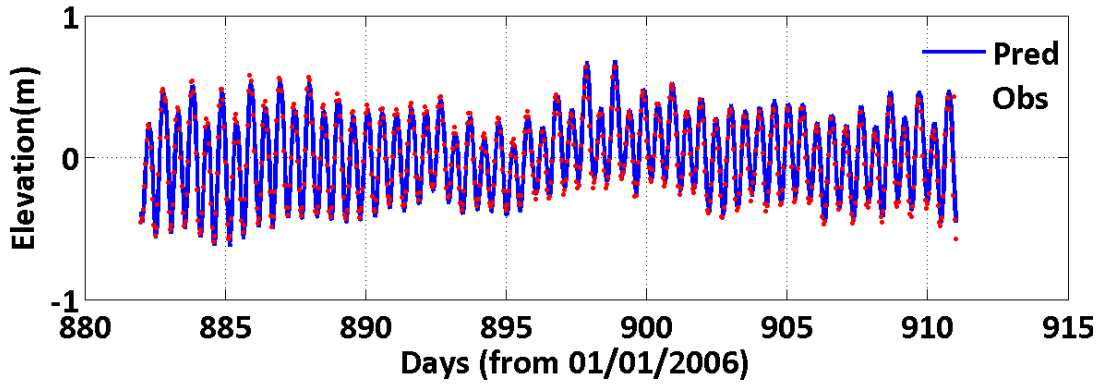
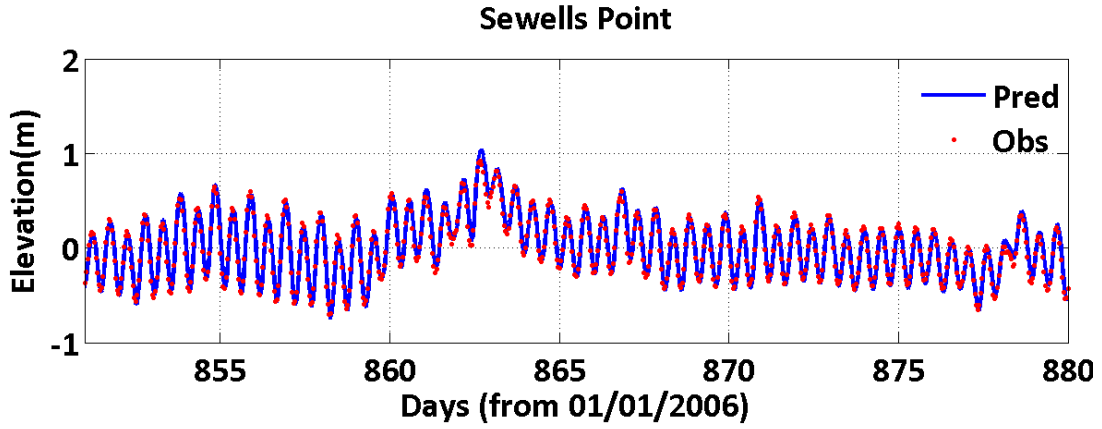


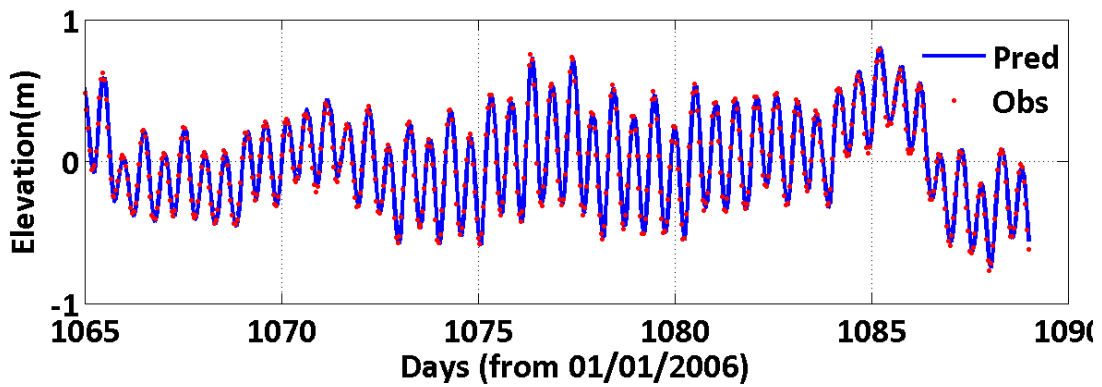
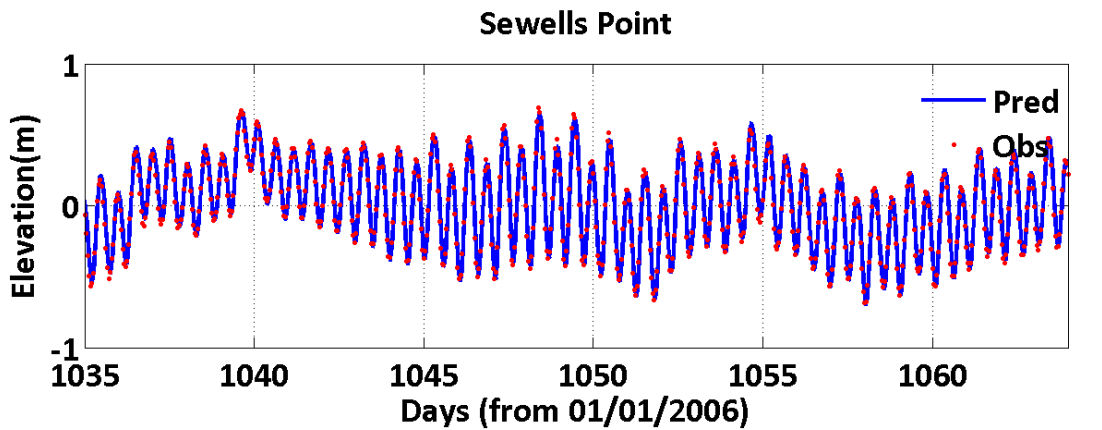
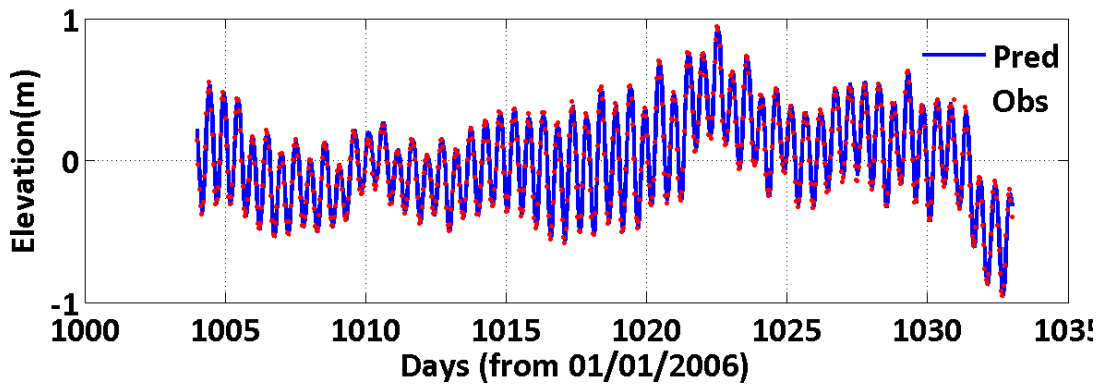
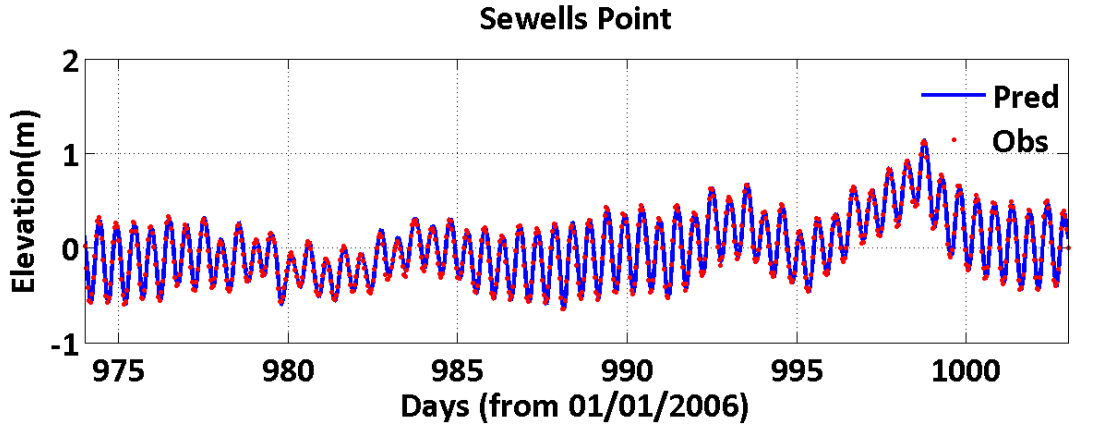
Sewells Point



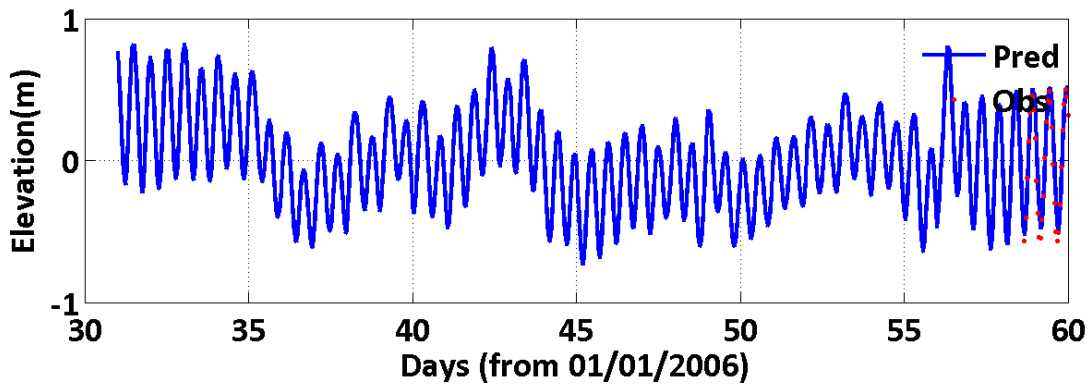
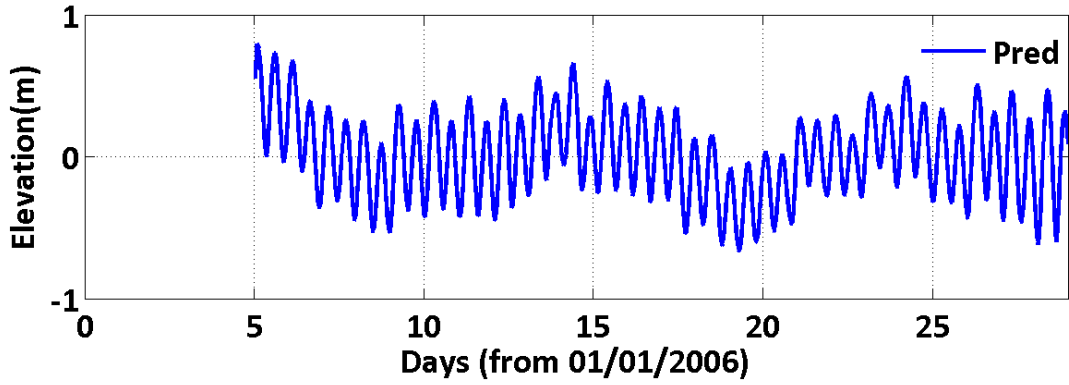
Sewells Point



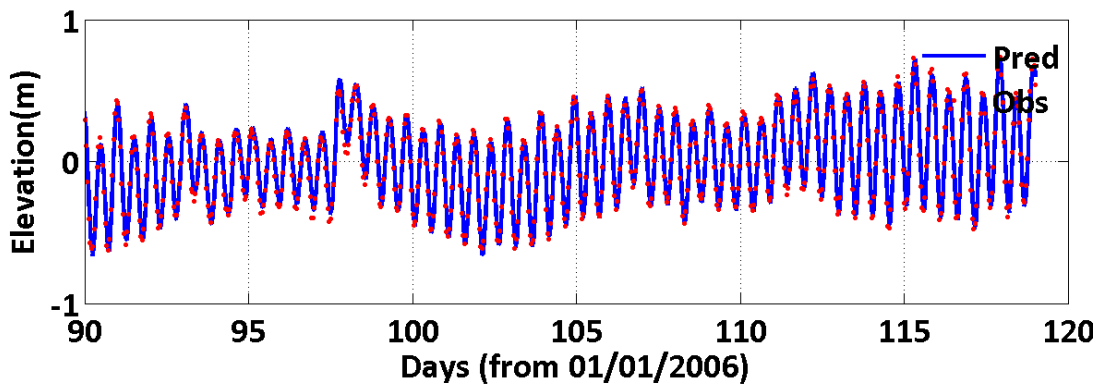
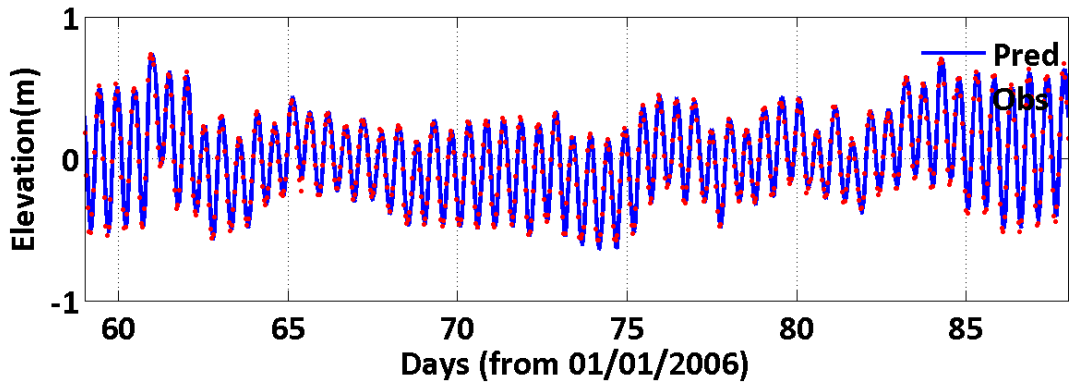




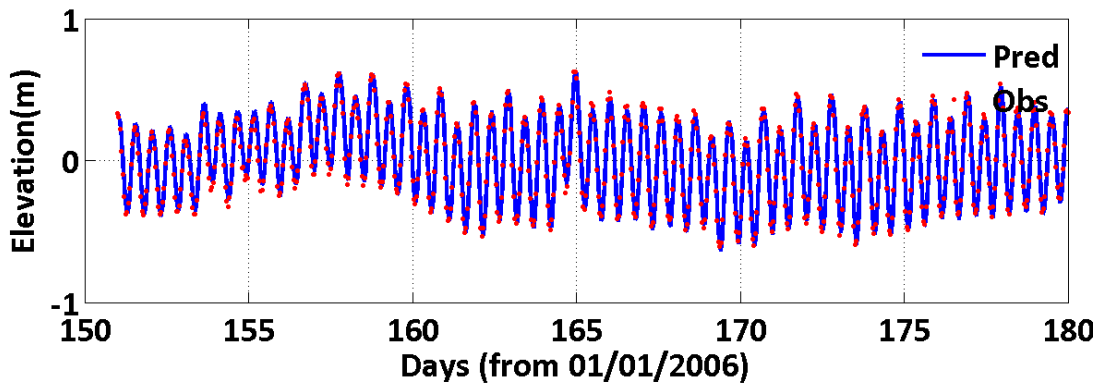
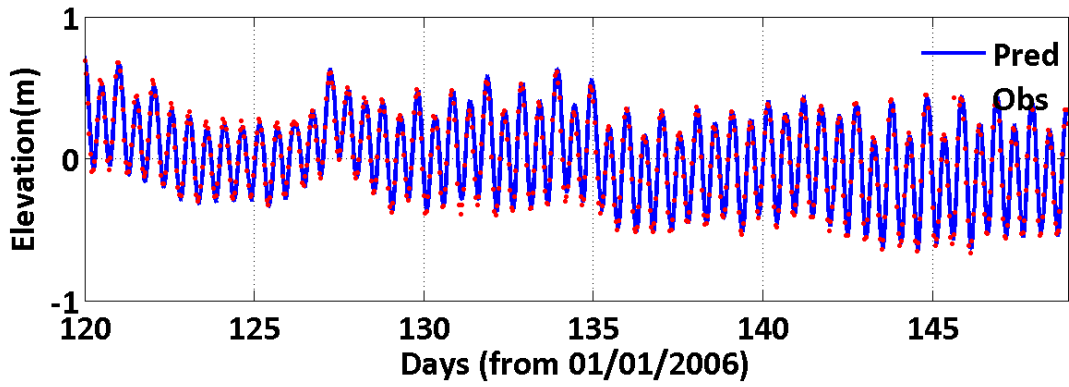
JMS002.55



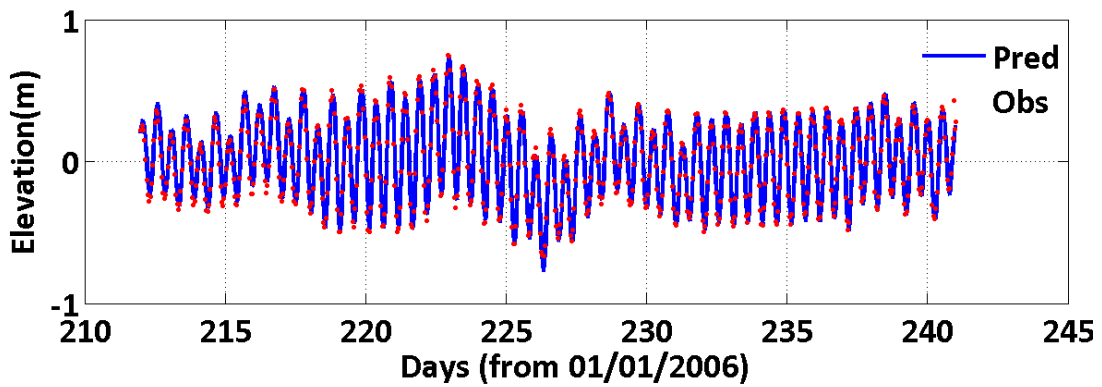
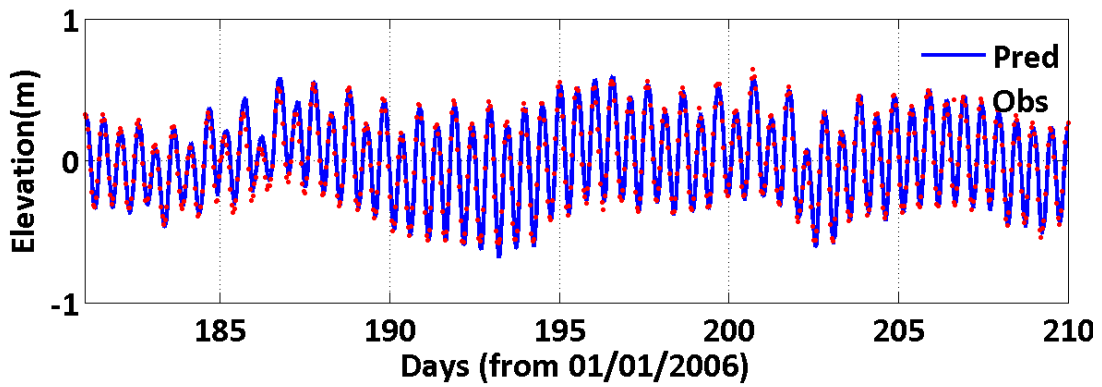
JMS002.55



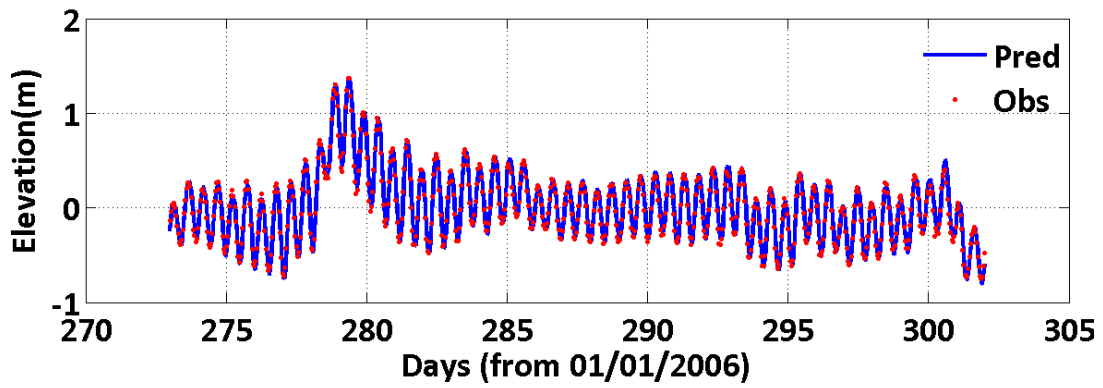
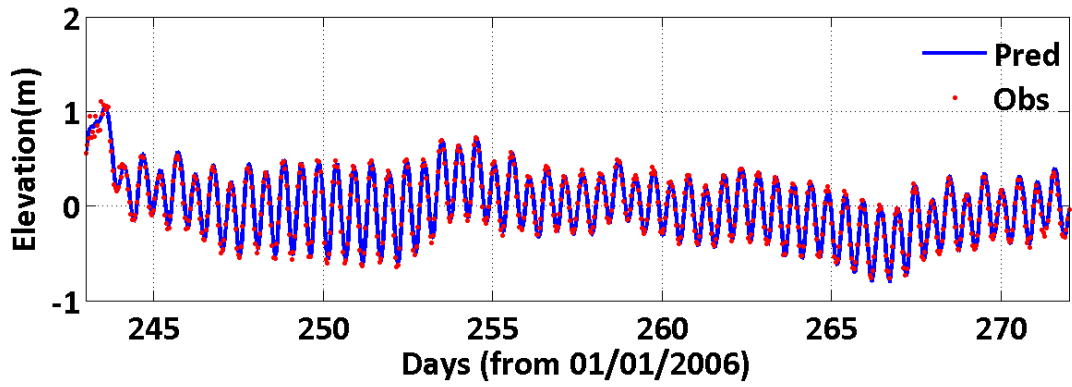
JMS002.55



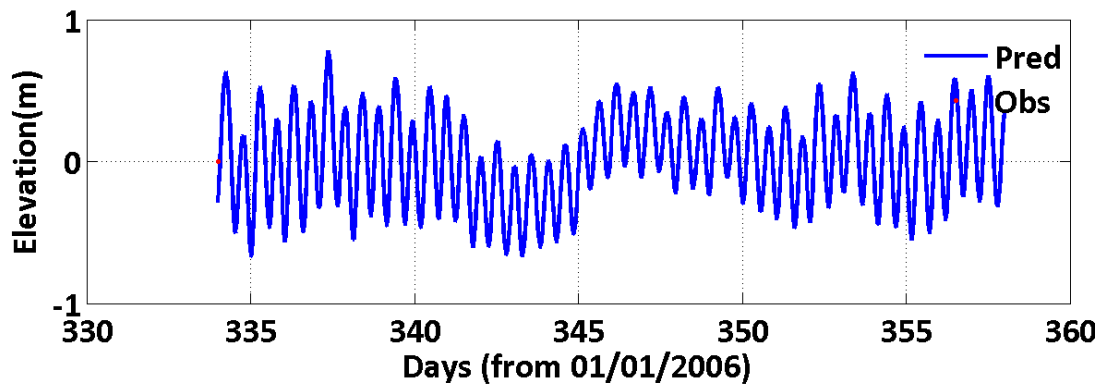
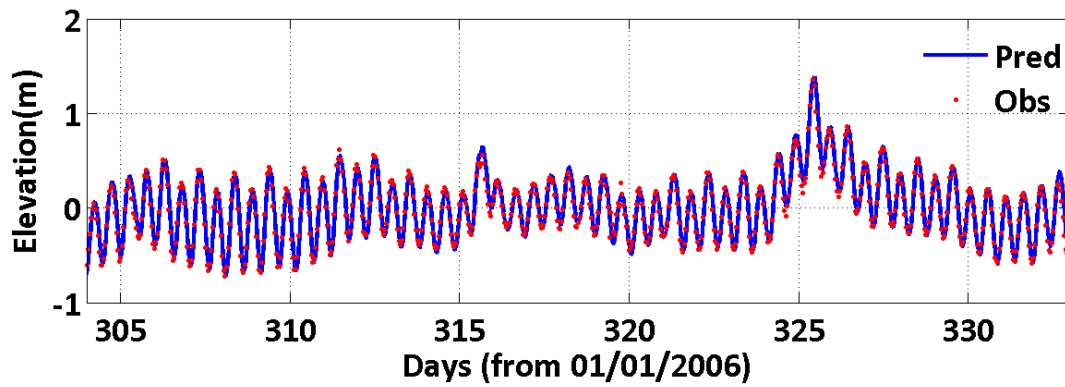
JMS002.55

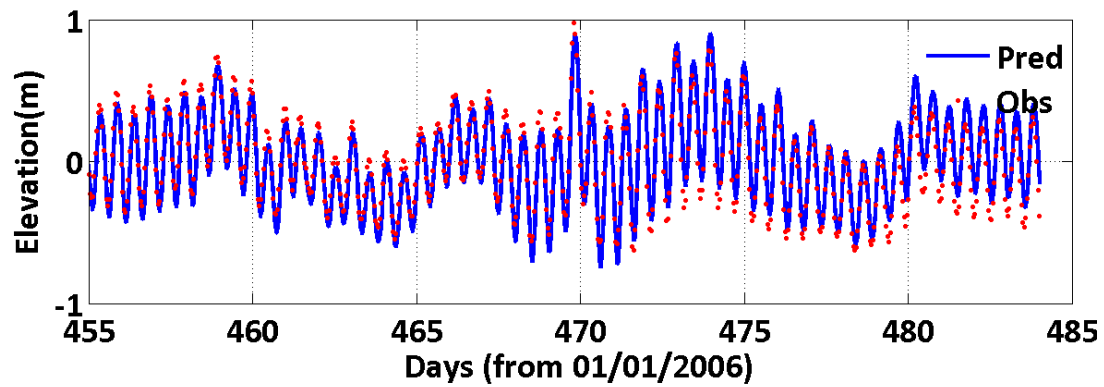
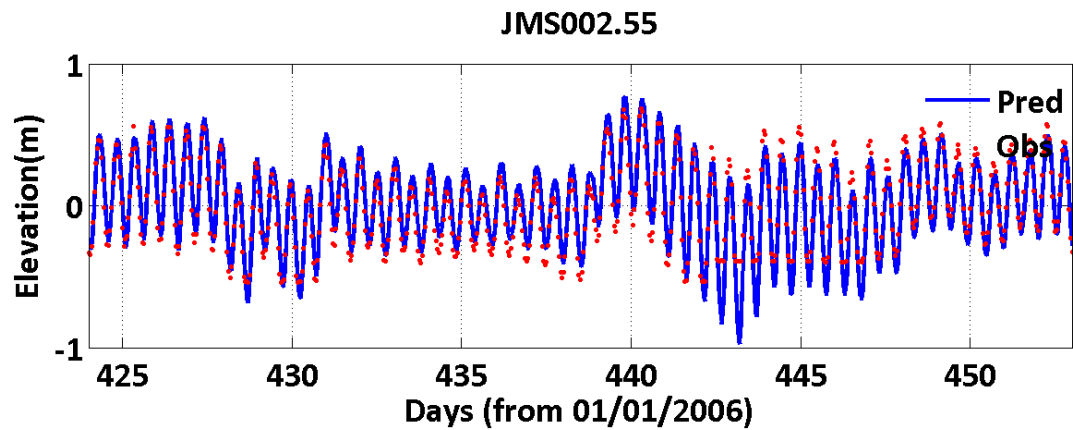
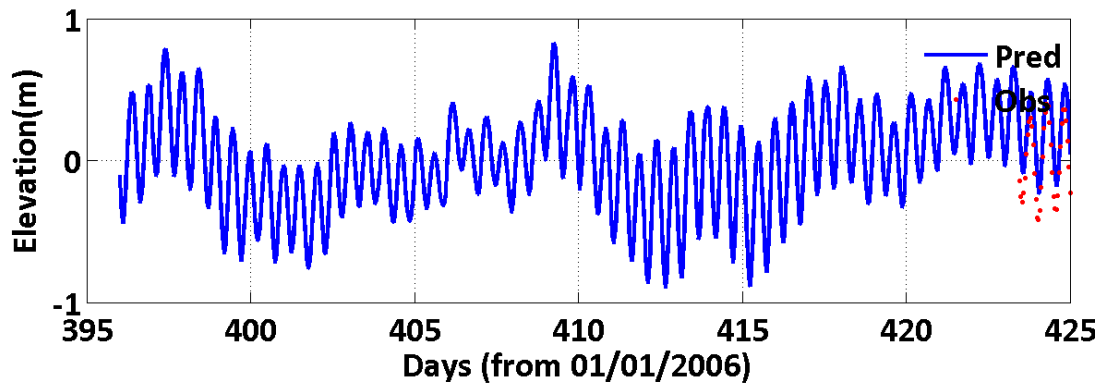
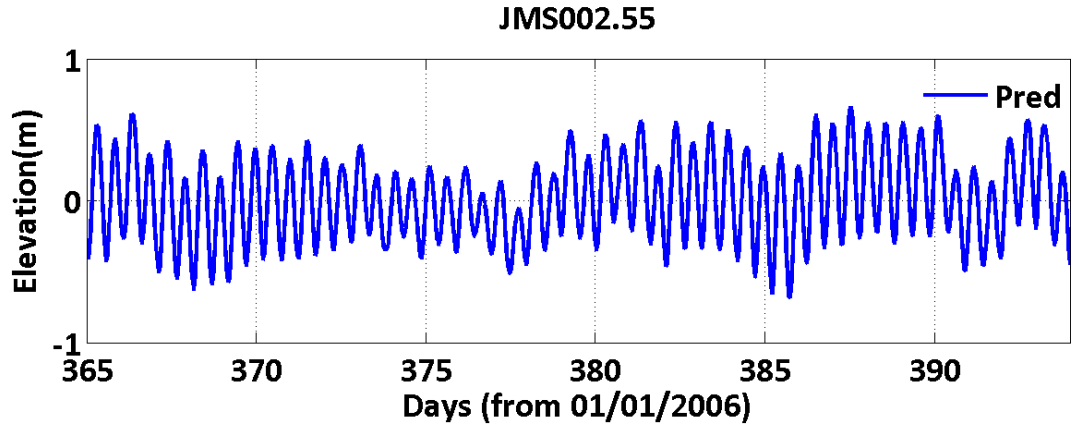


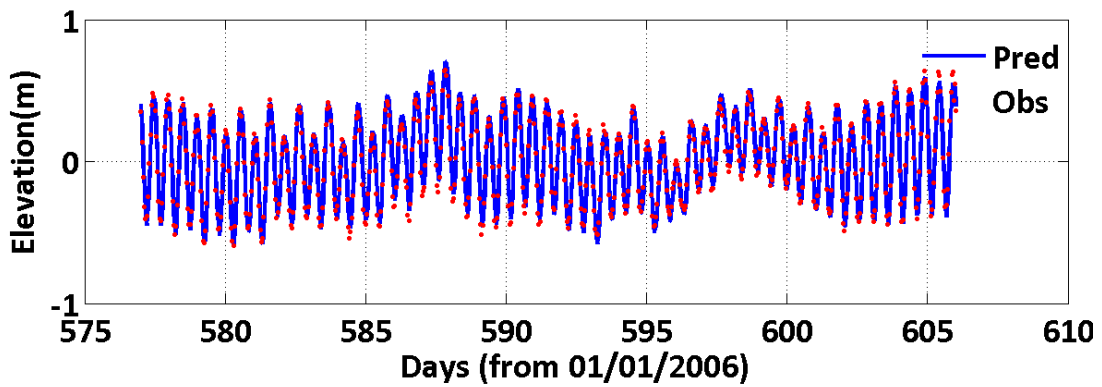
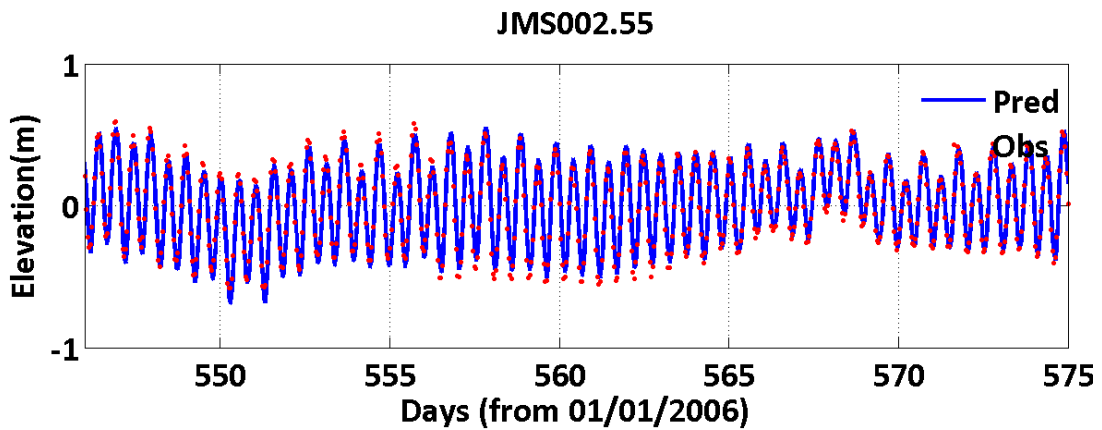
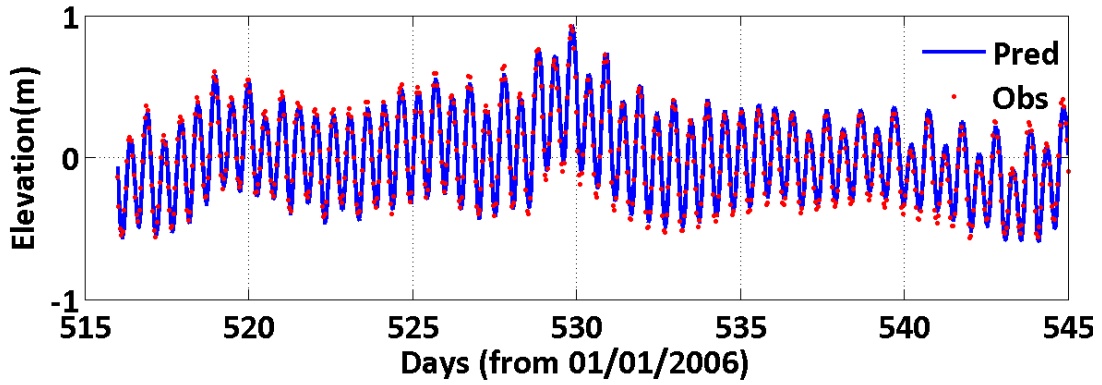
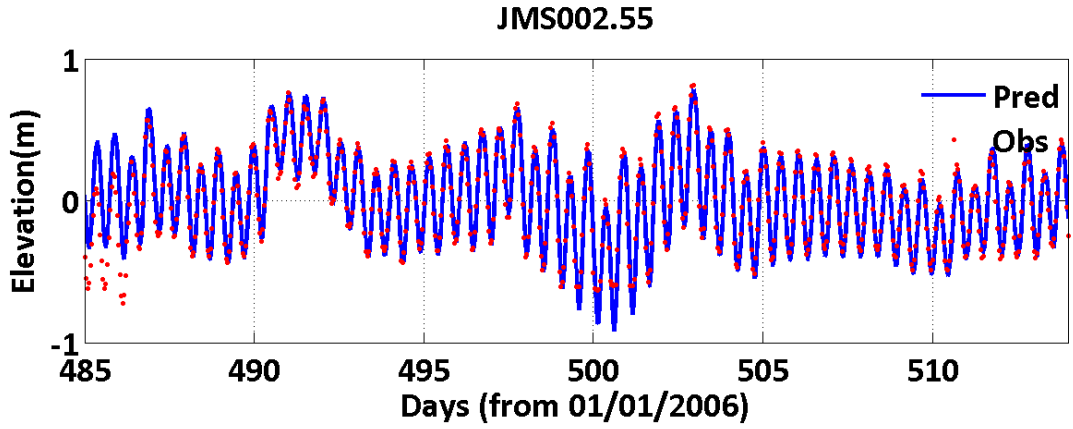
JMS002.55

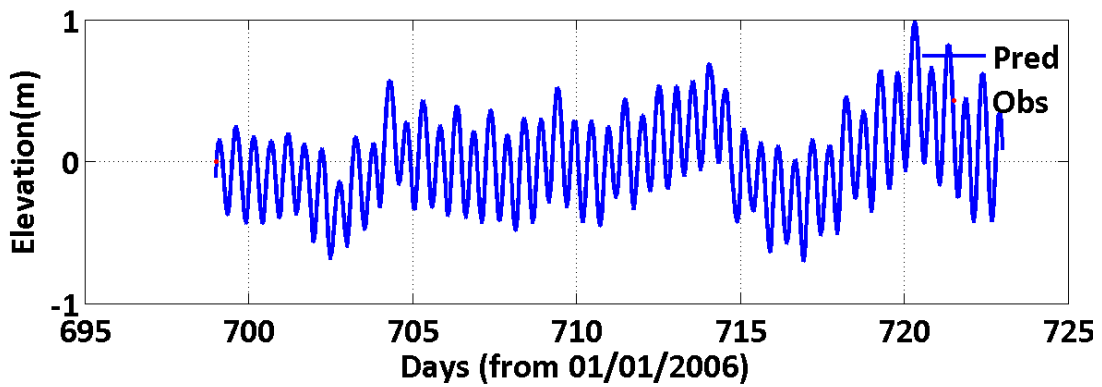
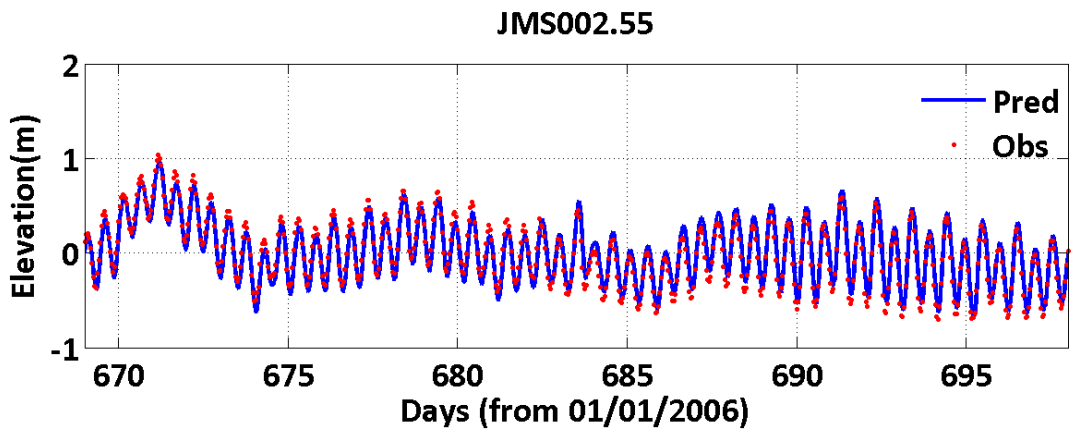
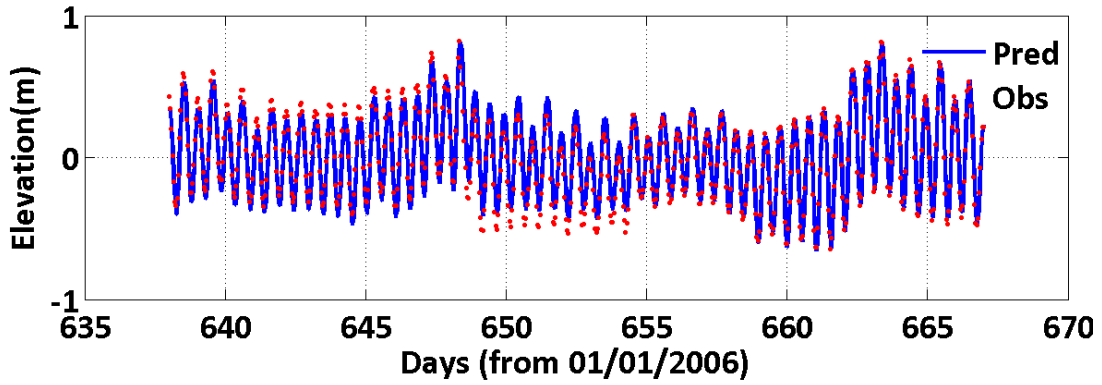
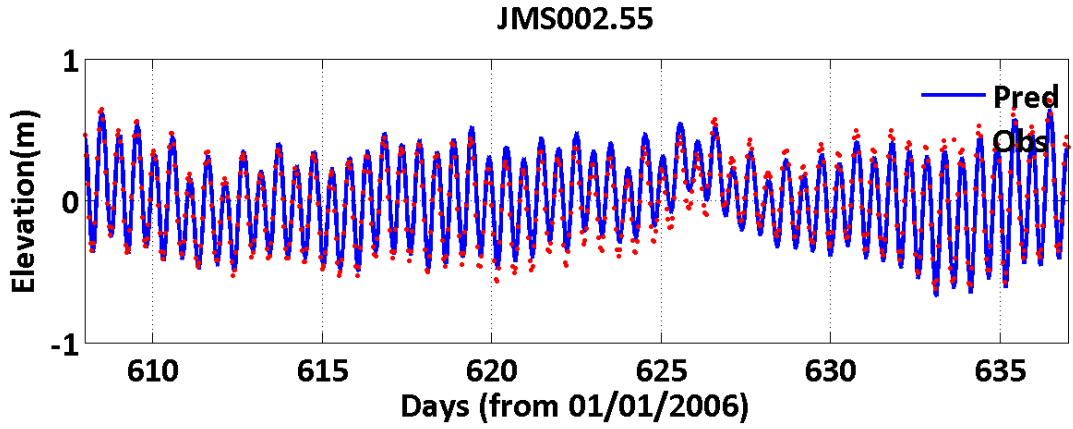


JMS002.55

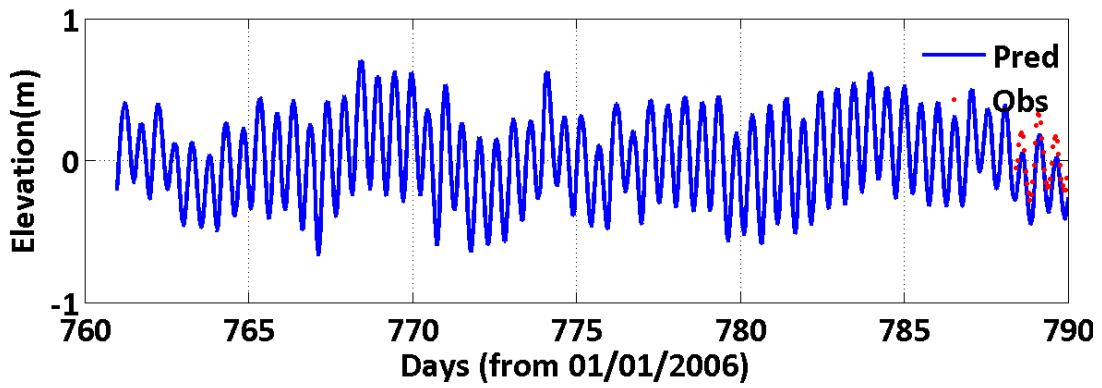
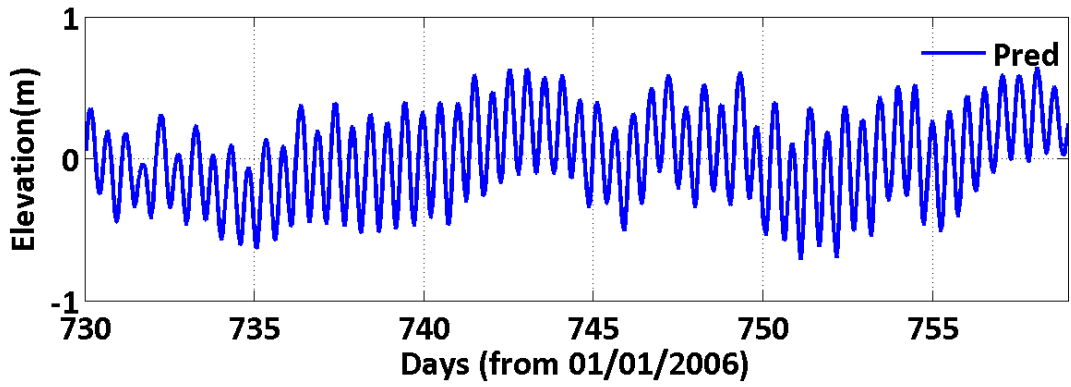




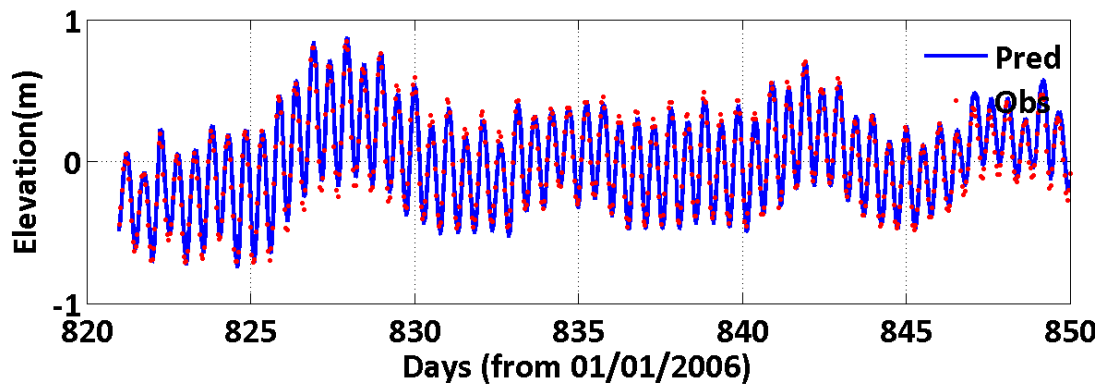
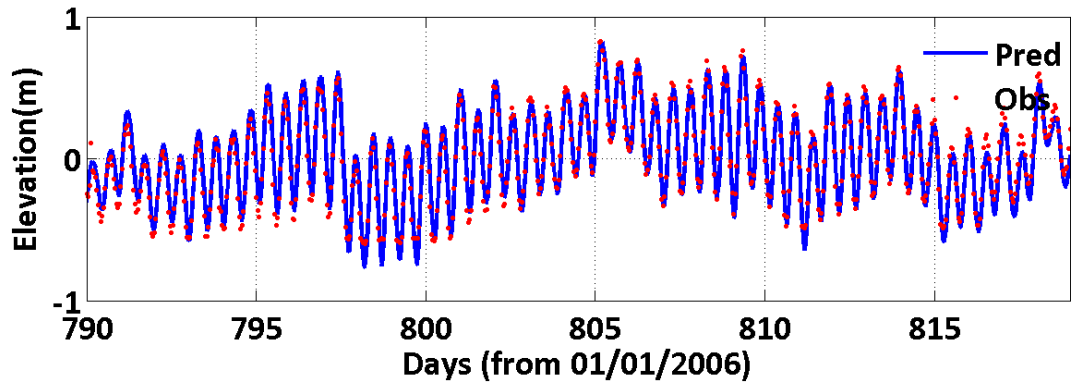




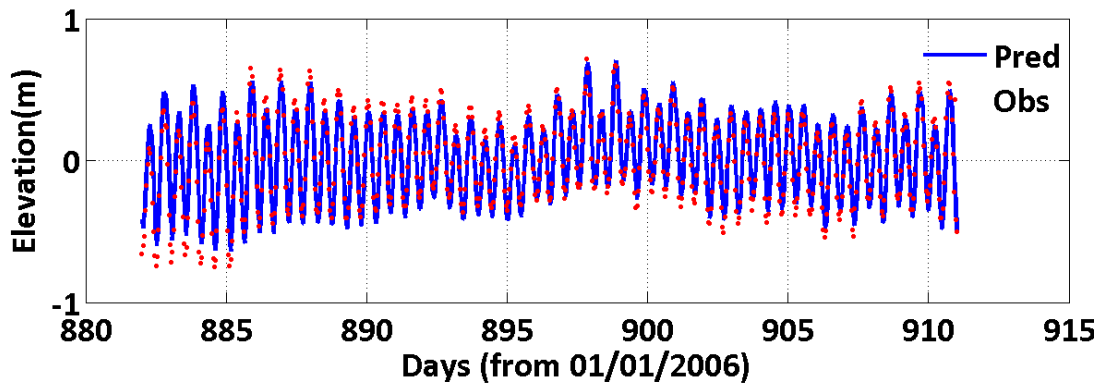
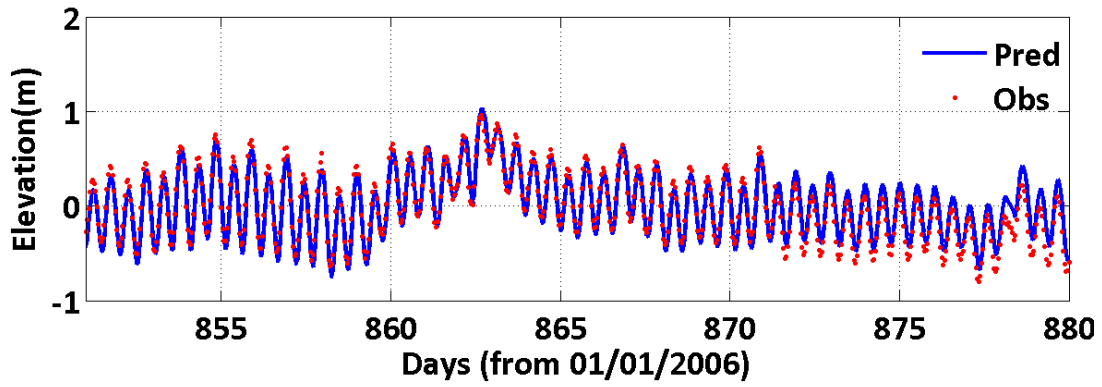
JMS002.55



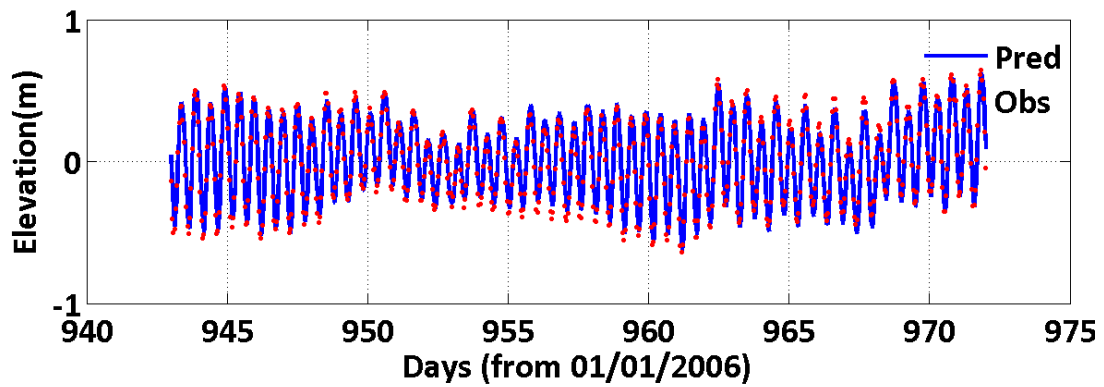
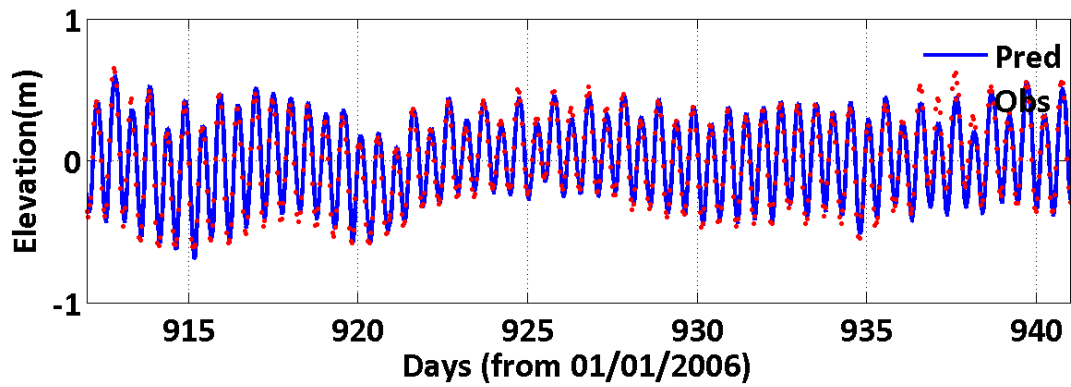
JMS002.55

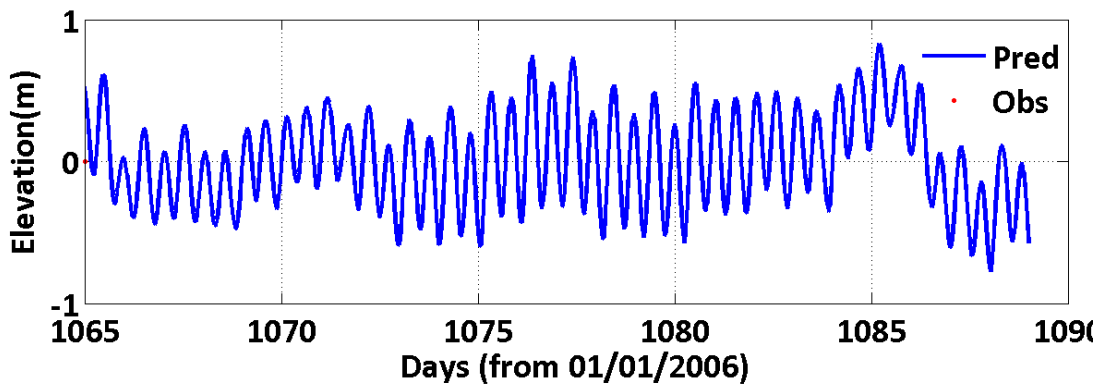
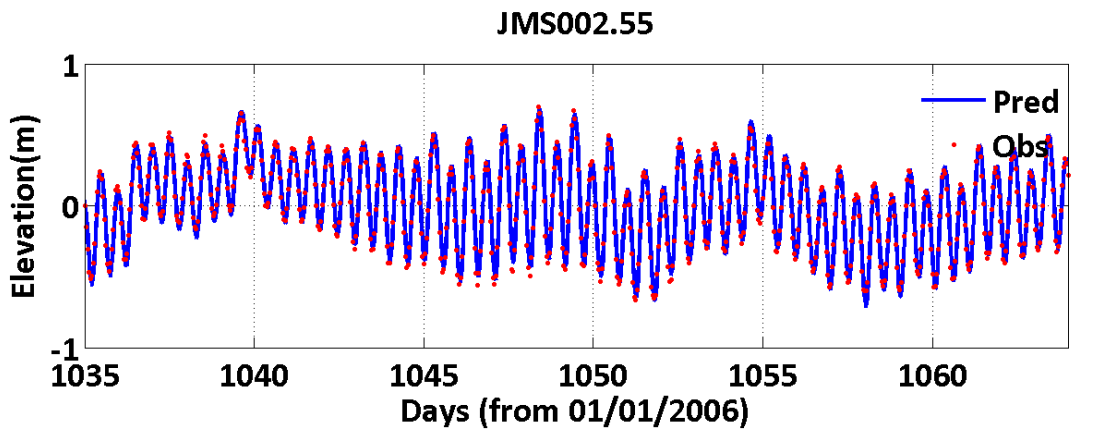
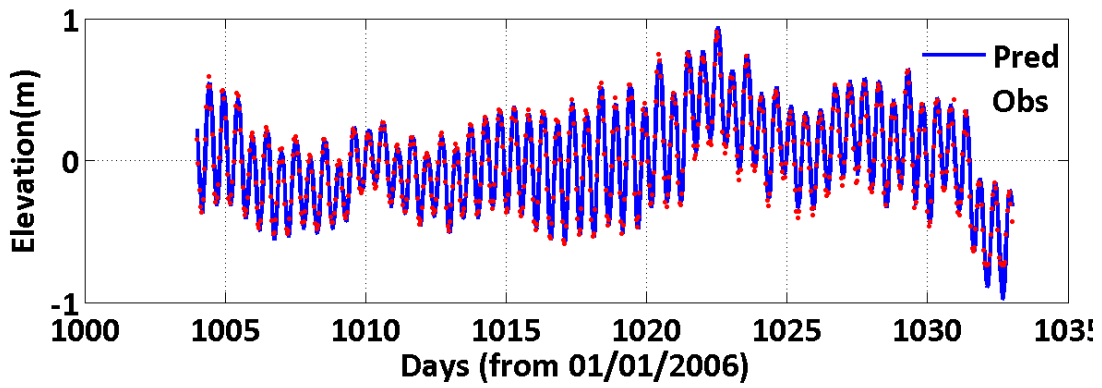
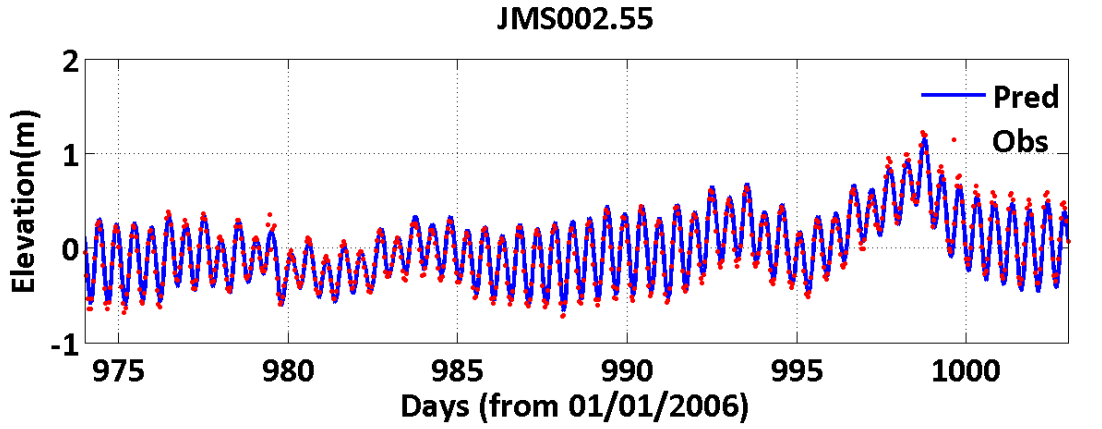


JMS002.55

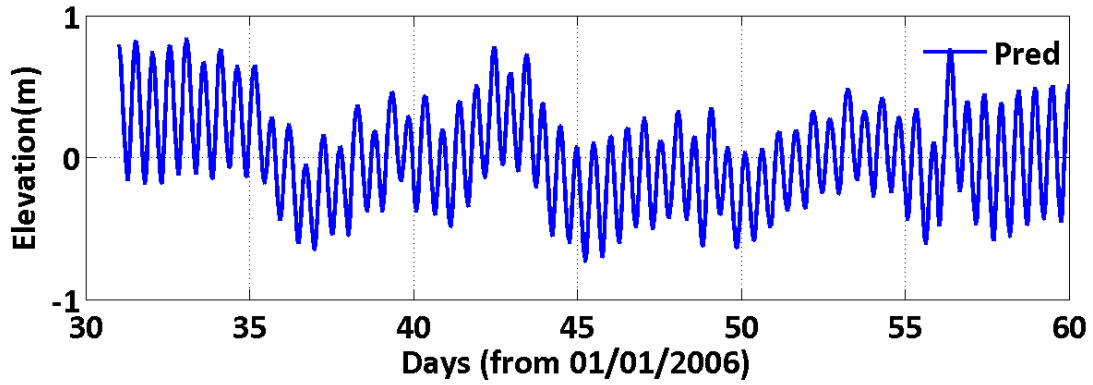
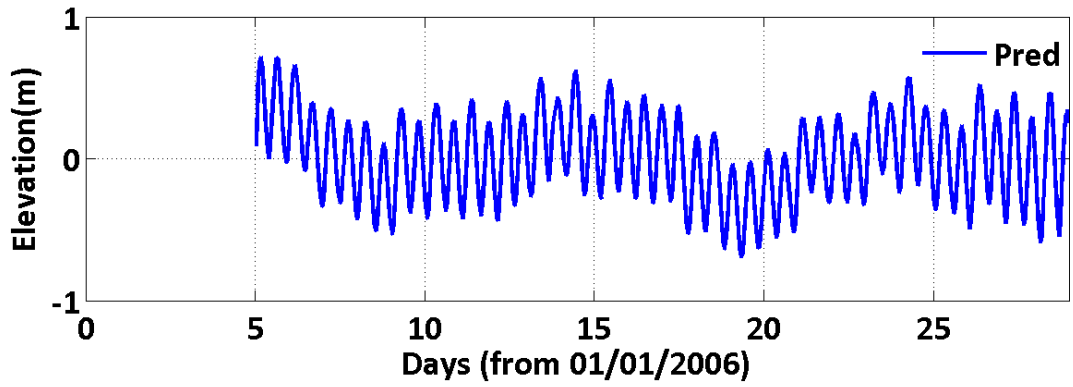


JMS002.55

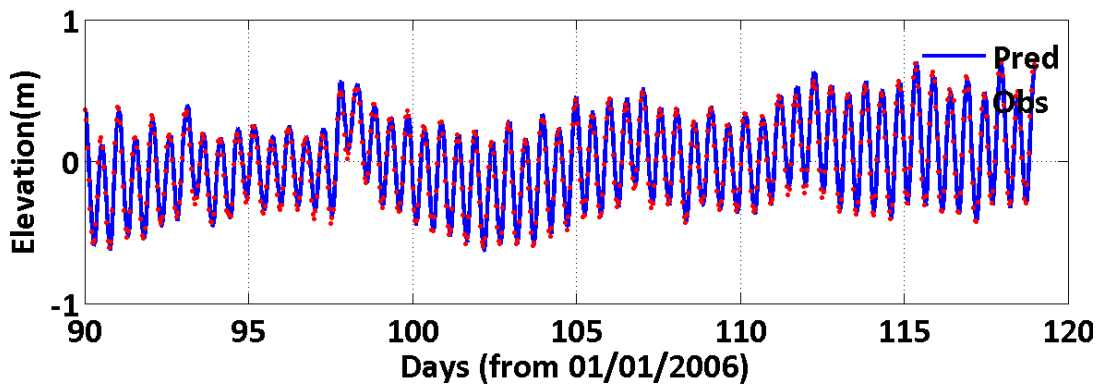
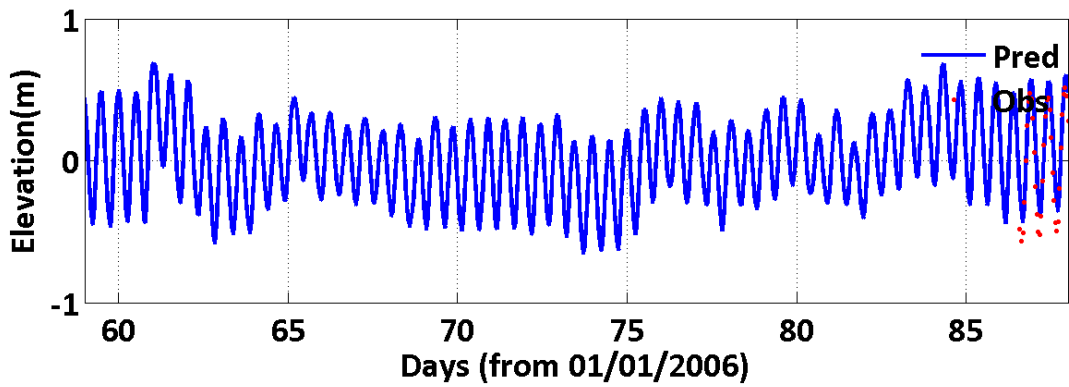




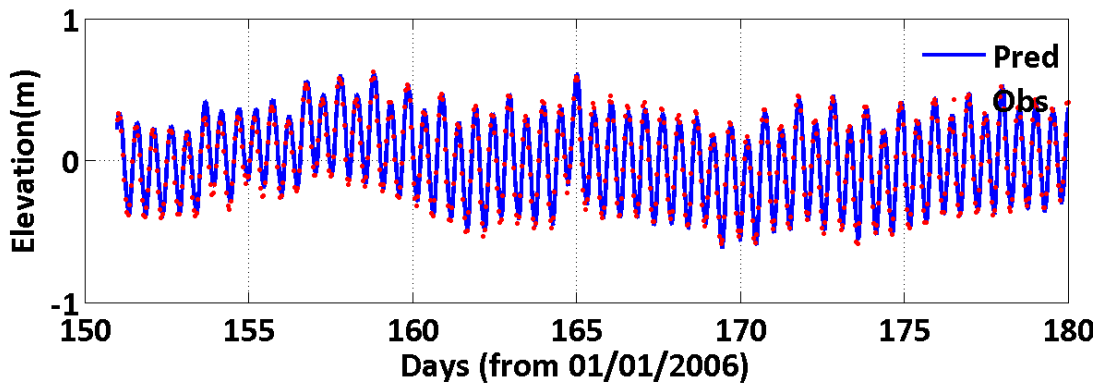
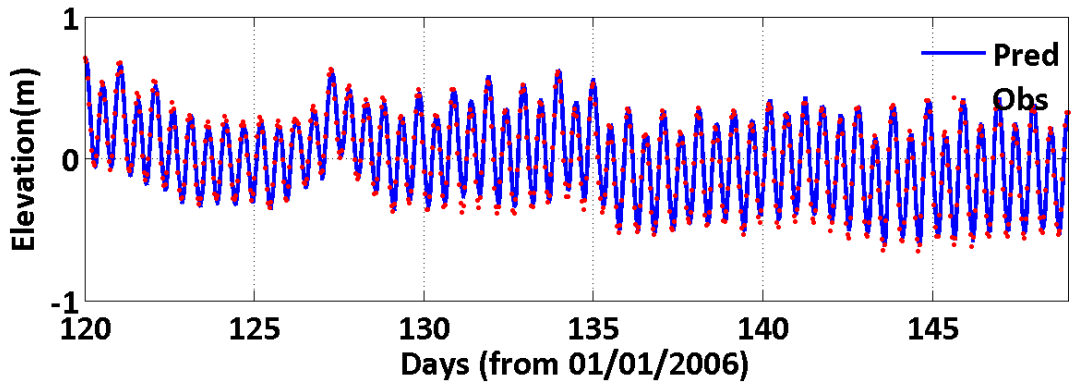
JMS018.23



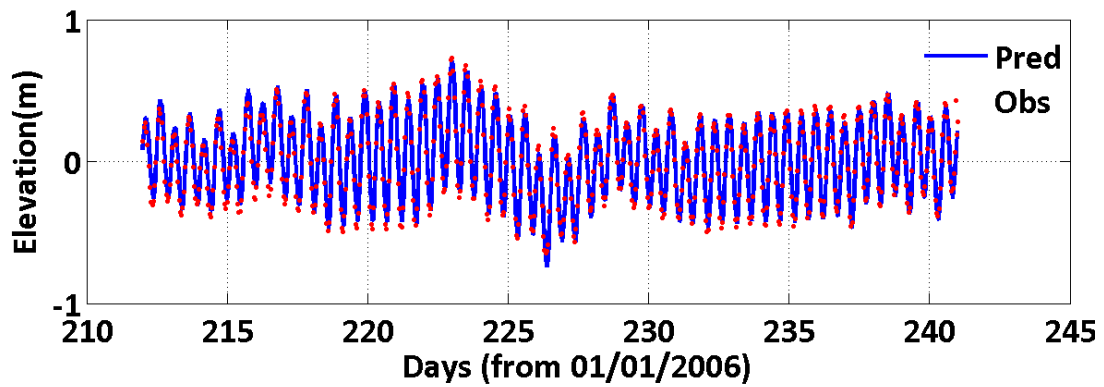
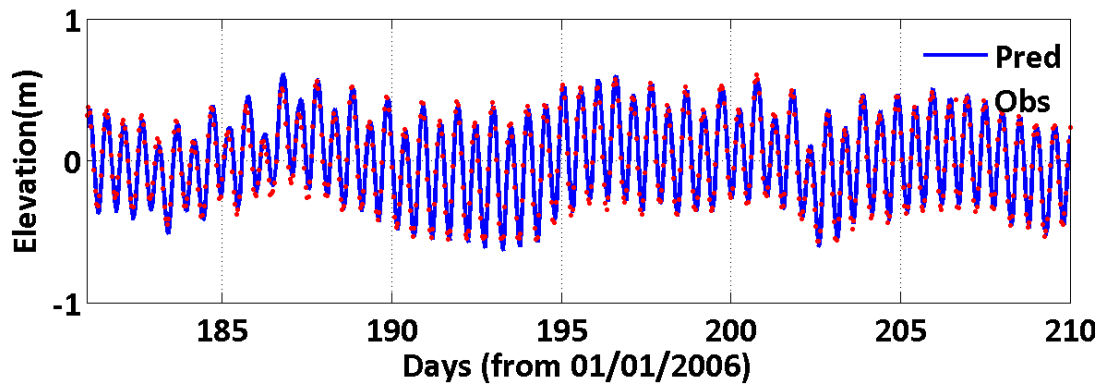
JMS018.23



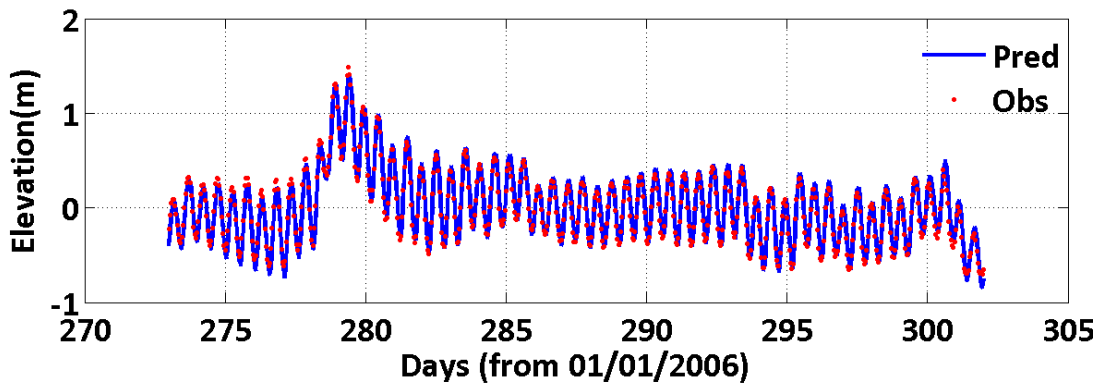
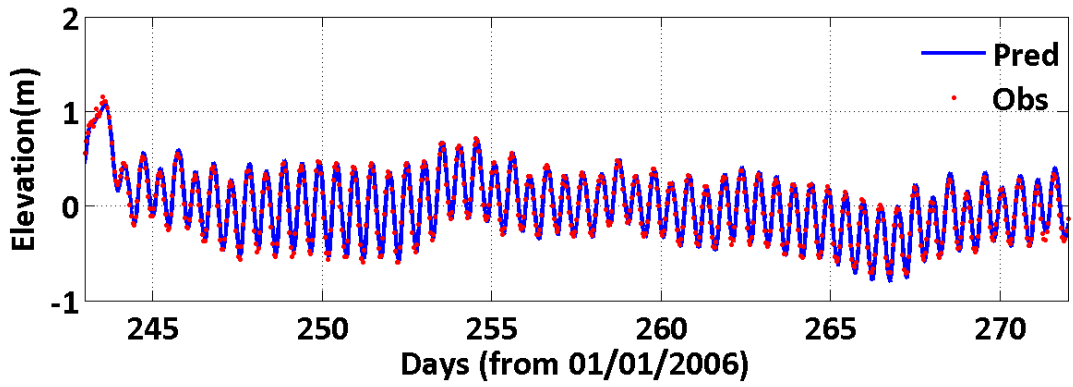
JMS018.23



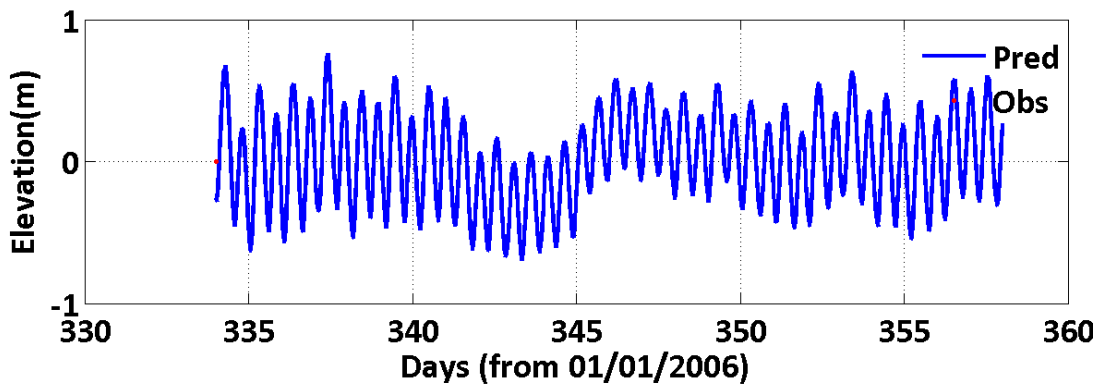
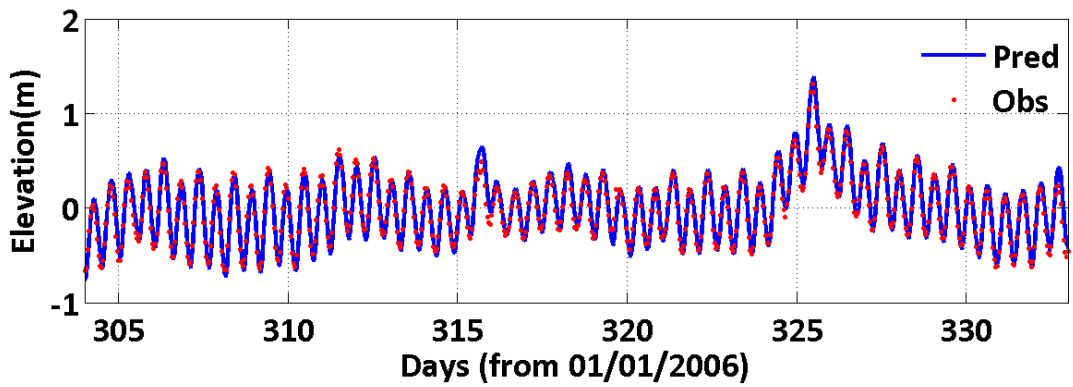
JMS018.23



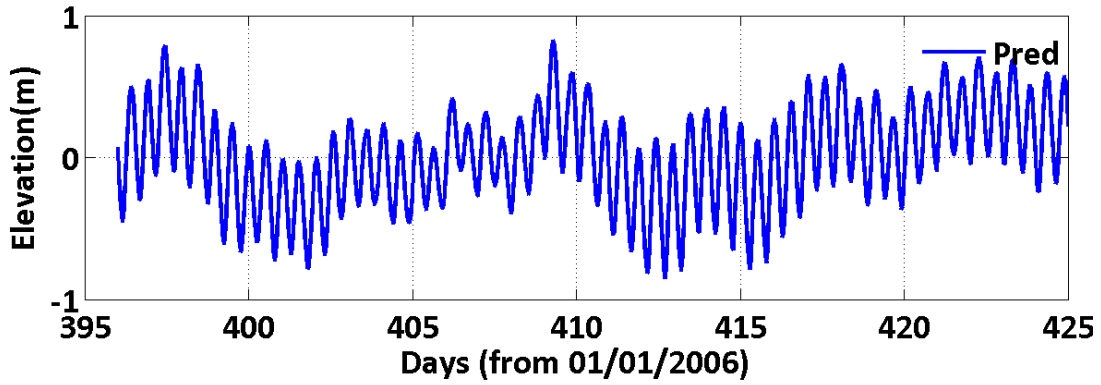
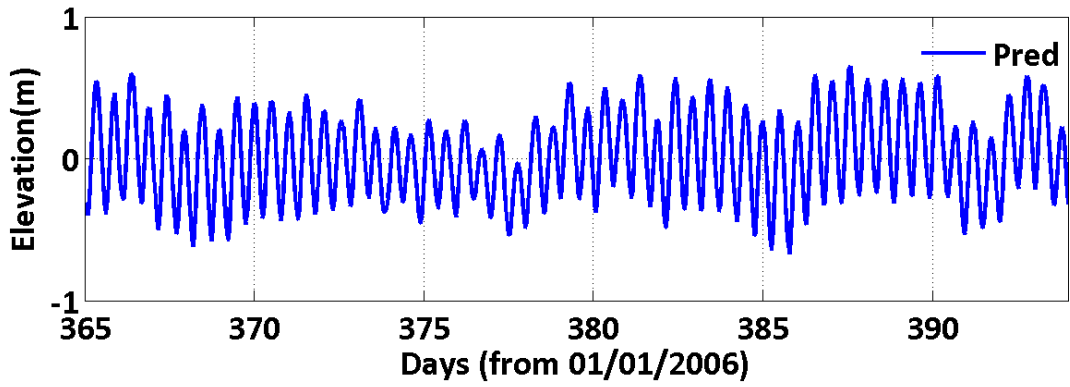
JMS018.23



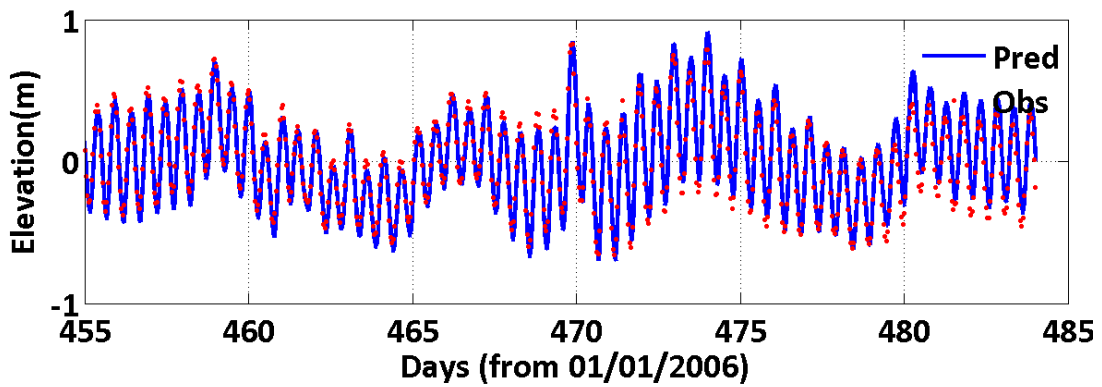
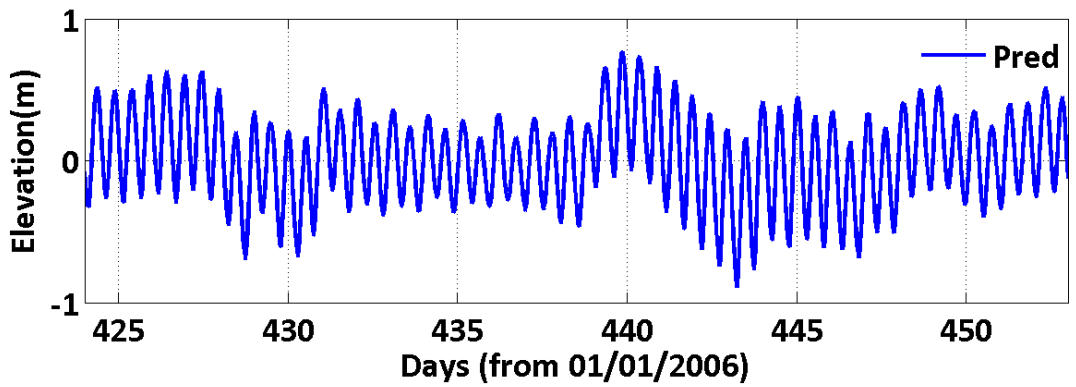
JMS018.23



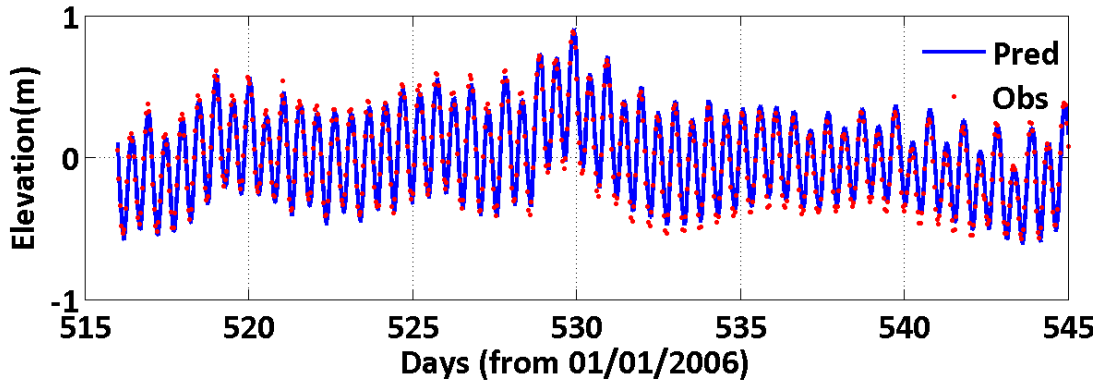
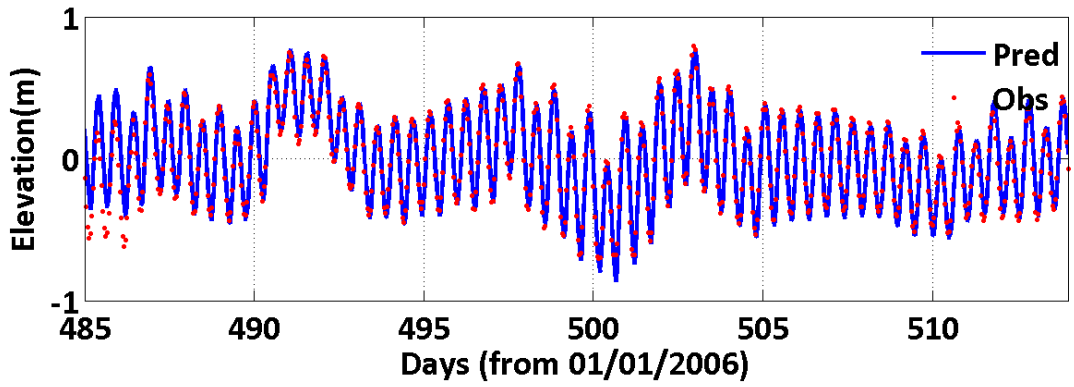
JMS018.23



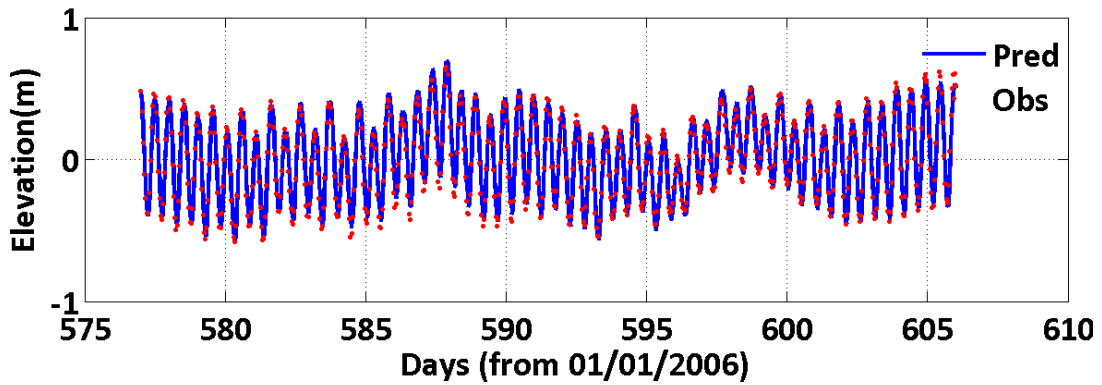
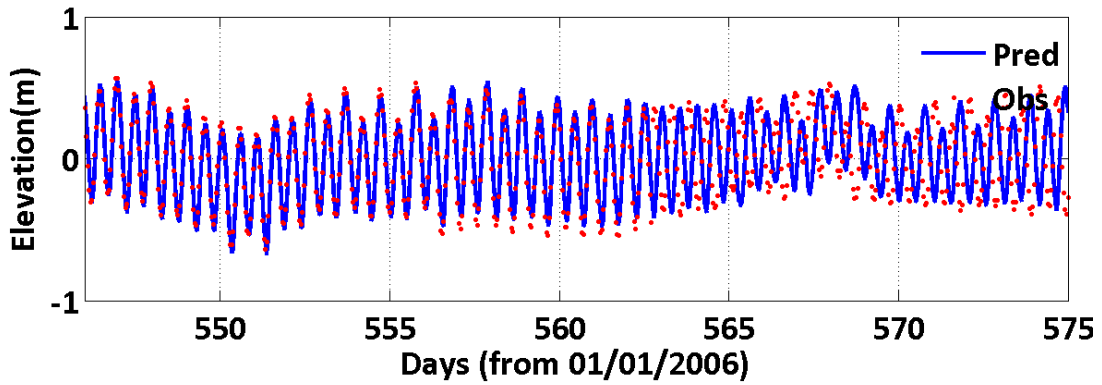
JMS018.23

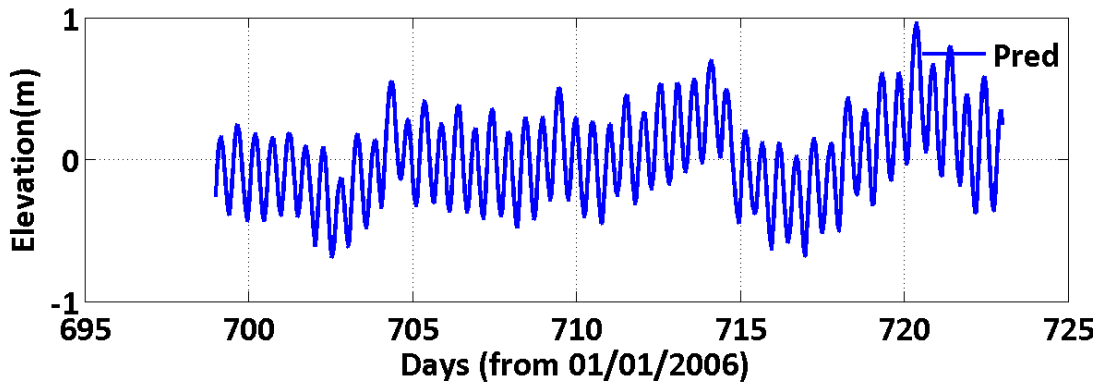
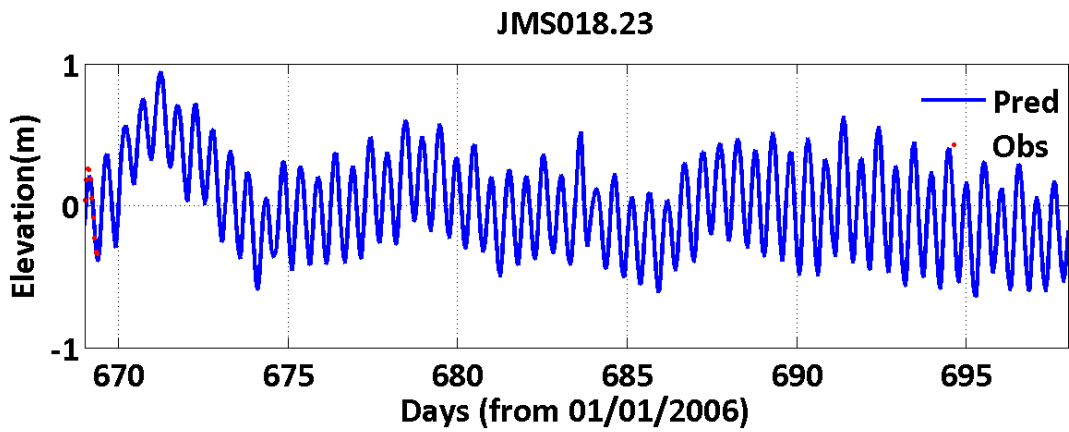
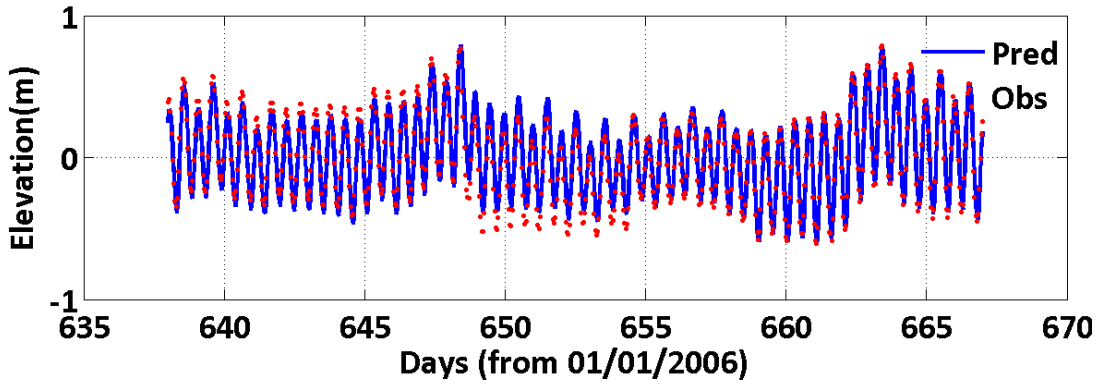
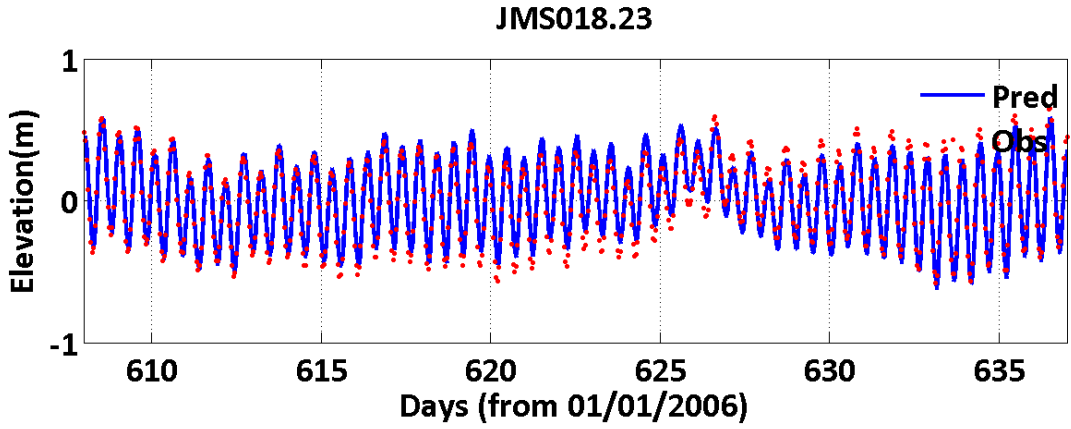


JMS018.23

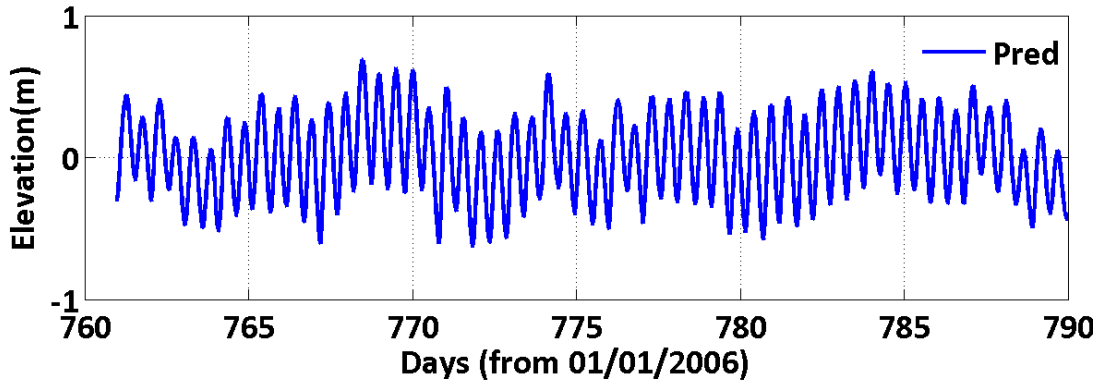
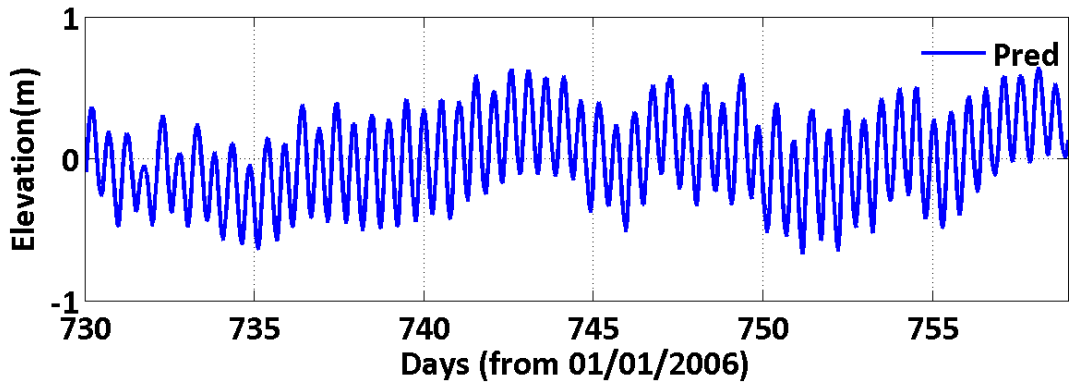


JMS018.23

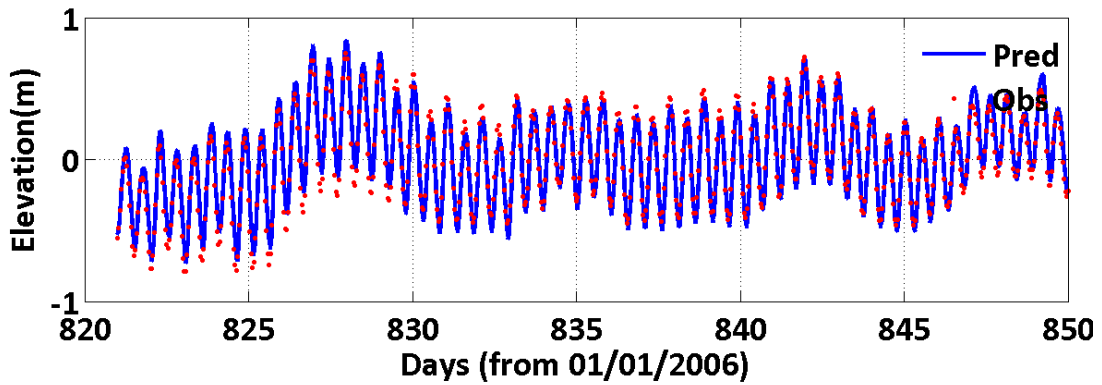
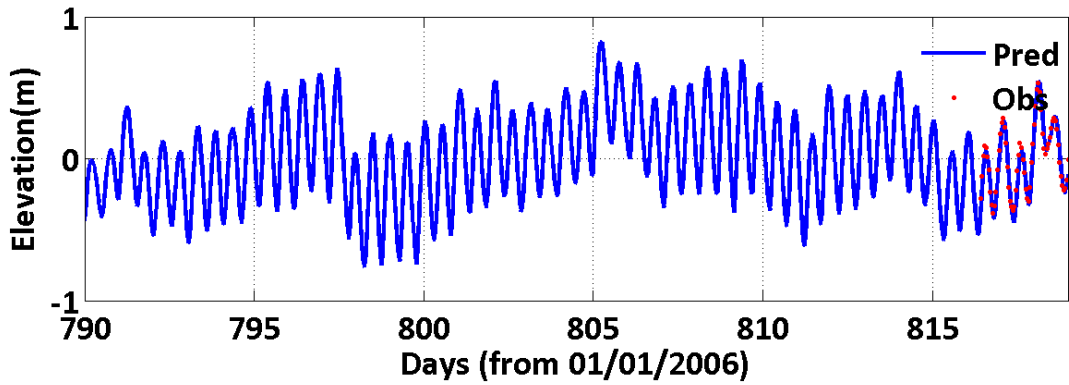




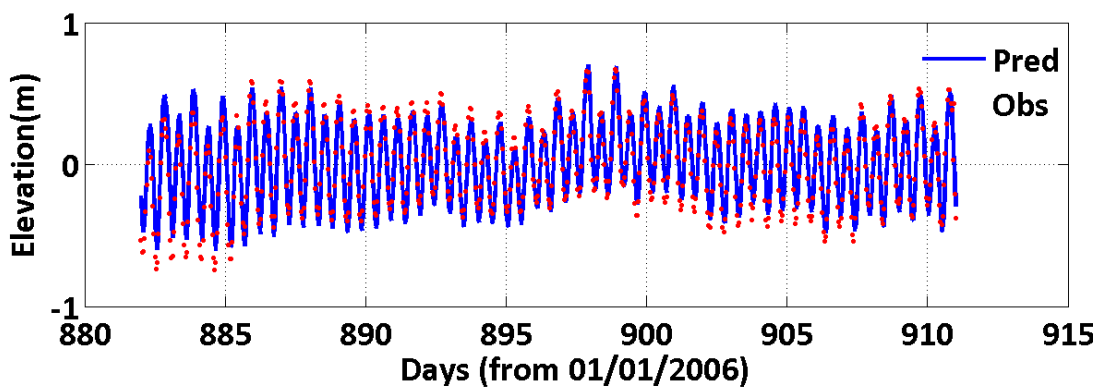
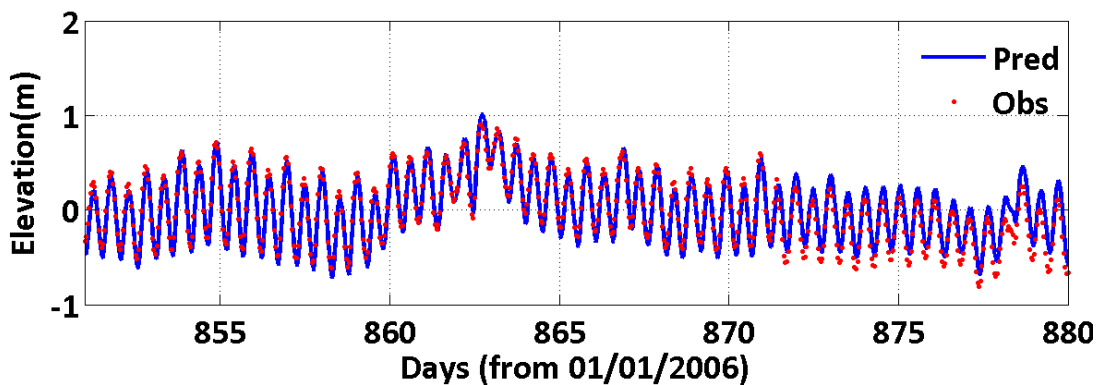
JMS018.23



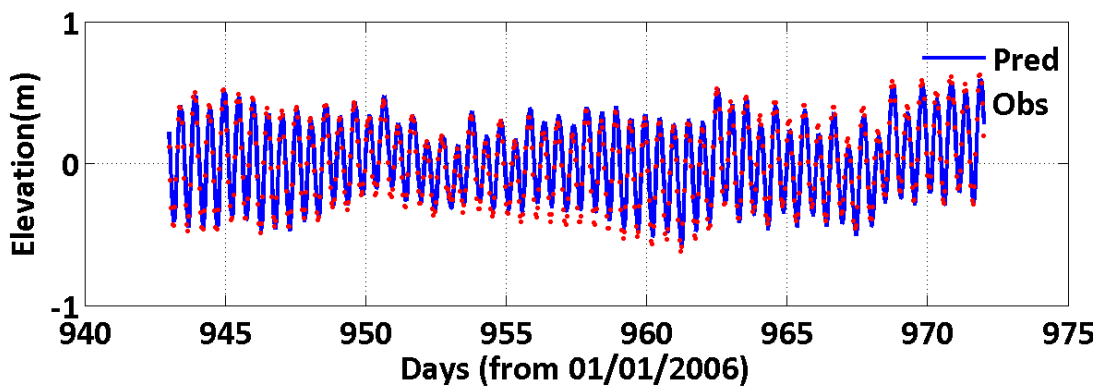
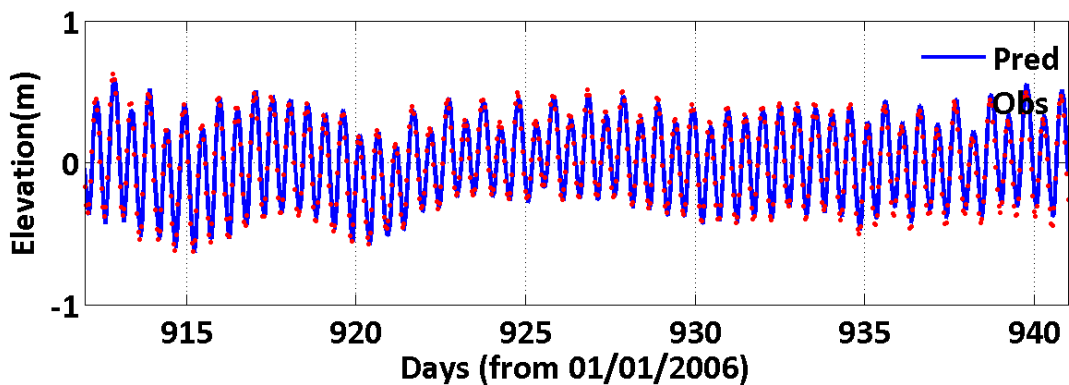
JMS018.23



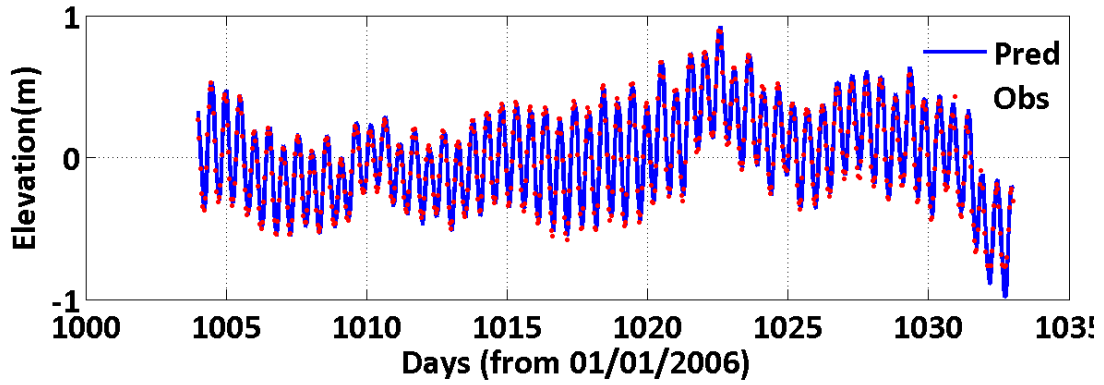
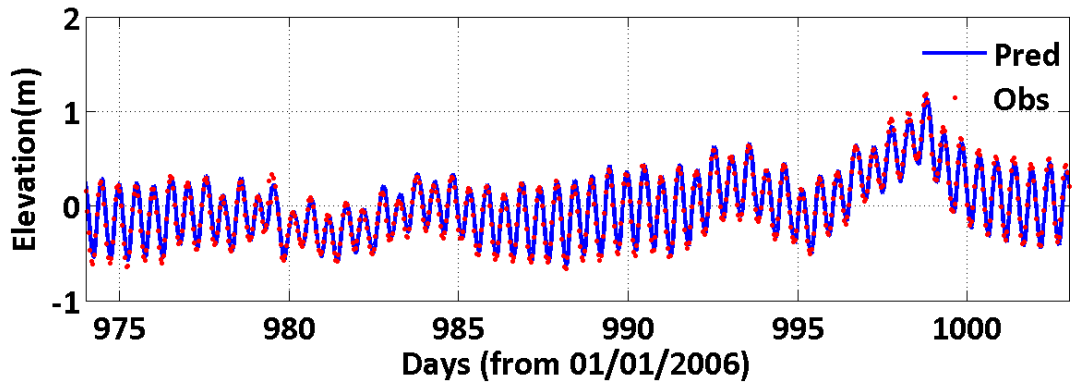
JMS018.23



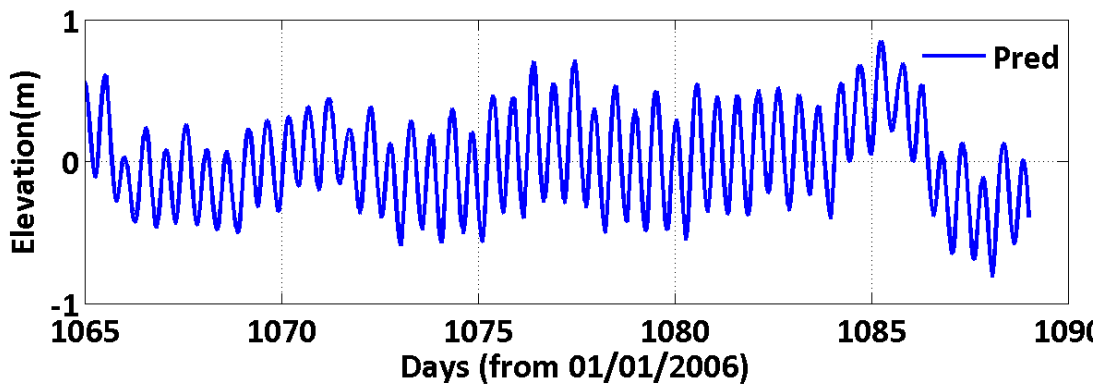
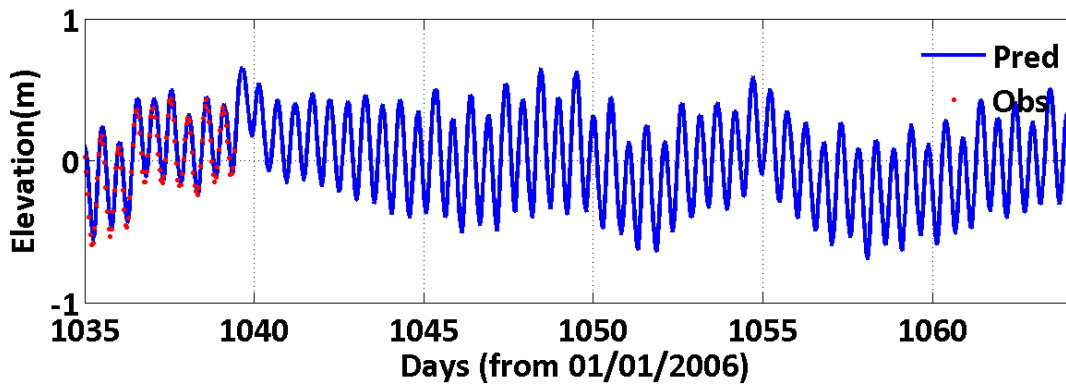
JMS018.23



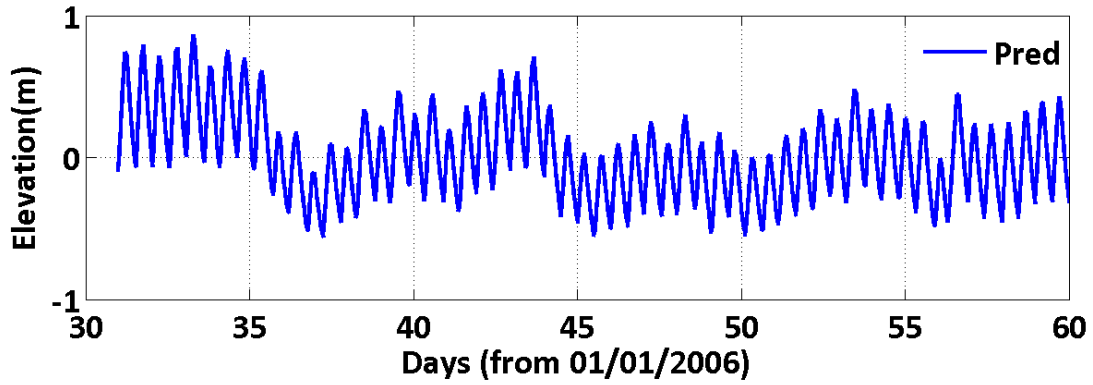
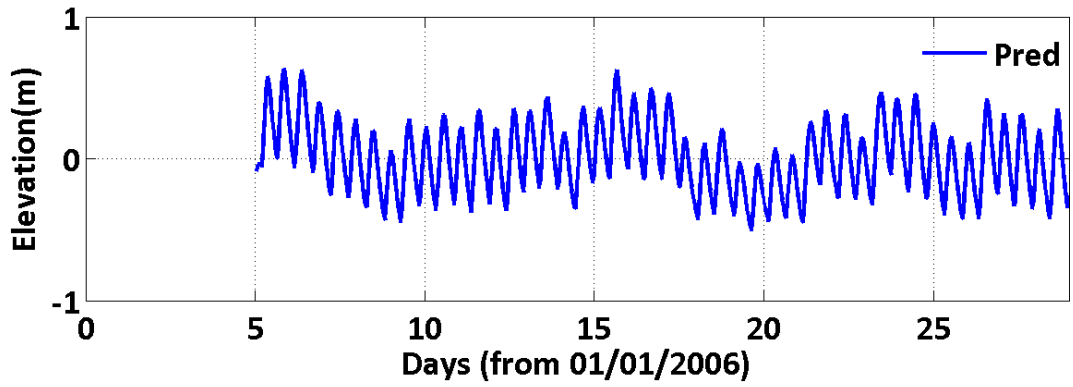
JMS018.23



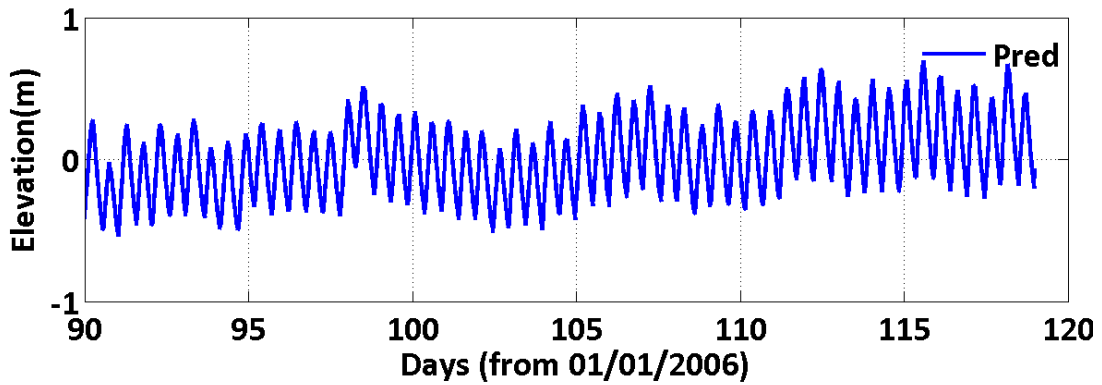
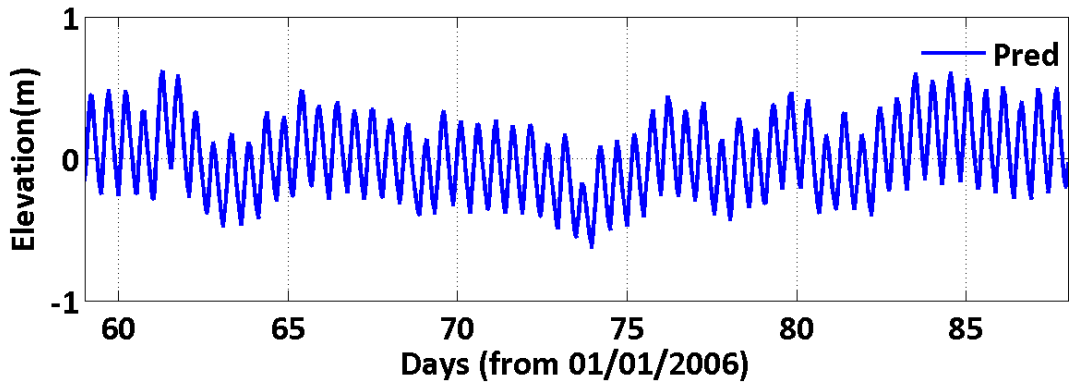
JMS018.23



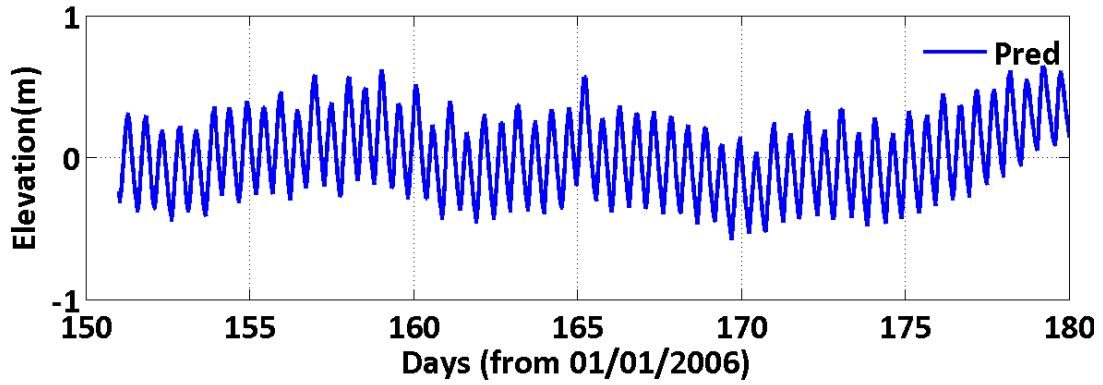
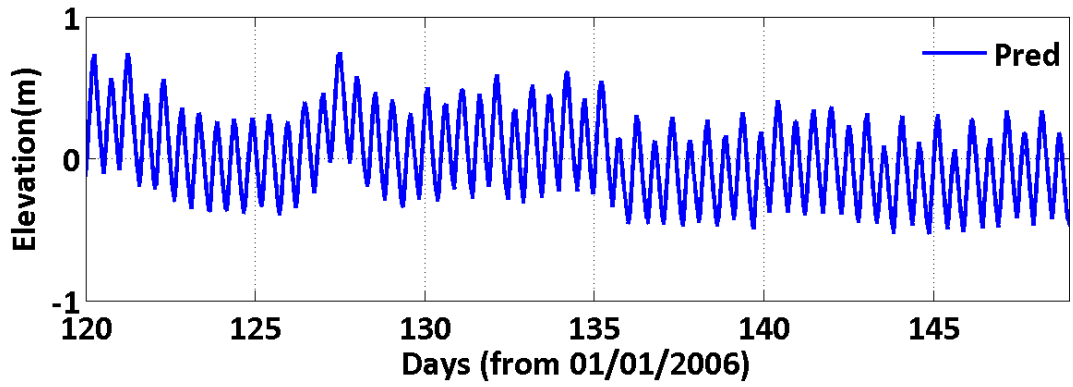
APP001.83



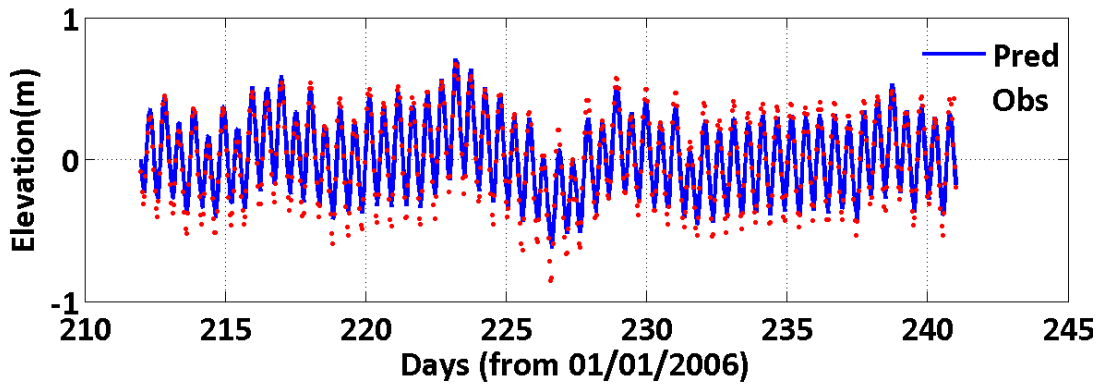
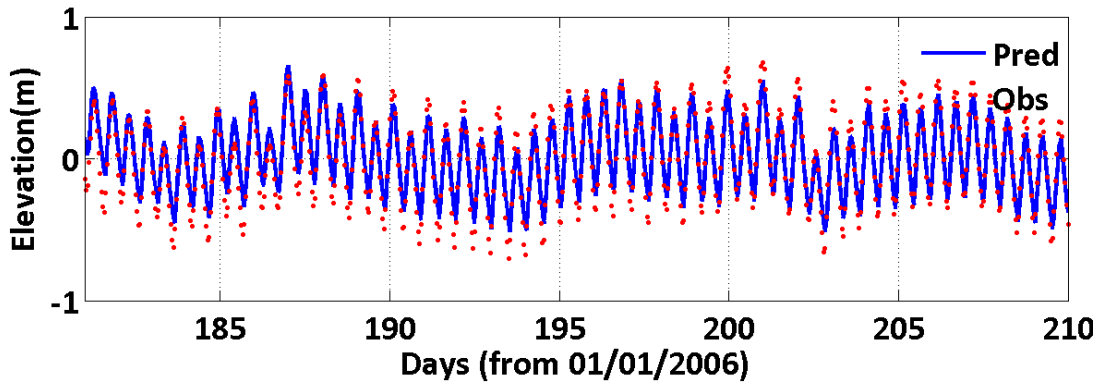
APP001.83



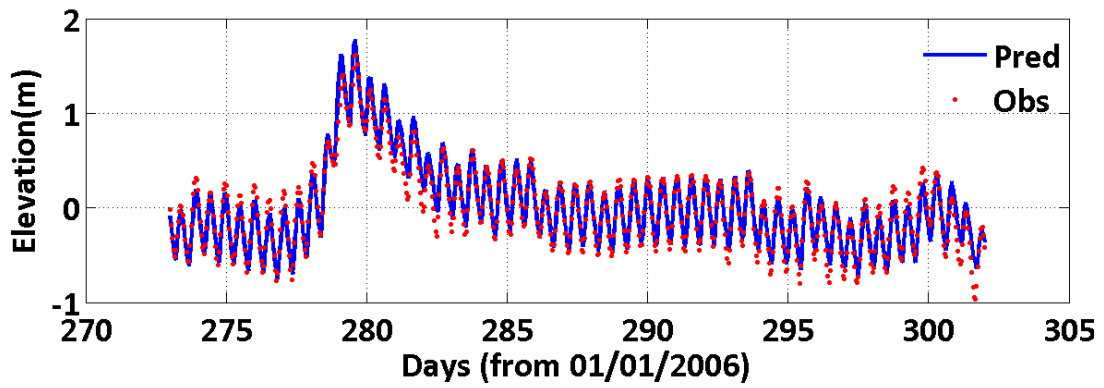
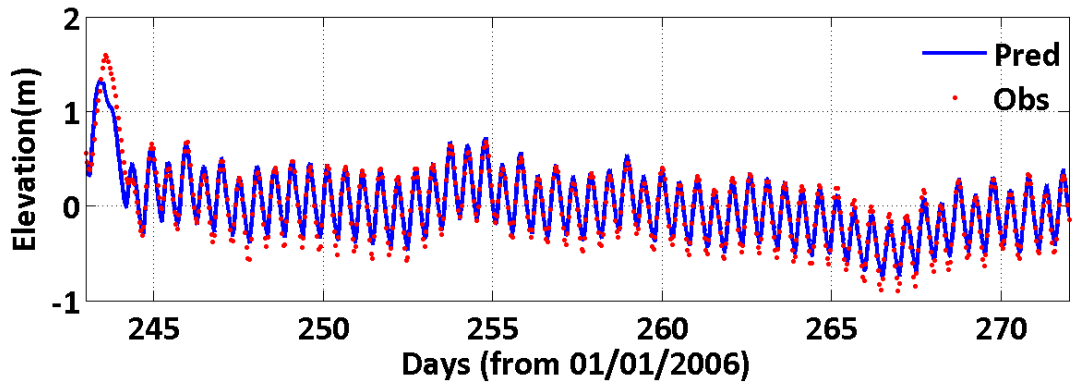
APP001.83



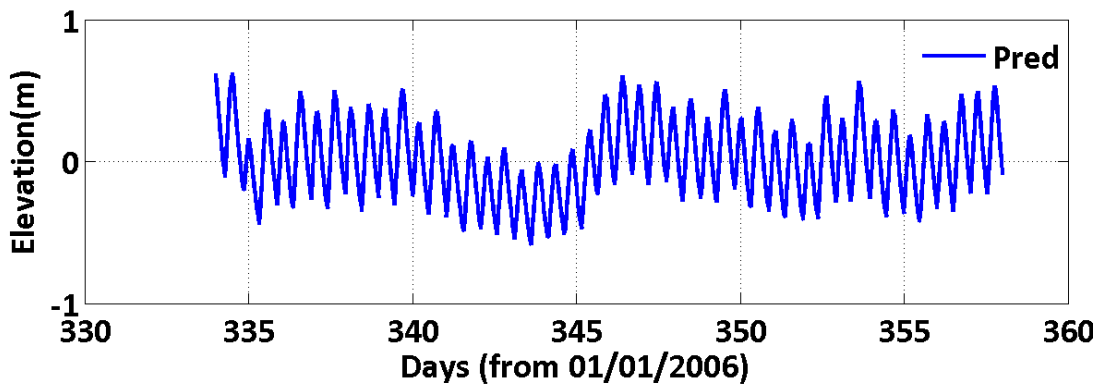
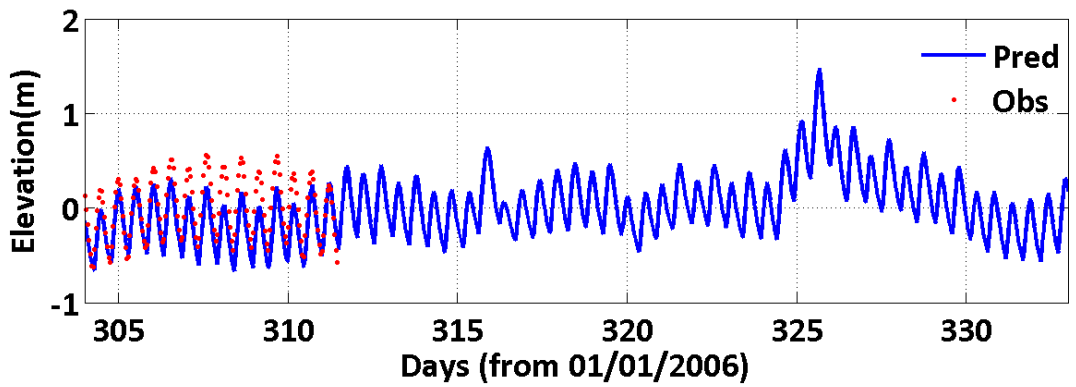
APP001.83

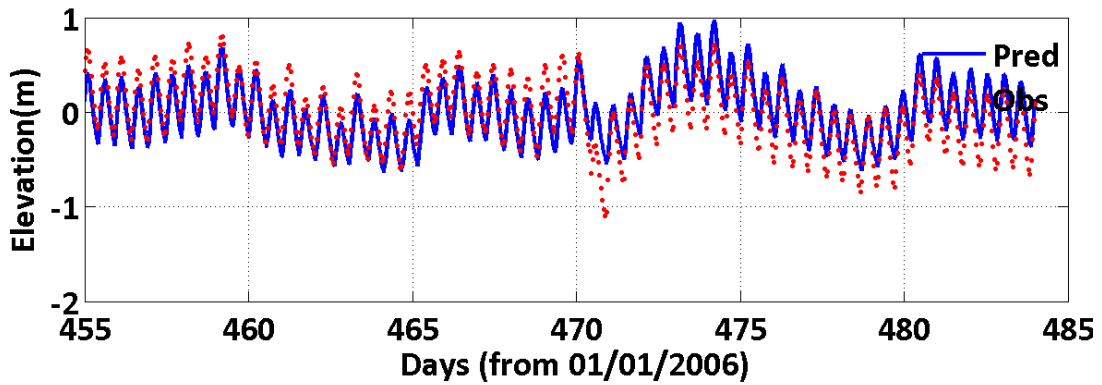
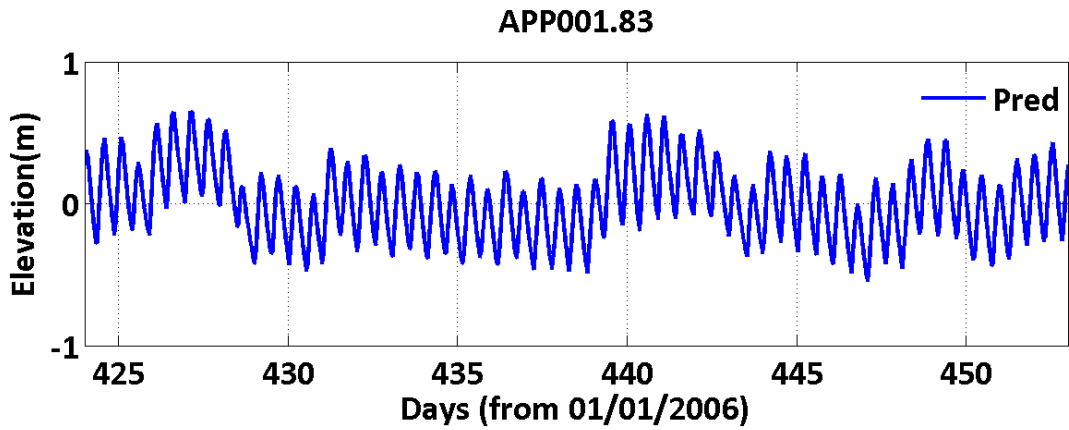
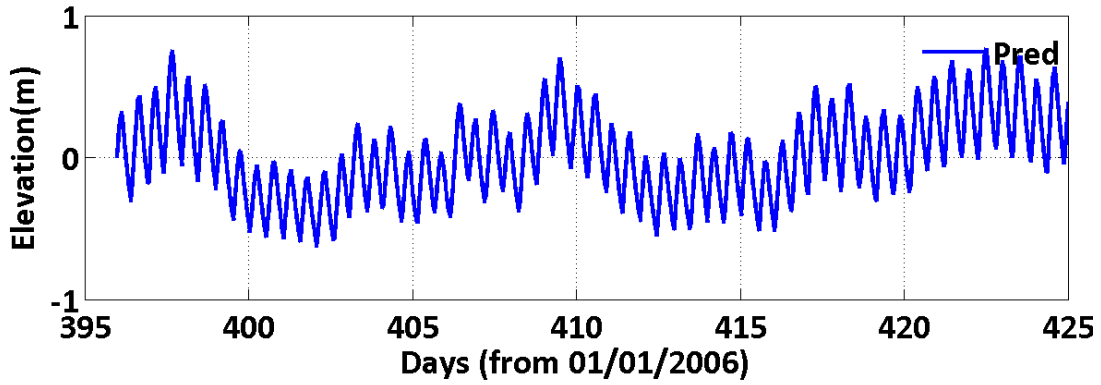
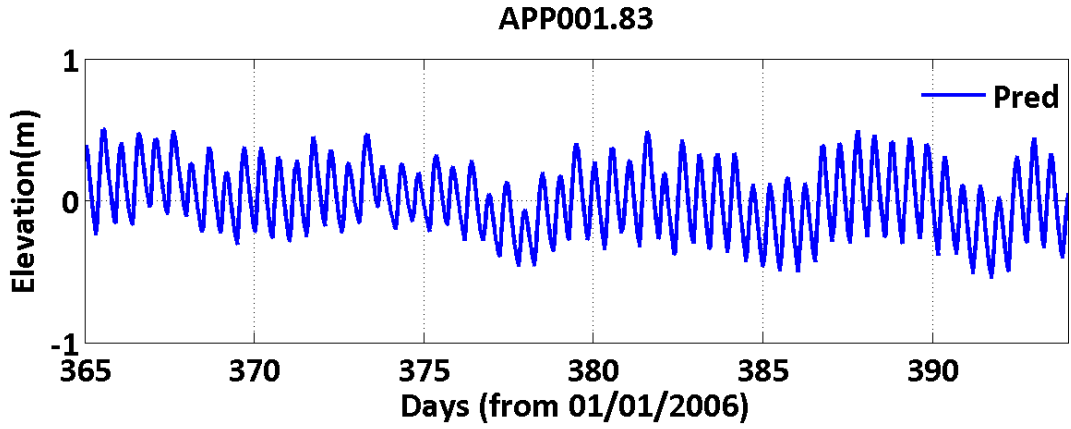


APP001.83

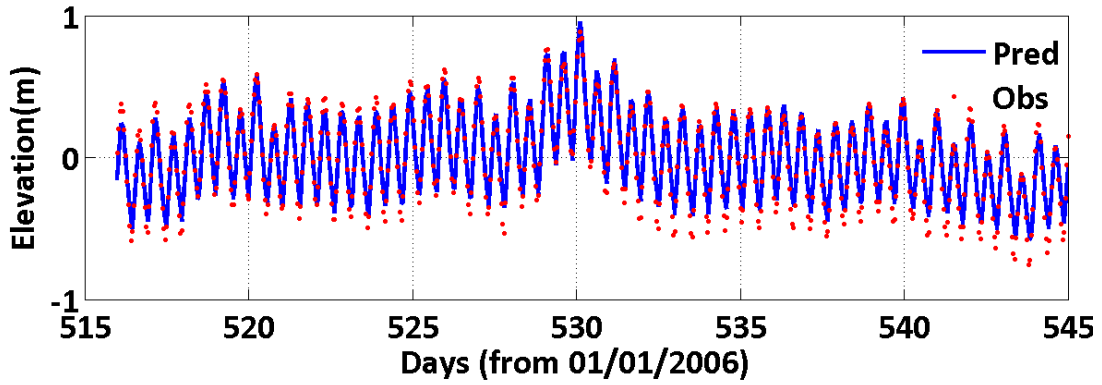
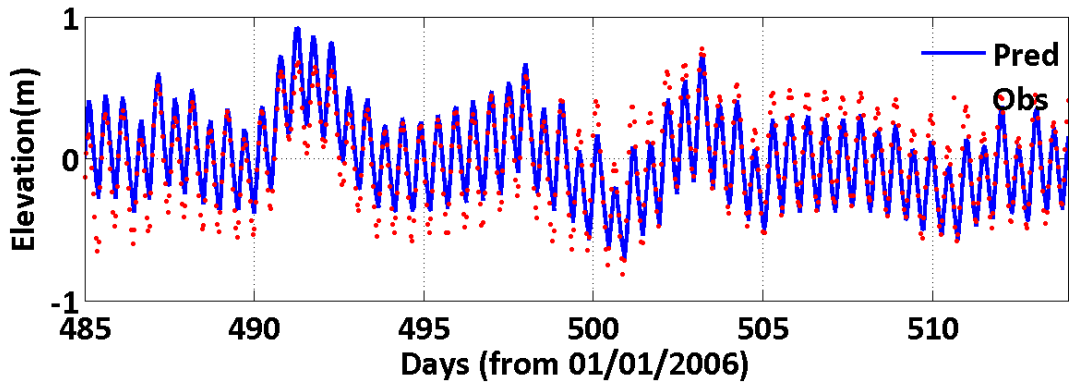


APP001.83

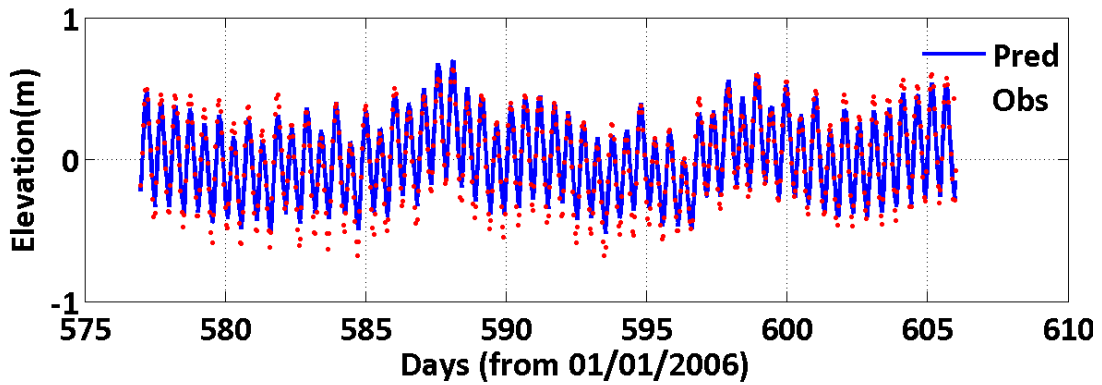
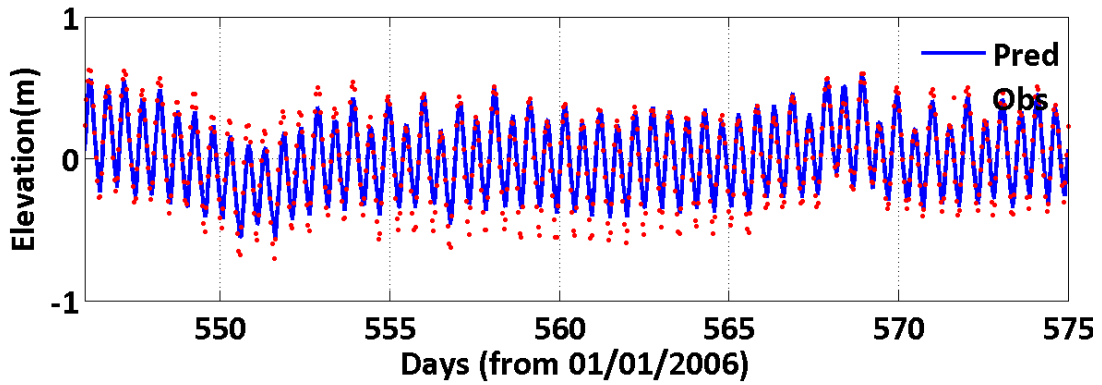




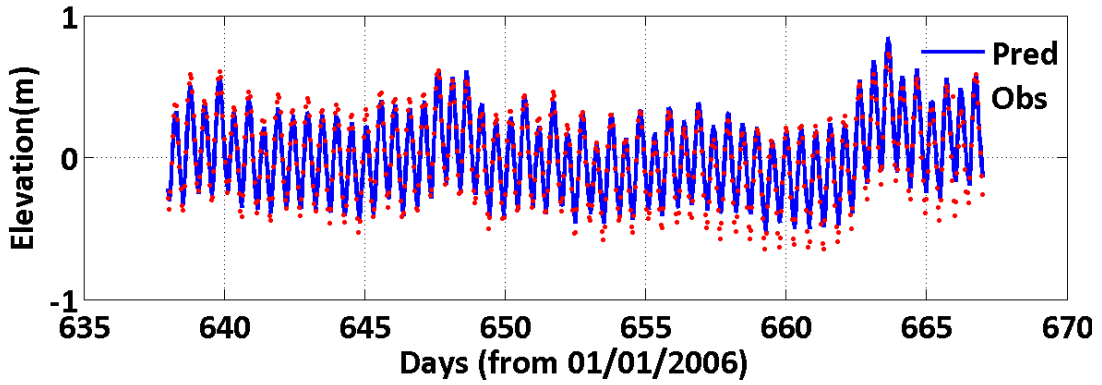
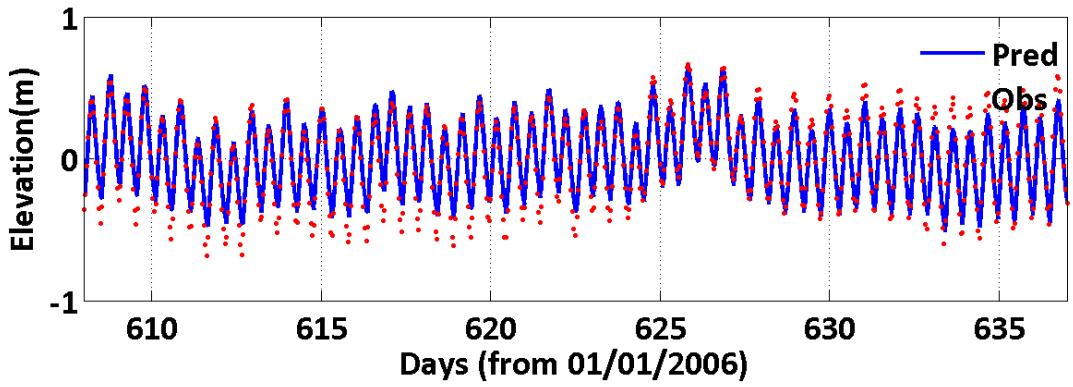
APP001.83



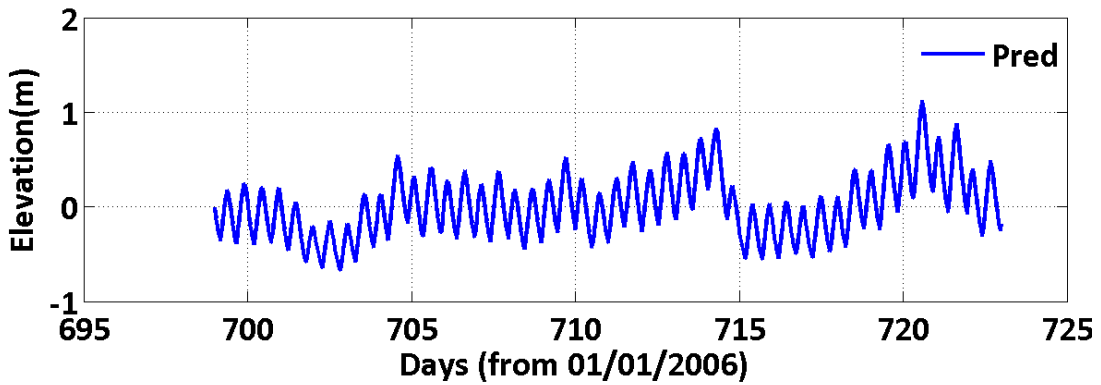
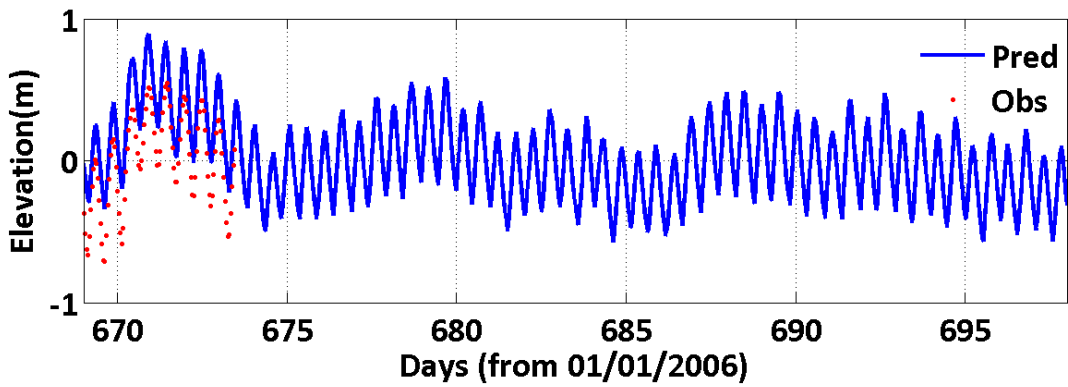
APP001.83



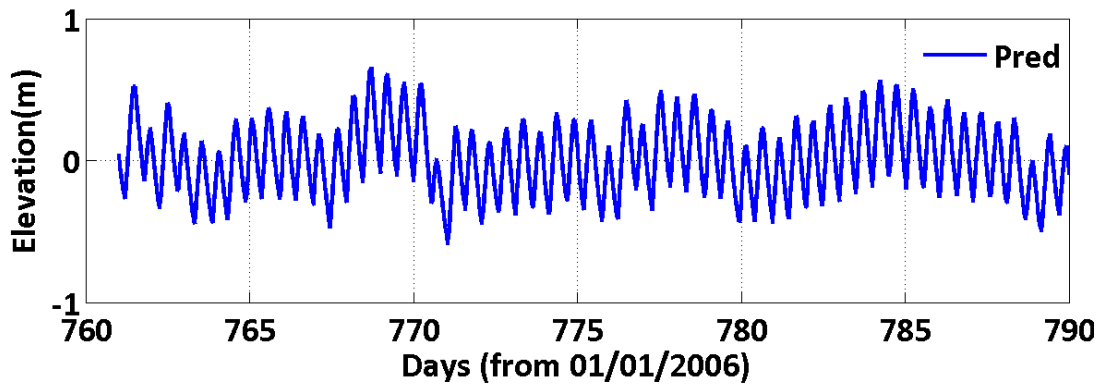
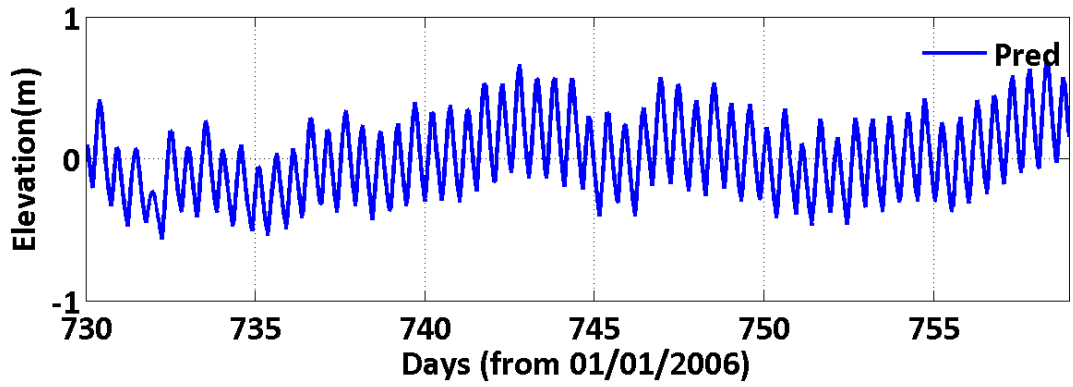
APP001.83



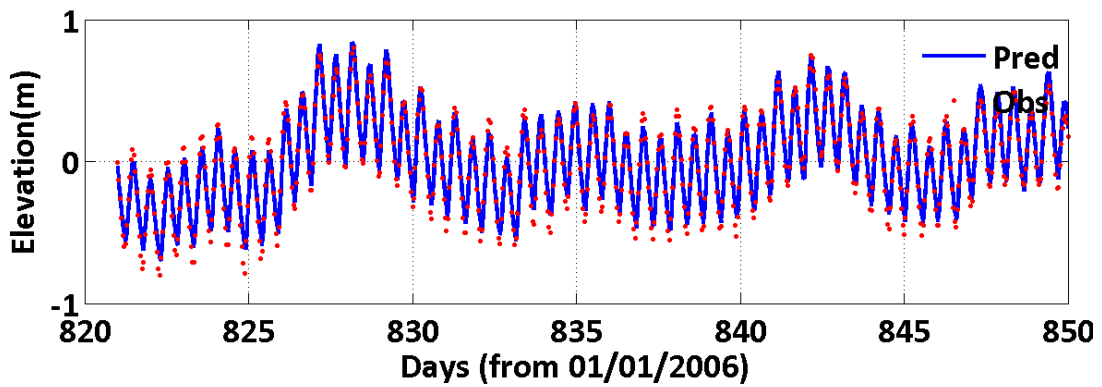
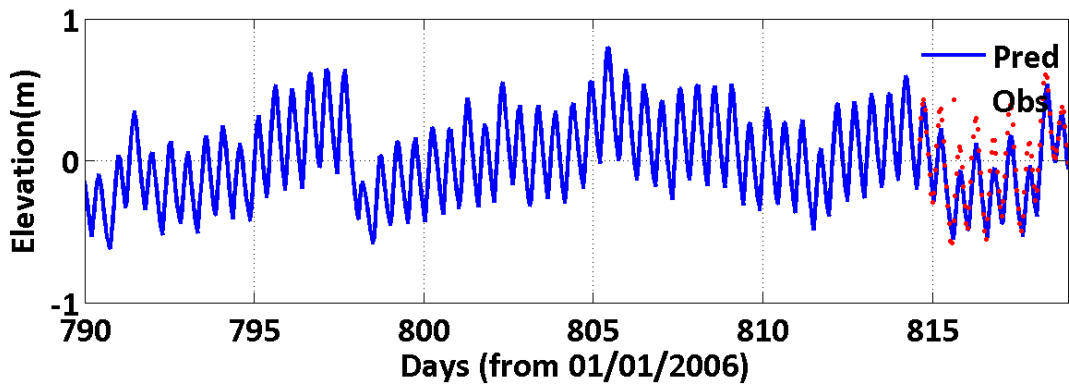
APP001.83

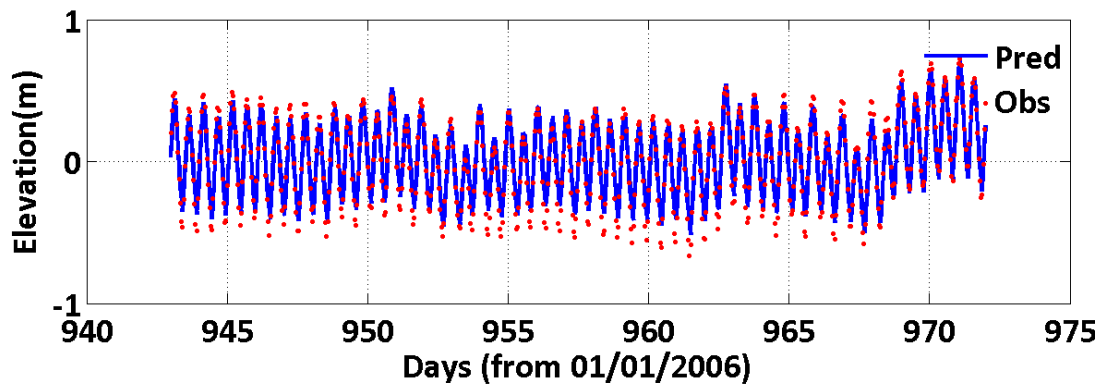
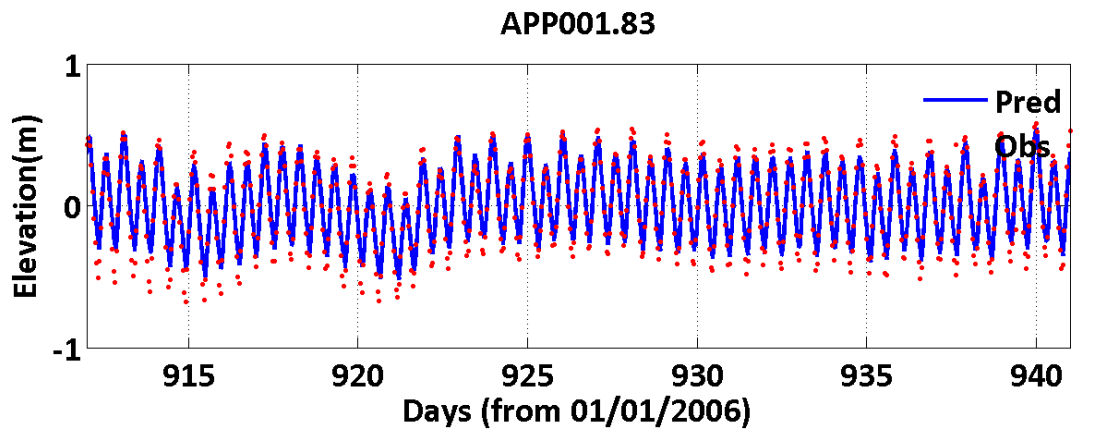
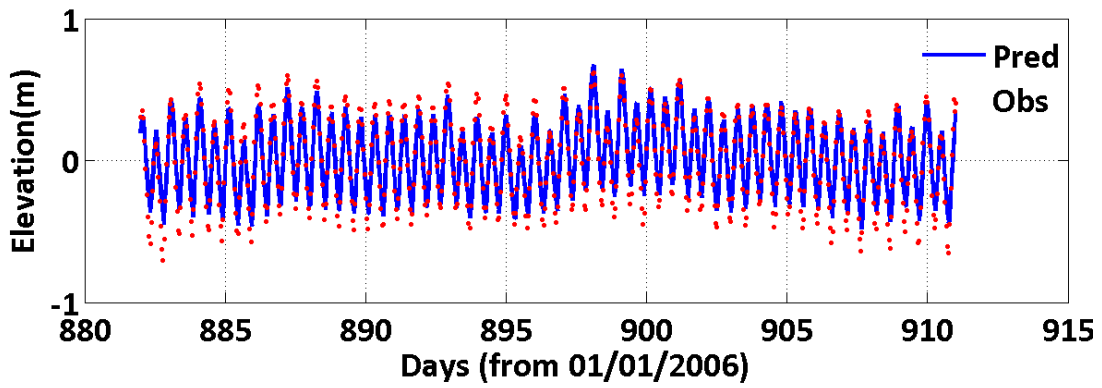
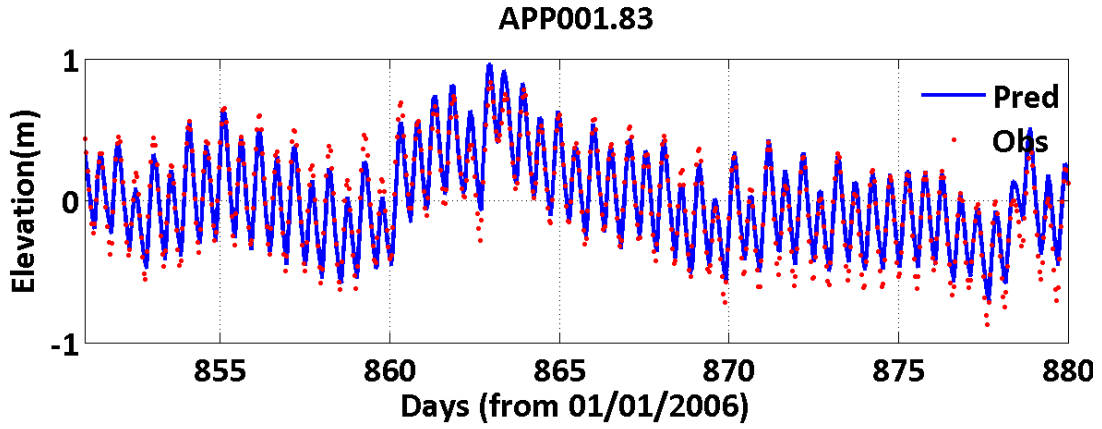


APP001.83

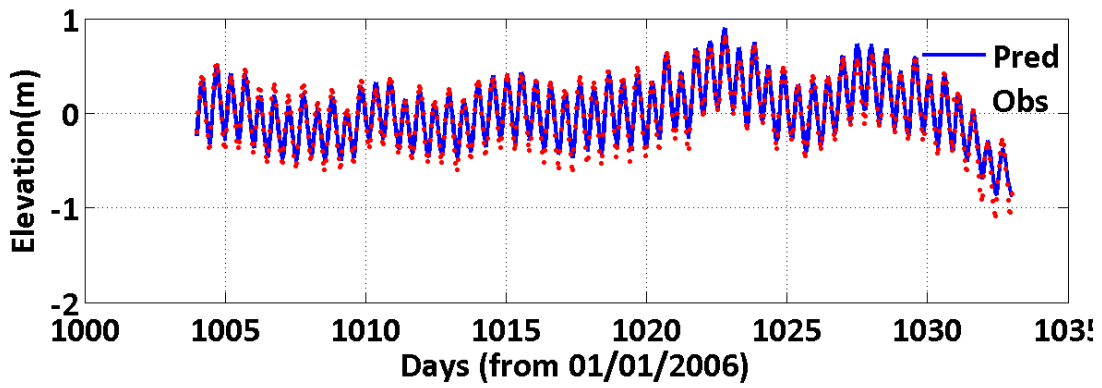
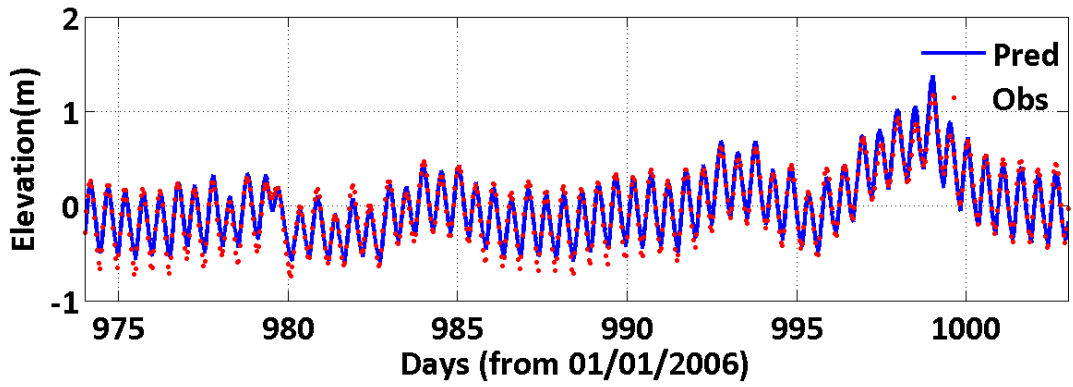


APP001.83

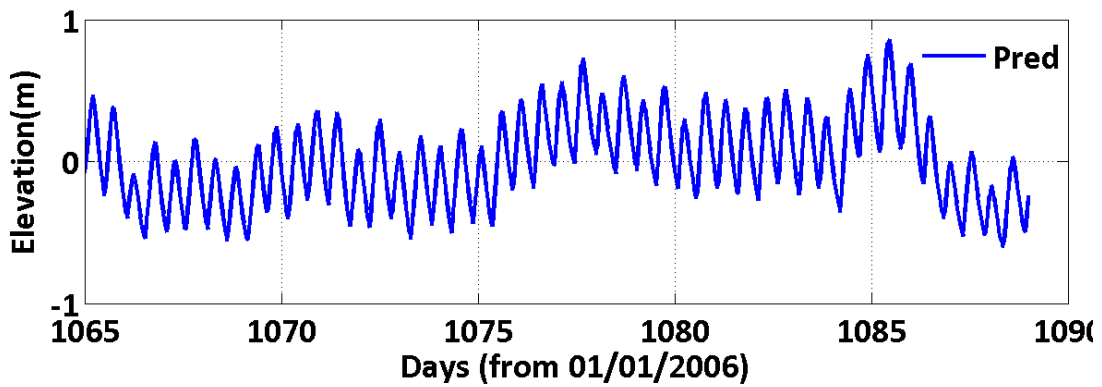
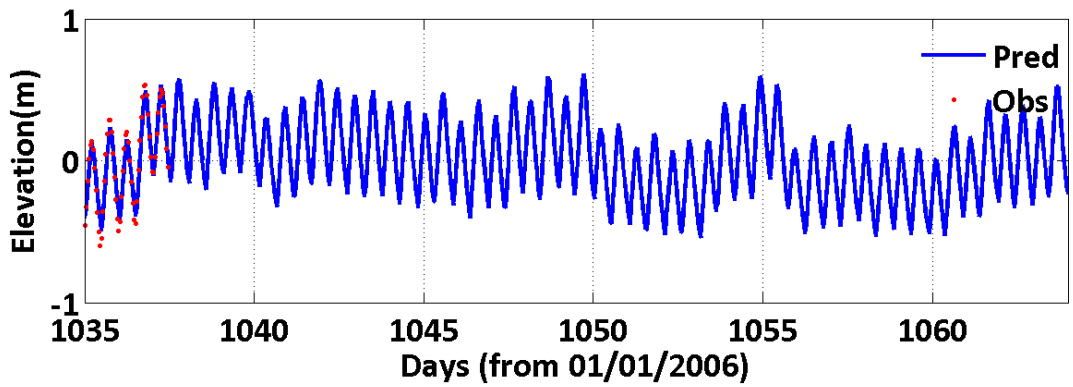




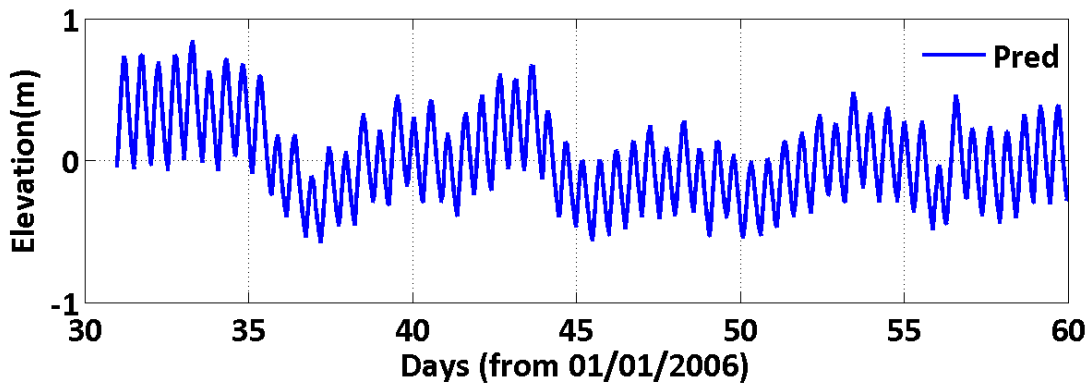
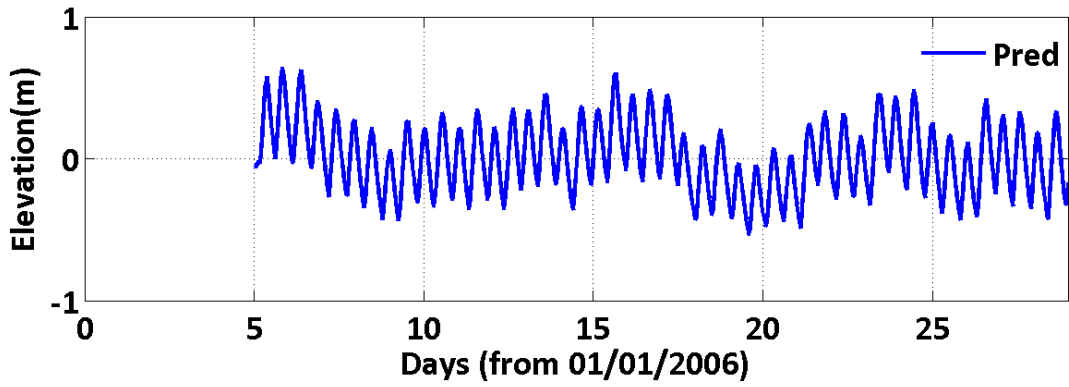
APP001.83



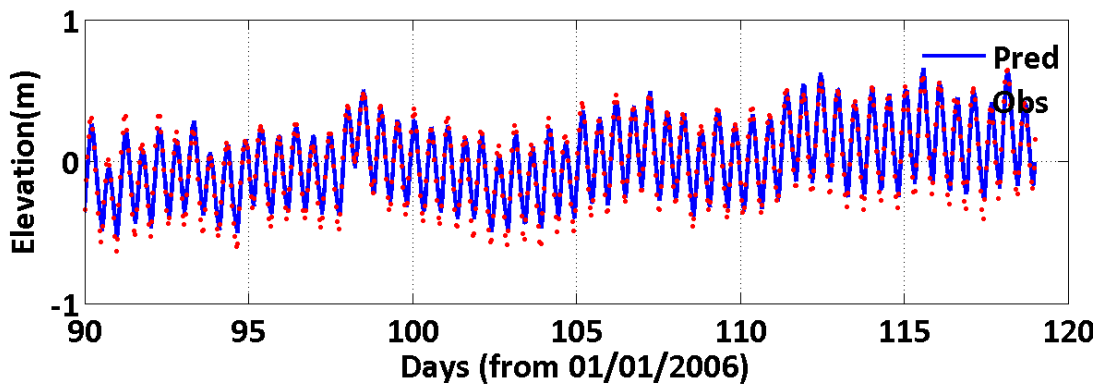
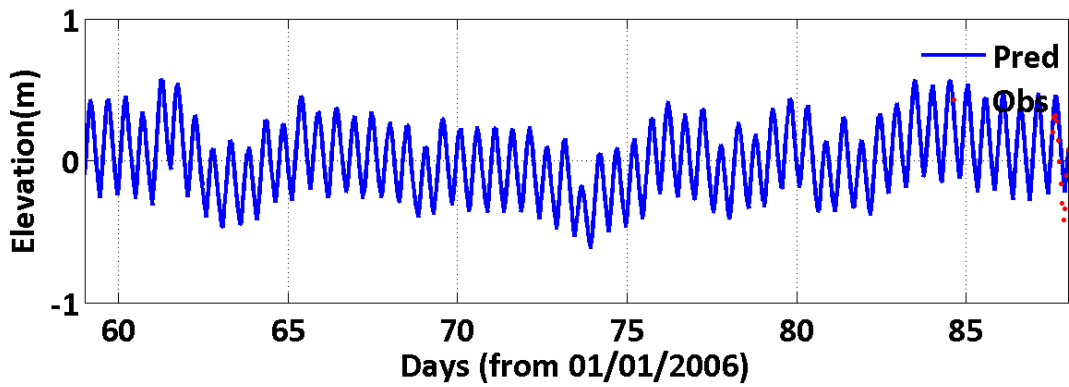
APP001.83



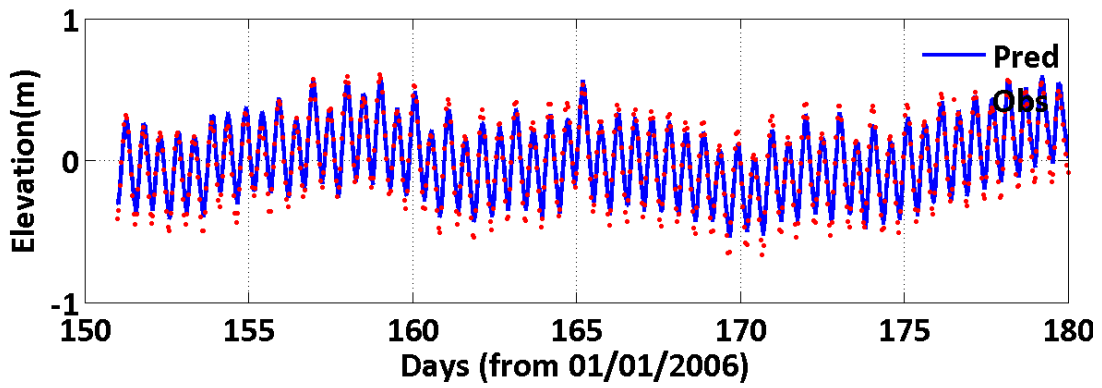
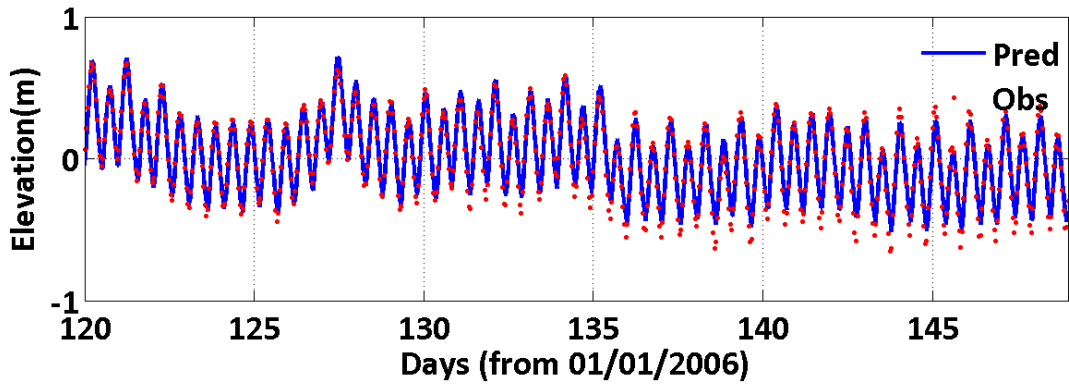
JMS073.37



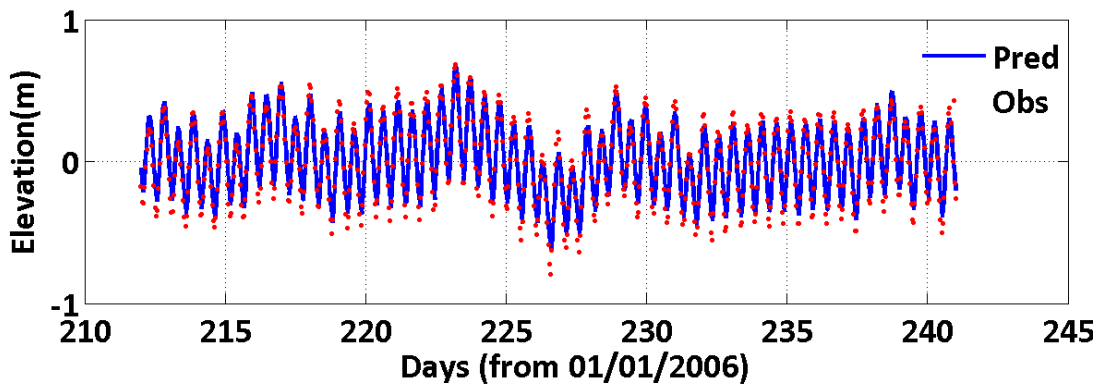
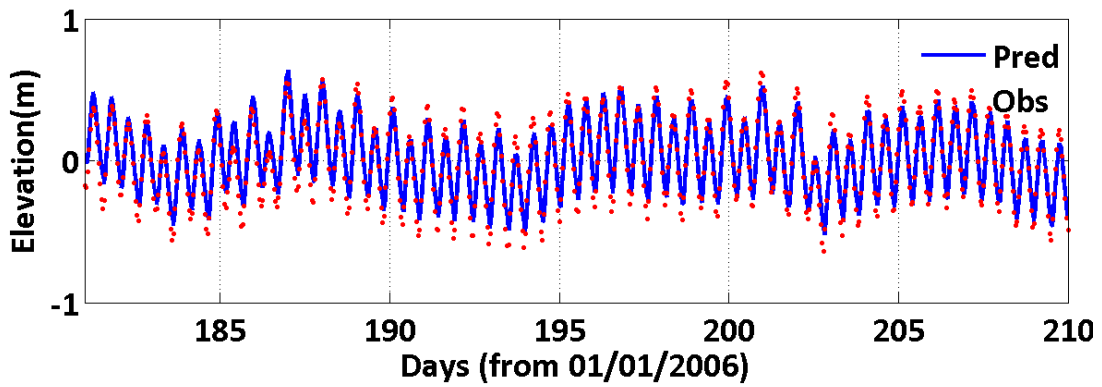
JMS073.37



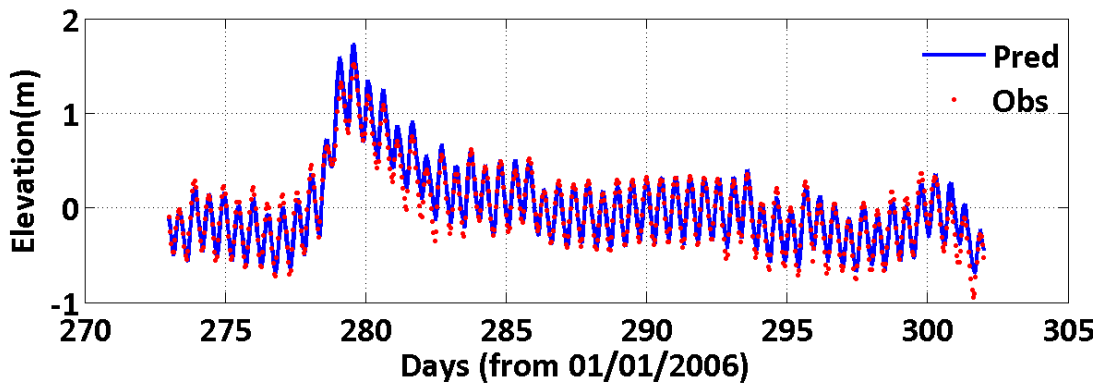
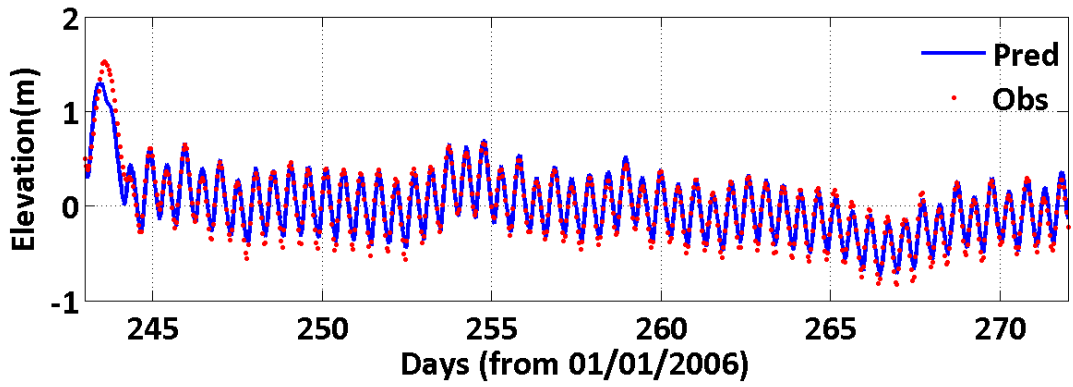
JMS073.37



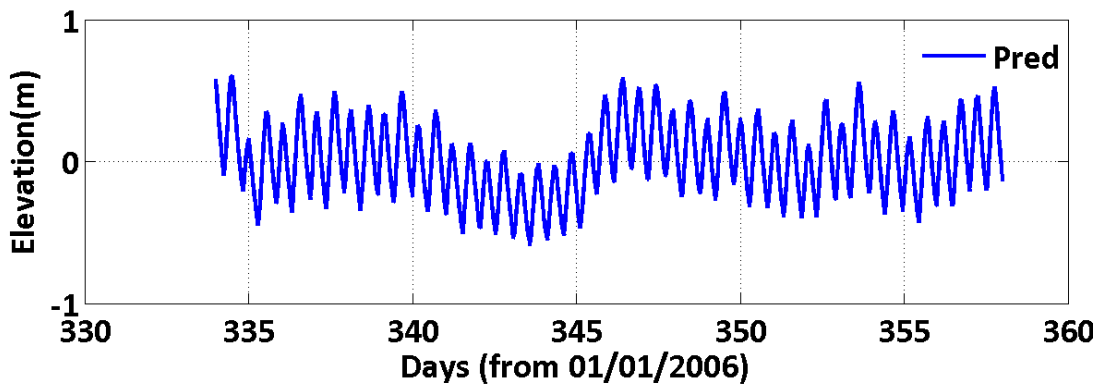
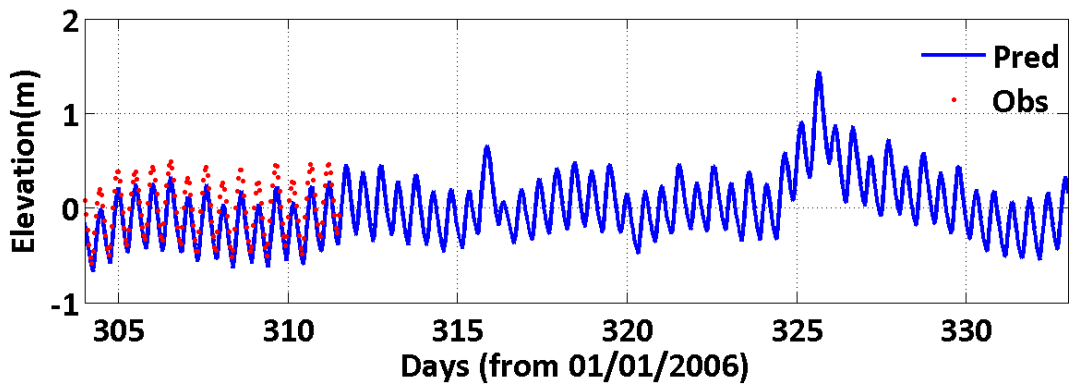
JMS073.37



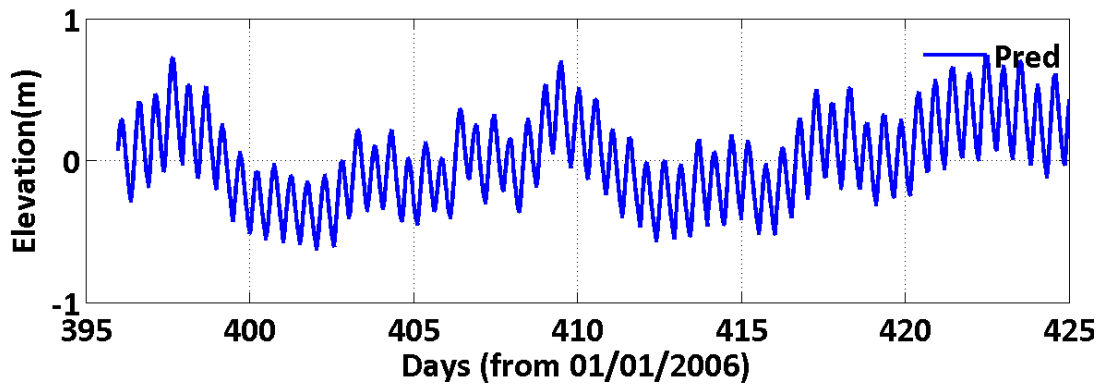
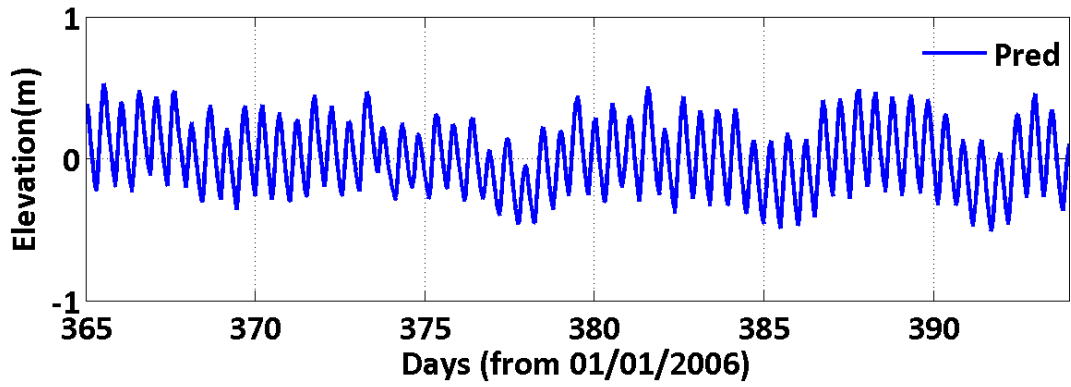
JMS073.37



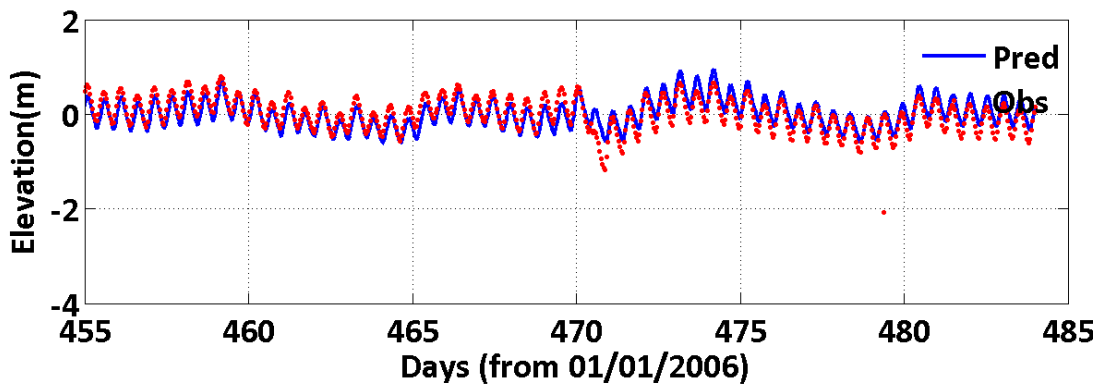
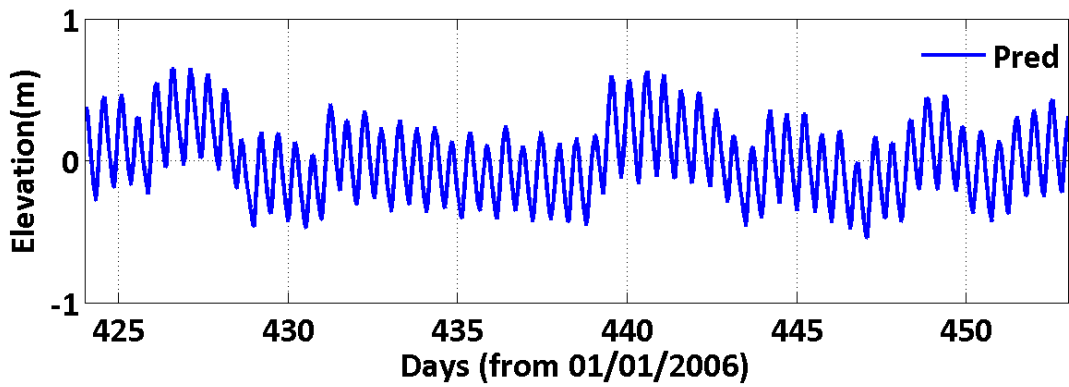
JMS073.37



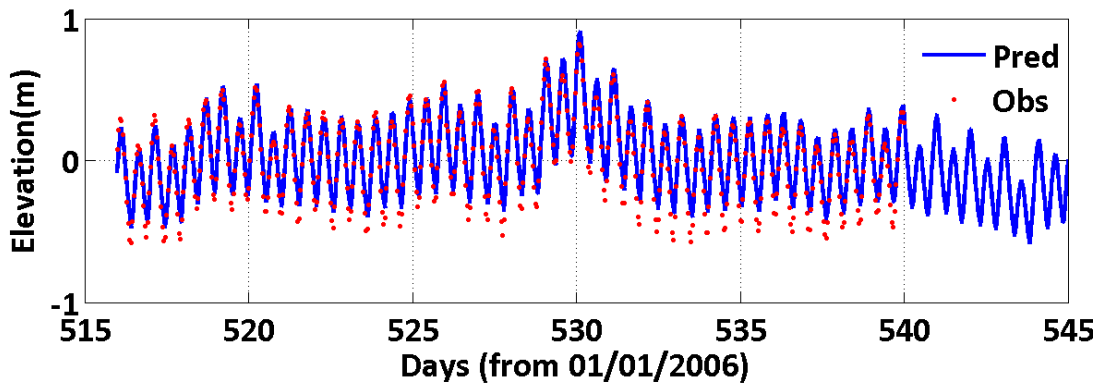
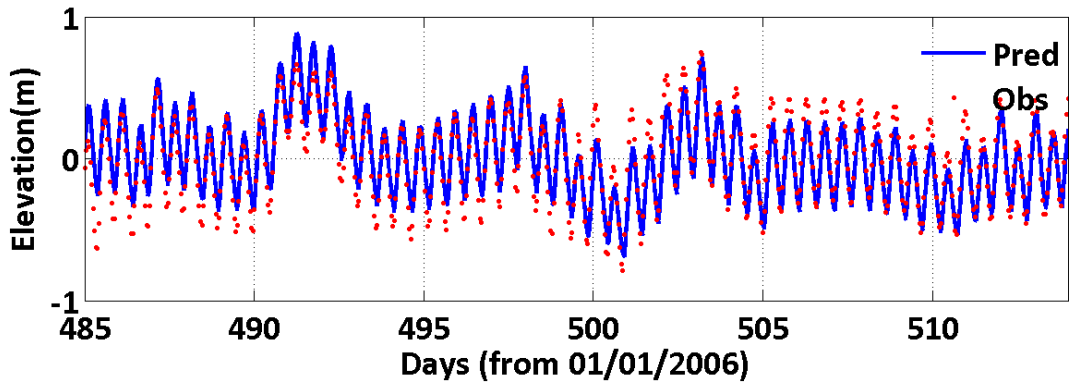
JMS073.37



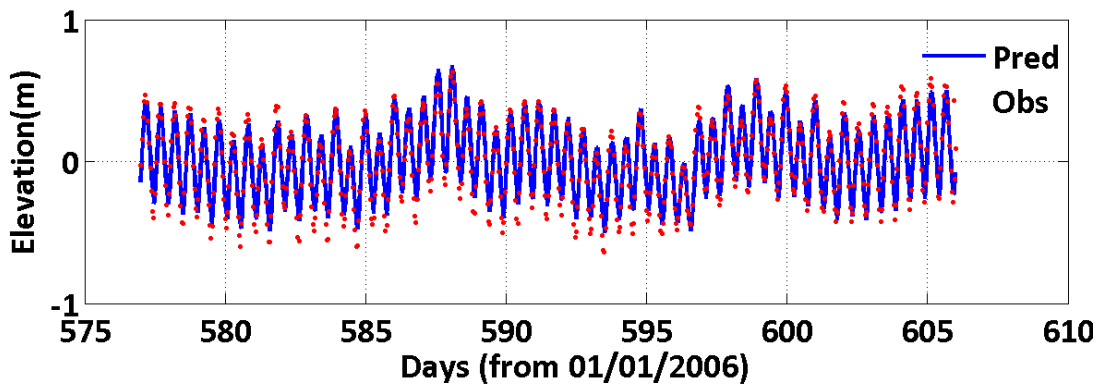
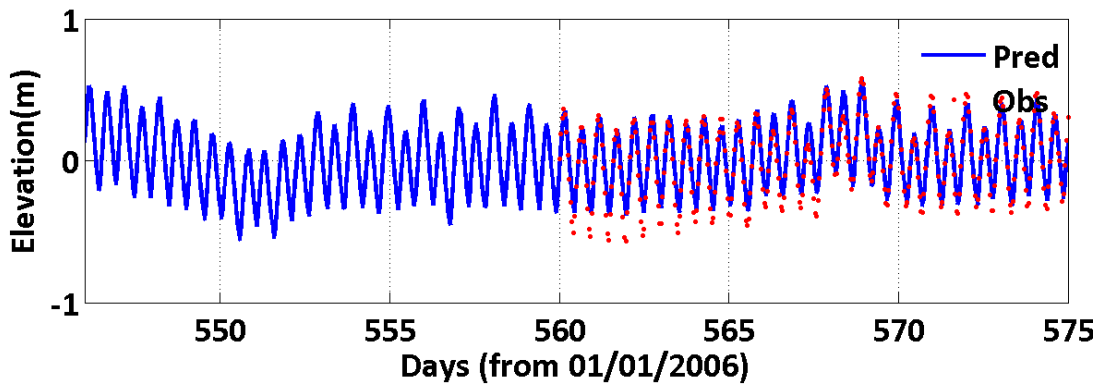
JMS073.37

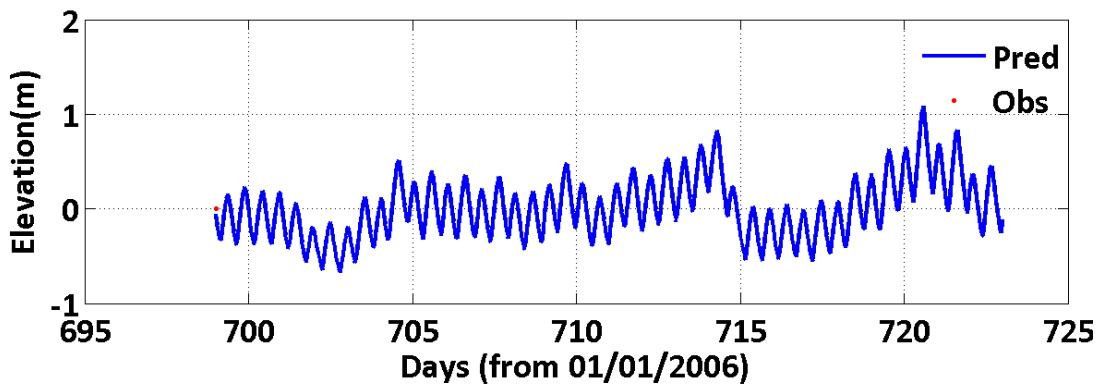
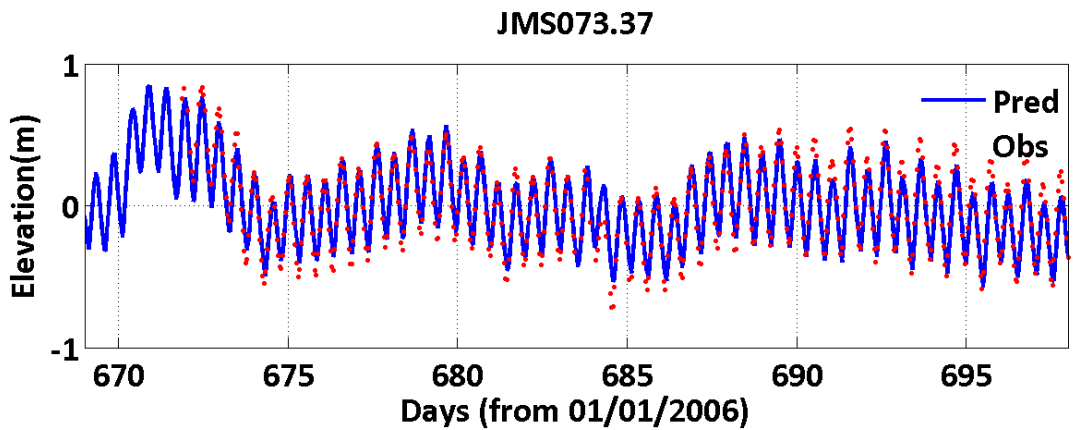
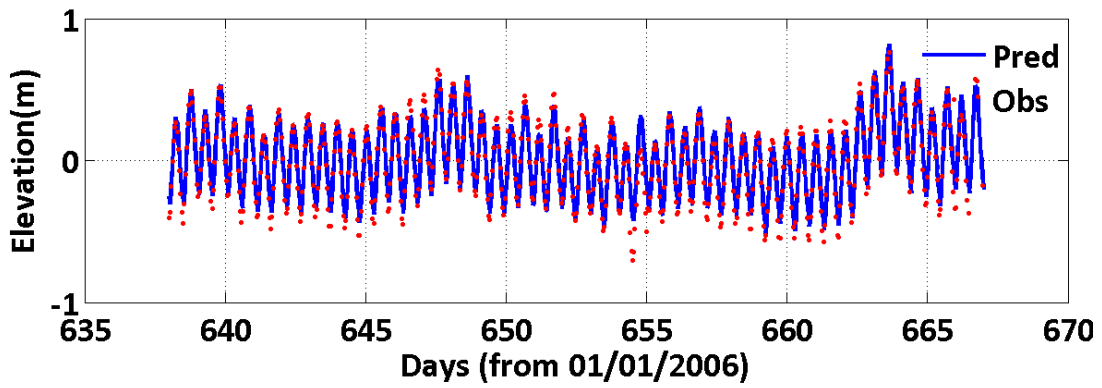
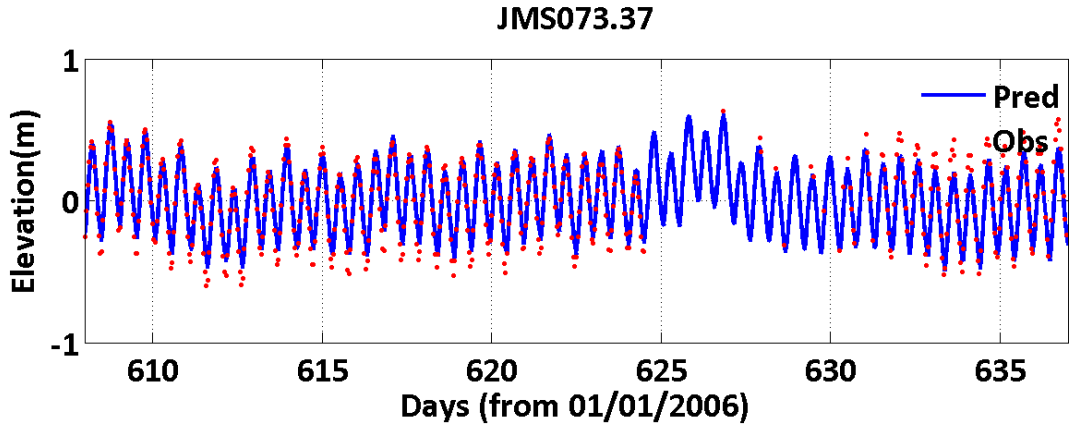


JMS073.37

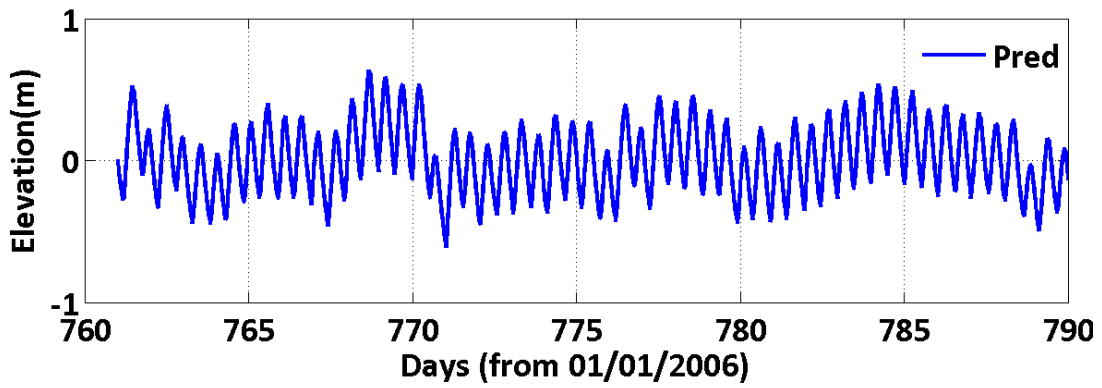
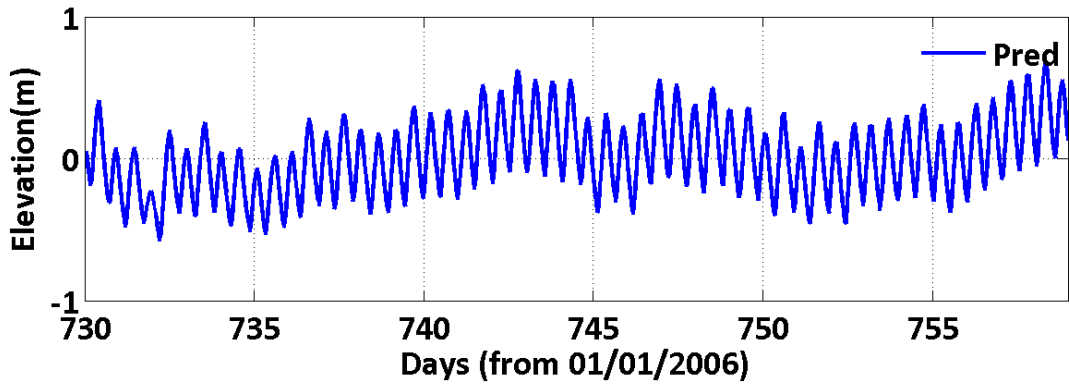


JMS073.37

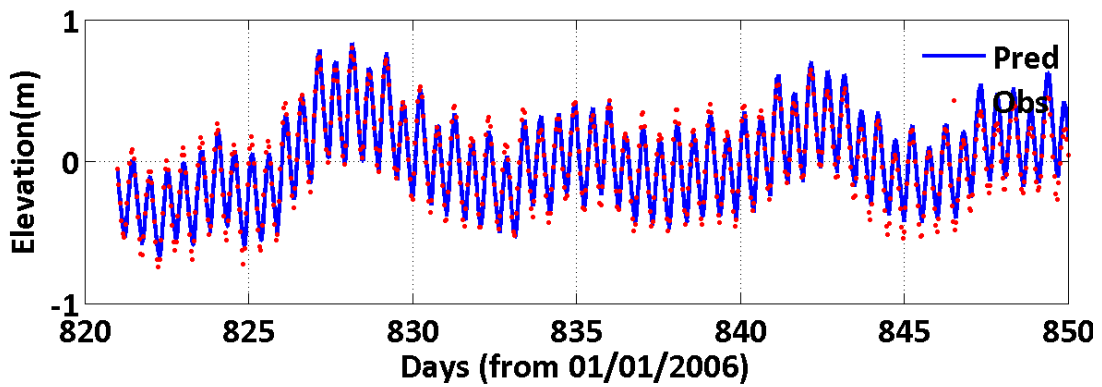
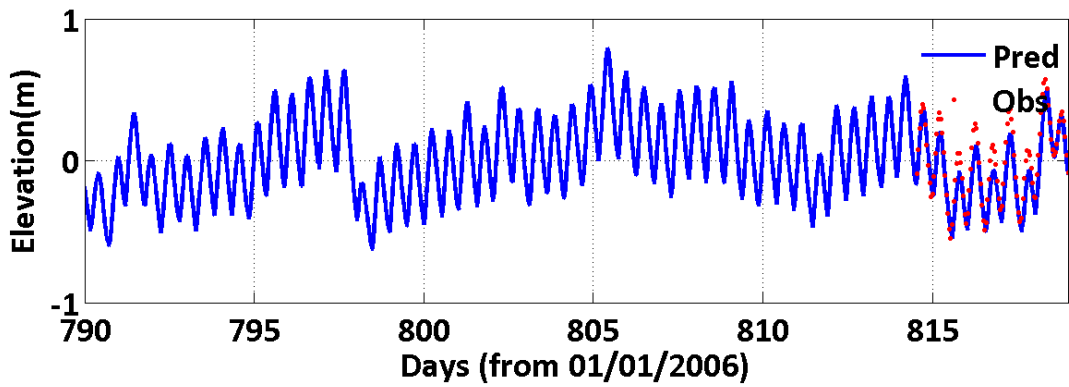


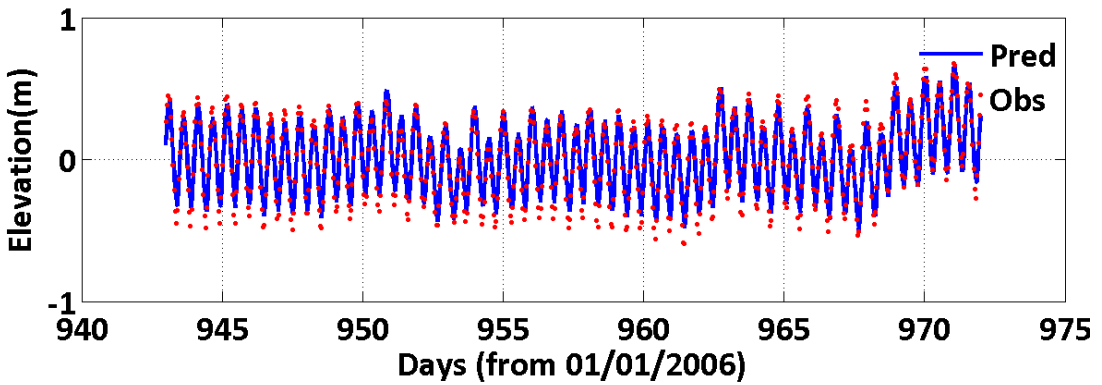
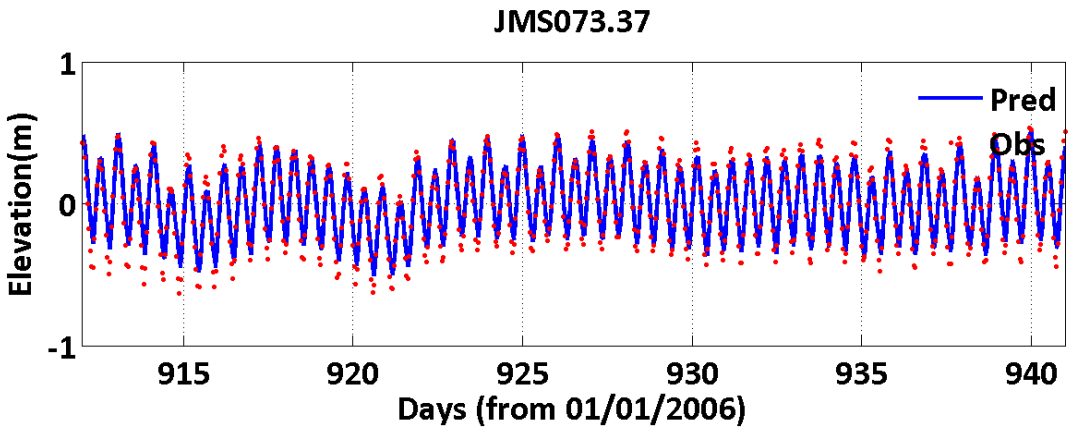
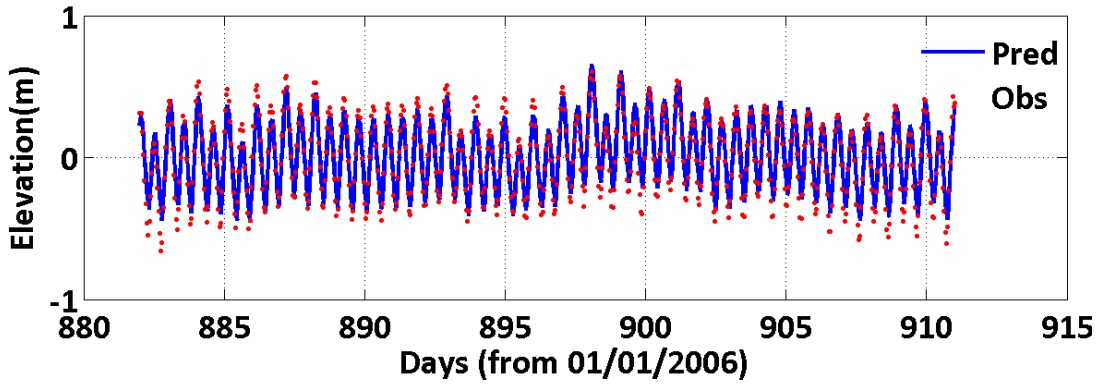
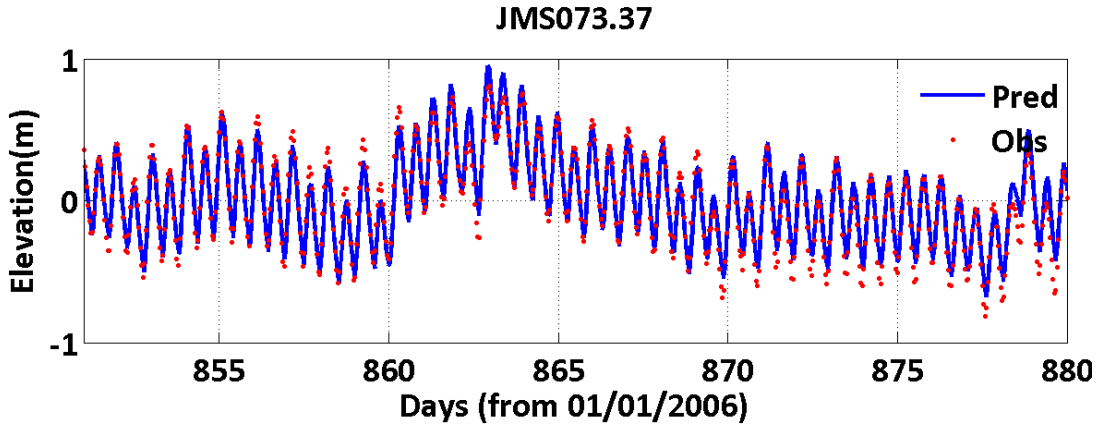


JMS073.37

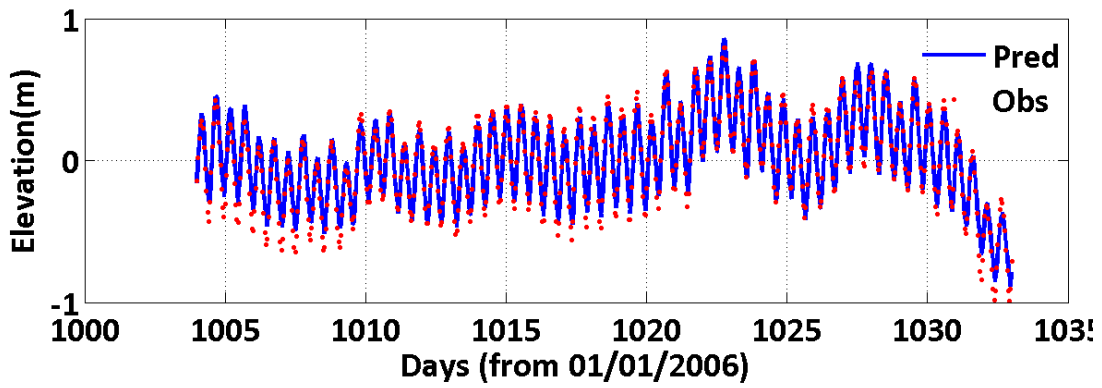
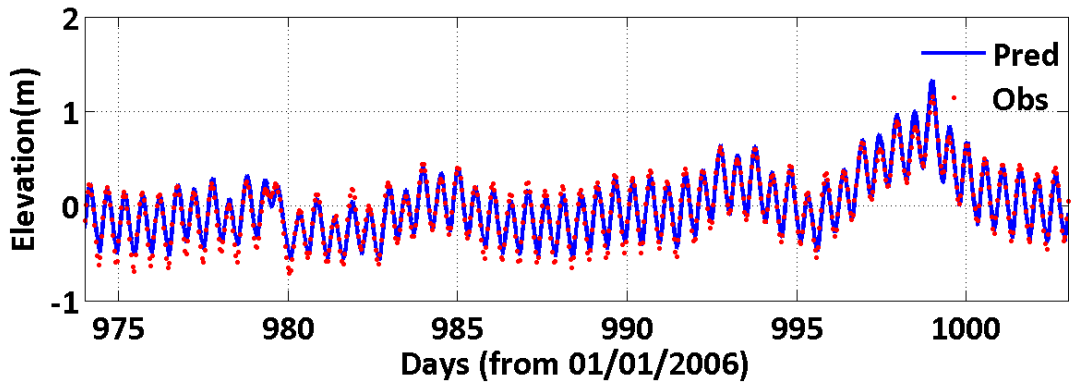


JMS073.37

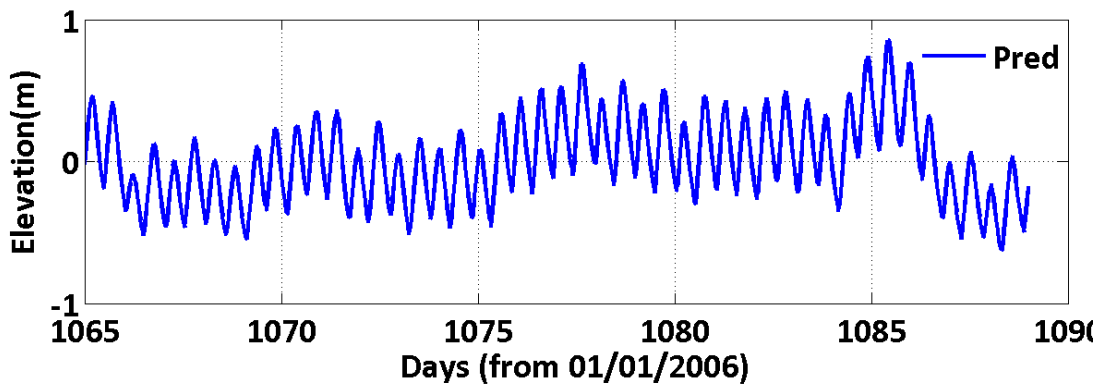
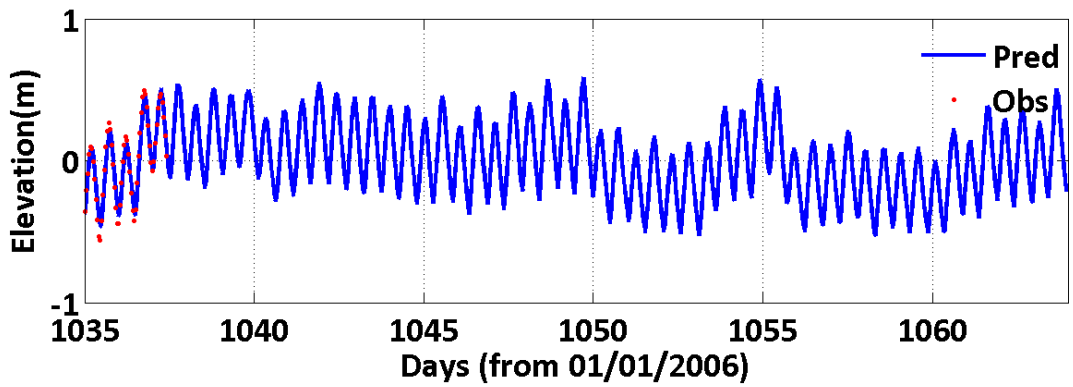




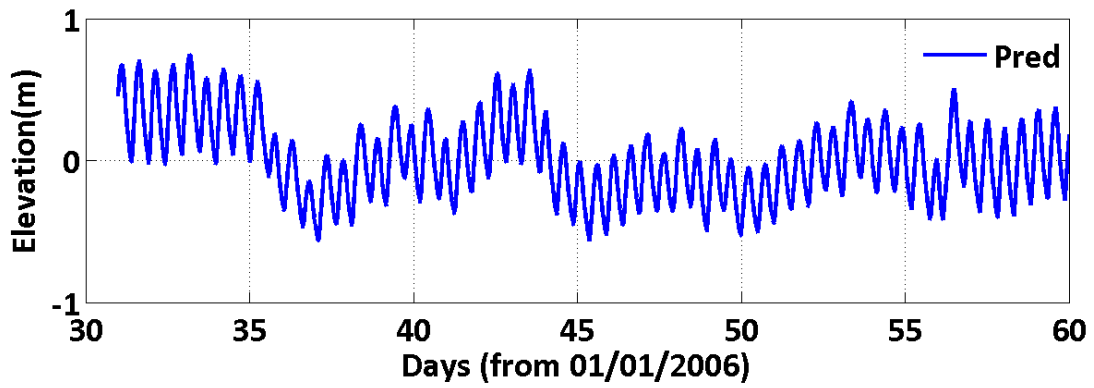
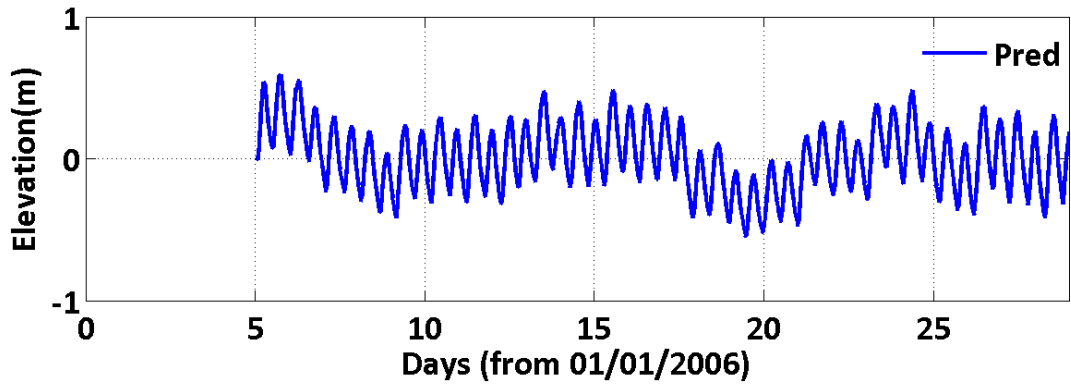
JMS073.37



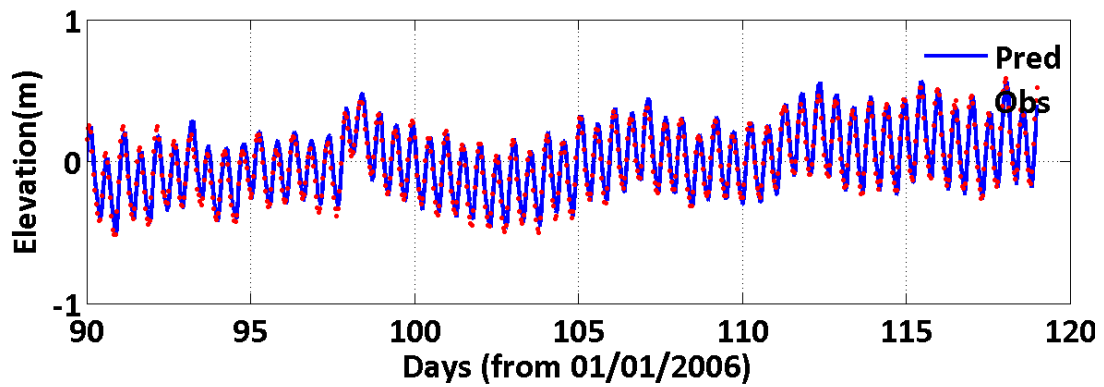
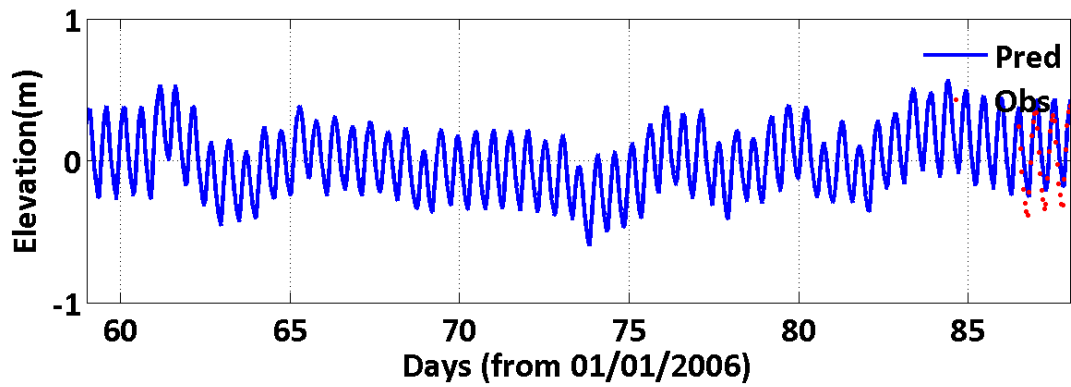
JMS073.37



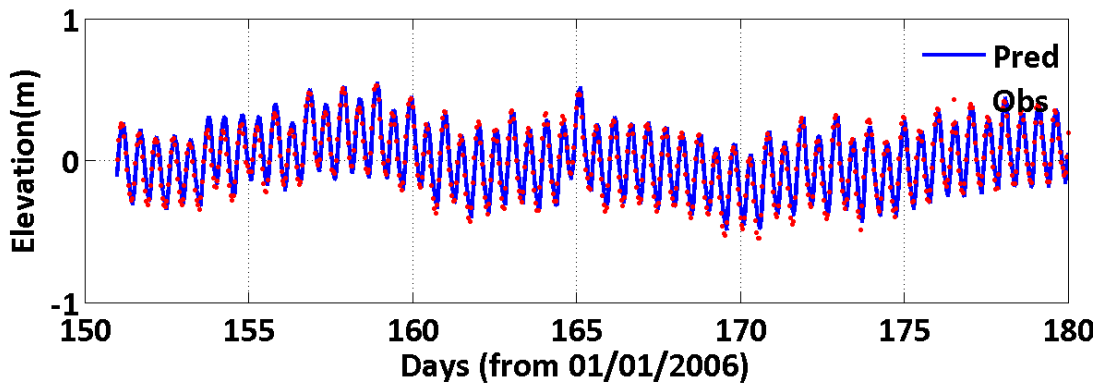
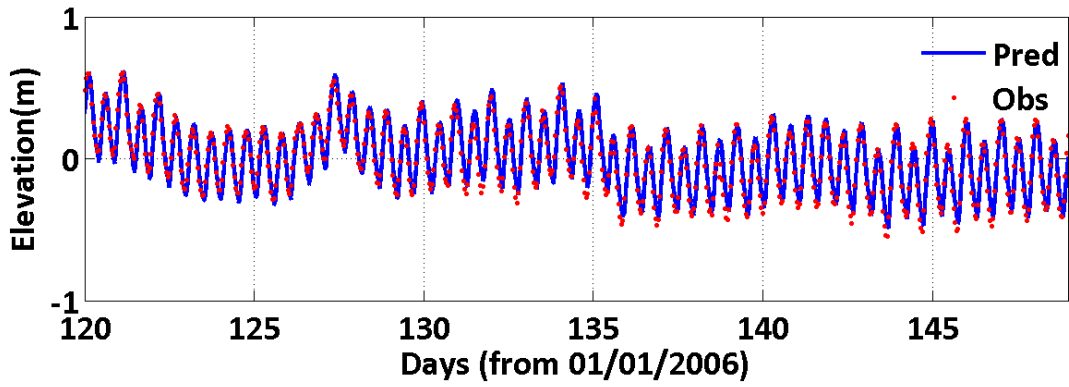
JMS043.78



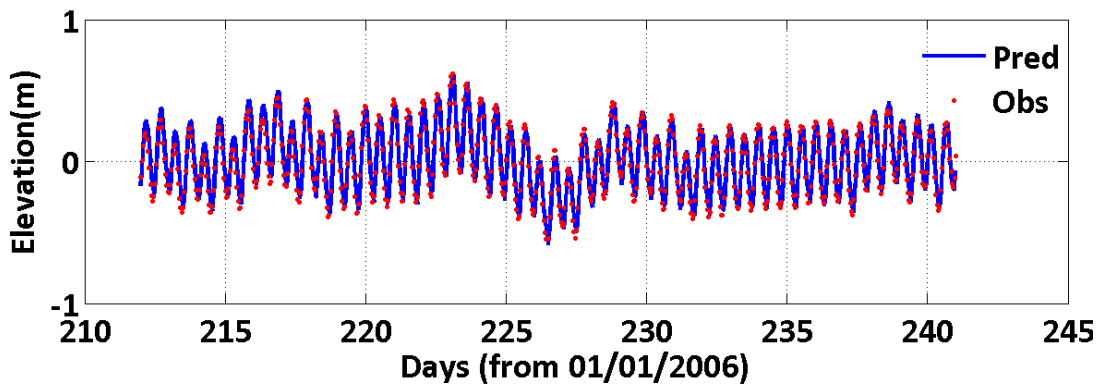
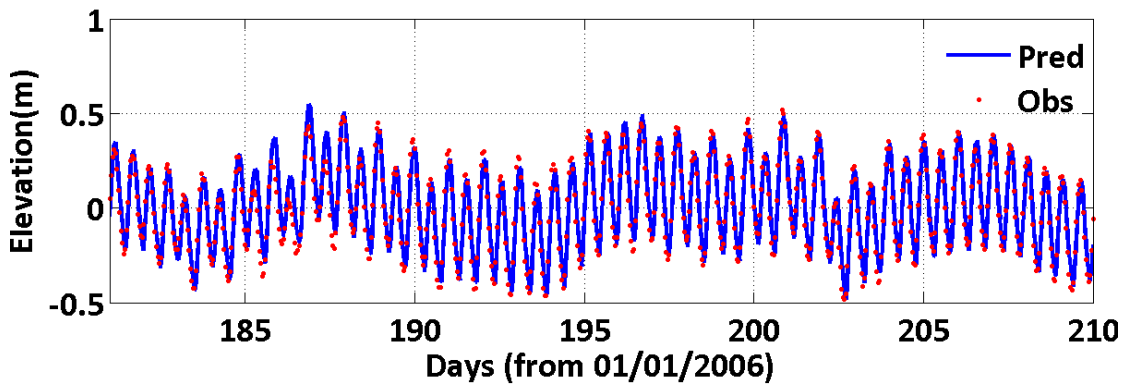
JMS043.78



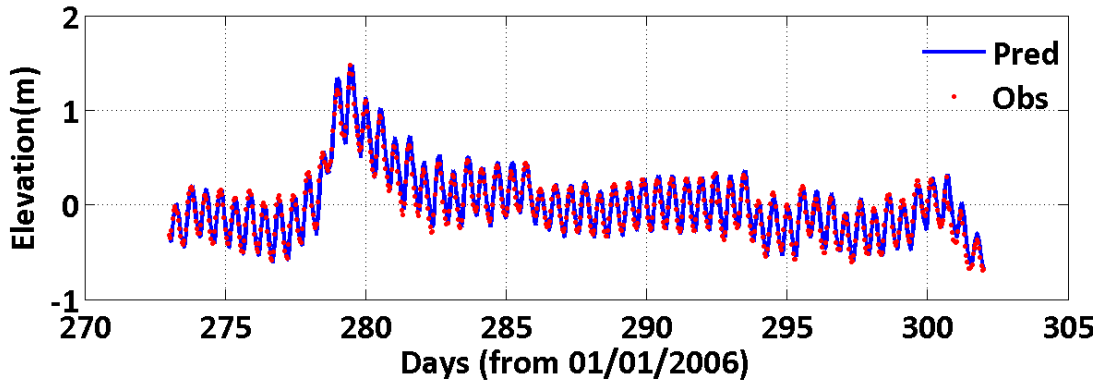
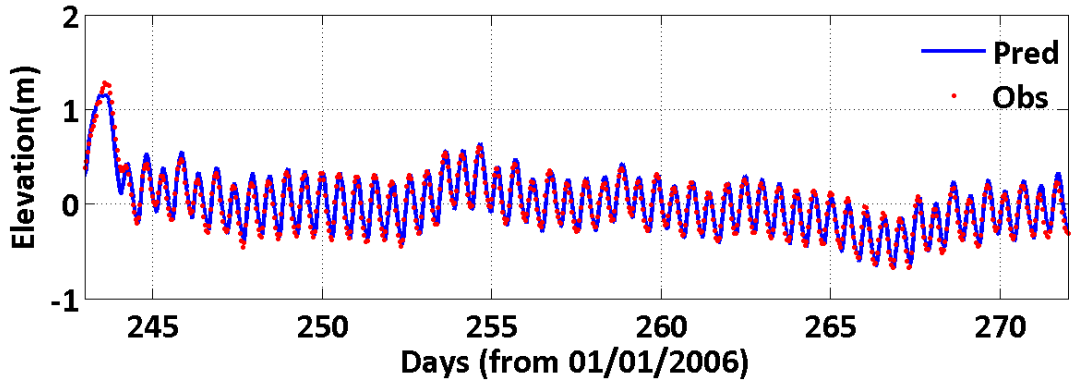
JMS043.78



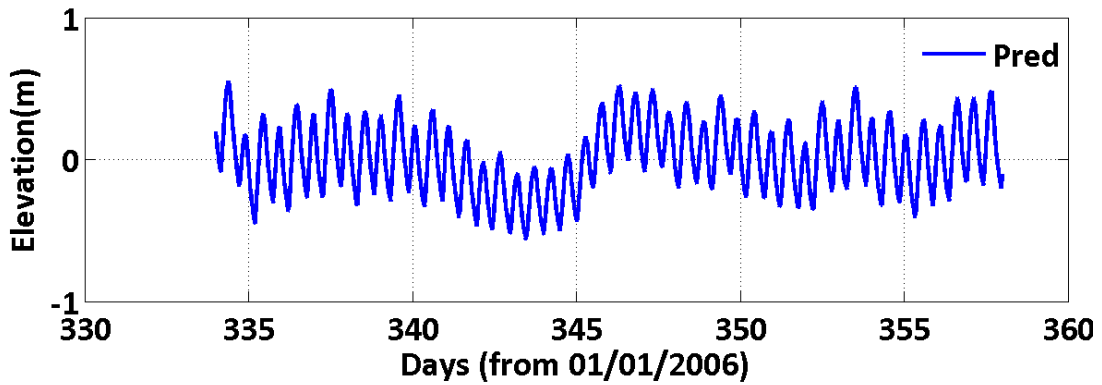
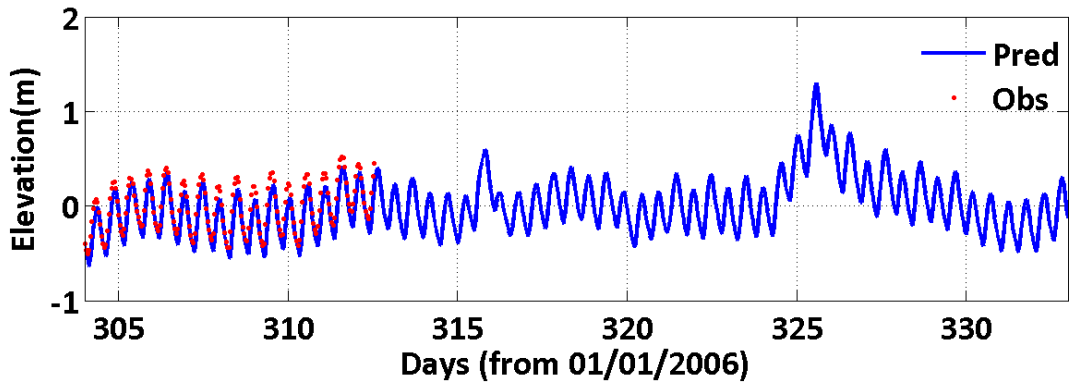
JMS043.78

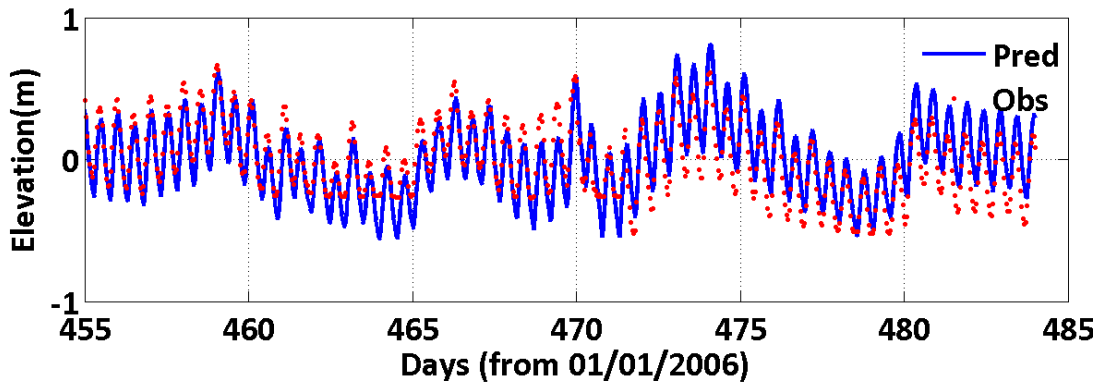
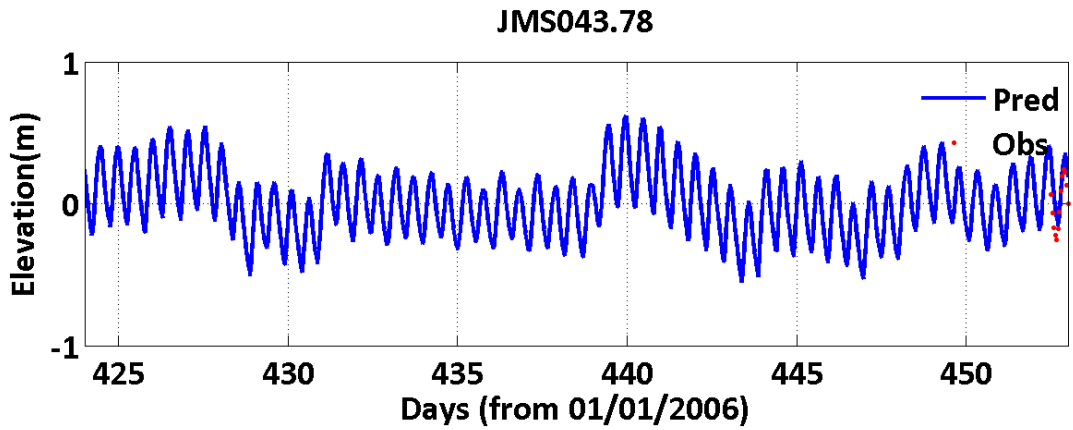
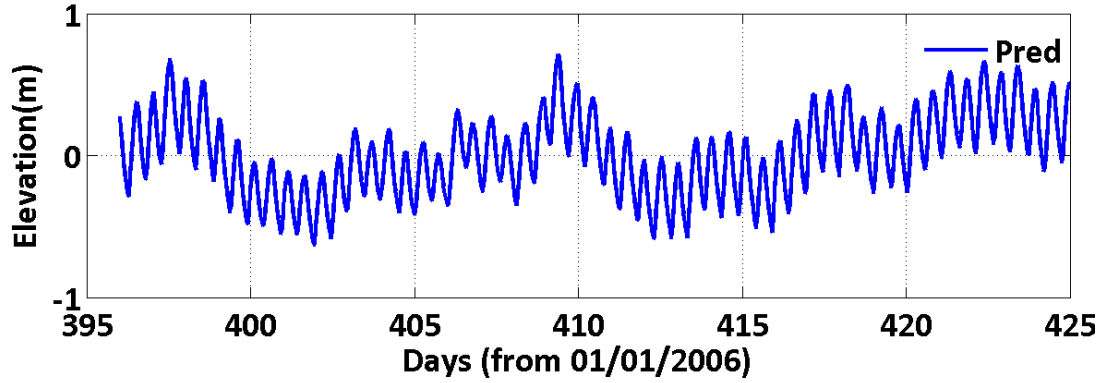
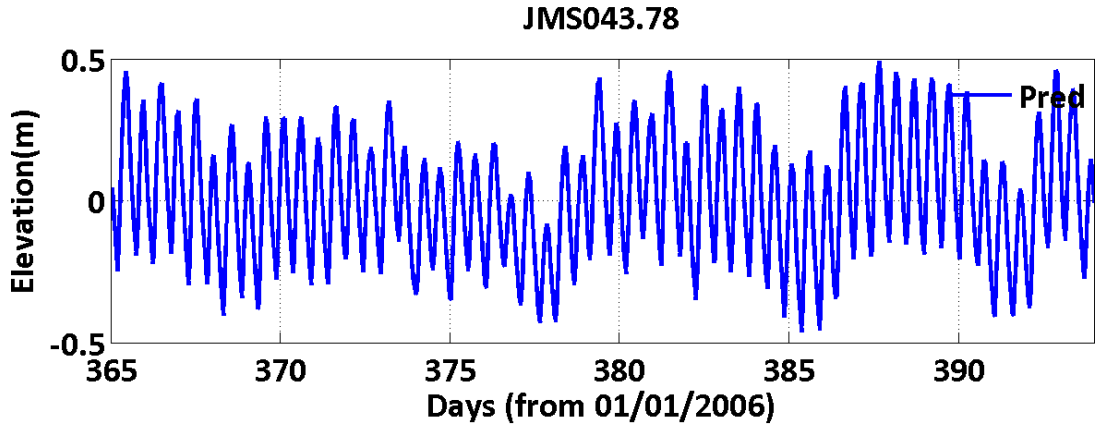


JMS043.78

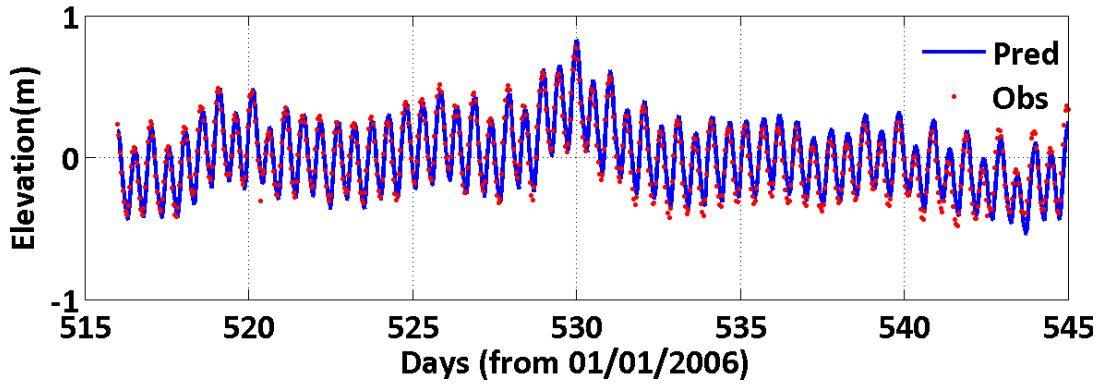
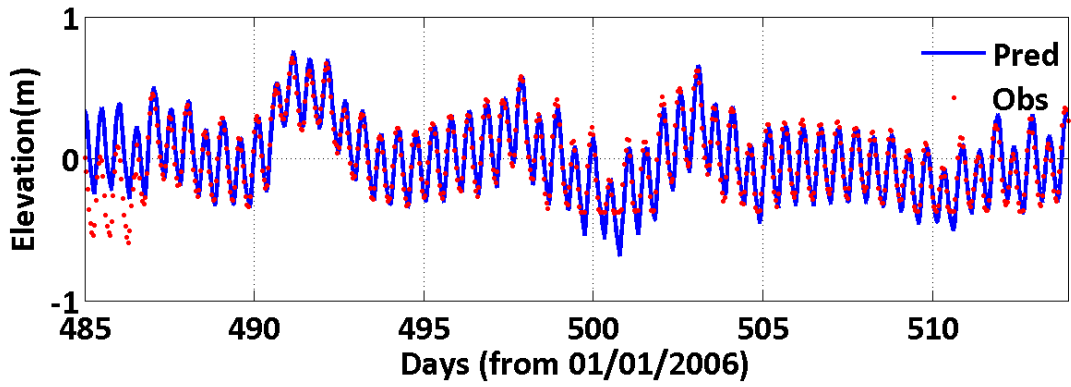


JMS043.78

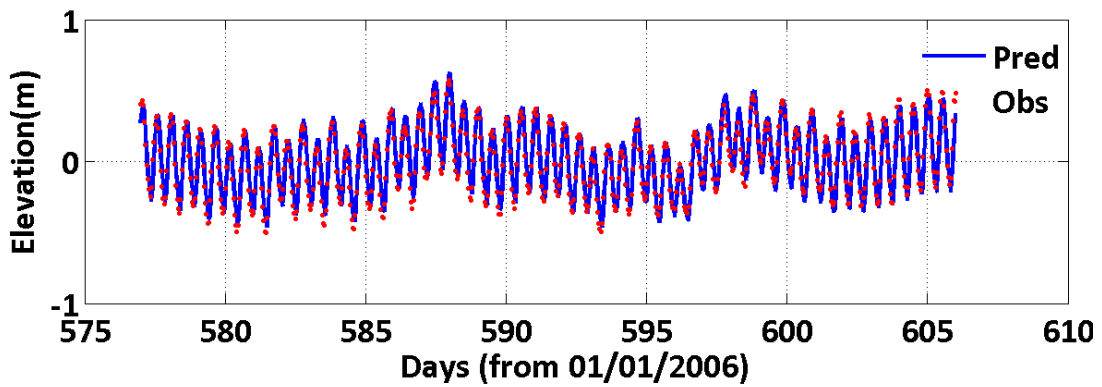
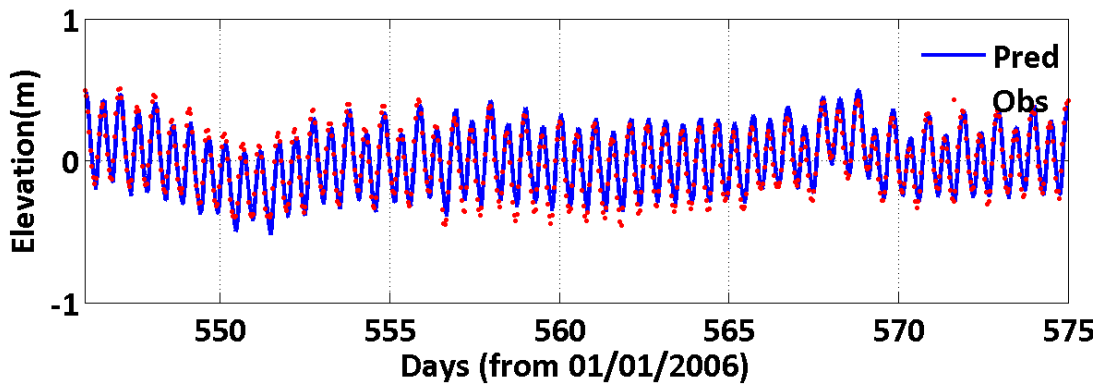


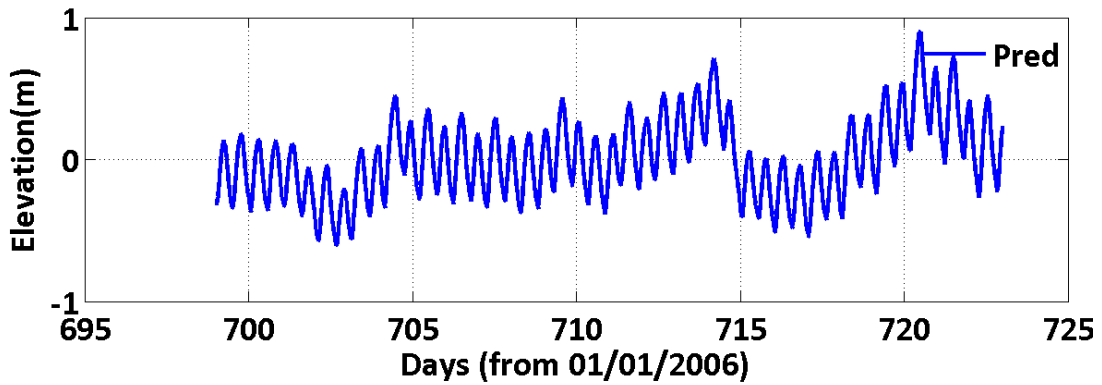
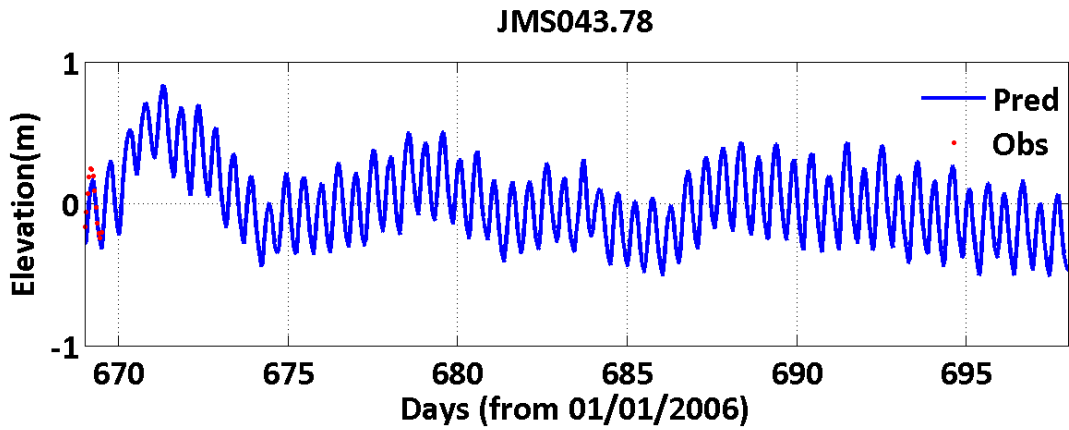
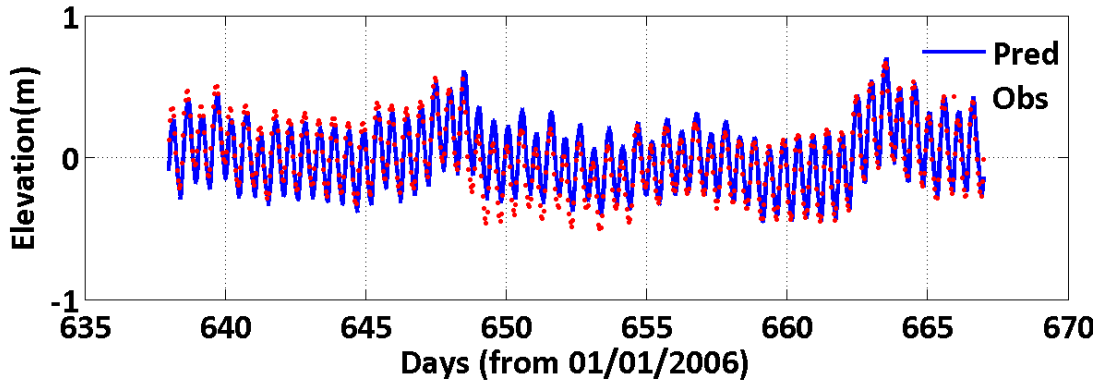
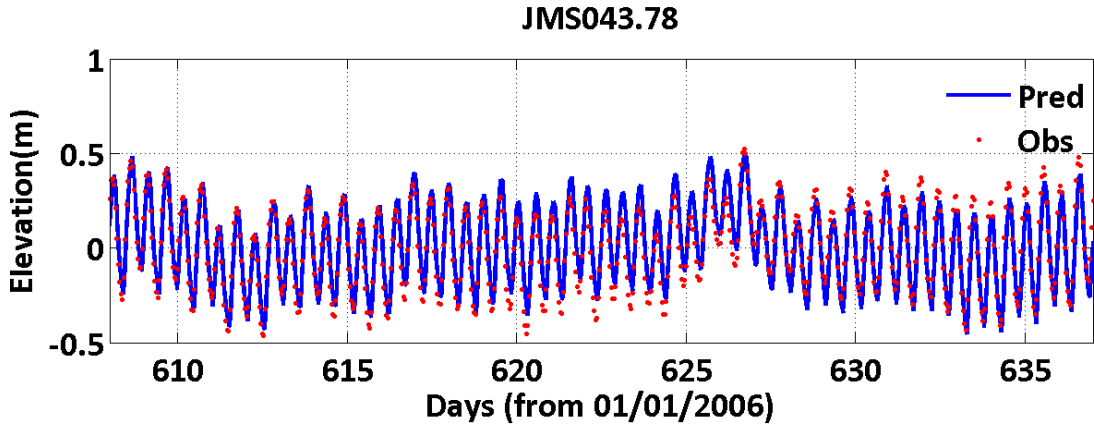


JMS043.78

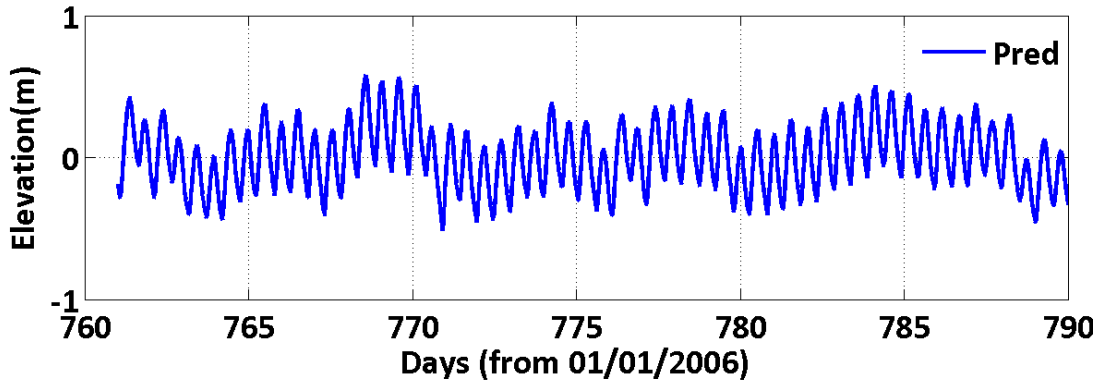
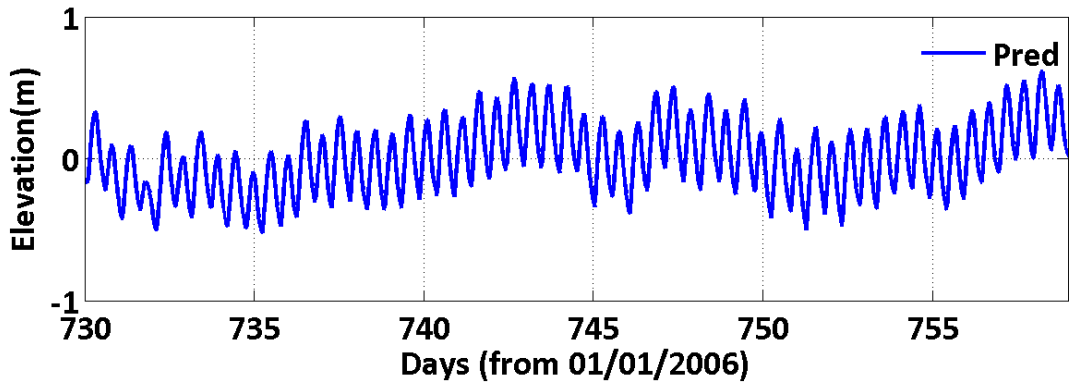


JMS043.78

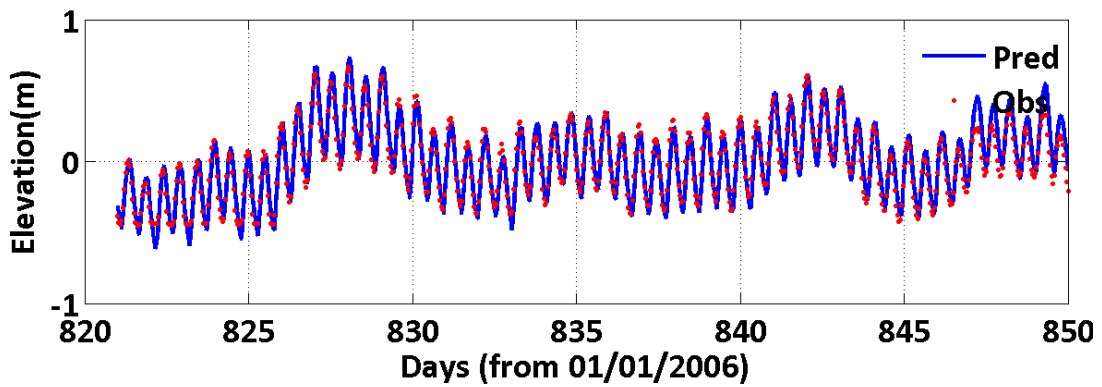
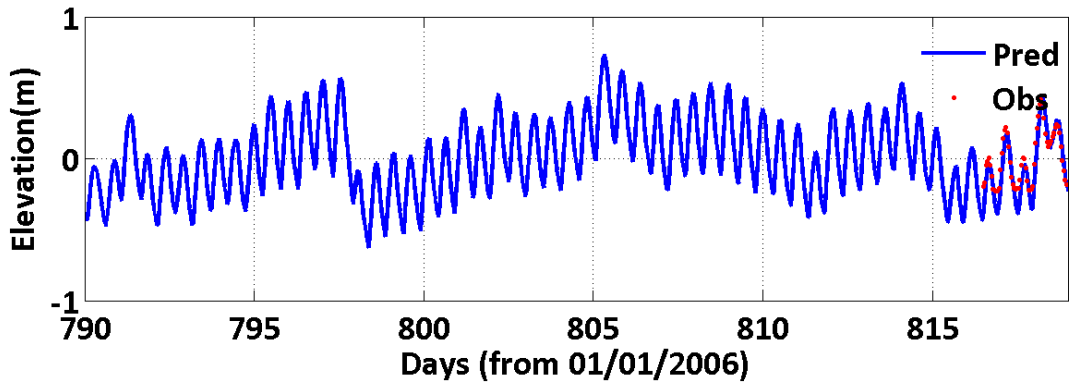




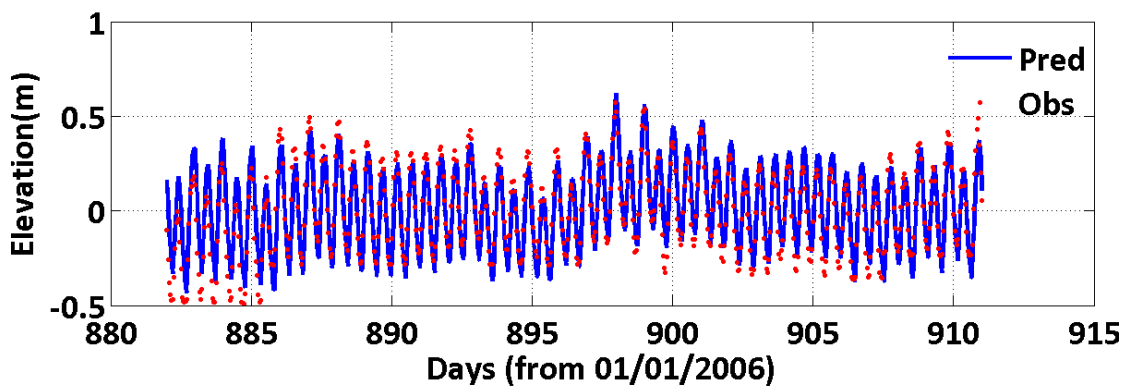
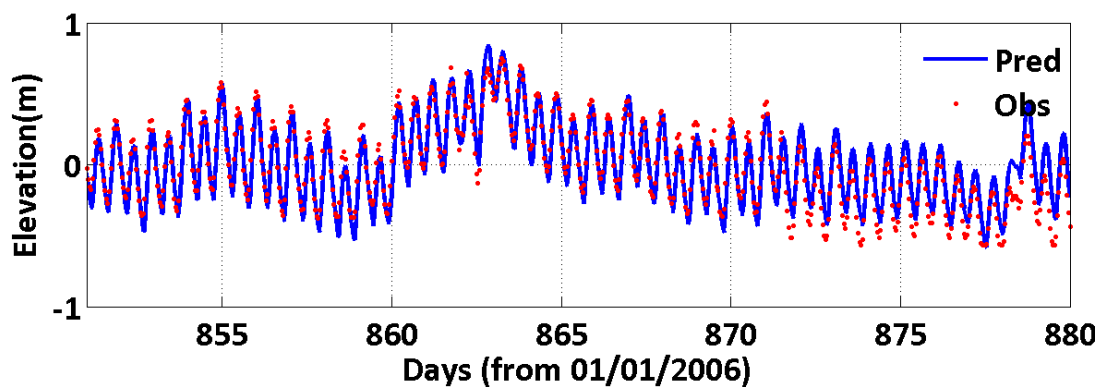
JMS043.78



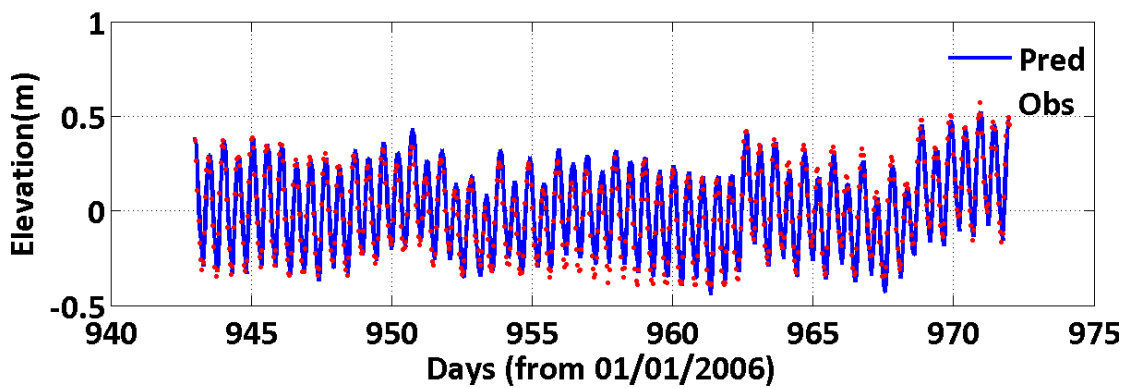
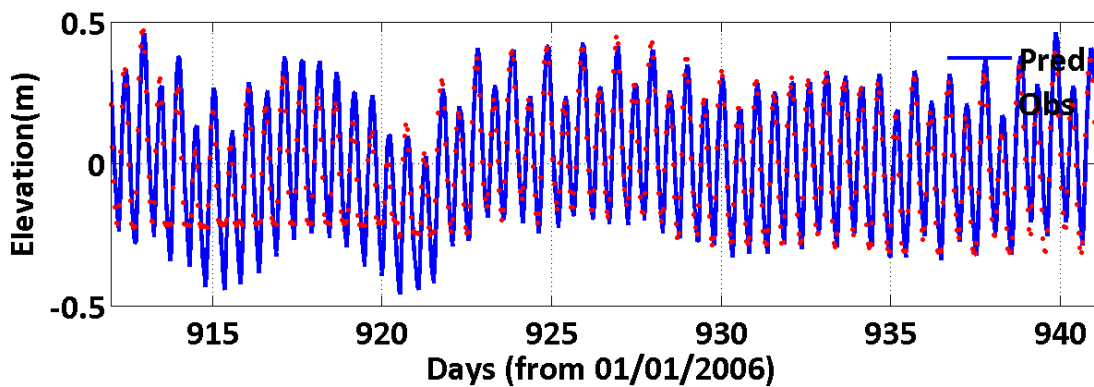
JMS043.78



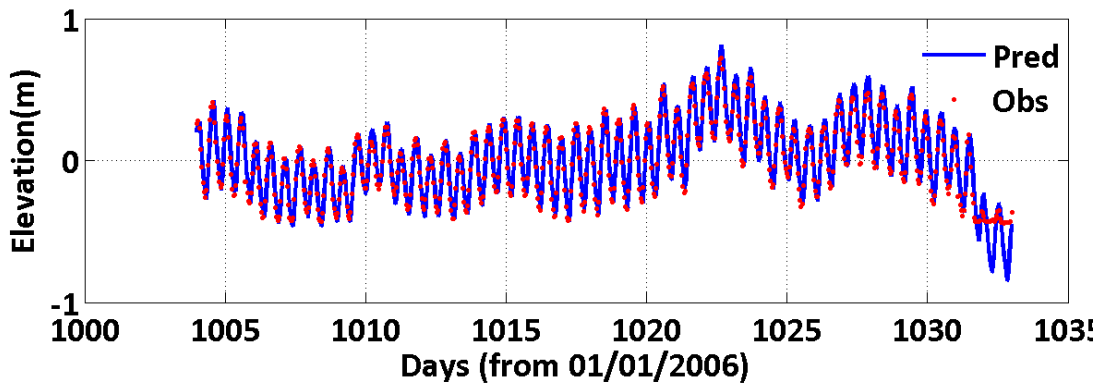
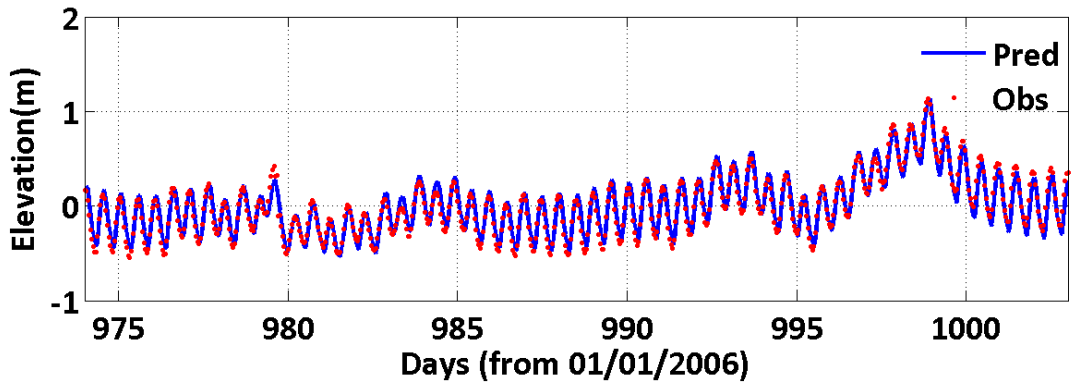
JMS043.78



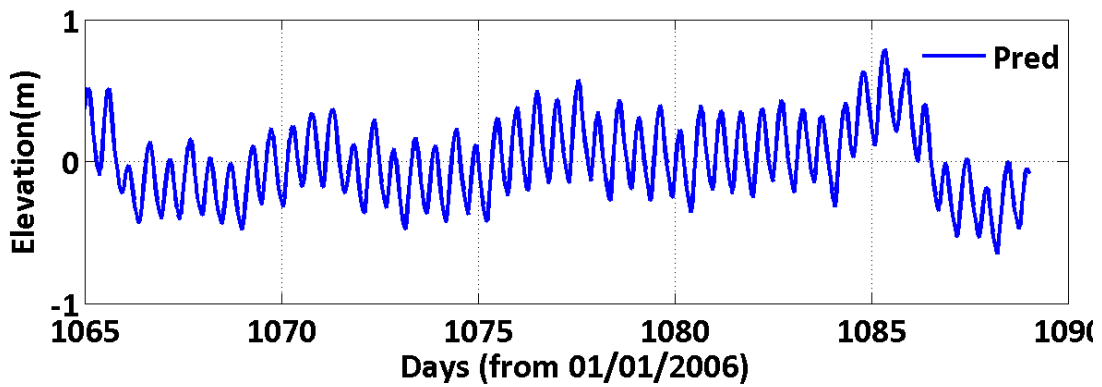
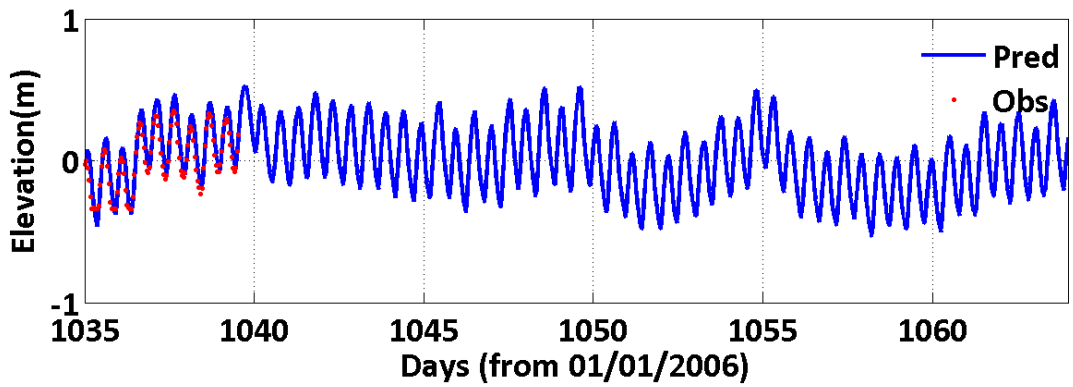
JMS043.78



JMS043.78



JMS043.78



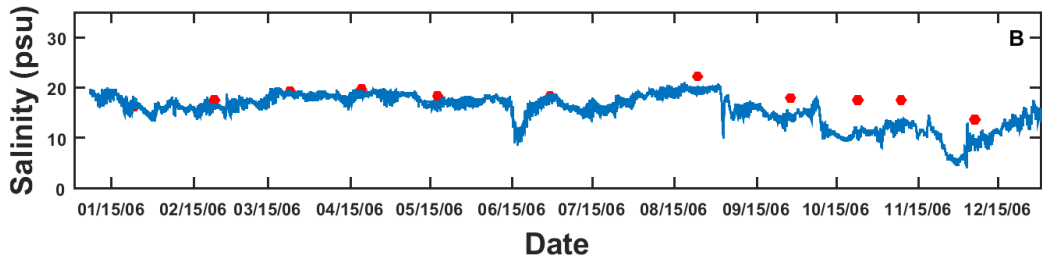
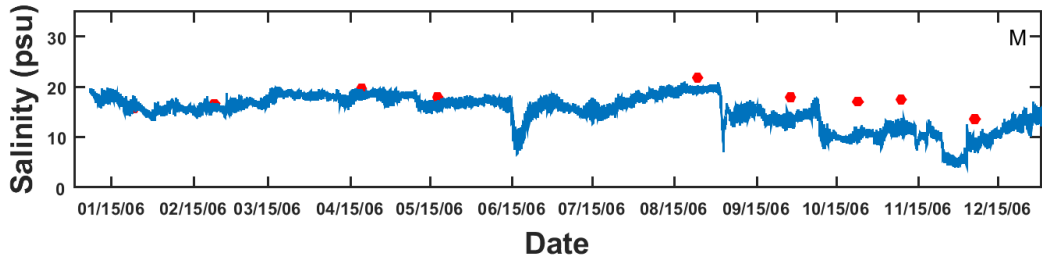
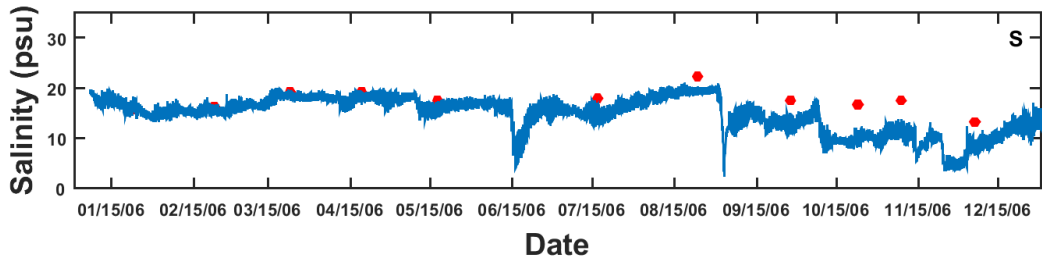
1. Appendix C

Salinity calibration results

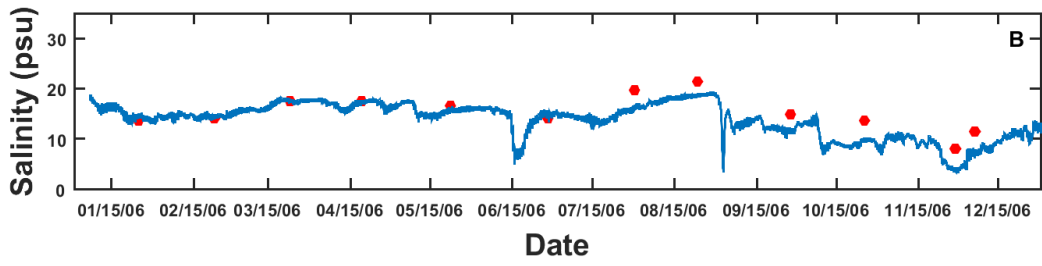
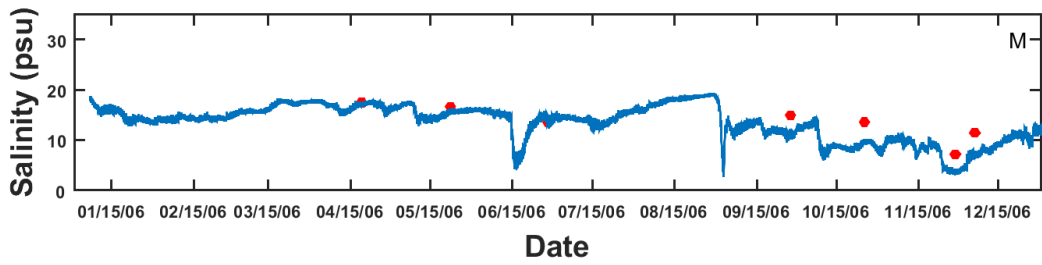
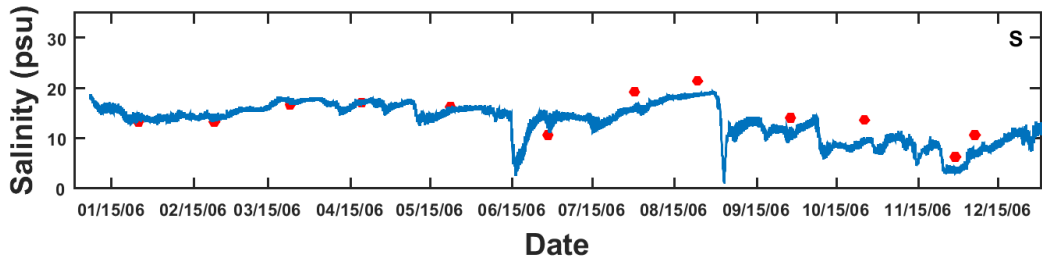
Model predicted salinities were compared to observed salinities from Chesapeake Bay stations that were monitored monthly from 2006-2008. The locations of monitoring stations are shown in Figure 3-2. Model predictions were compared against observations for each station as shown in the following figures. Blue lines are model results and red dots are observations in these figures. Labels ‘S’, ‘M’, and ‘B’ represent surface layer, middle layer, and bottom layer, respectively.

<u>Simulation Year</u>	<u>Pages</u>
2006	C2-C12
2007	C13-C23
2008	C24-C34

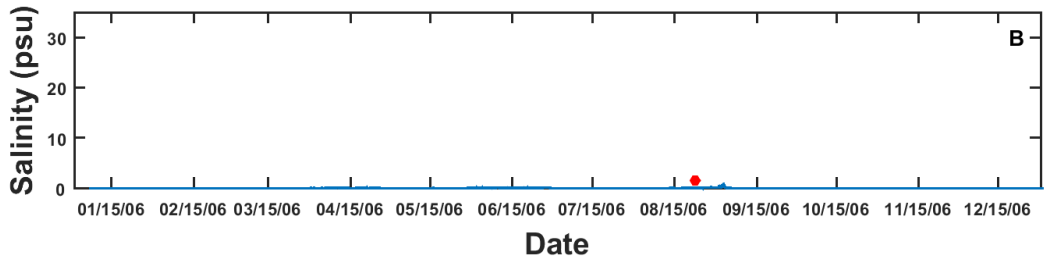
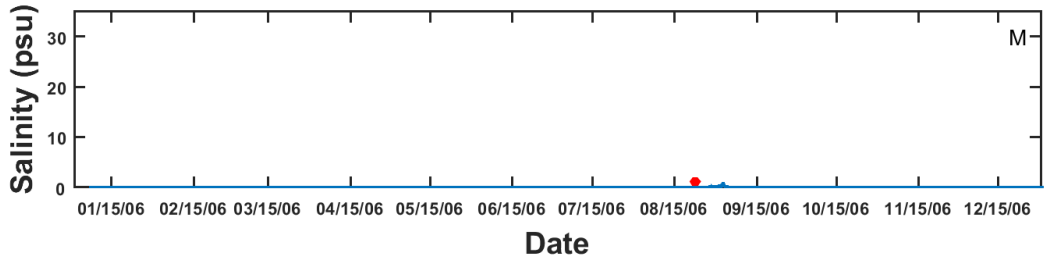
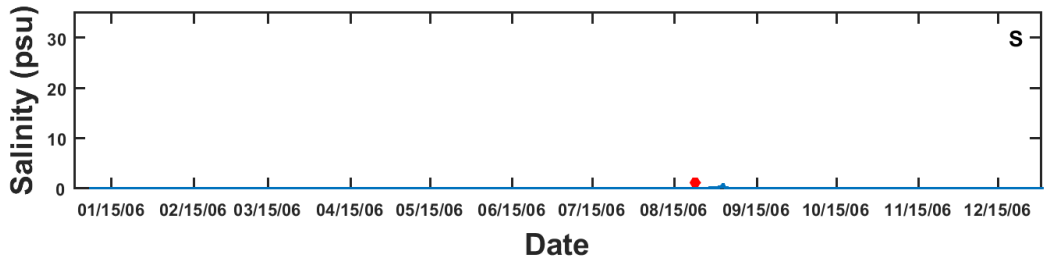
WBE1



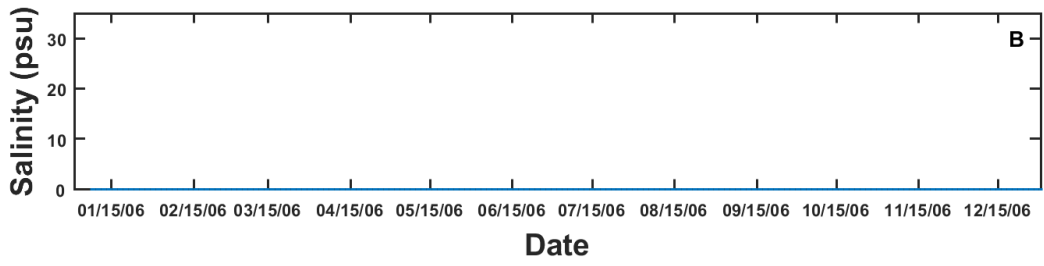
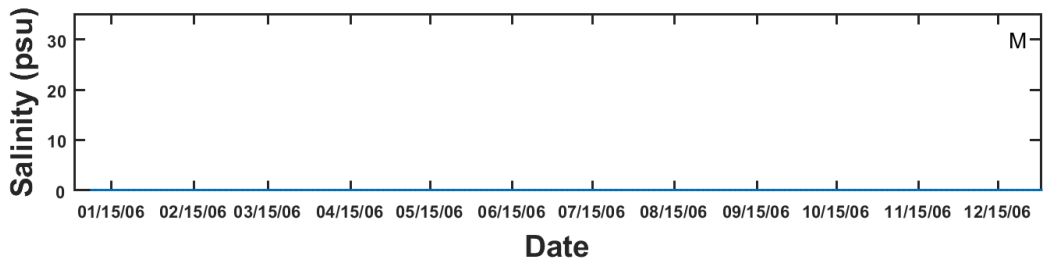
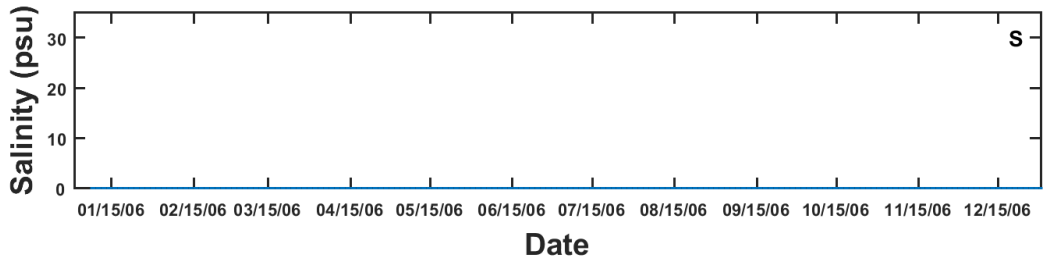
WBB05



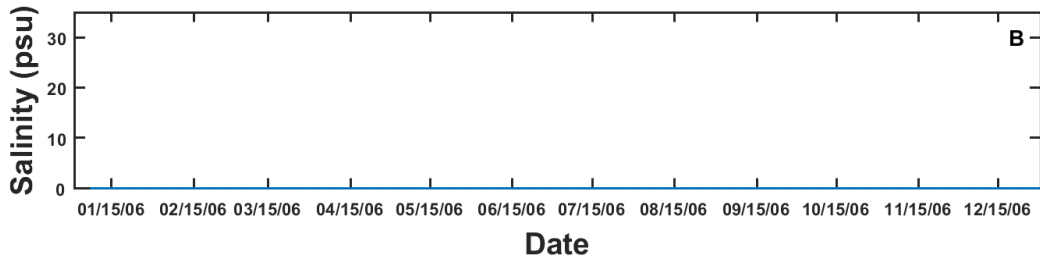
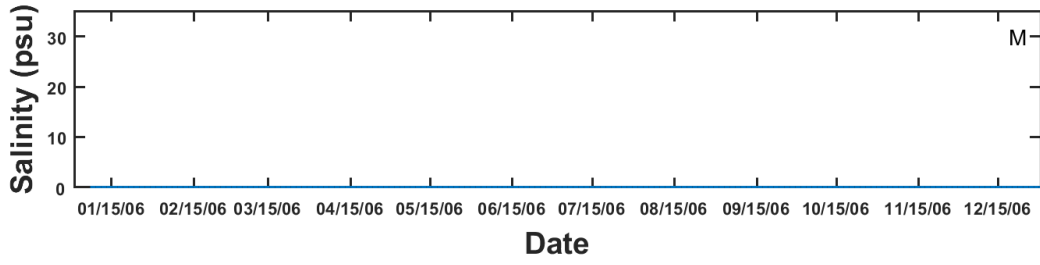
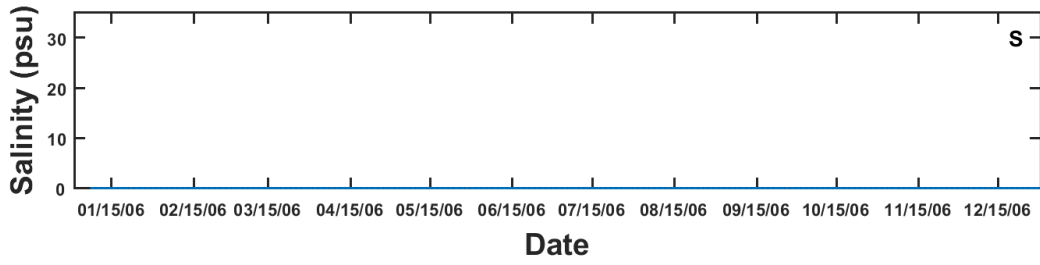
TF5.6



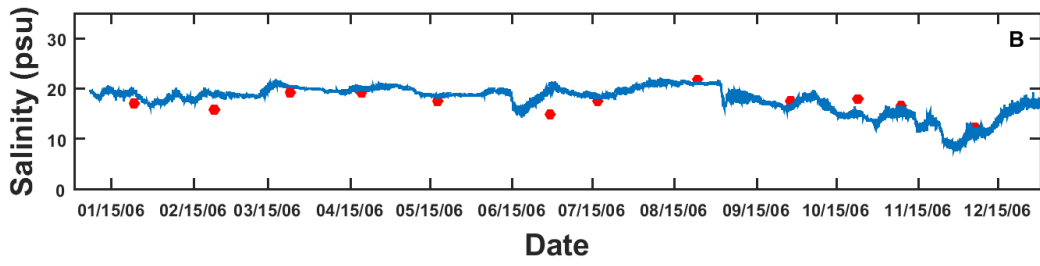
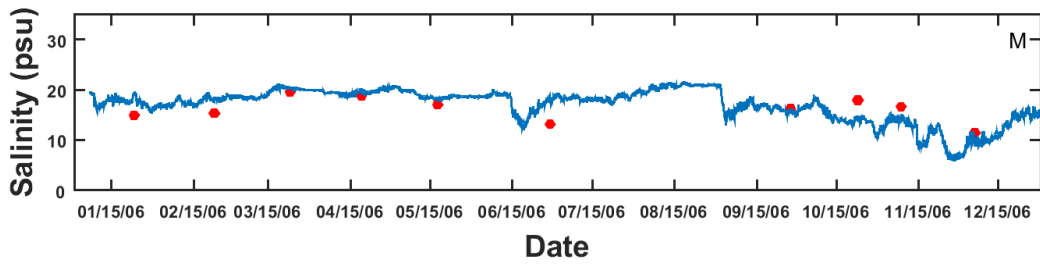
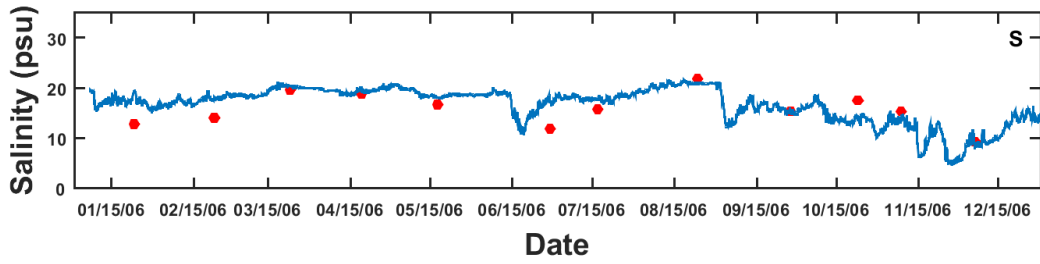
TF5.5A



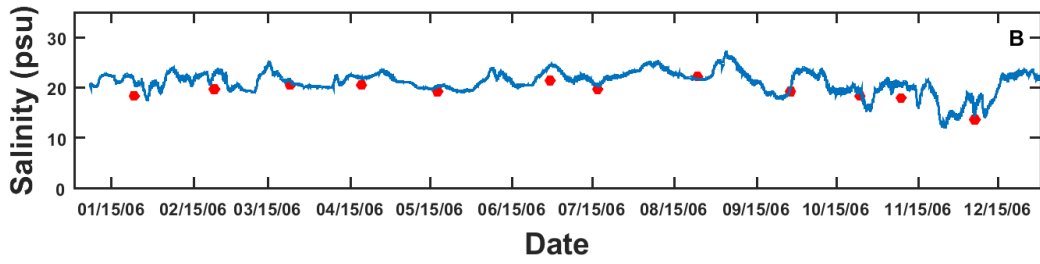
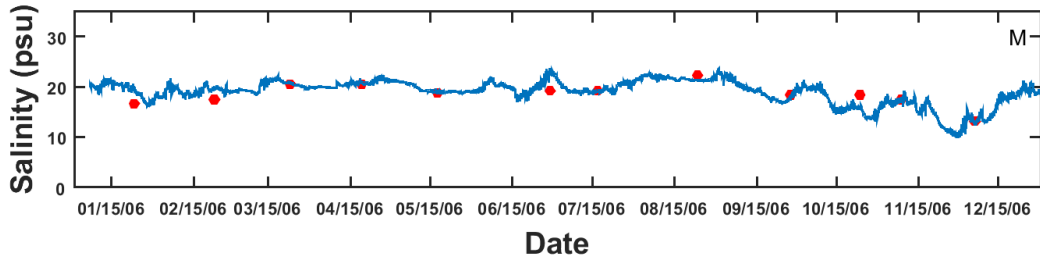
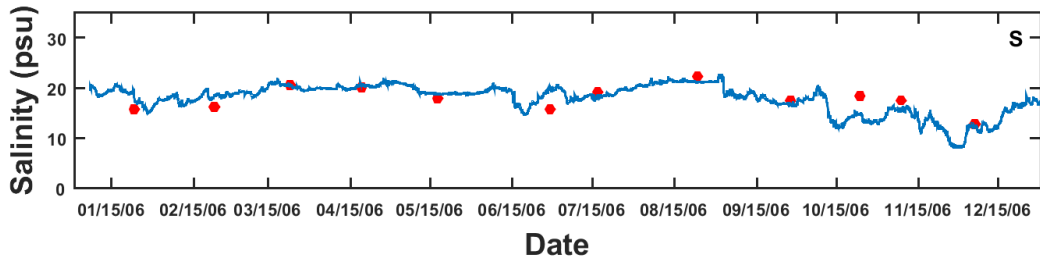
TF5.5



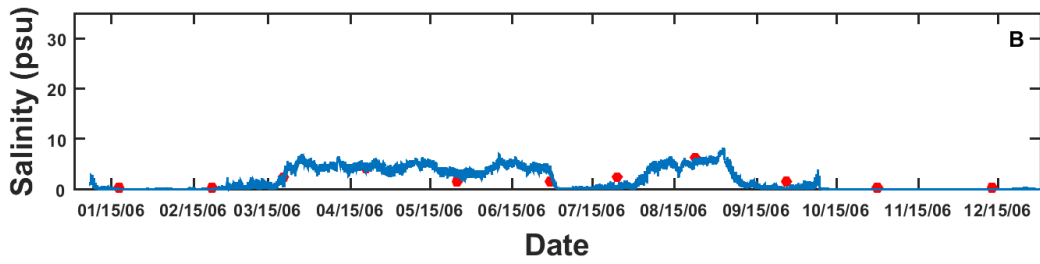
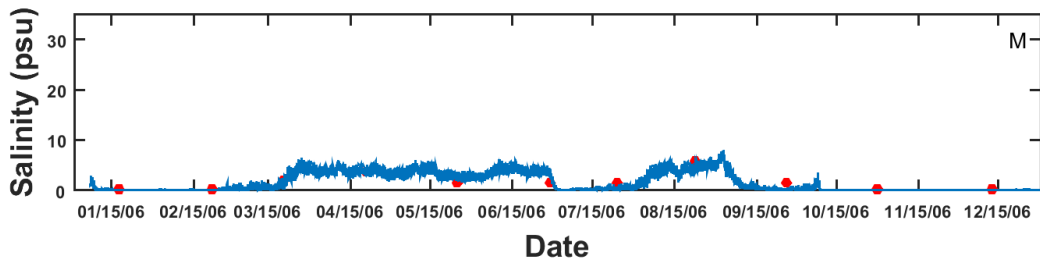
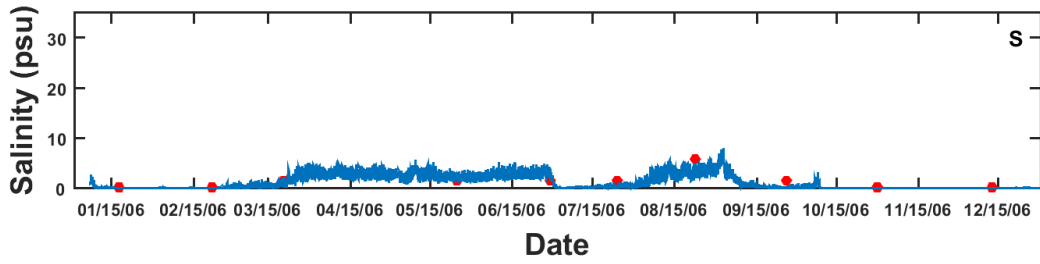
SBE5



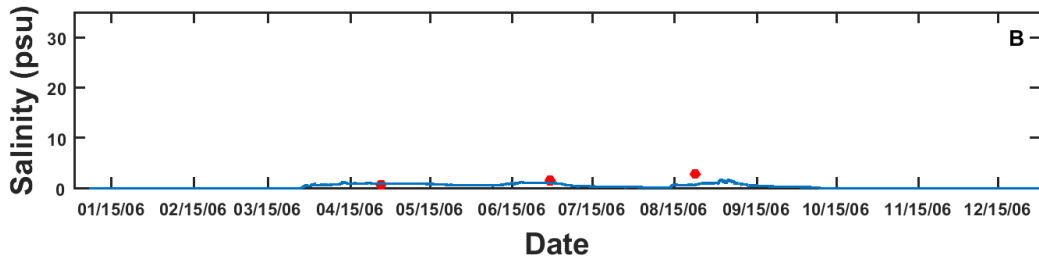
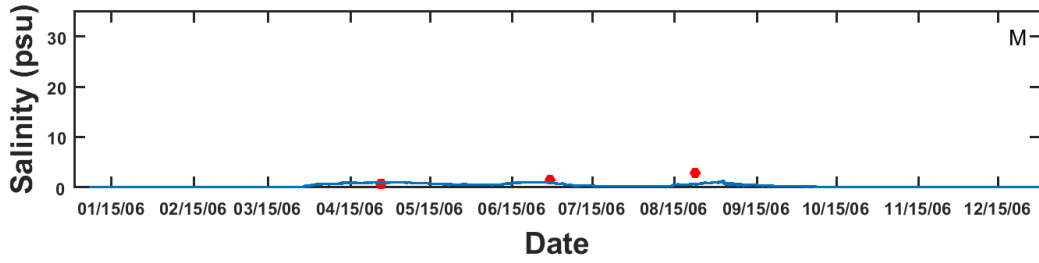
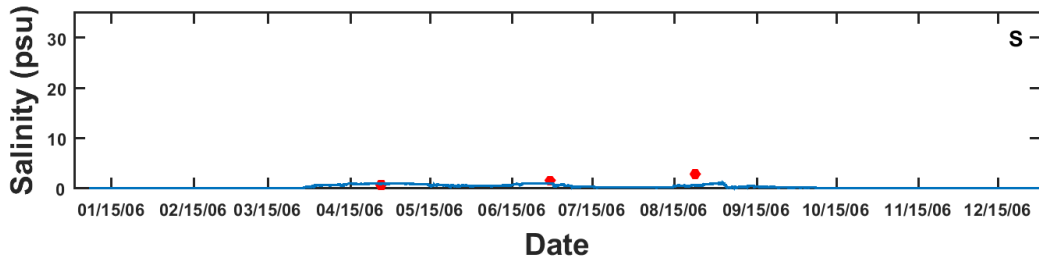
SBE2



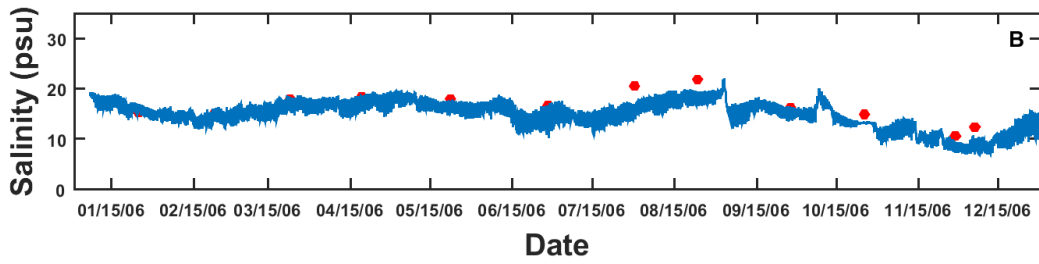
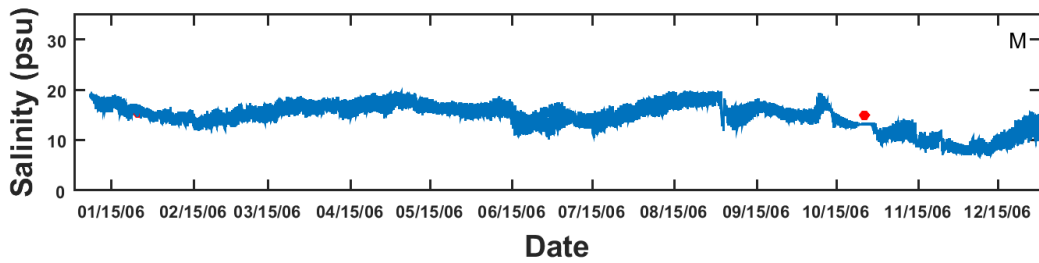
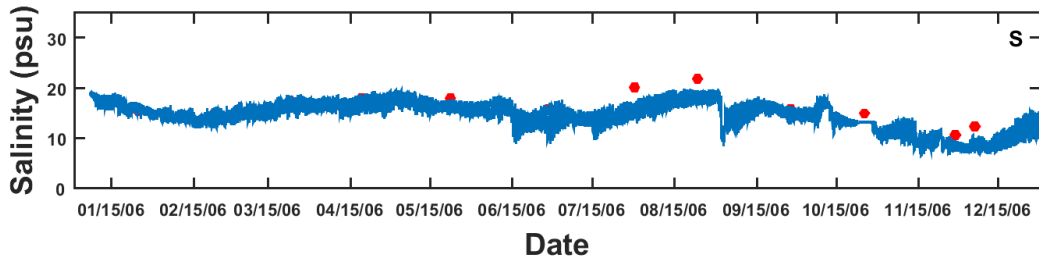
RET5.2



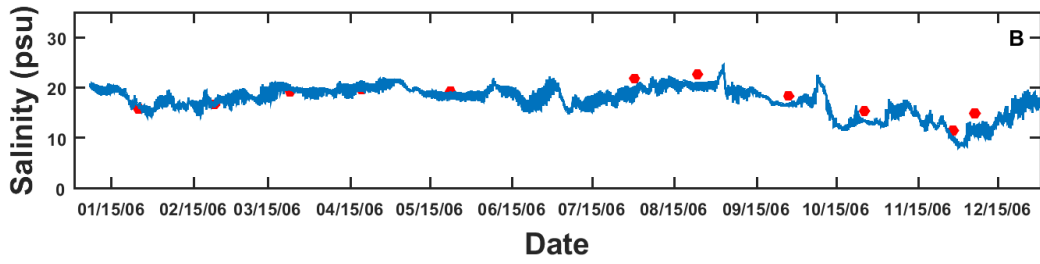
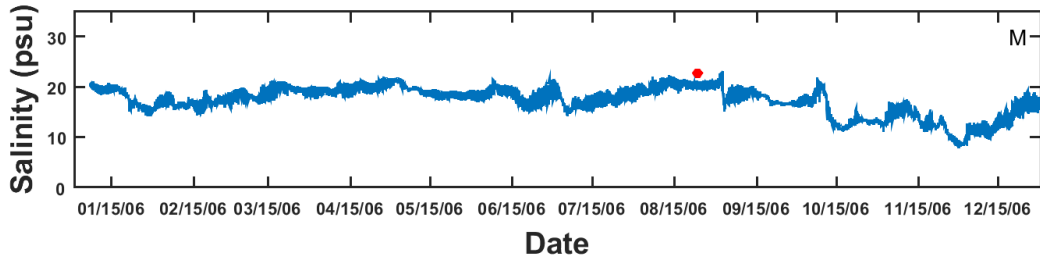
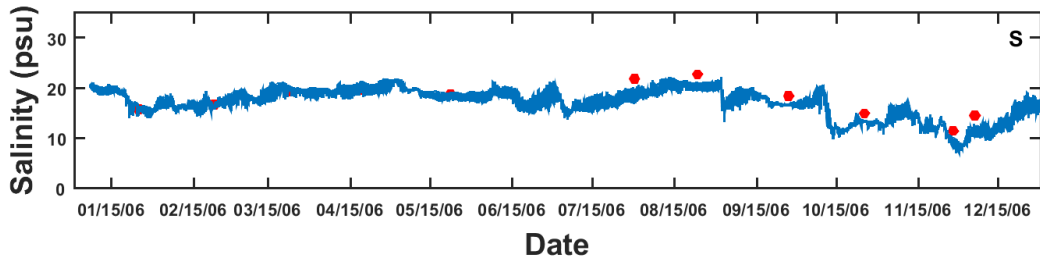
RET5.1A



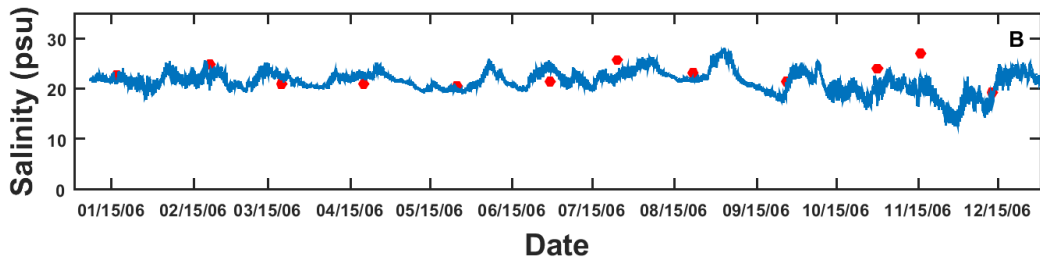
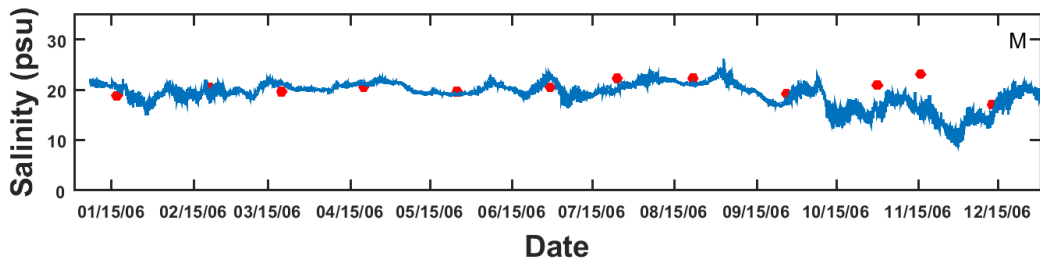
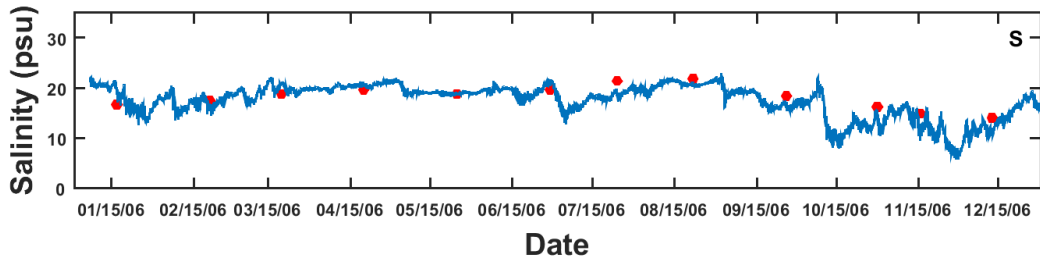
LFB01



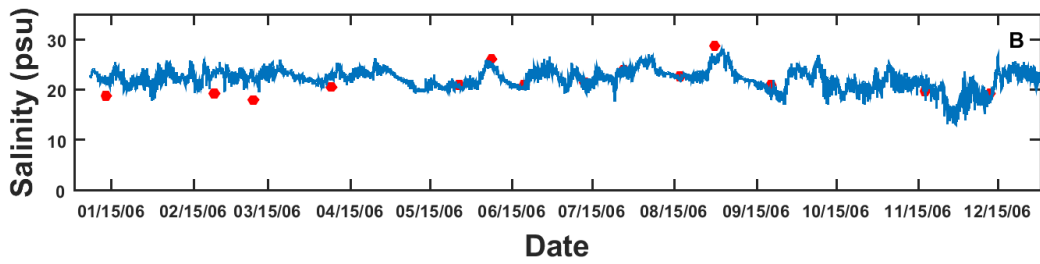
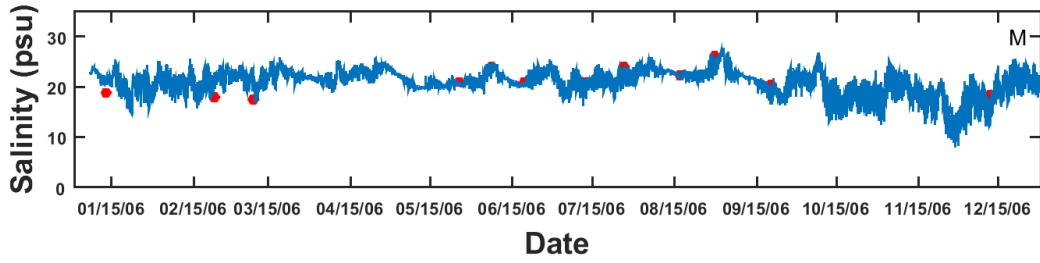
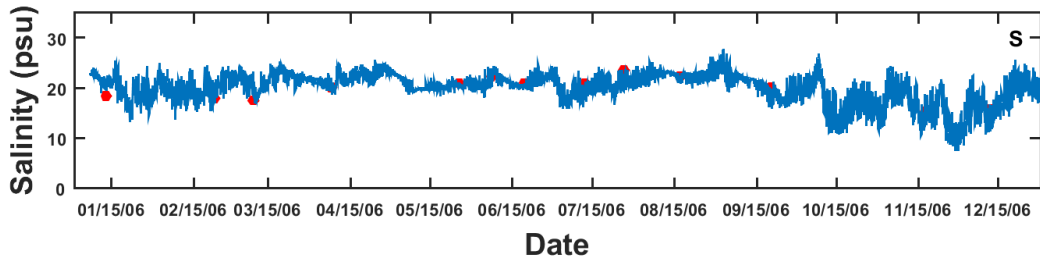
LFA01



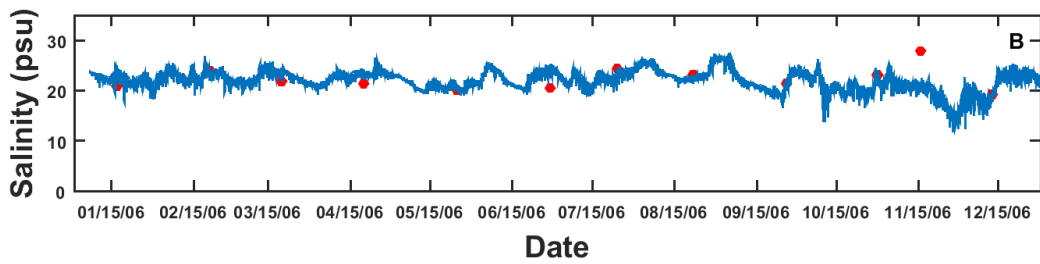
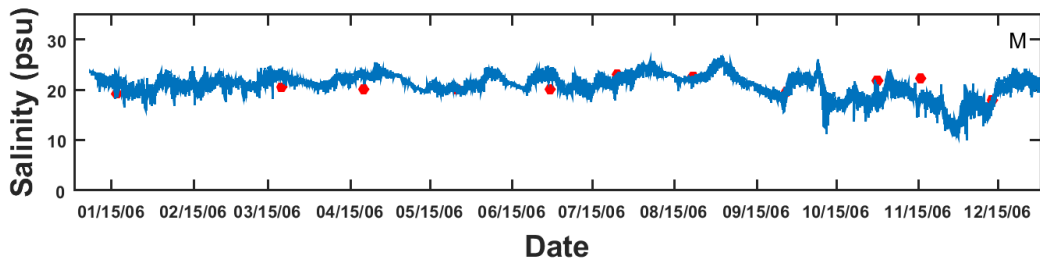
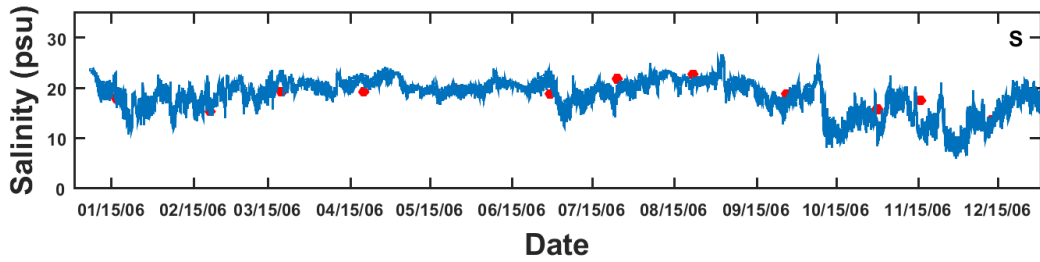
LE5.6



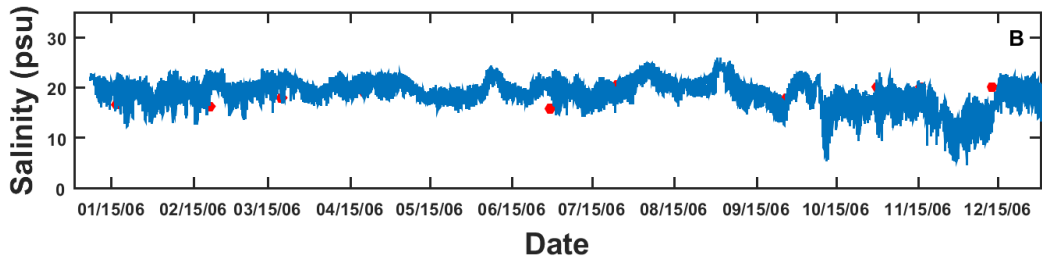
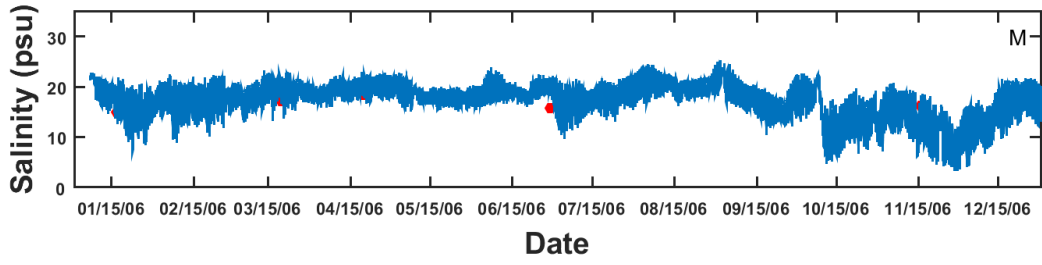
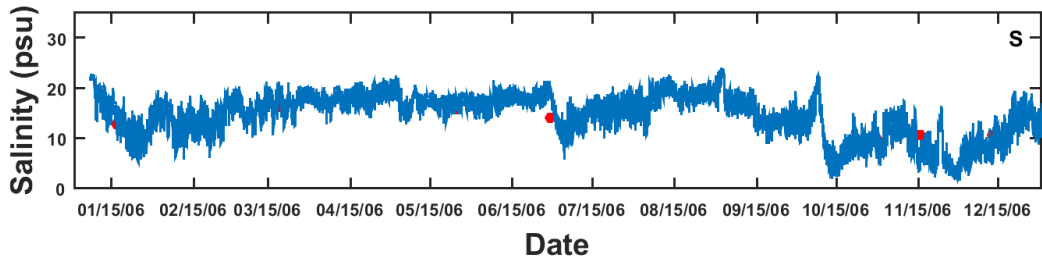
LE5.5-W



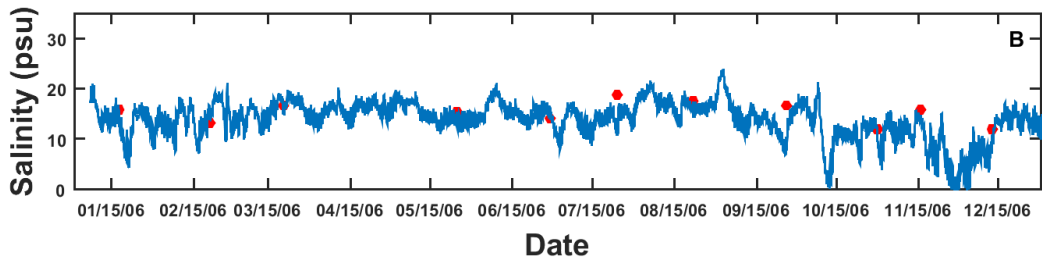
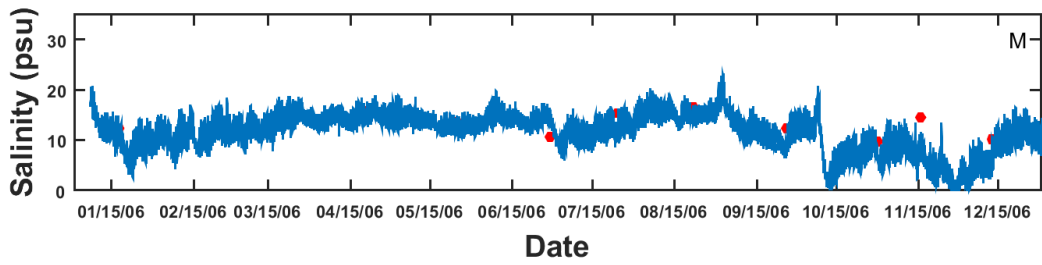
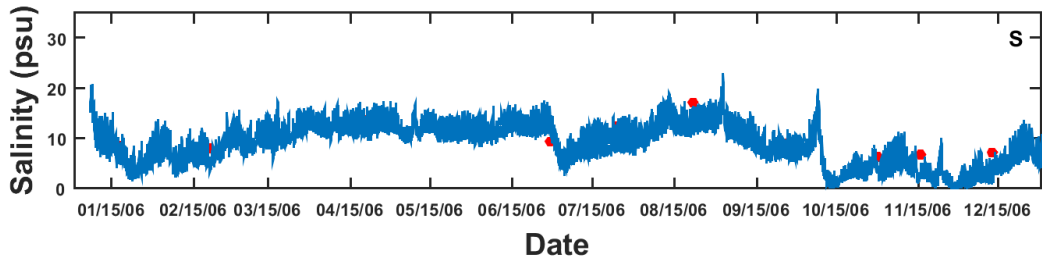
LE5.4



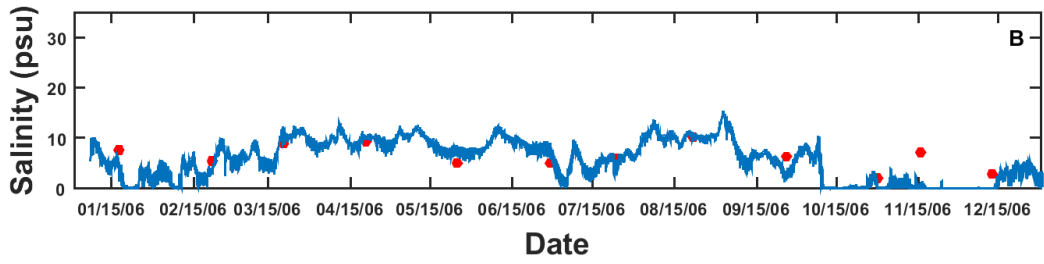
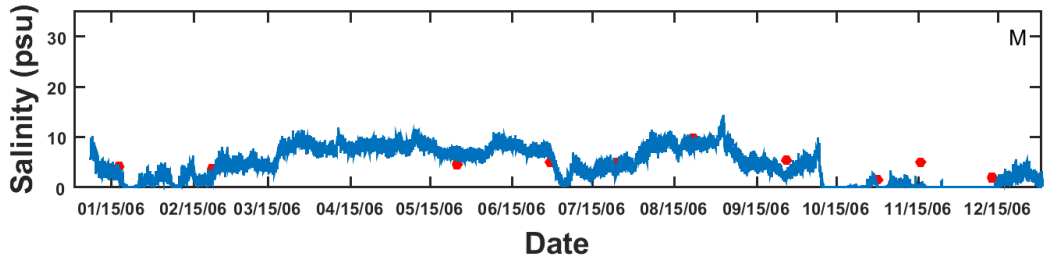
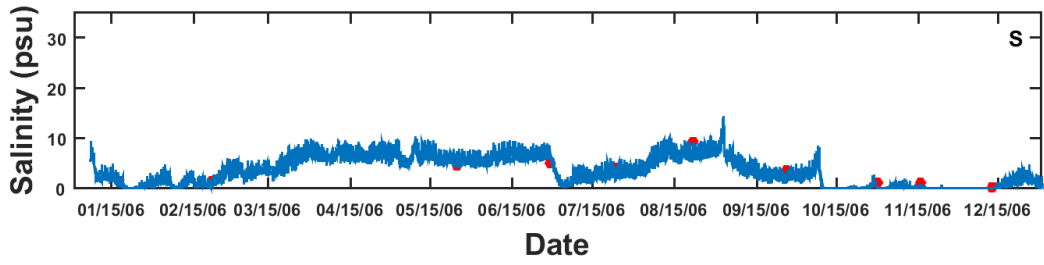
LE5.3



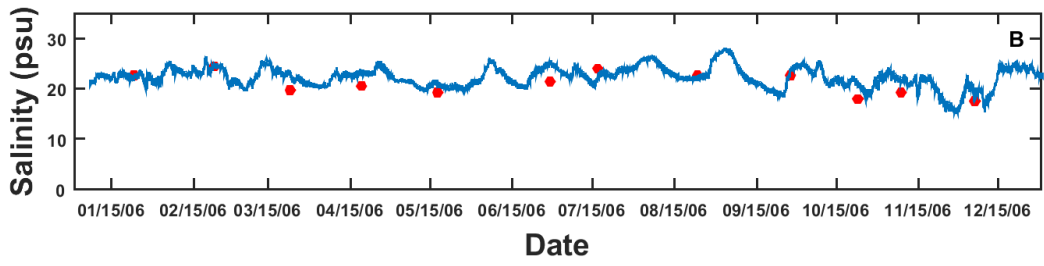
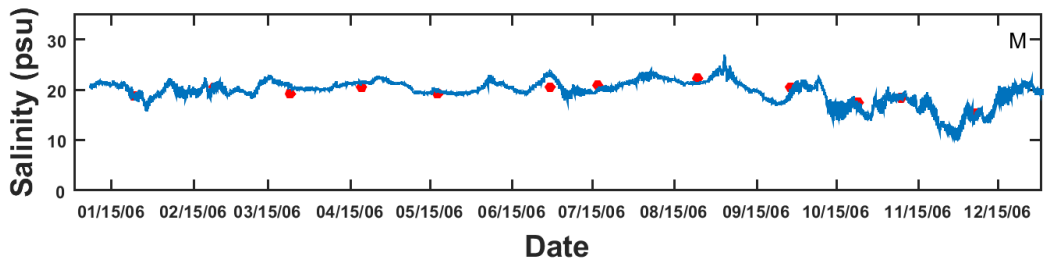
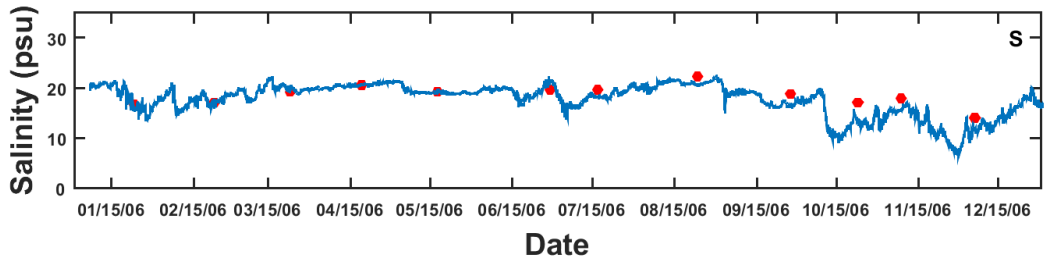
LE5.2



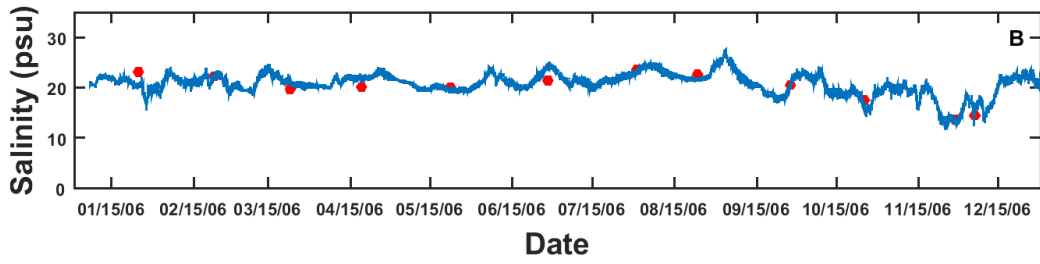
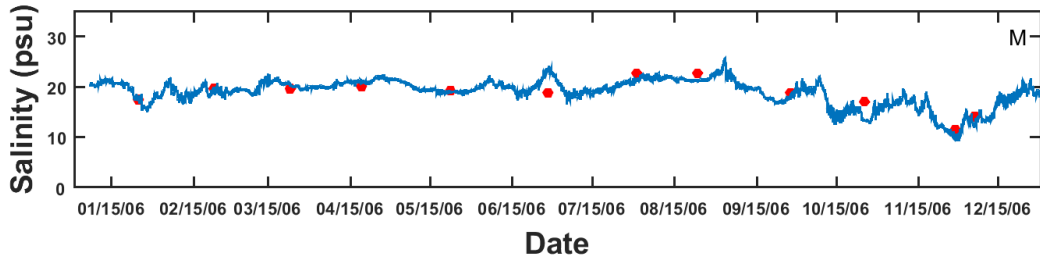
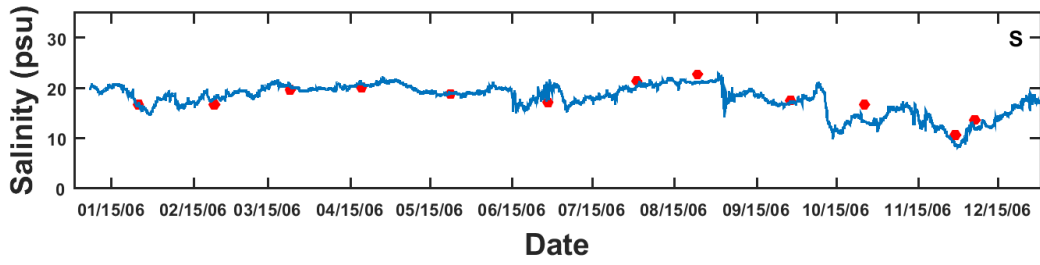
LE5.1



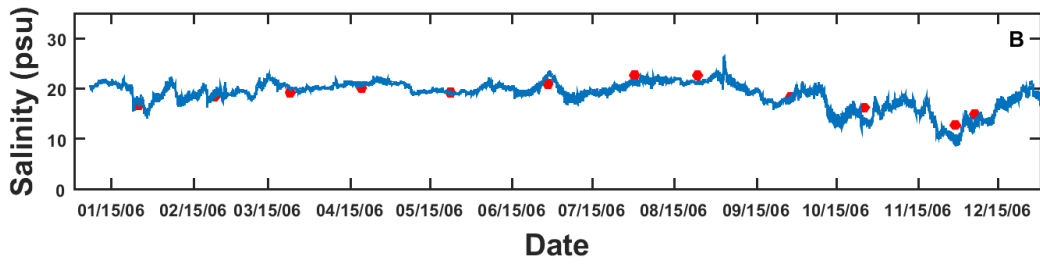
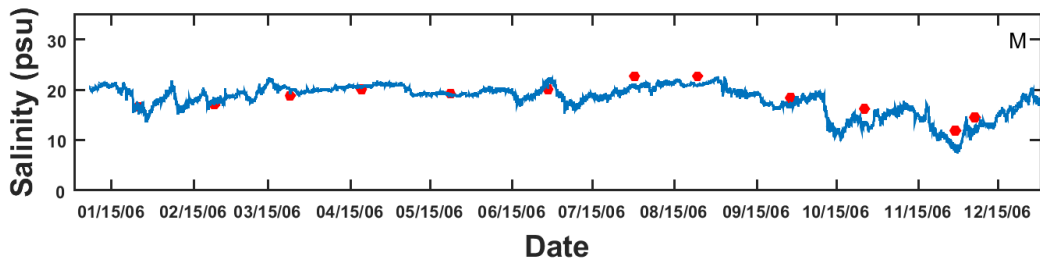
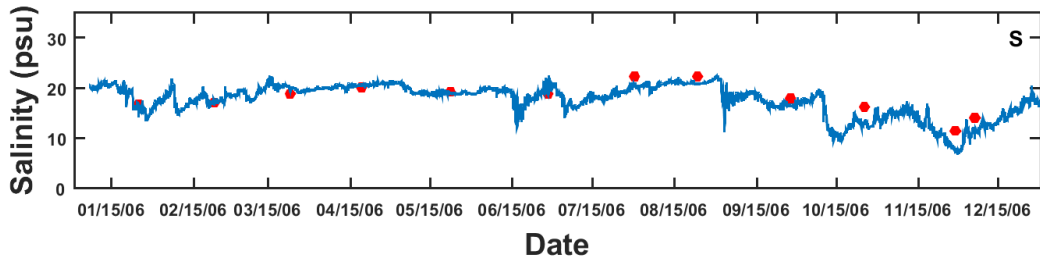
ELI2



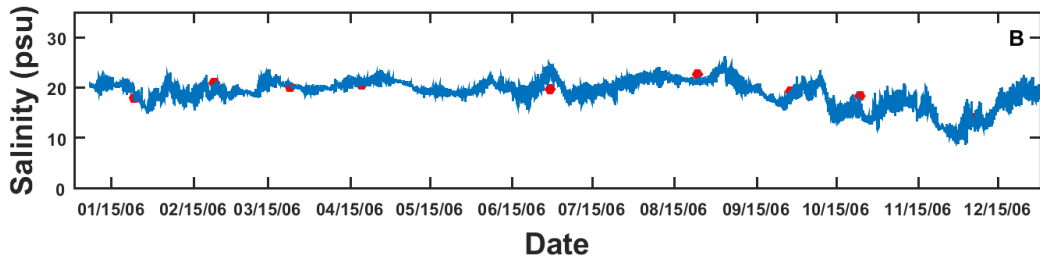
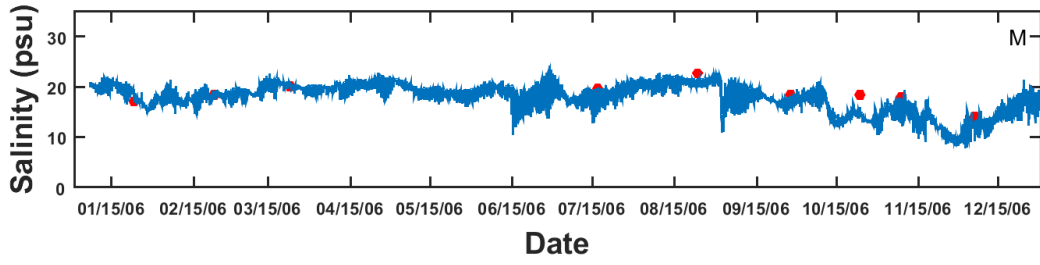
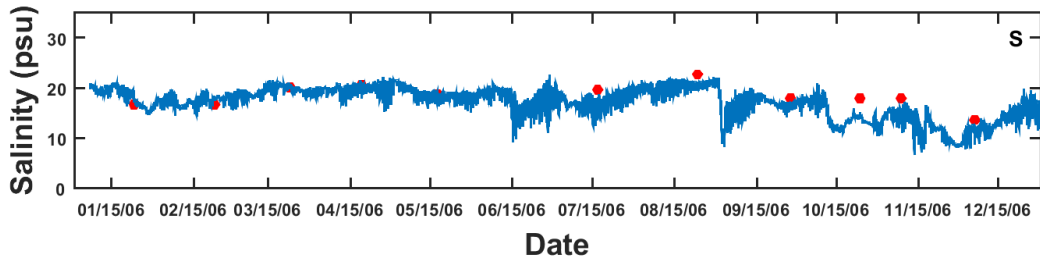
ELE01



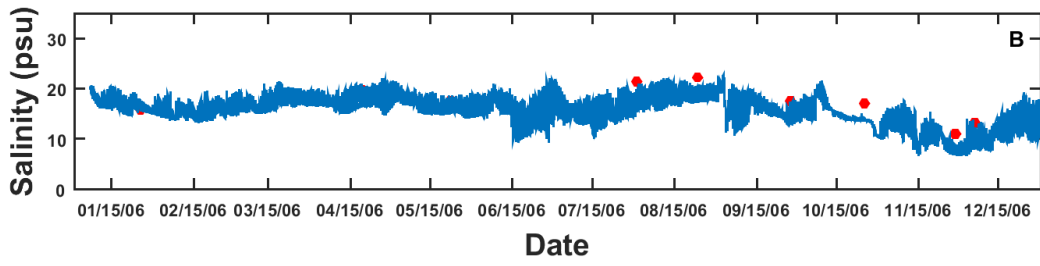
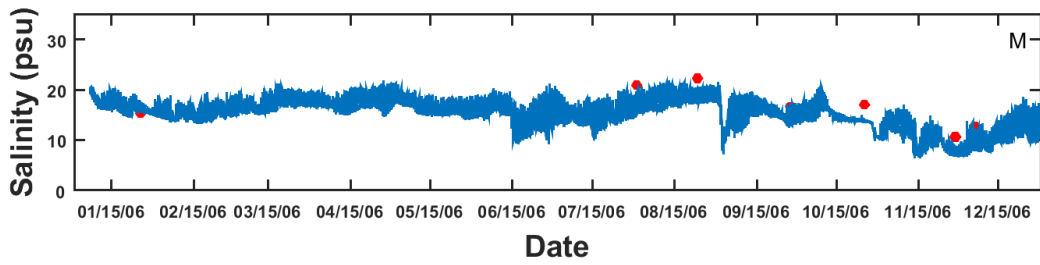
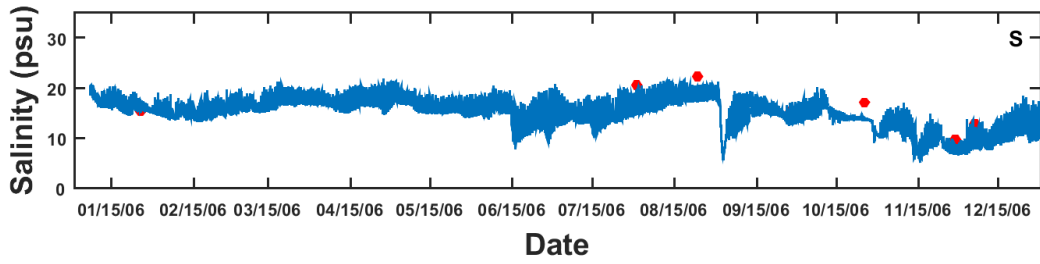
ELD01



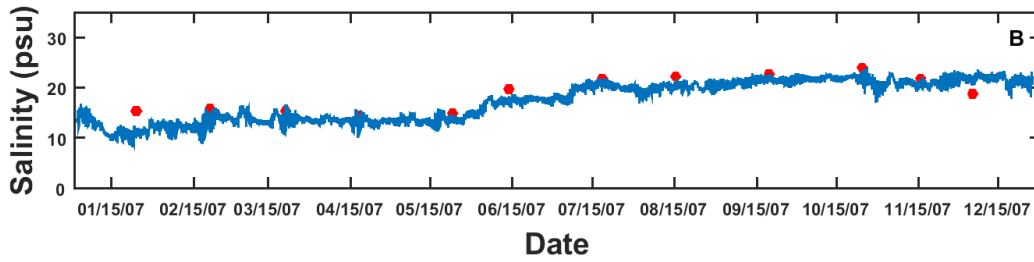
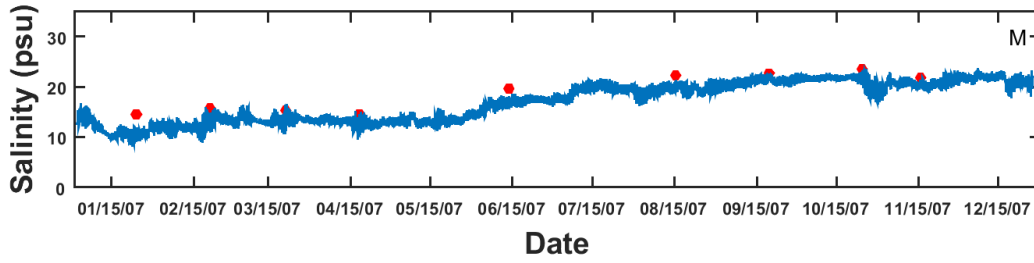
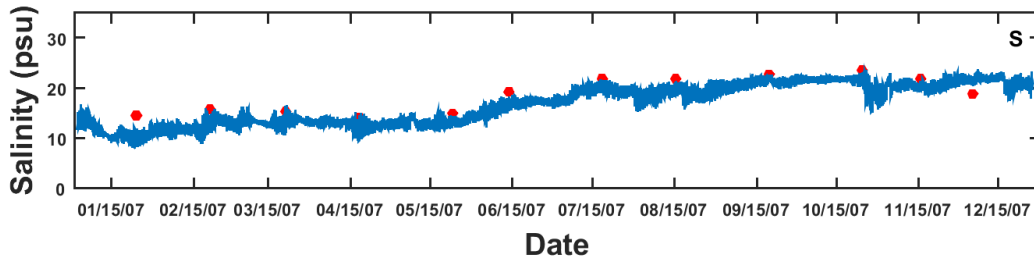
EBE1



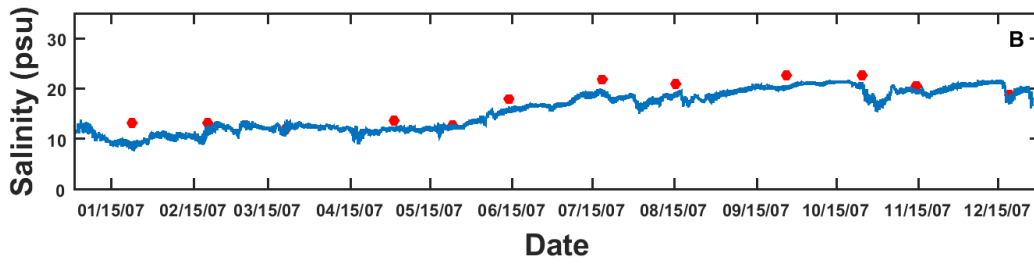
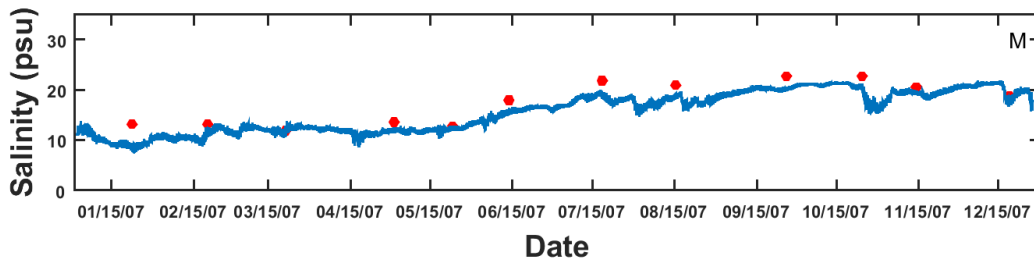
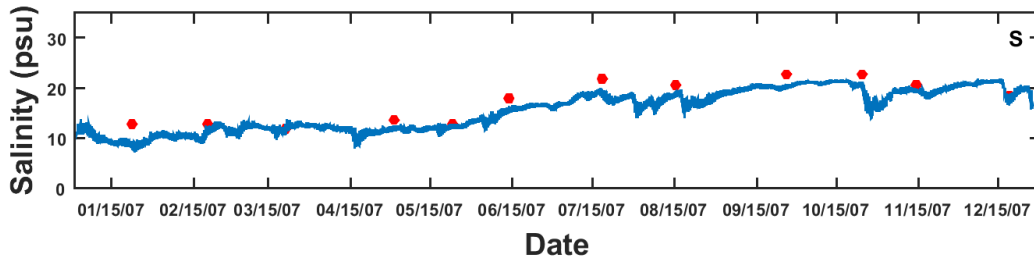
EBB01



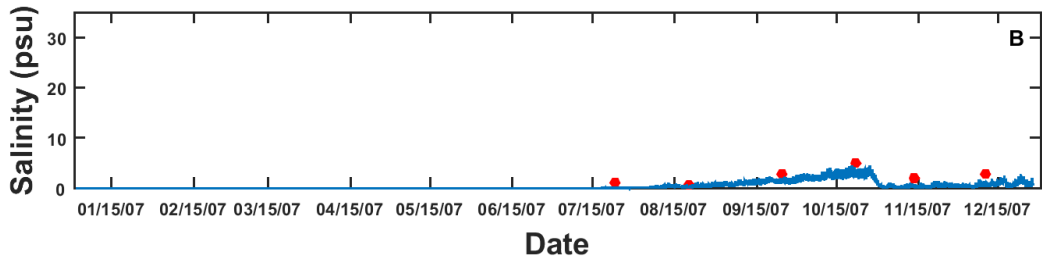
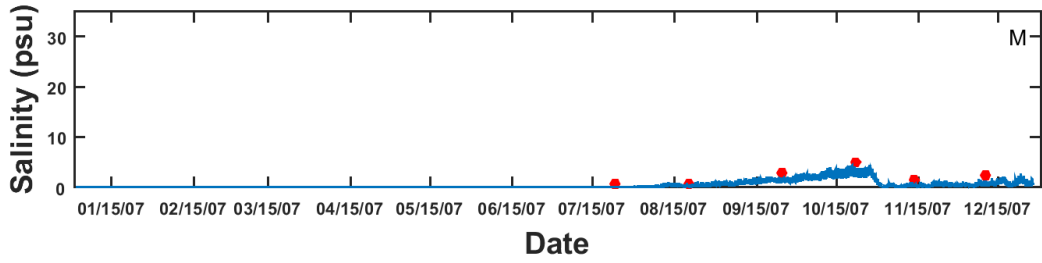
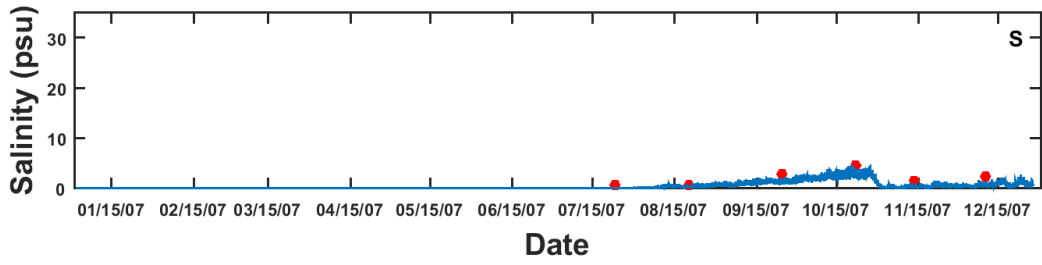
WBE1



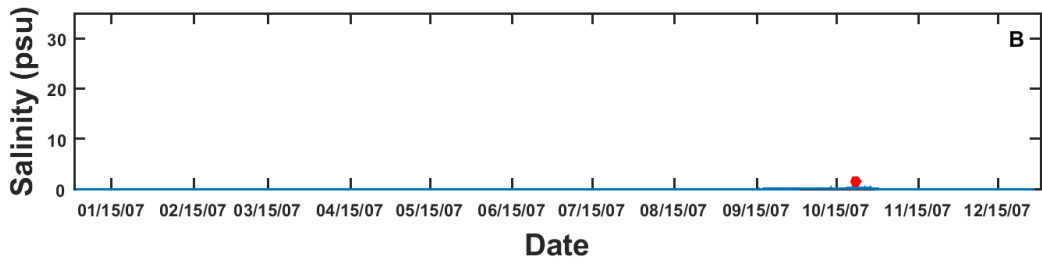
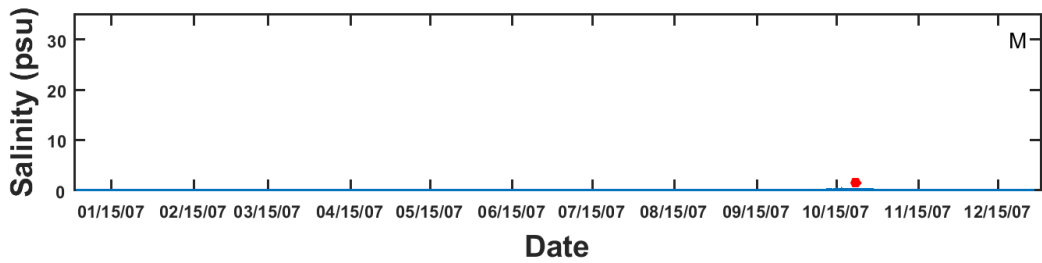
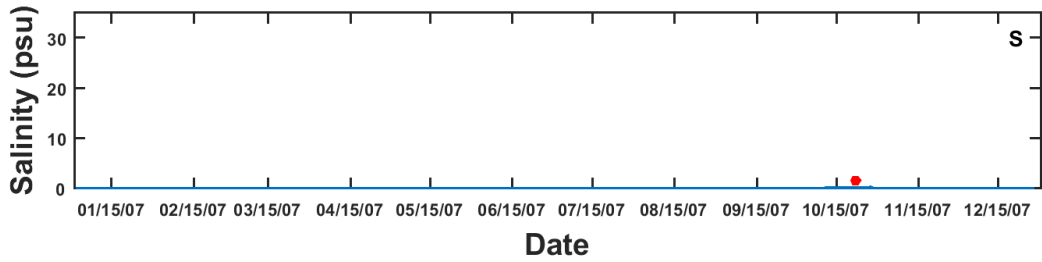
WBB05



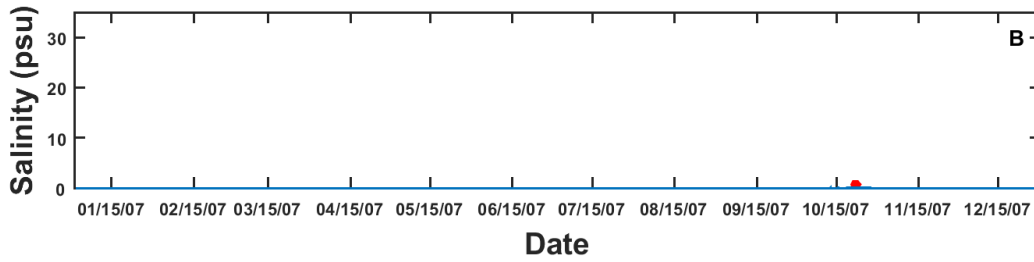
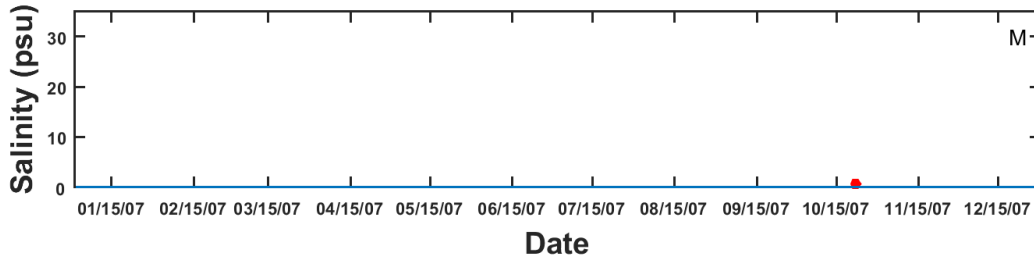
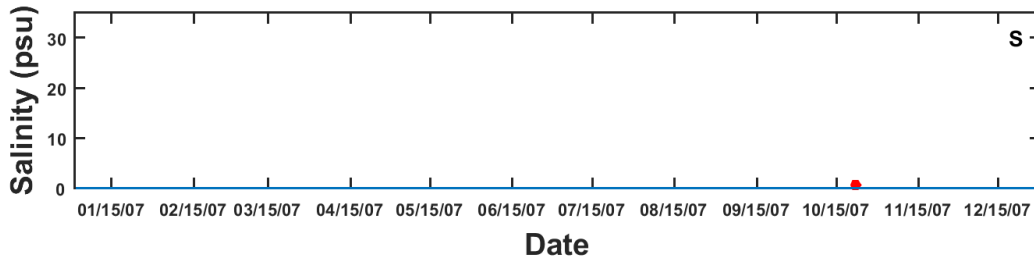
TF5.6



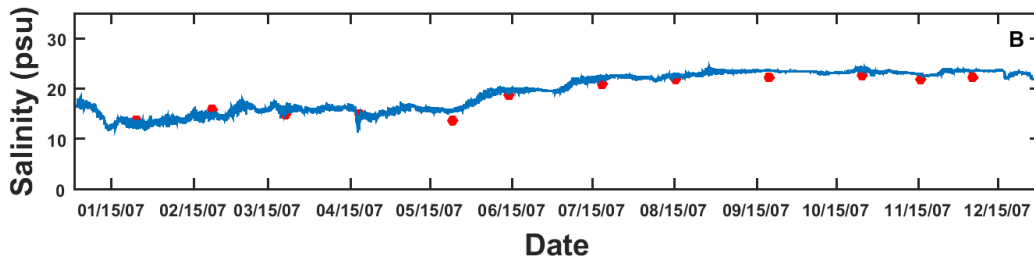
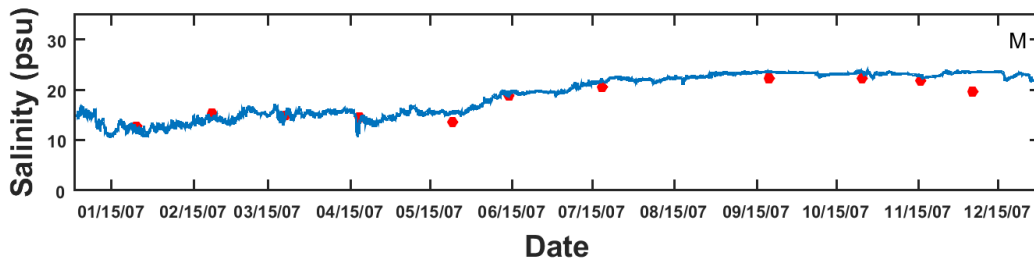
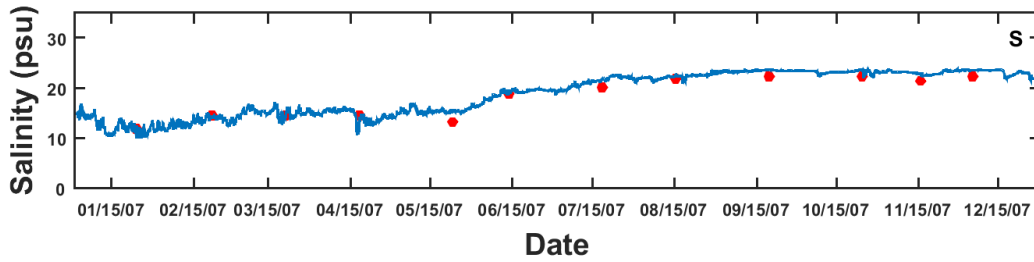
TF5.5A



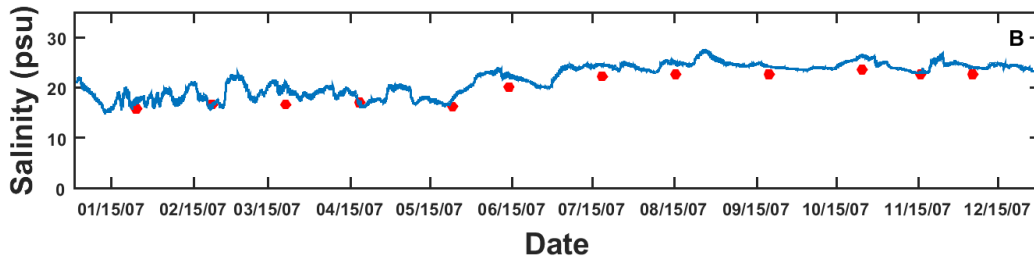
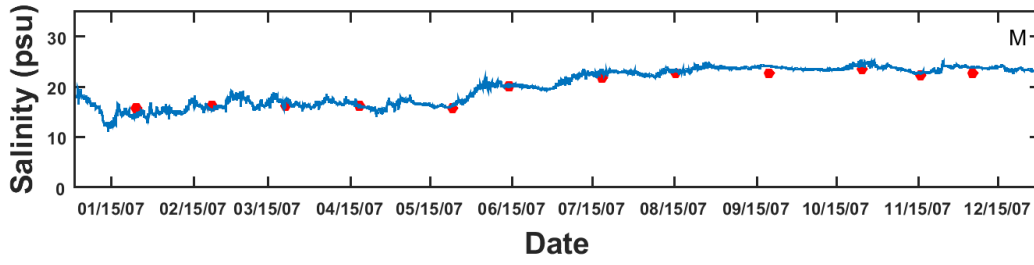
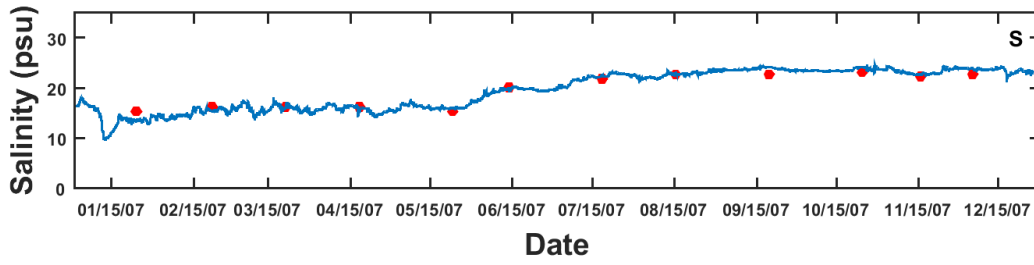
TF5.5



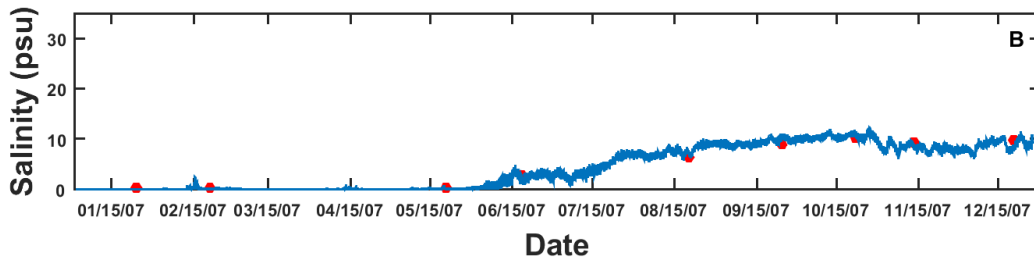
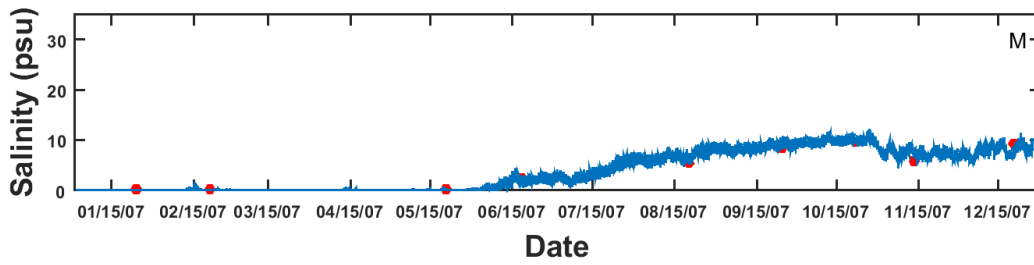
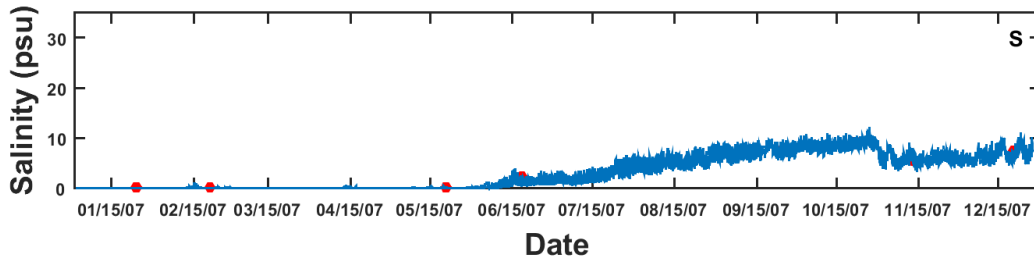
SBE5



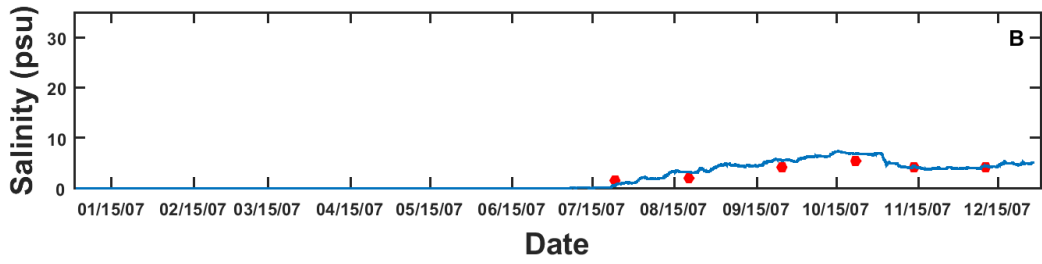
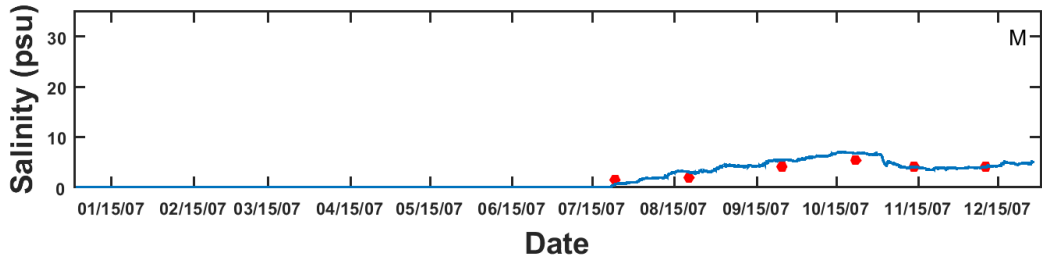
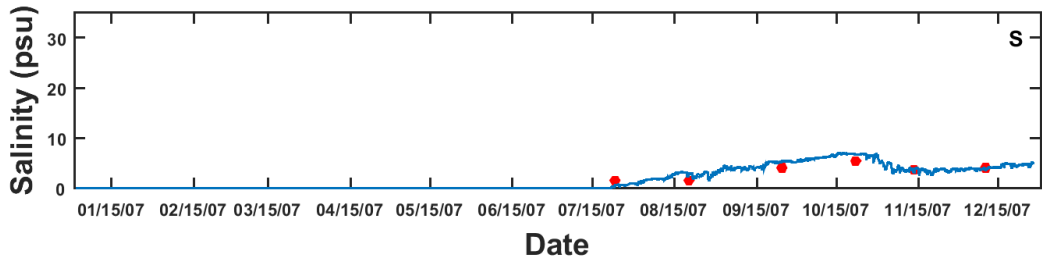
SBE2



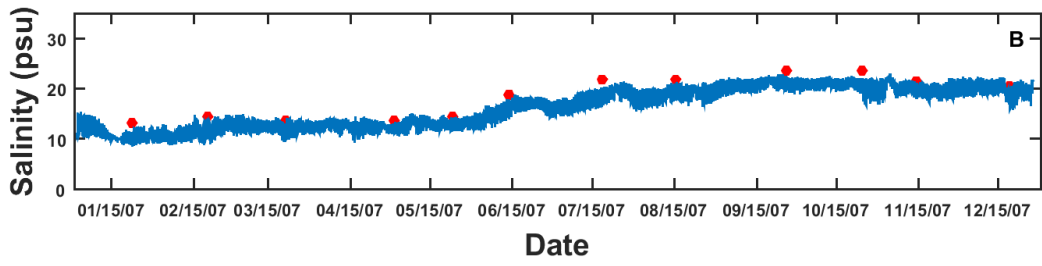
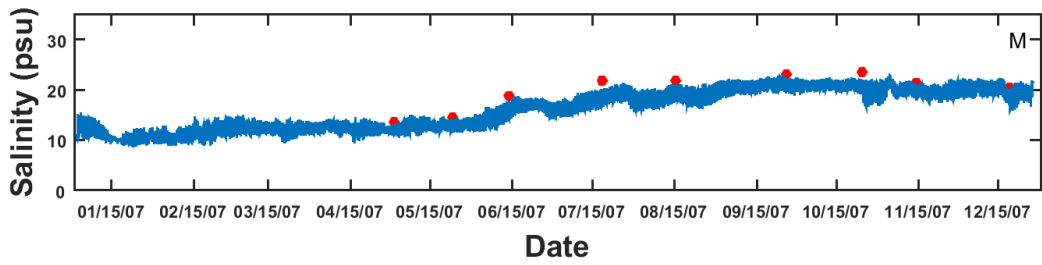
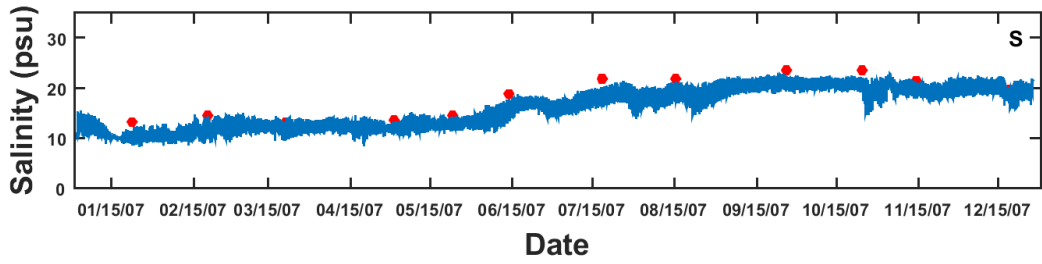
RET5.2



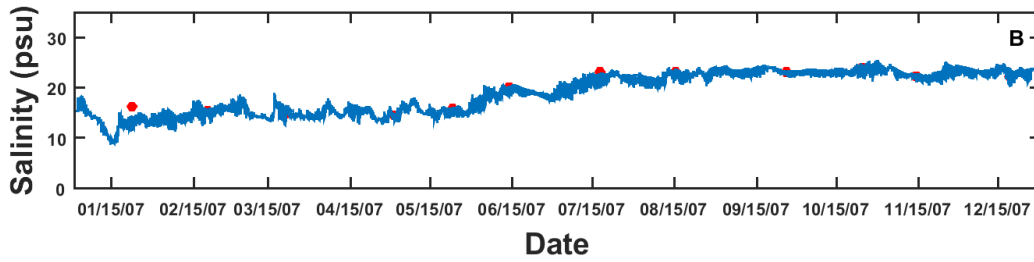
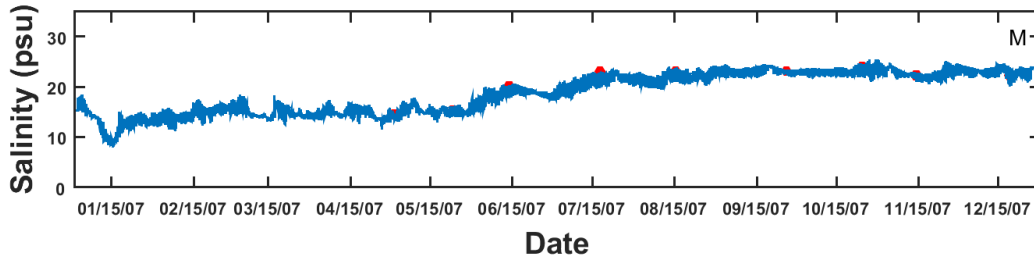
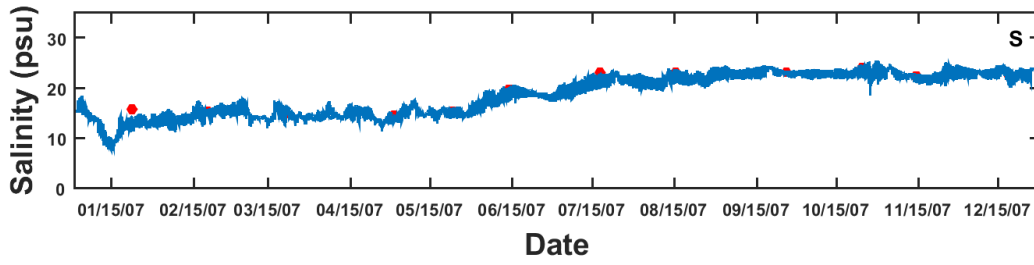
RET5.1A



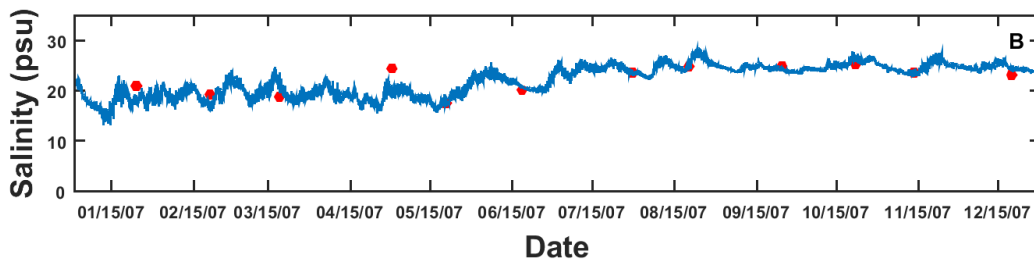
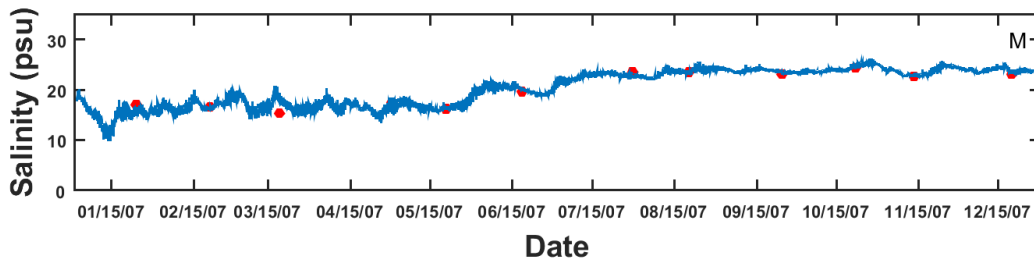
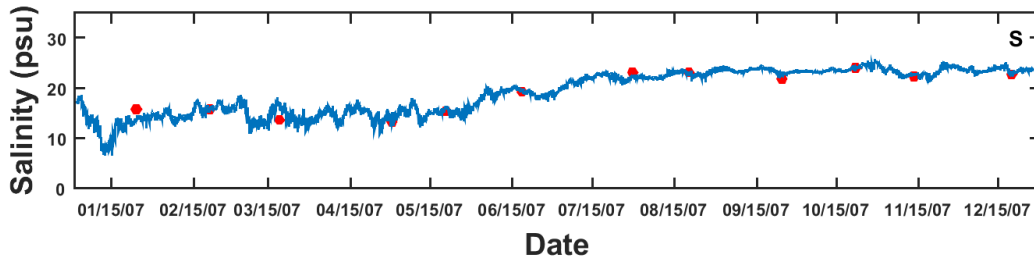
LFB01



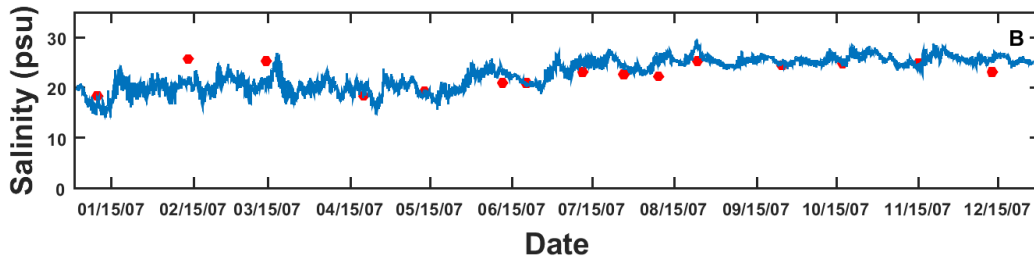
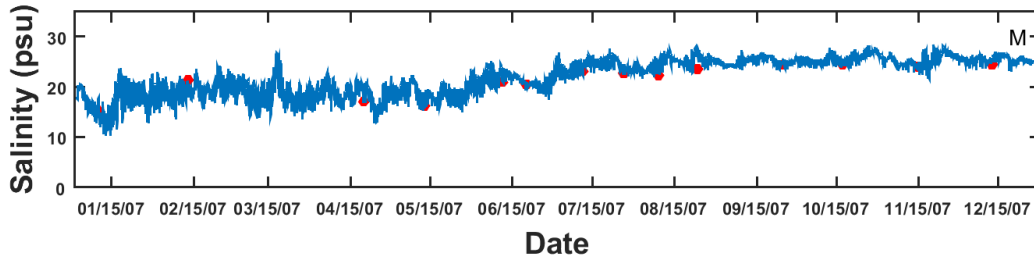
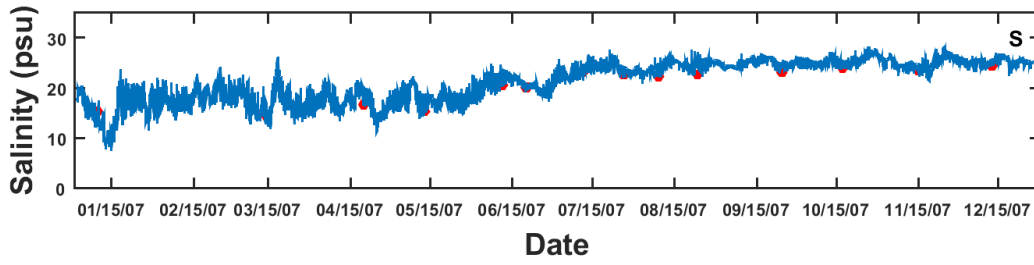
LFA01



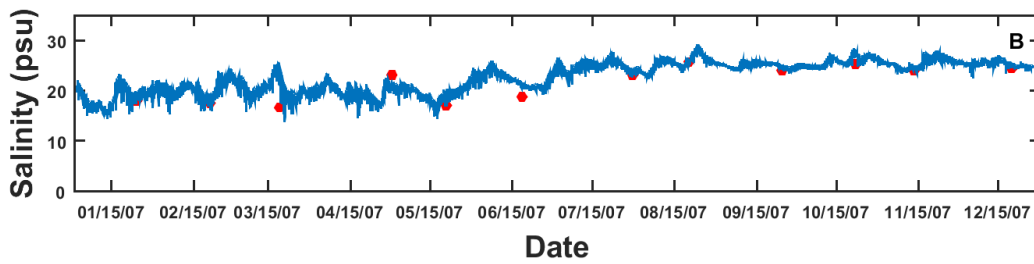
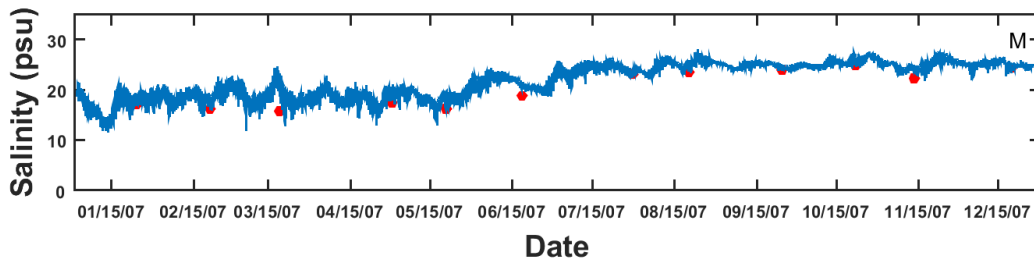
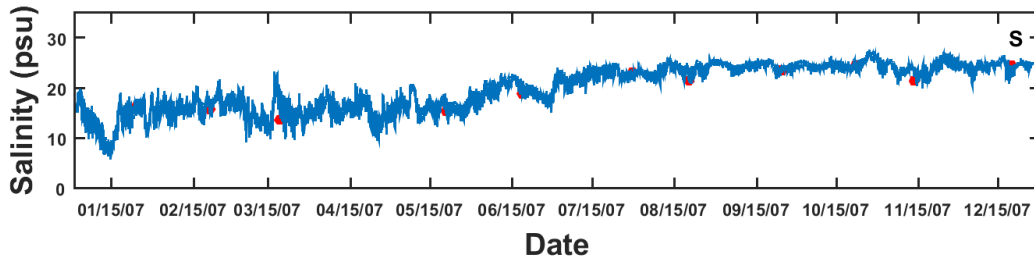
LE5.6



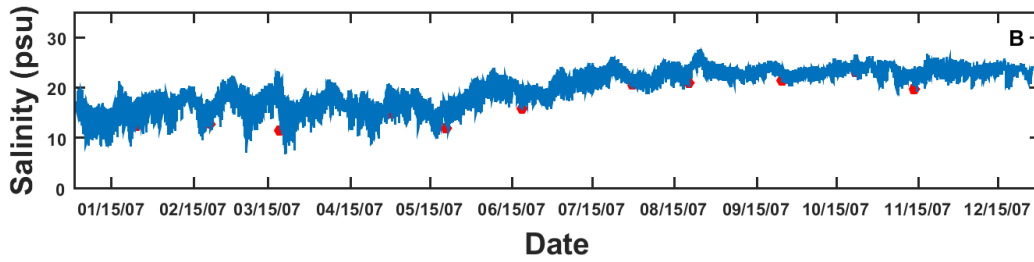
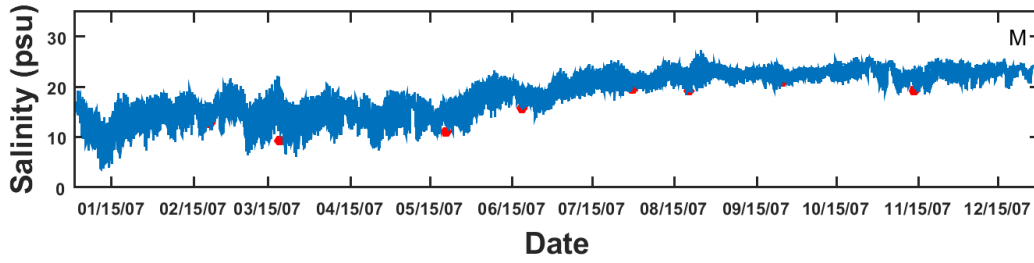
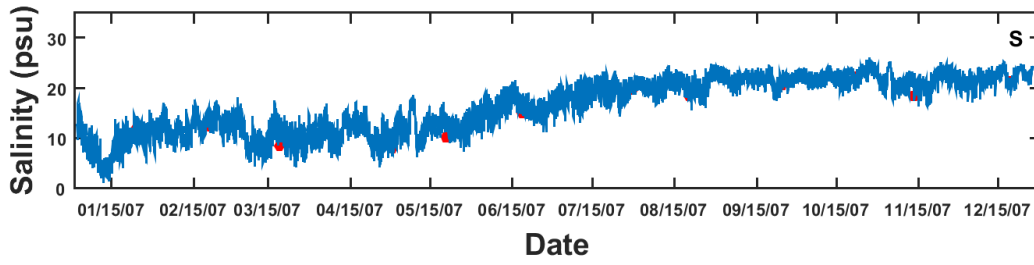
LE5.5-W



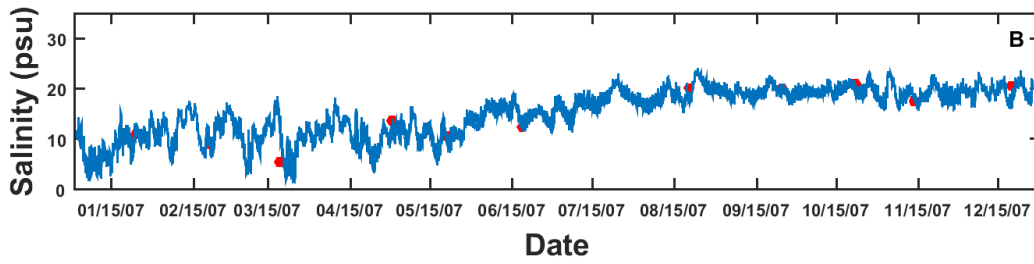
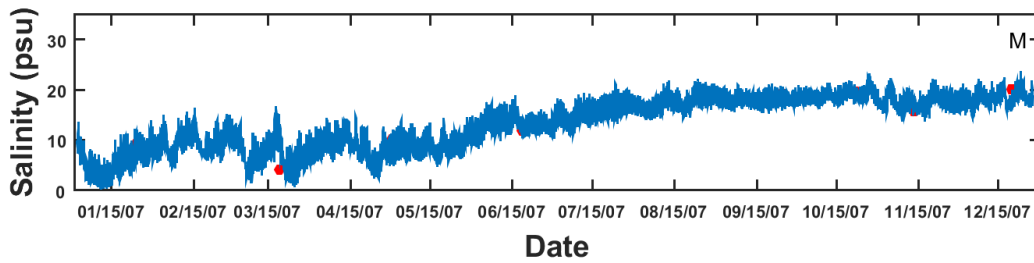
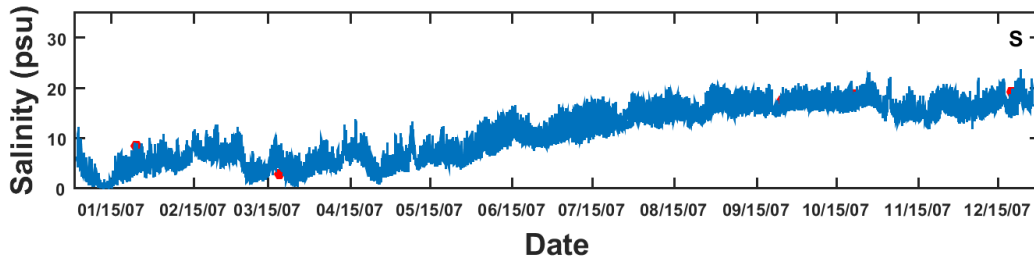
LE5.4



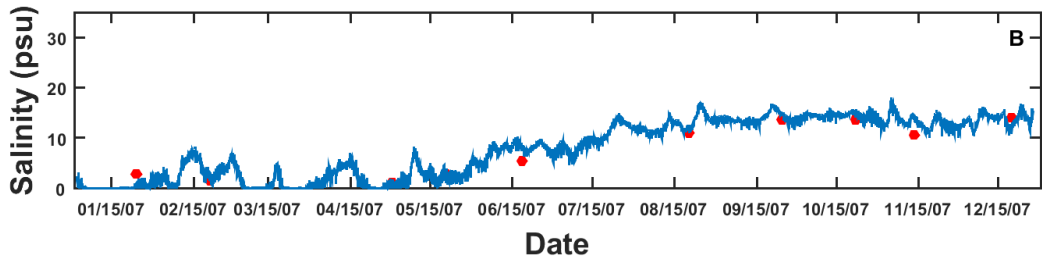
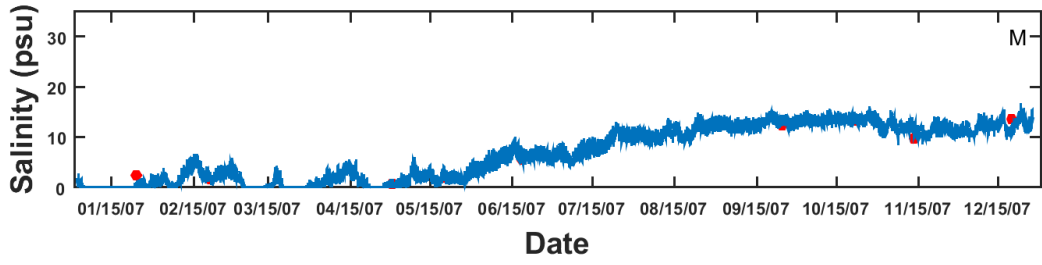
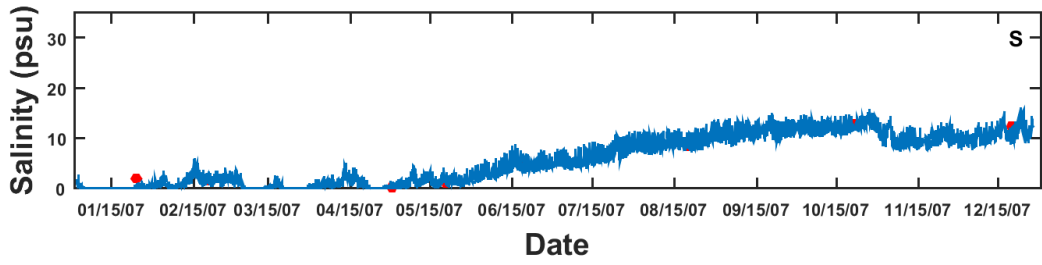
LE5.3



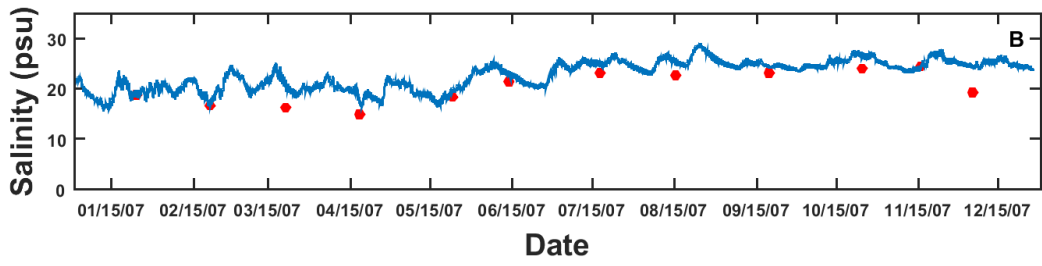
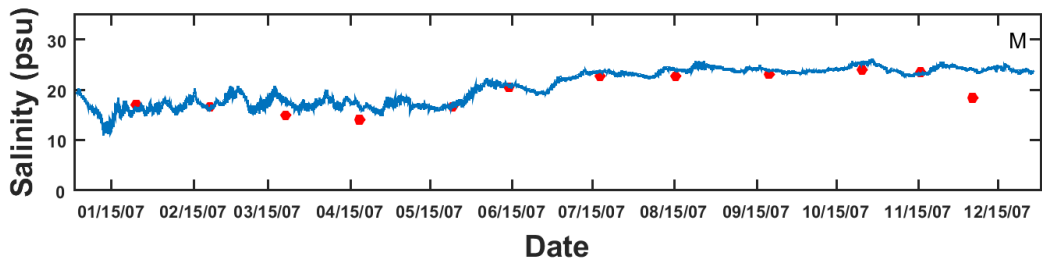
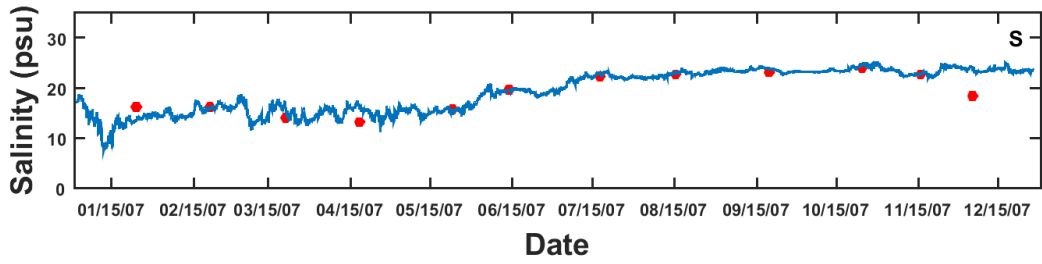
LE5.2



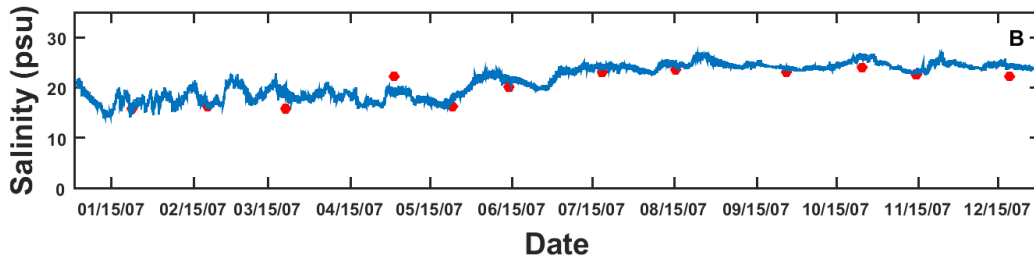
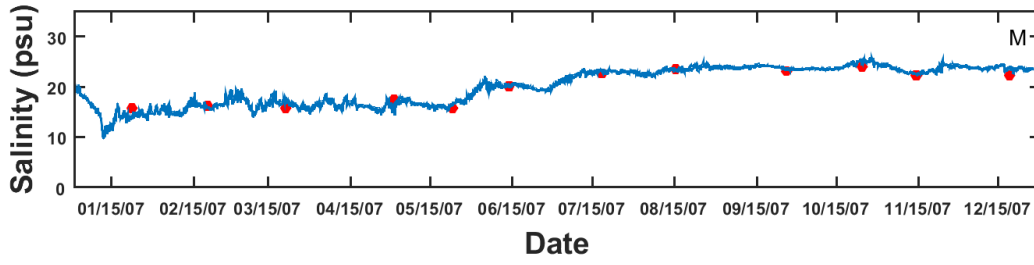
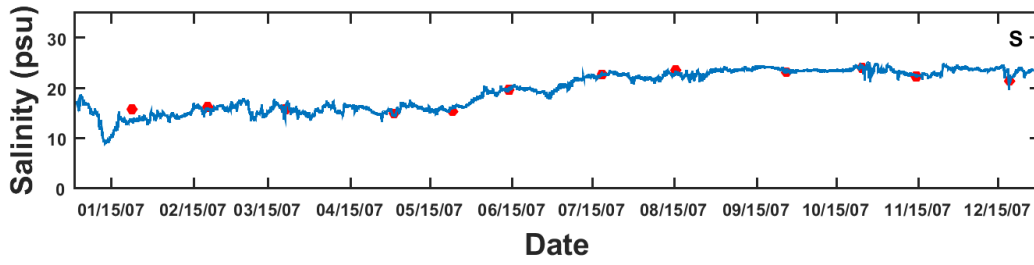
LE5.1



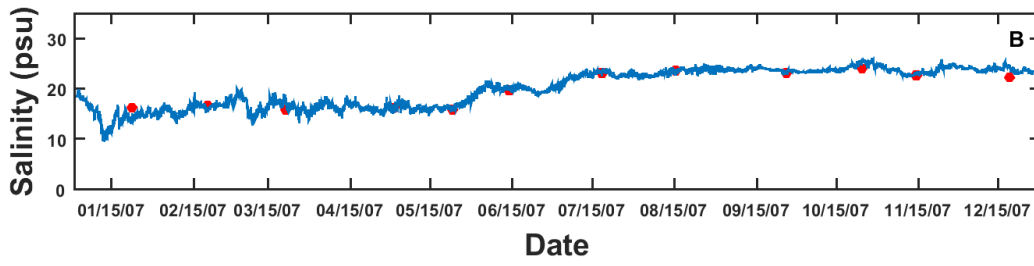
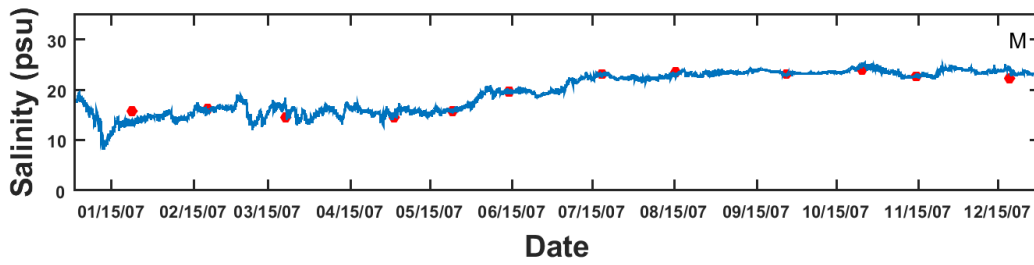
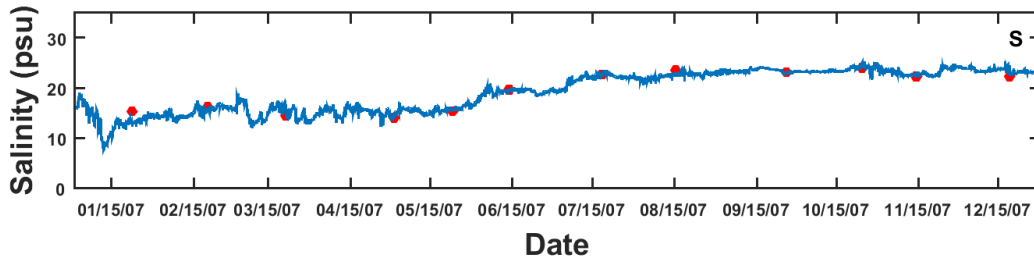
ELI2



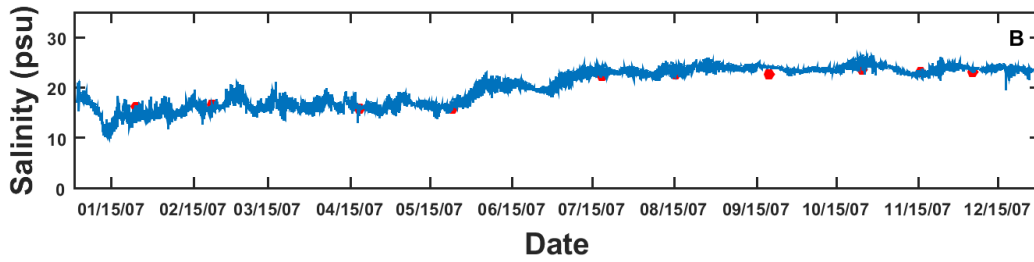
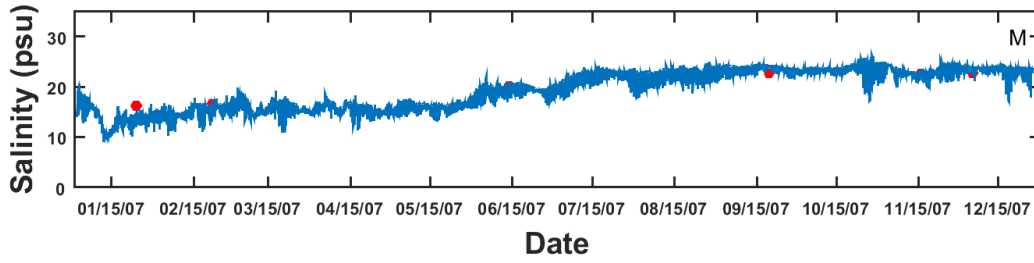
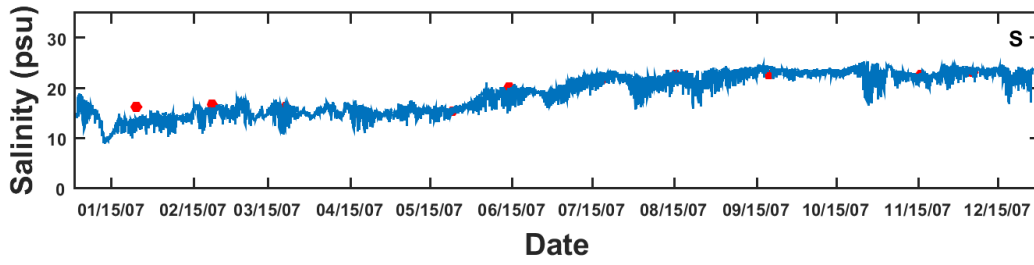
ELE01



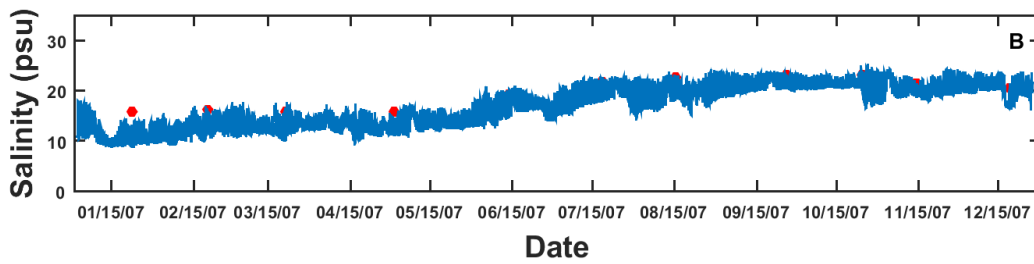
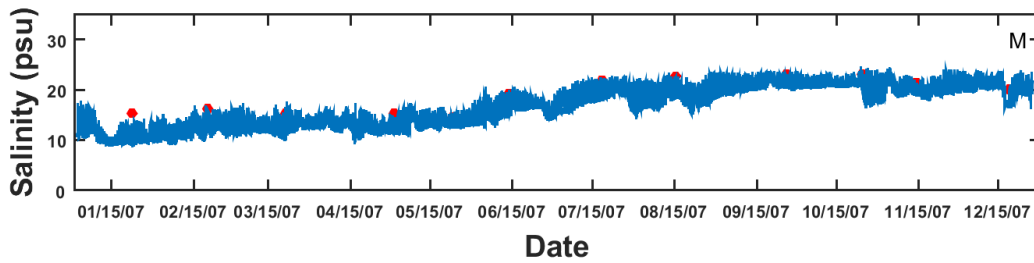
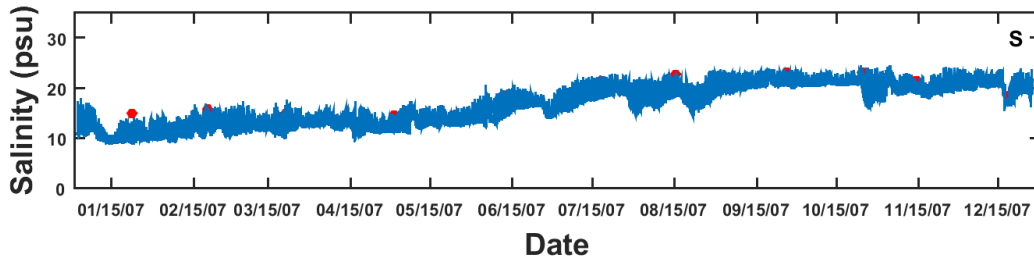
ELD01



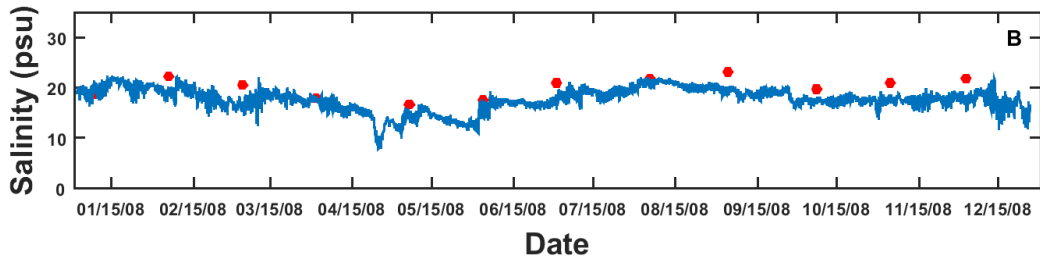
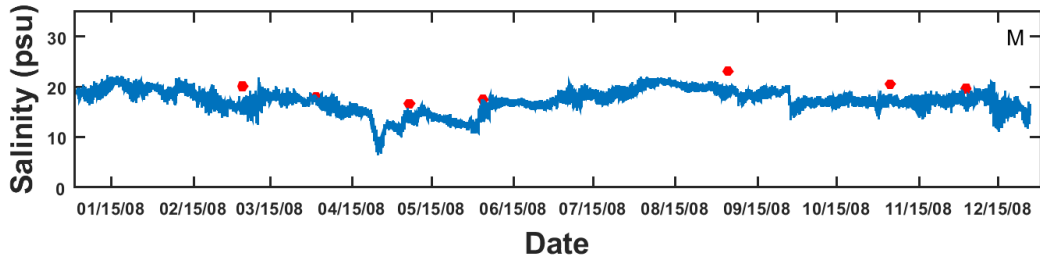
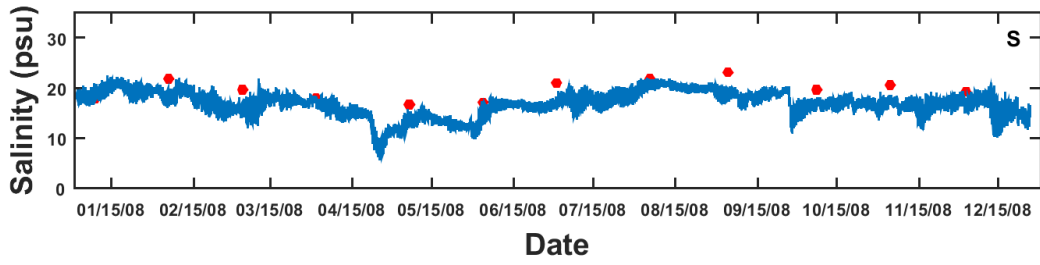
EBE1



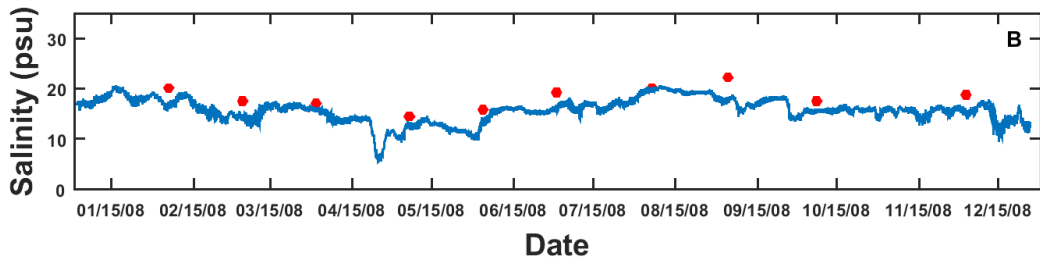
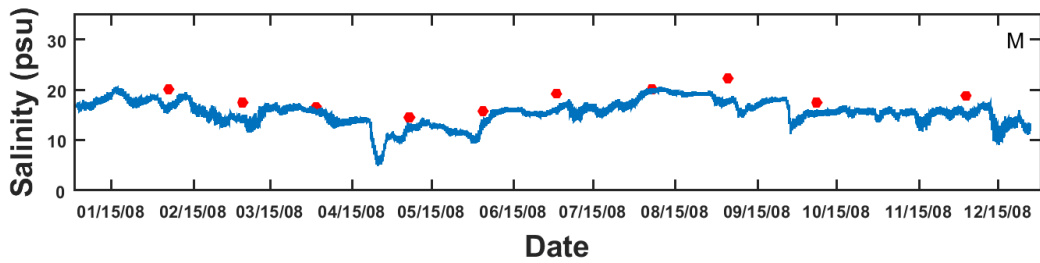
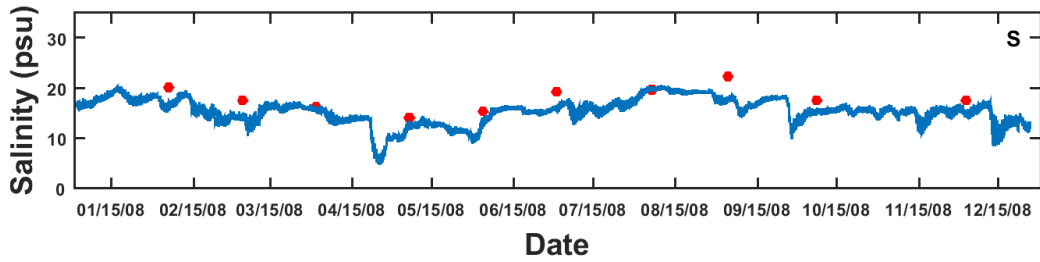
EBB01



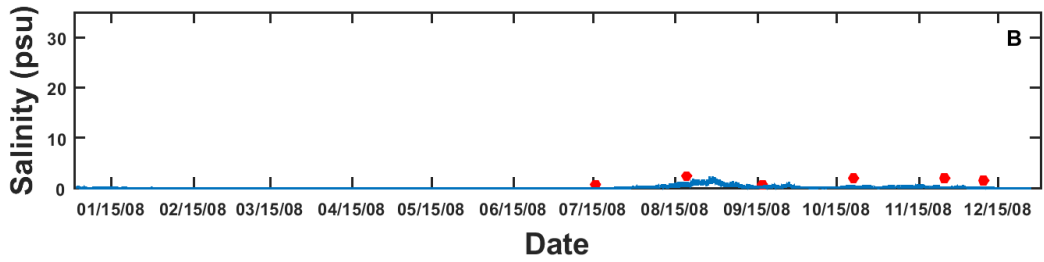
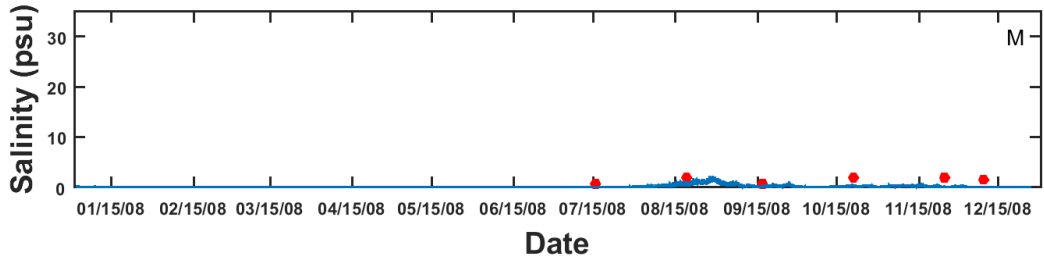
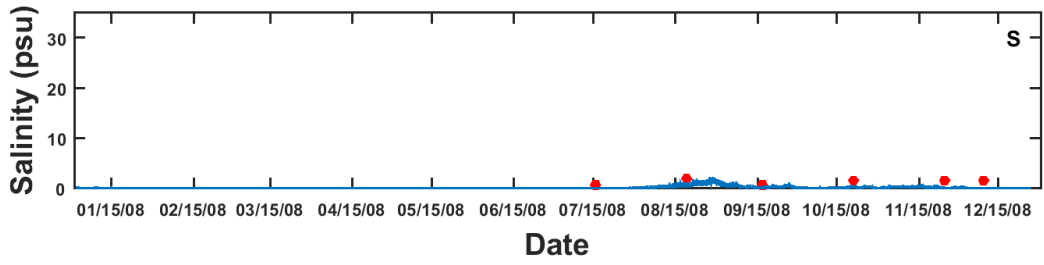
WBE1



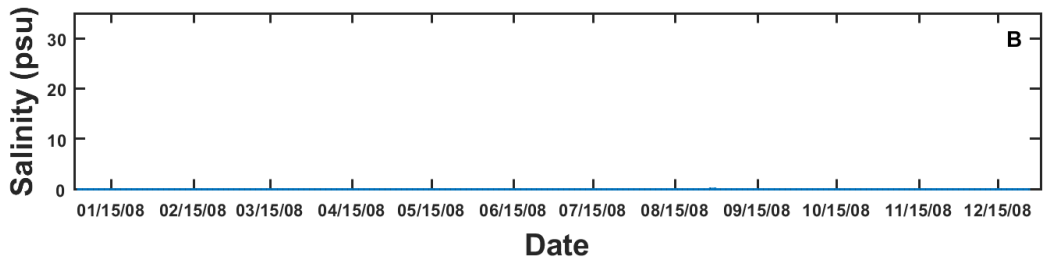
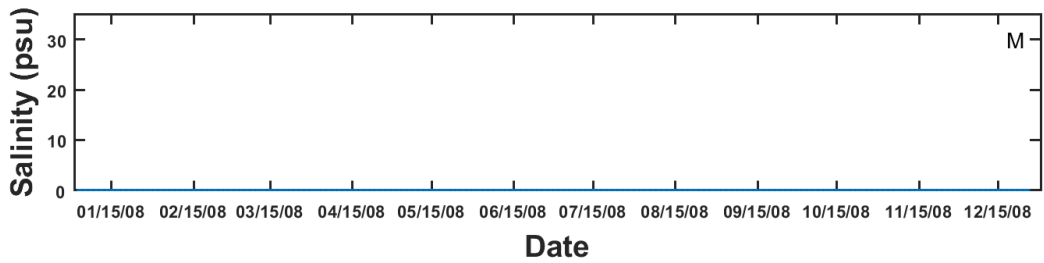
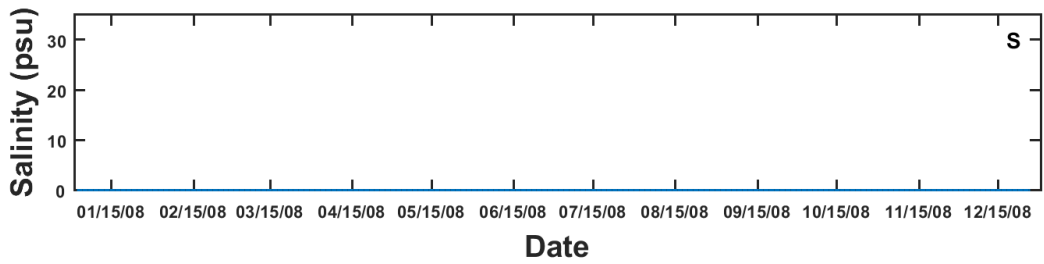
WBB05



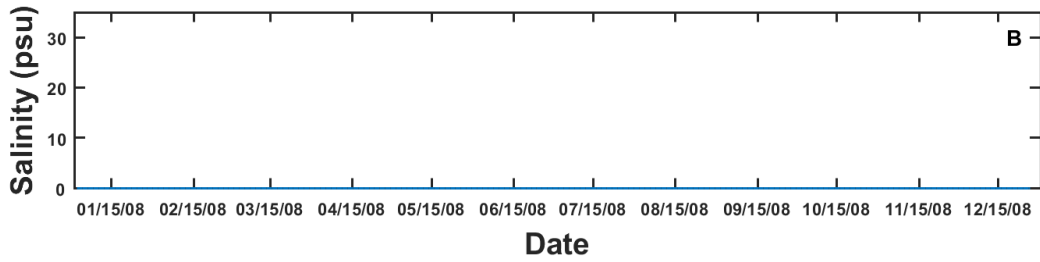
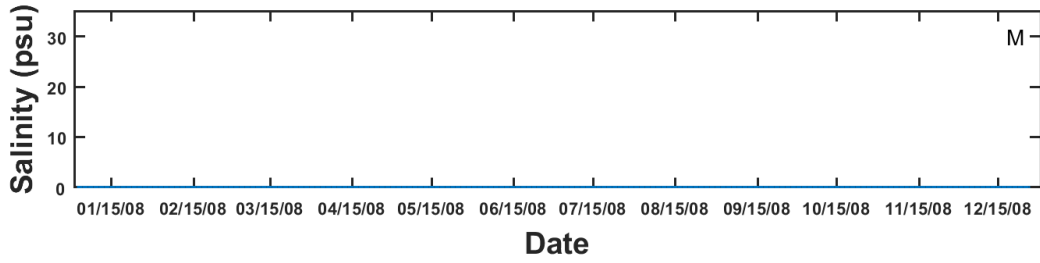
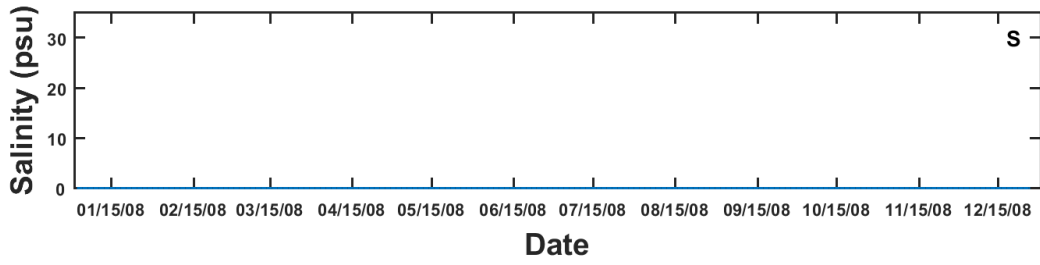
TF5.6



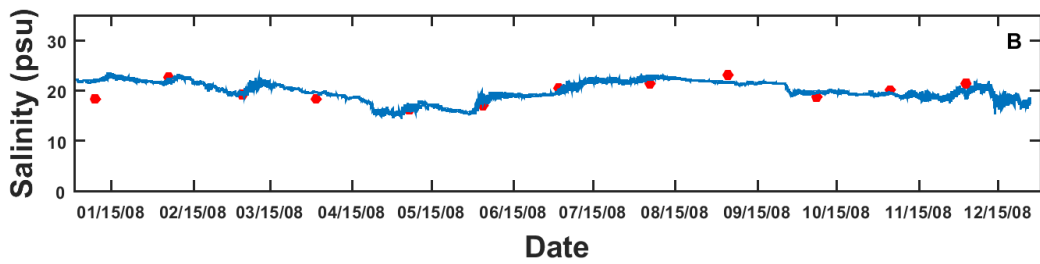
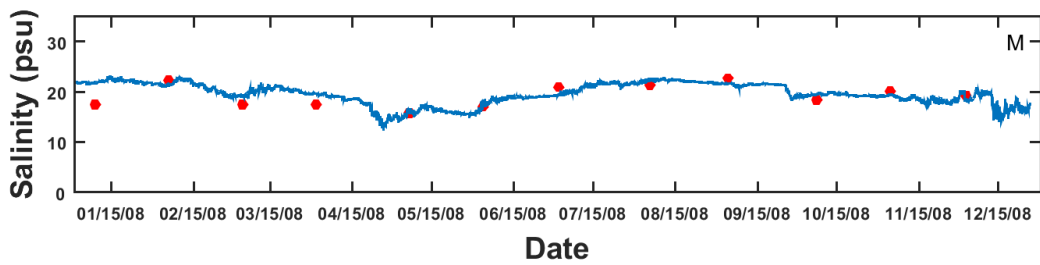
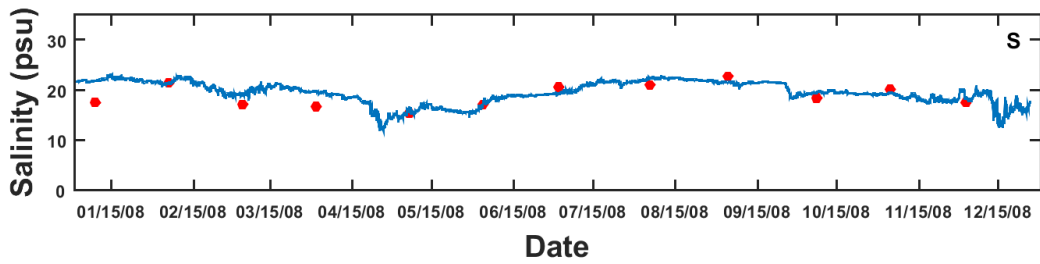
TF5.5A



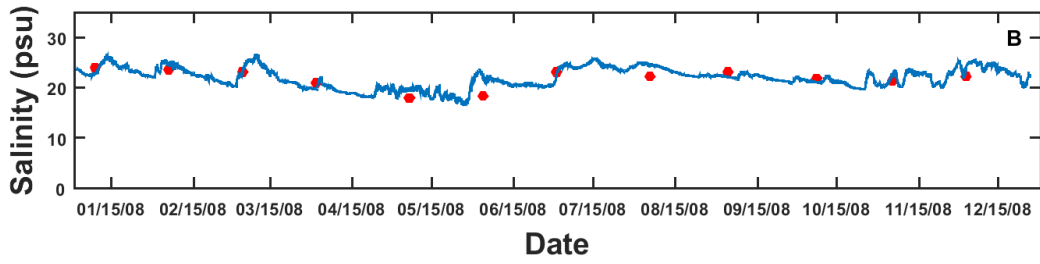
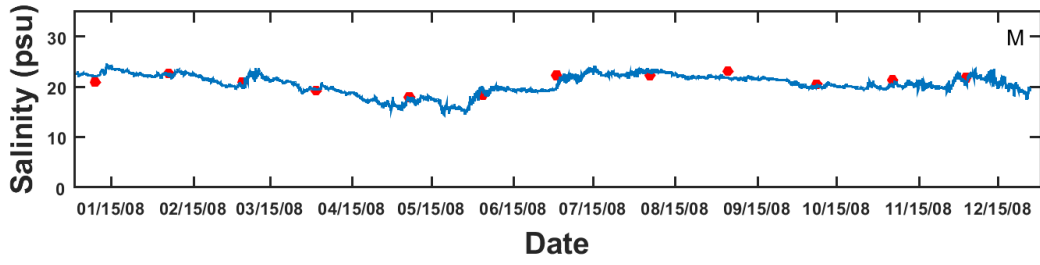
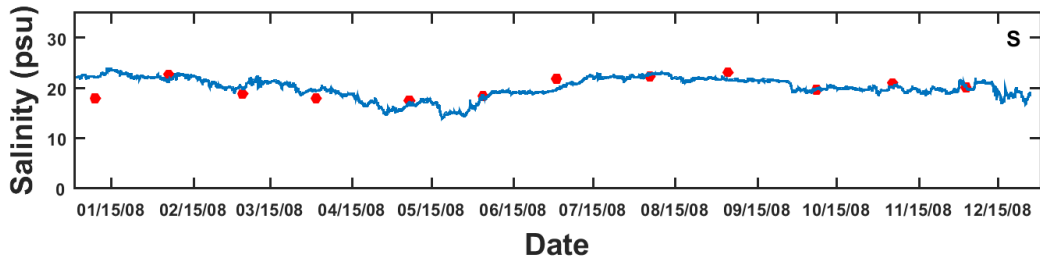
TF5.5



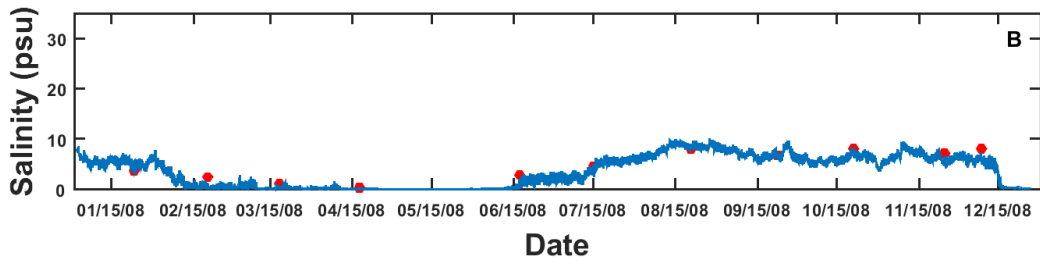
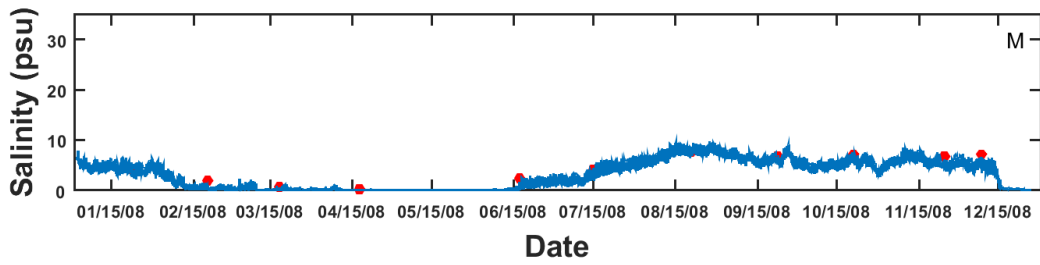
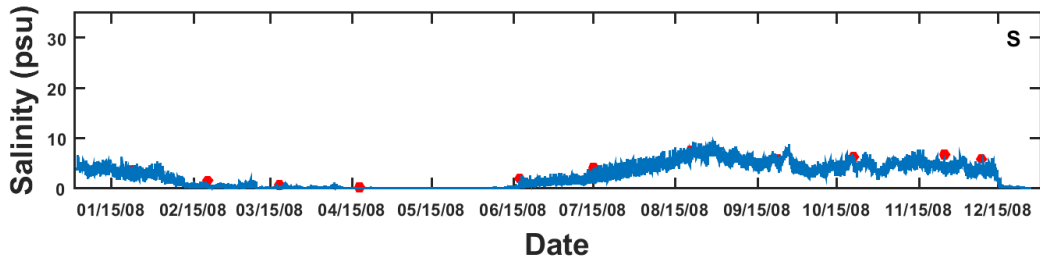
SBE5



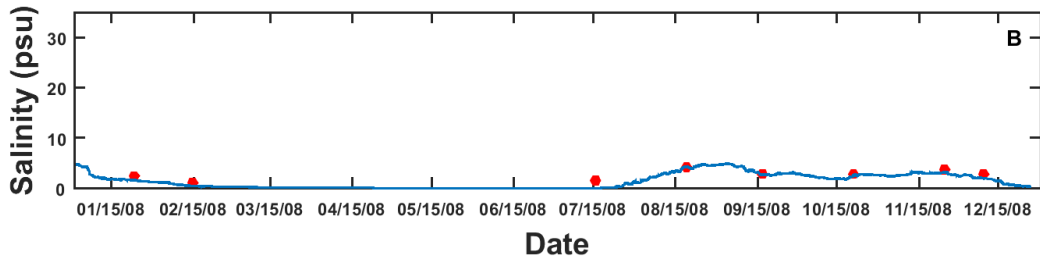
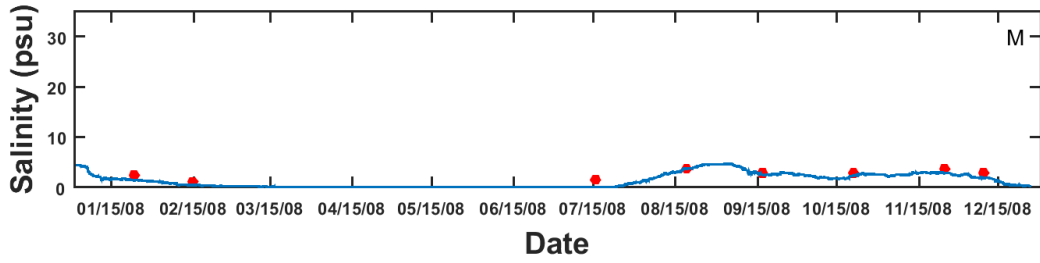
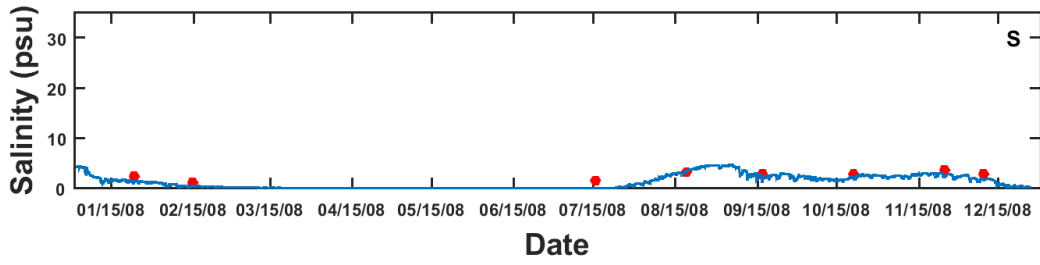
SBE2



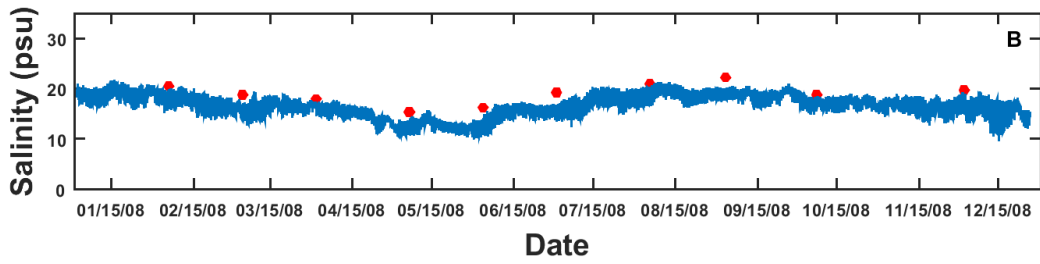
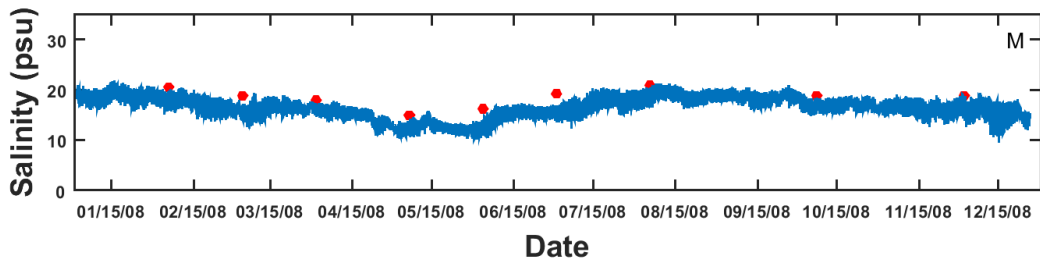
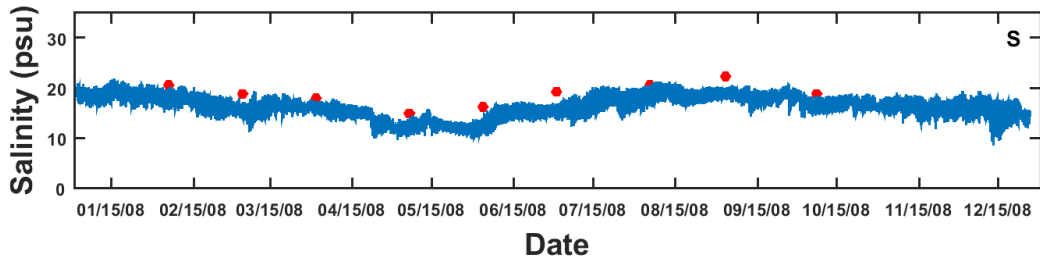
RET5.2



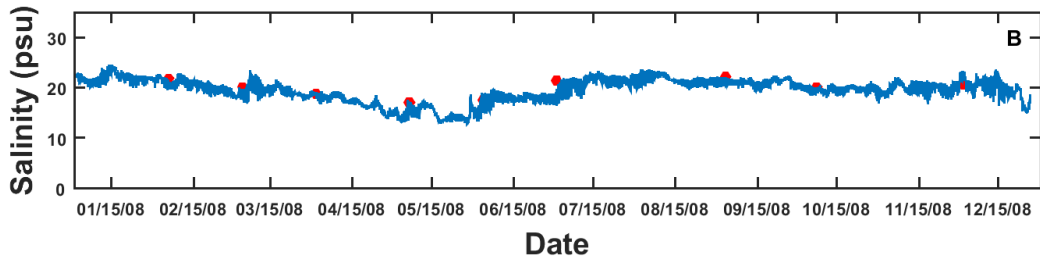
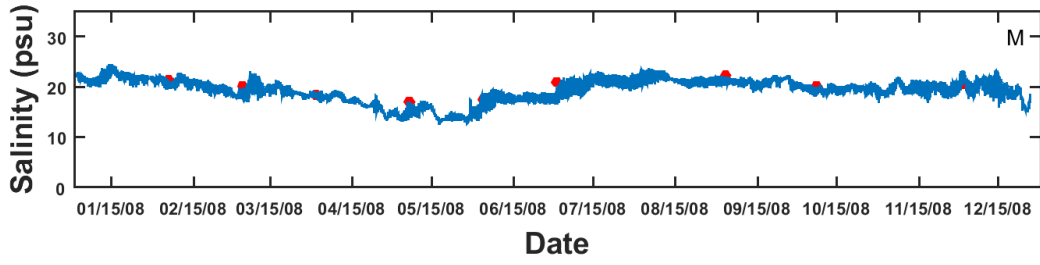
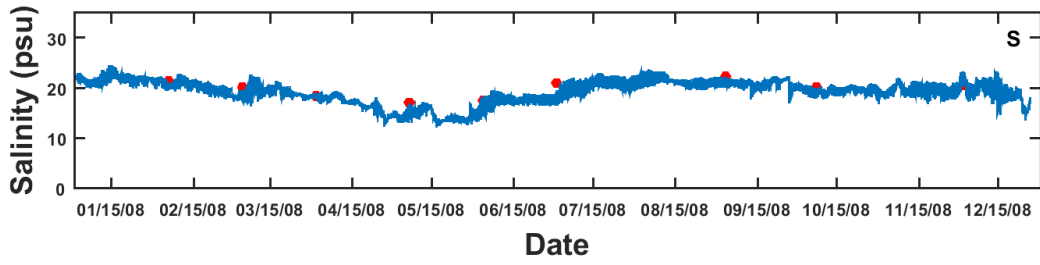
RET5.1A



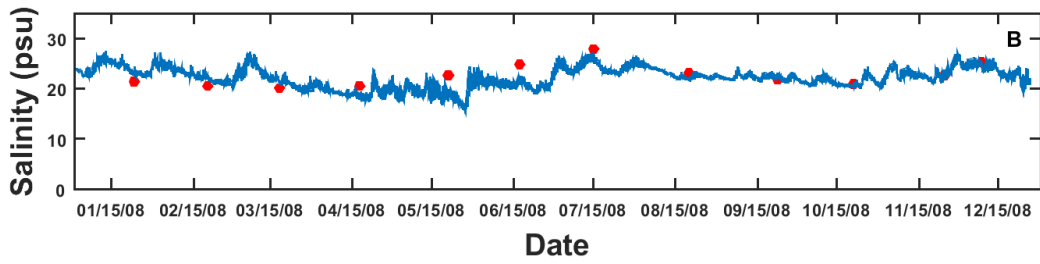
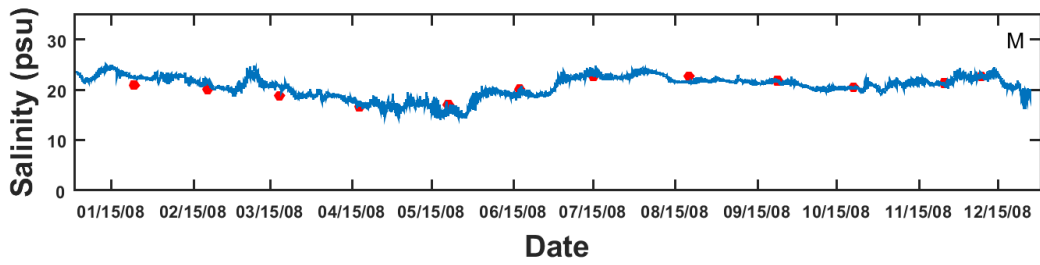
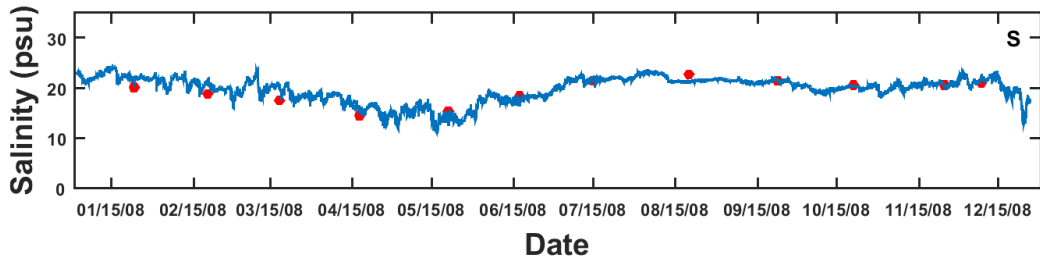
LFB01



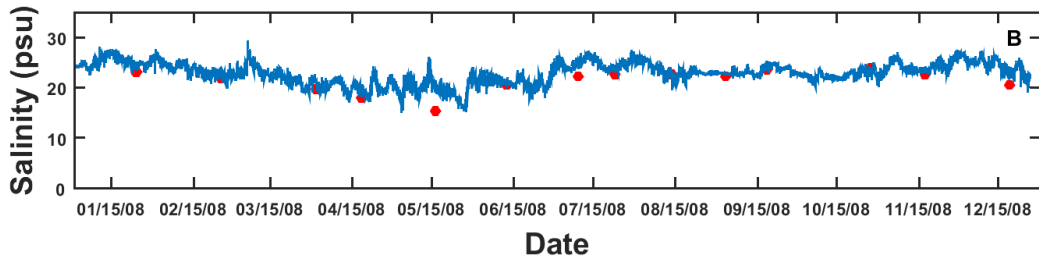
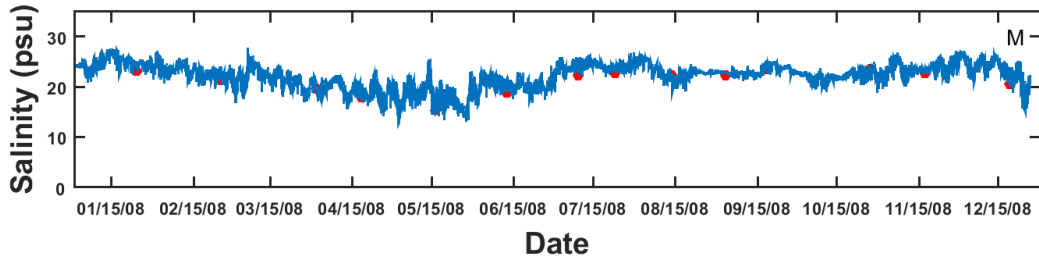
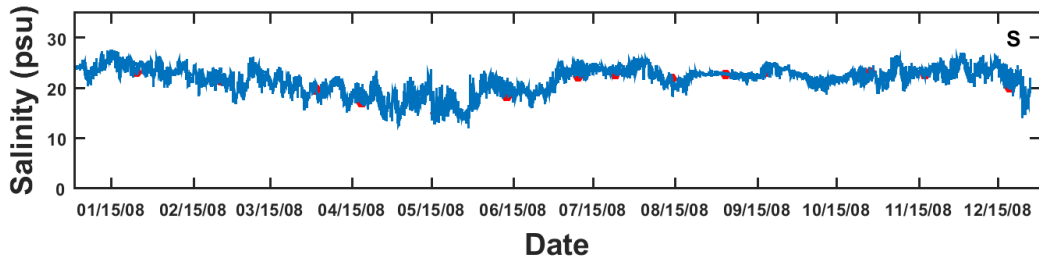
LFA01



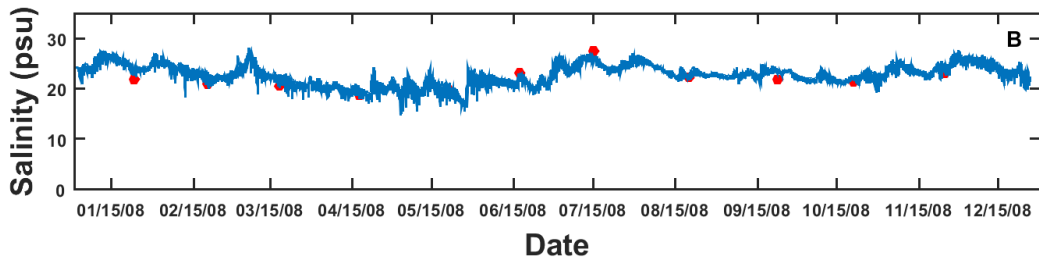
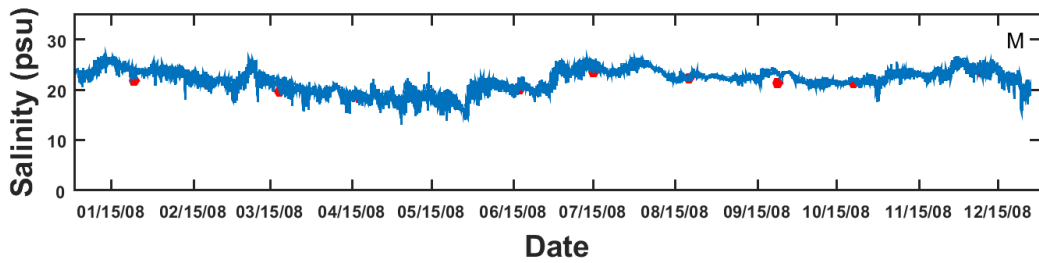
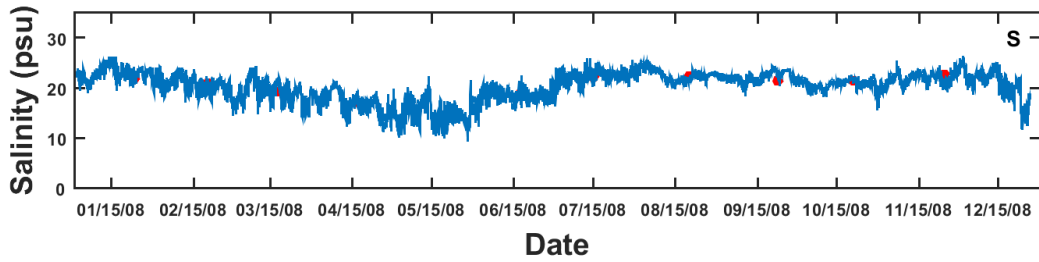
LE5.6



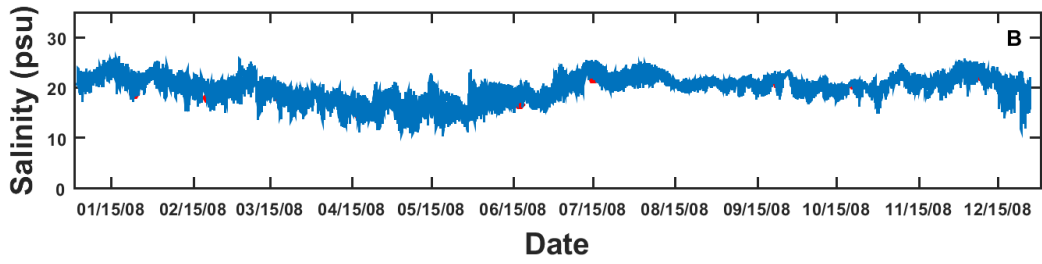
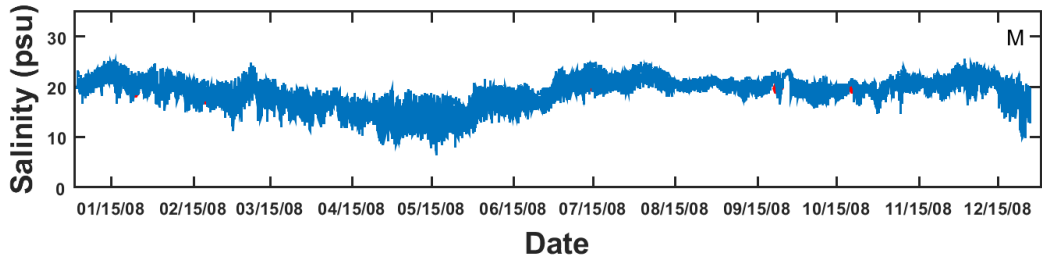
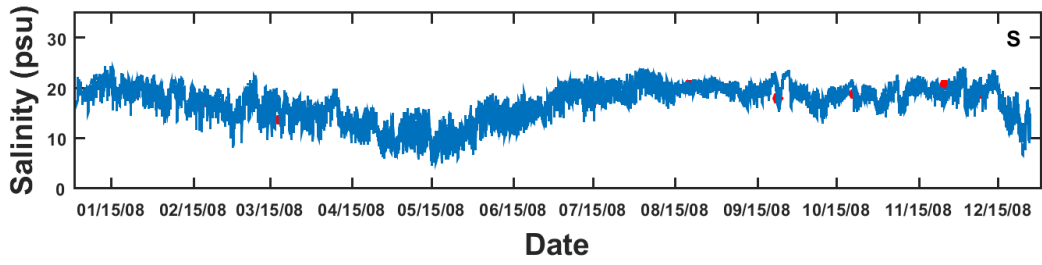
LE5.5-W



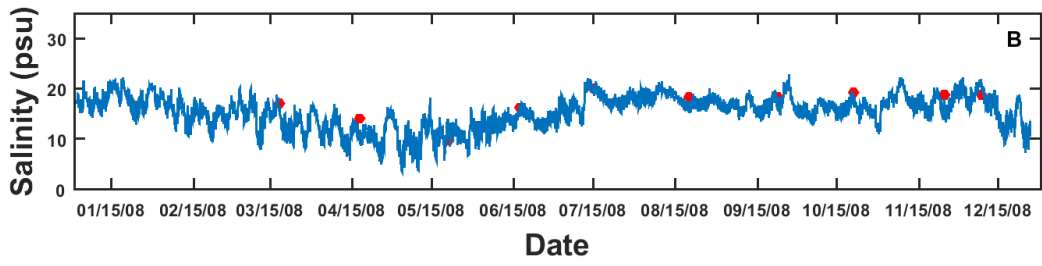
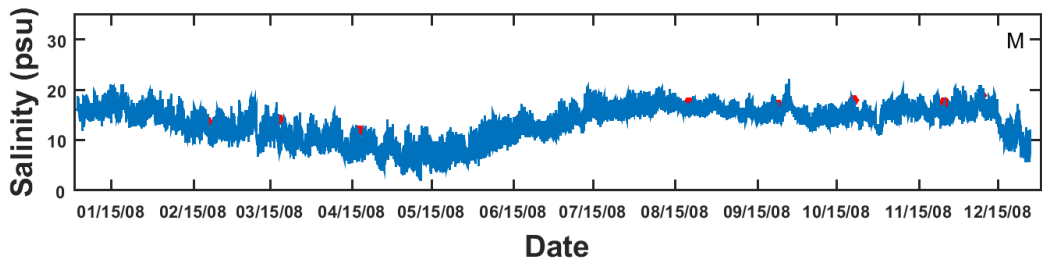
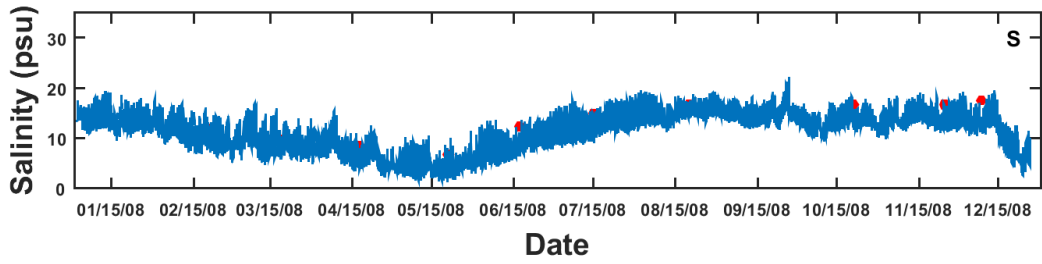
LE5.4



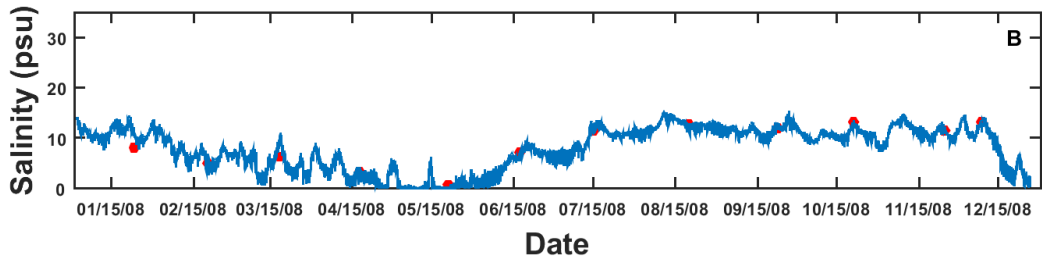
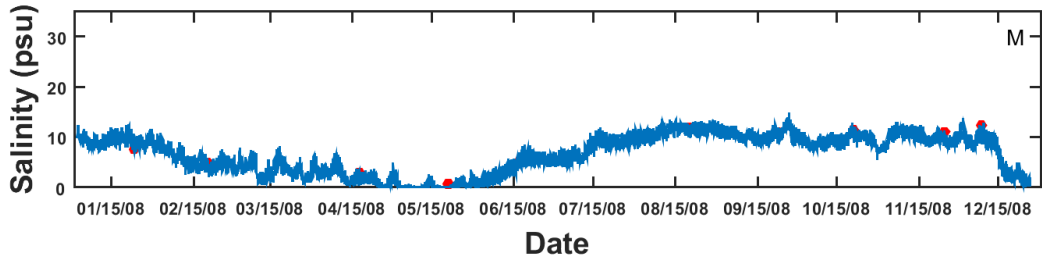
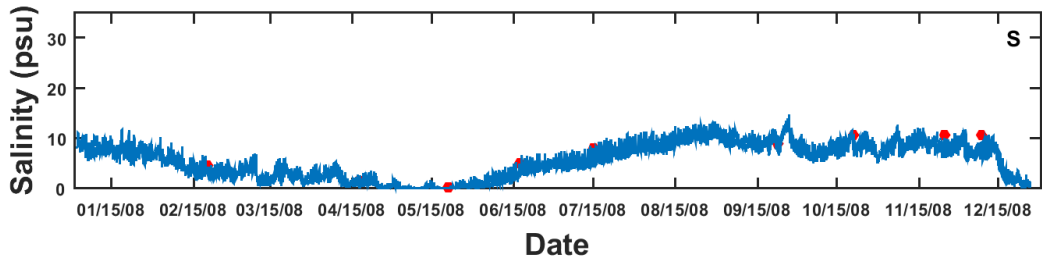
LE5.3



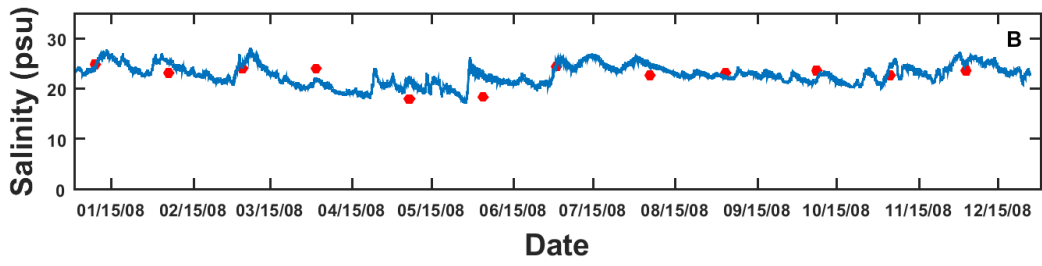
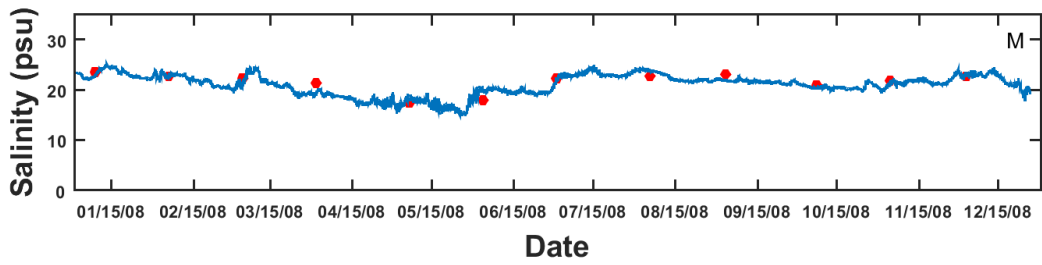
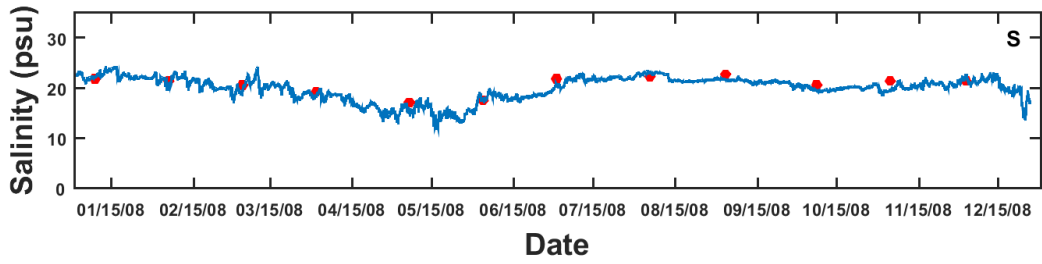
LE5.2



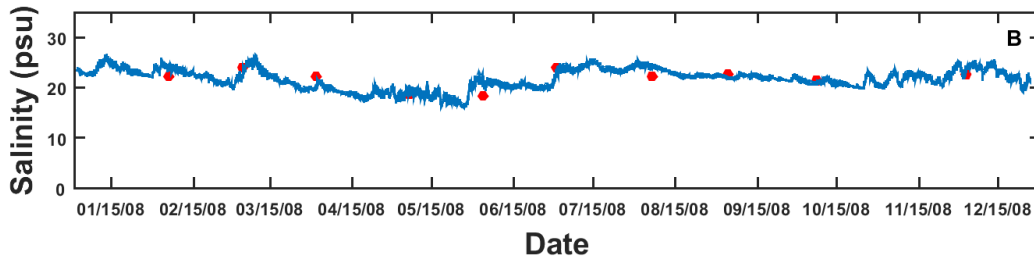
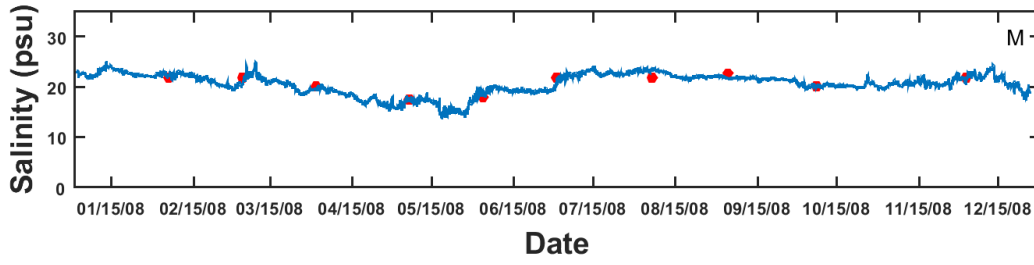
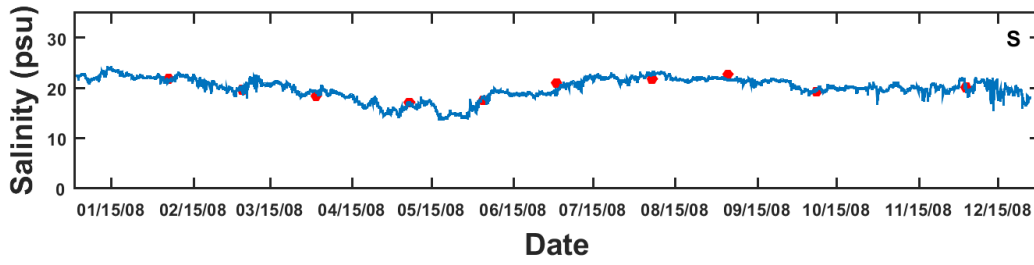
LE5.1



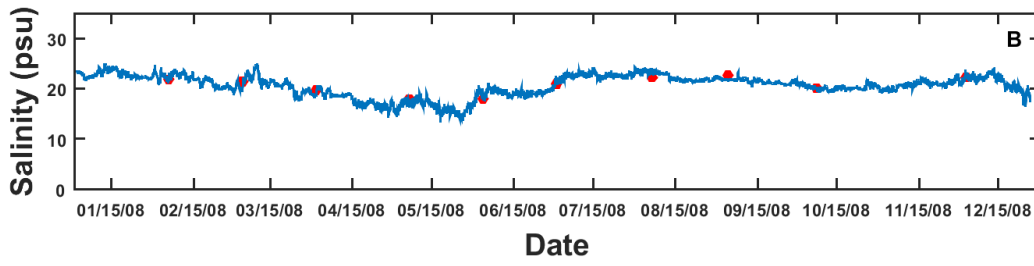
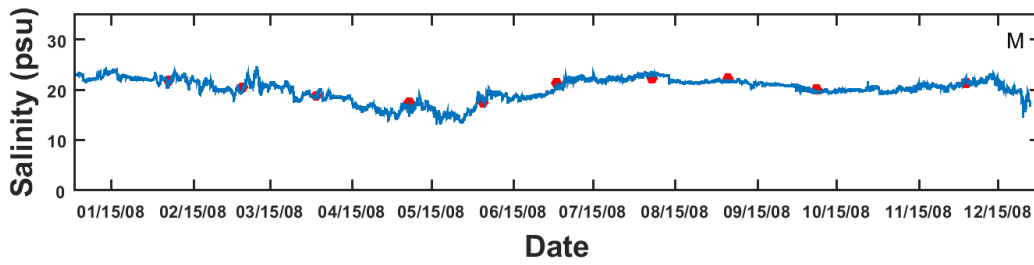
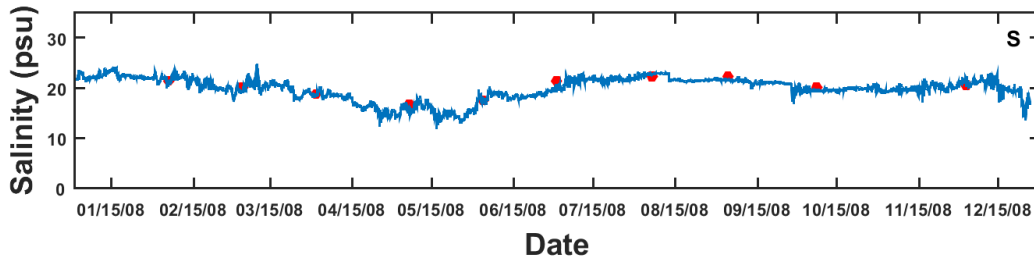
ELI2



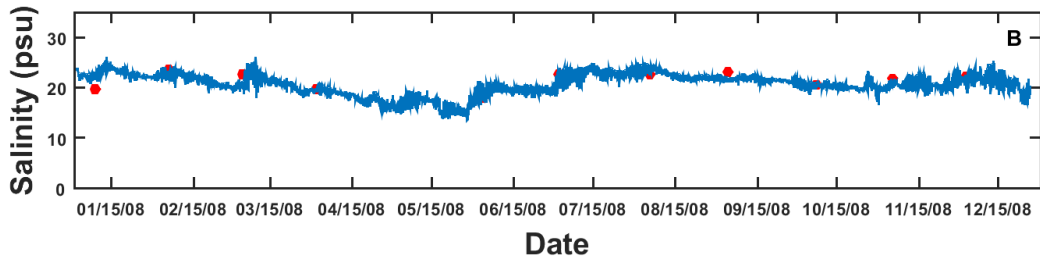
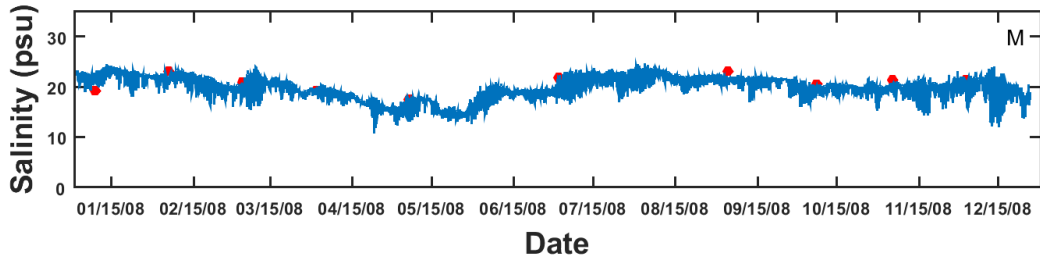
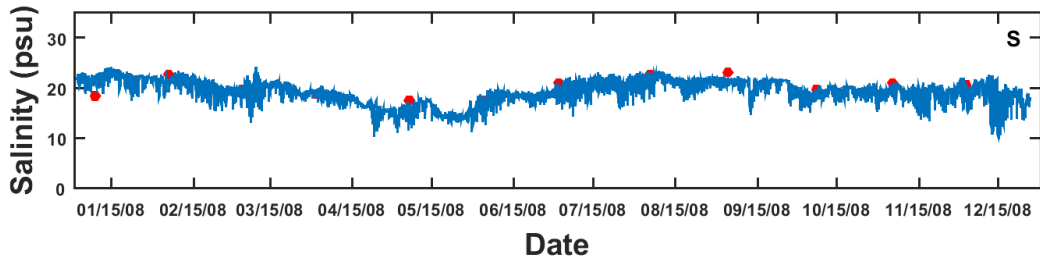
ELE01



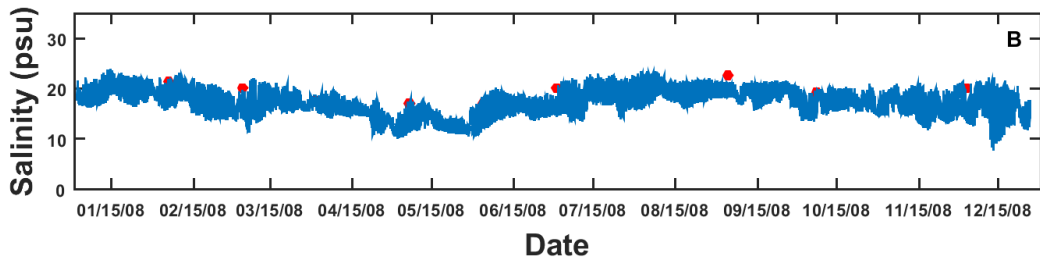
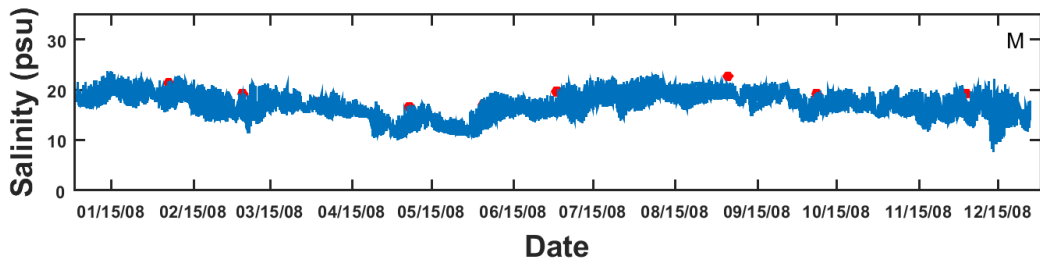
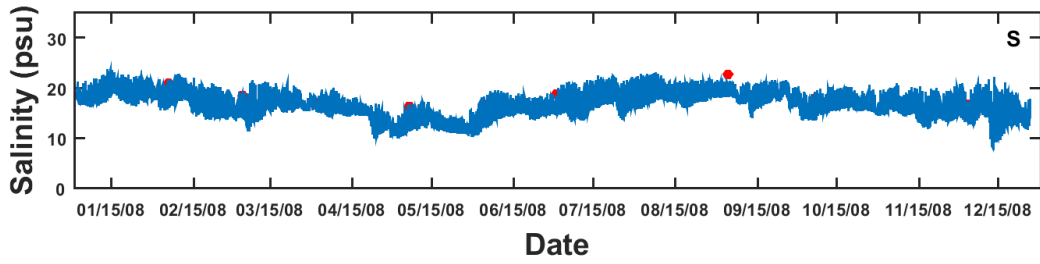
ELD01



EBE1



EBB01



1. Appendix D

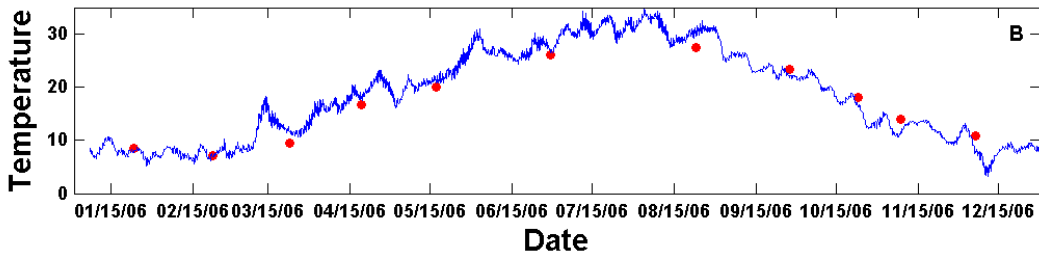
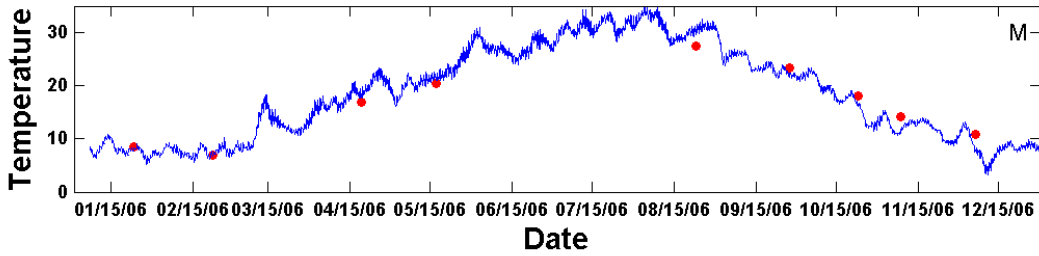
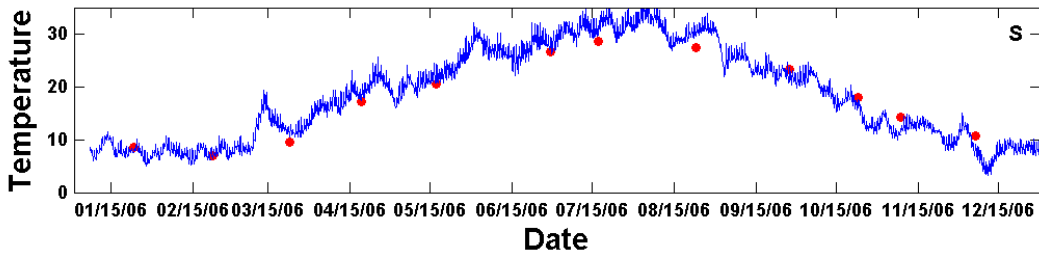
Temperature calibration results

Temperature values predicted by the model were compared with observed temperatures at Chesapeake Bay stations from 2006-2008. Locations of monitoring stations are shown in Figure 3-2. Model simulations were compared against the observation for each as shown in the following figures. Blue lines show model results and red dots show observations in figures. Labels 'S', 'M', and 'B' represent surface layer, middle layer, and bottom layer, respectively.

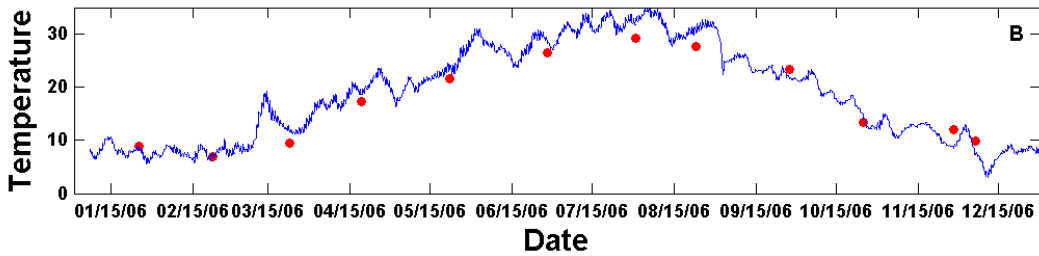
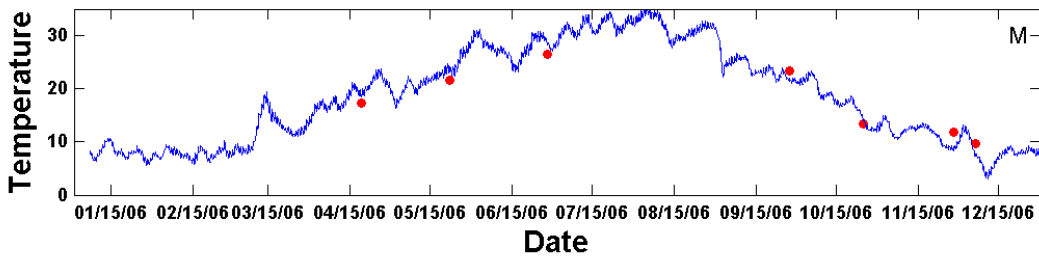
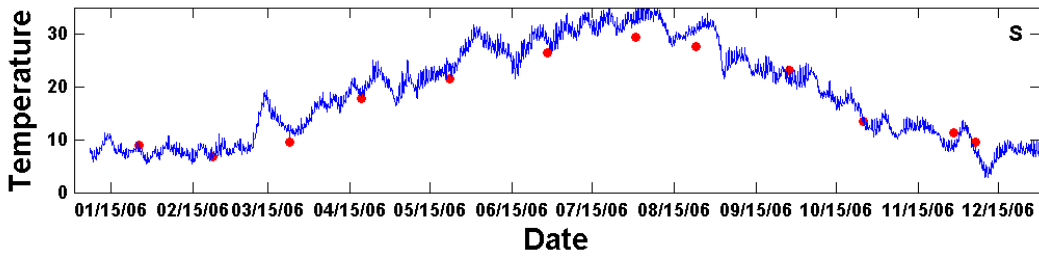
<u>Simulation Year</u>	<u>Pages</u>
2006	D2-D13
2007	D14-D25
2008	D26-D37

2.

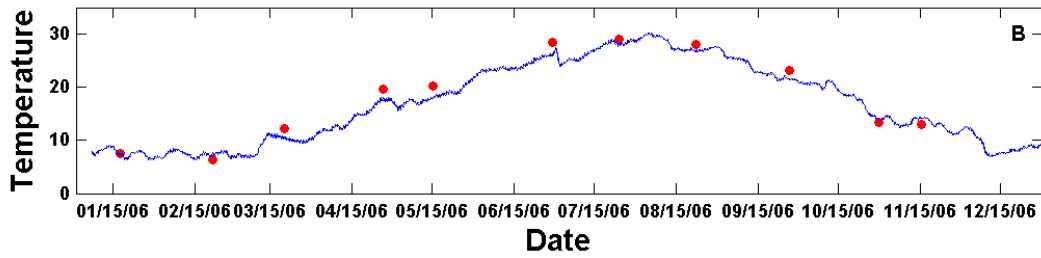
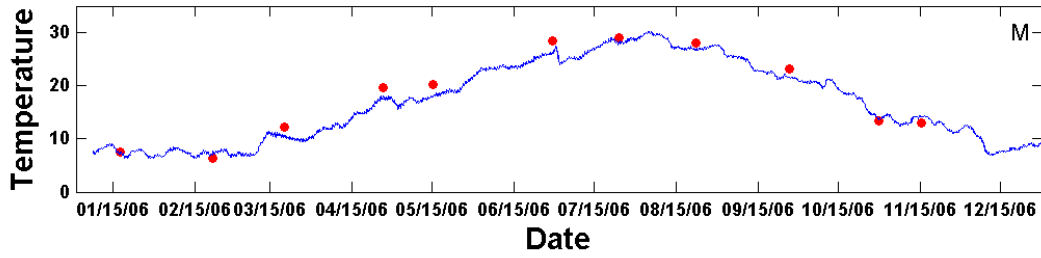
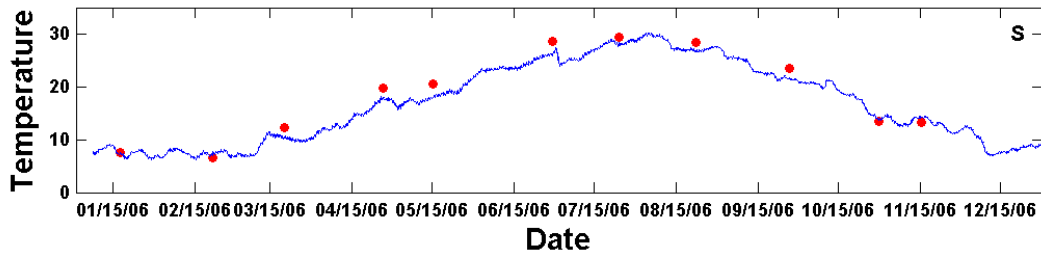
WBE1



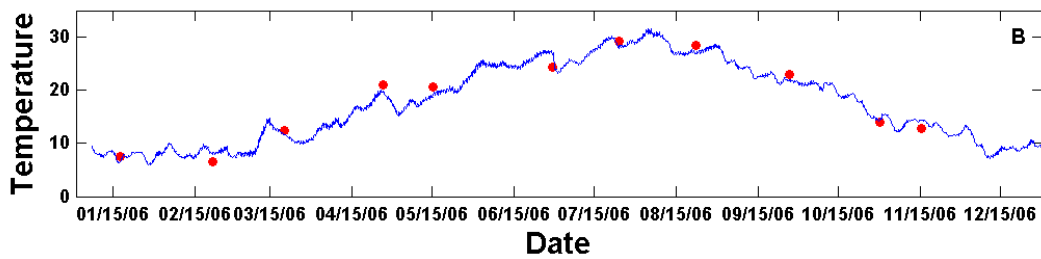
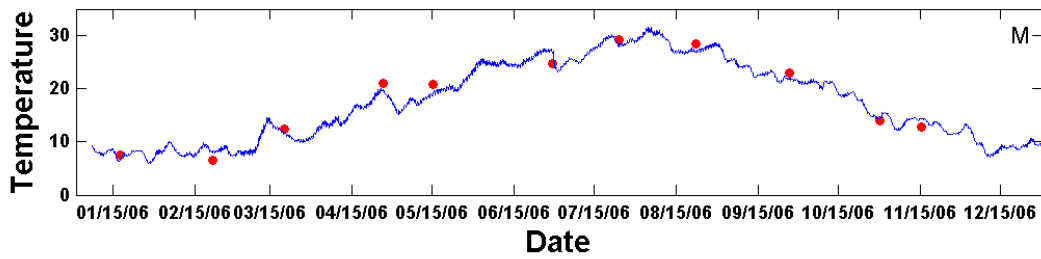
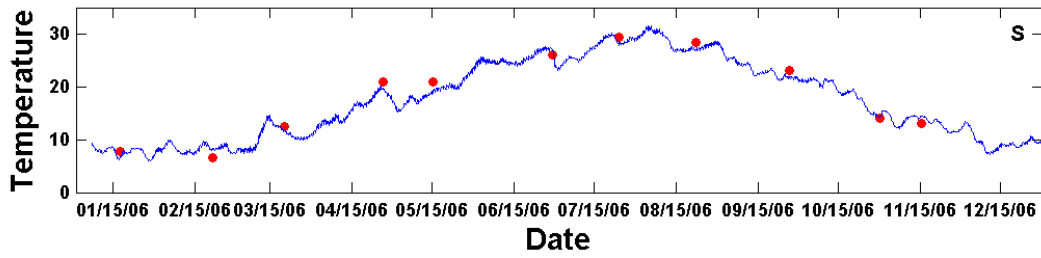
WBB05



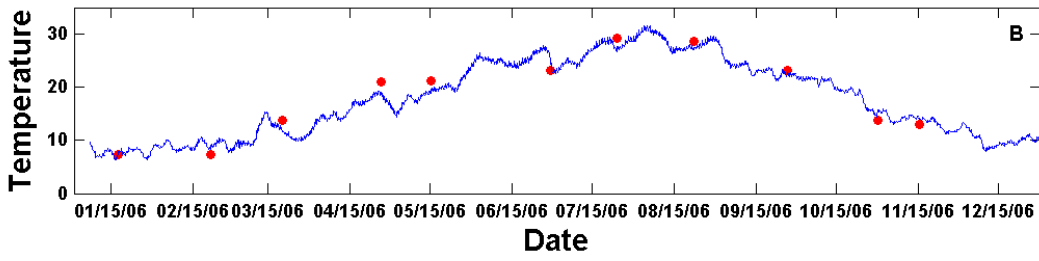
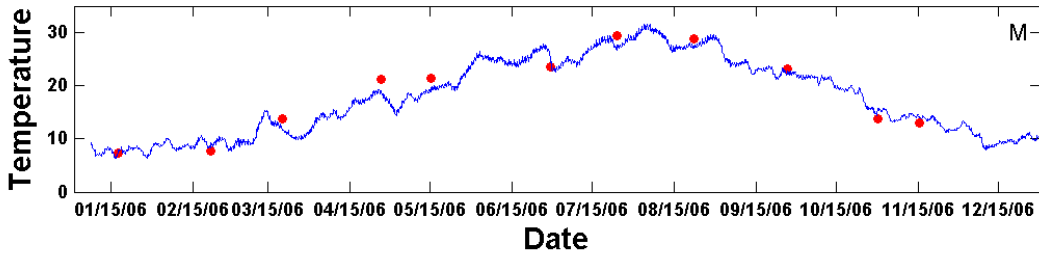
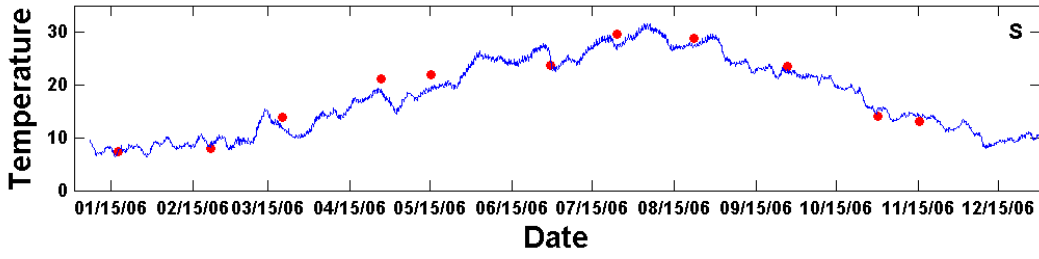
TF5.6



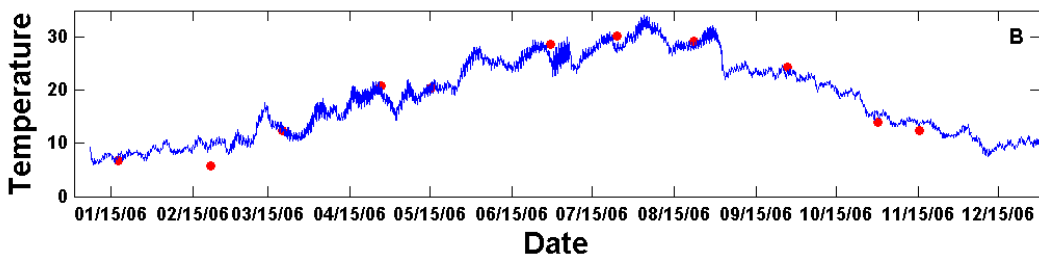
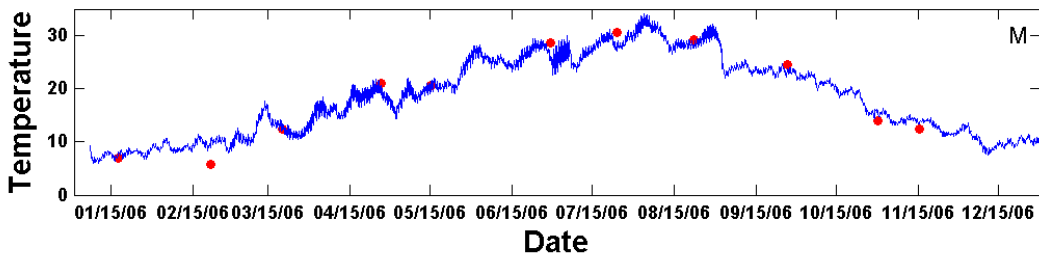
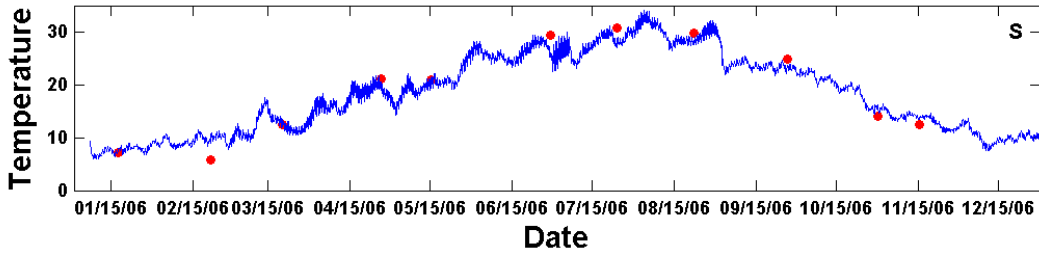
TF5.5A



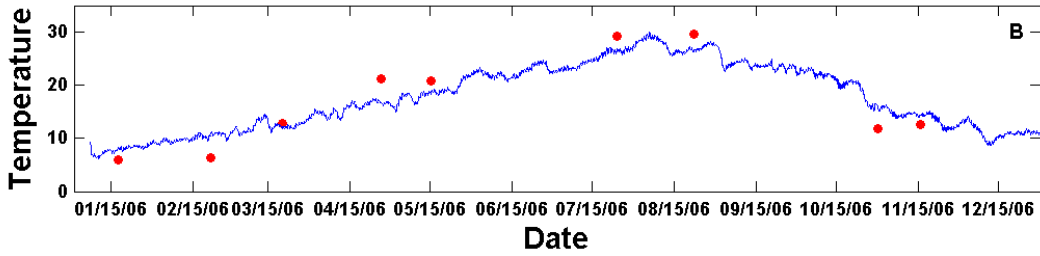
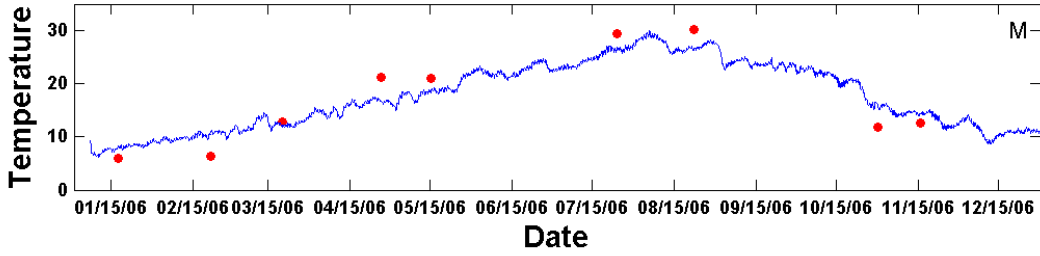
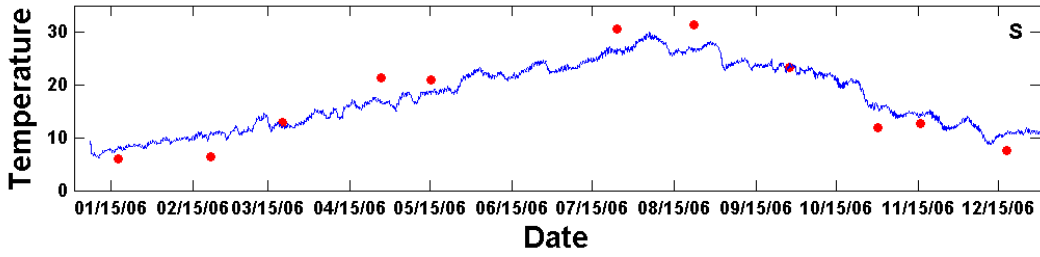
TF5.5



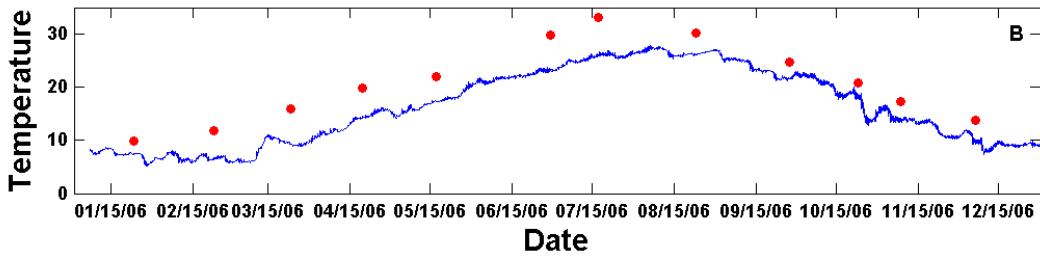
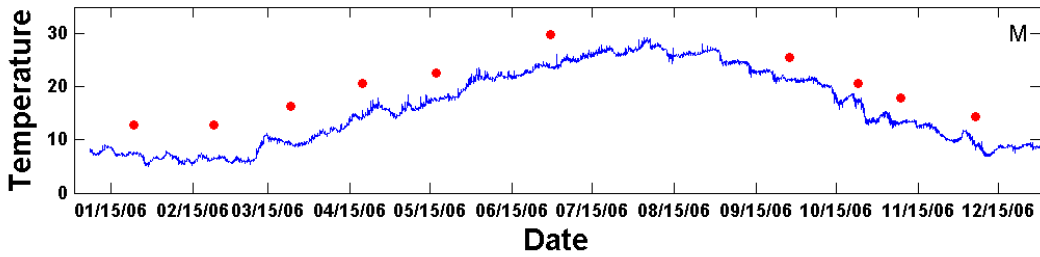
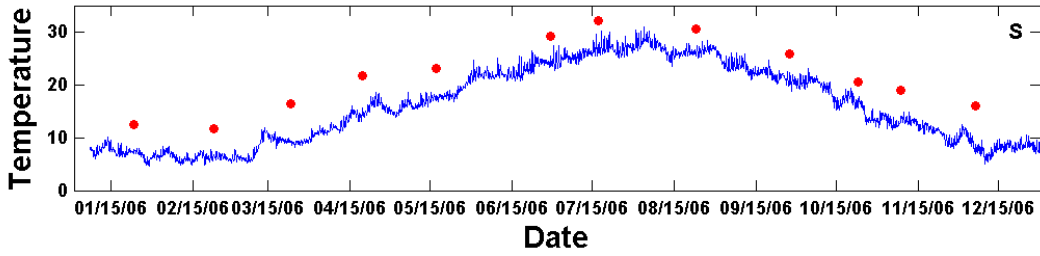
TF5.4



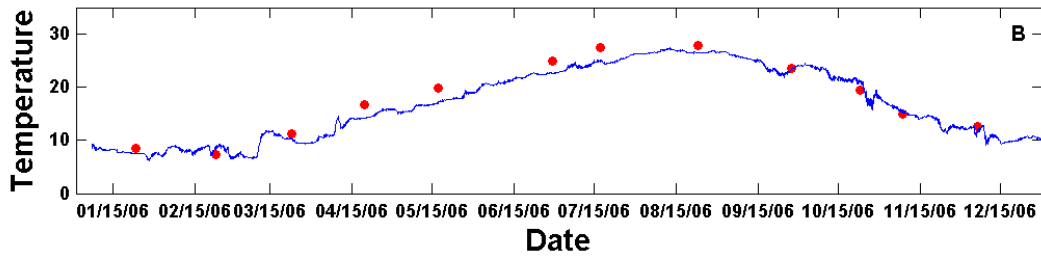
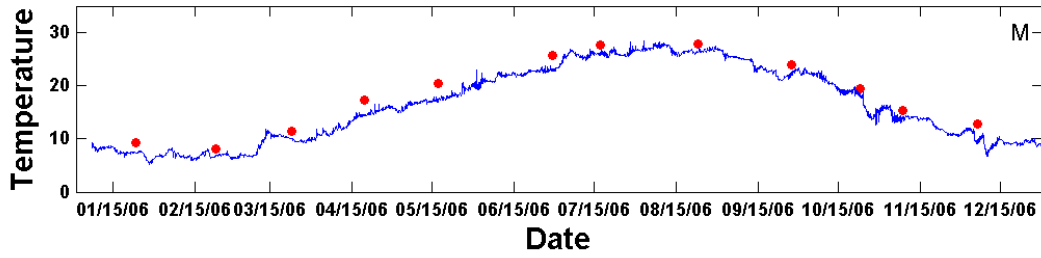
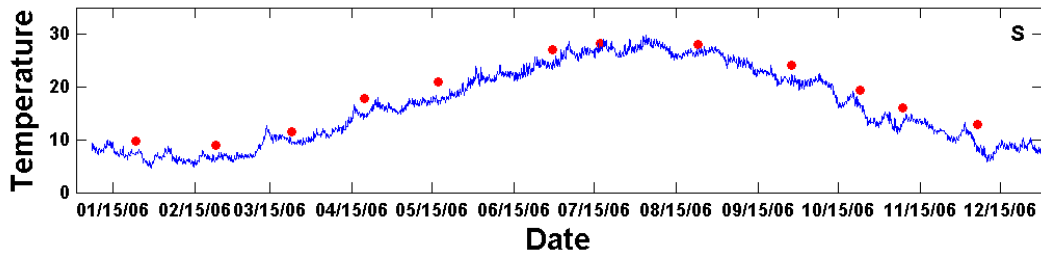
TF5.3



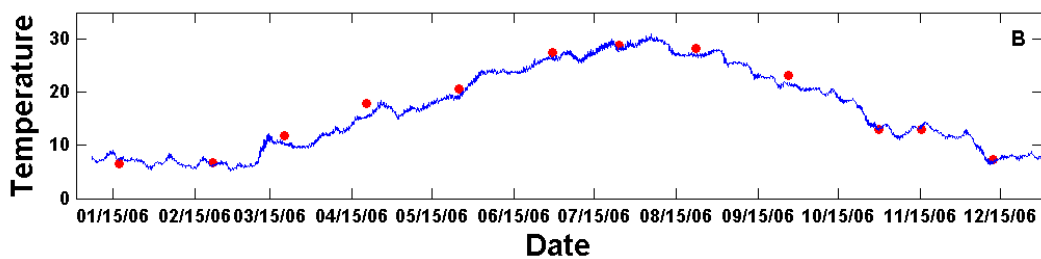
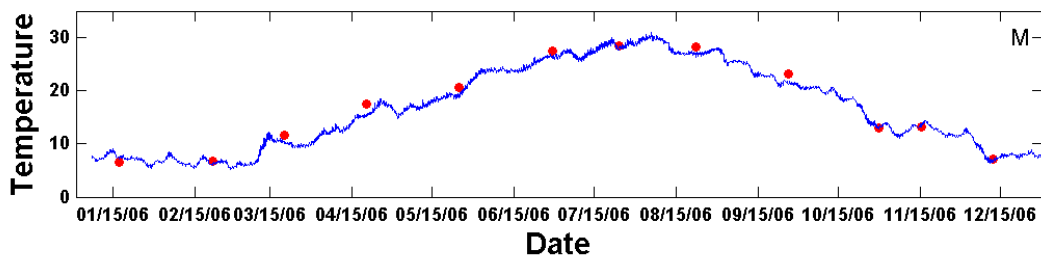
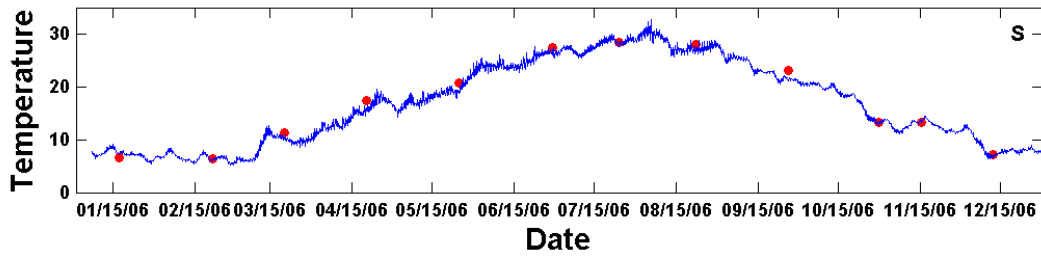
SBE5



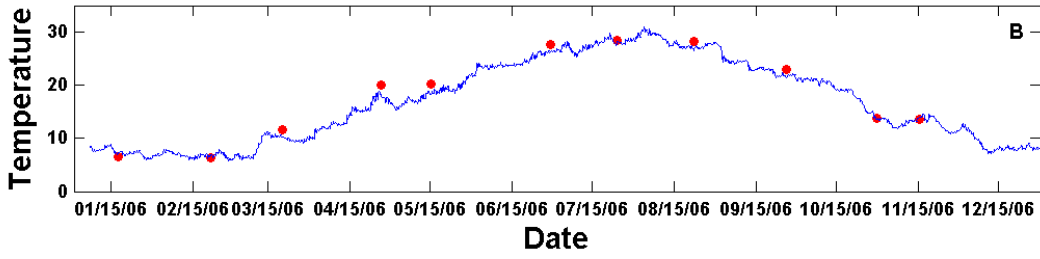
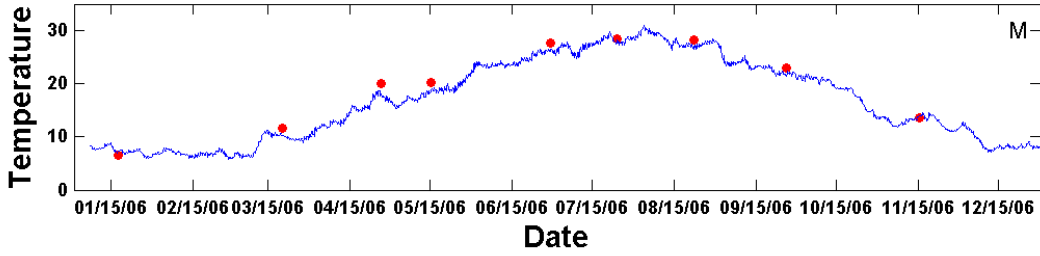
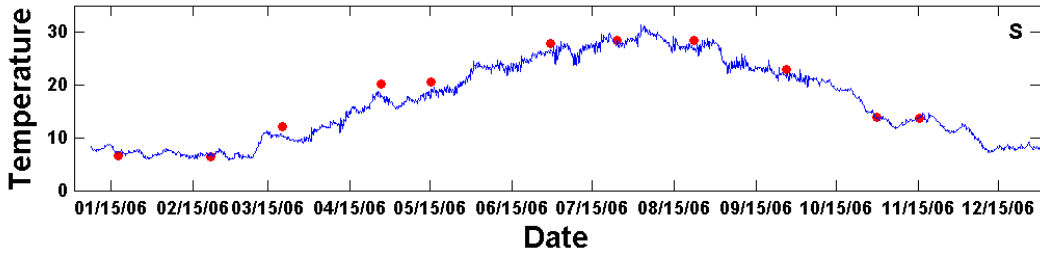
SBE2



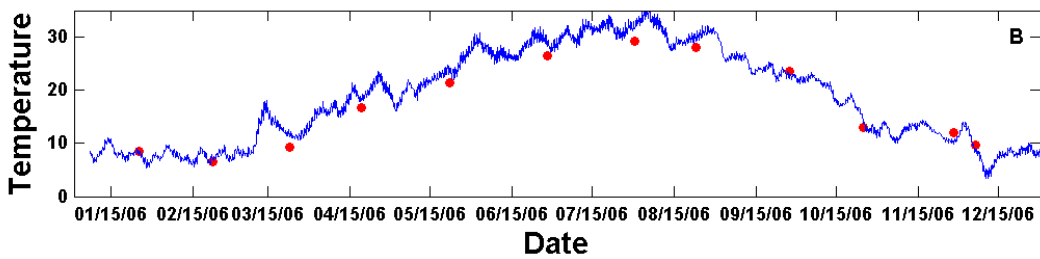
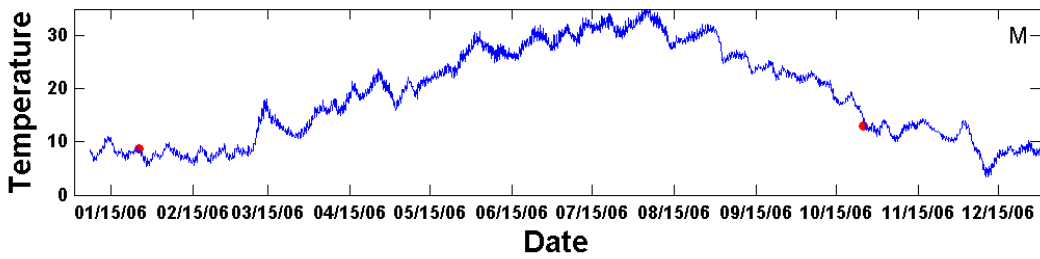
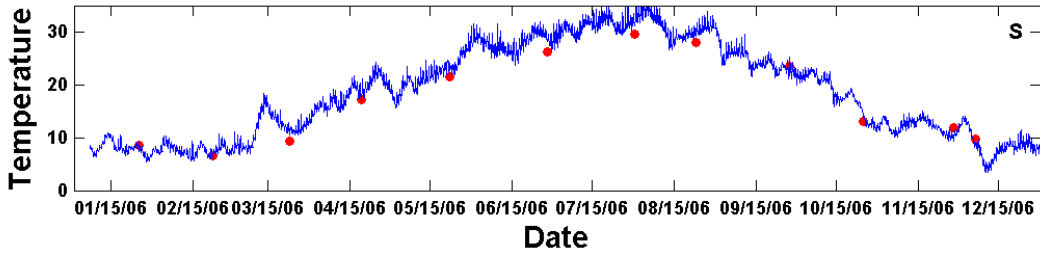
RET5.2



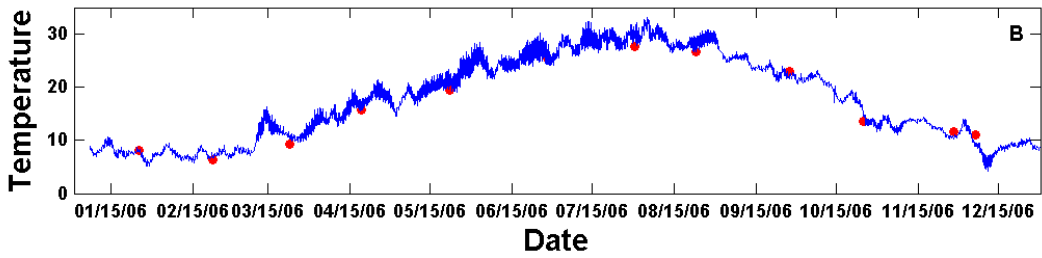
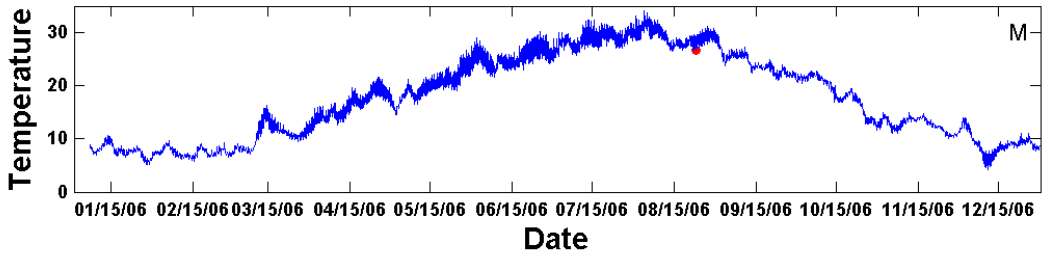
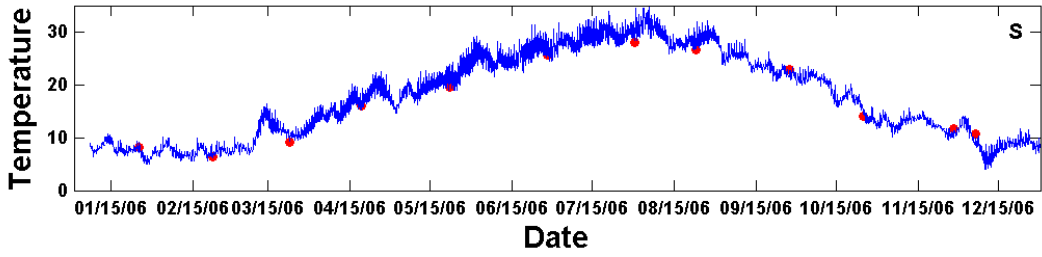
RET5.1A



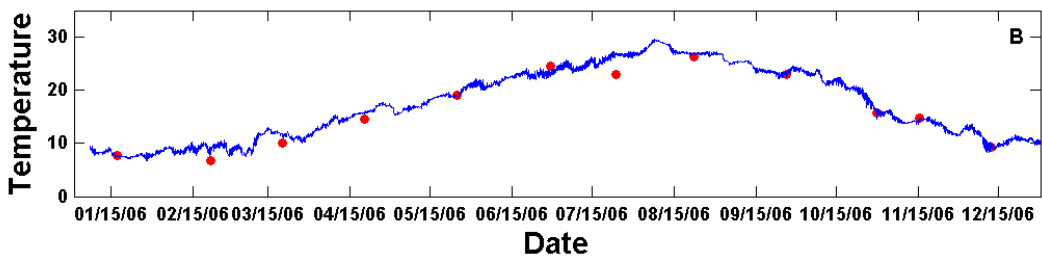
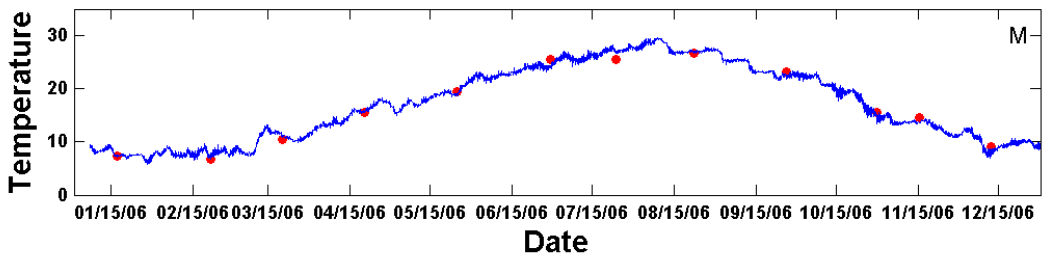
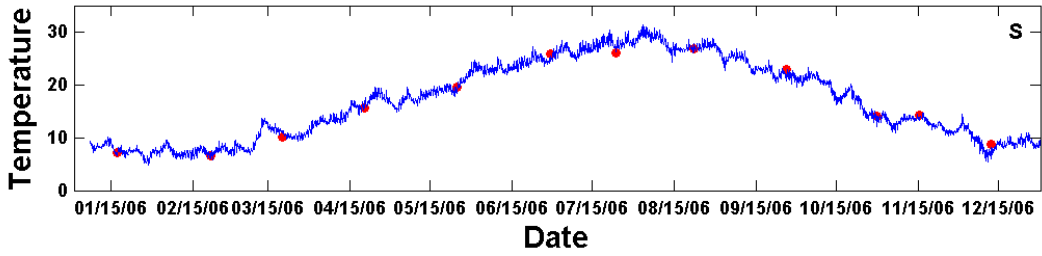
LFB01



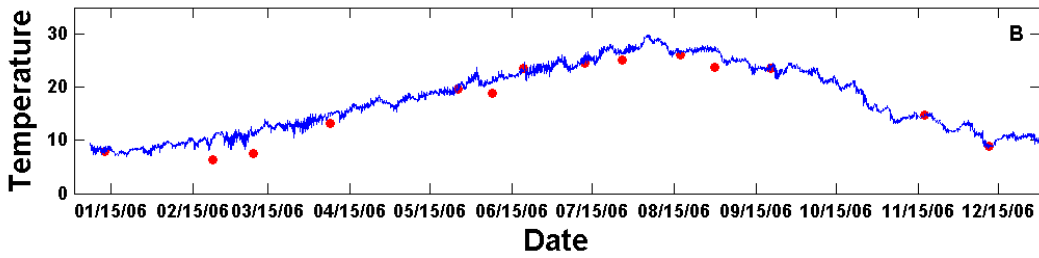
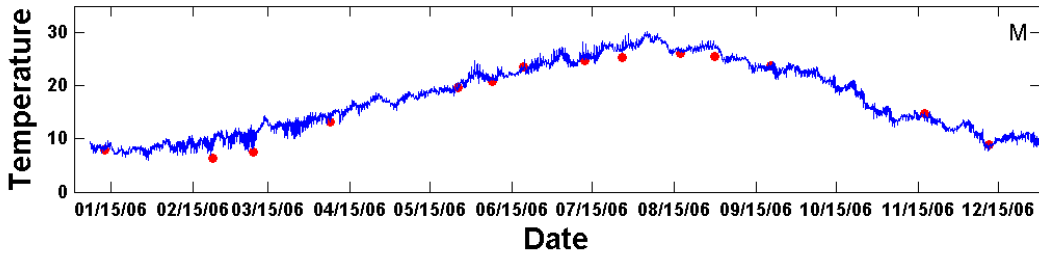
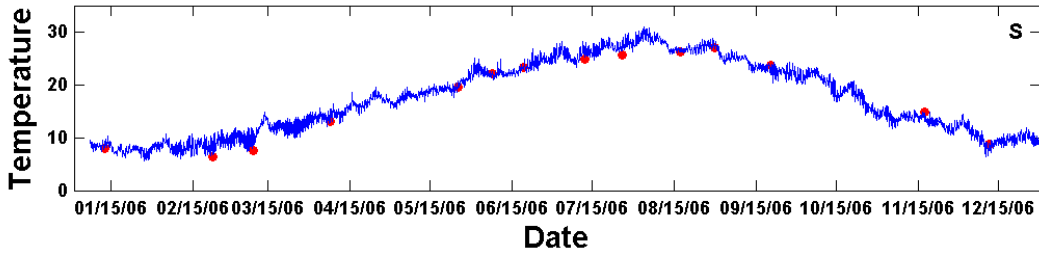
LFA01



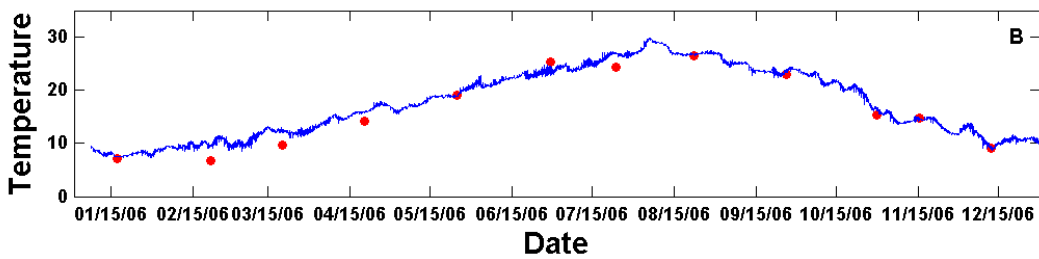
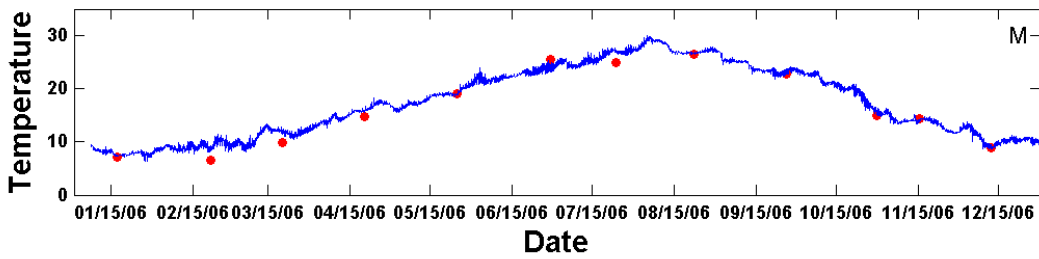
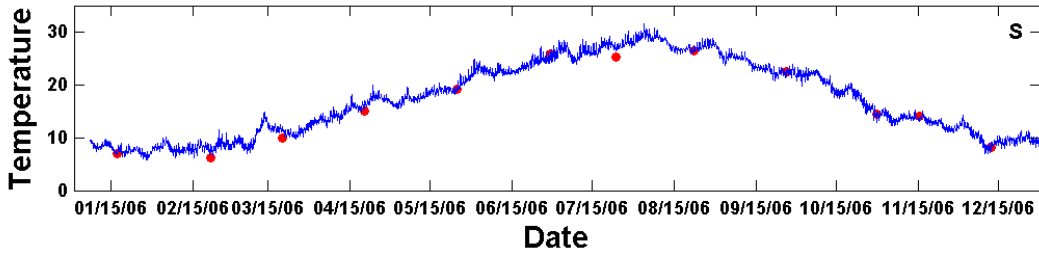
LE5.6



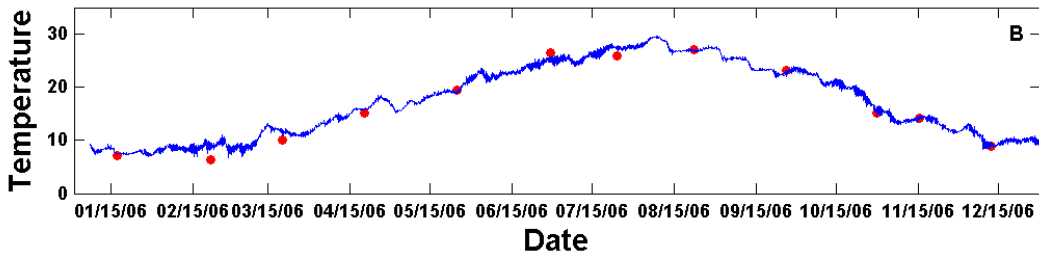
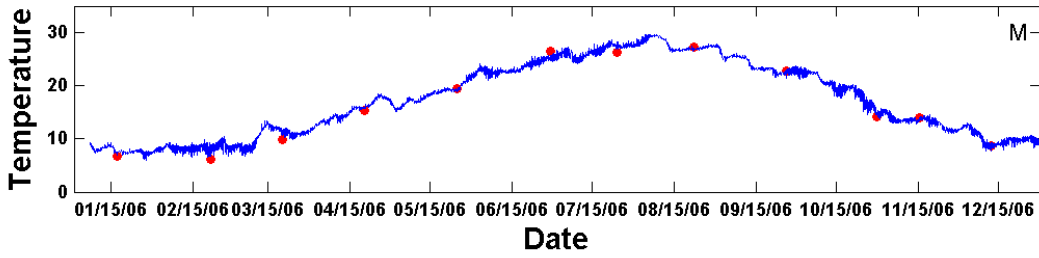
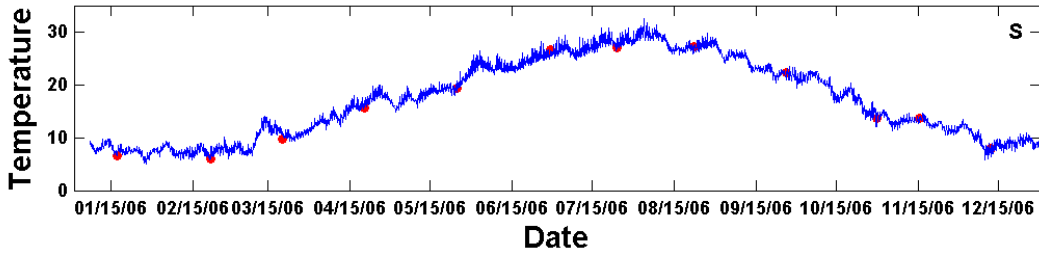
LE5.5-W



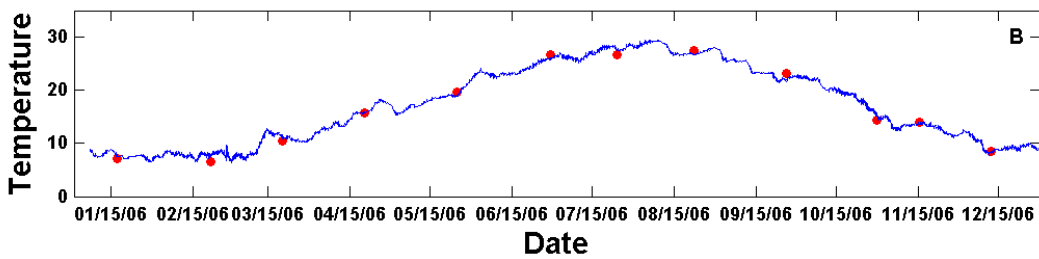
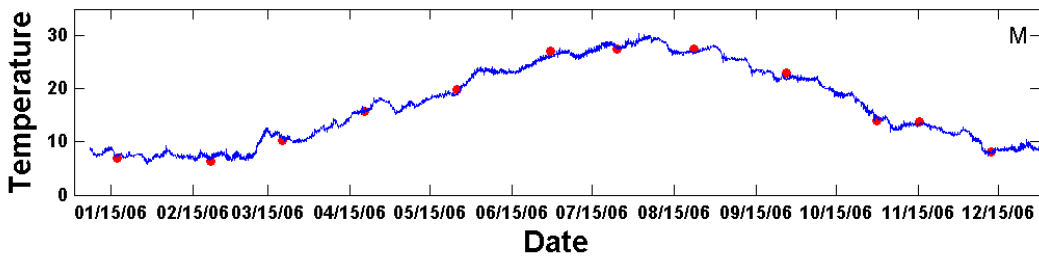
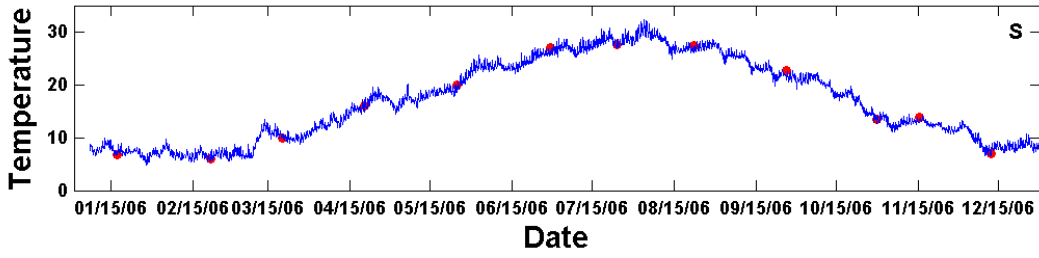
LE5.4



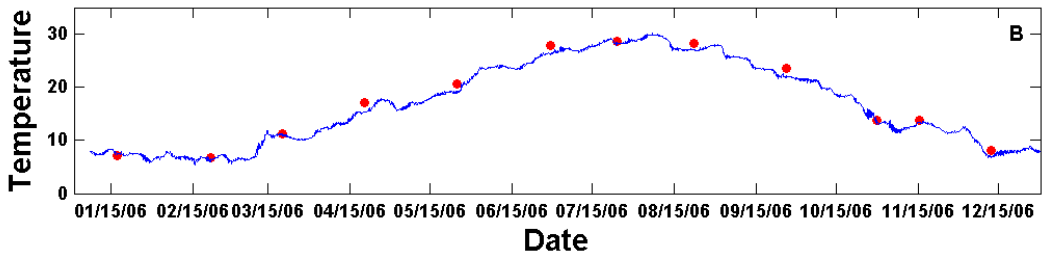
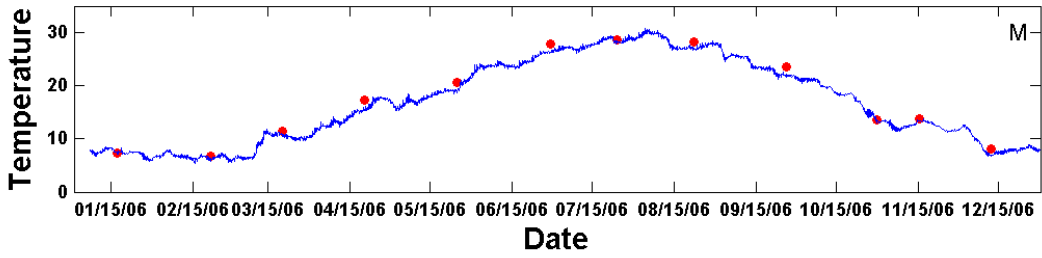
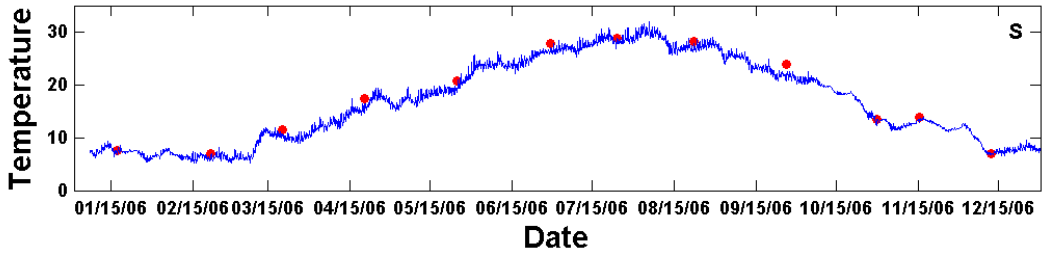
LE5.3



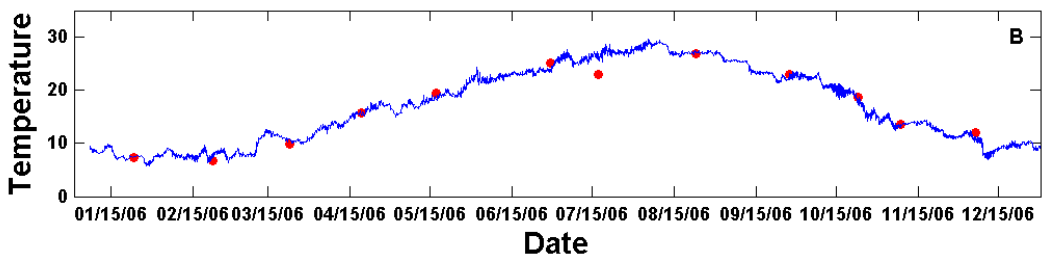
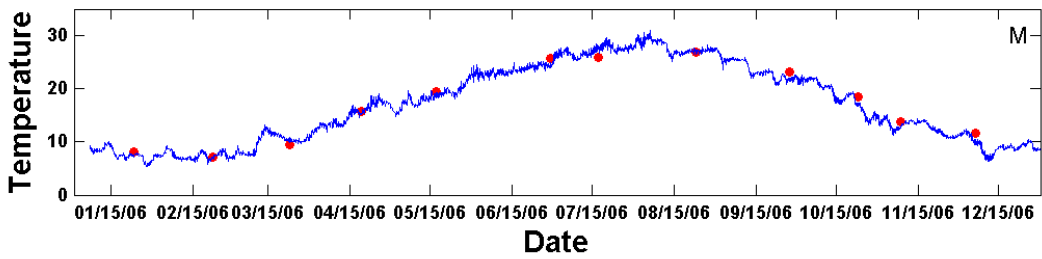
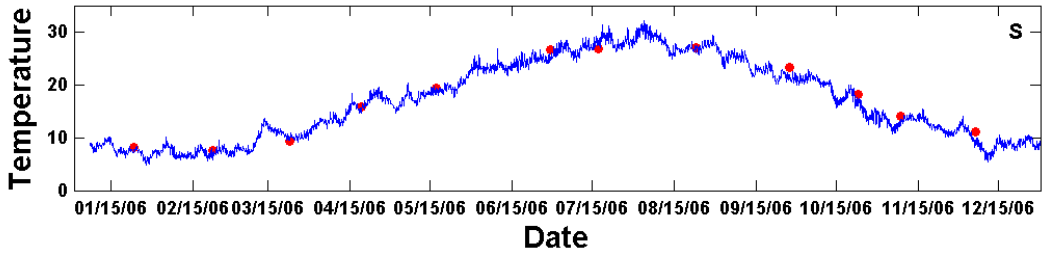
LE5.2



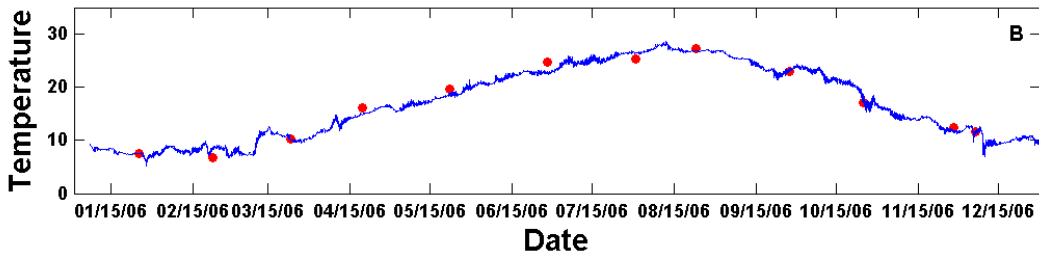
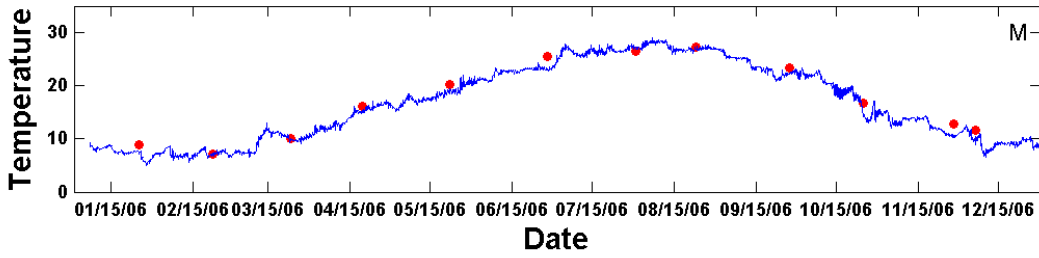
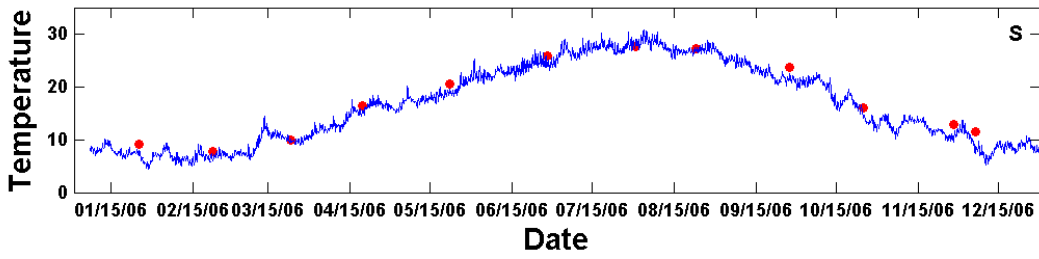
LE5.1



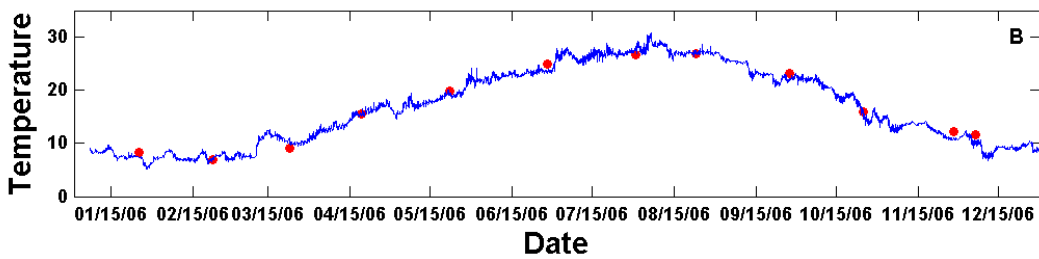
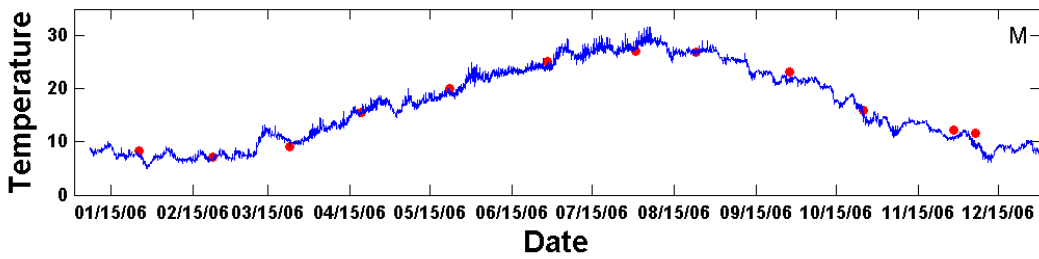
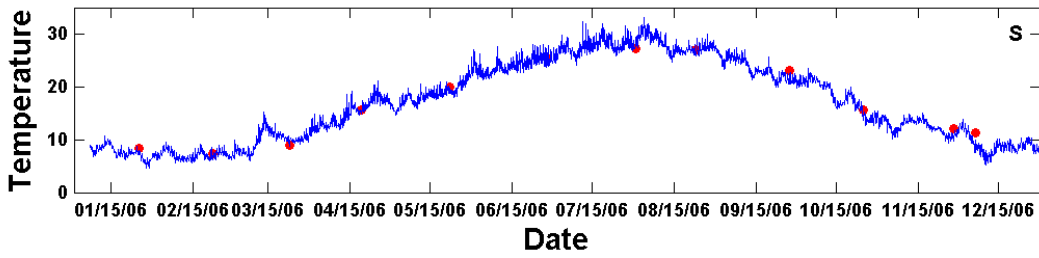
ELI2



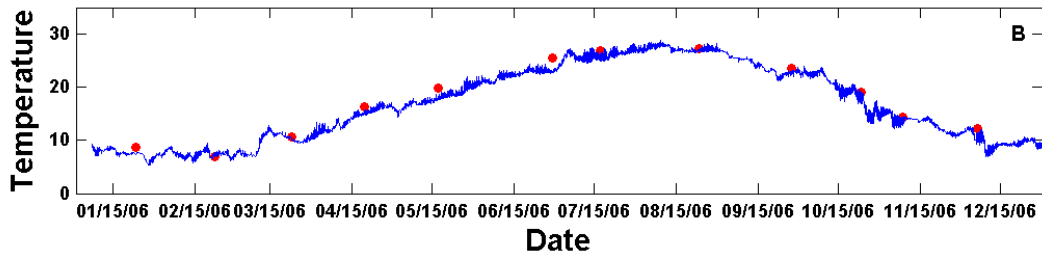
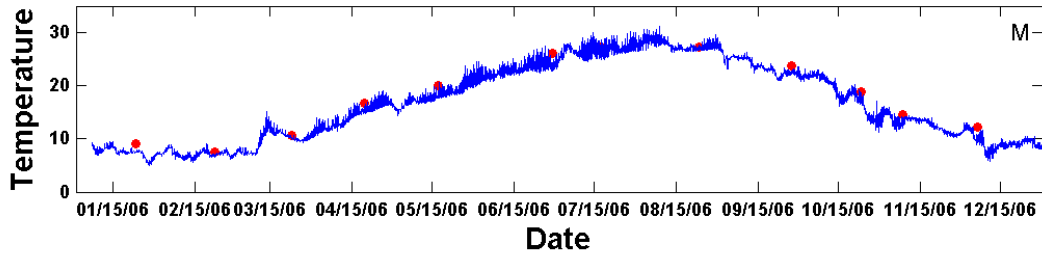
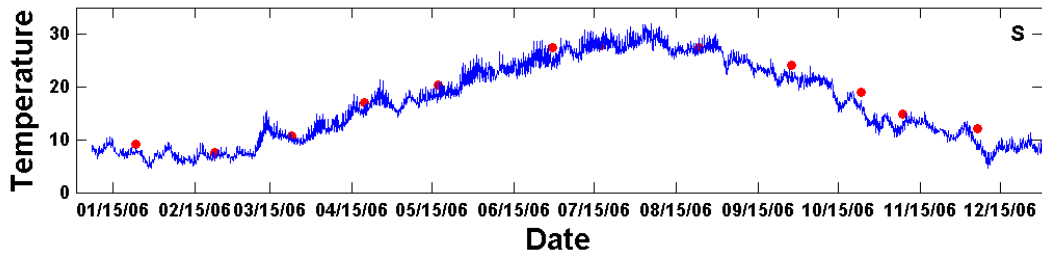
ELE01



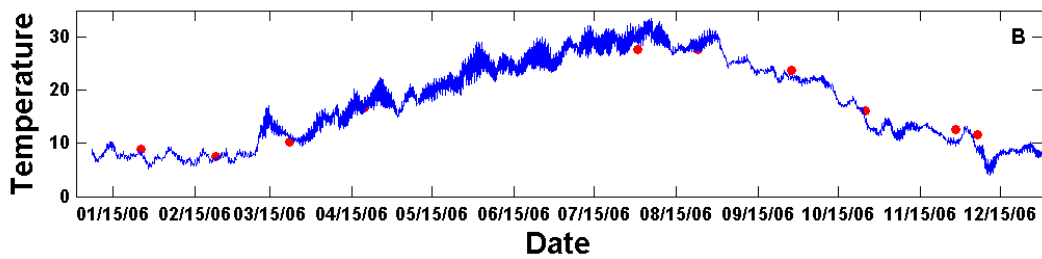
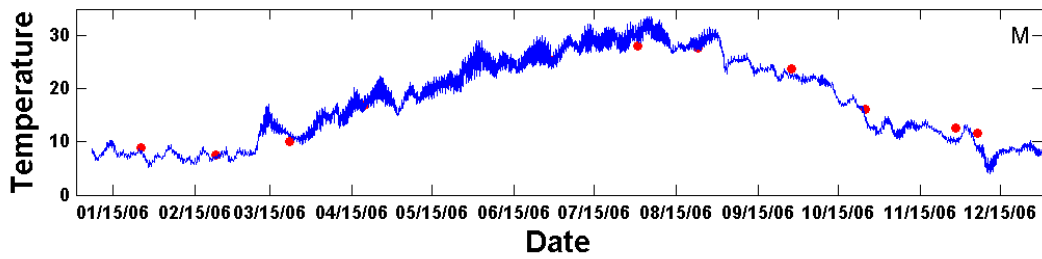
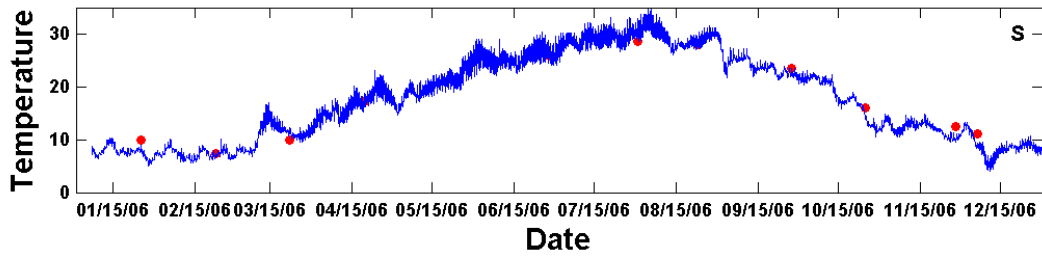
ELD01



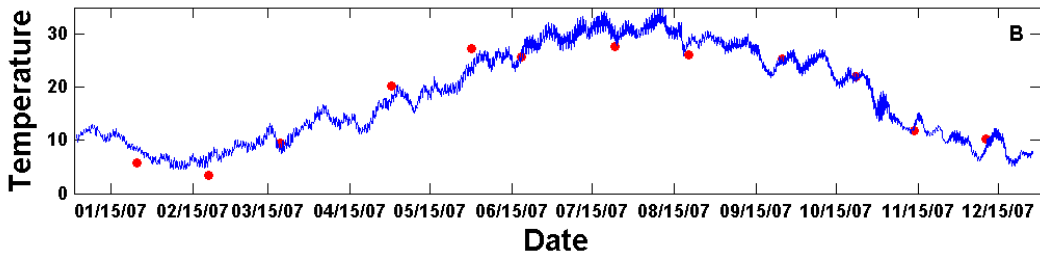
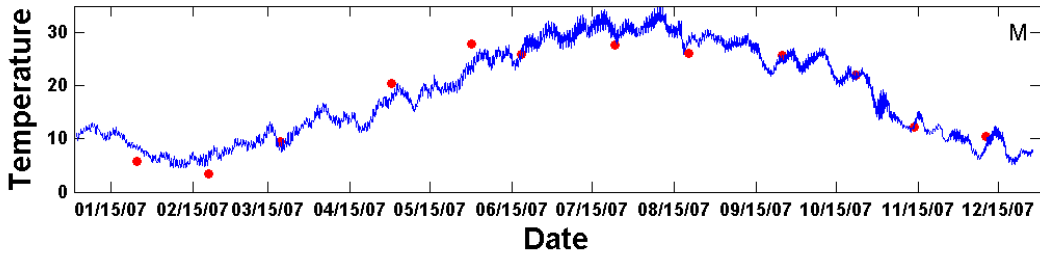
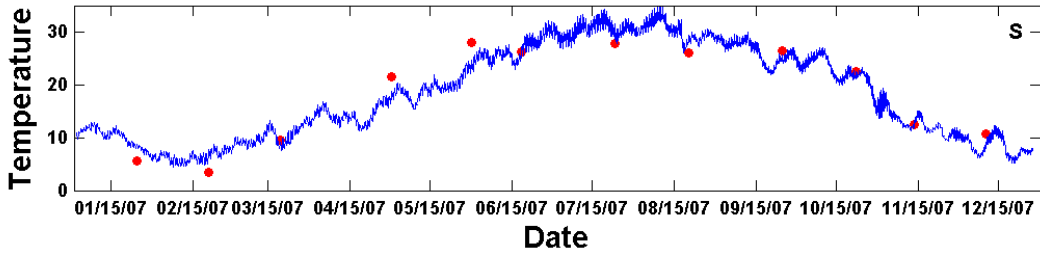
EBE1



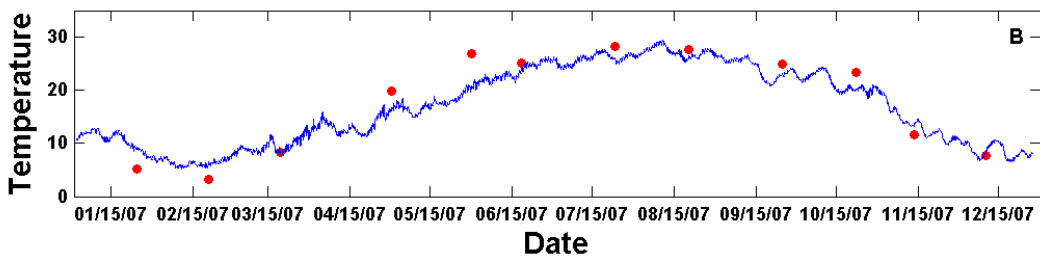
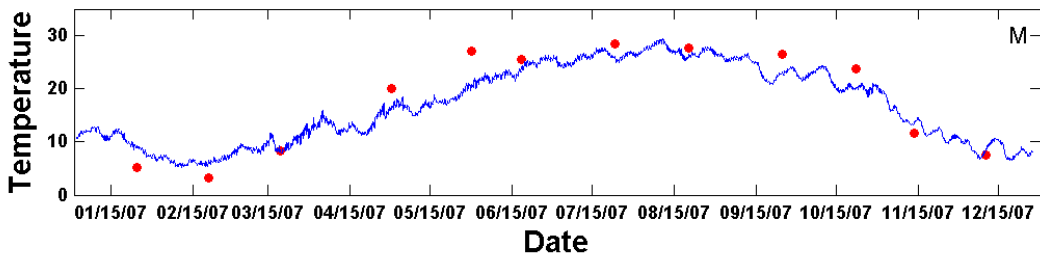
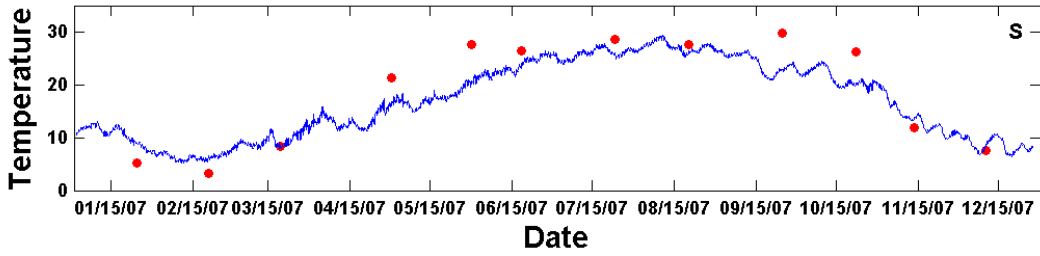
EBB01



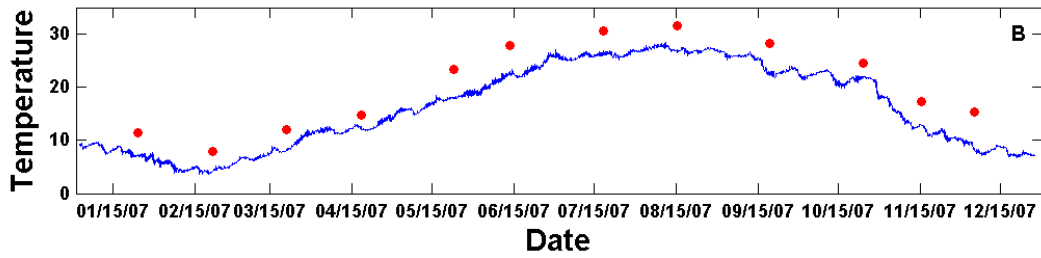
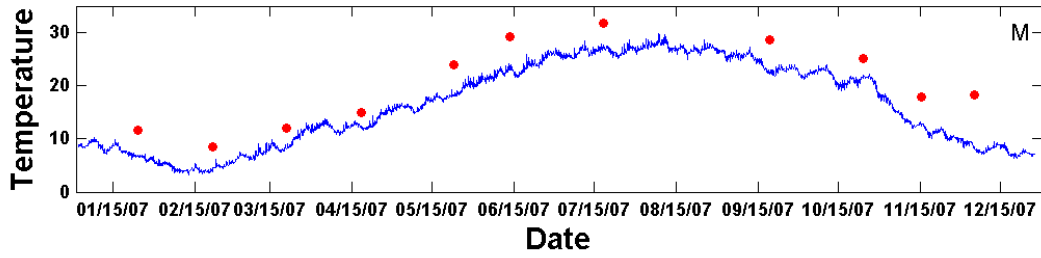
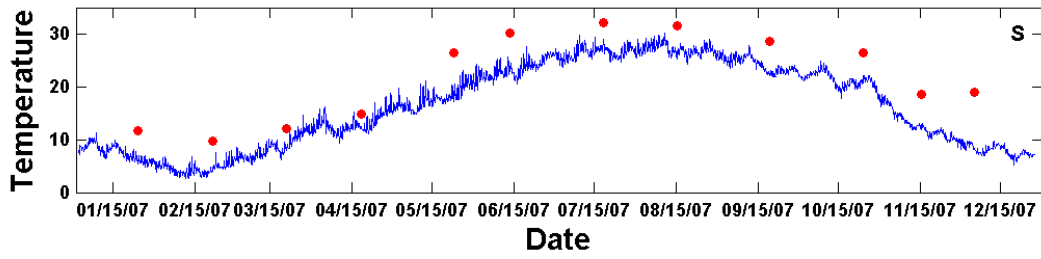
TF5.4



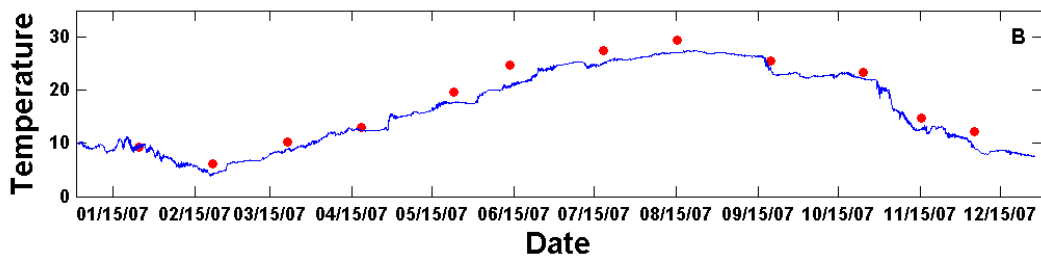
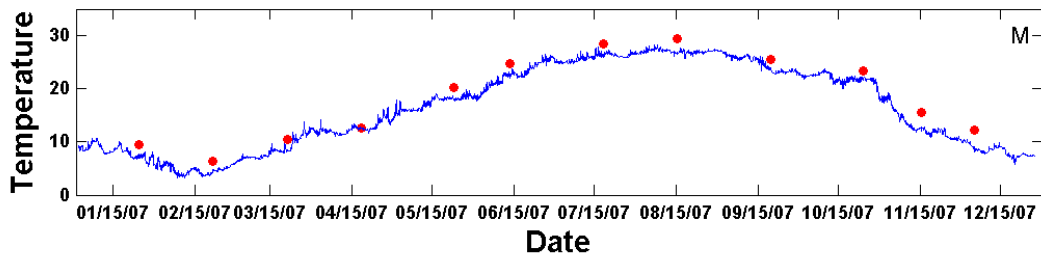
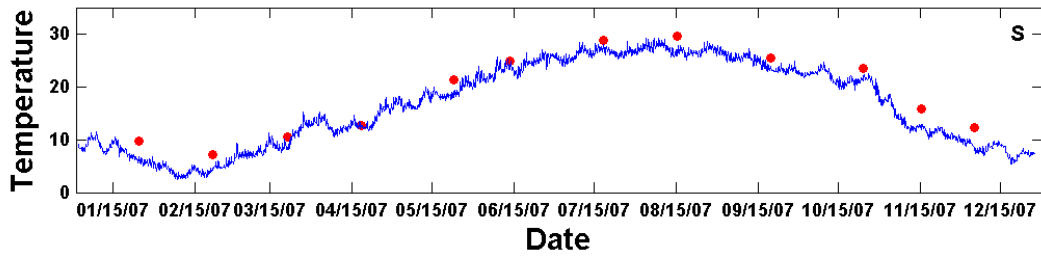
TF5.3



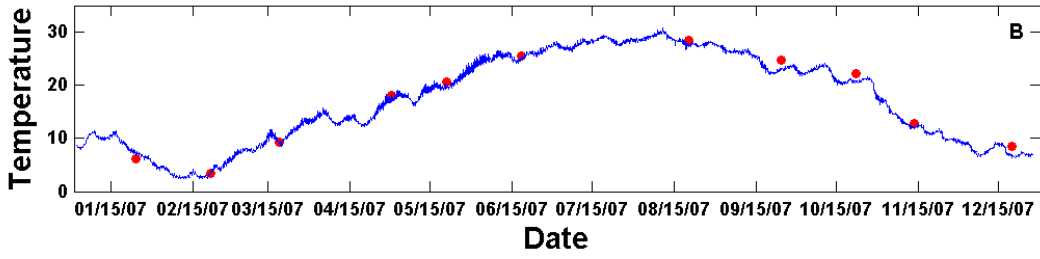
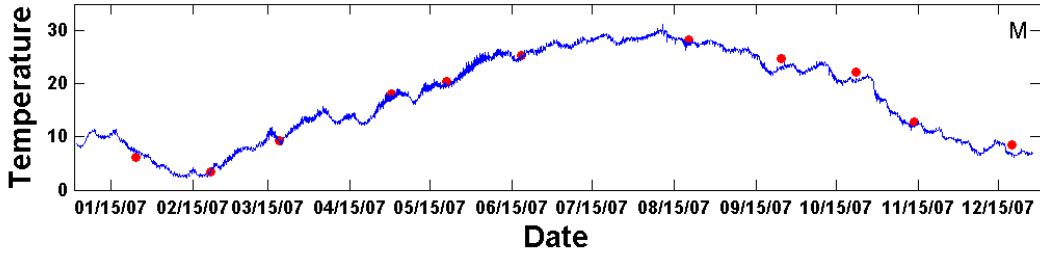
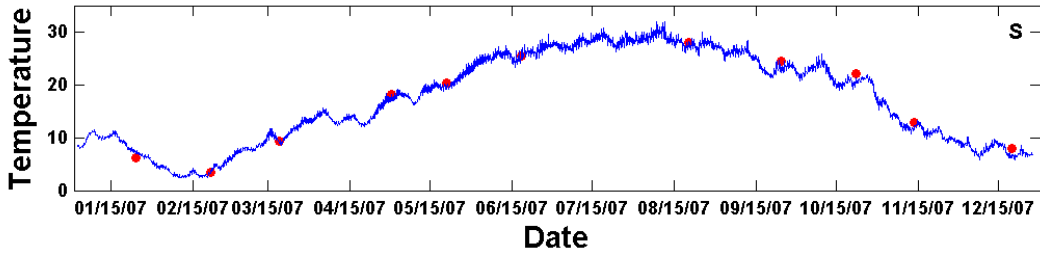
SBE5



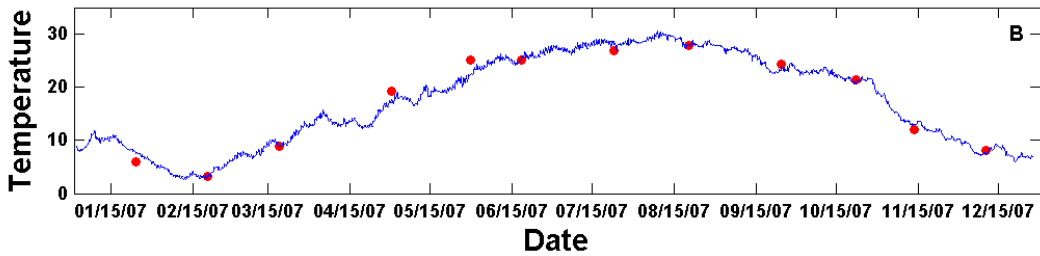
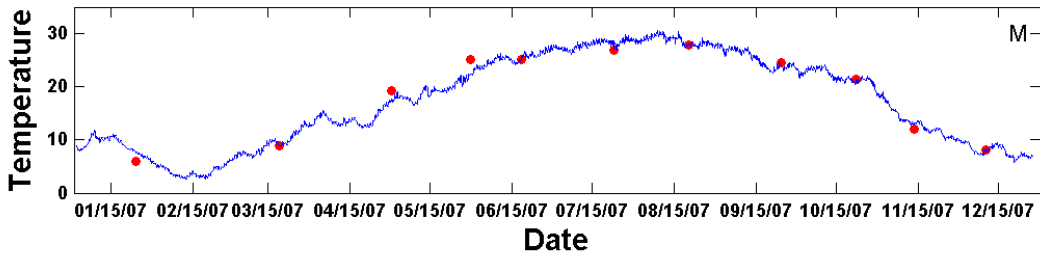
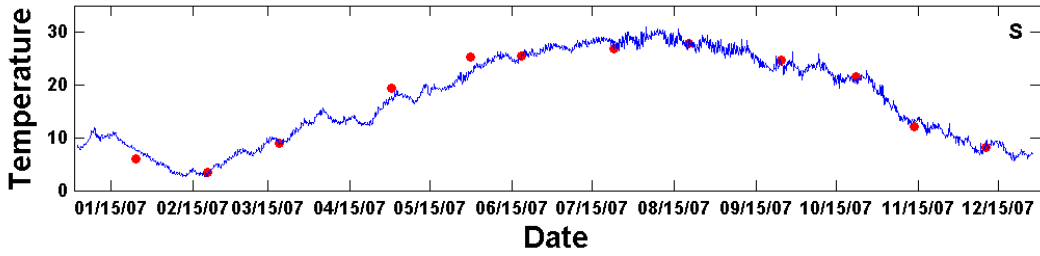
SBE2



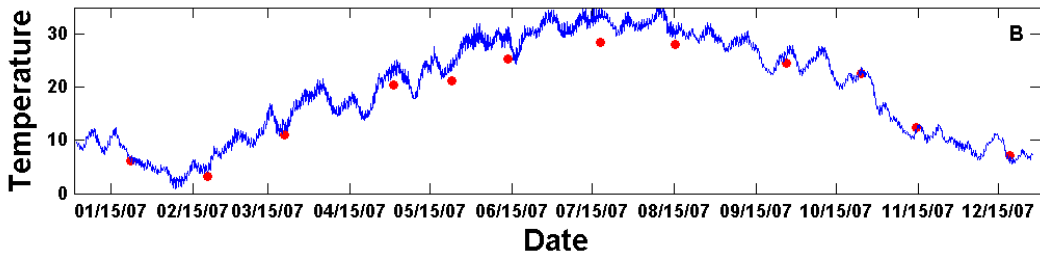
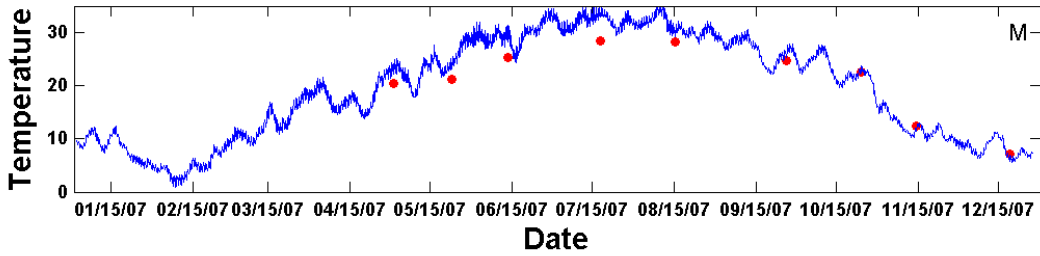
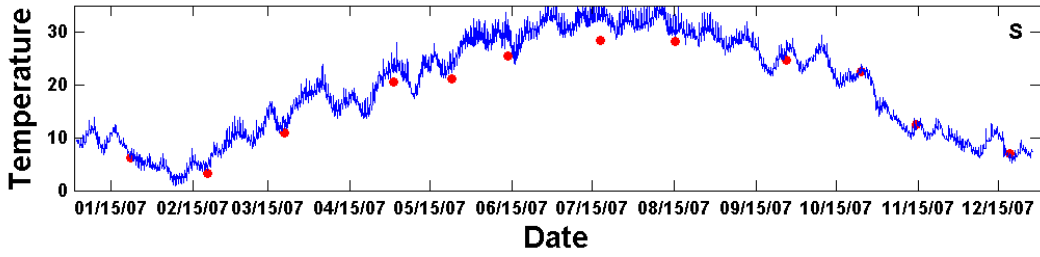
RET5.2



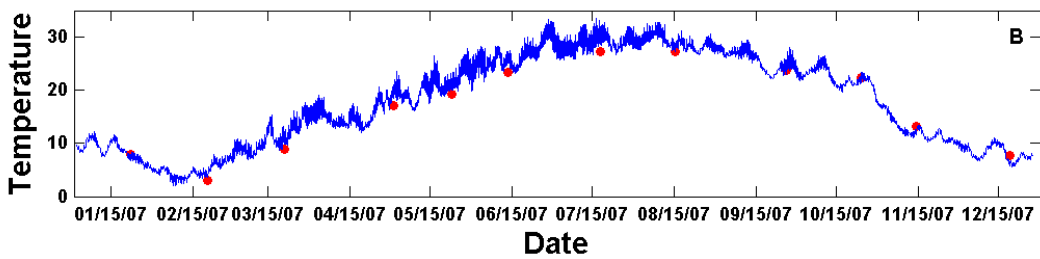
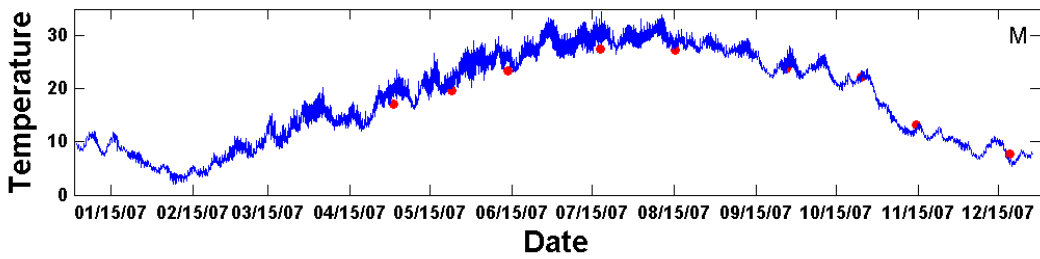
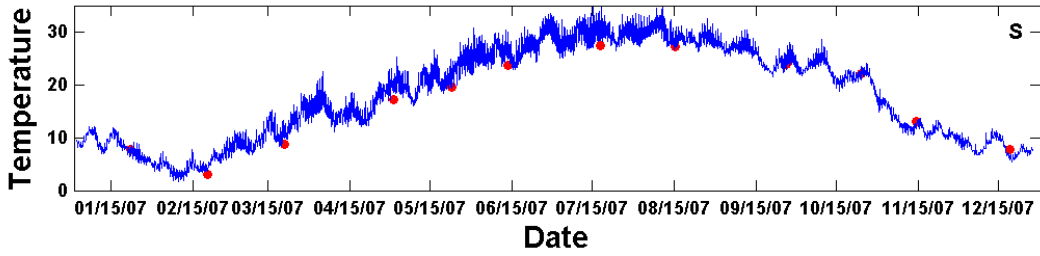
RET5.1A



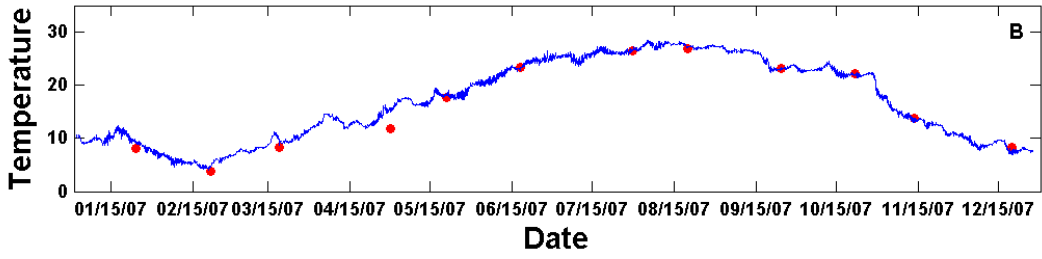
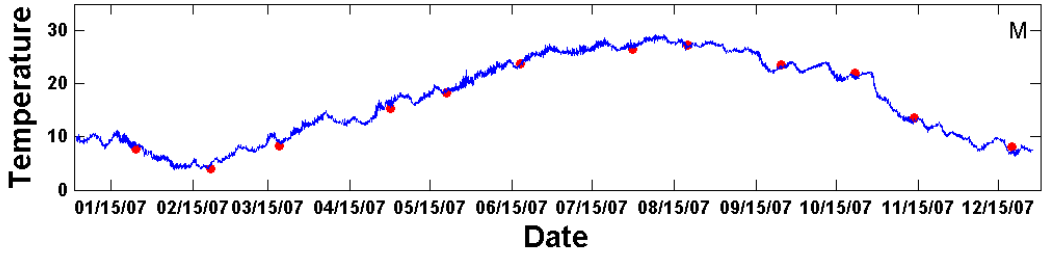
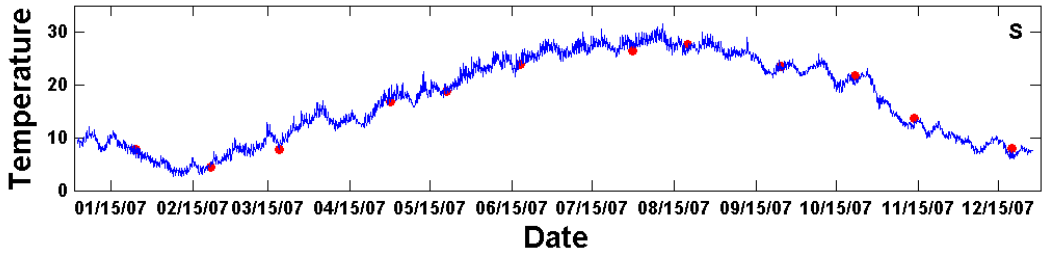
LFB01



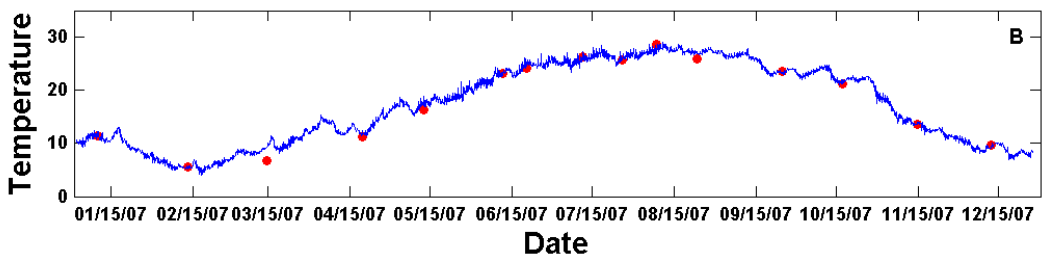
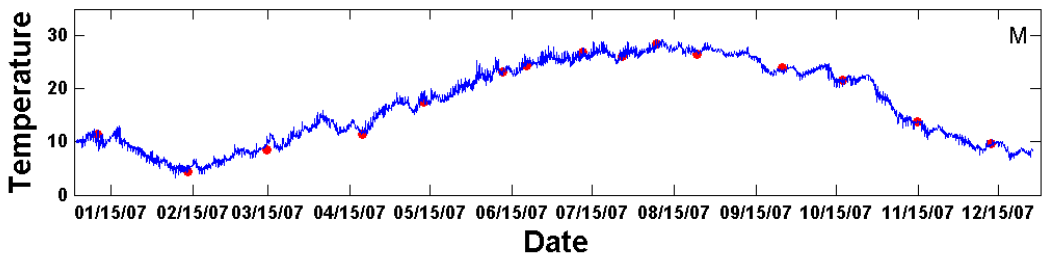
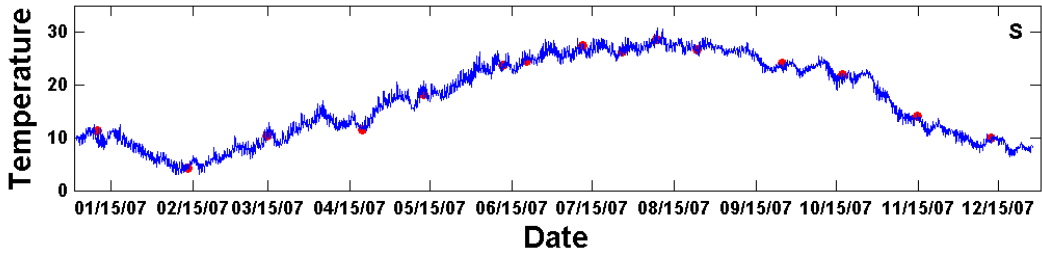
LFA01



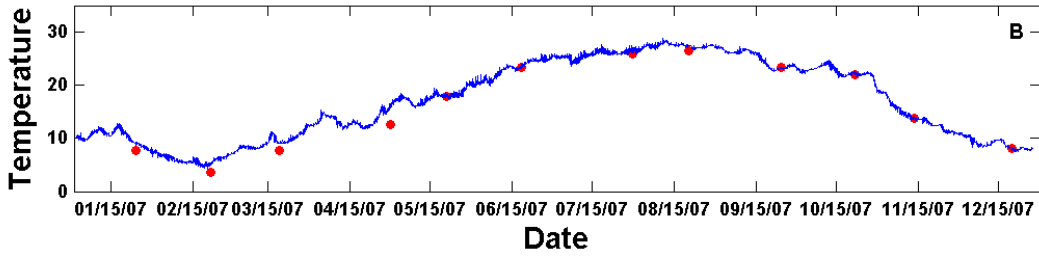
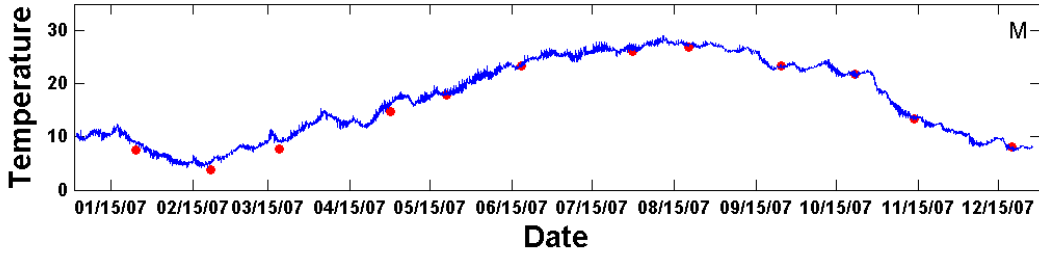
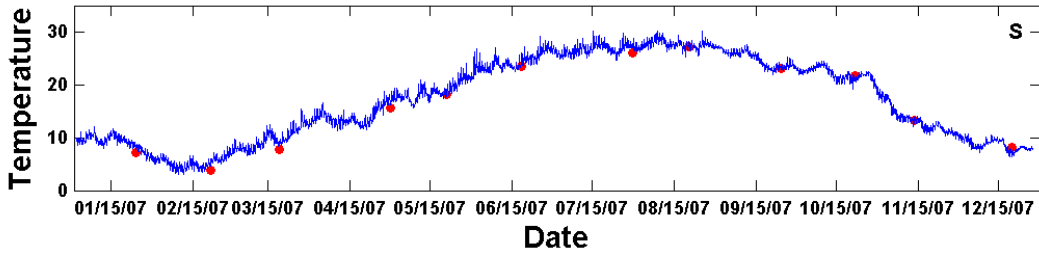
LE5.6



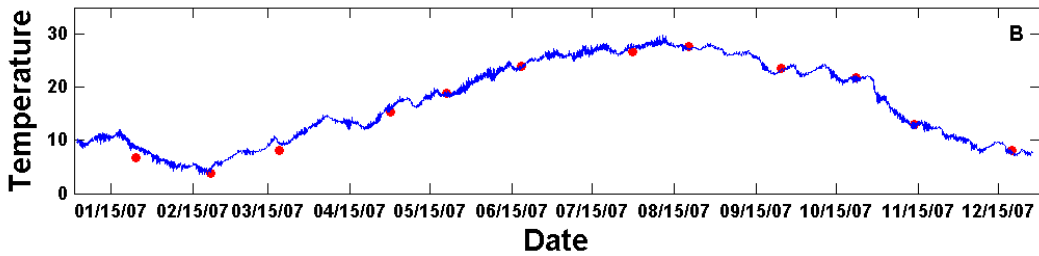
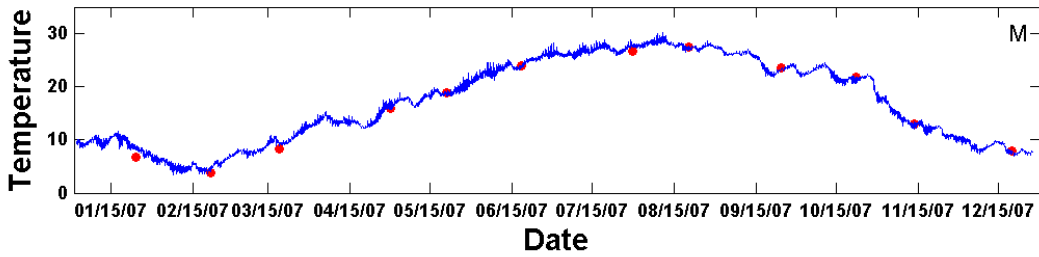
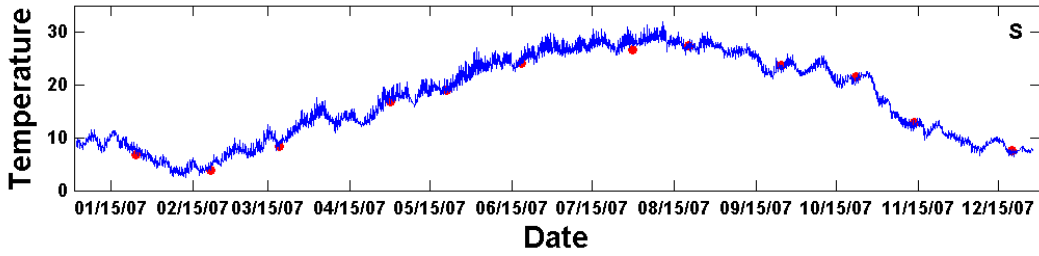
LE5.5-W



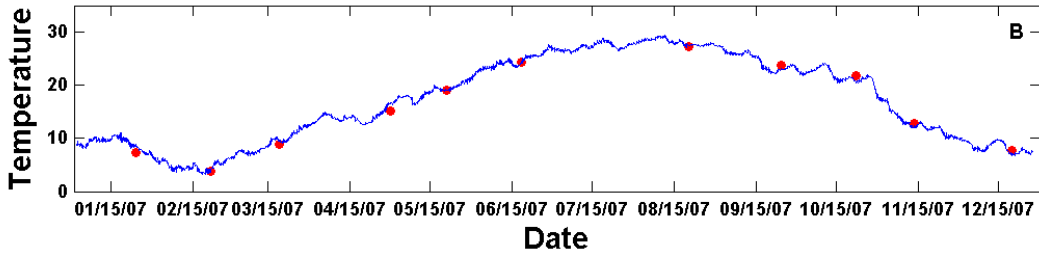
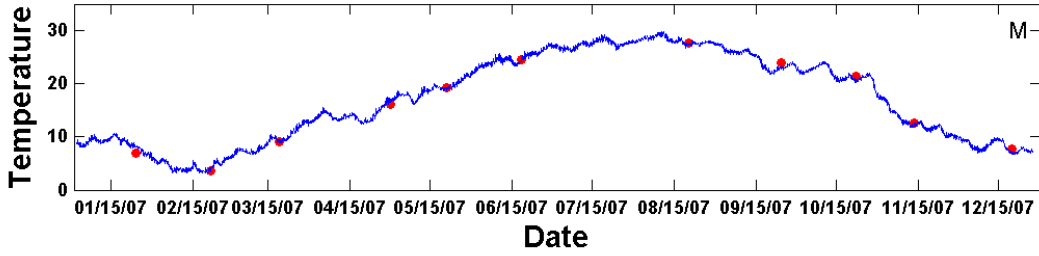
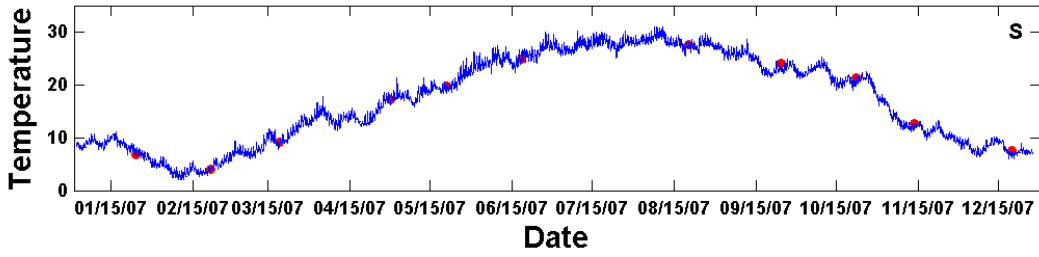
LE5.4



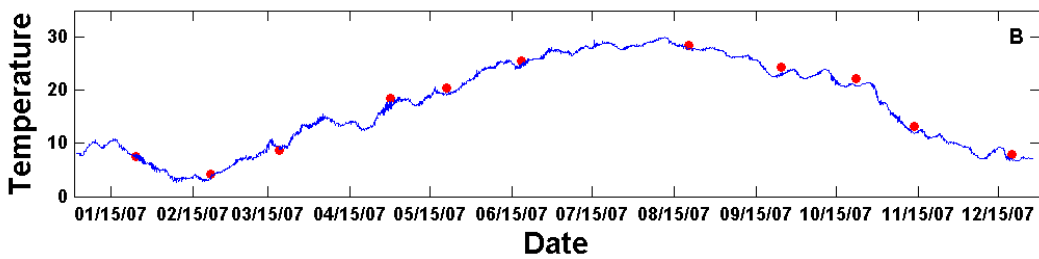
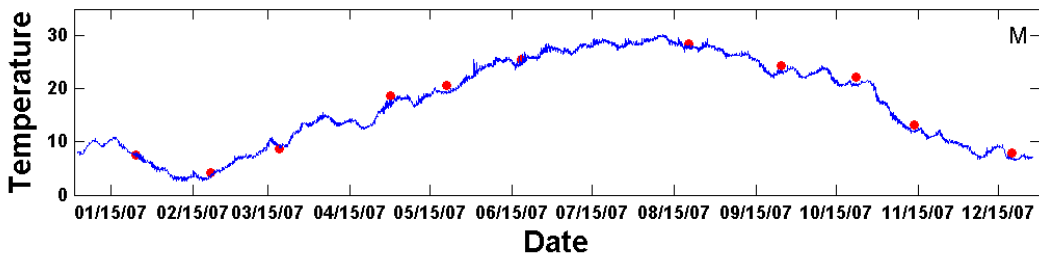
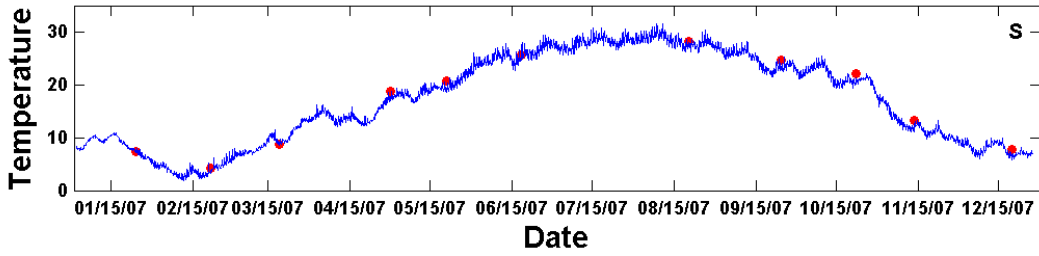
LE5.3



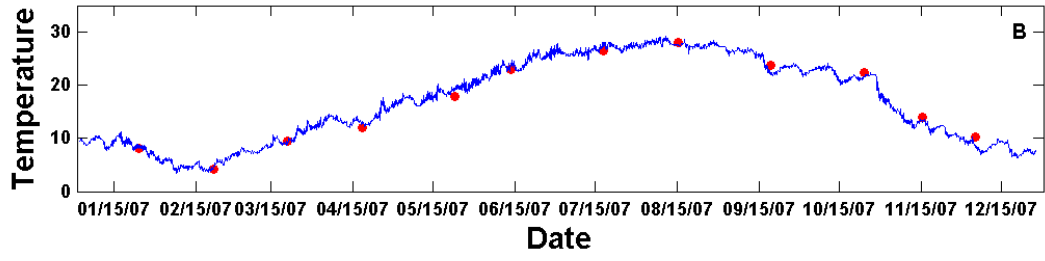
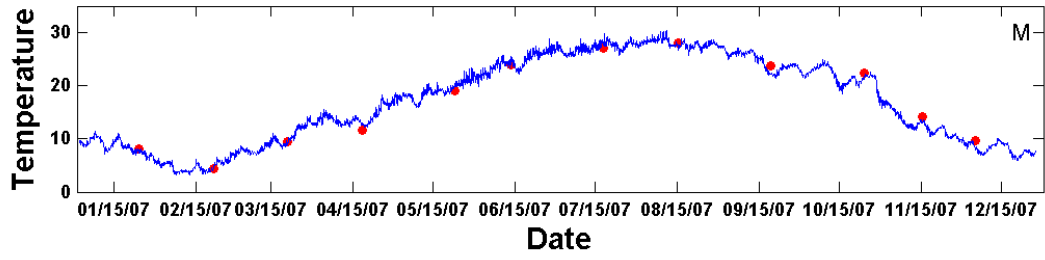
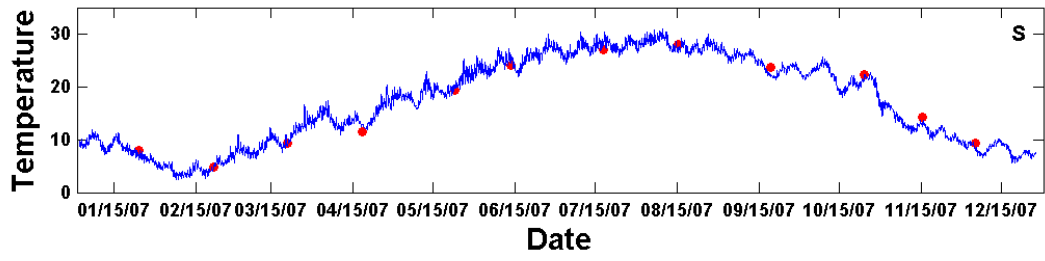
LE5.2



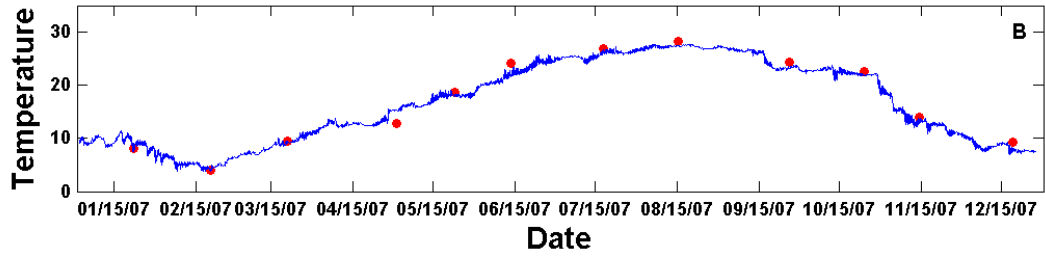
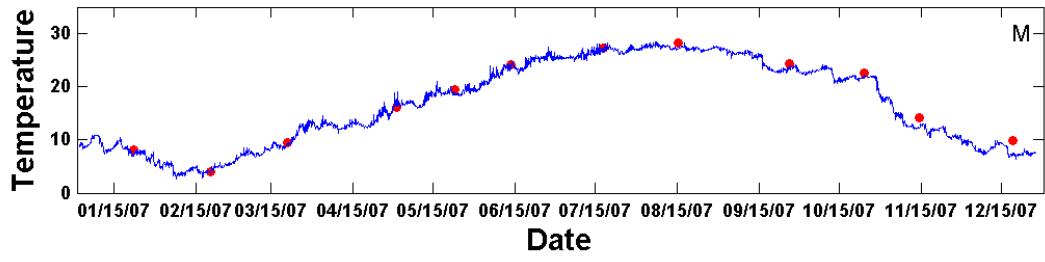
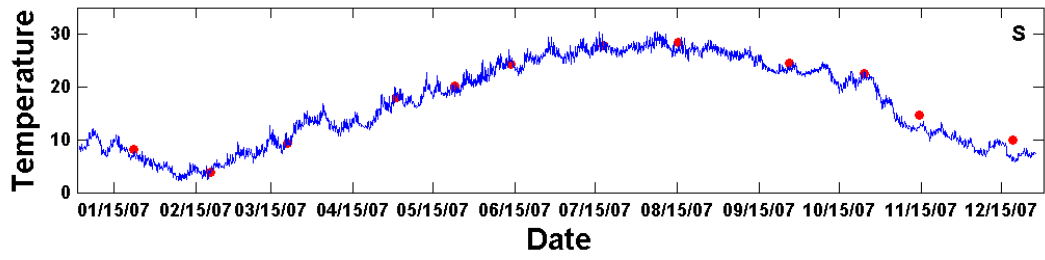
LE5.1



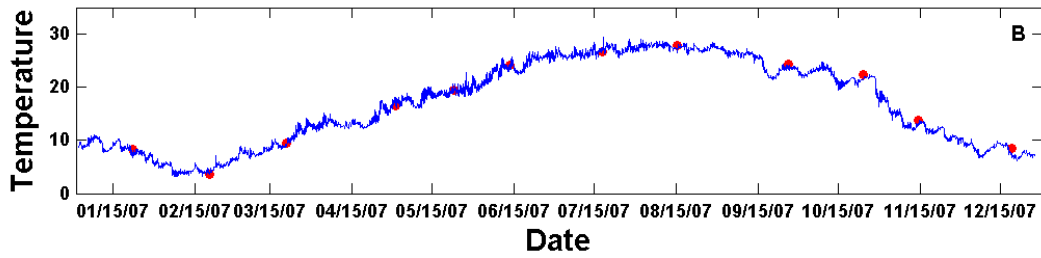
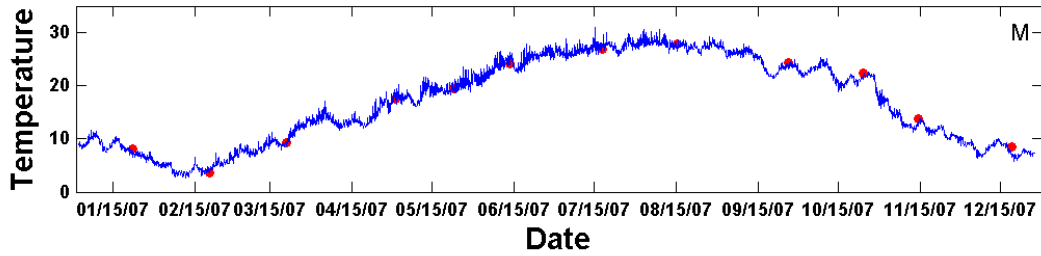
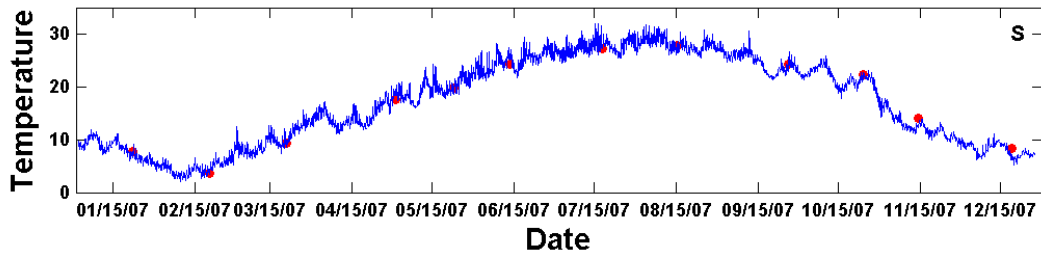
ELI2



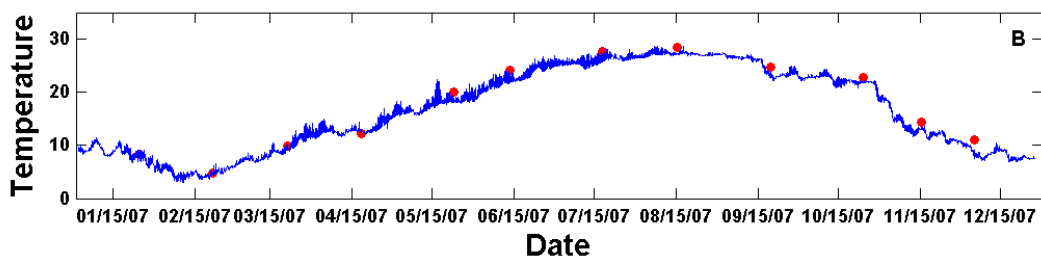
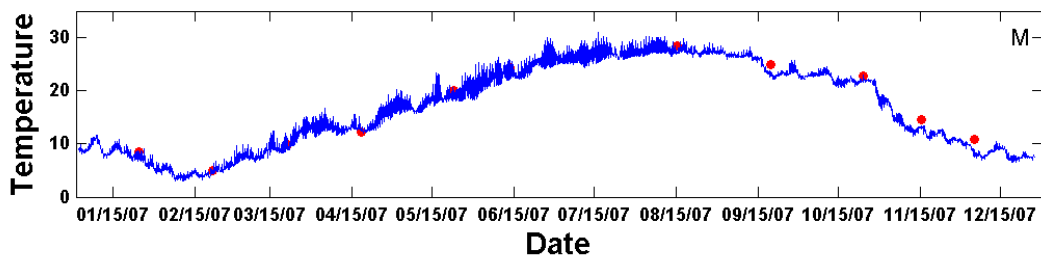
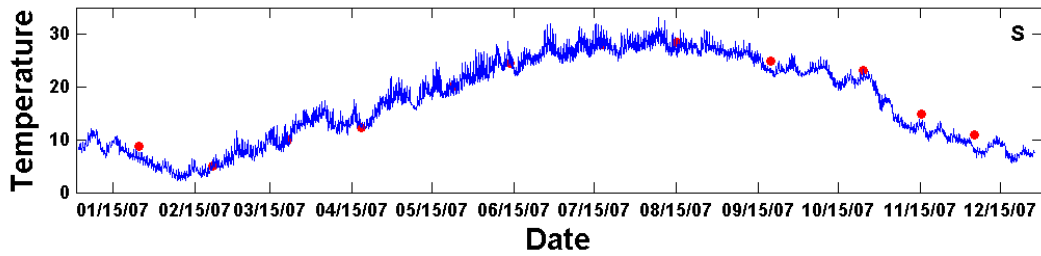
ELE01



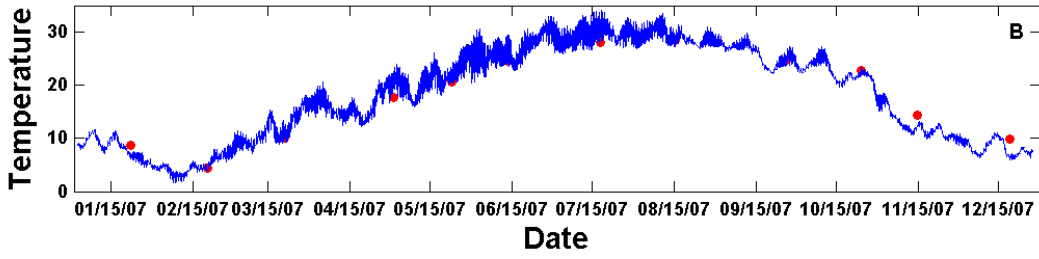
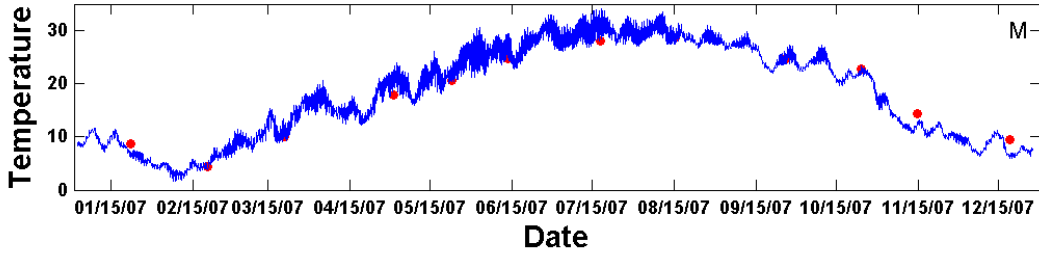
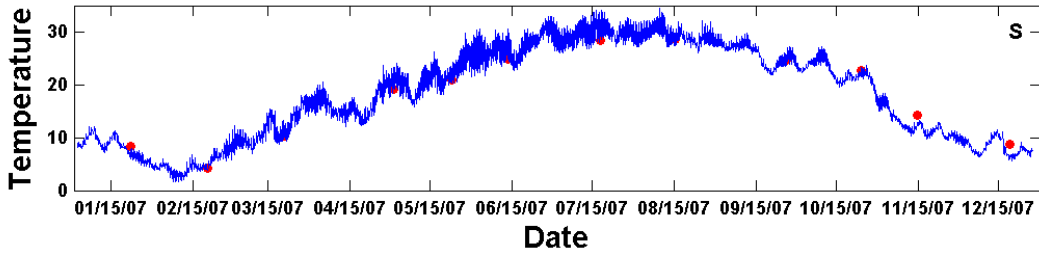
ELD01



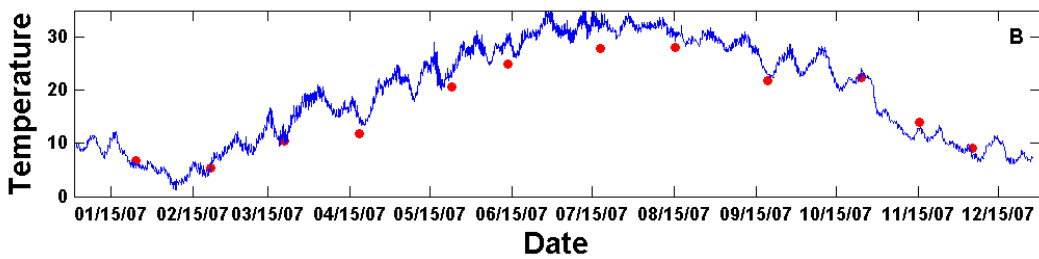
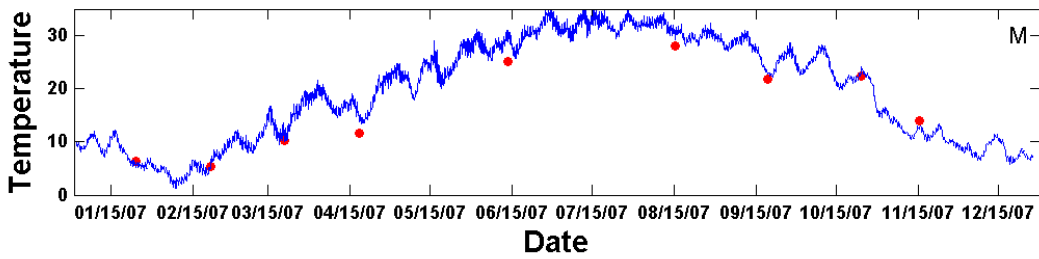
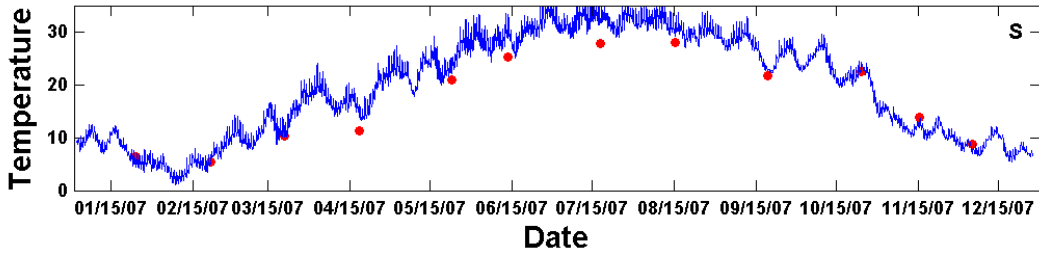
EBE1



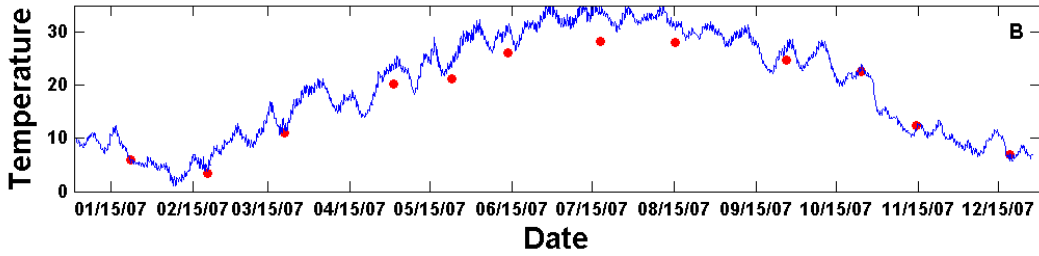
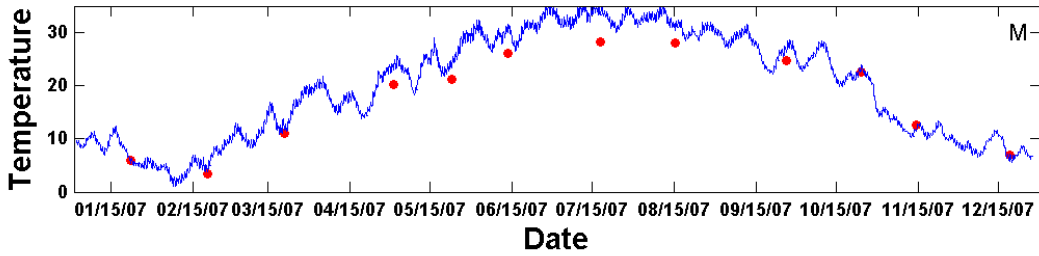
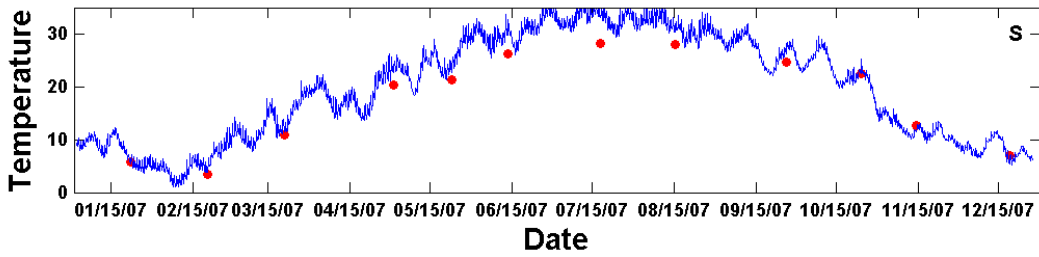
EBB01



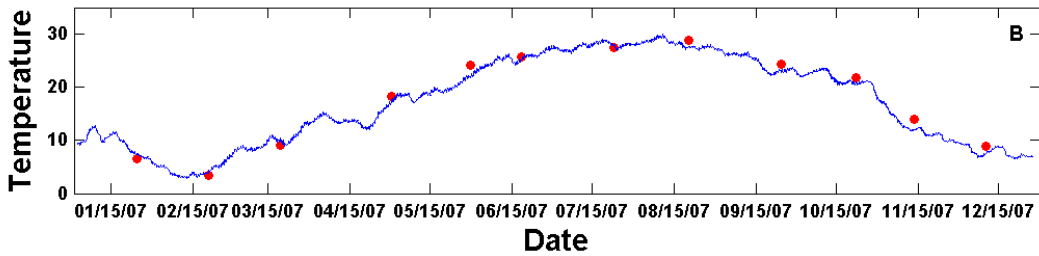
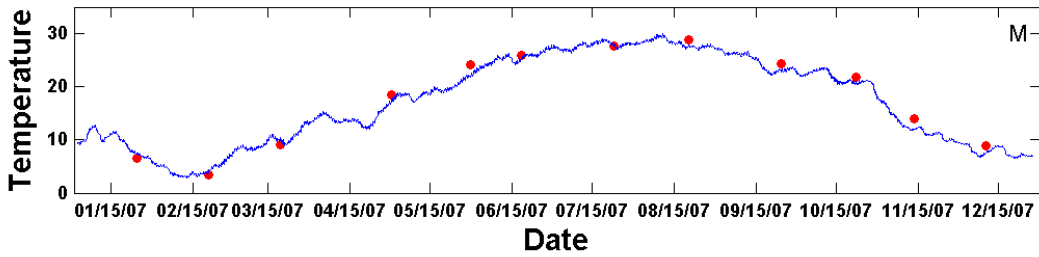
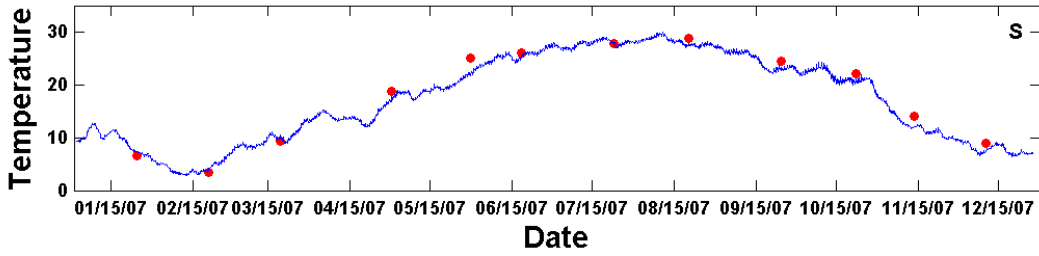
WBE1



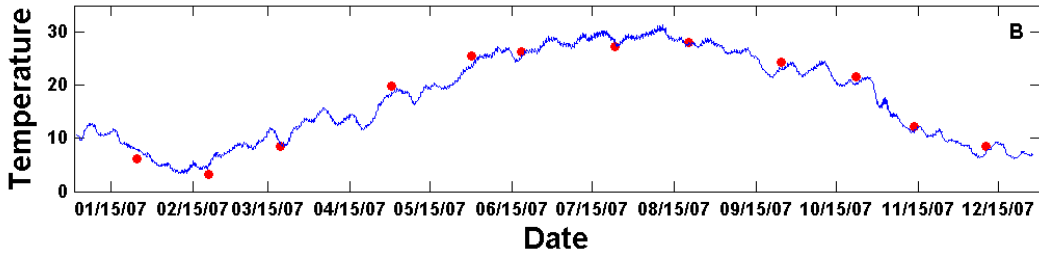
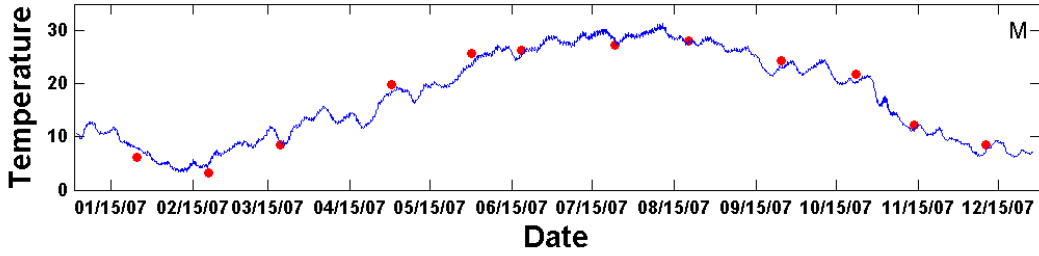
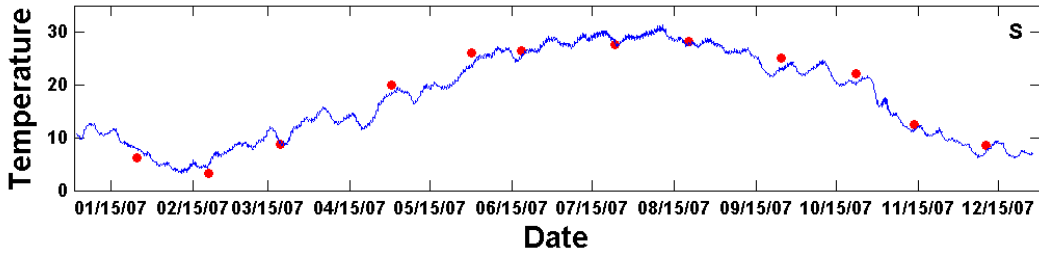
WBB05



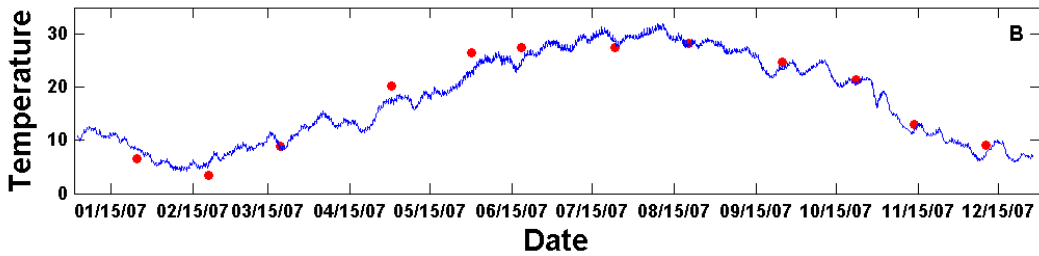
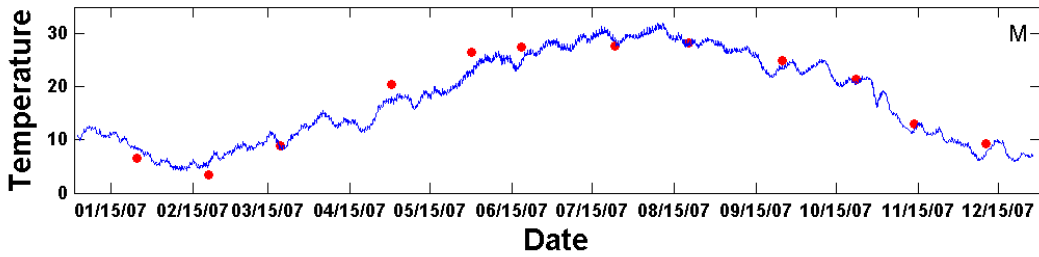
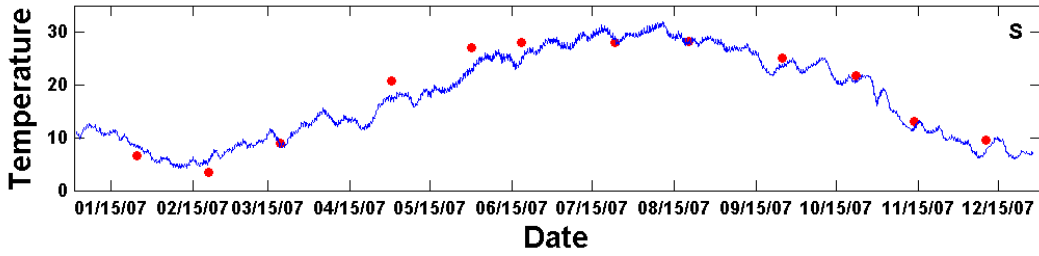
TF5.6



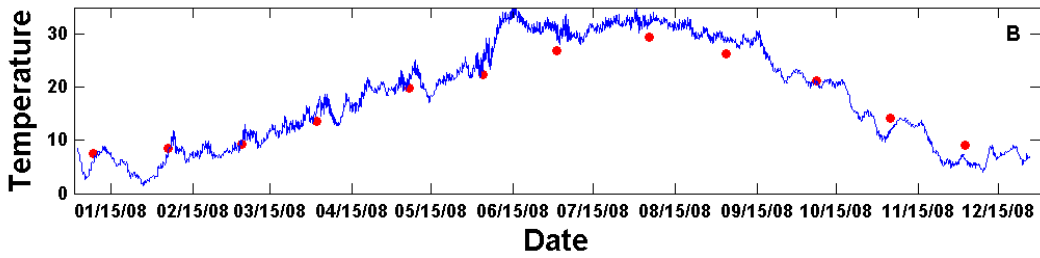
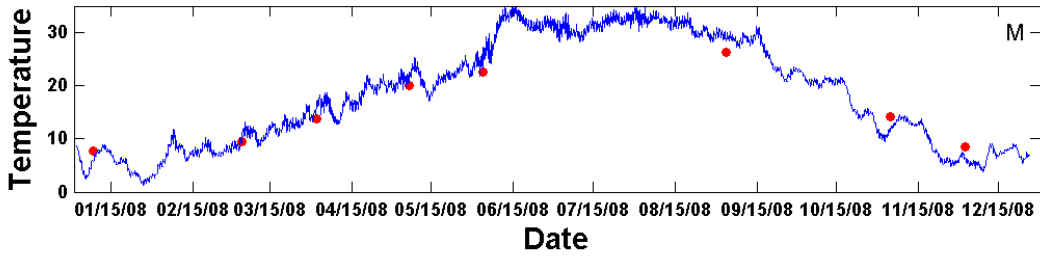
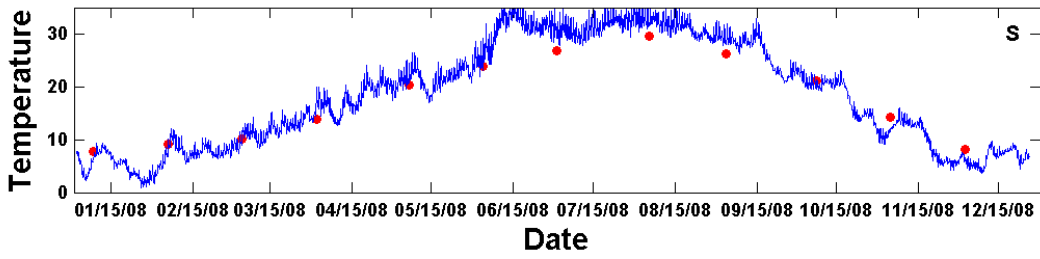
TF5.5A



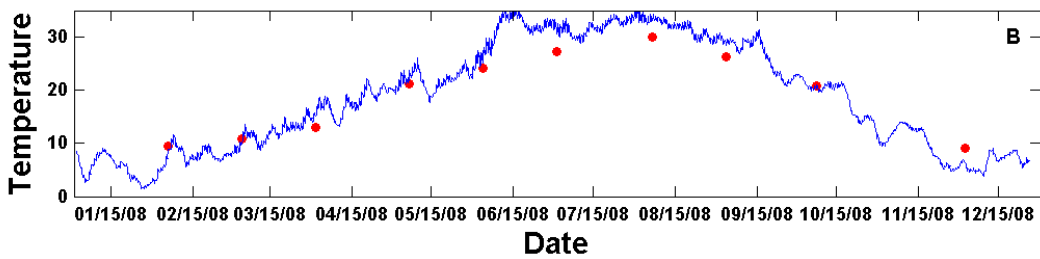
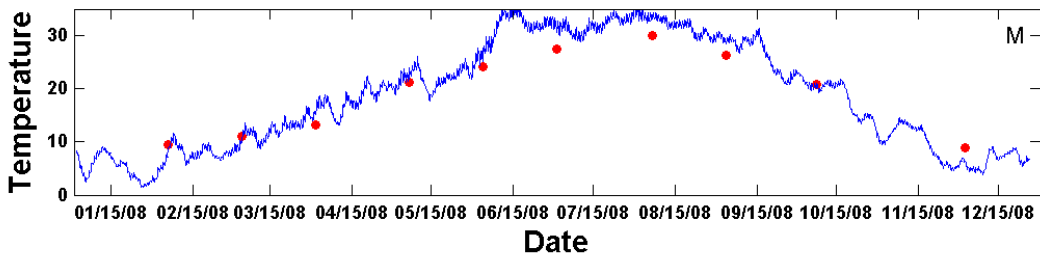
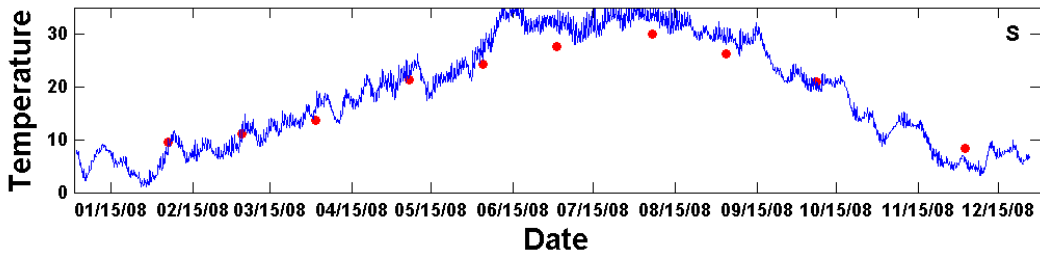
TF5.5



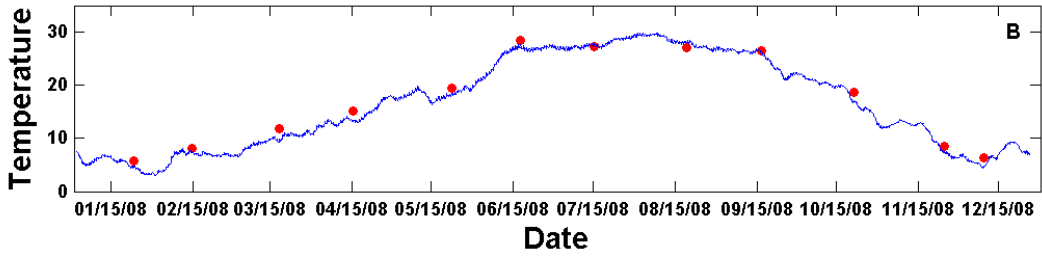
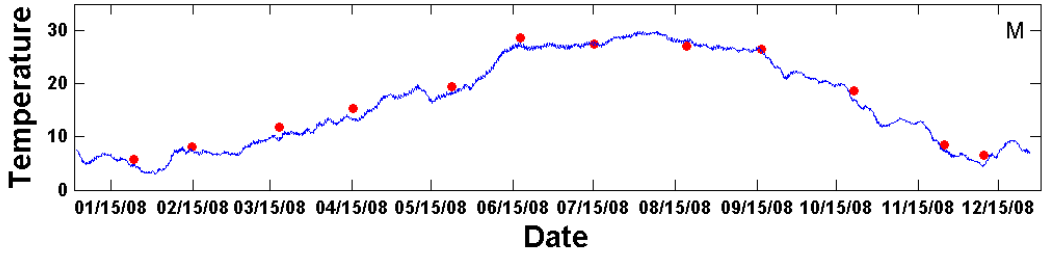
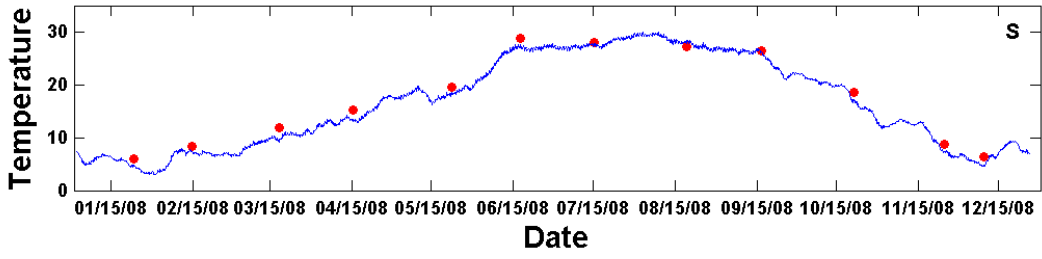
WBE1



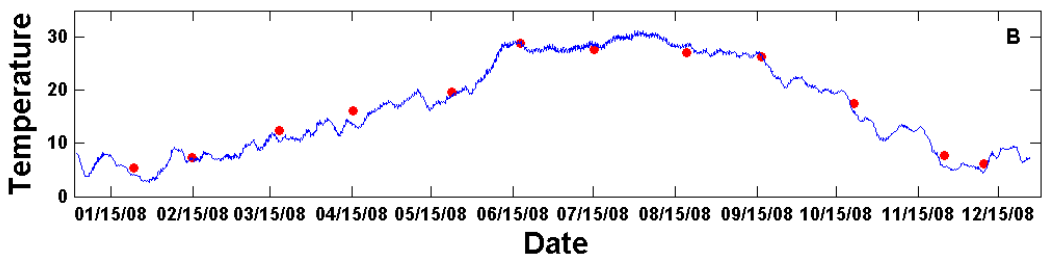
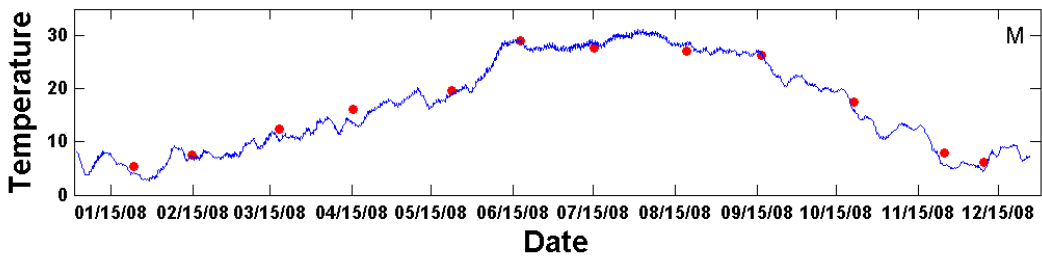
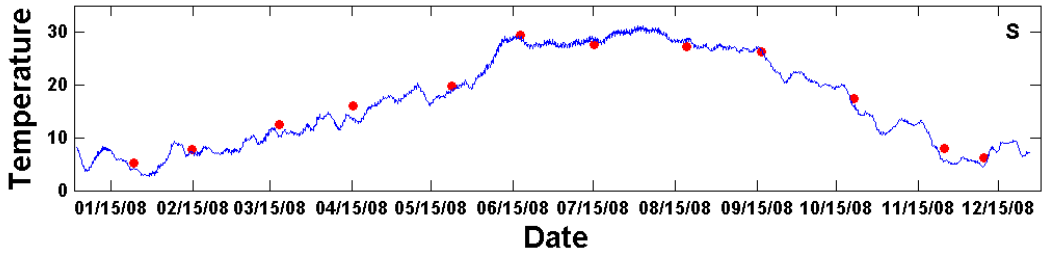
WBB05



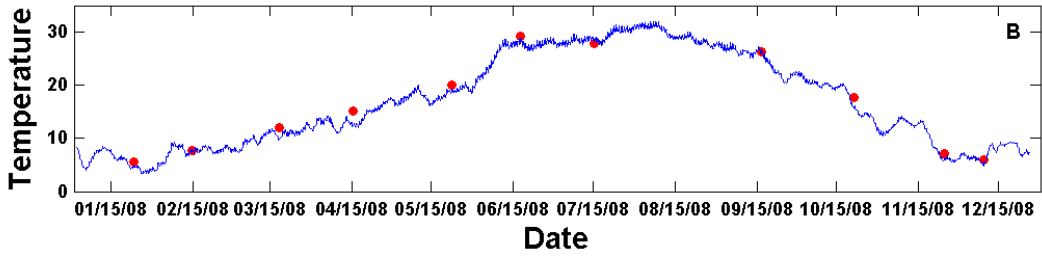
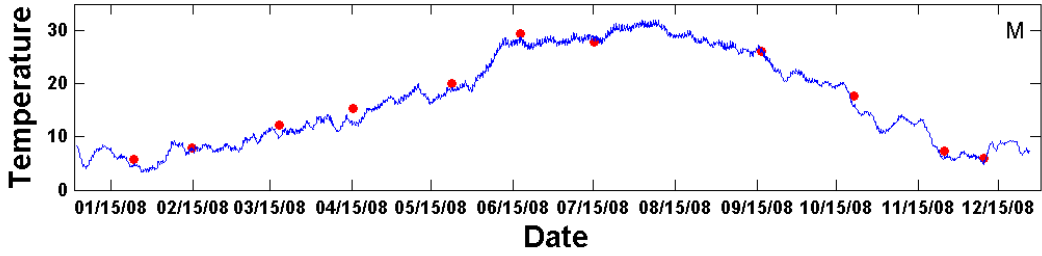
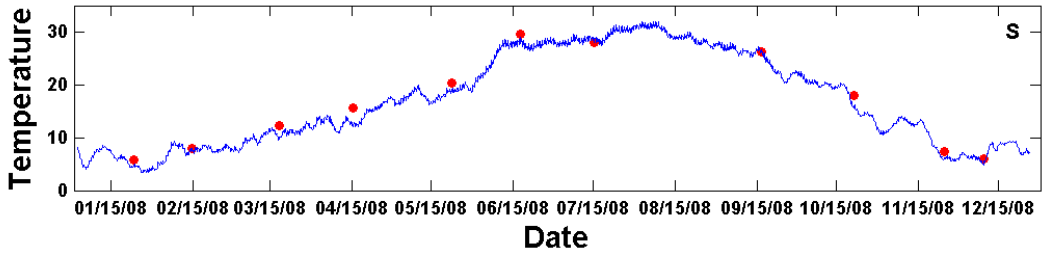
TF5.6



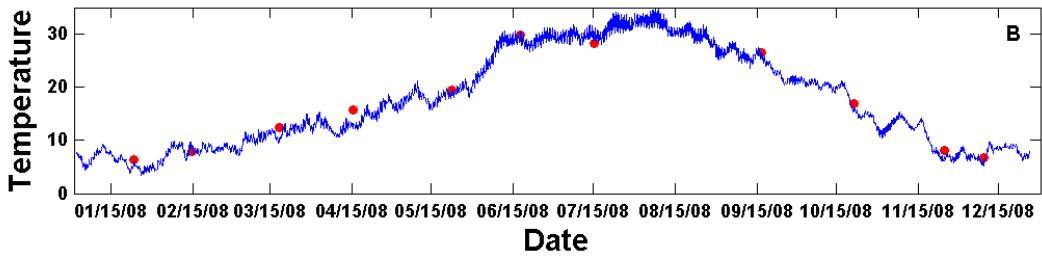
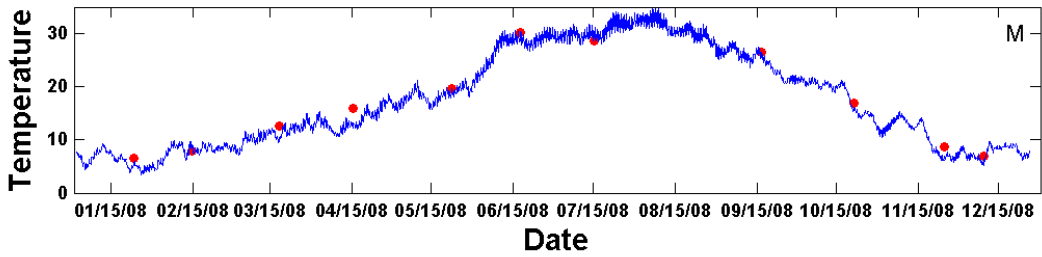
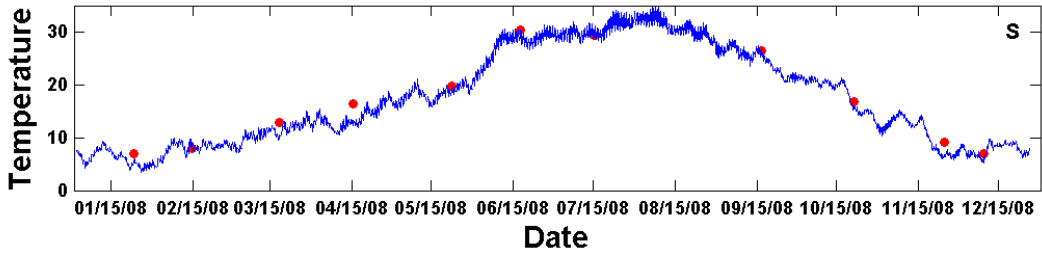
TF5.5A



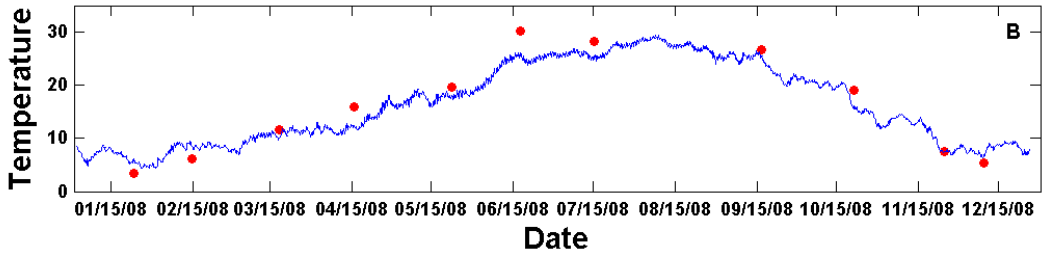
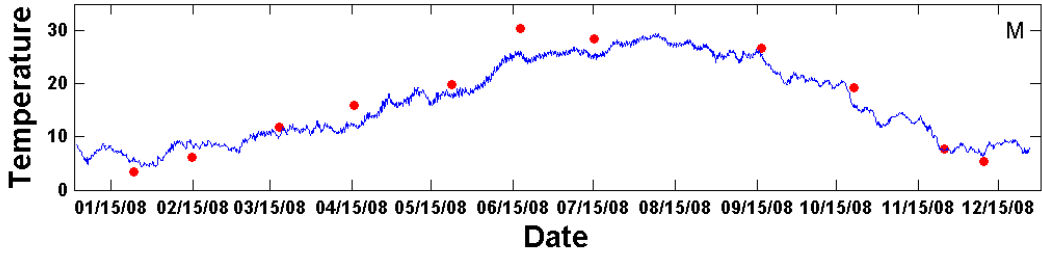
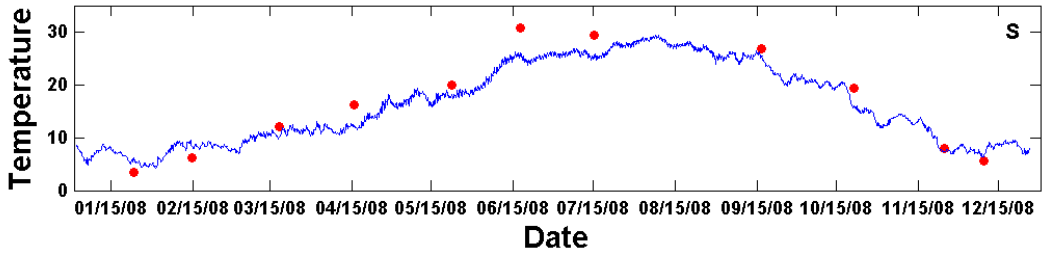
TF5.5



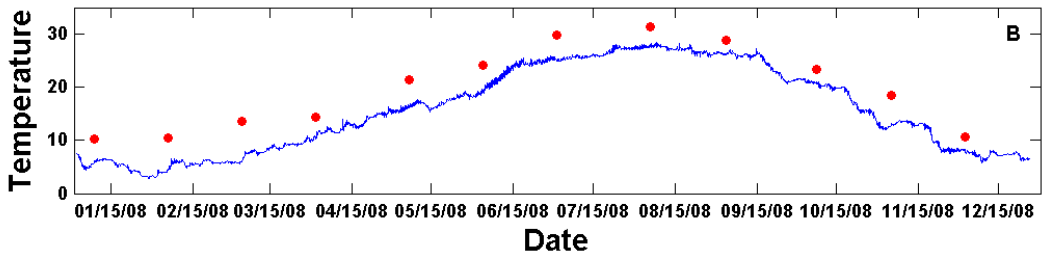
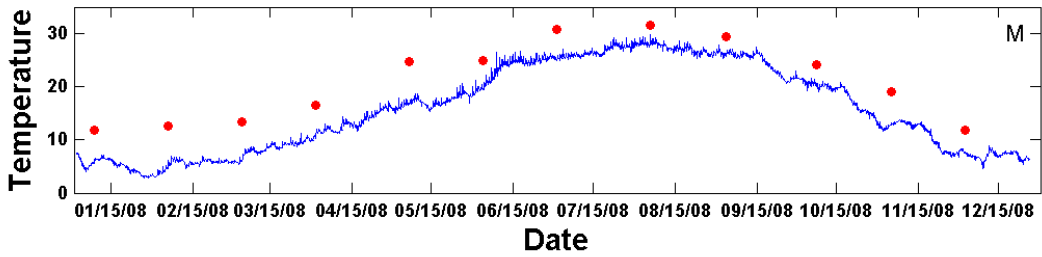
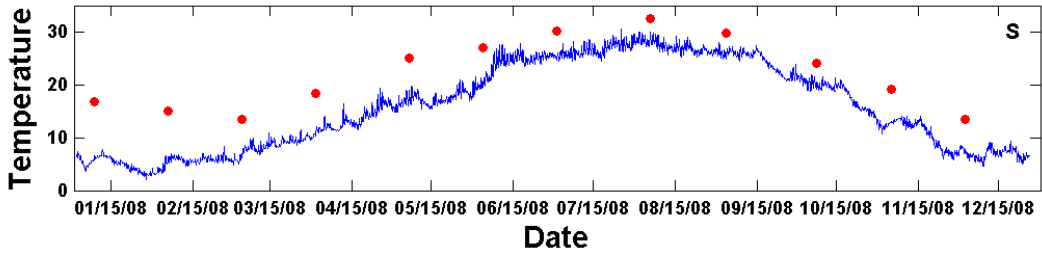
TF5.4



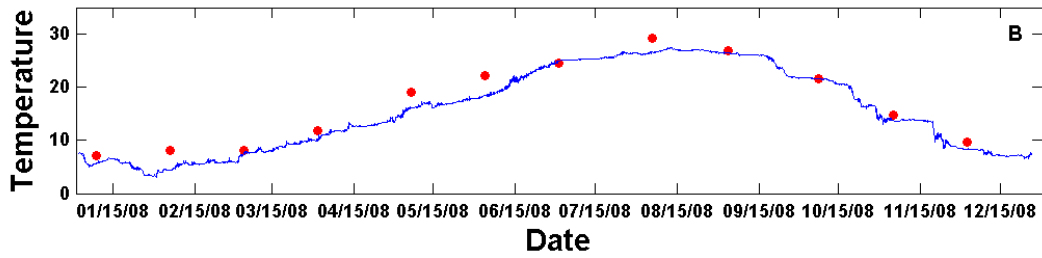
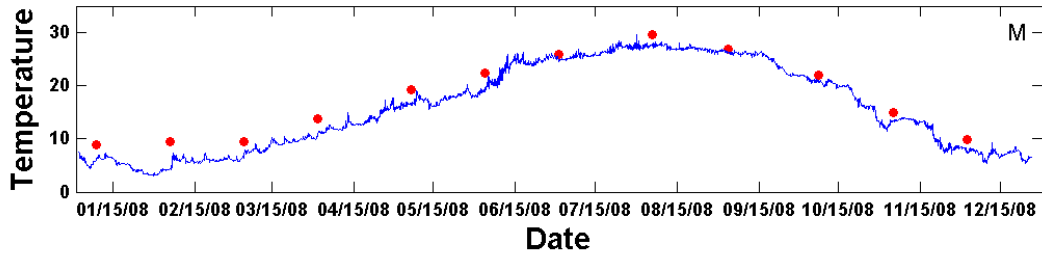
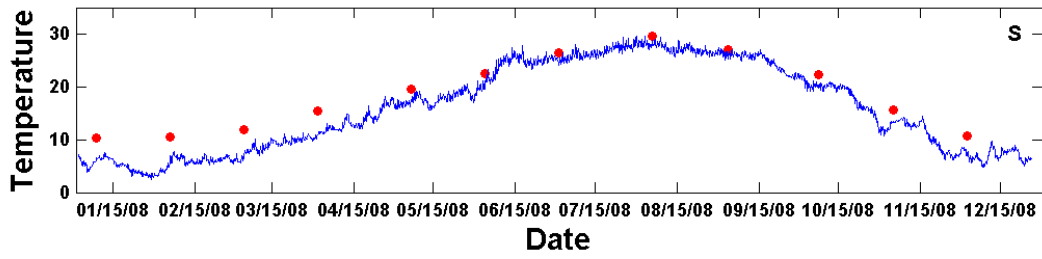
TF5.3



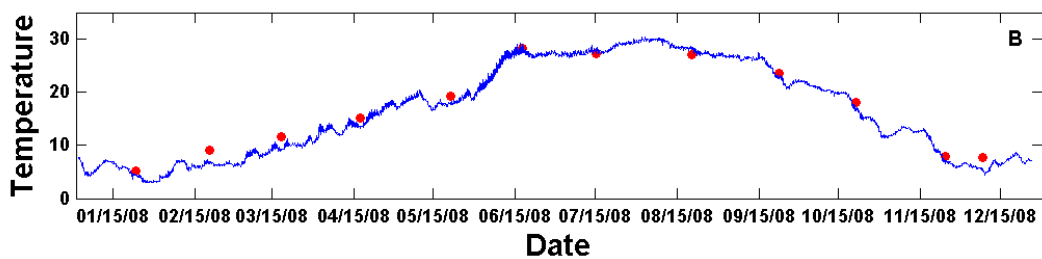
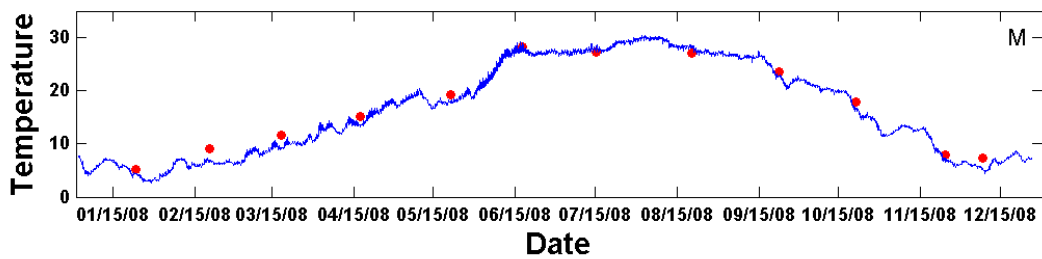
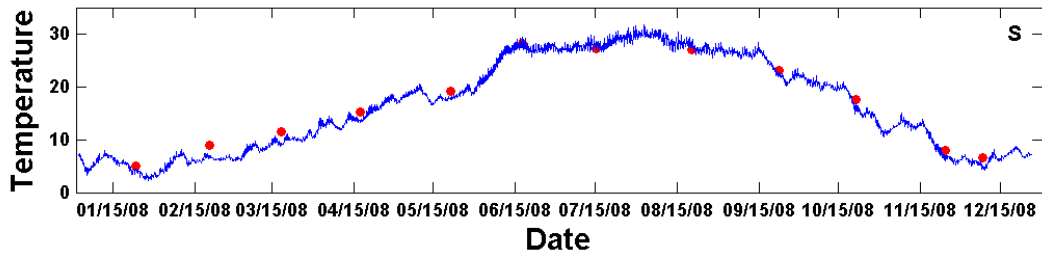
SBE5



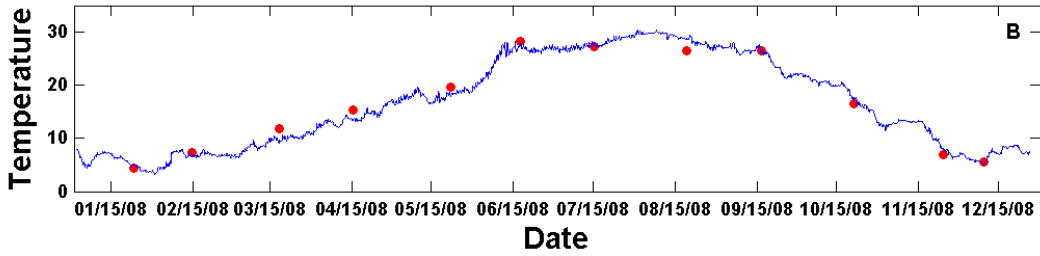
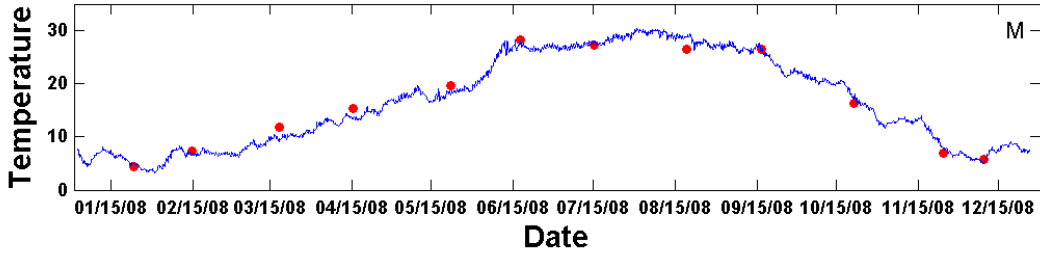
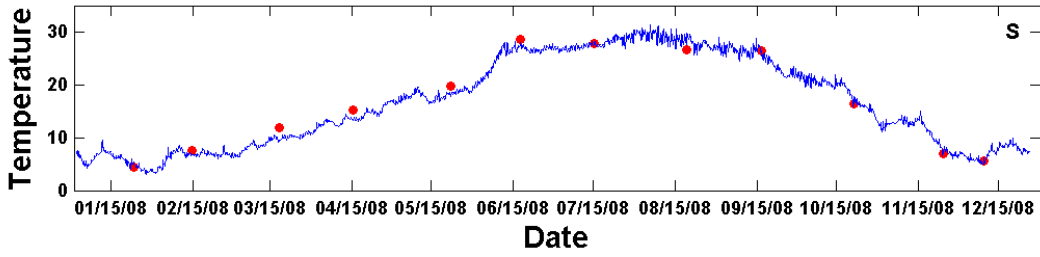
SBE2



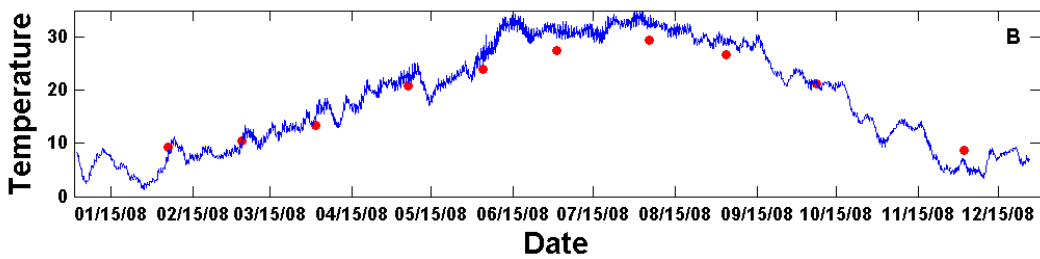
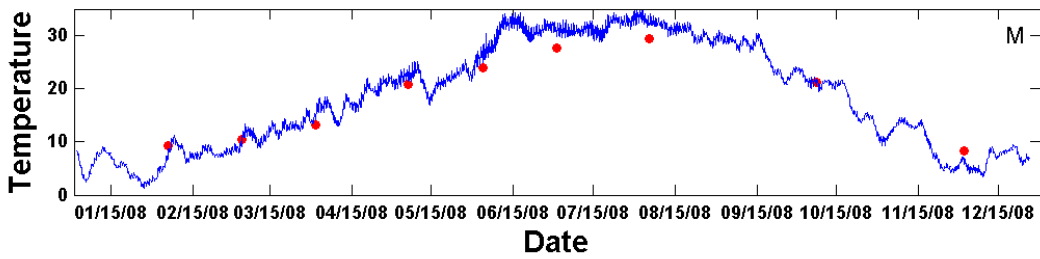
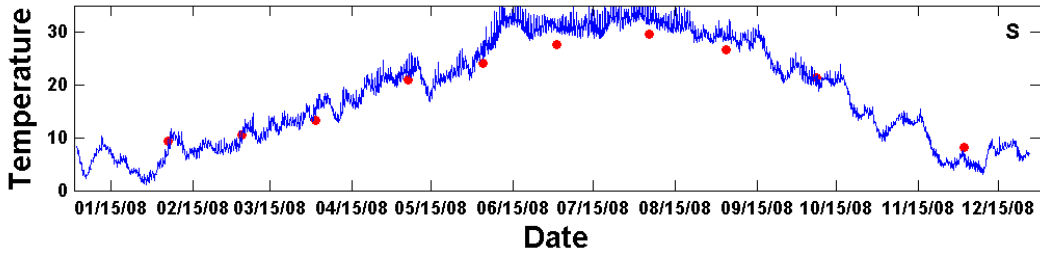
RET5.2



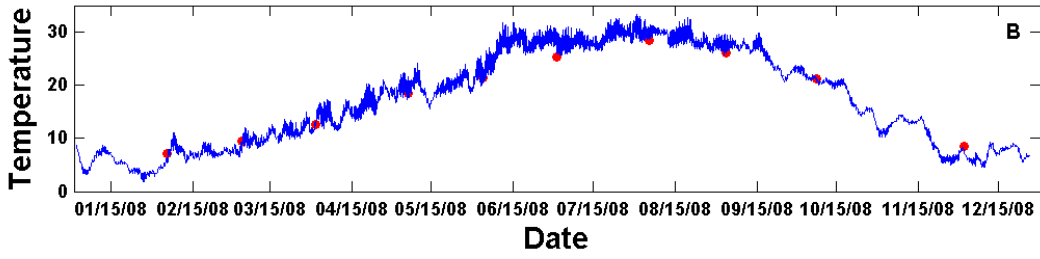
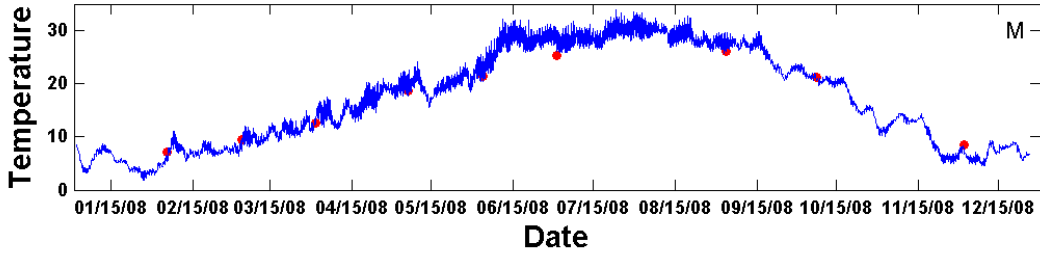
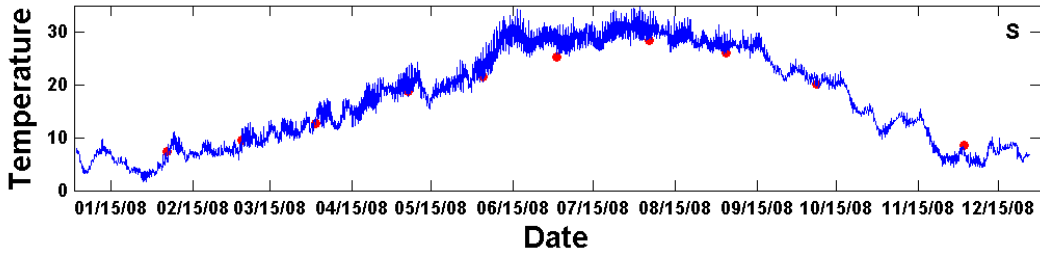
RET5.1A



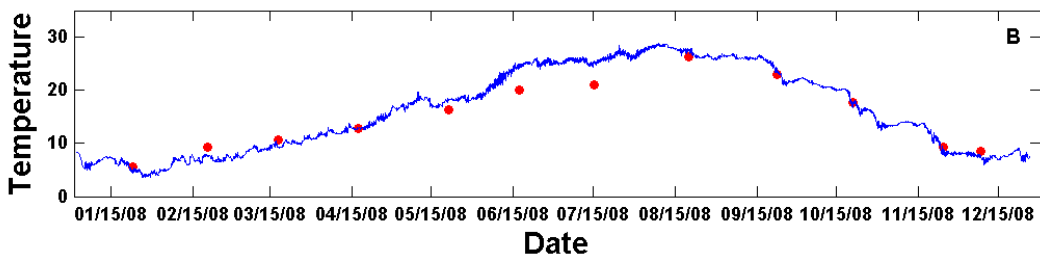
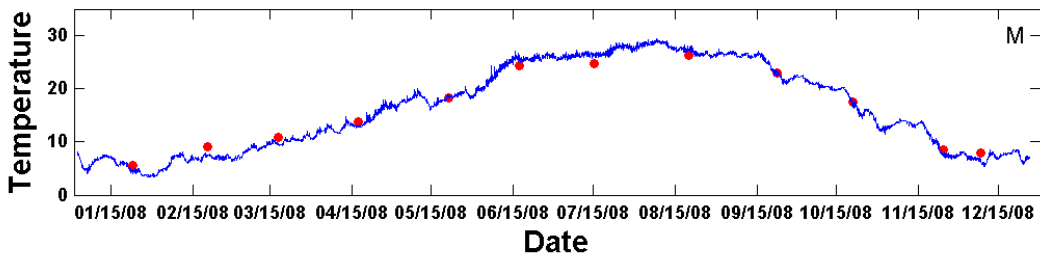
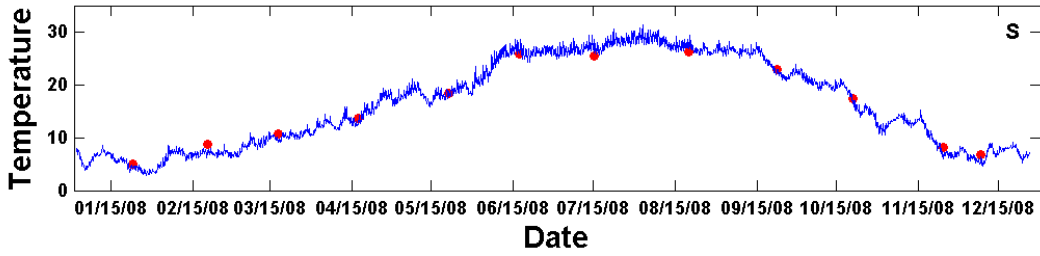
LFB01



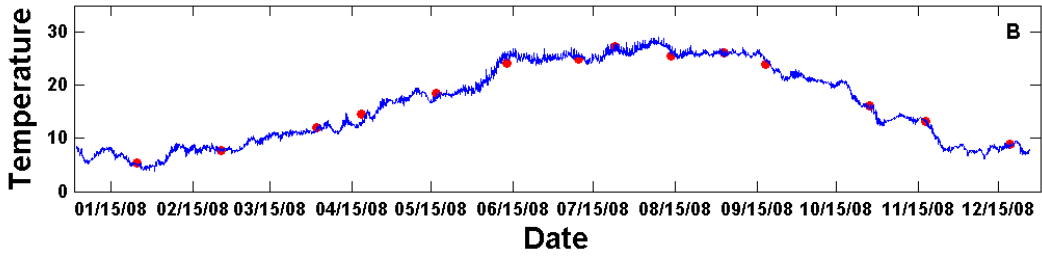
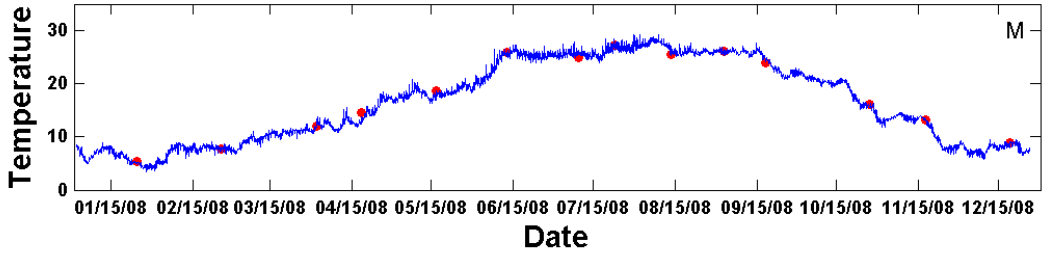
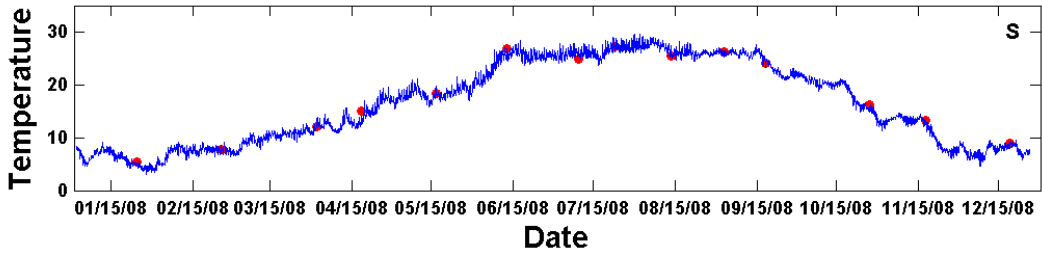
LFA01



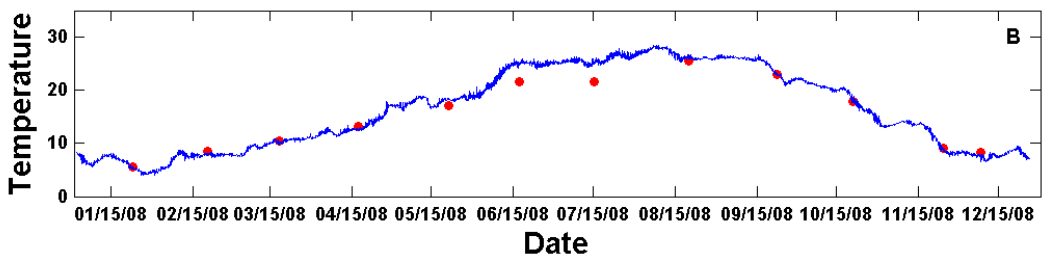
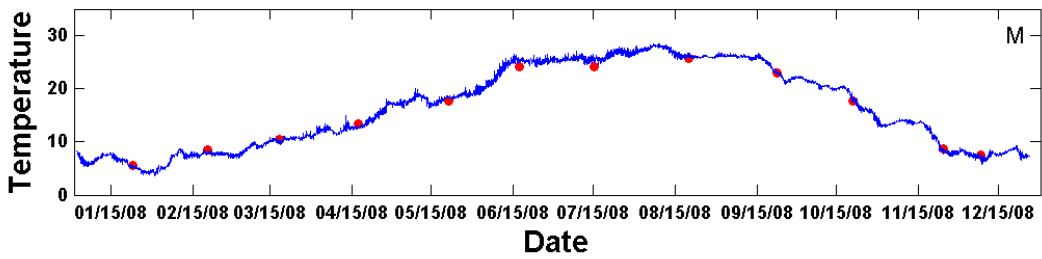
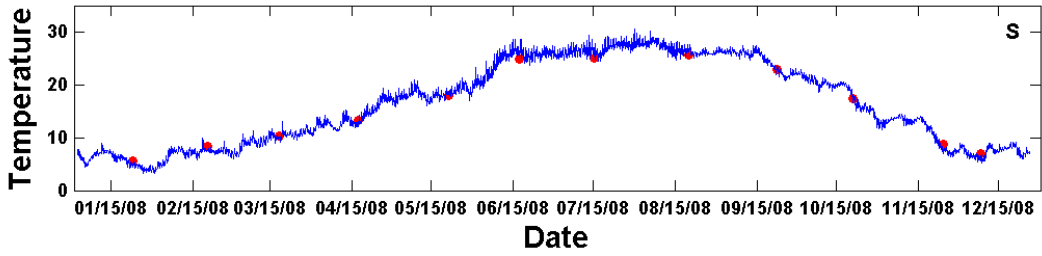
LE5.6



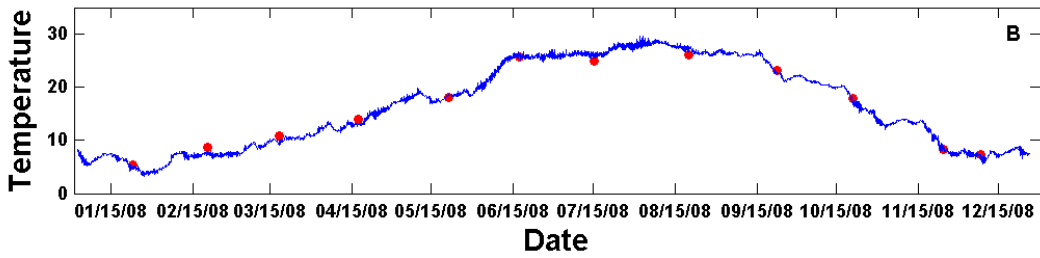
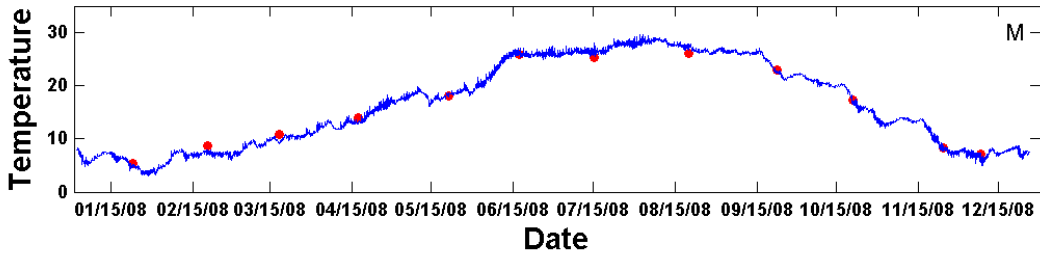
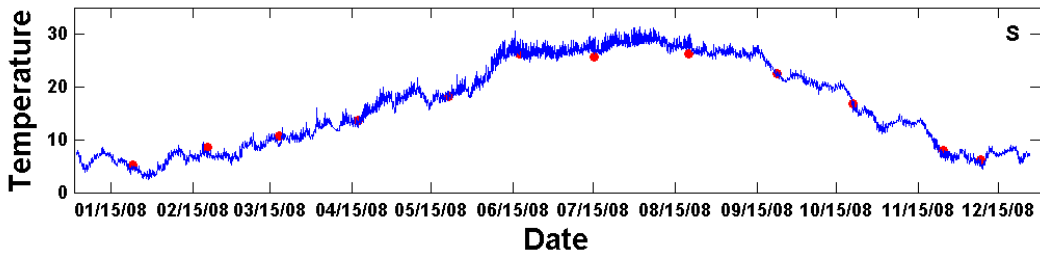
LE5.5-W



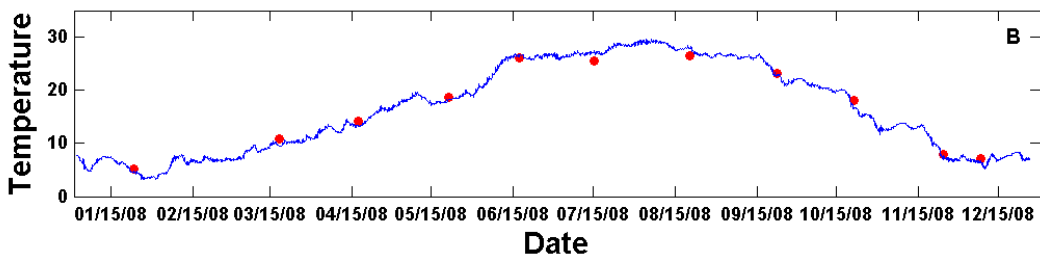
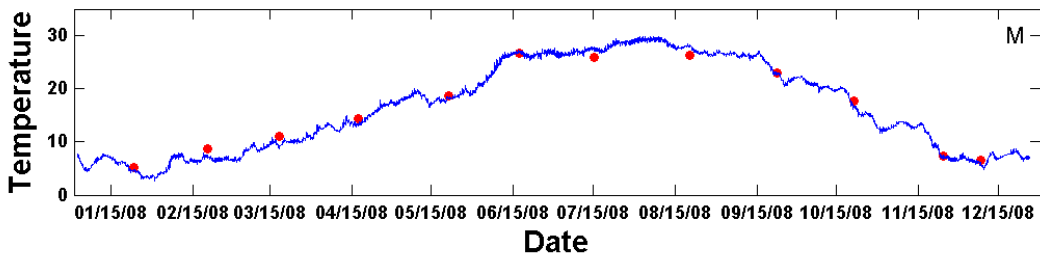
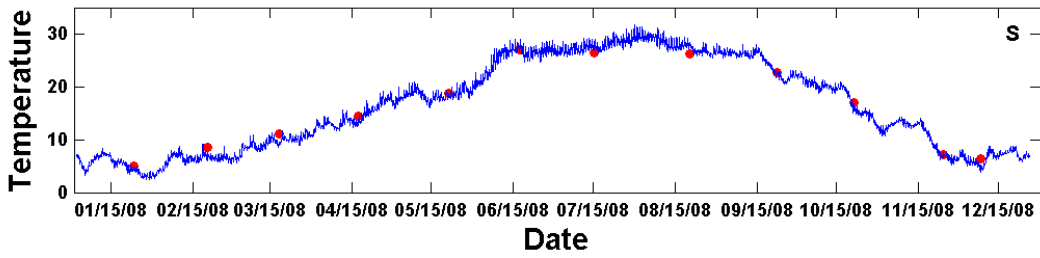
LE5.4



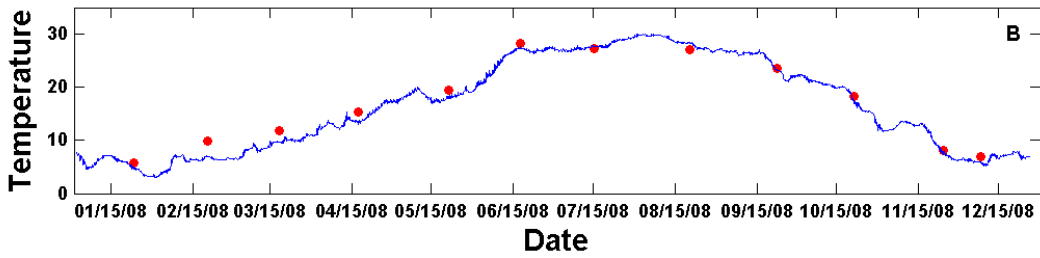
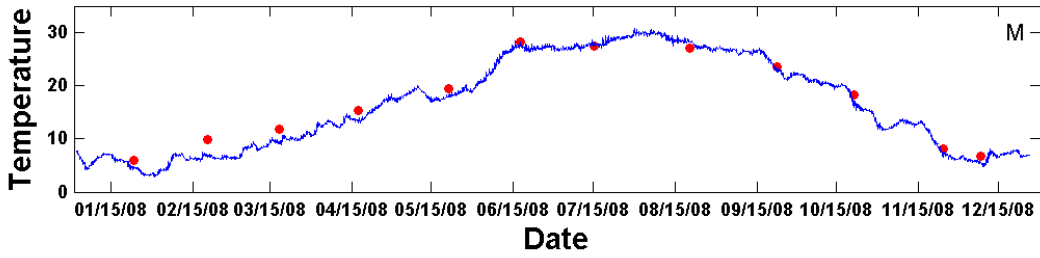
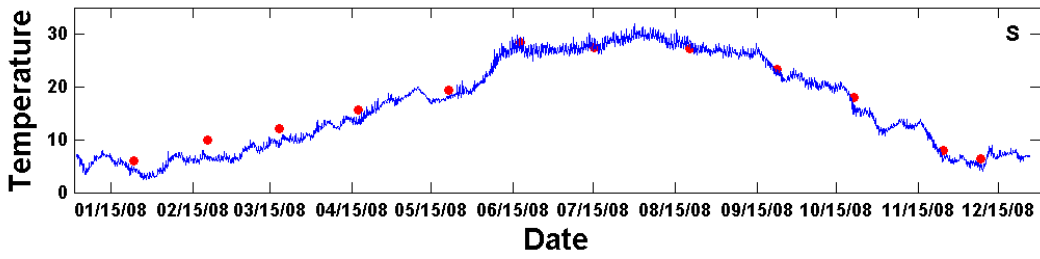
LE5.3



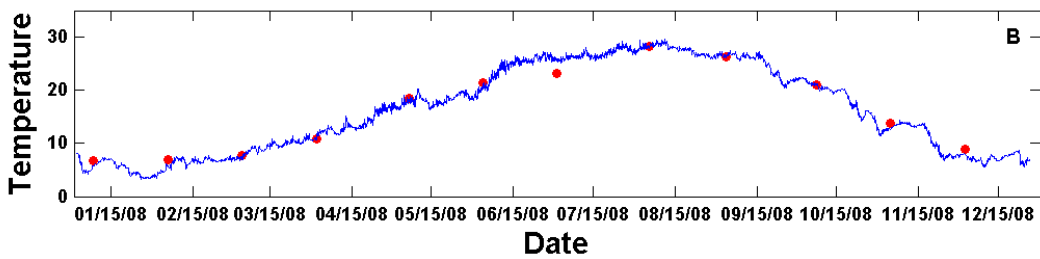
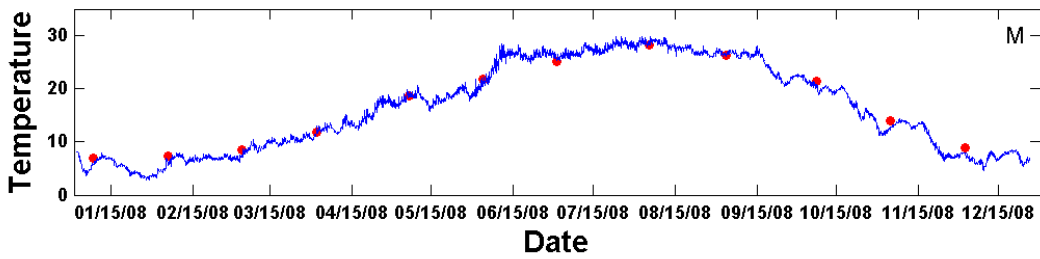
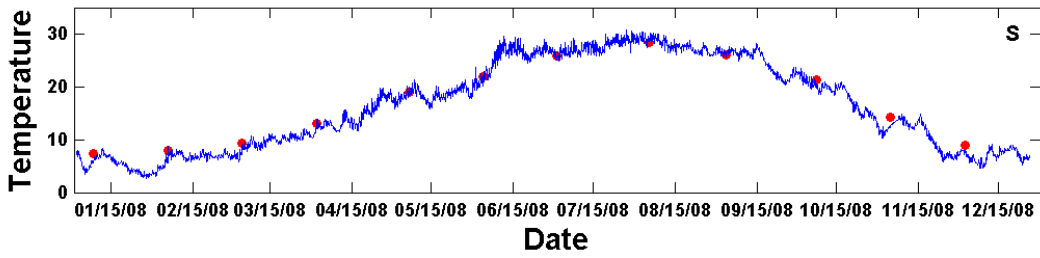
LE5.2



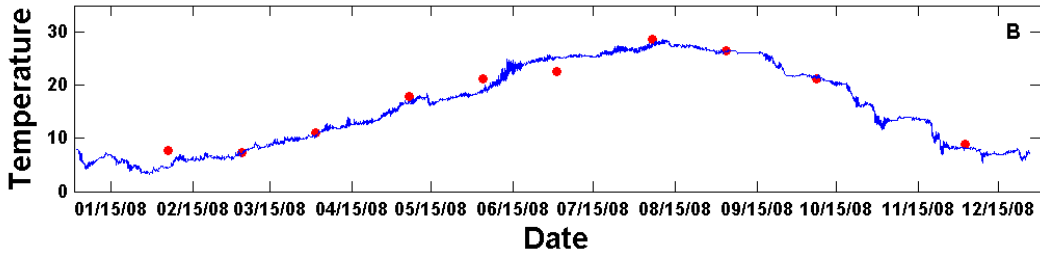
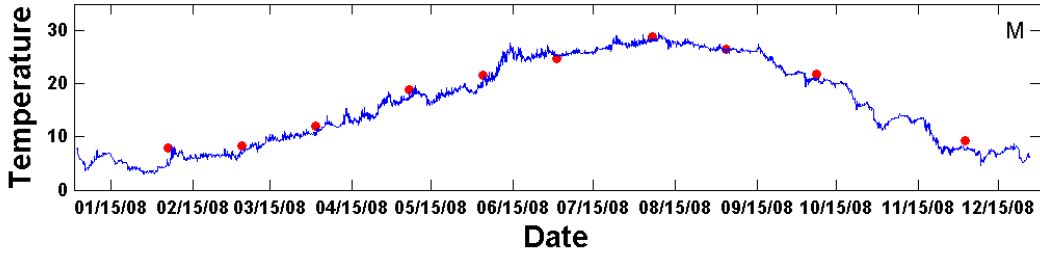
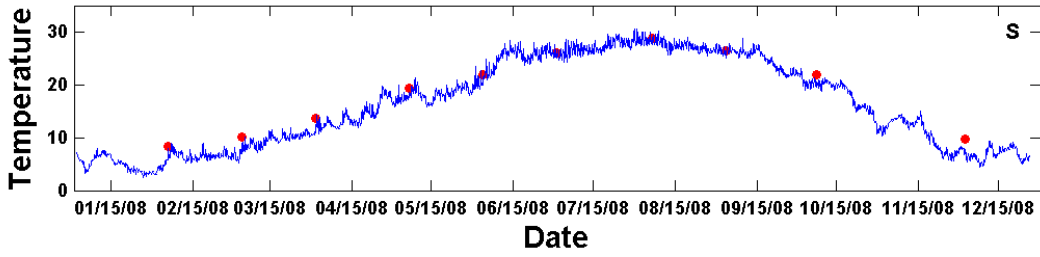
LE5.1



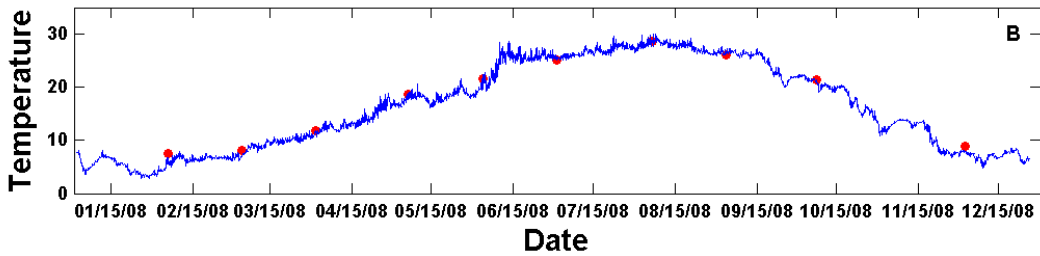
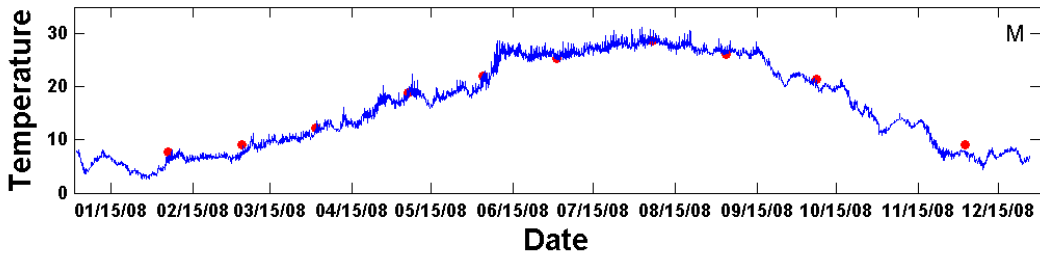
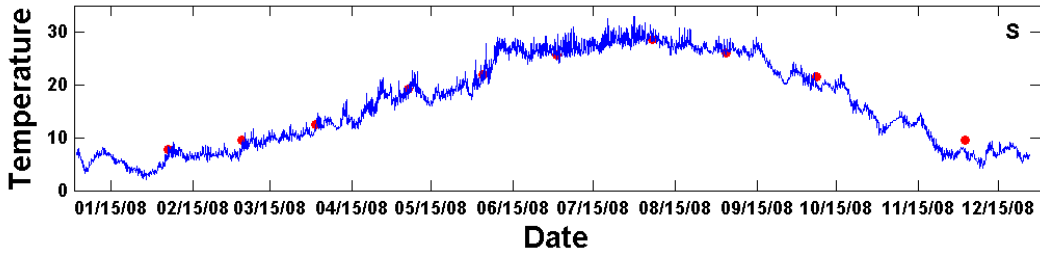
ELI2



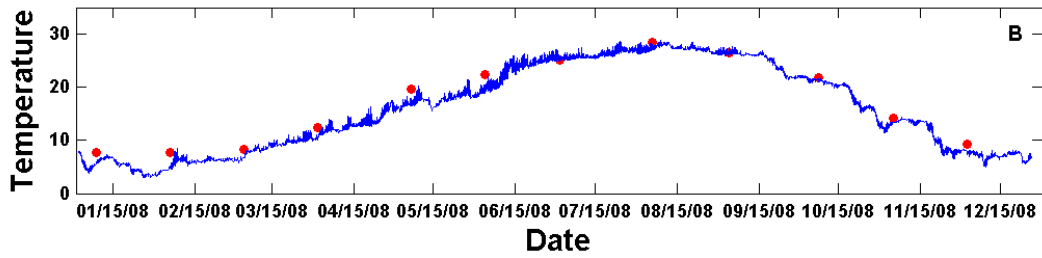
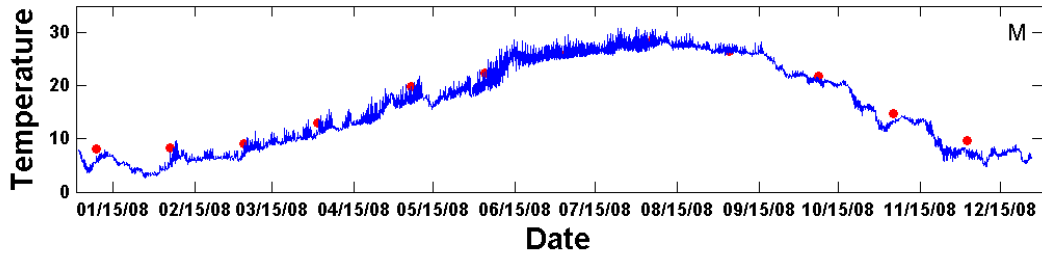
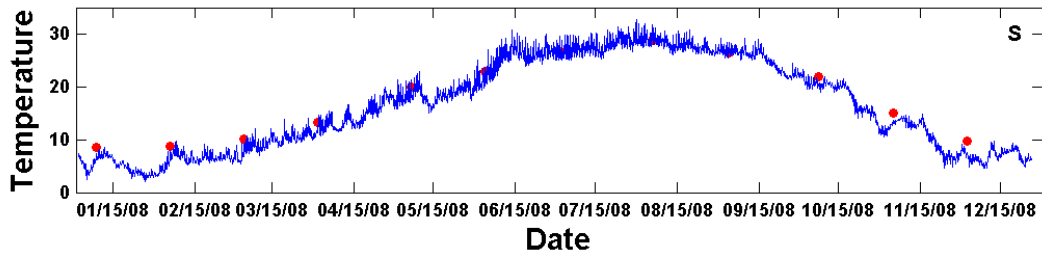
ELE01



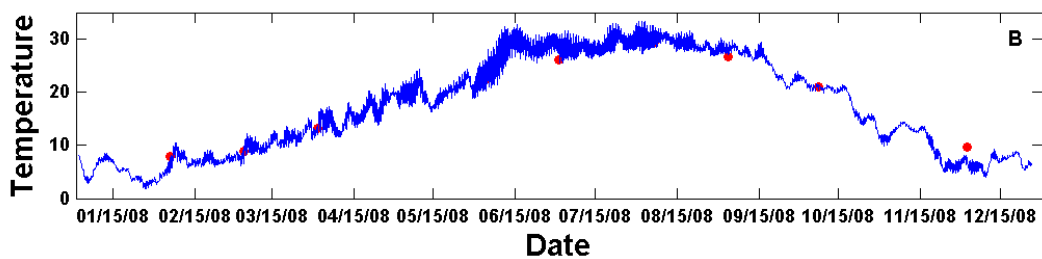
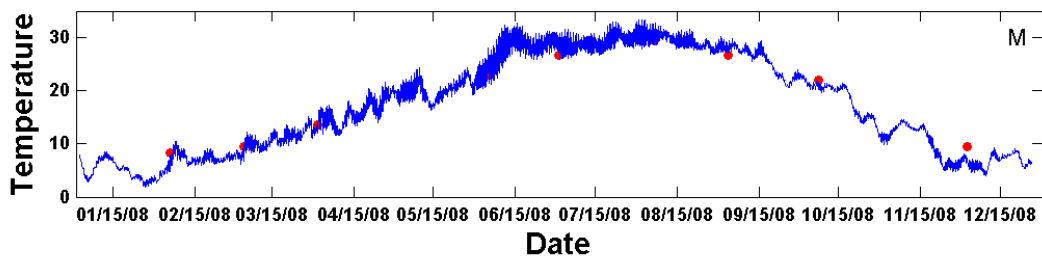
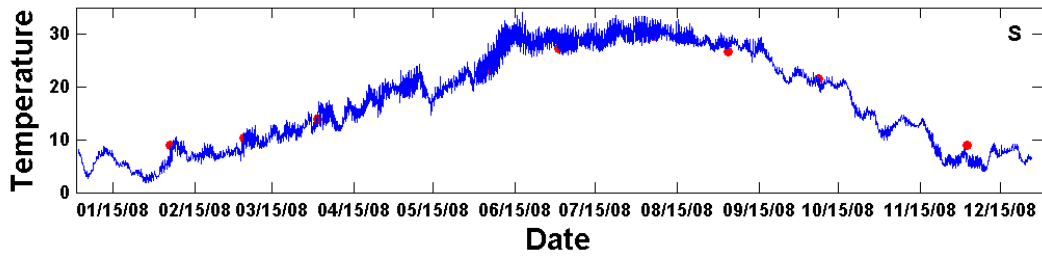
ELD01



EBE1



EBB01



1. Appendix E

This appendix includes time series plot of Water quality model results. The water quality time series comparison between different scenarios was plotted during the period from 2010 to 2013. The locations of monitoring stations are shown below in Figure E-1.

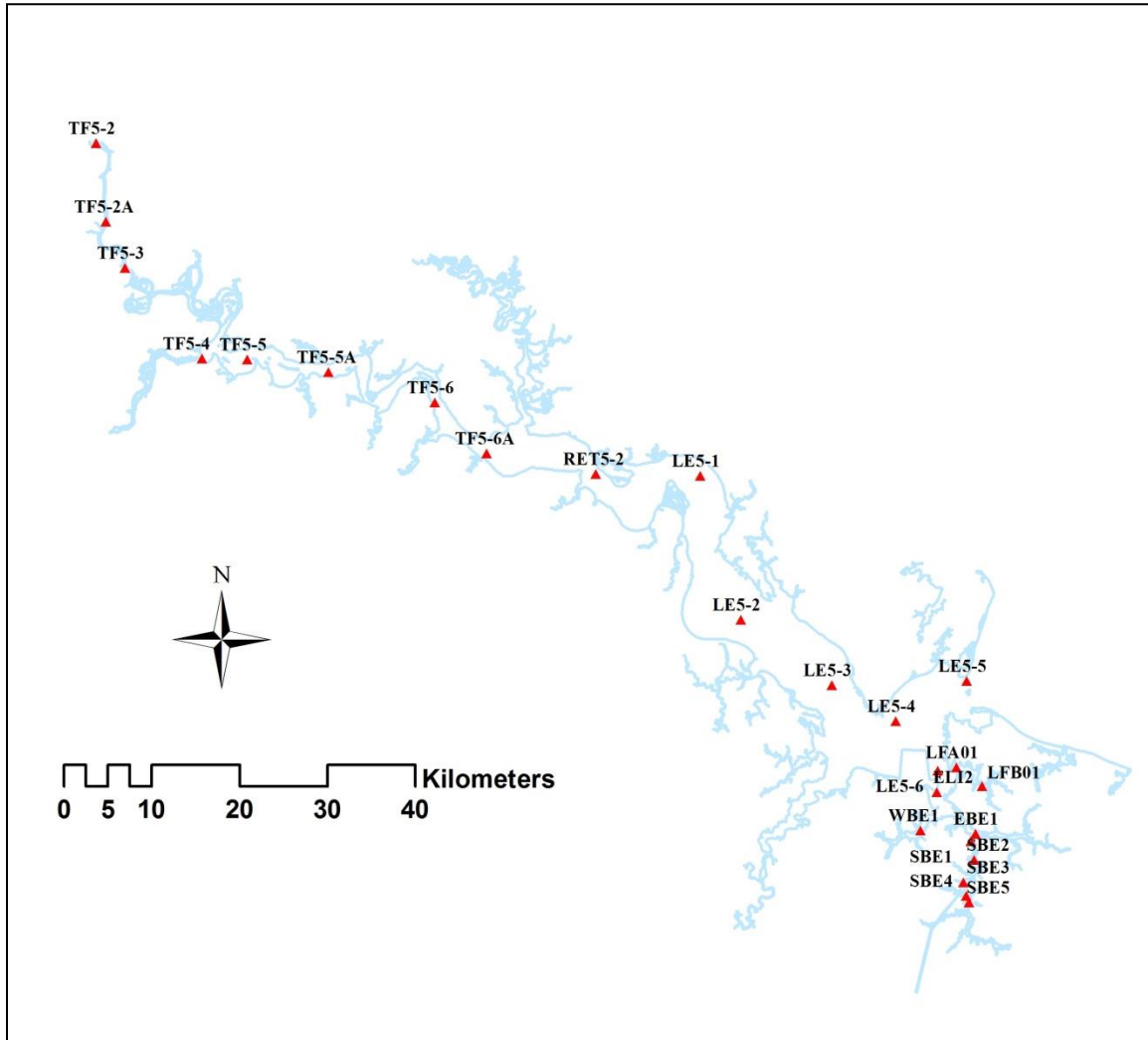
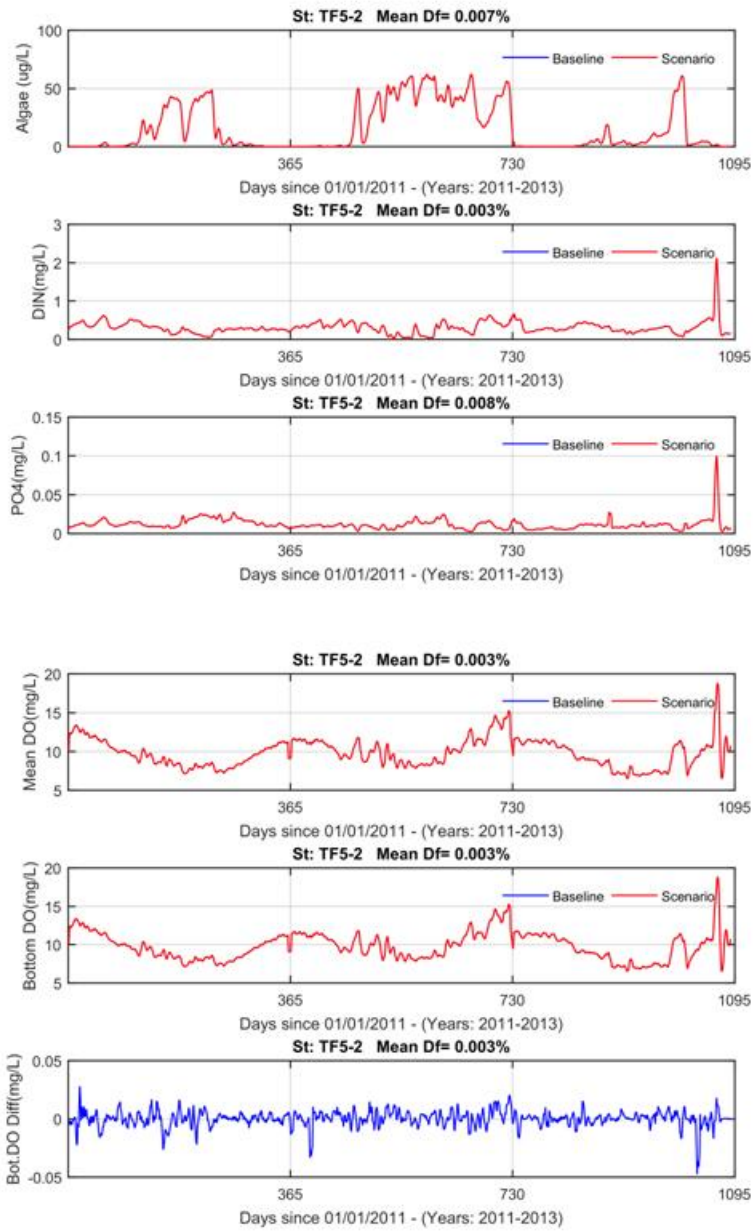
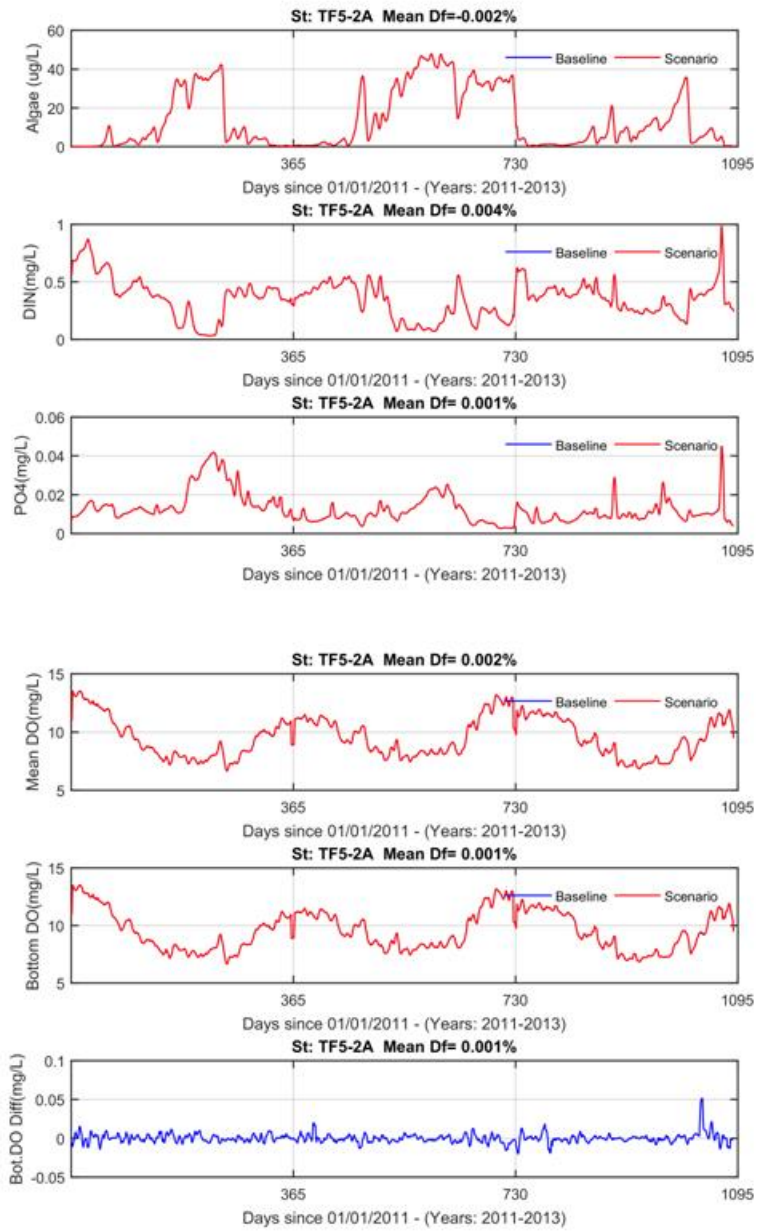
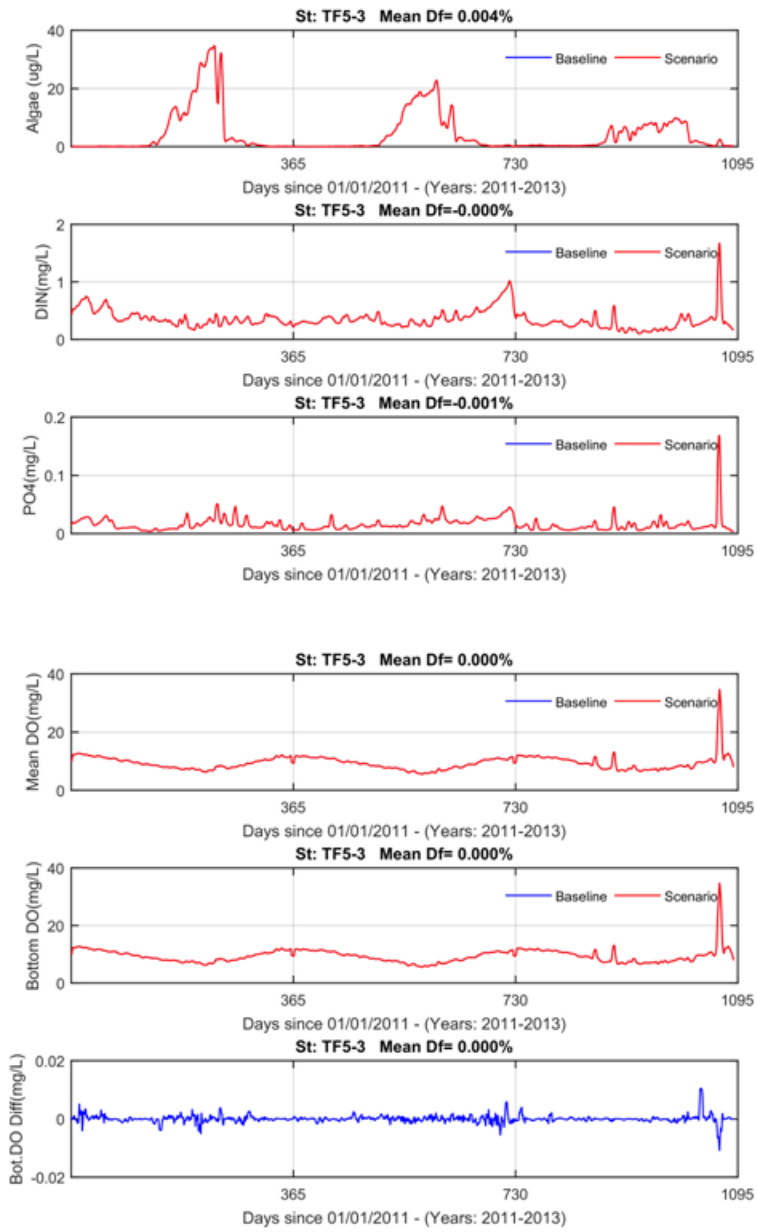


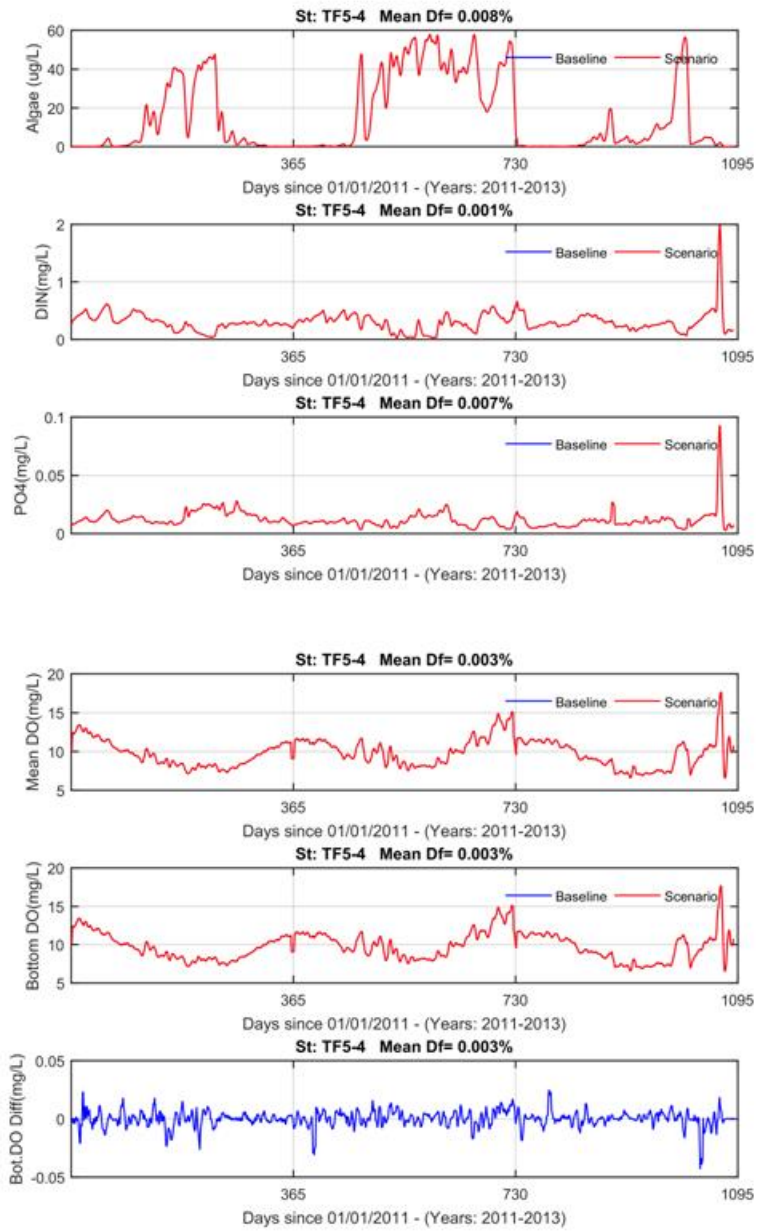
Figure E-1: Location of monitoring Stations.

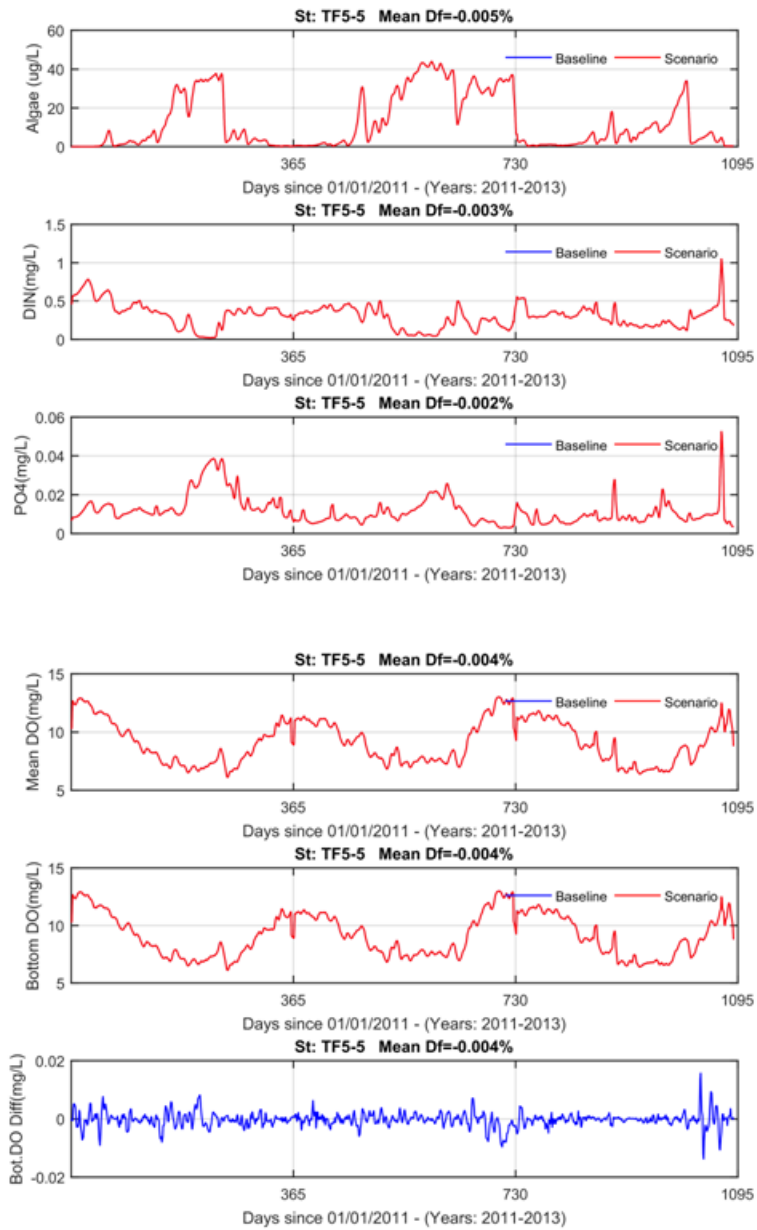
E1. Model Simulation of Baseline 1 and Baseline 2

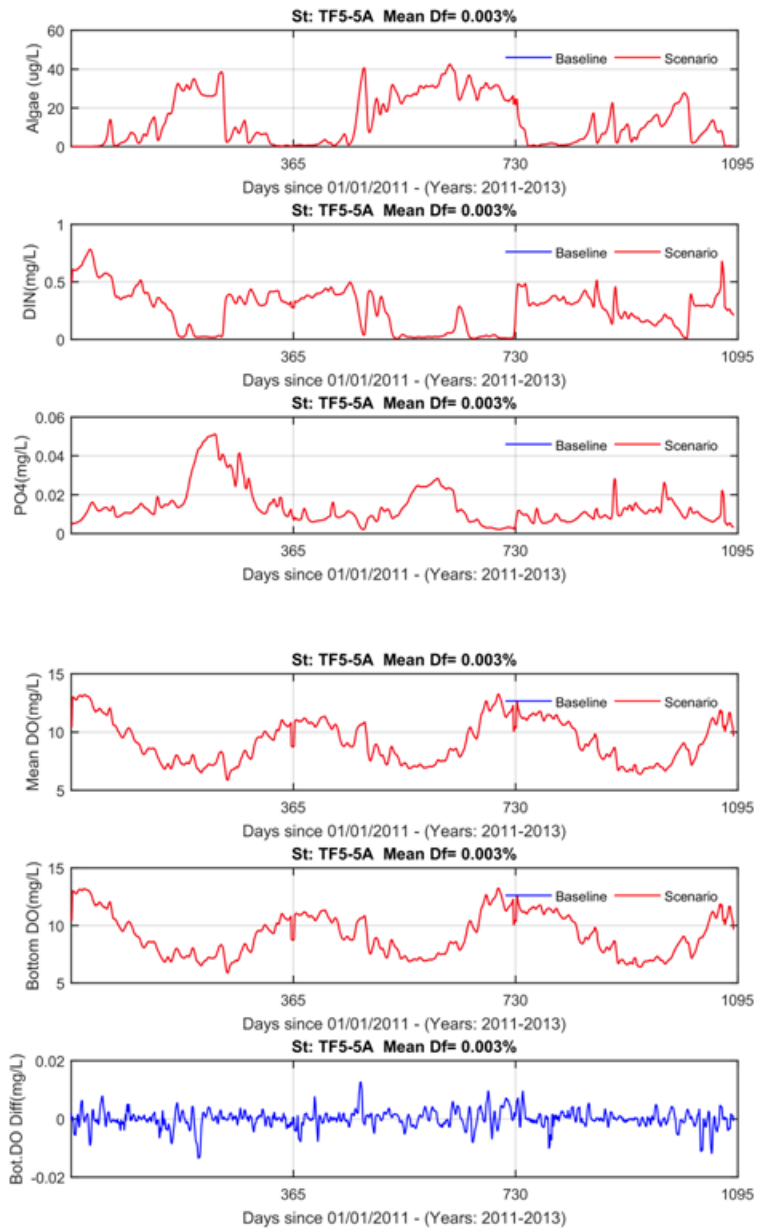


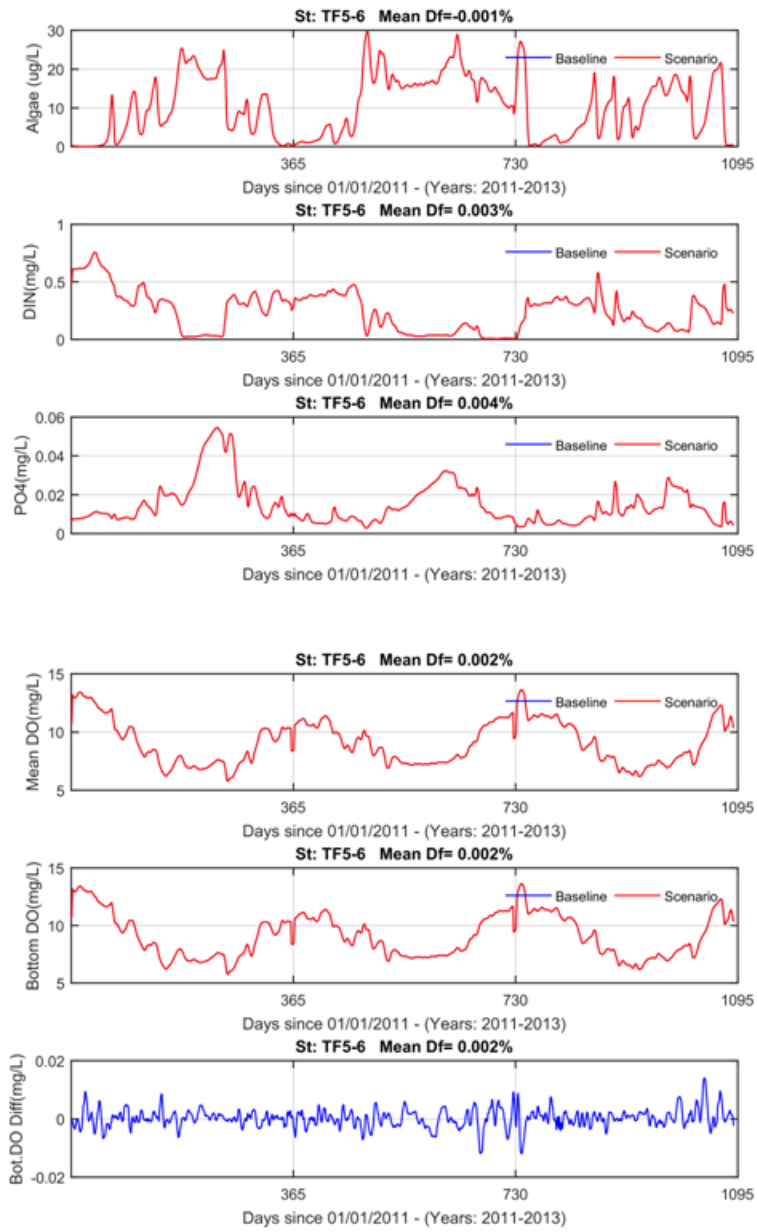


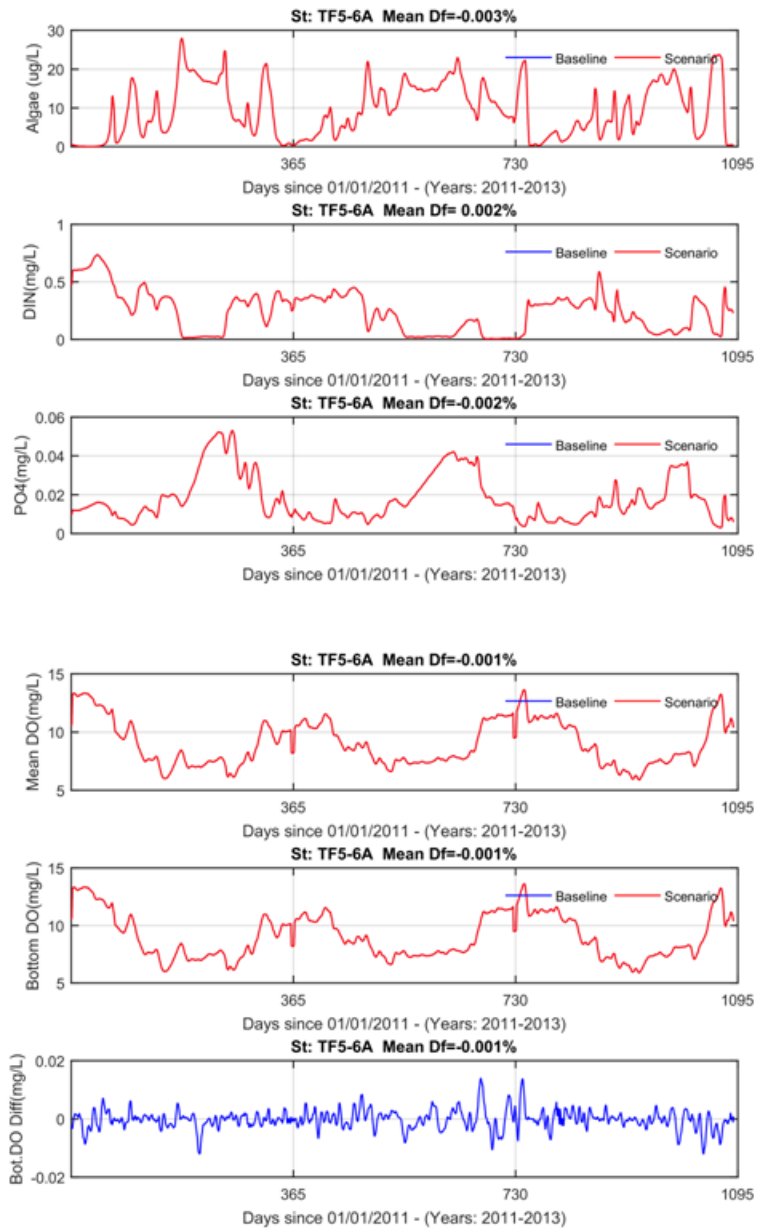


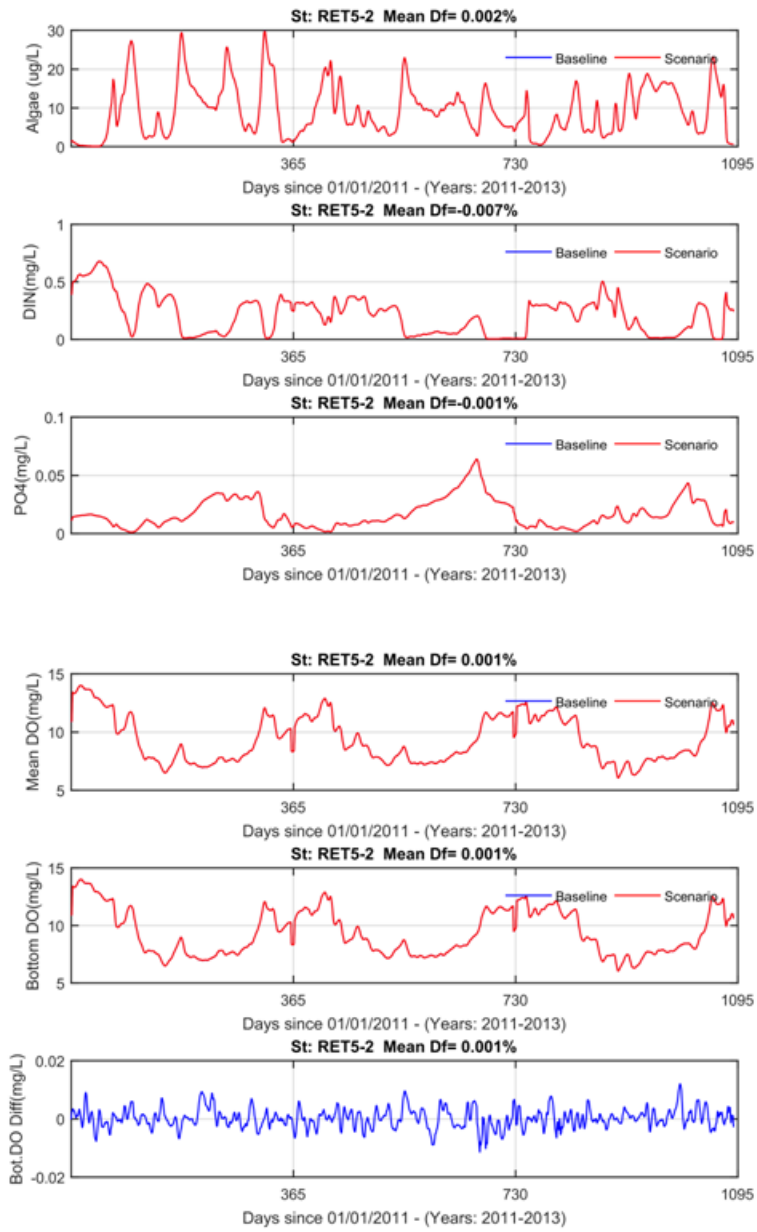


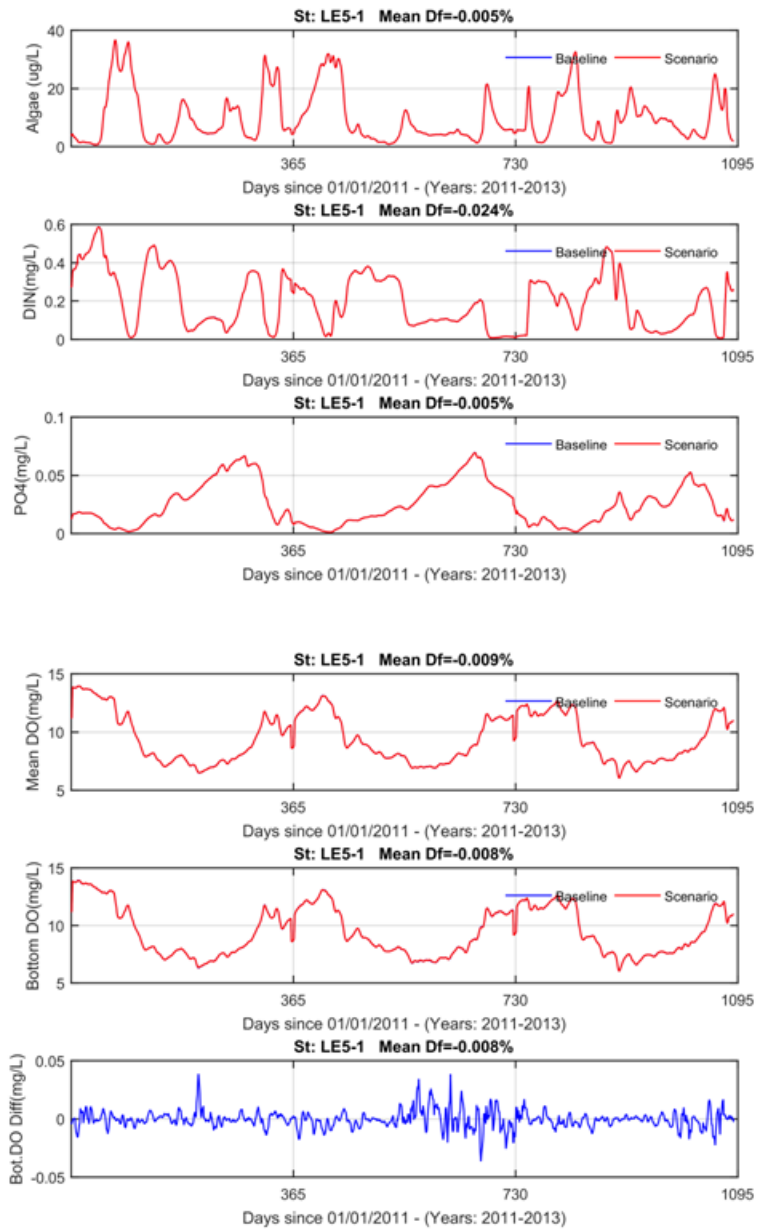


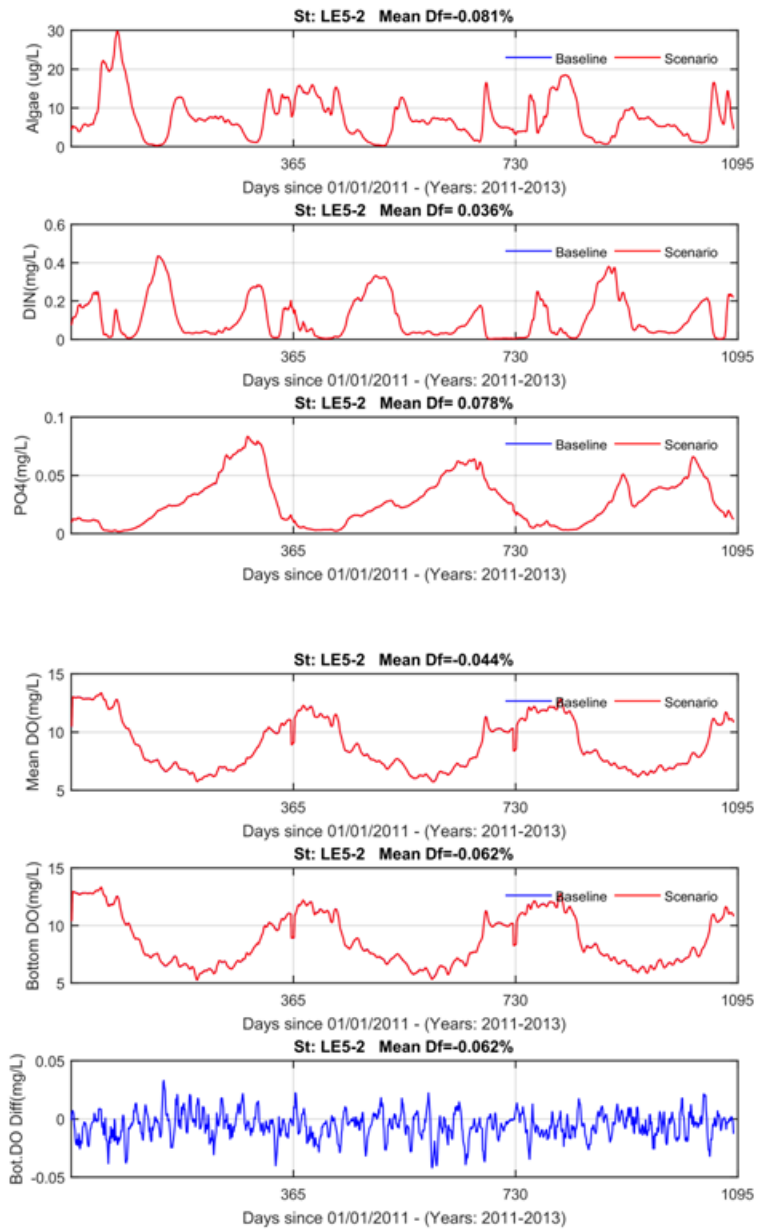


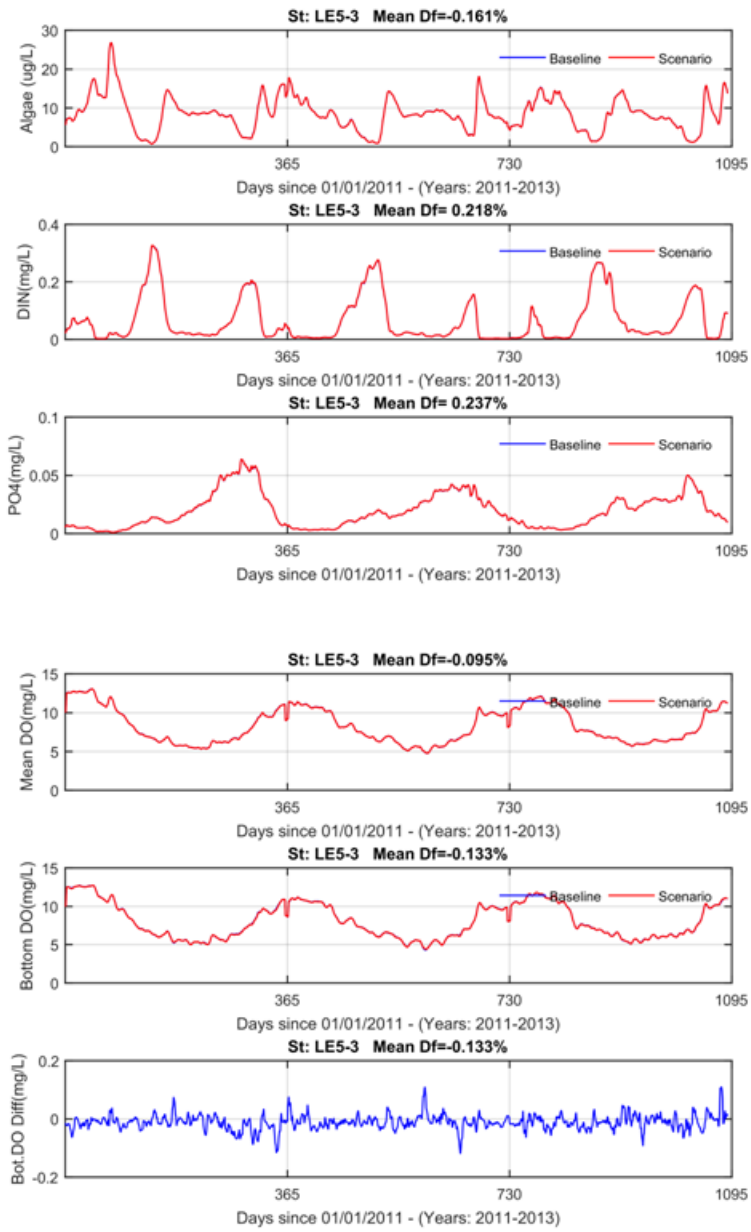


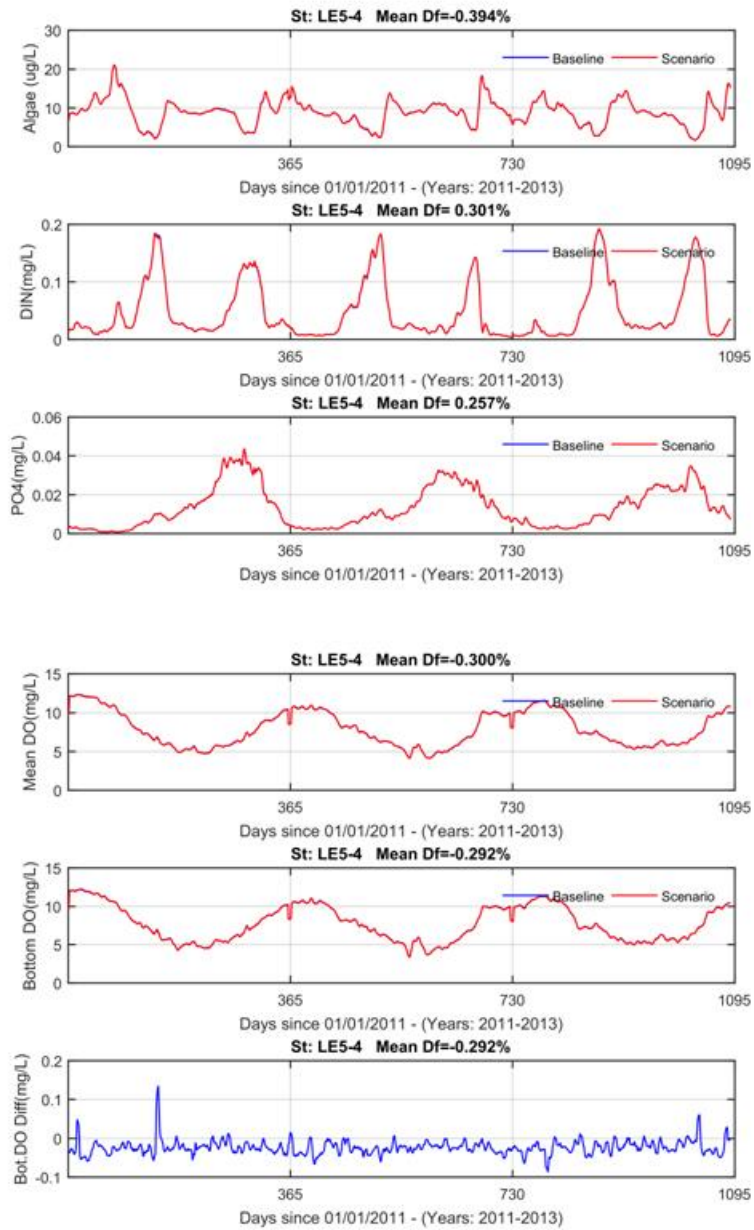


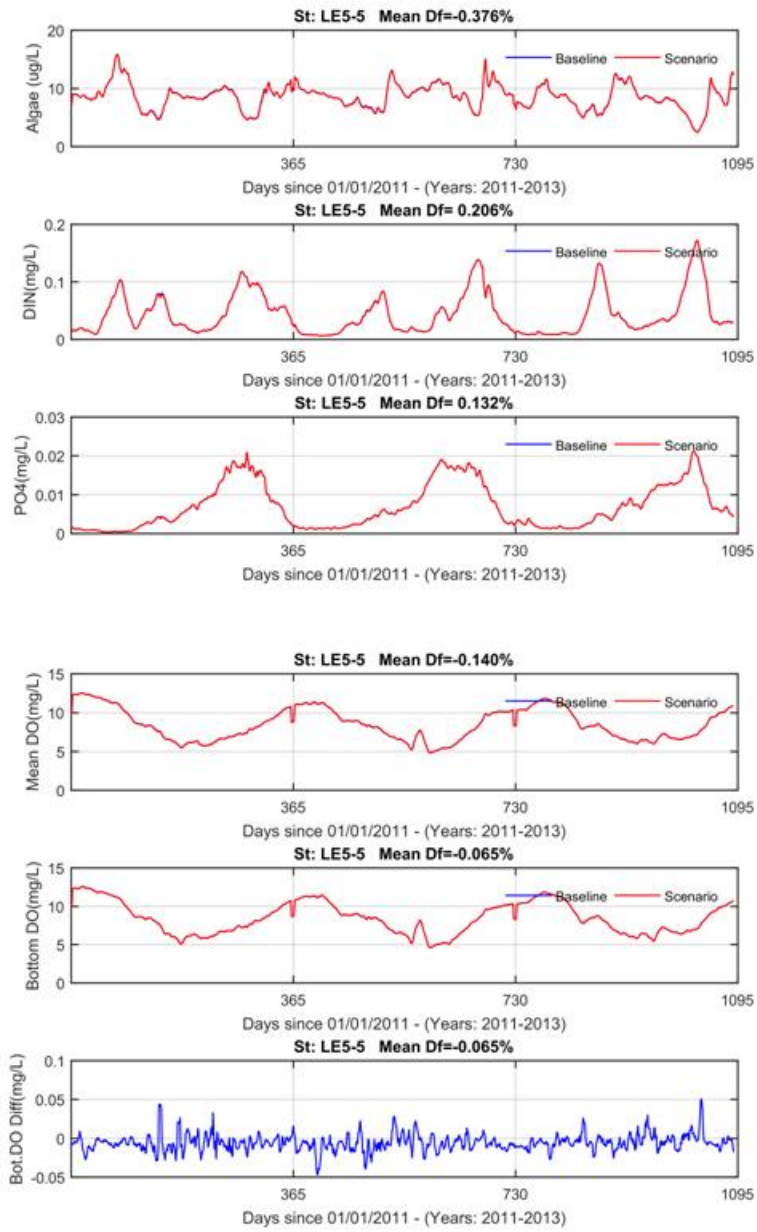


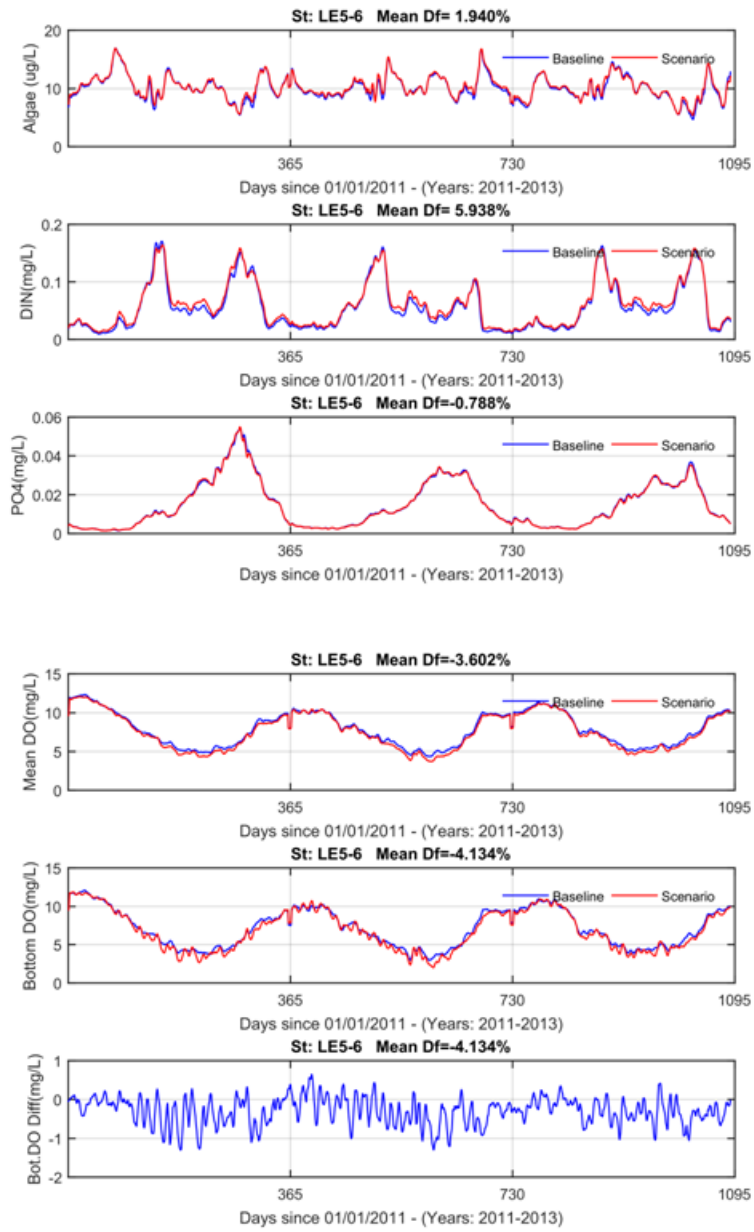


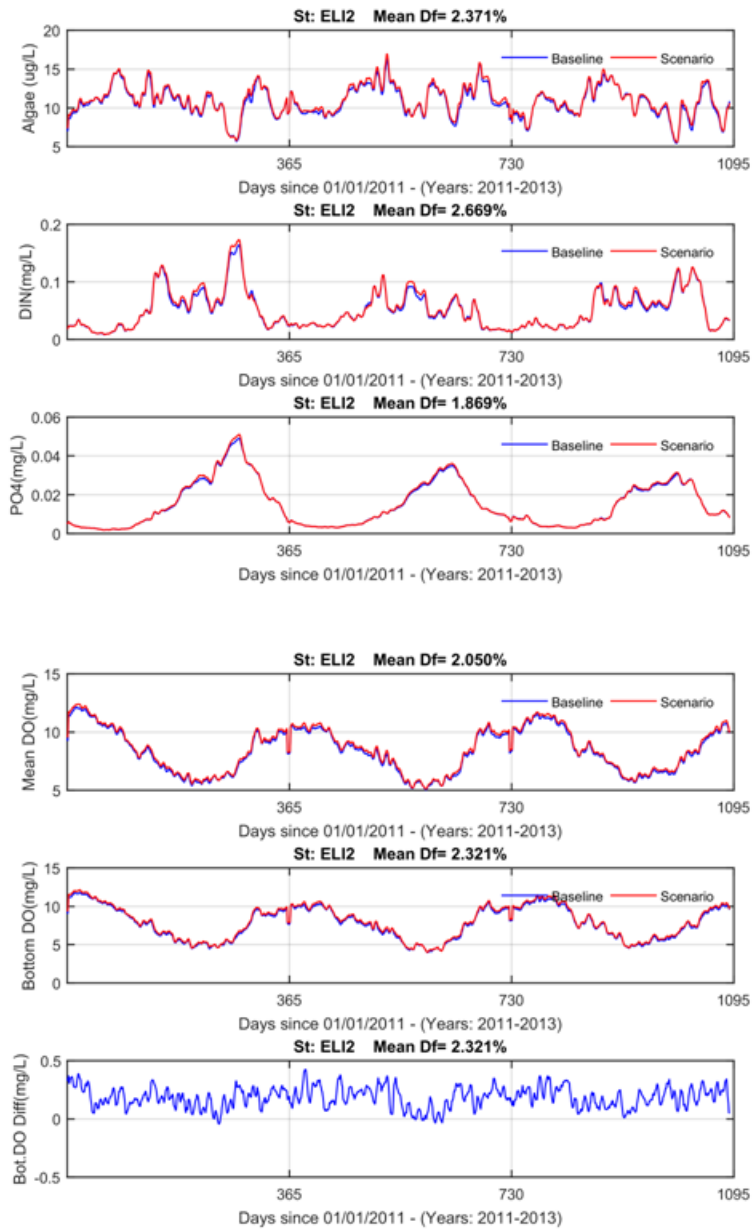


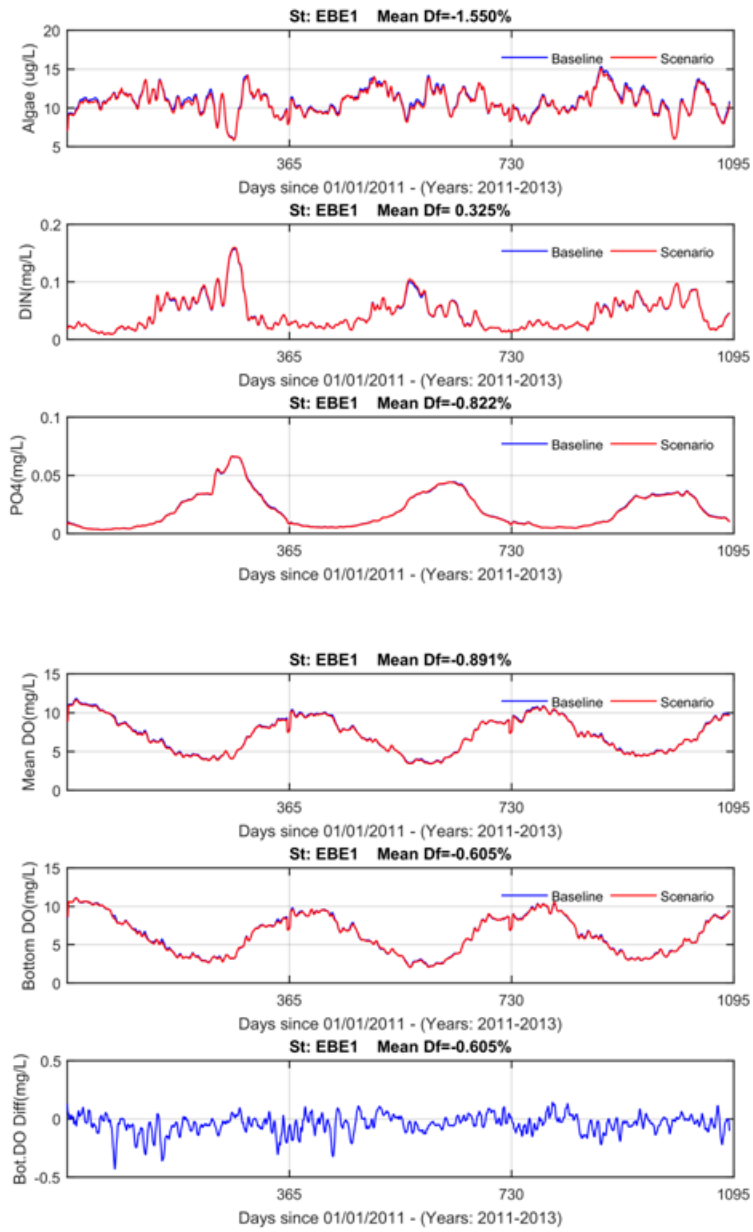


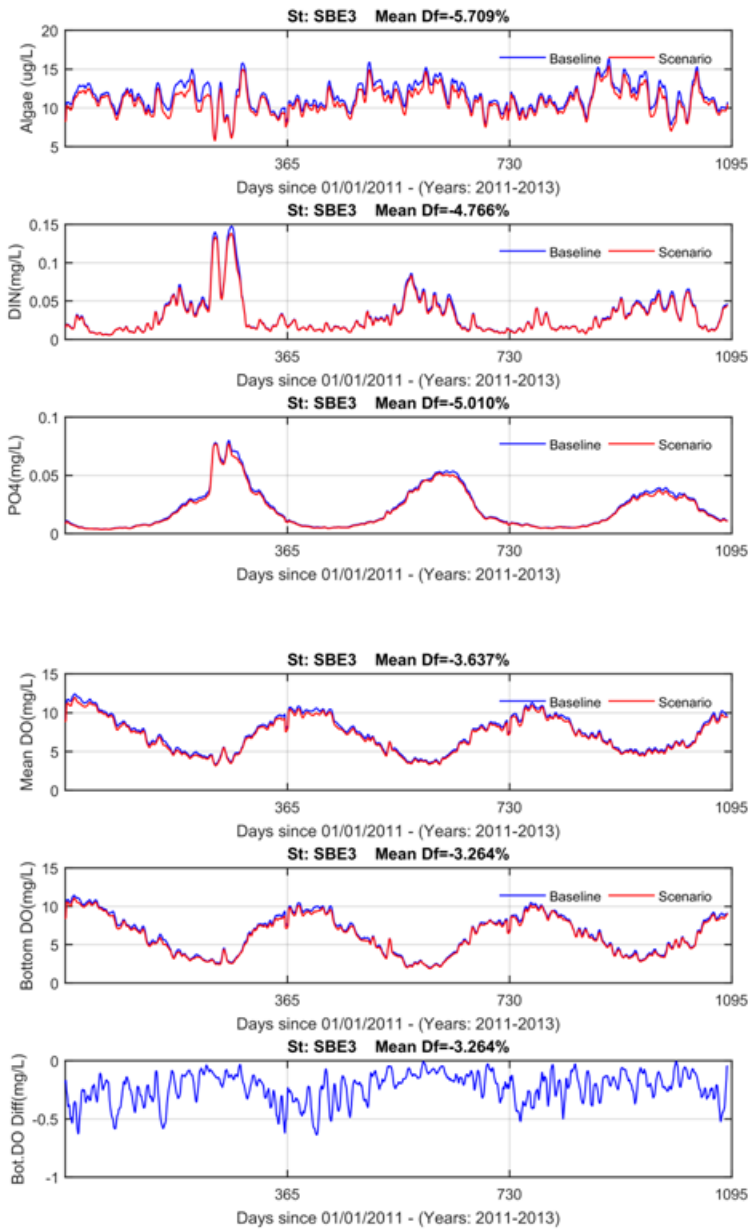


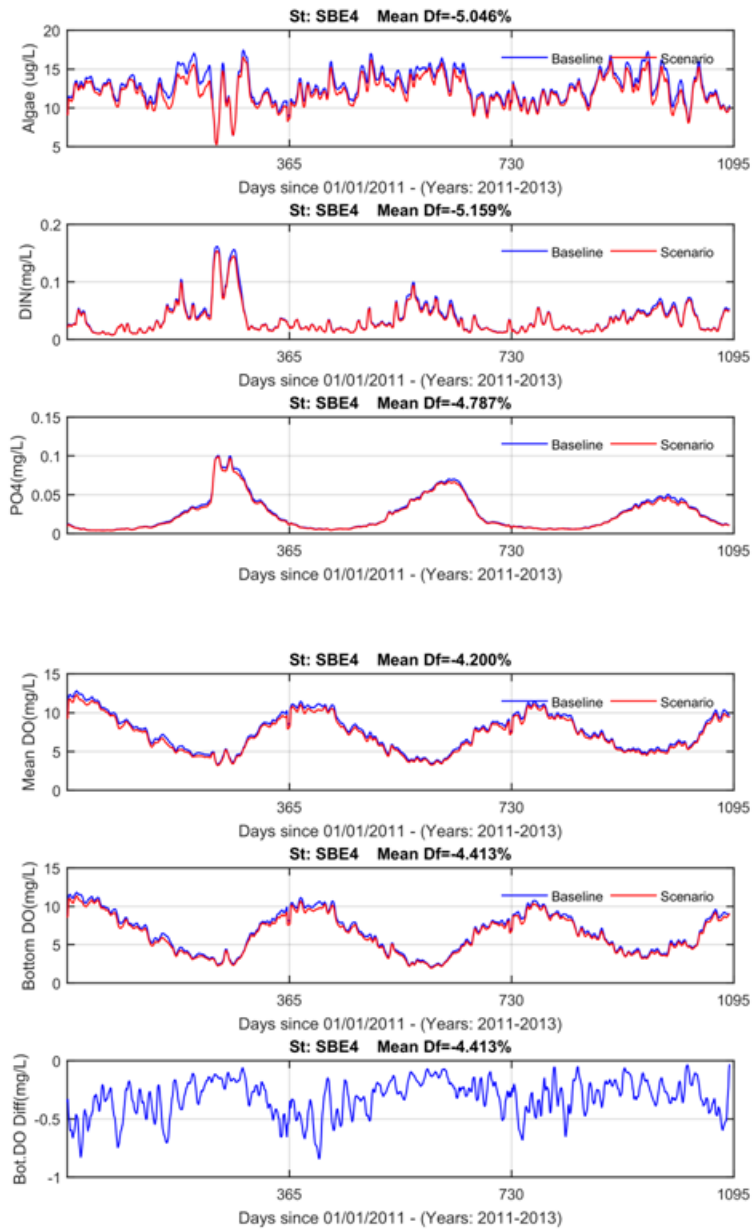


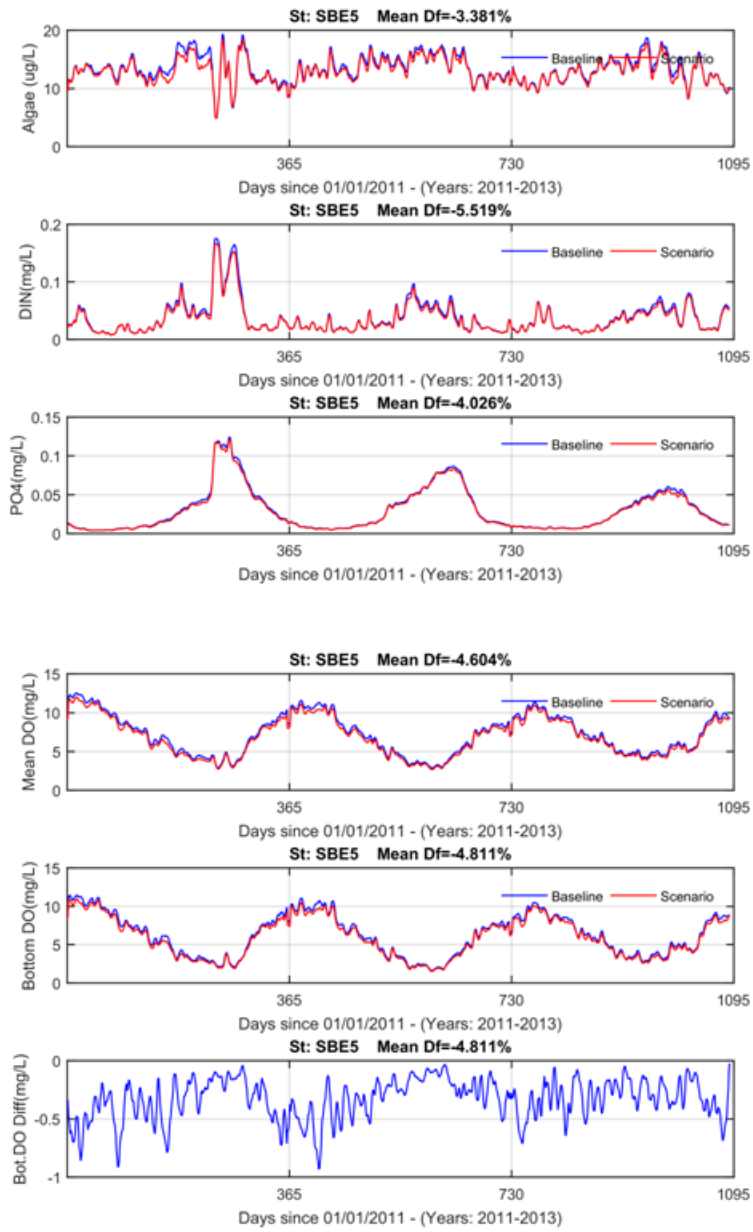


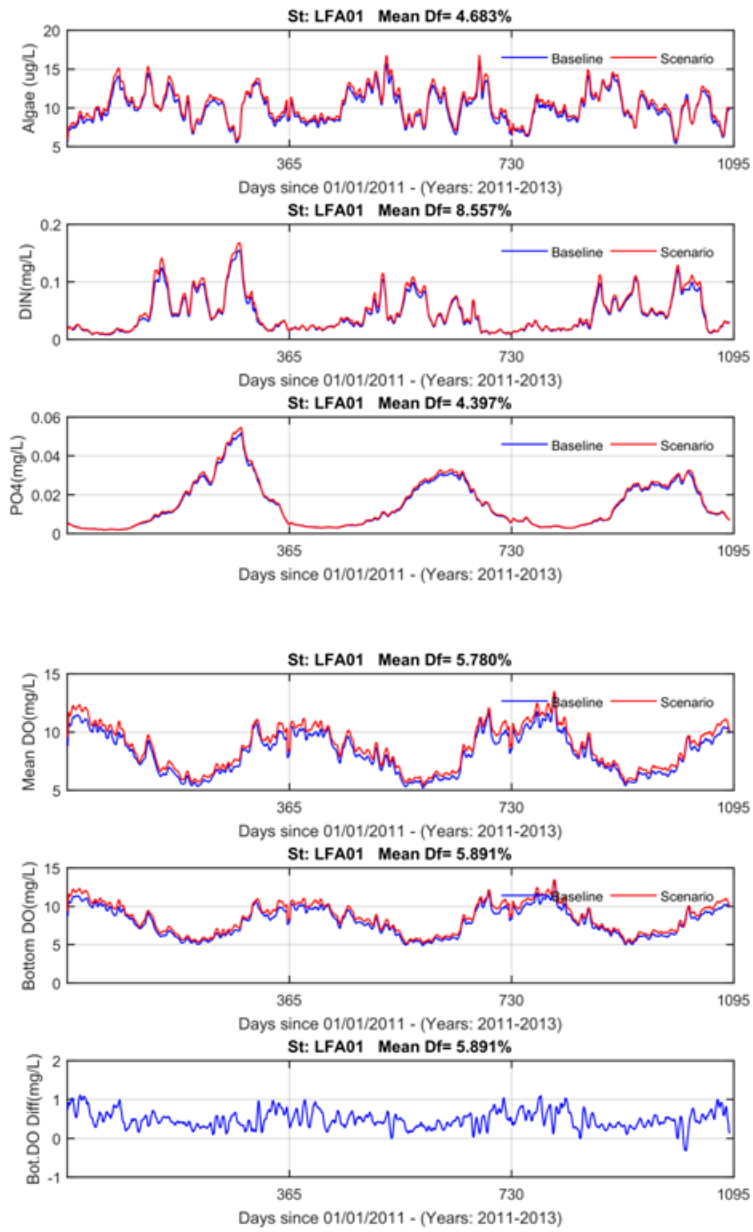


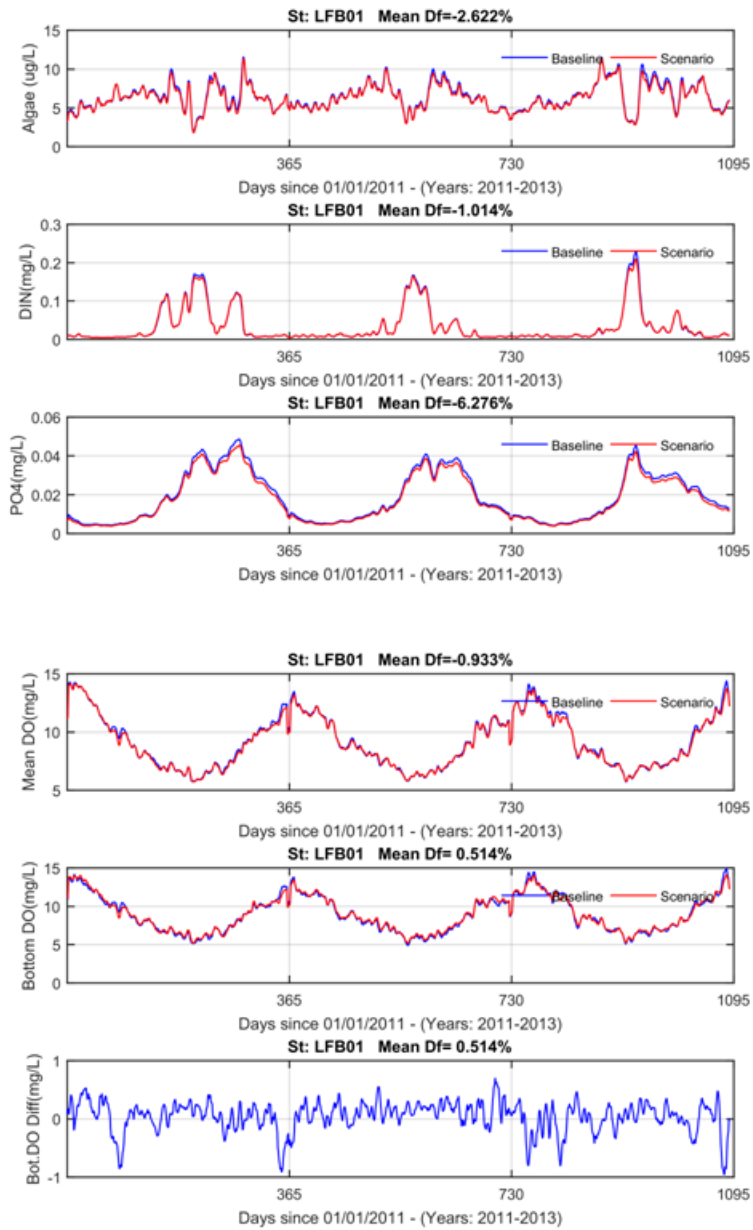


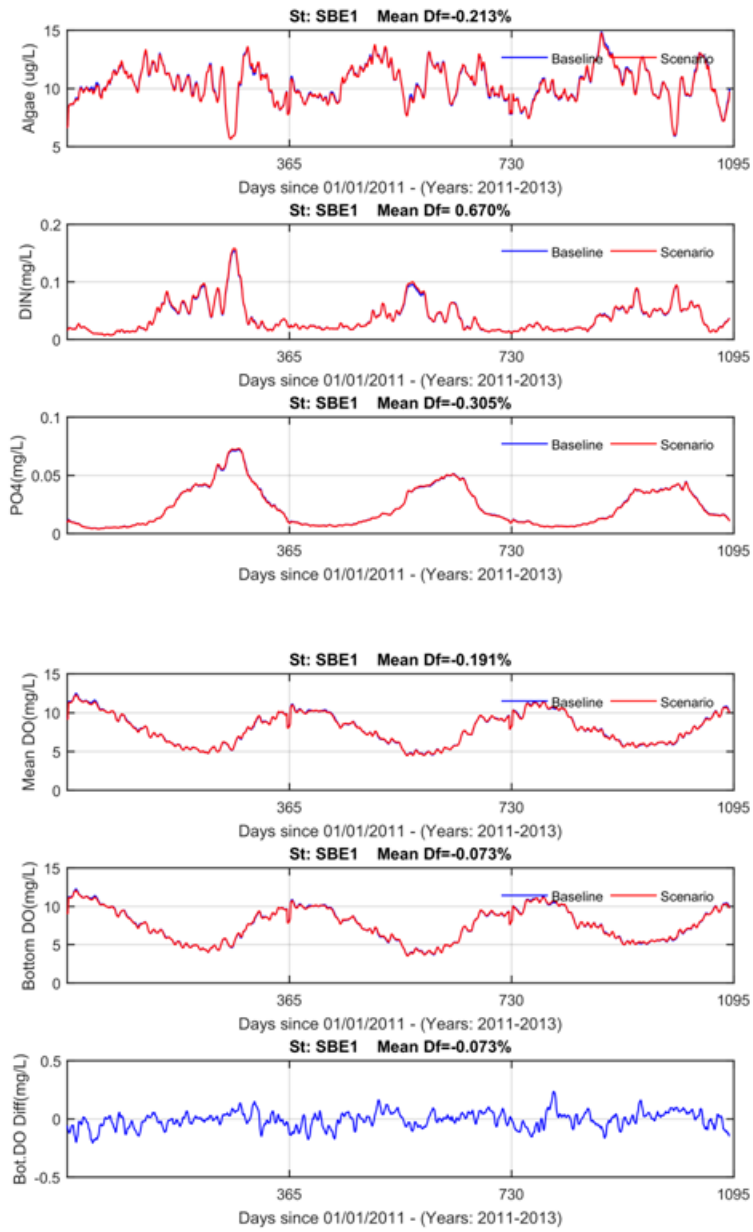


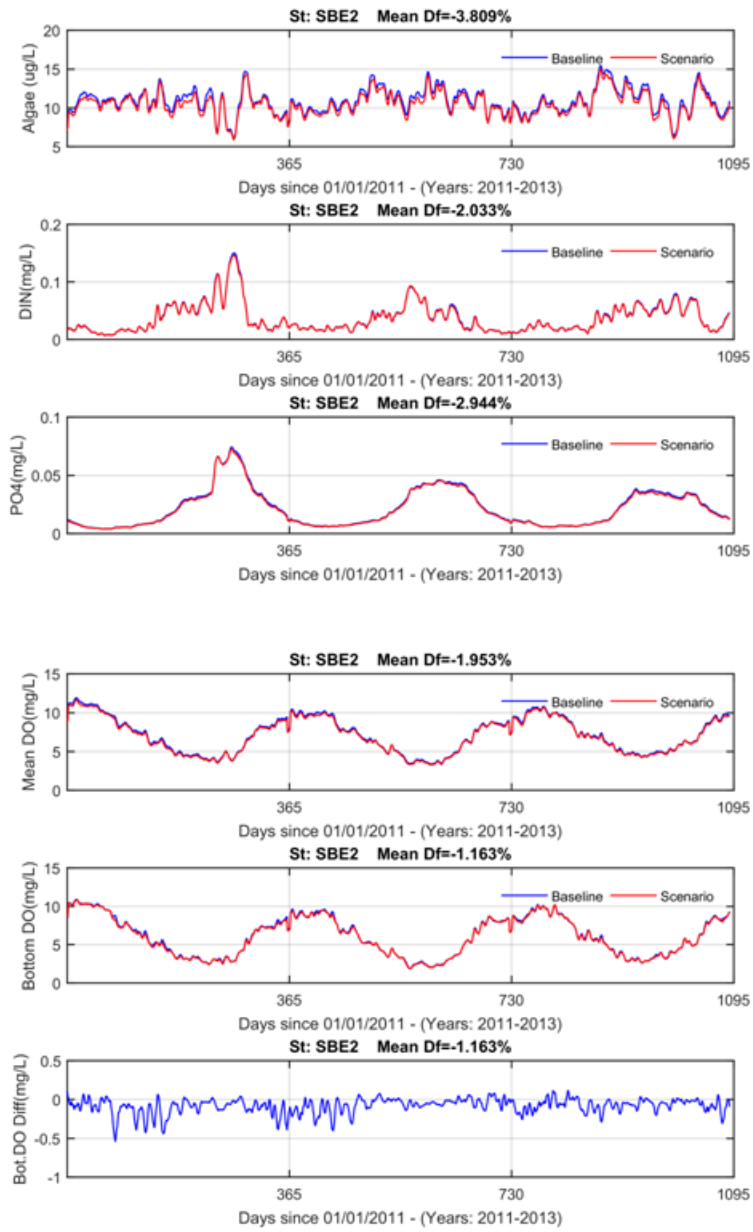


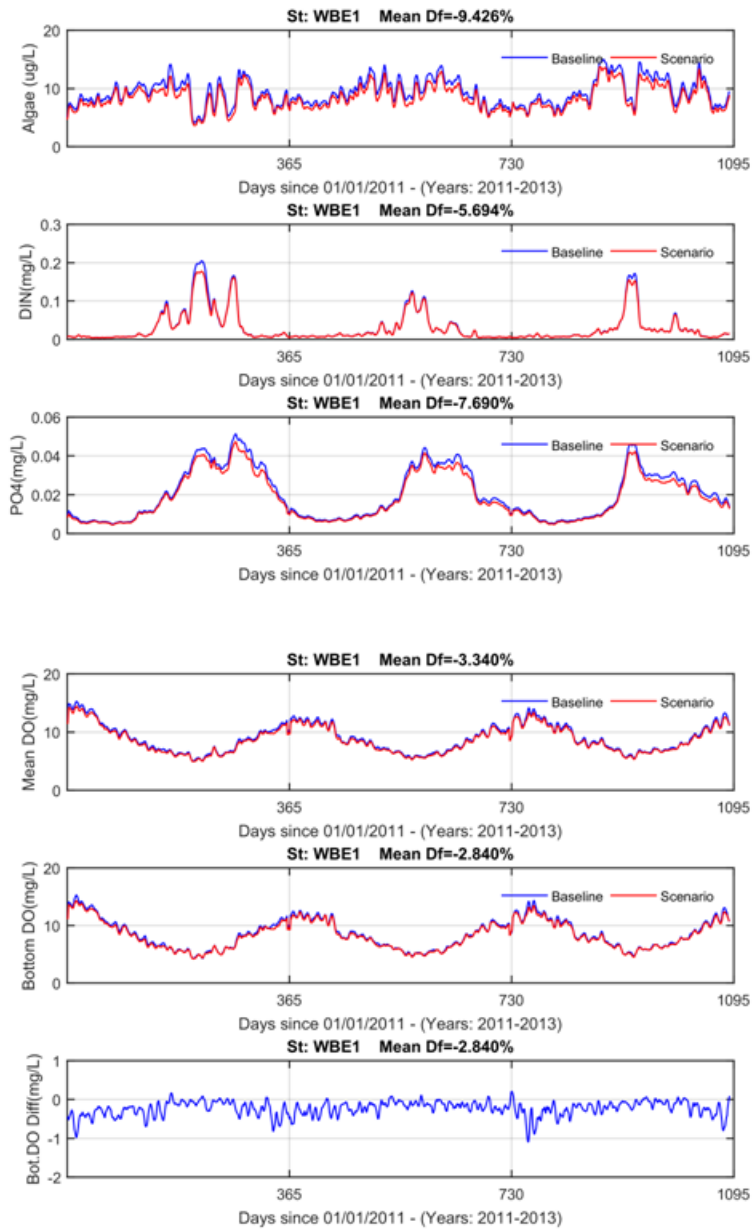






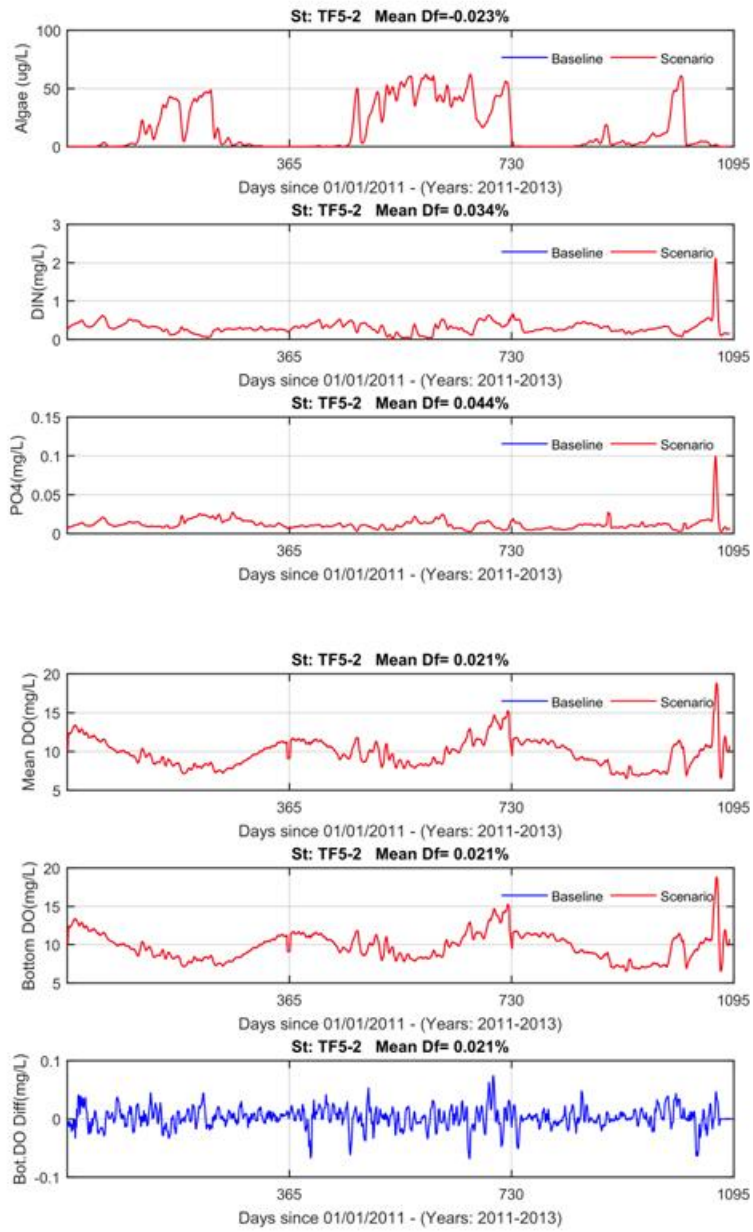


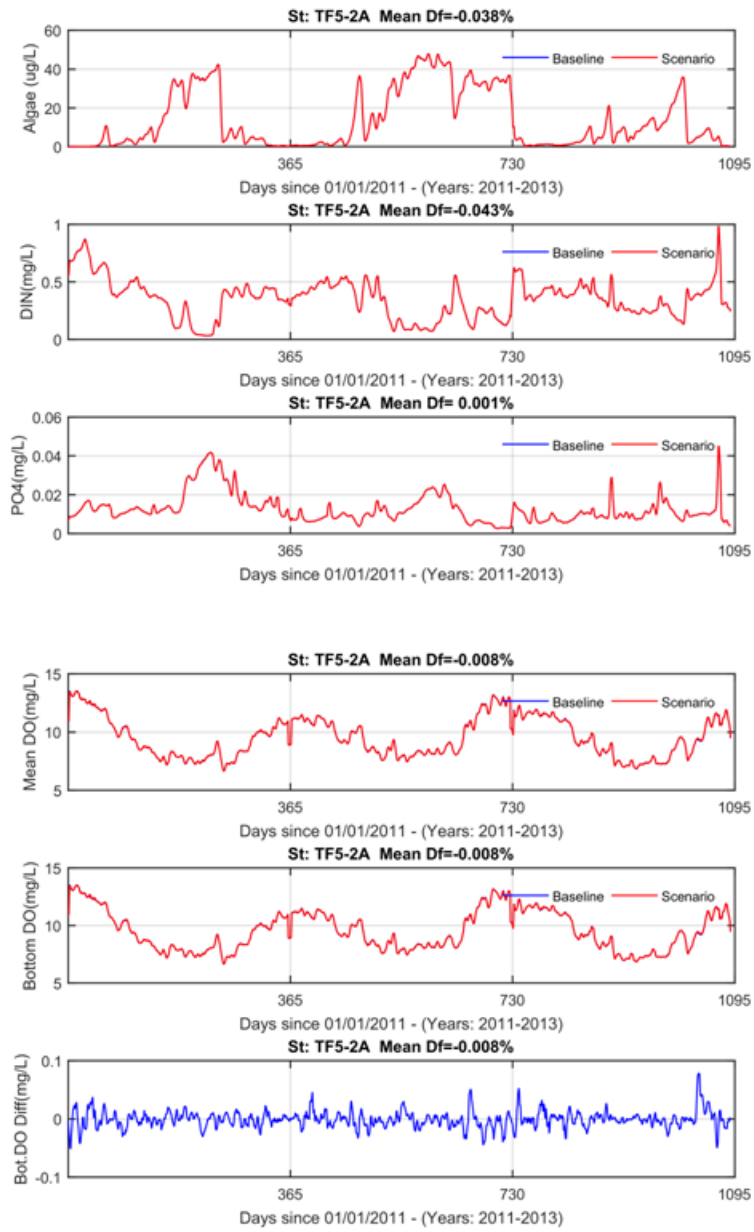


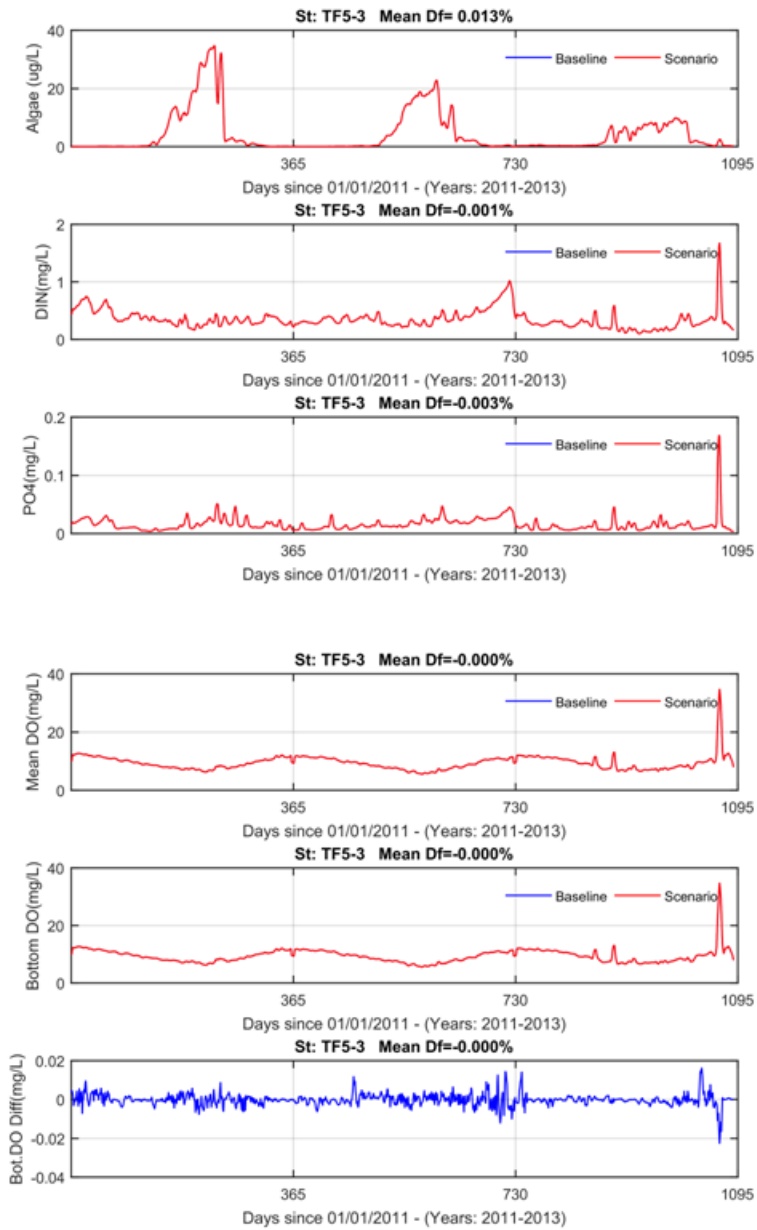


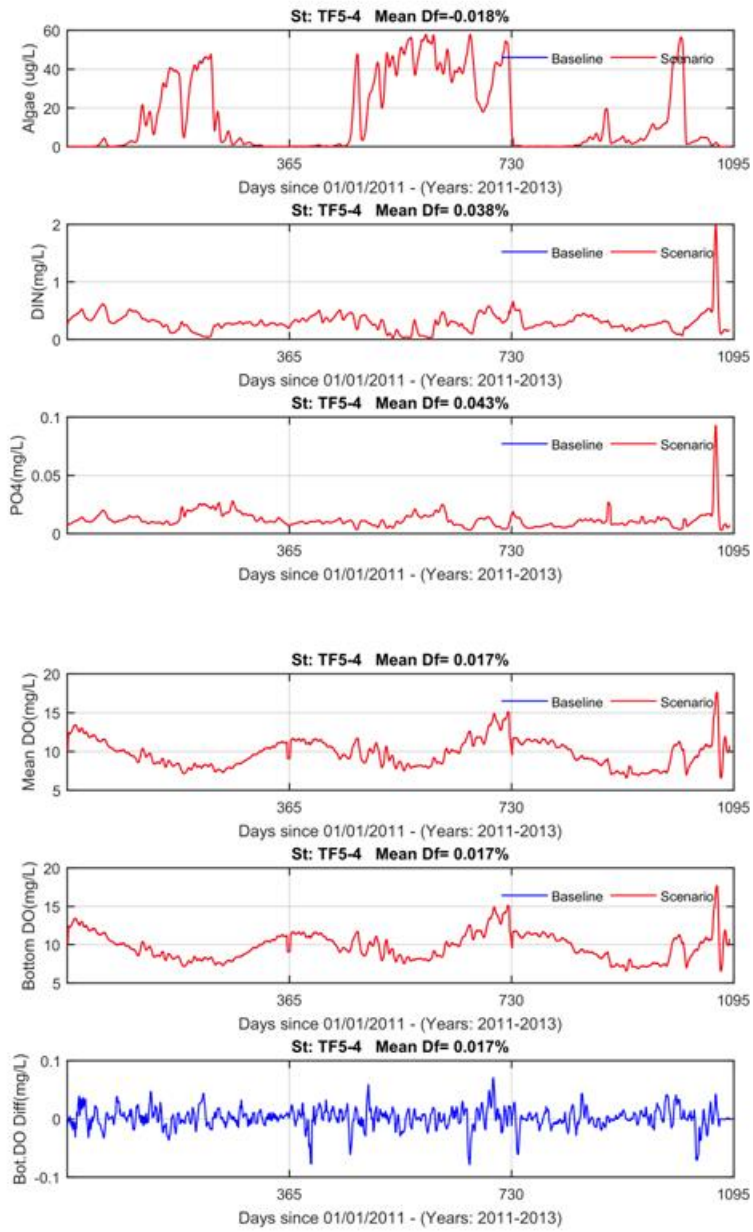
Model Simulation Baseline1 and Scenario 3-1

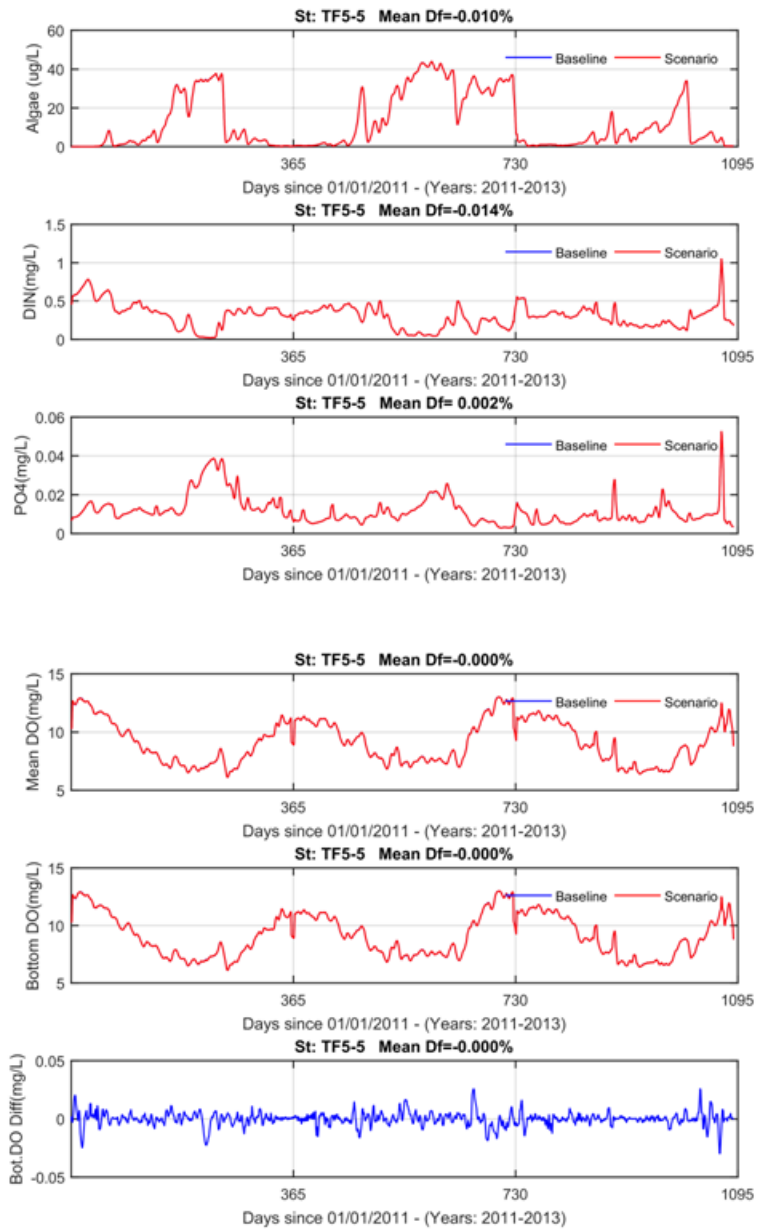
In the following plots. The Baseline is the results of baseline1 and Scenario is Scenario of 3-1.

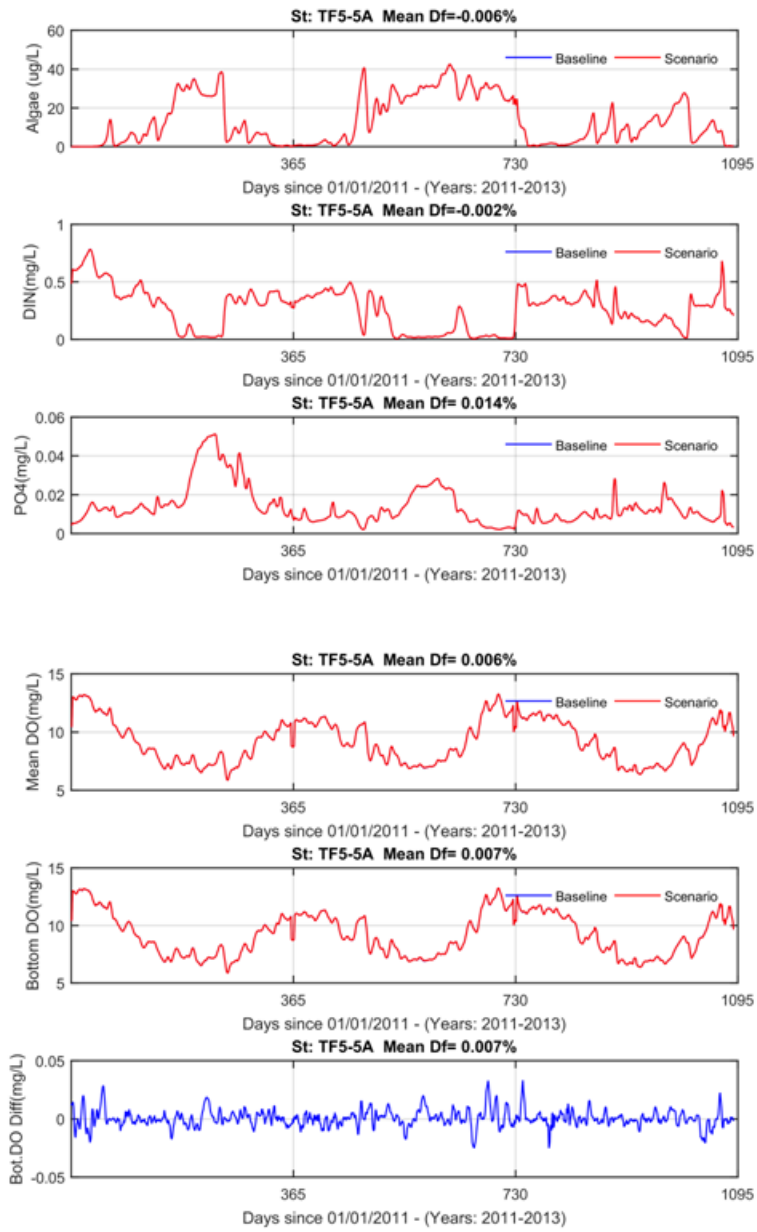


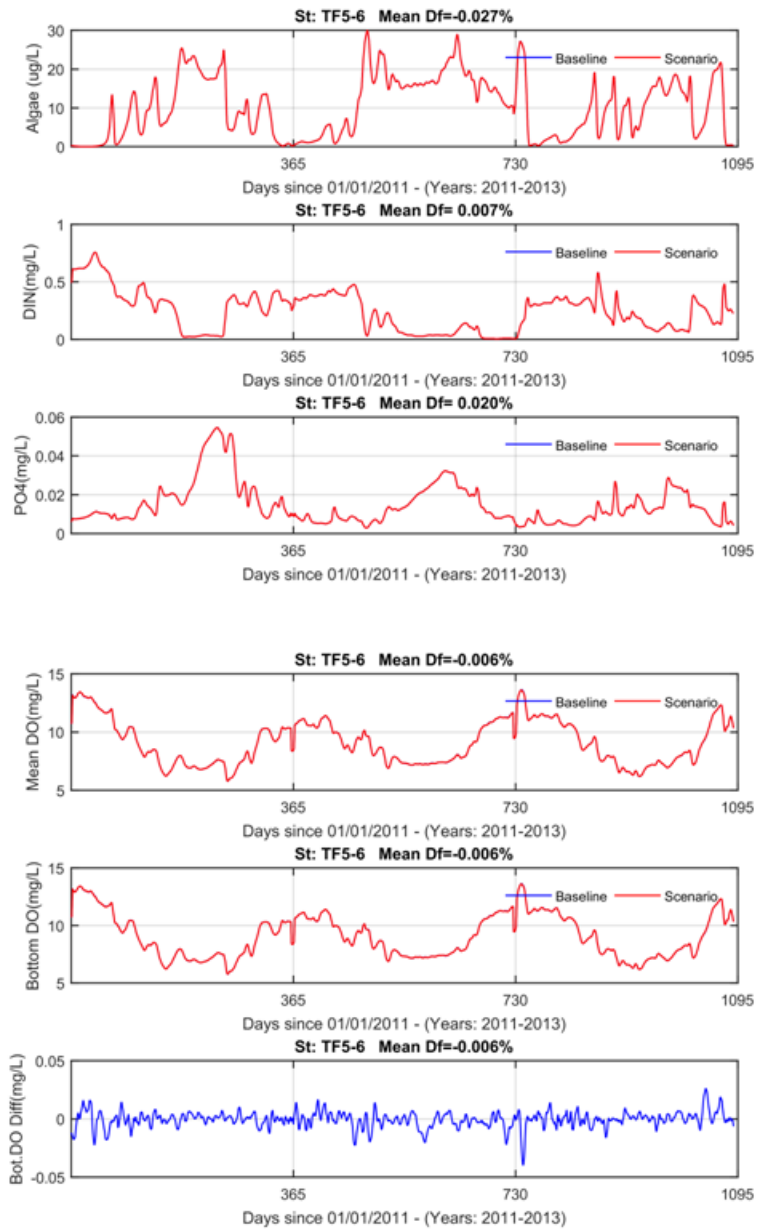


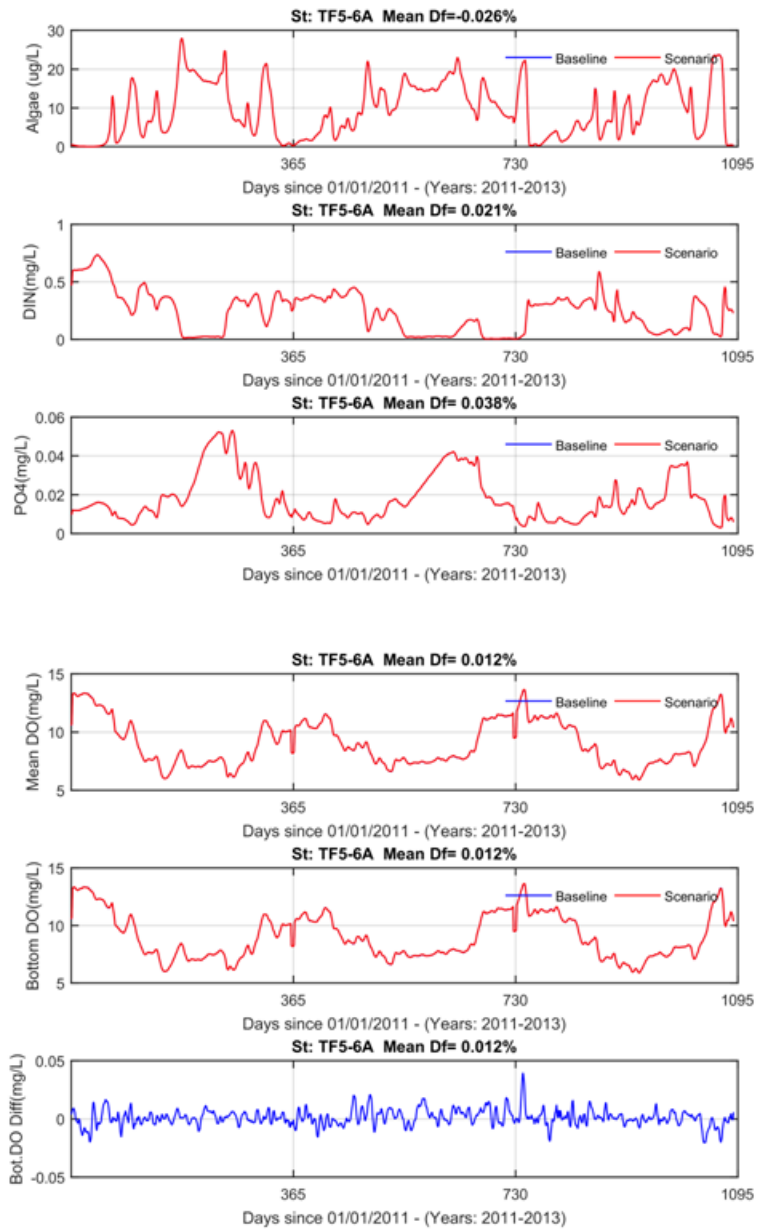


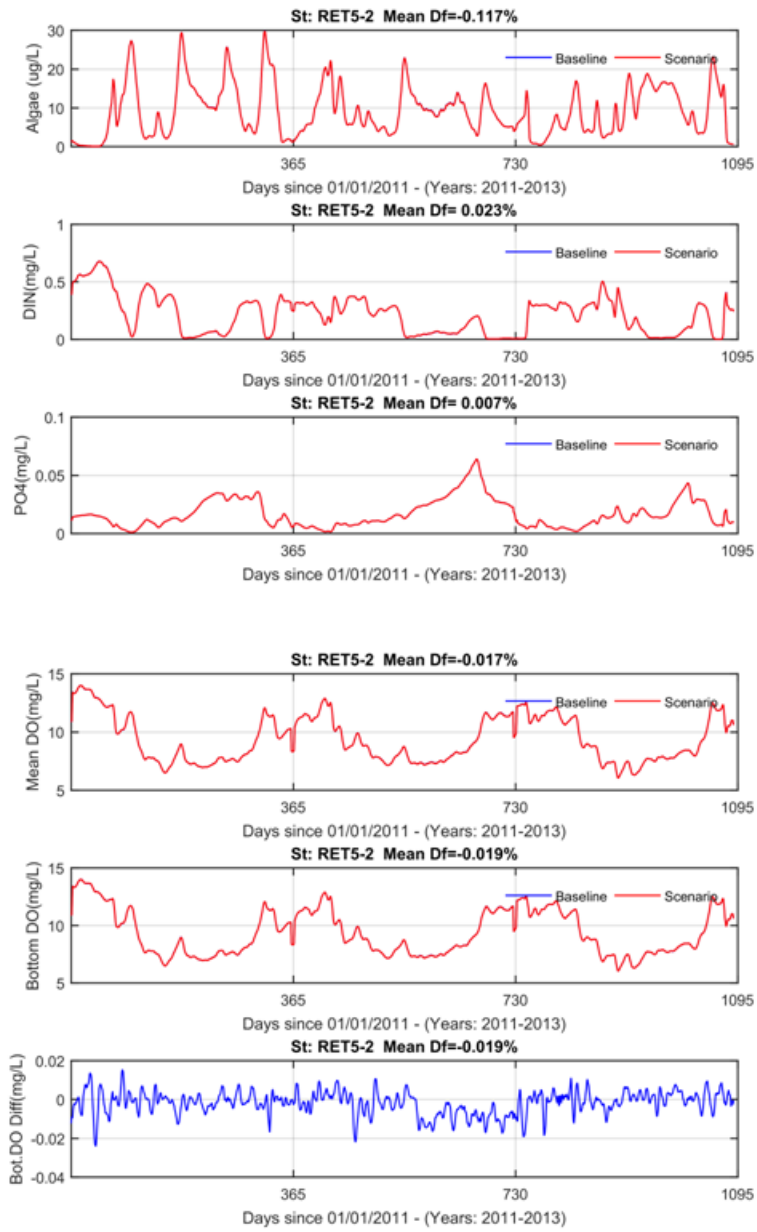


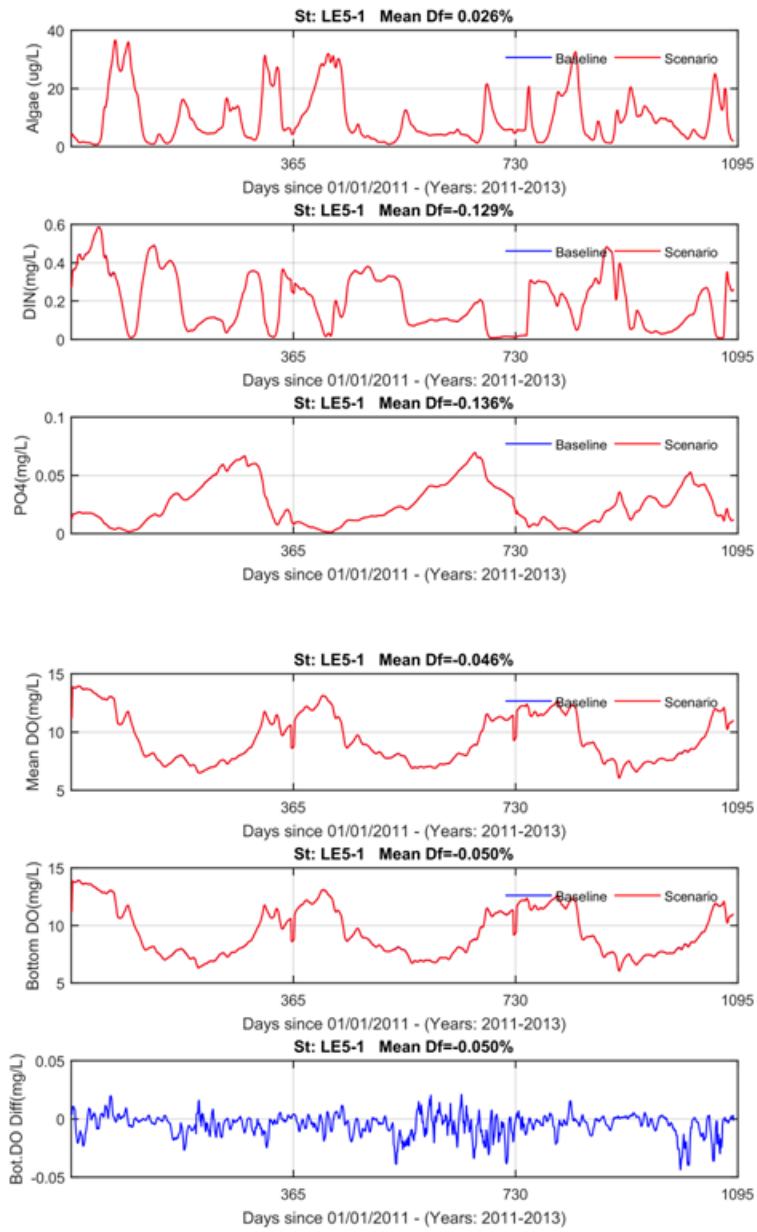


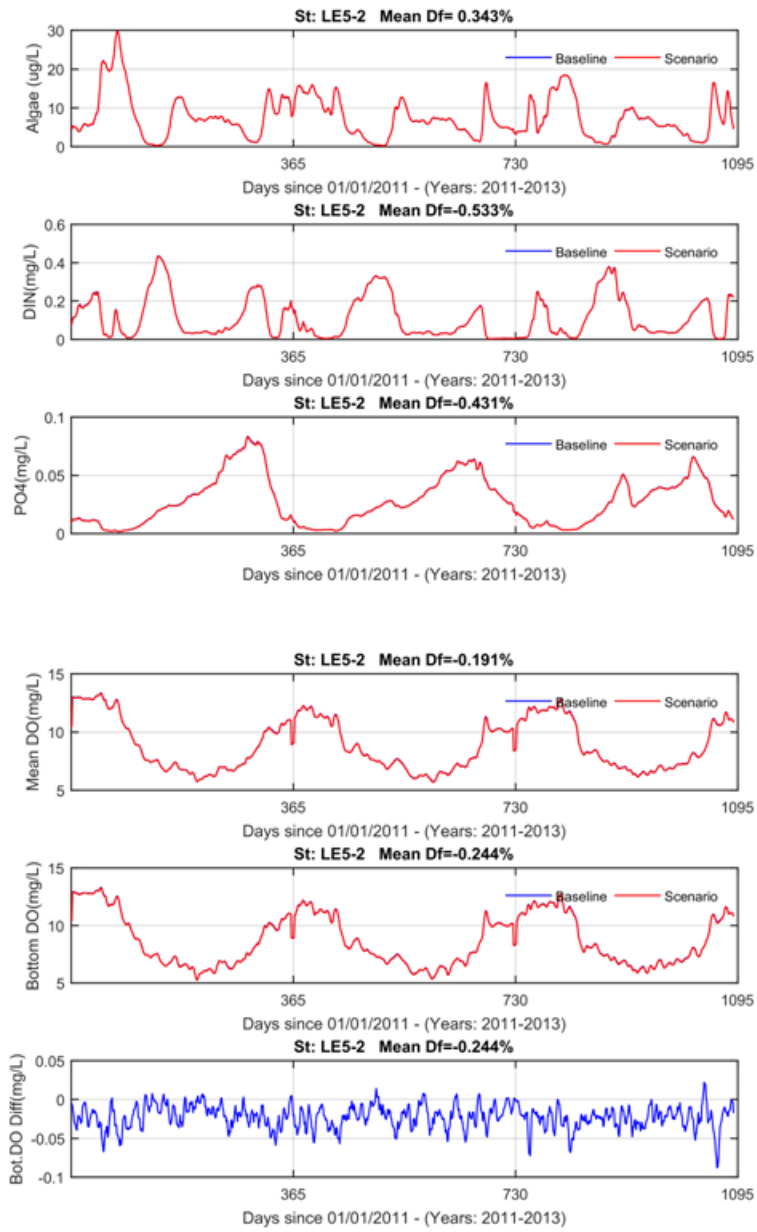


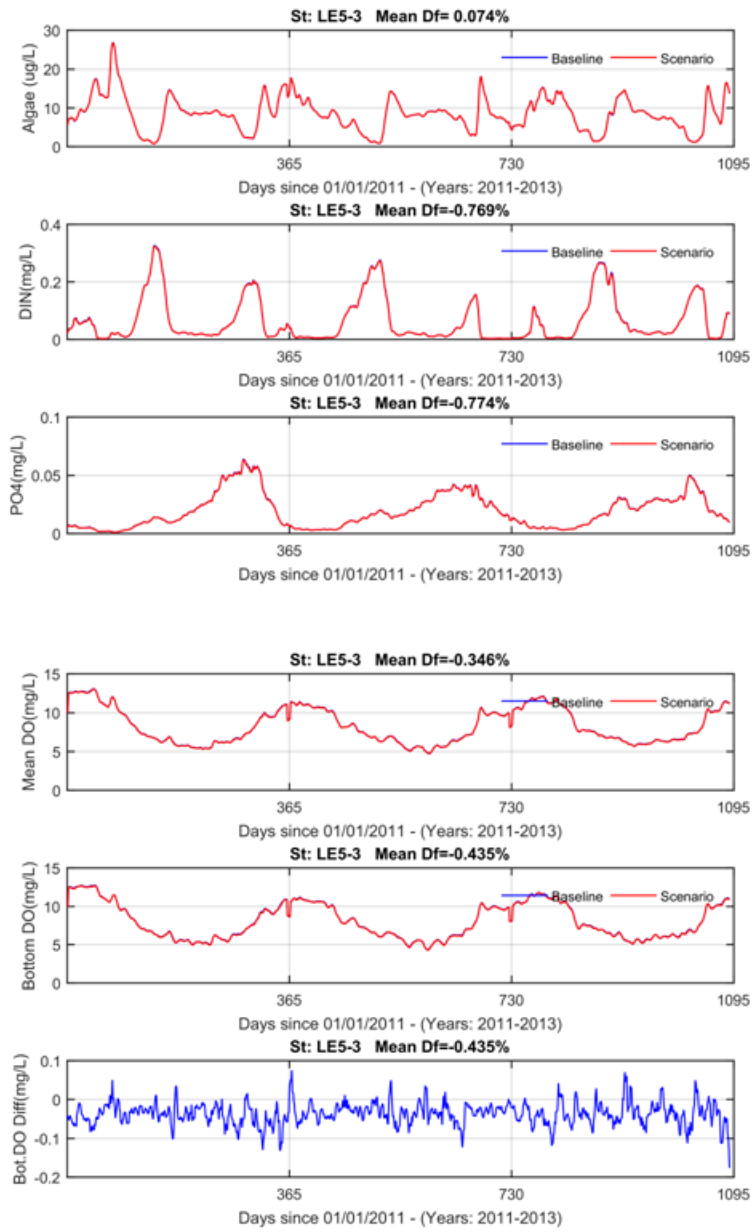


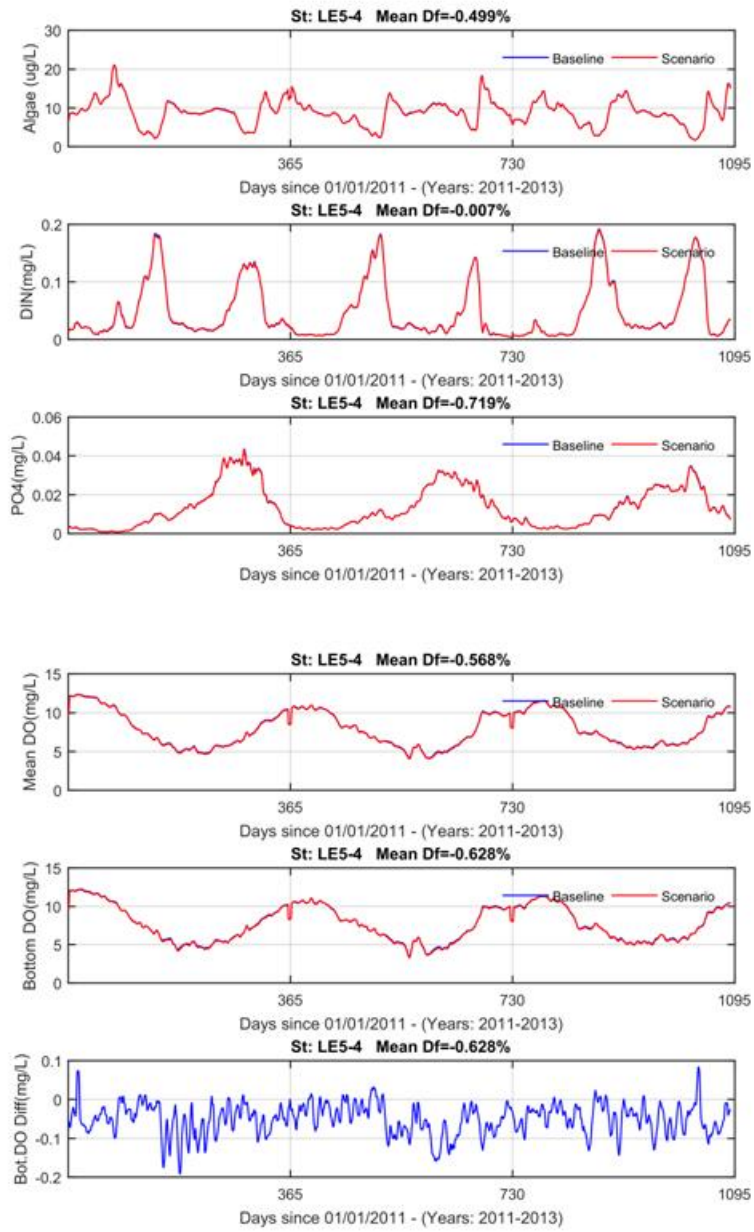


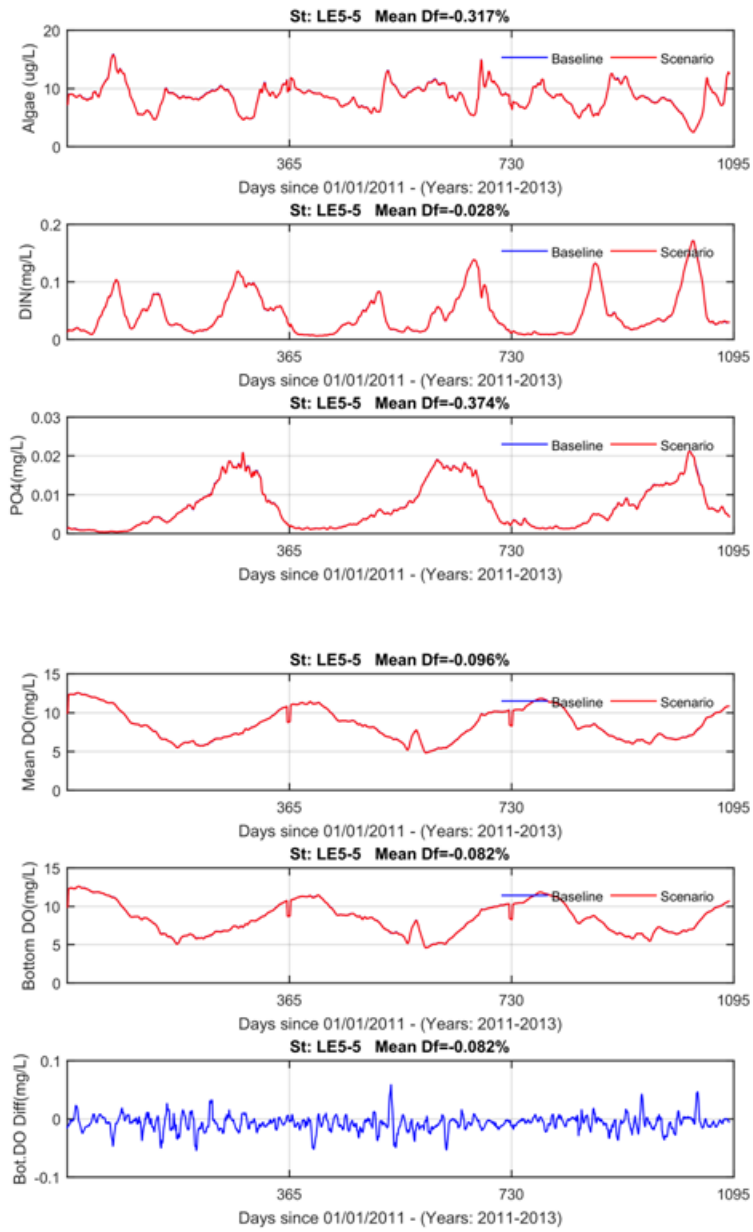


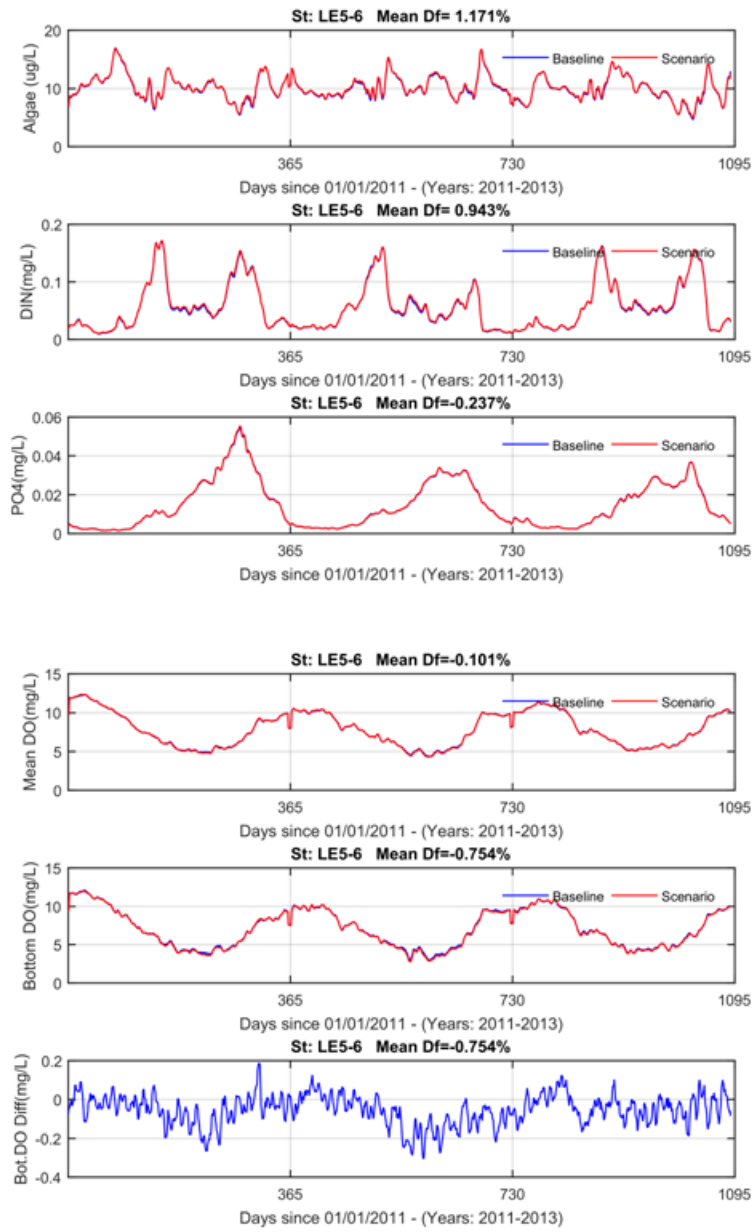


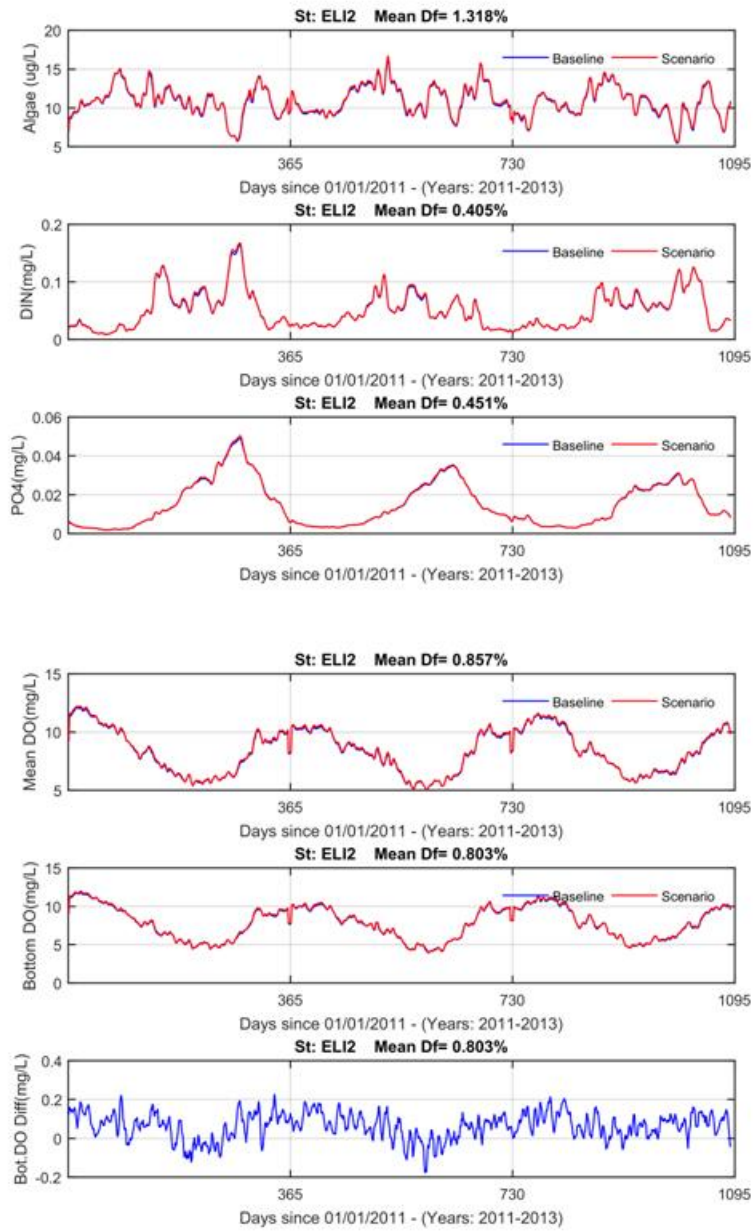


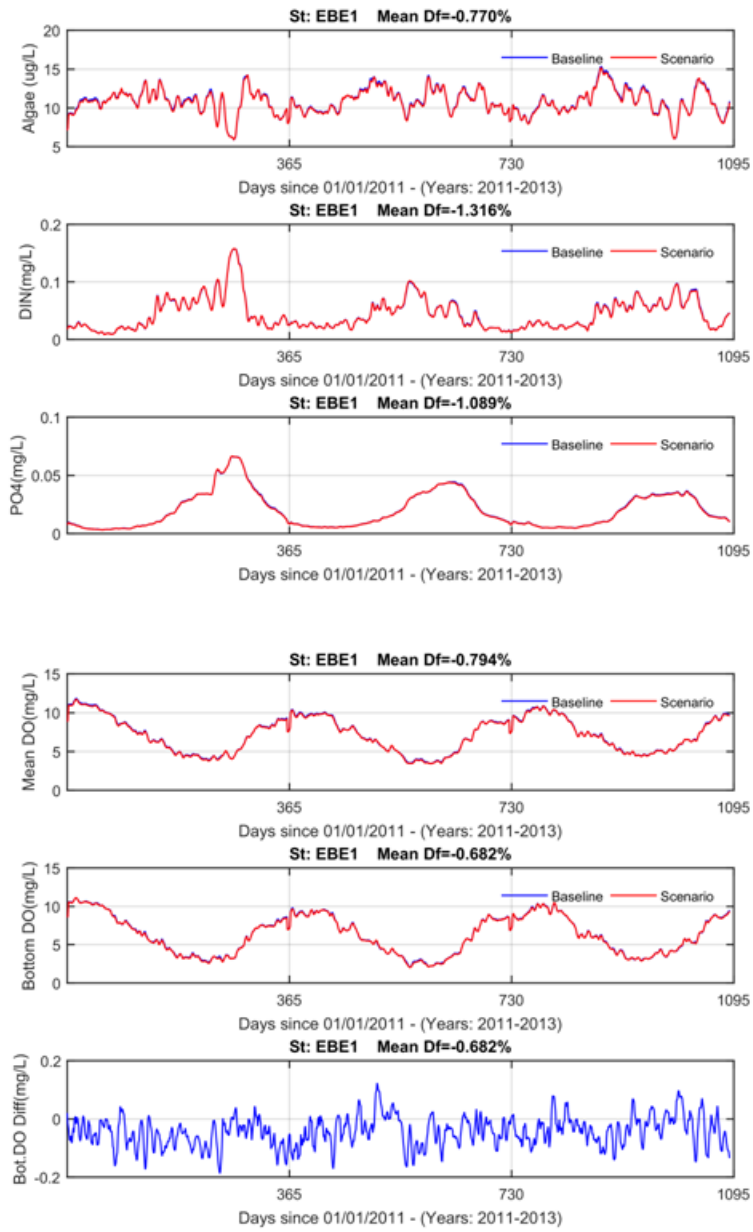


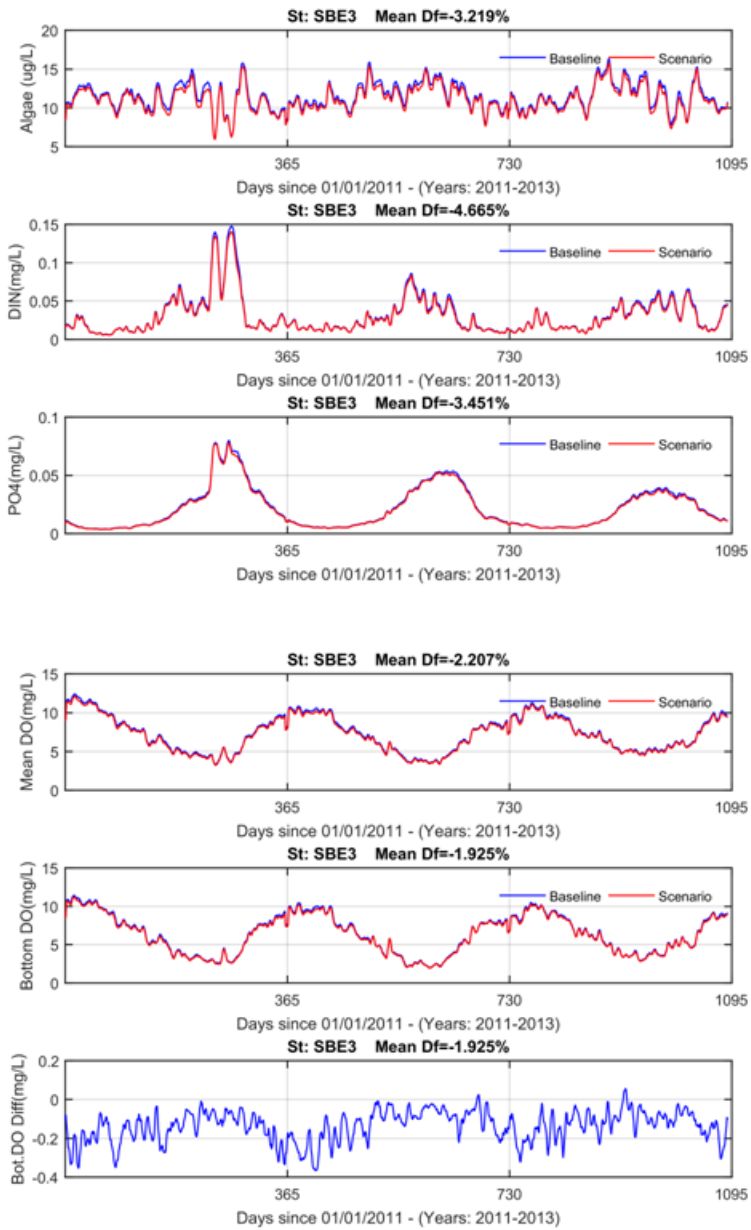


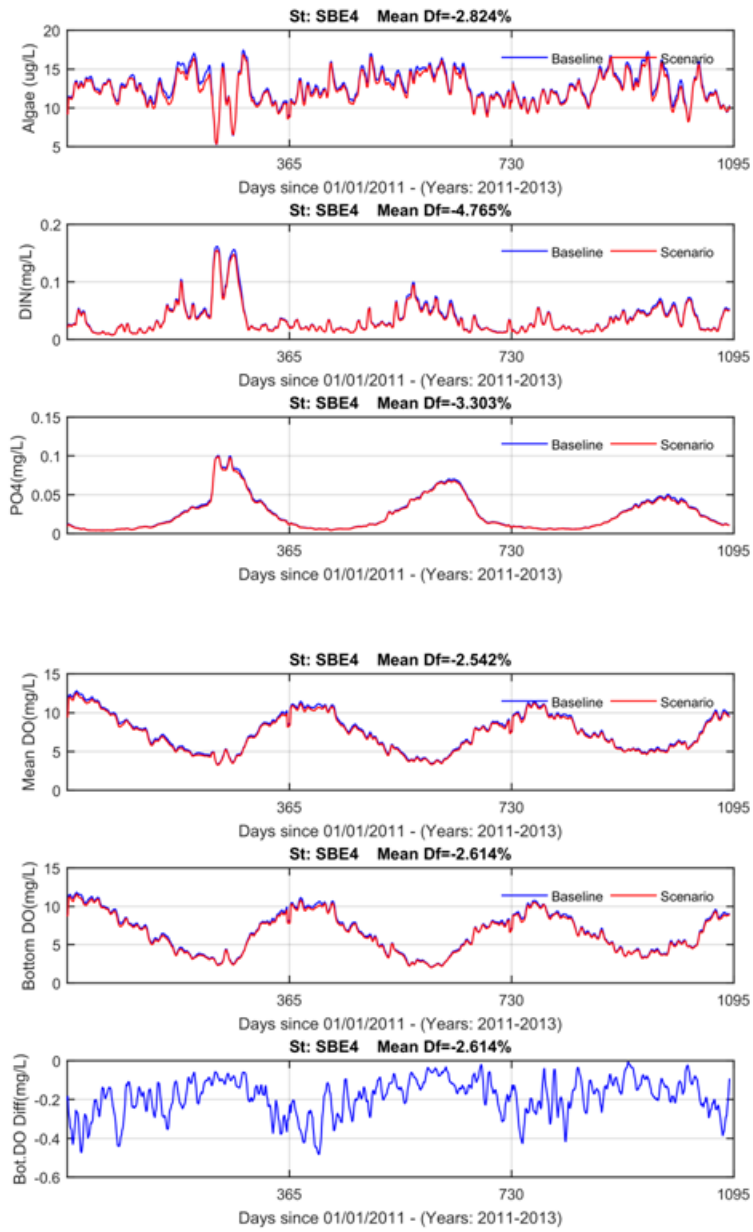


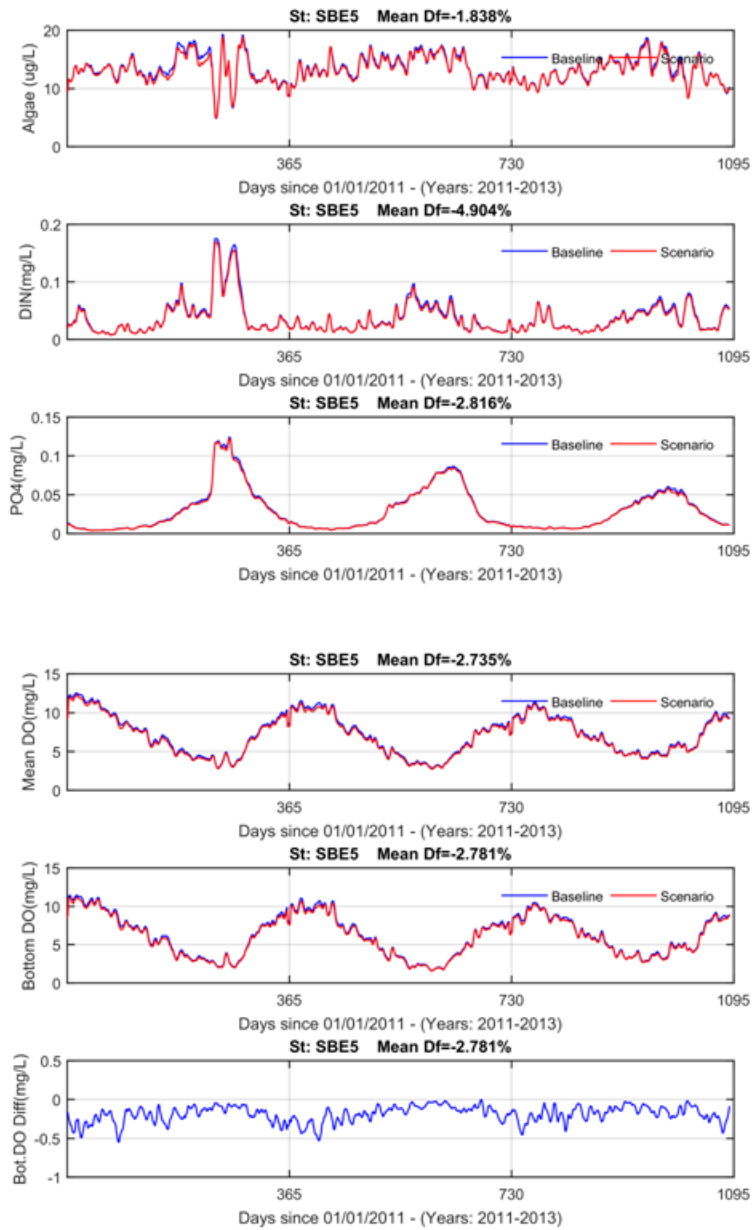


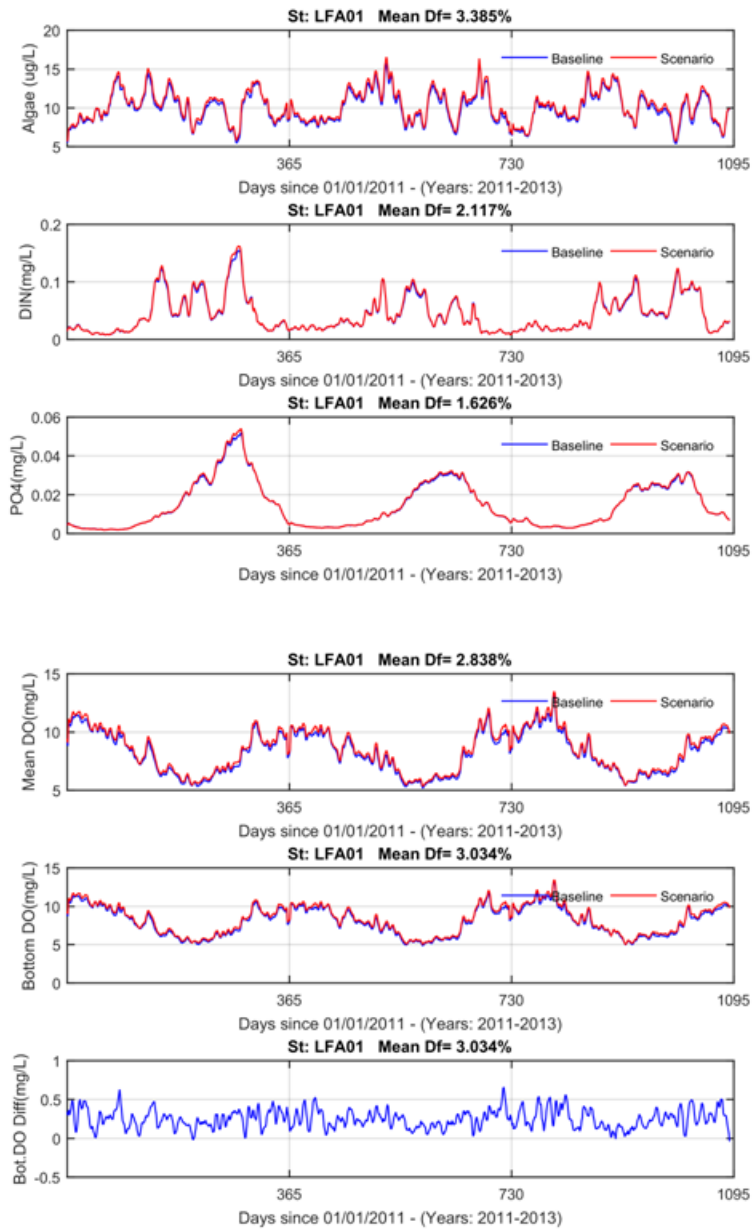


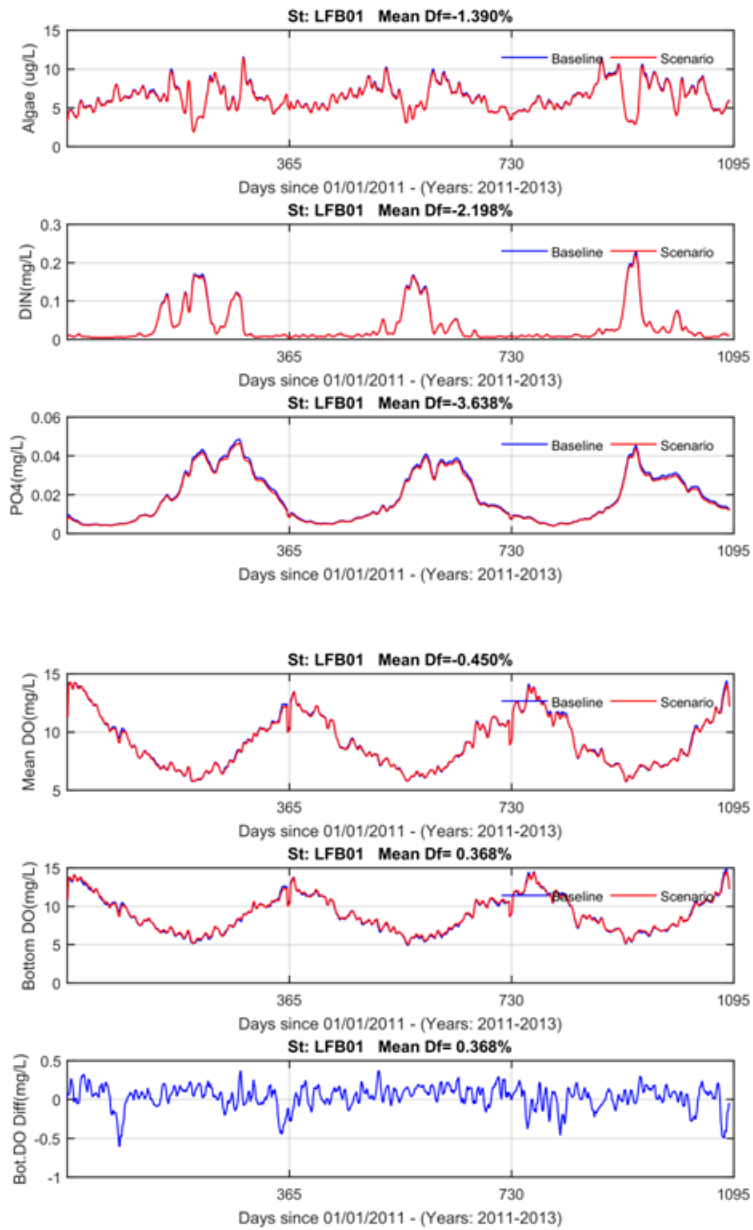


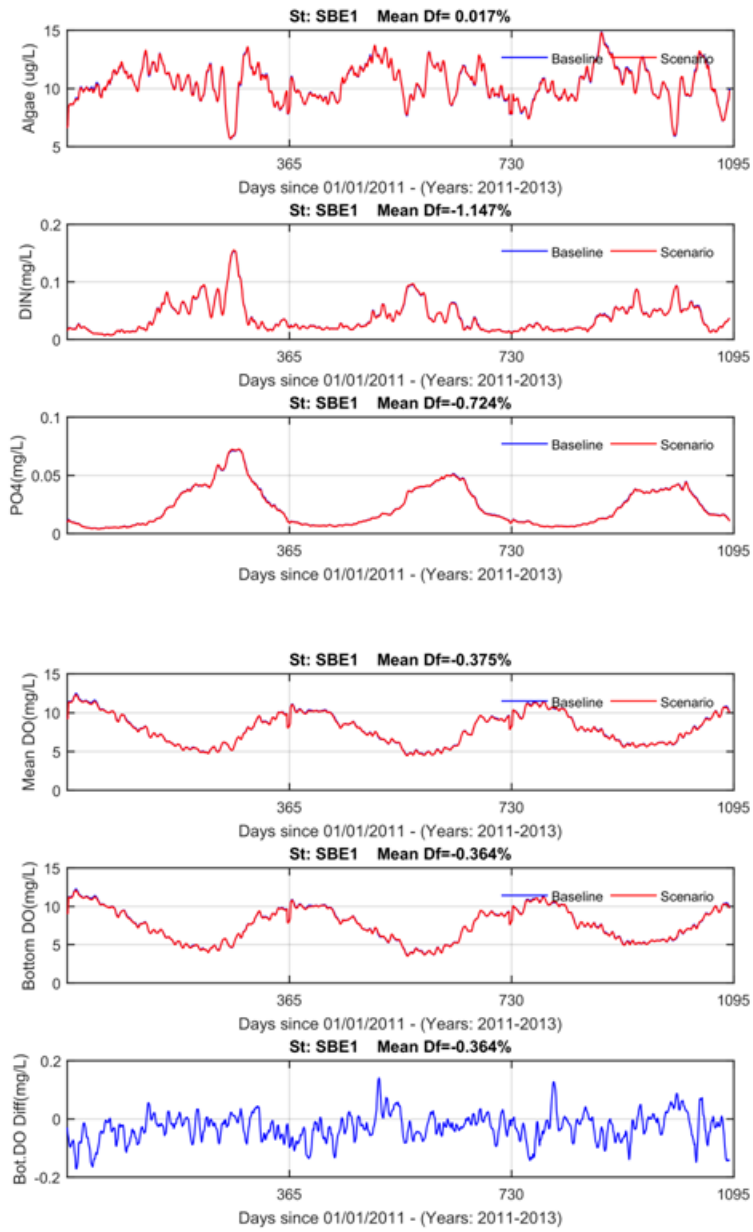


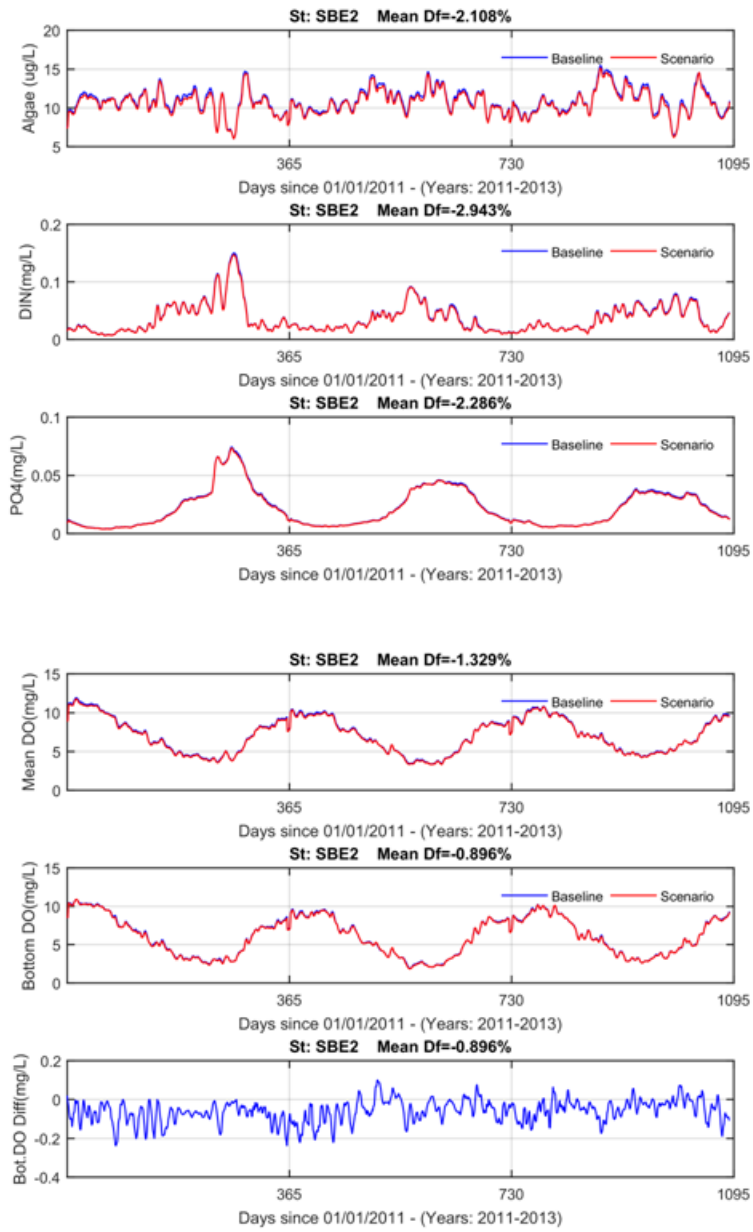


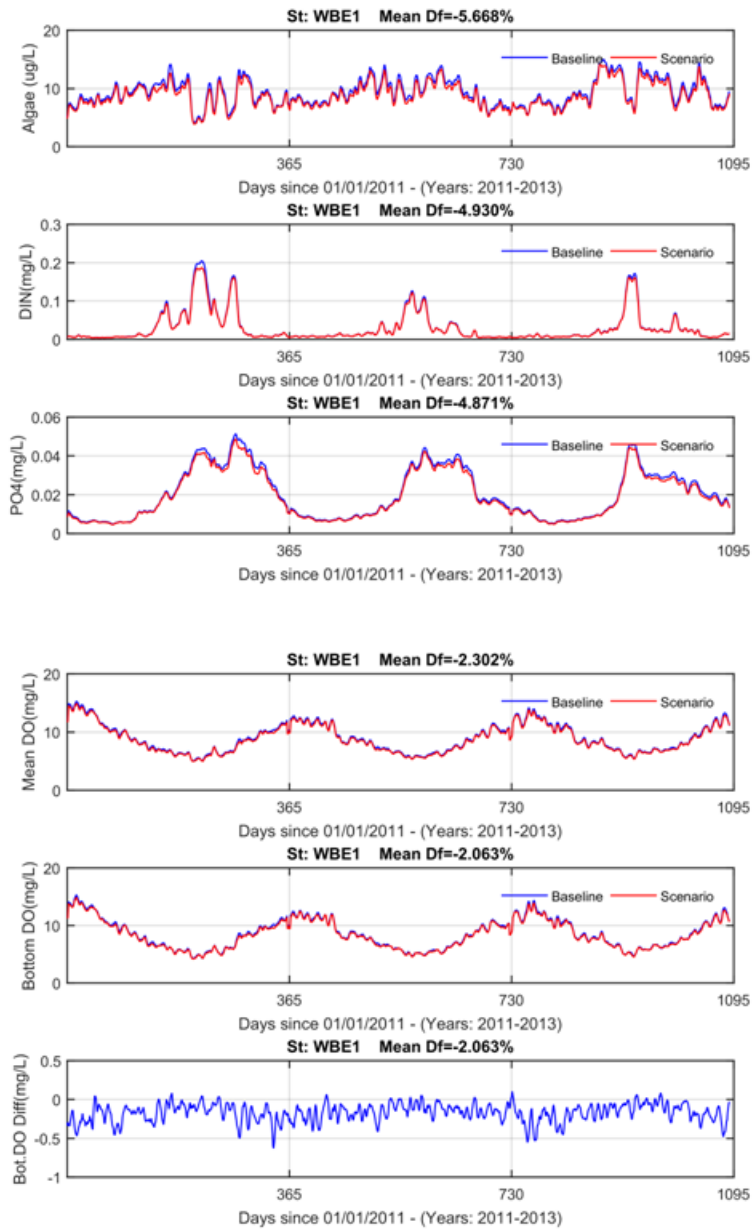






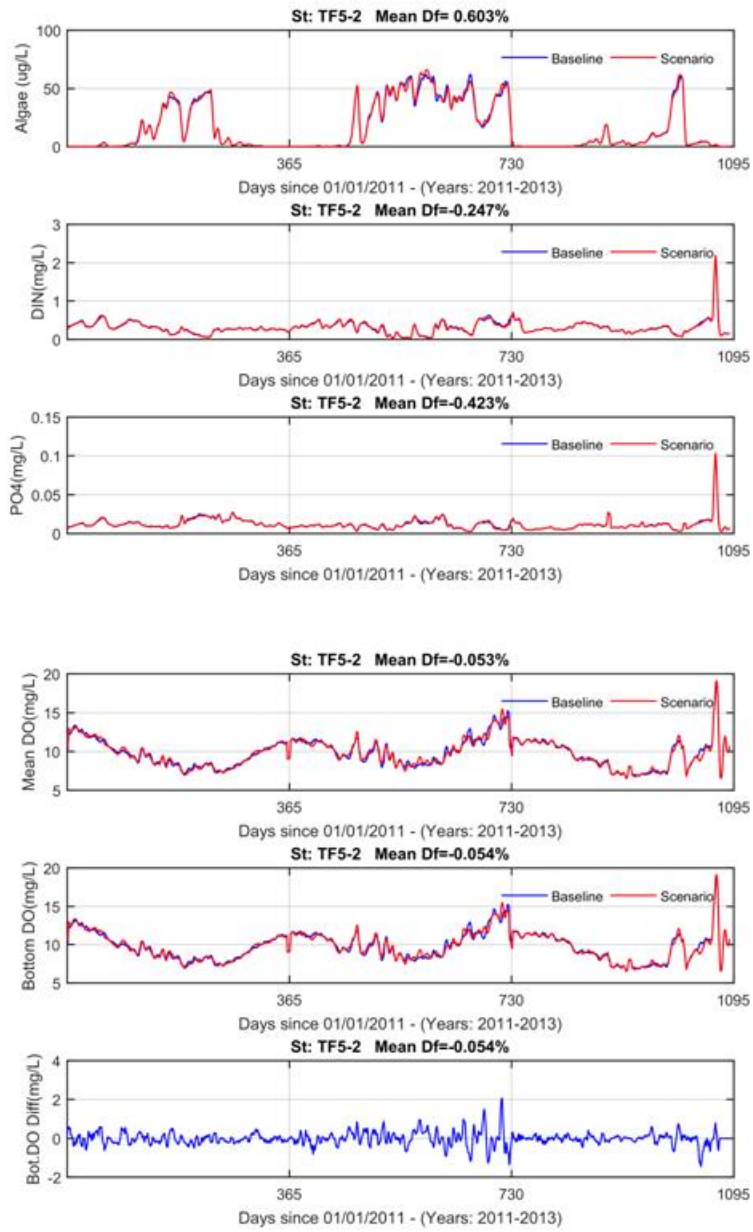


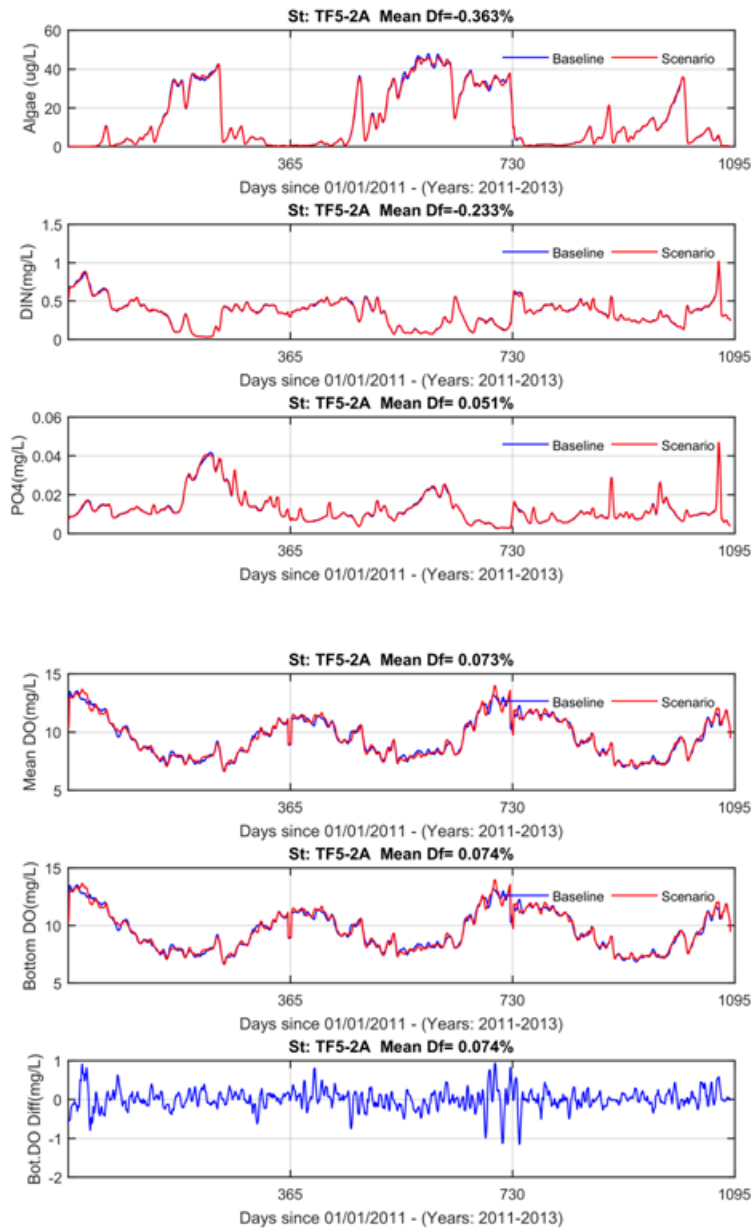


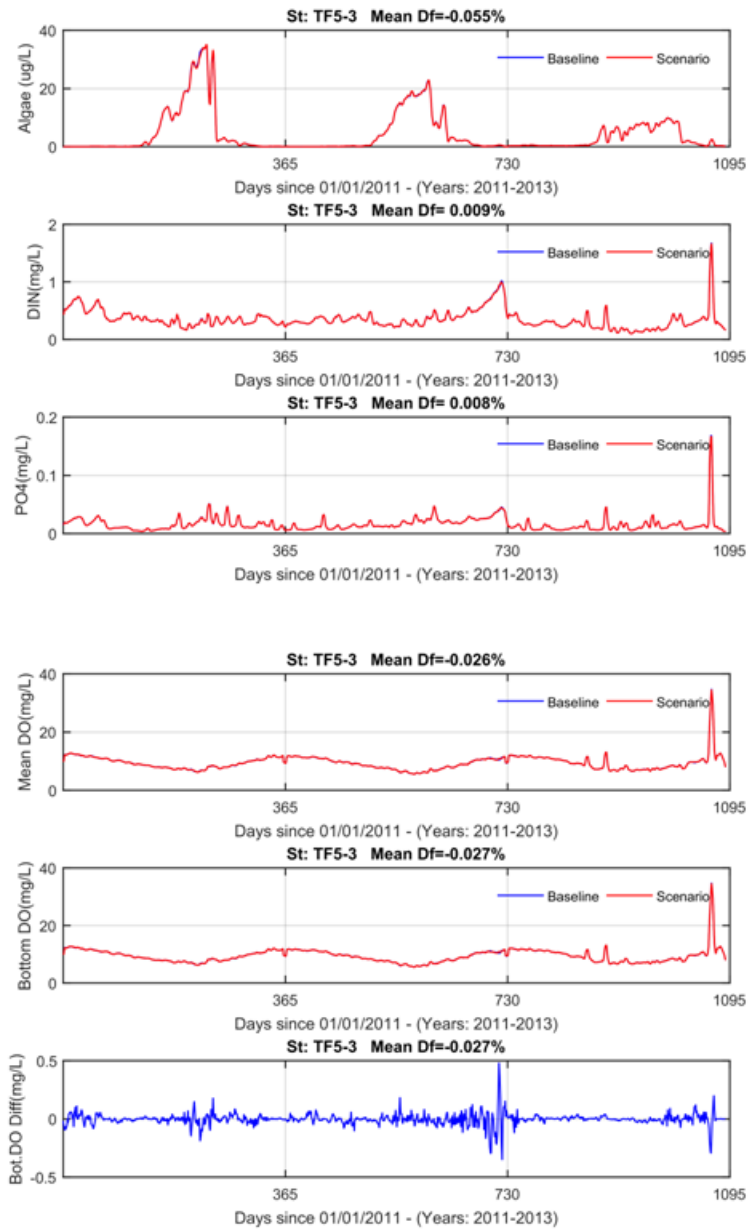


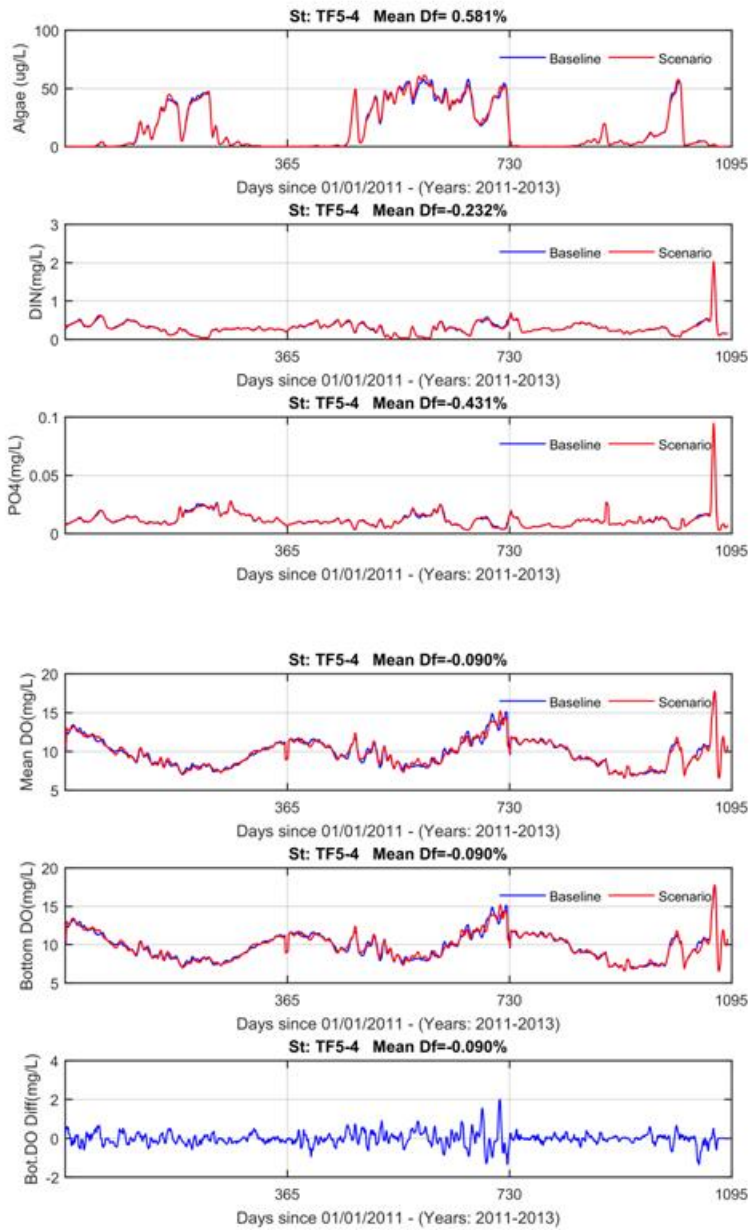
Model Simulation Baseline1 and Scenario 4-1

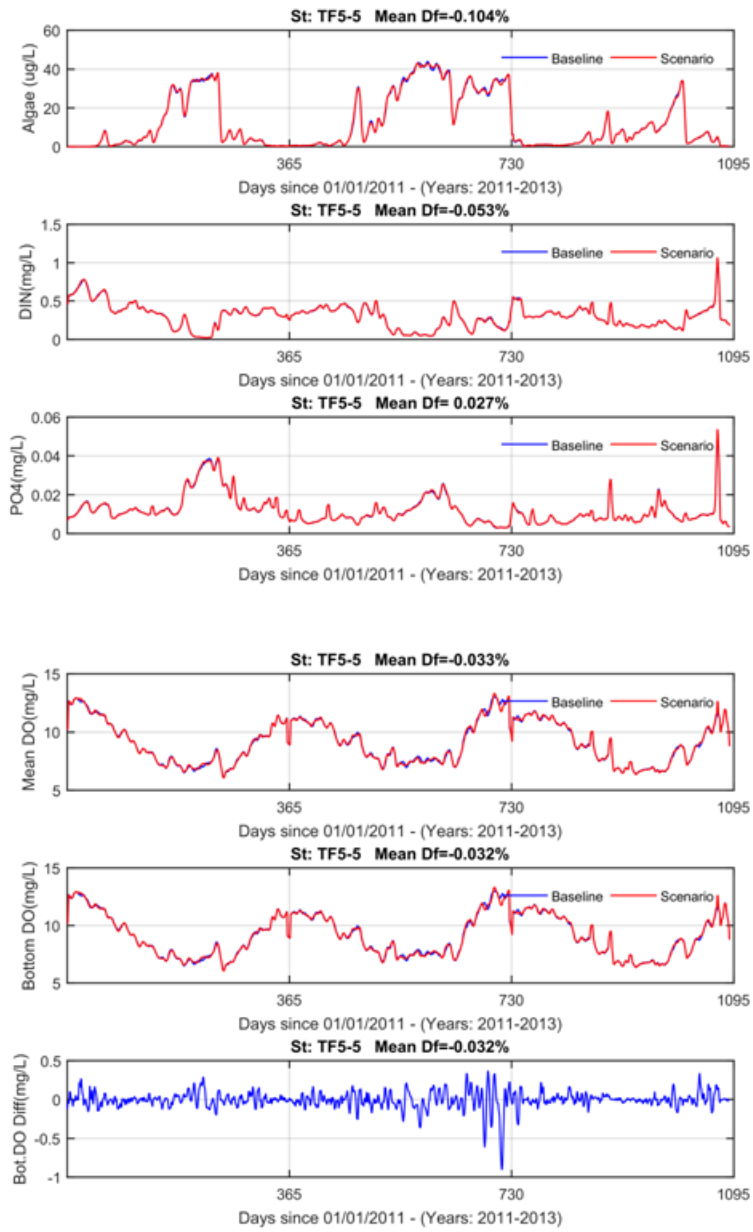
In the following plots. The Baseline is the results of baseline1 and Scenario is Scenario of 4-1.

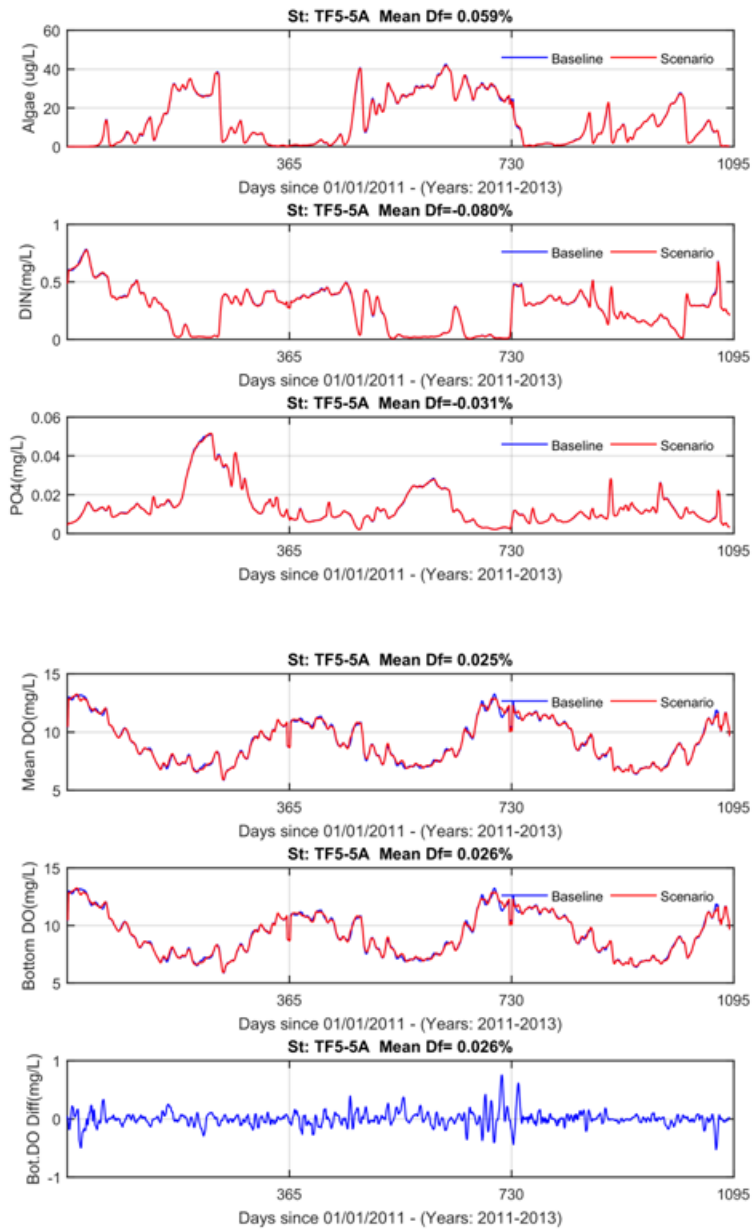


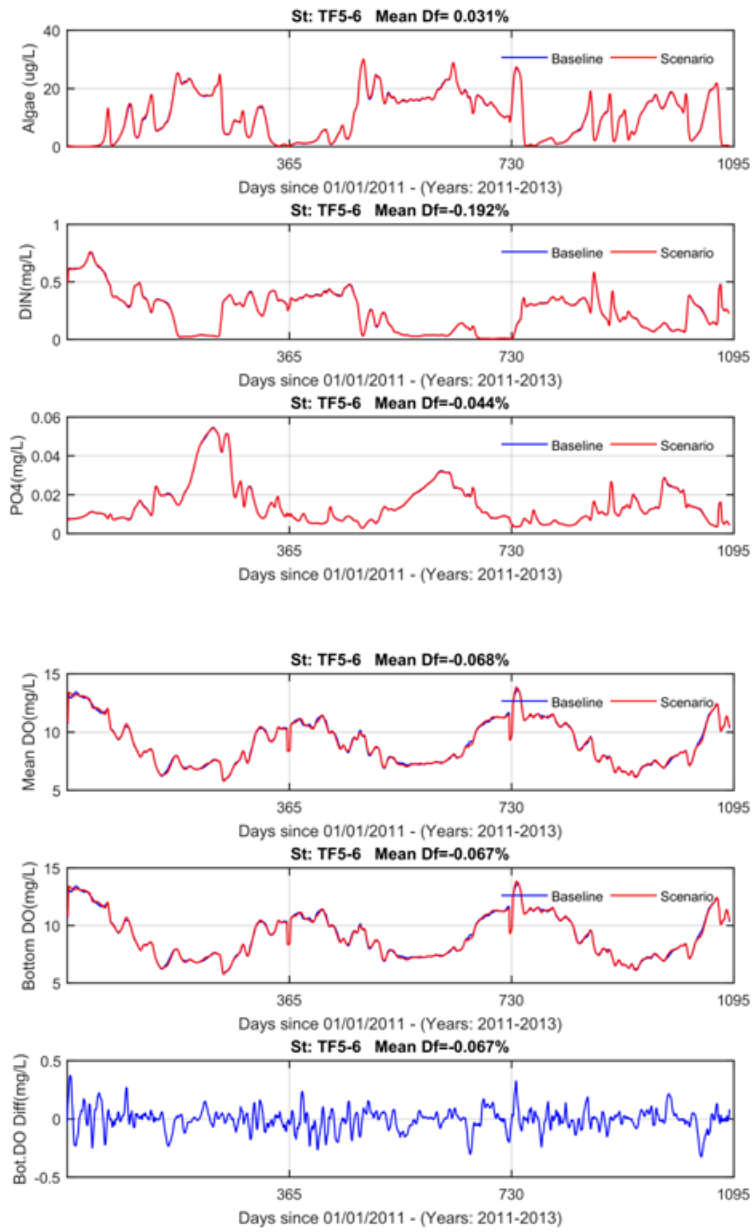


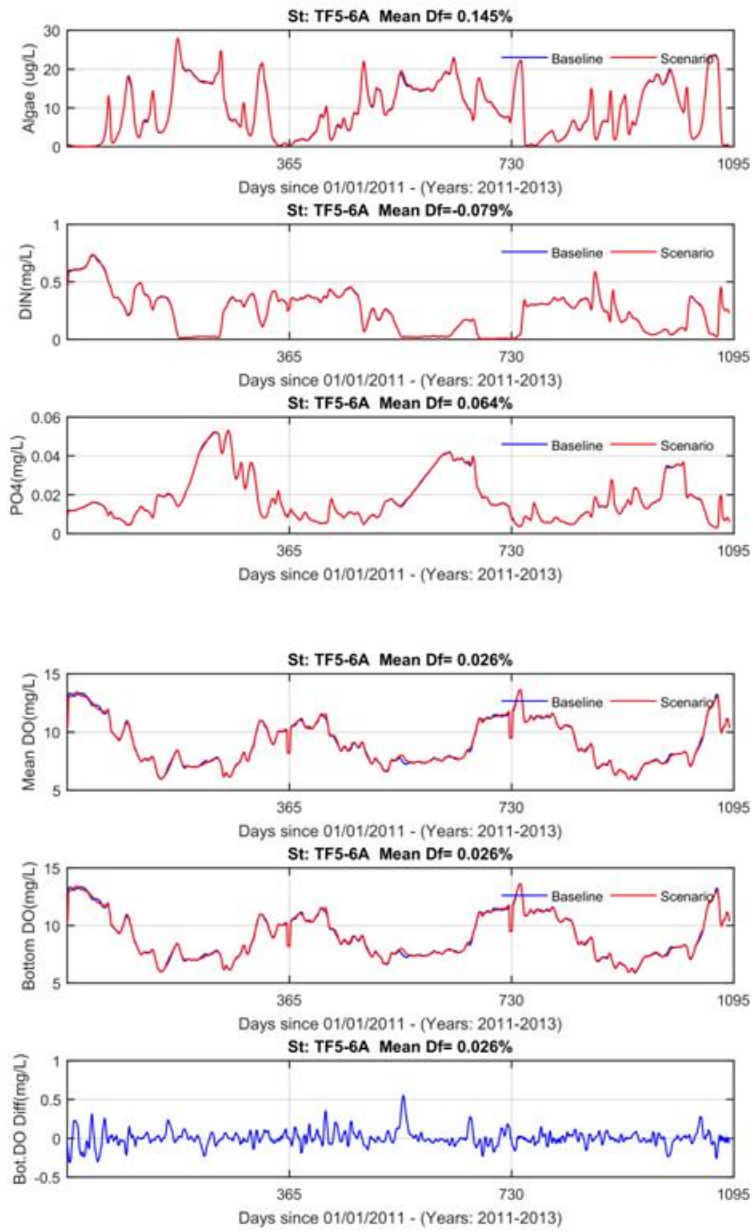


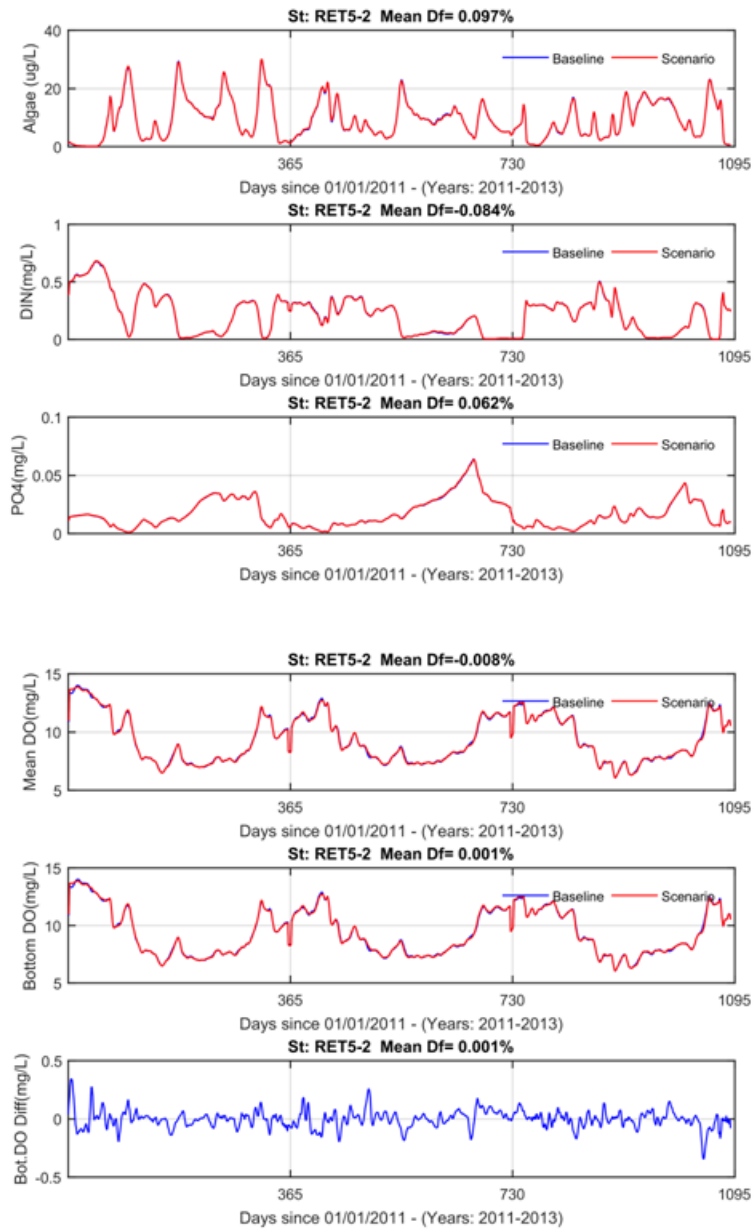


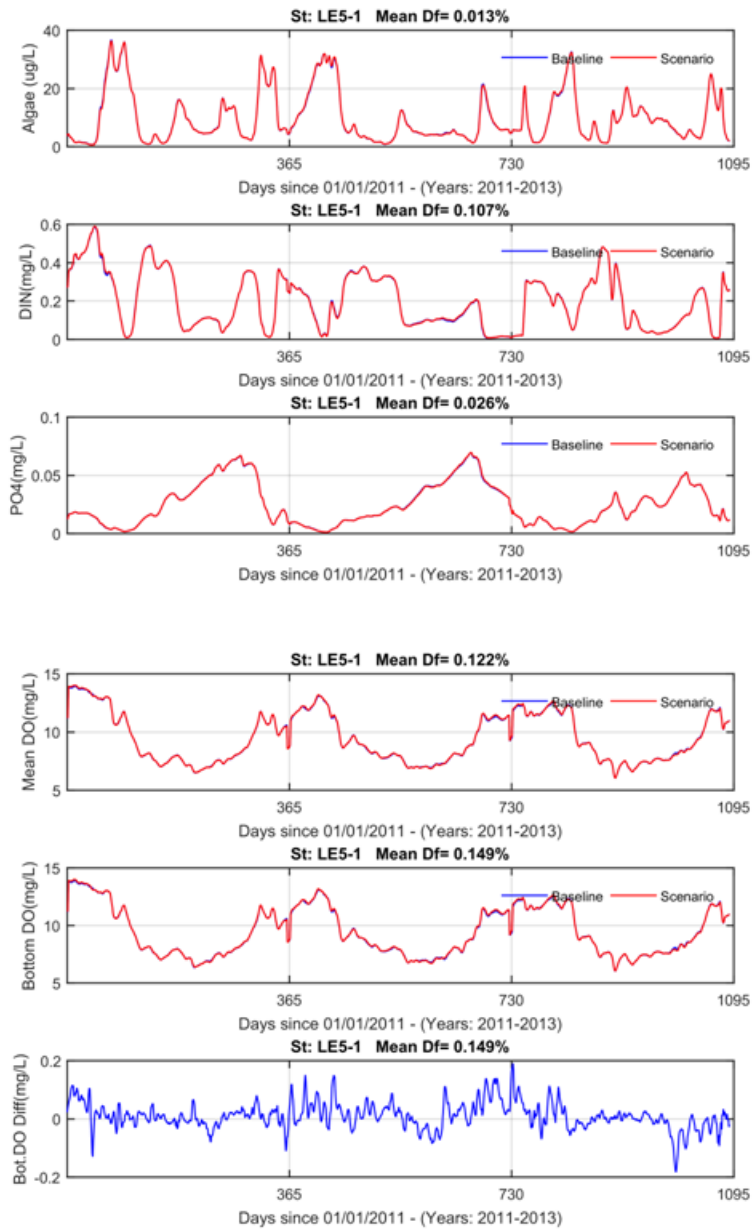


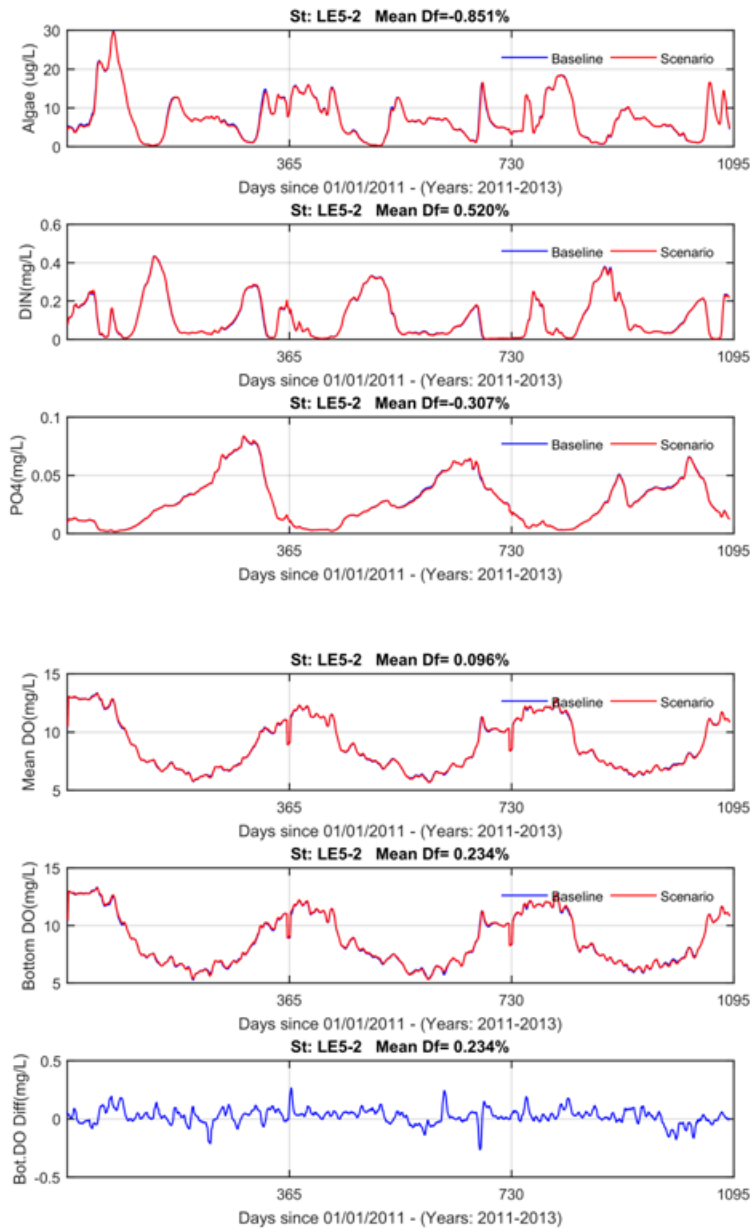


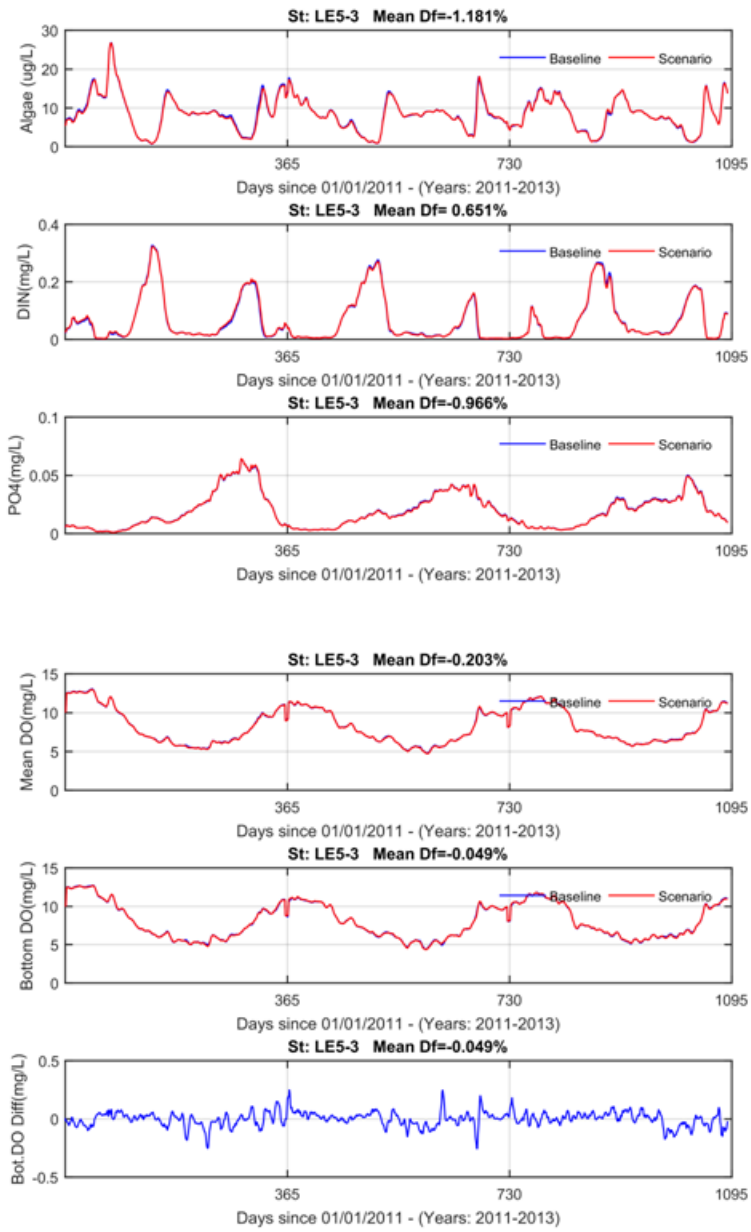


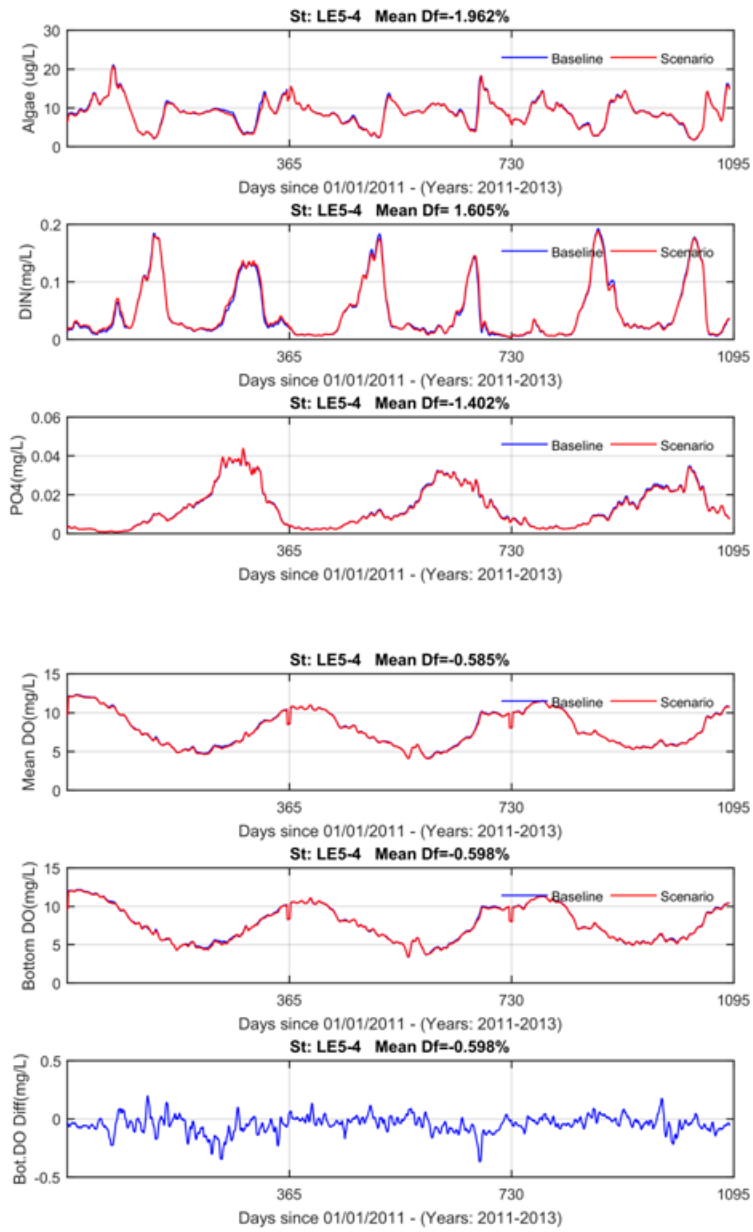


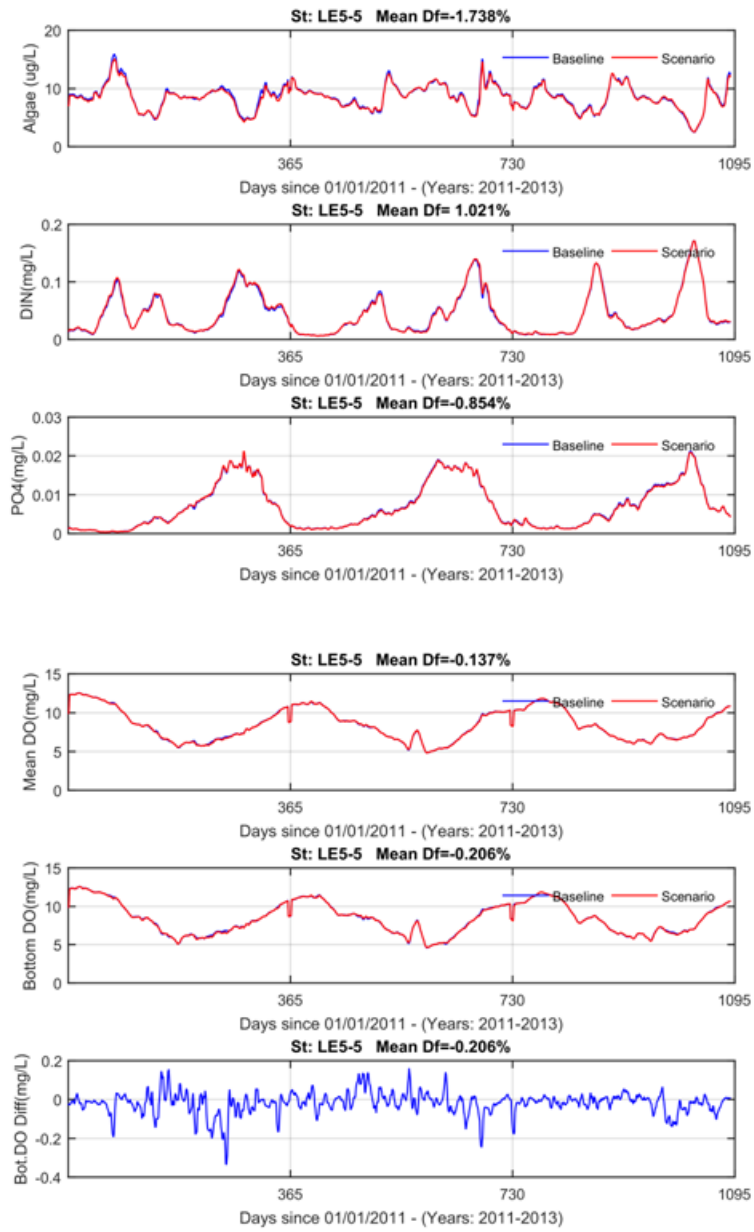


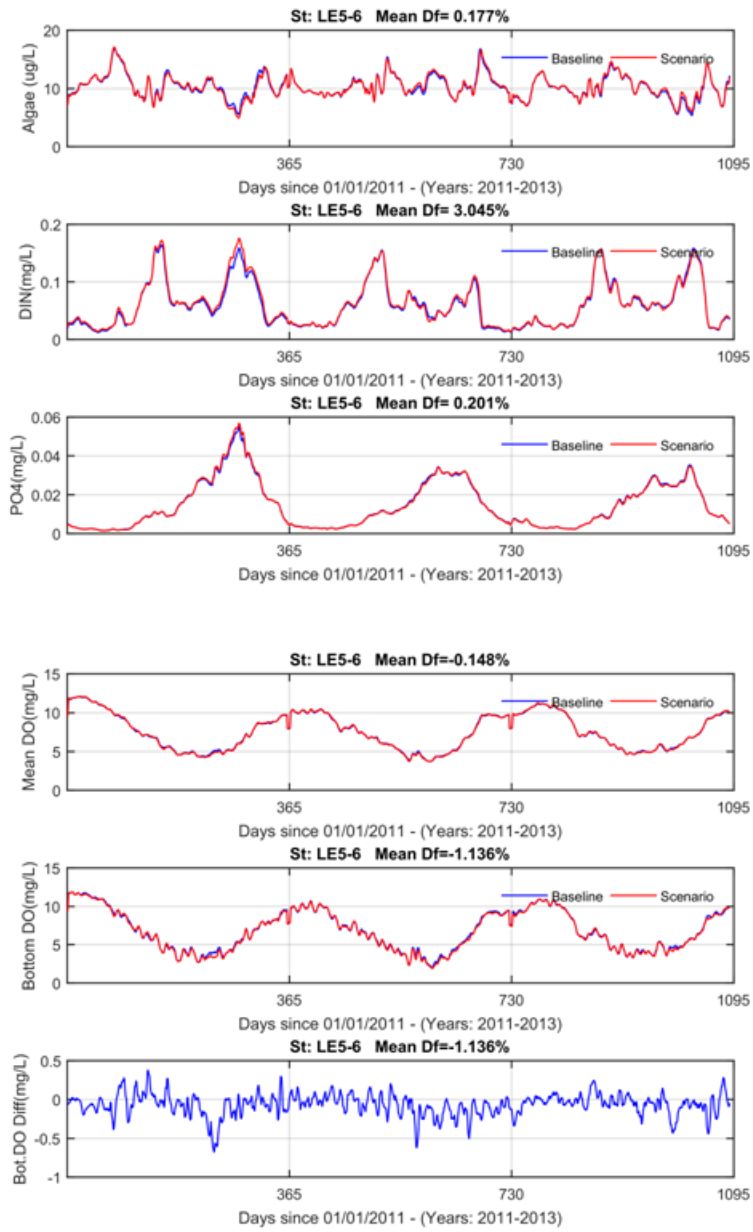


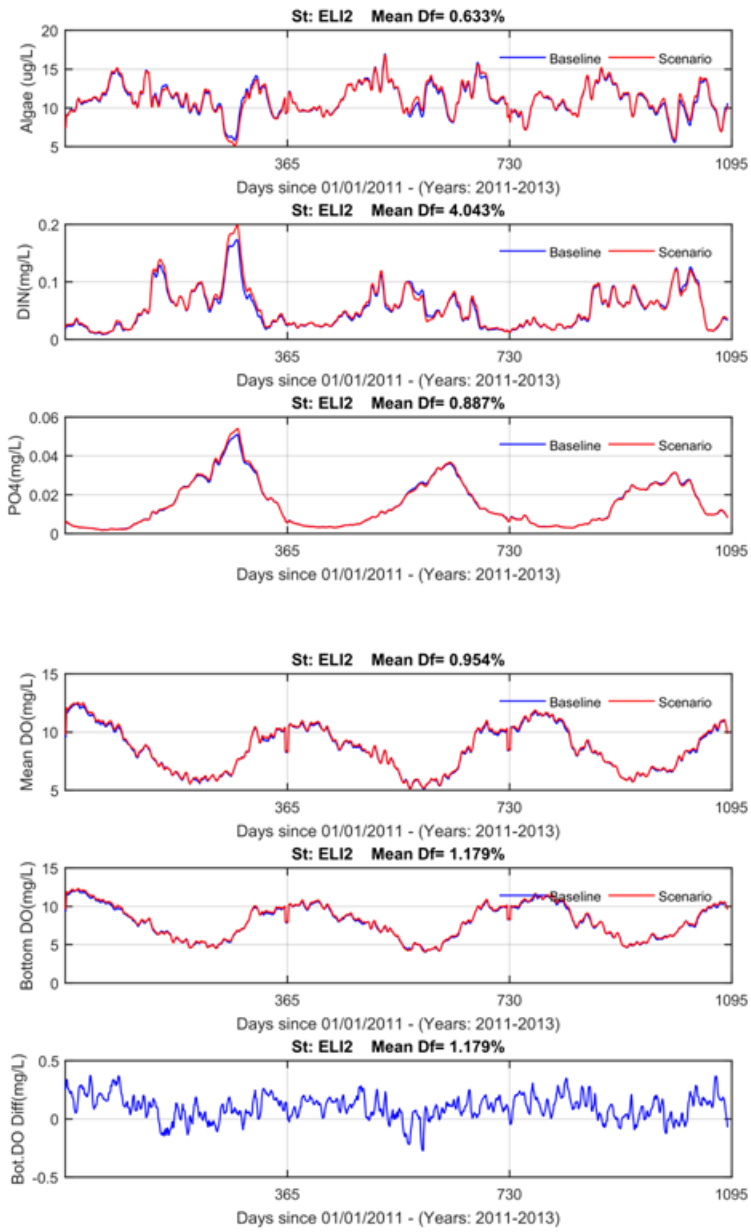


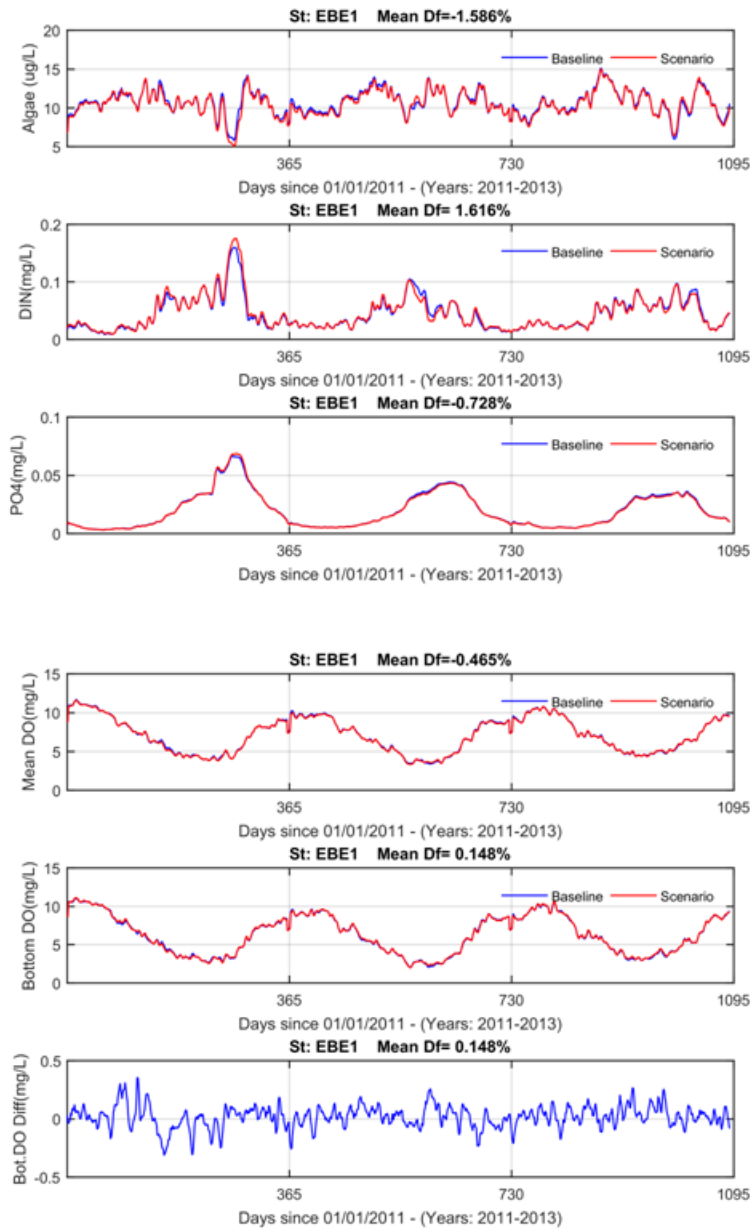


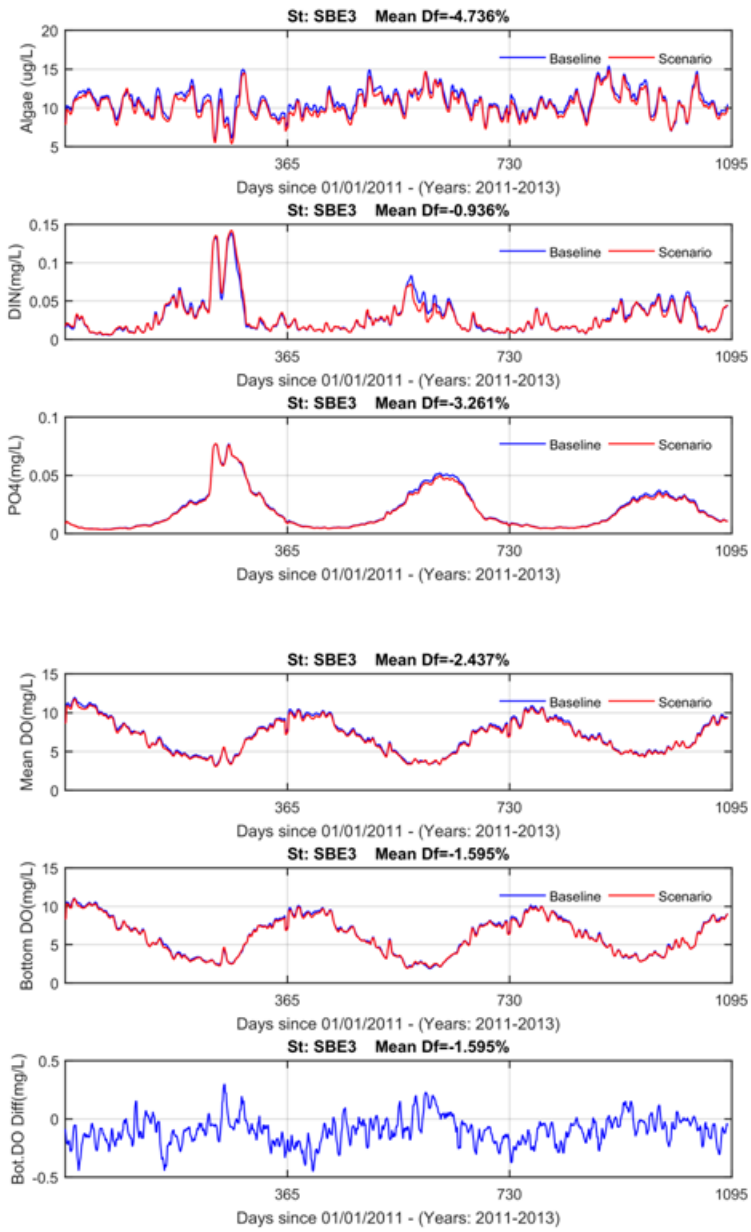


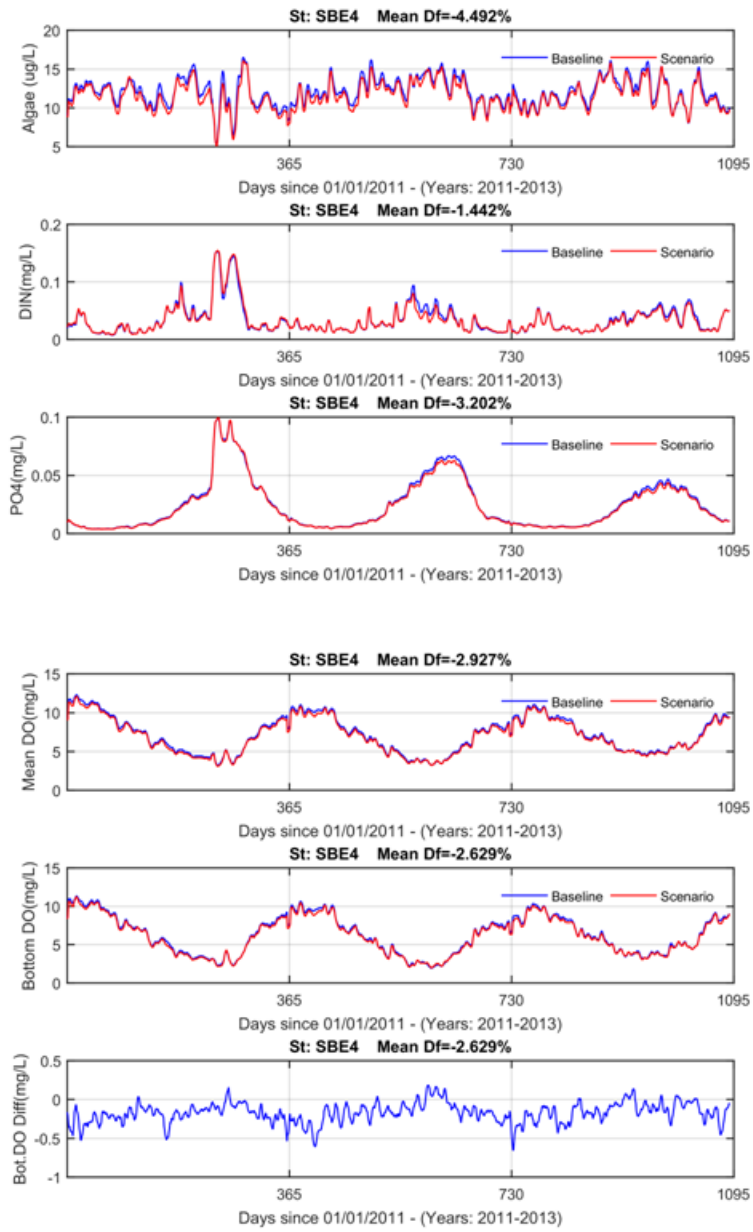


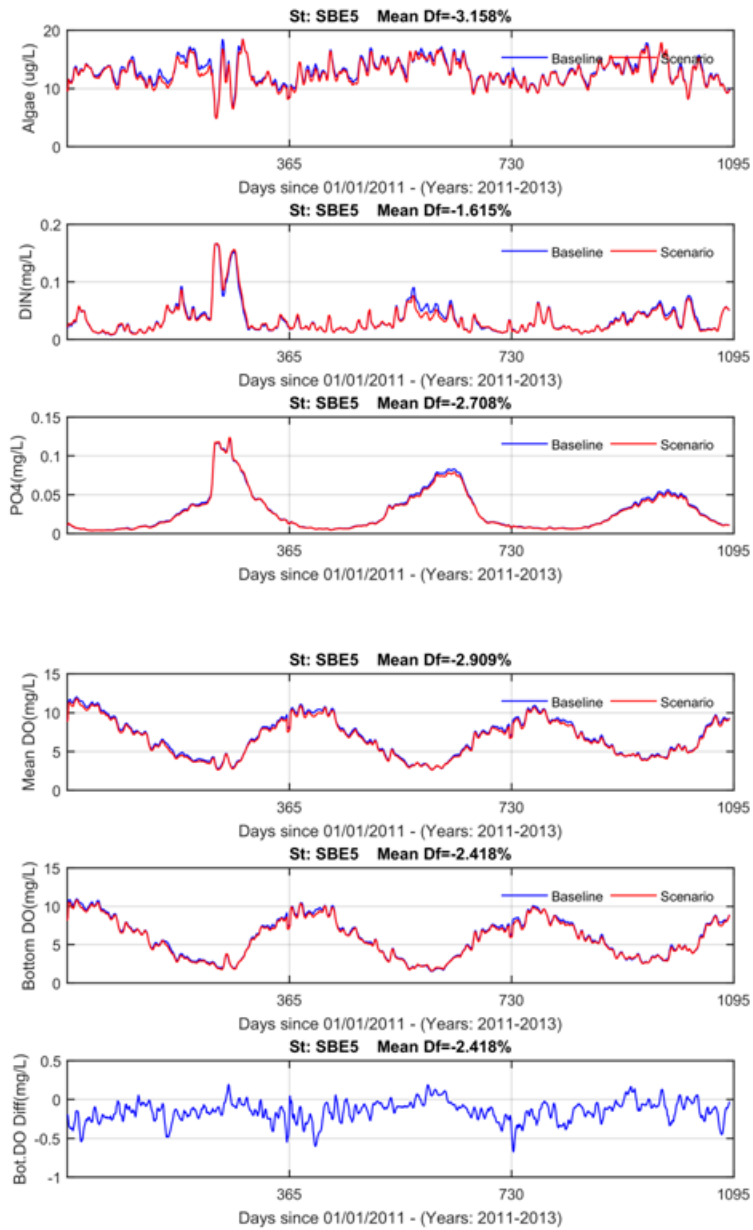


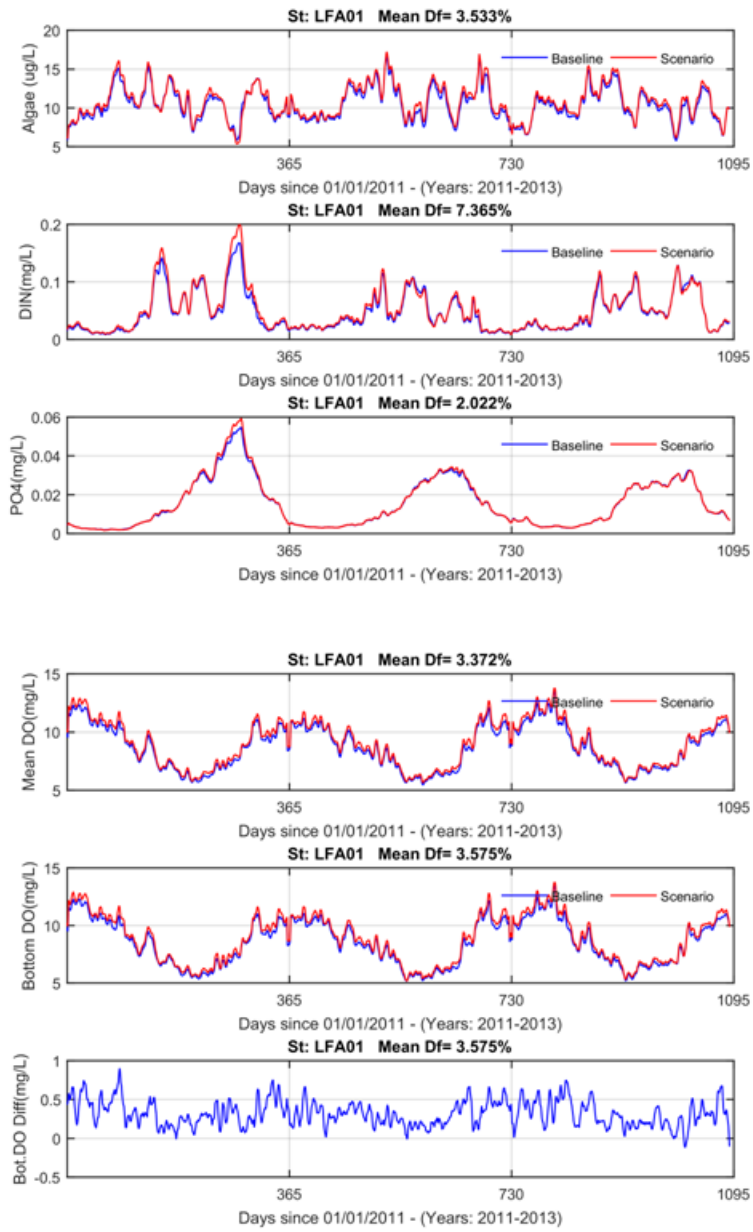


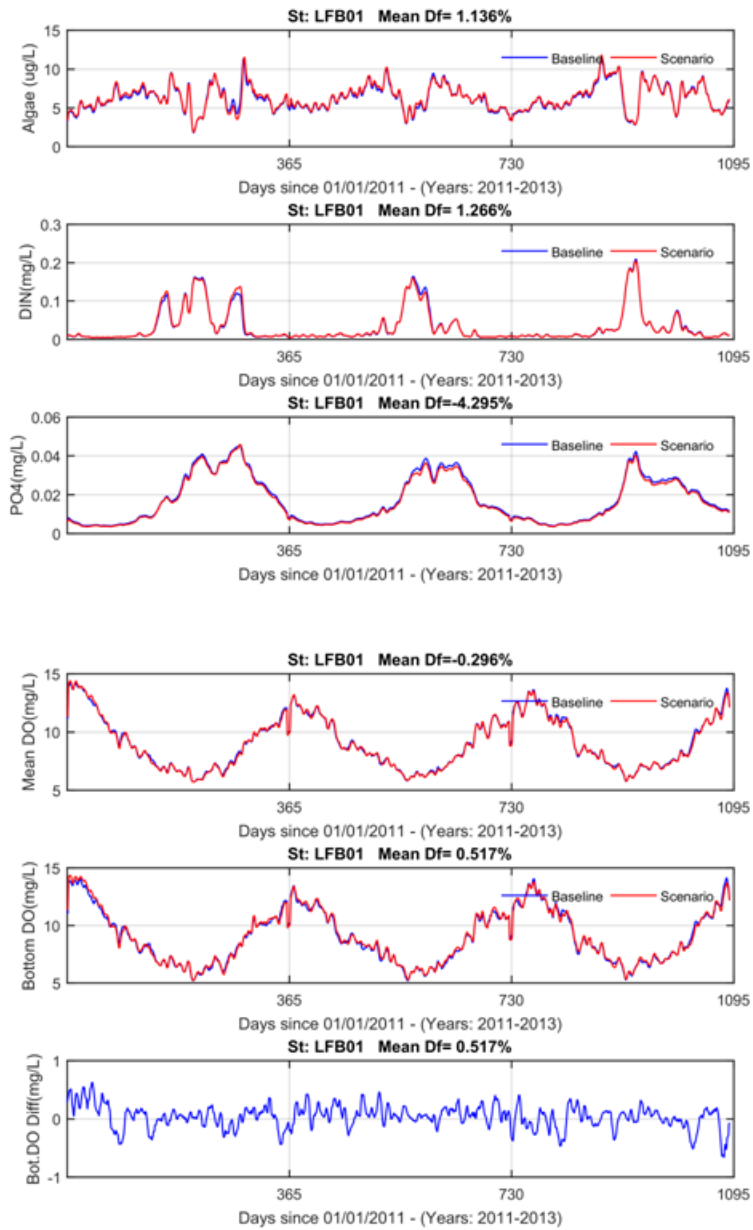


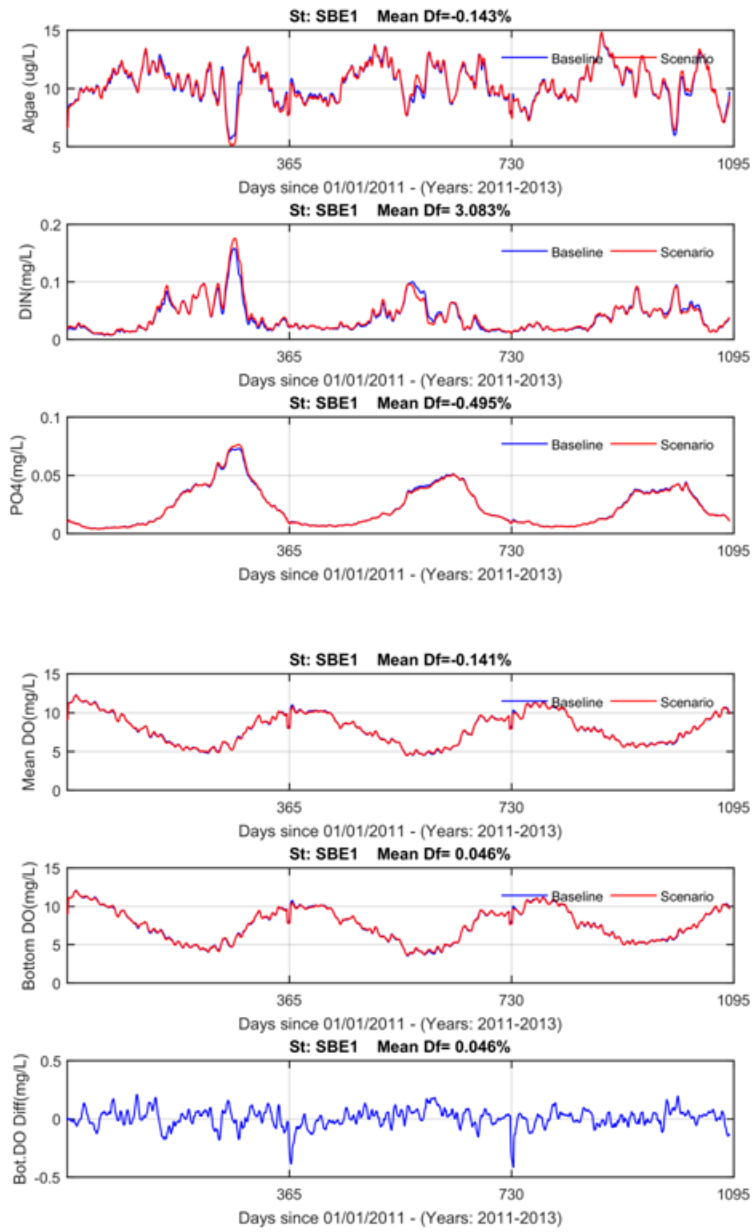


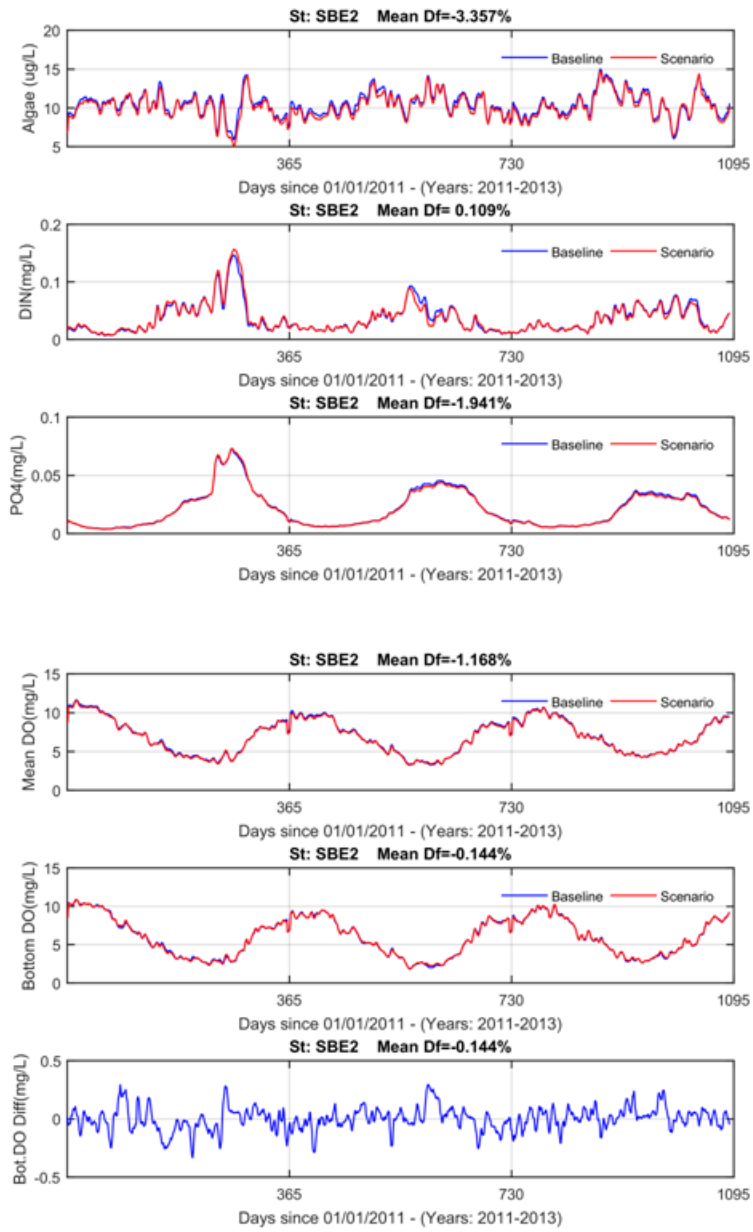


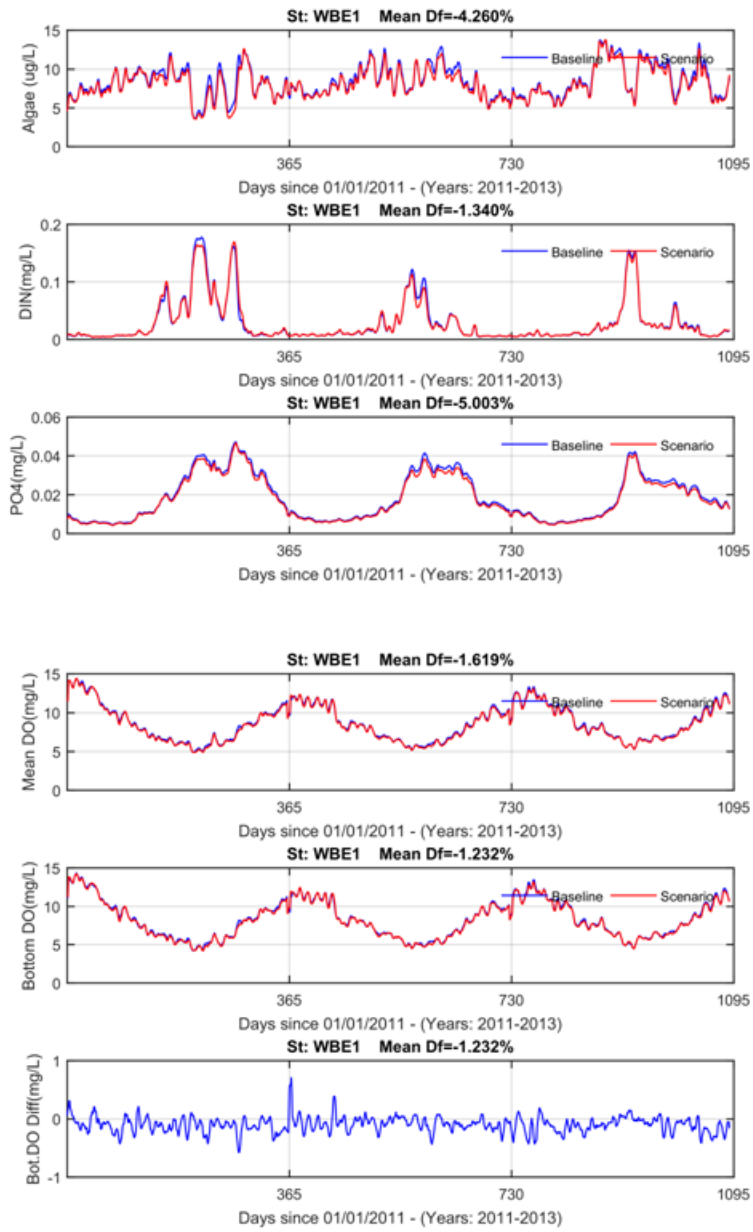






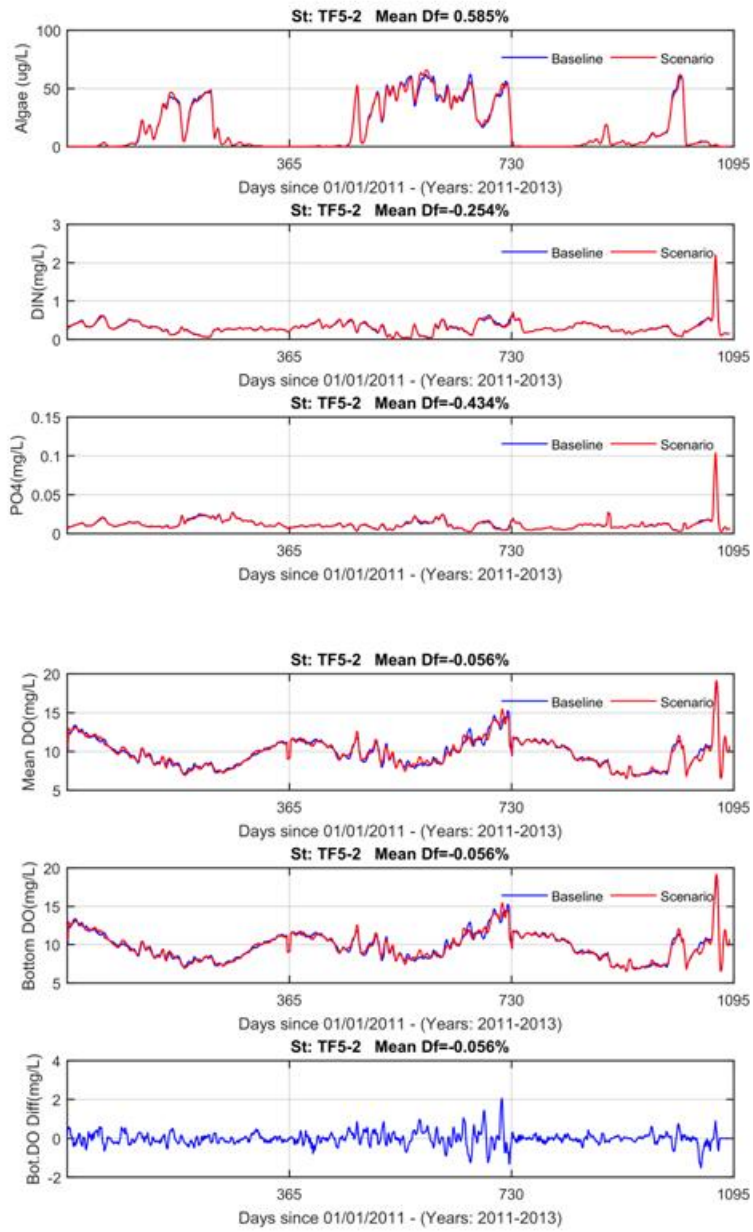


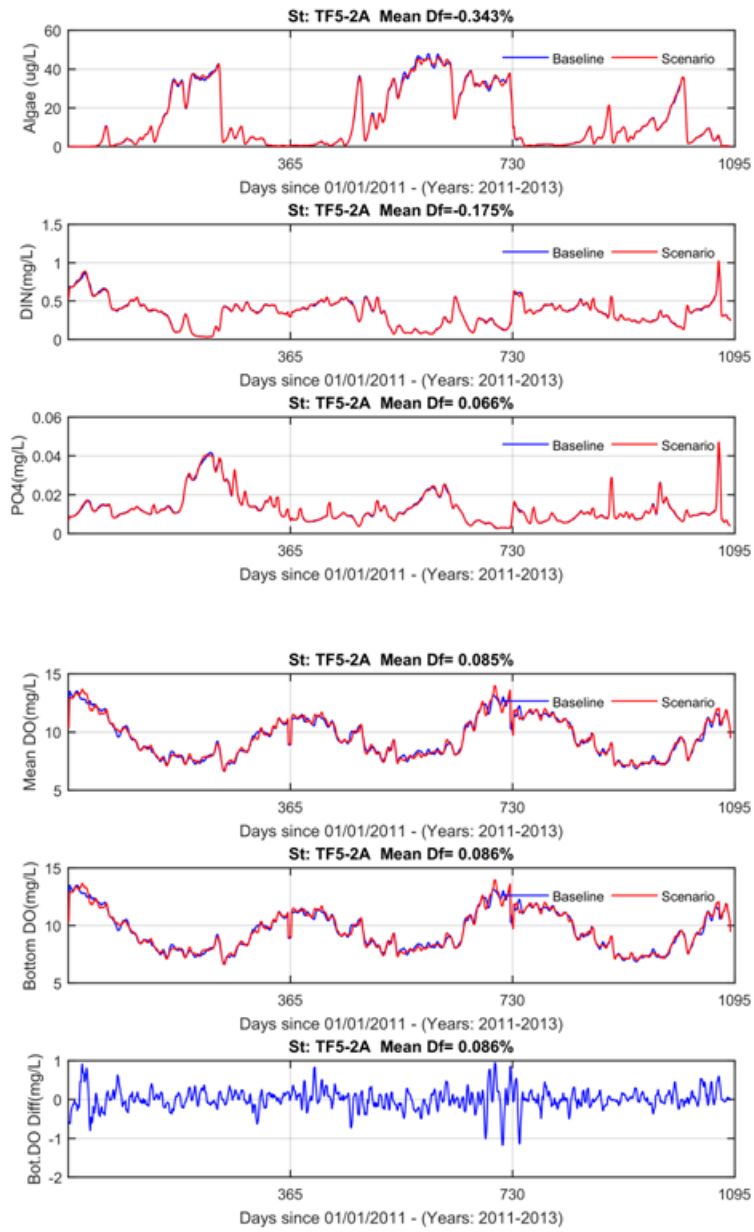


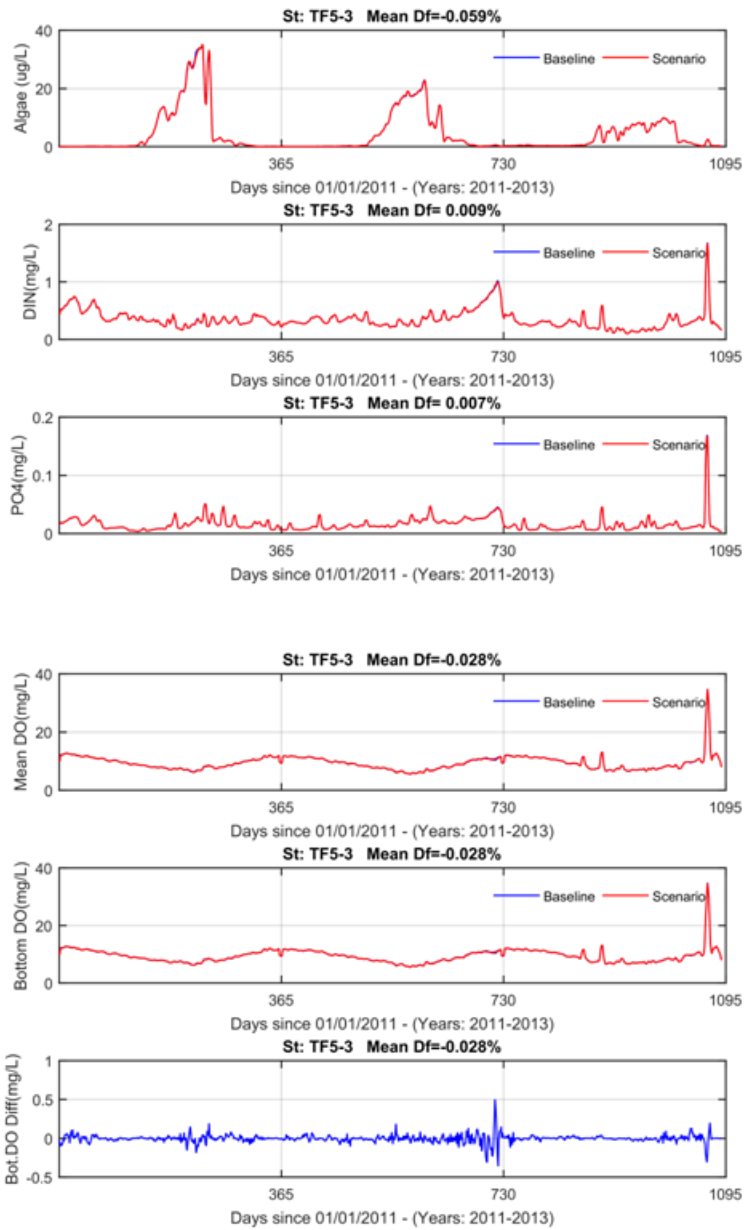


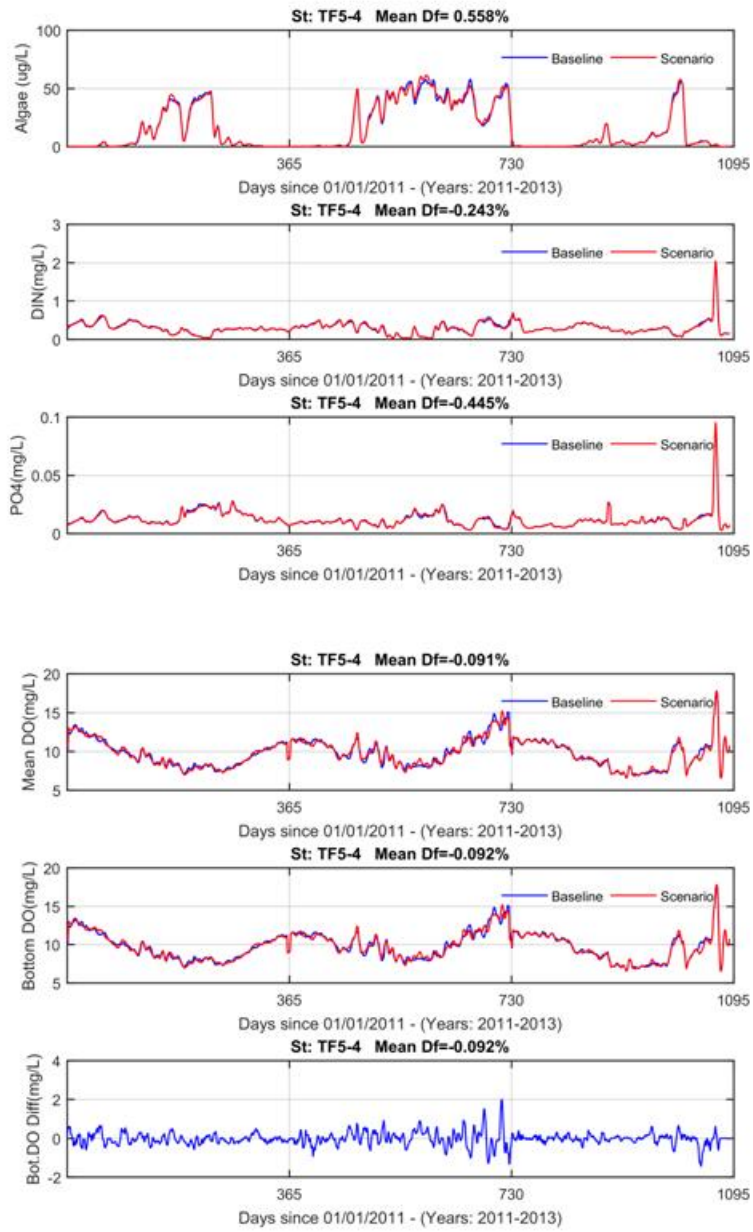
Model Simulation Baseline1 and Scenario 5-1

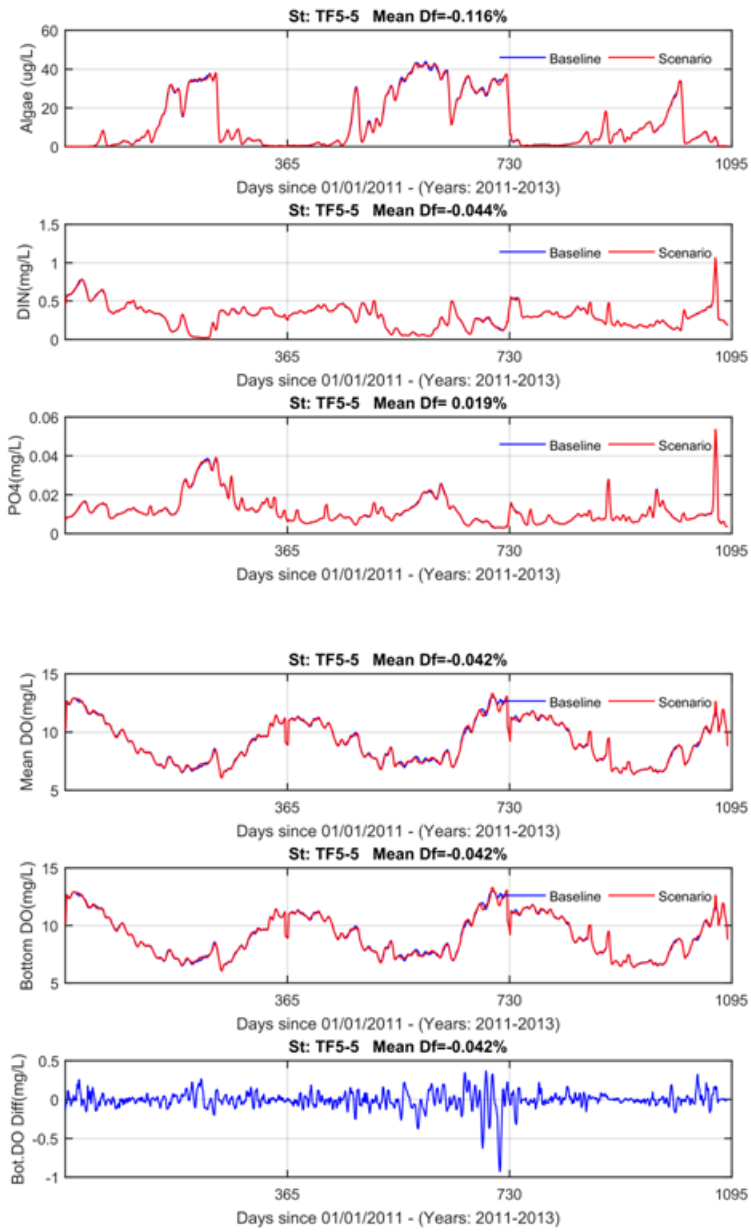
In the following plots. The Baseline is the results of baseline1 and Scenario is Scenario of 5-1.

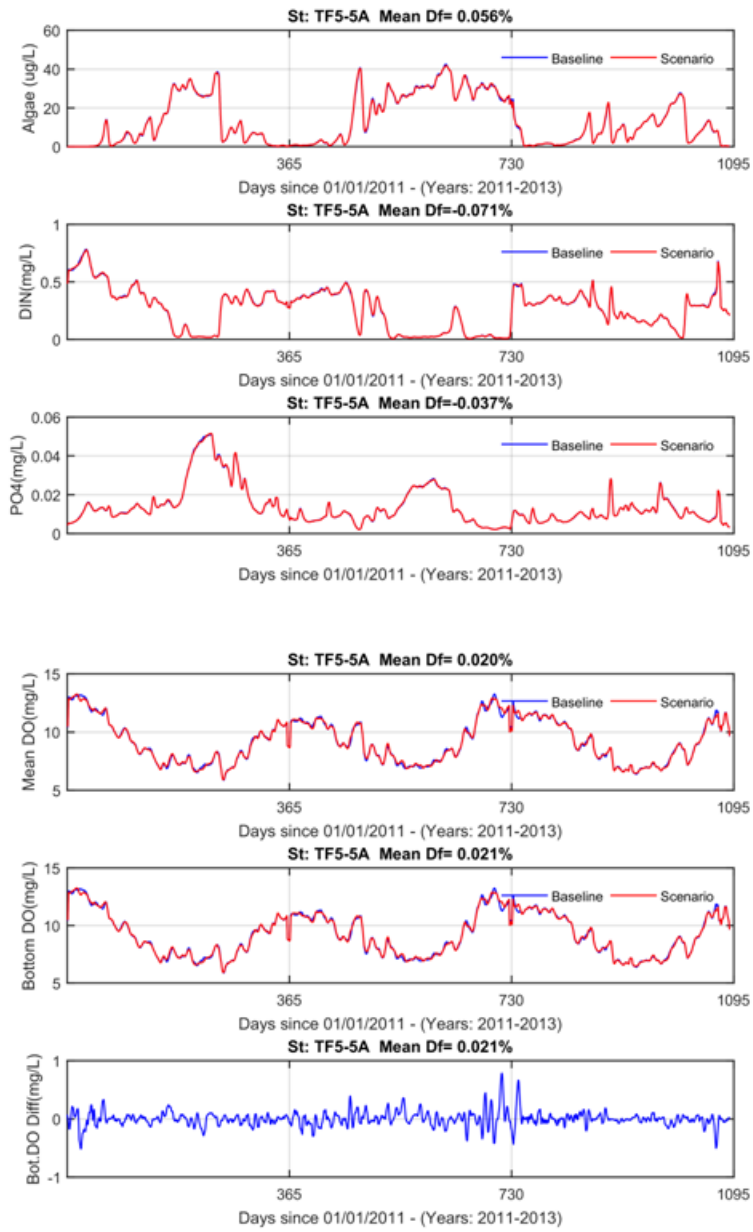


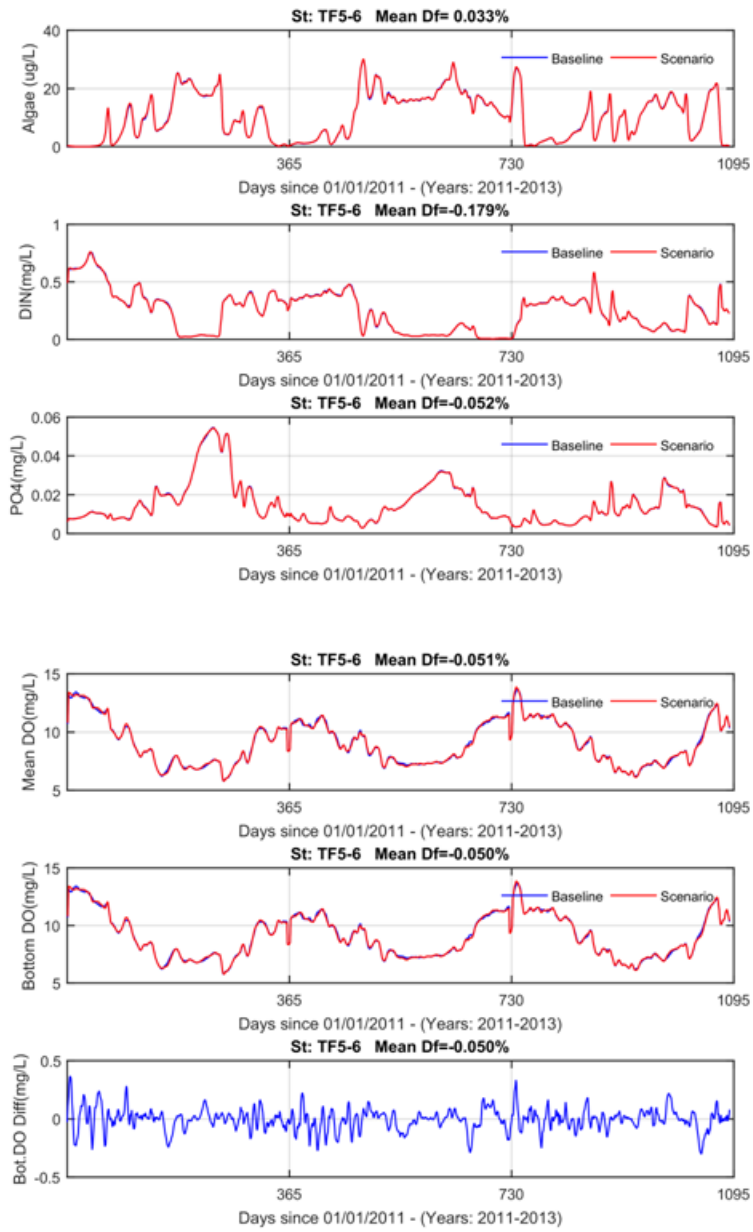


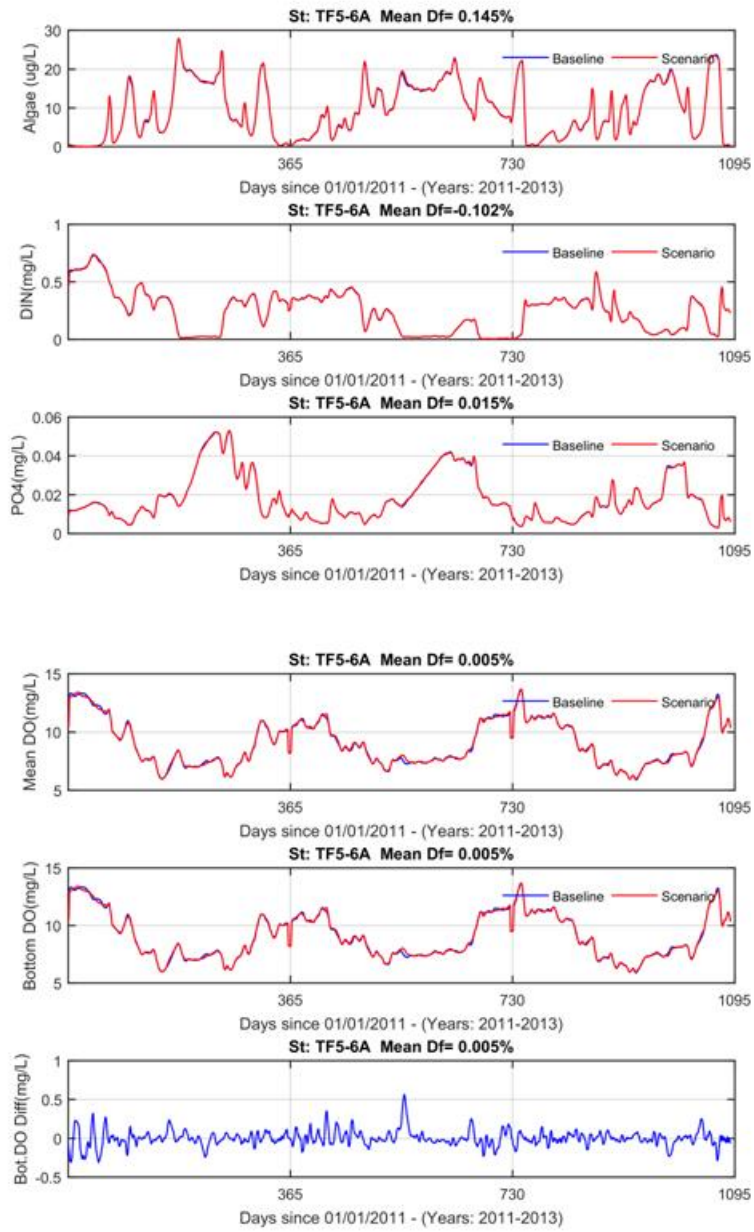


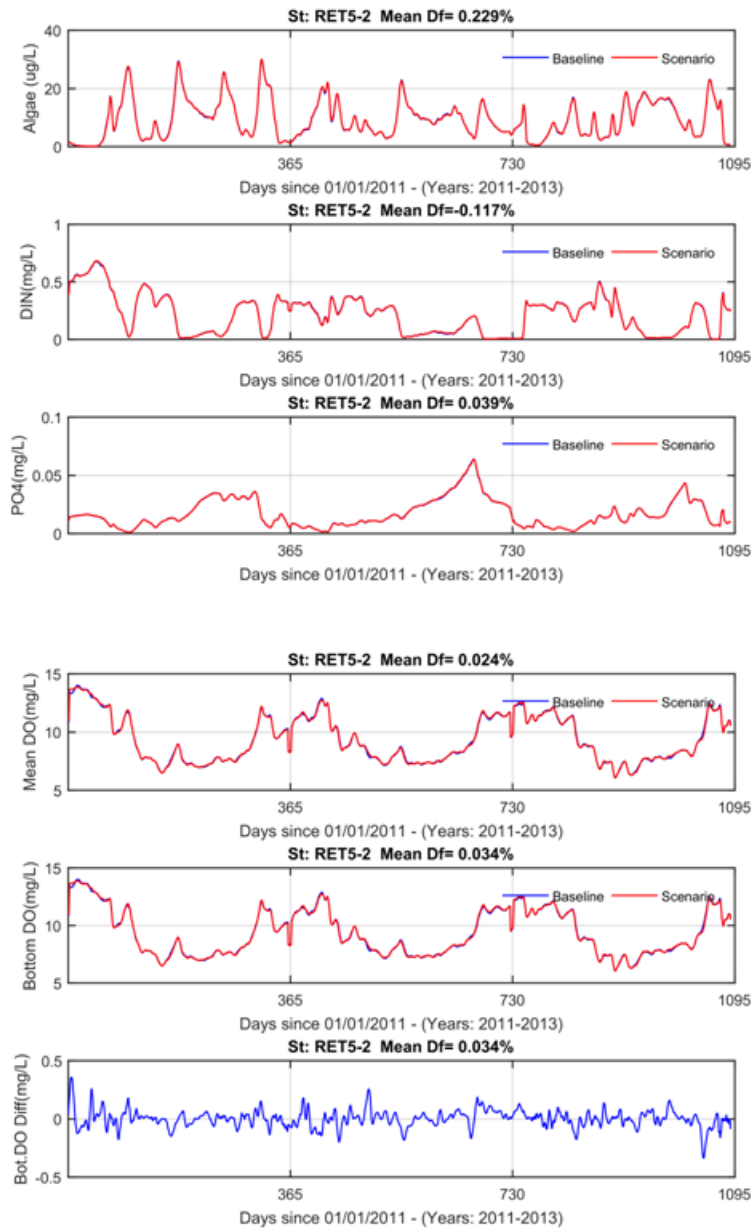


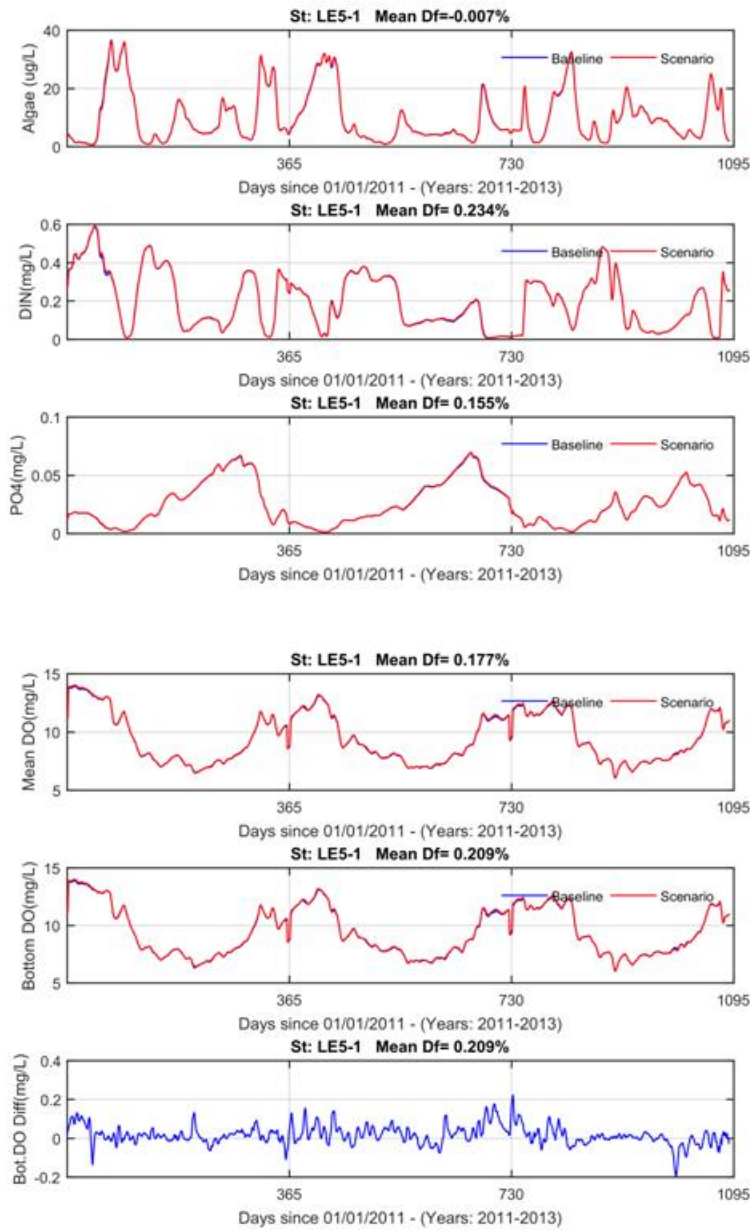


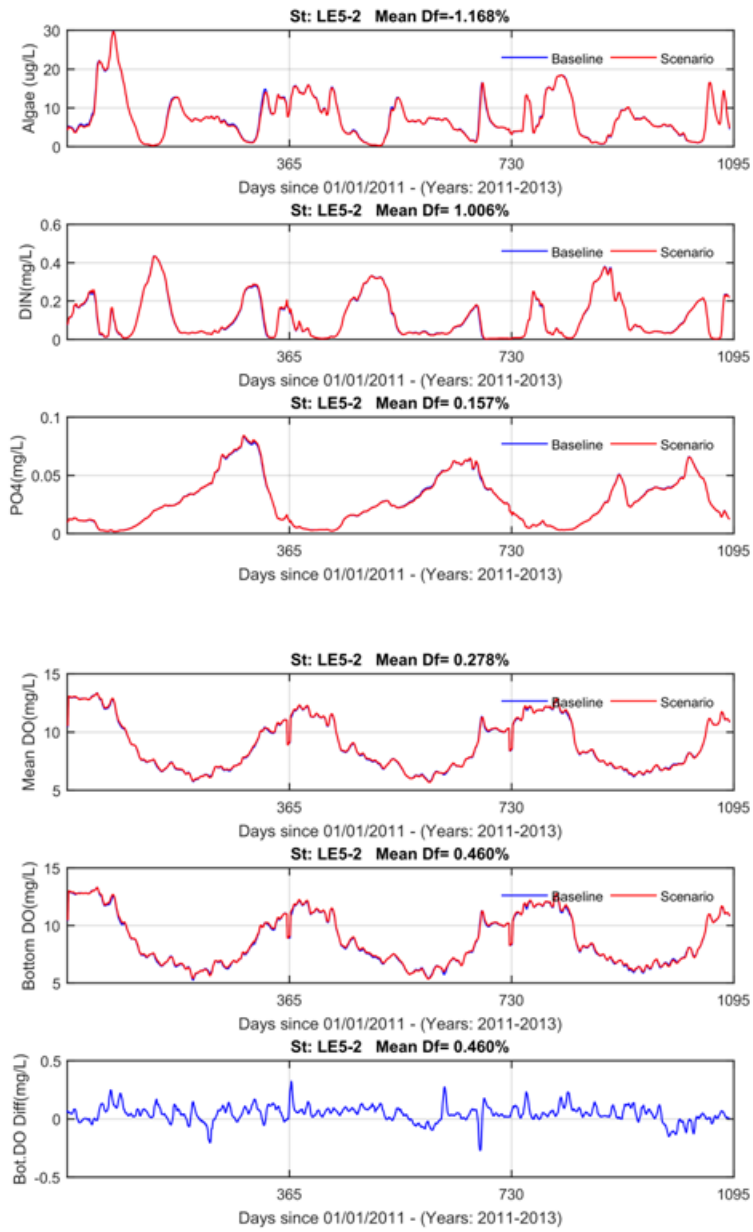


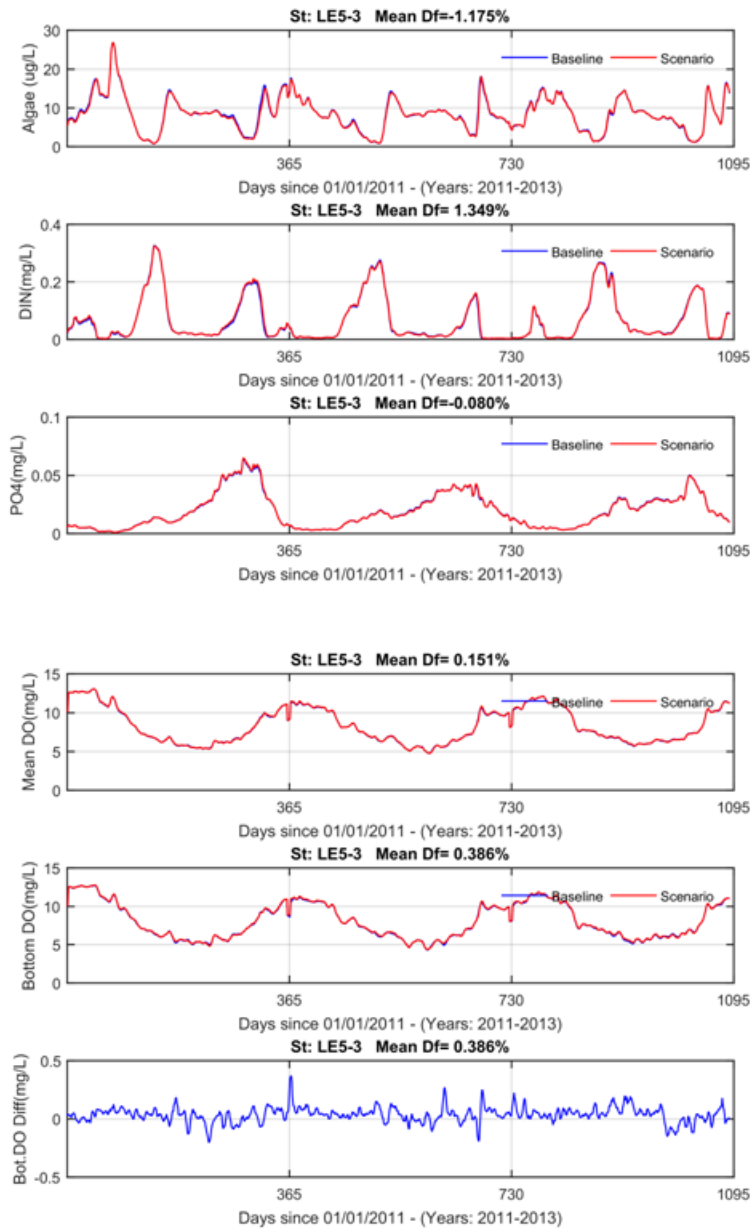


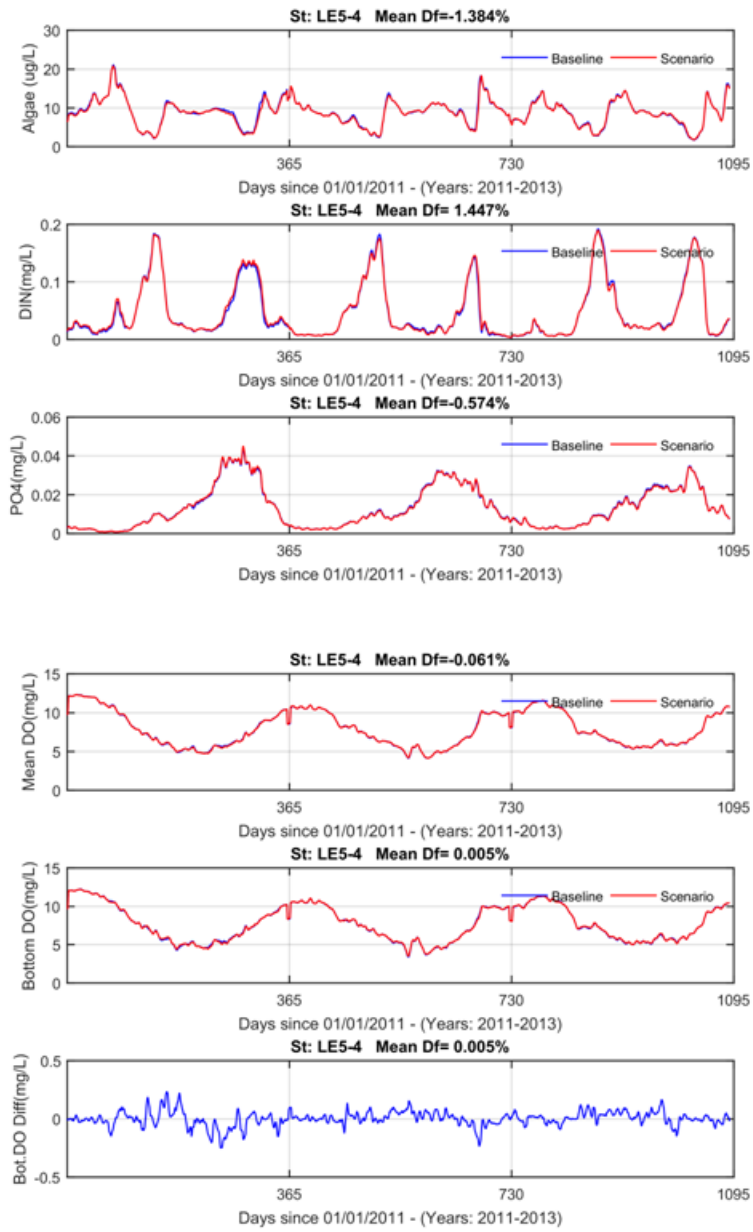


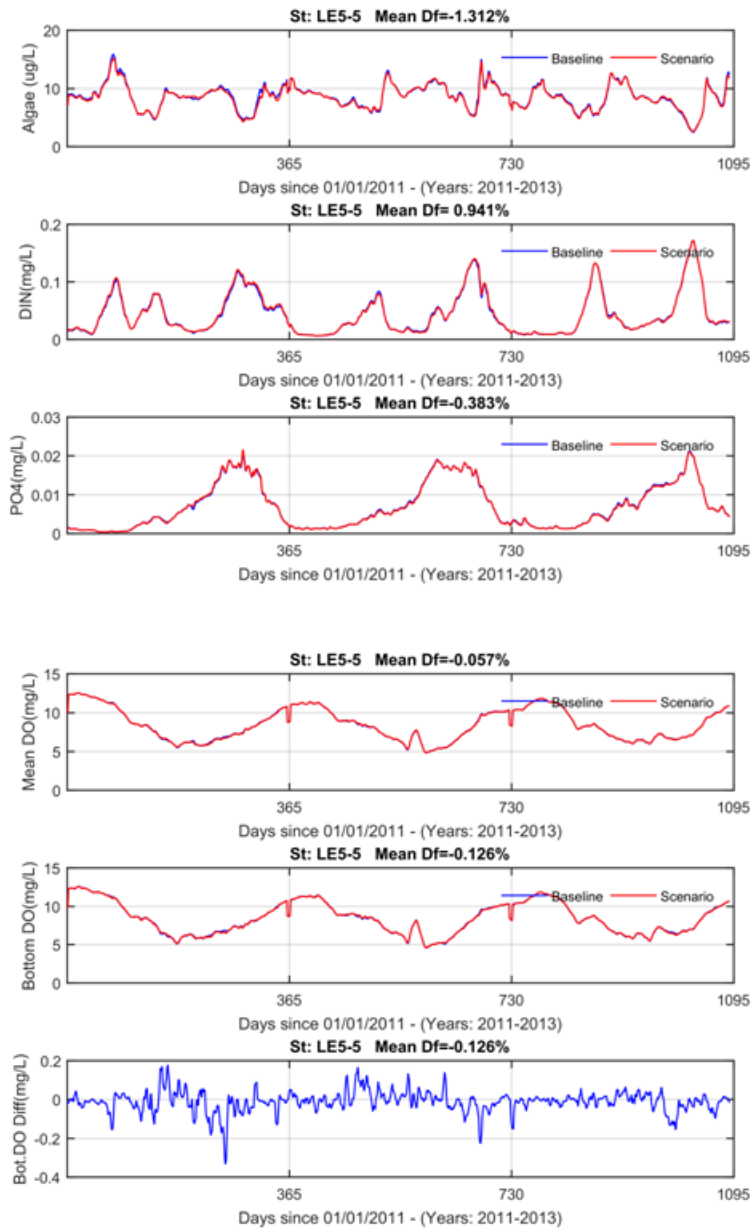


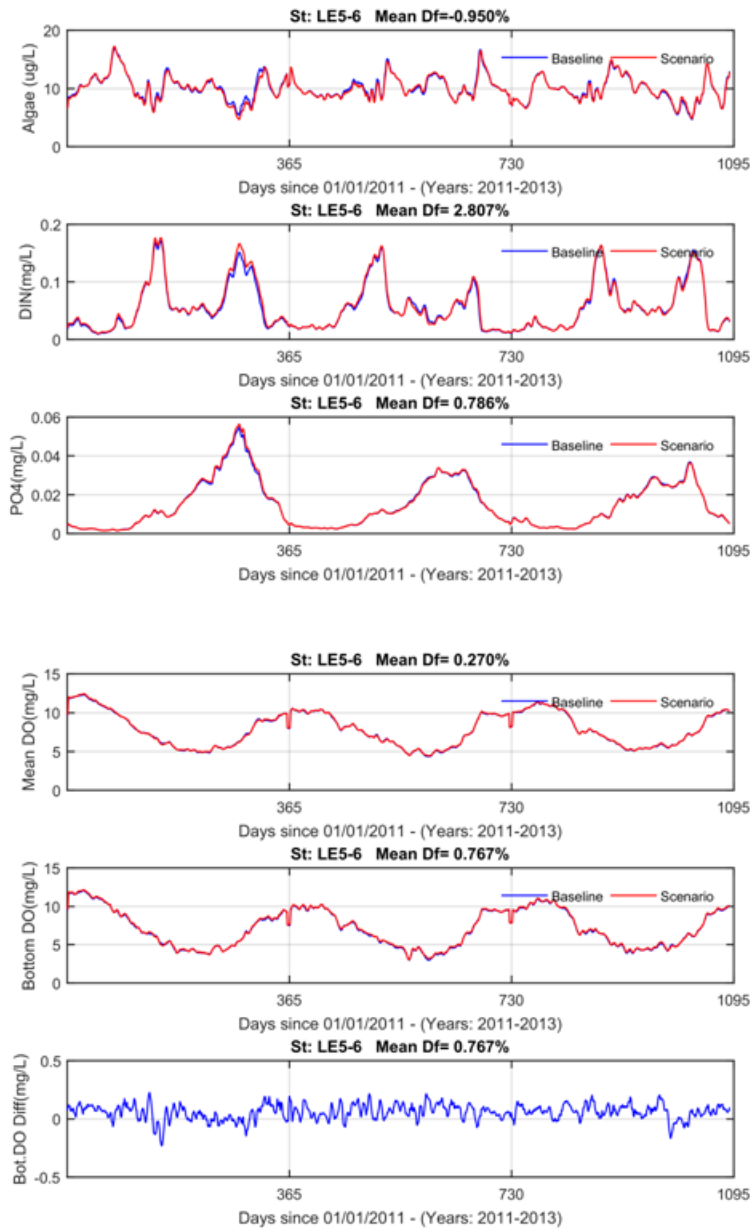


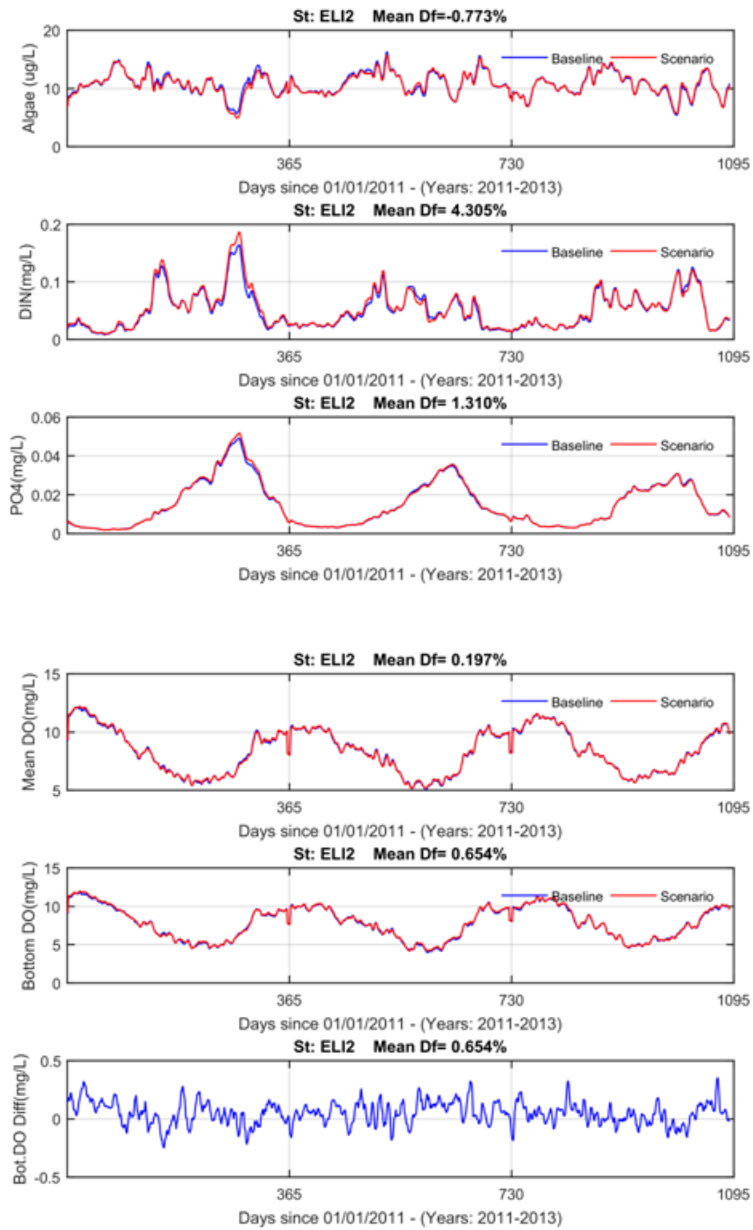


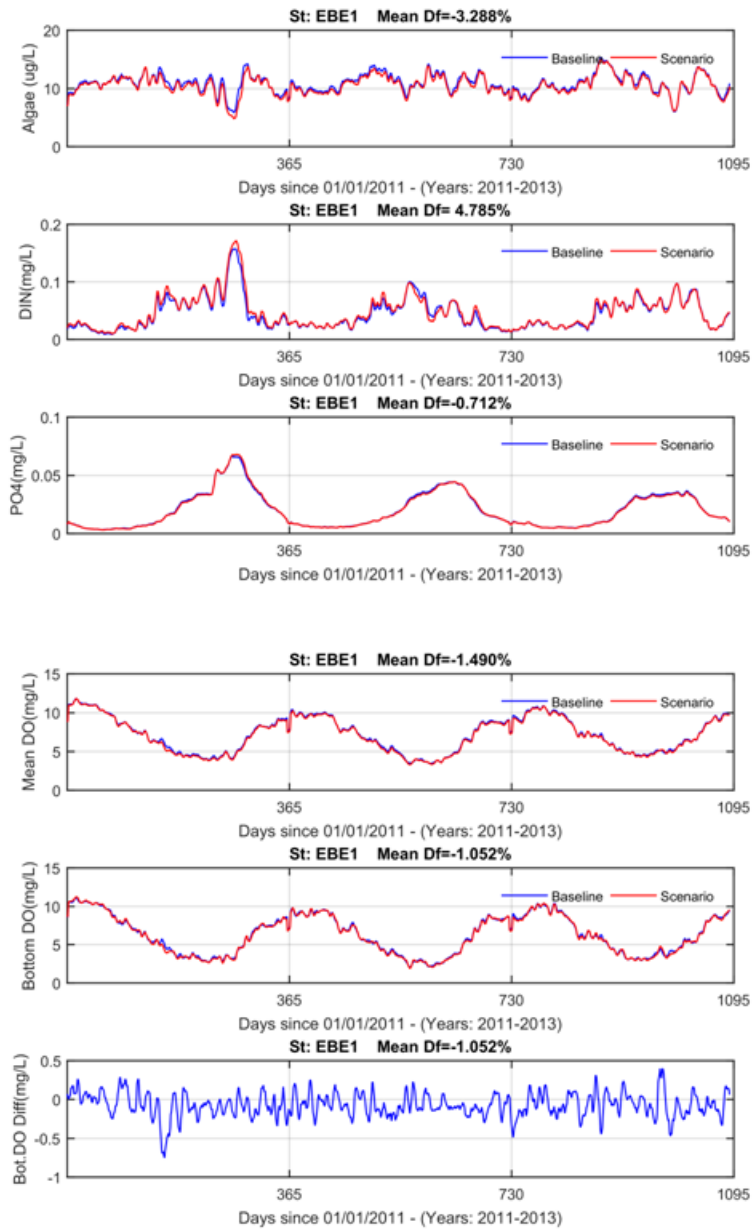


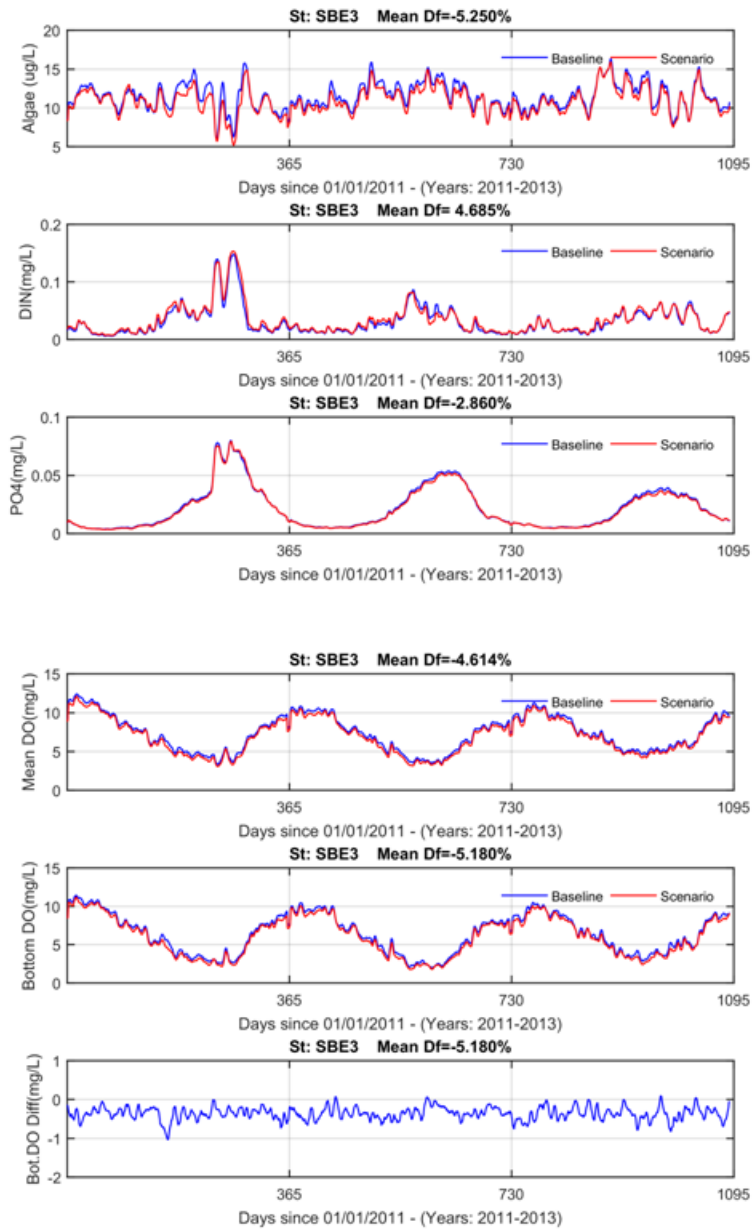


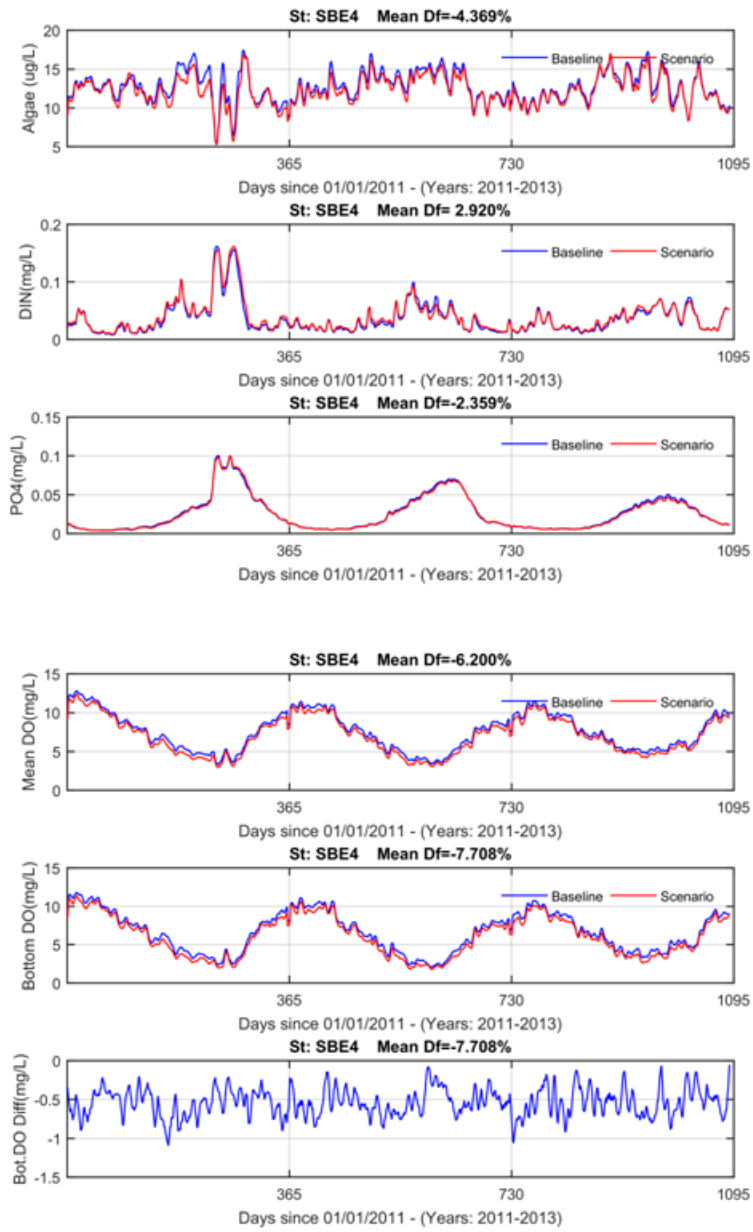


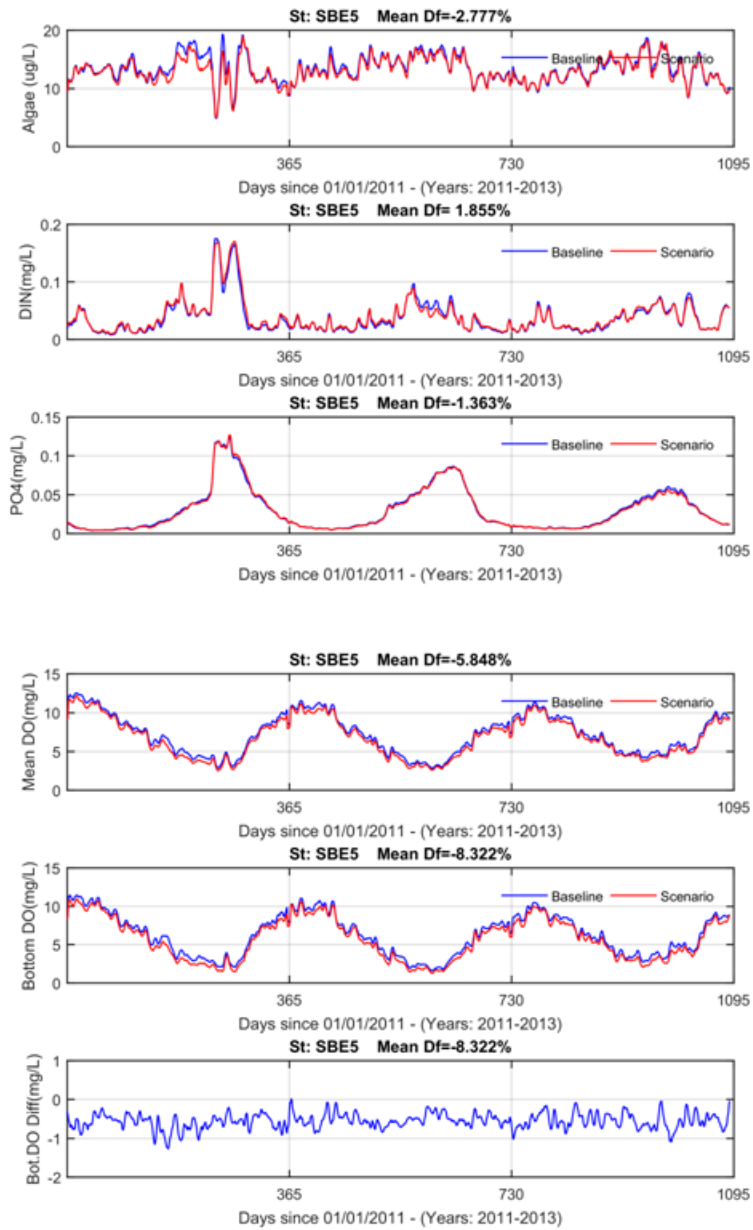


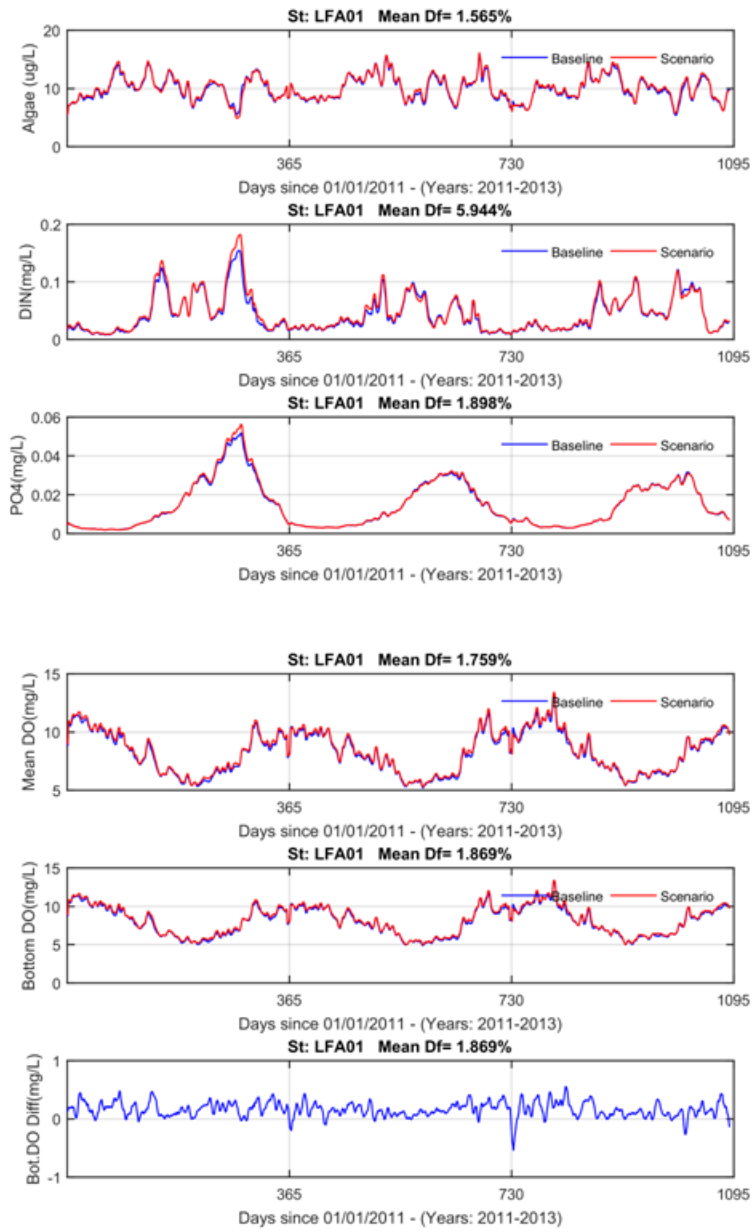


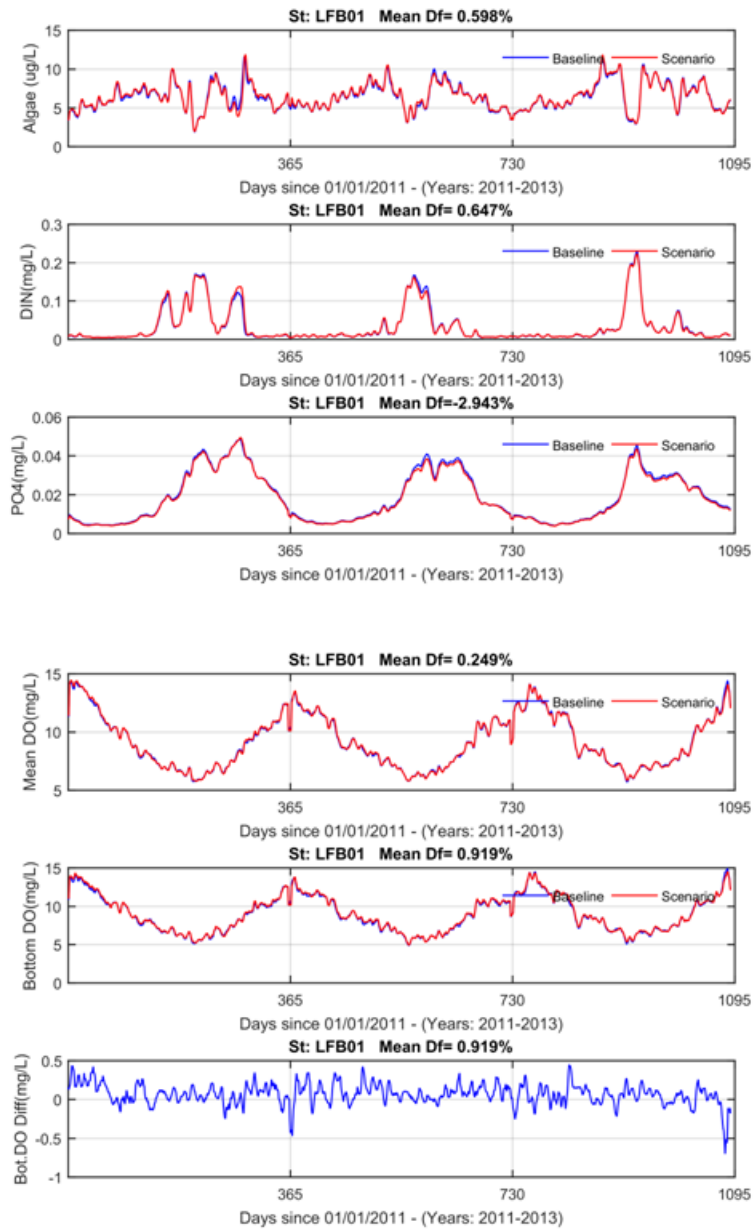


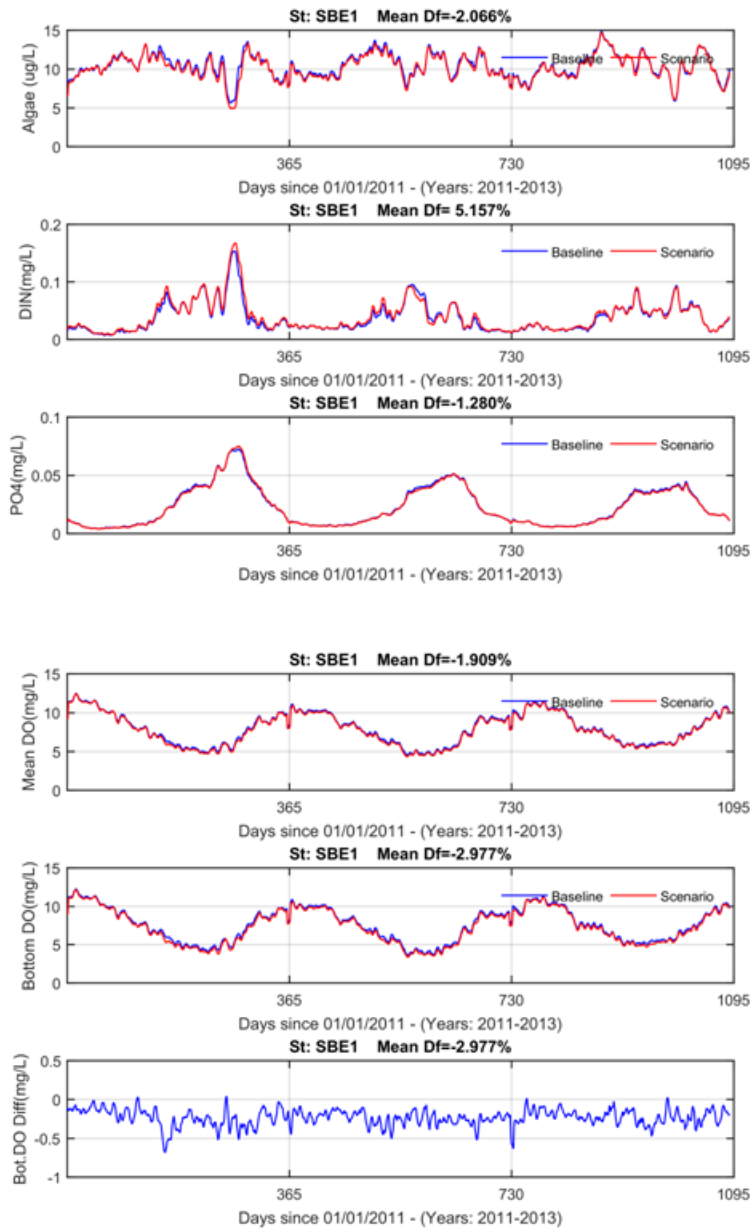


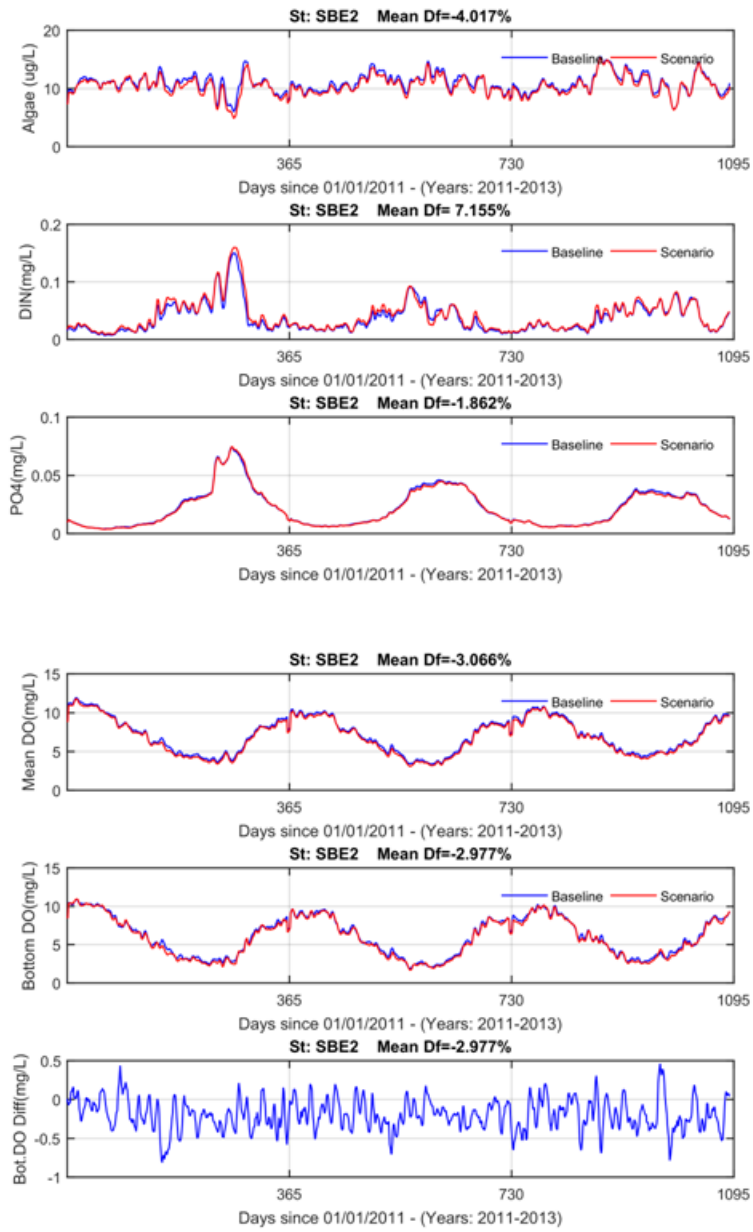


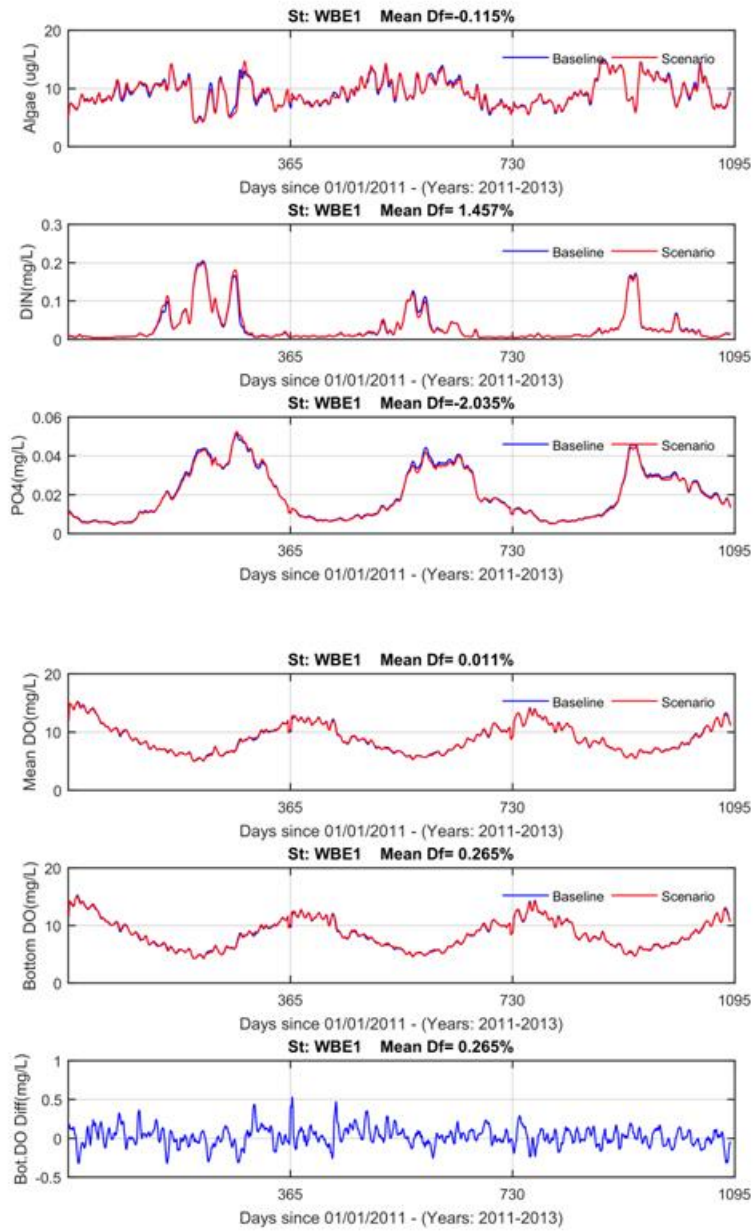






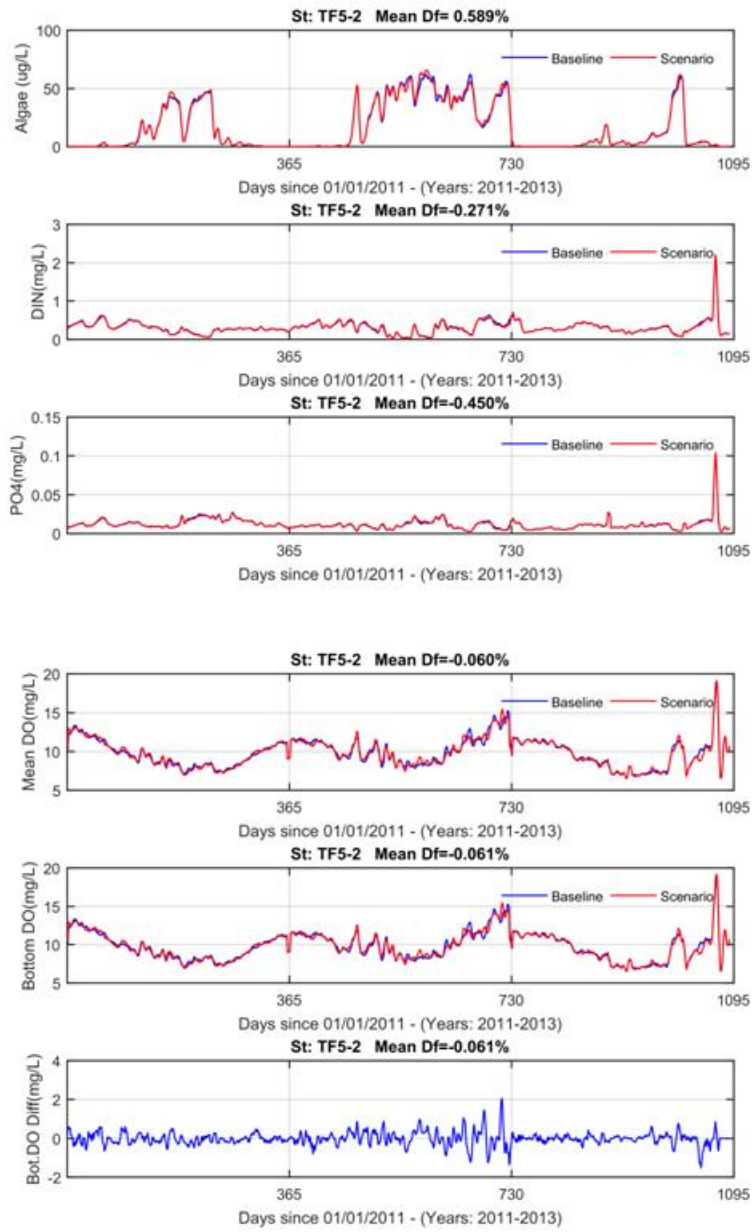


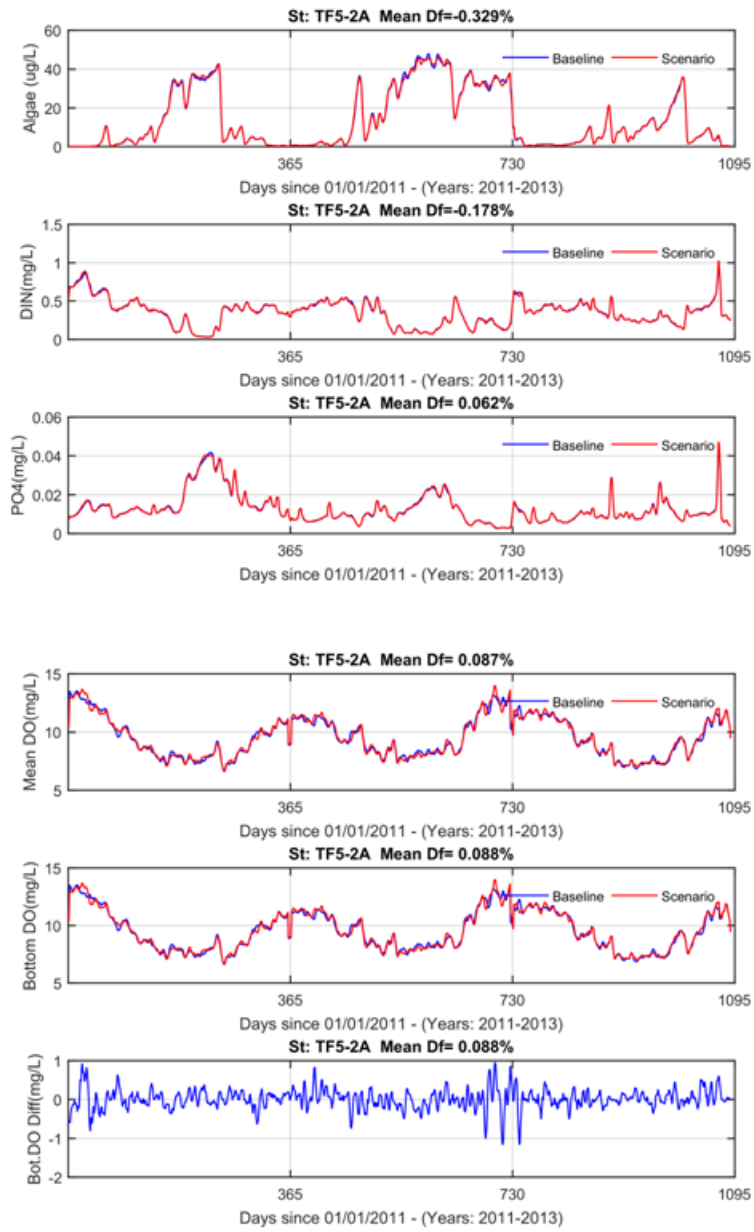


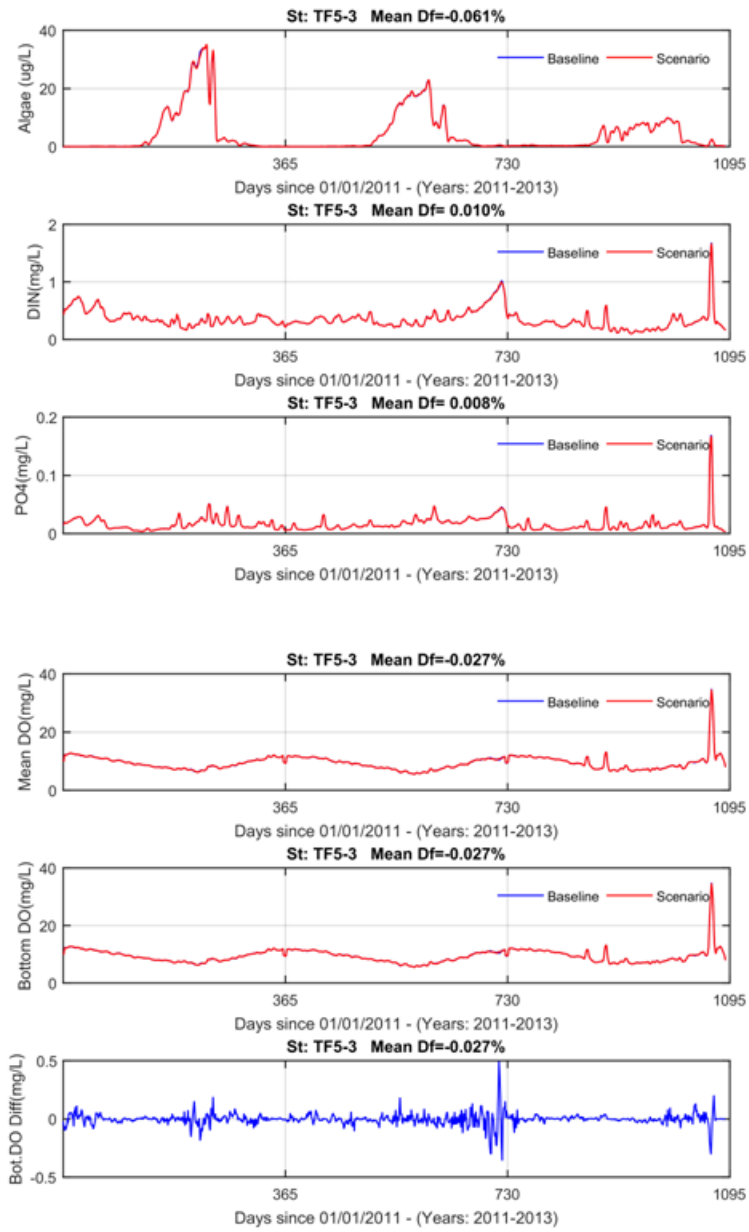


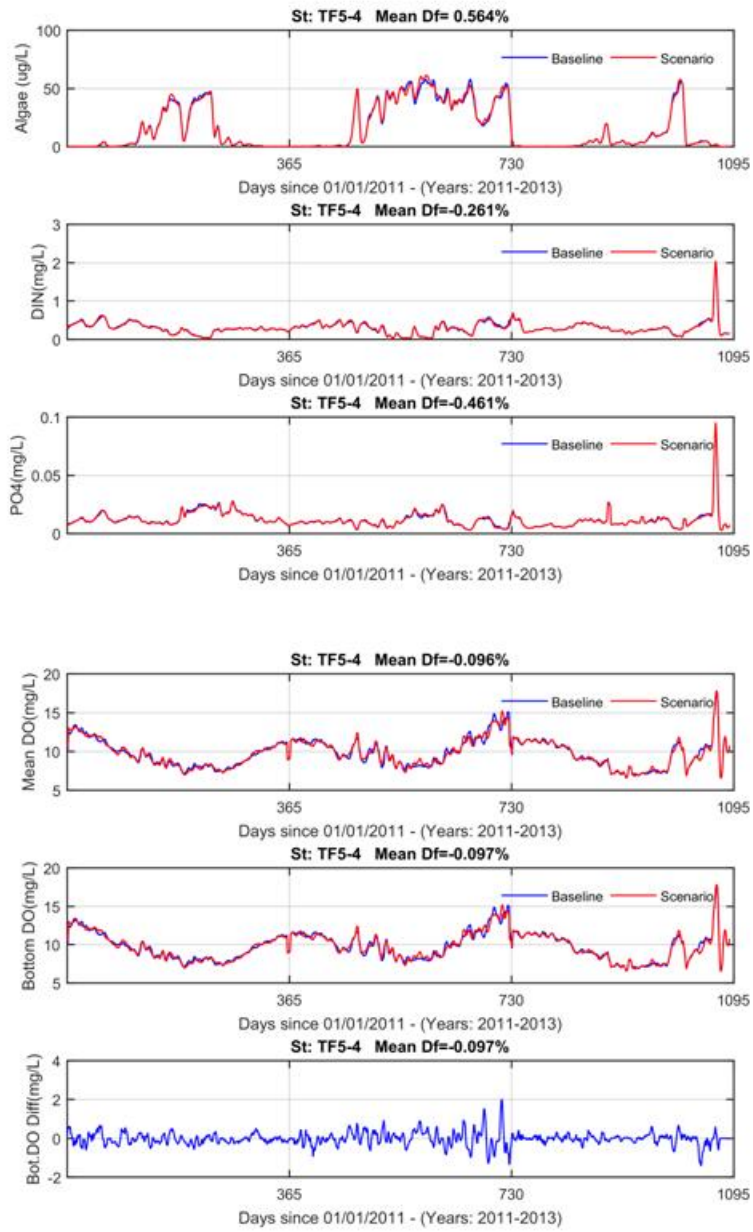
Model Simulation Baseline2 and Scenario 3-2

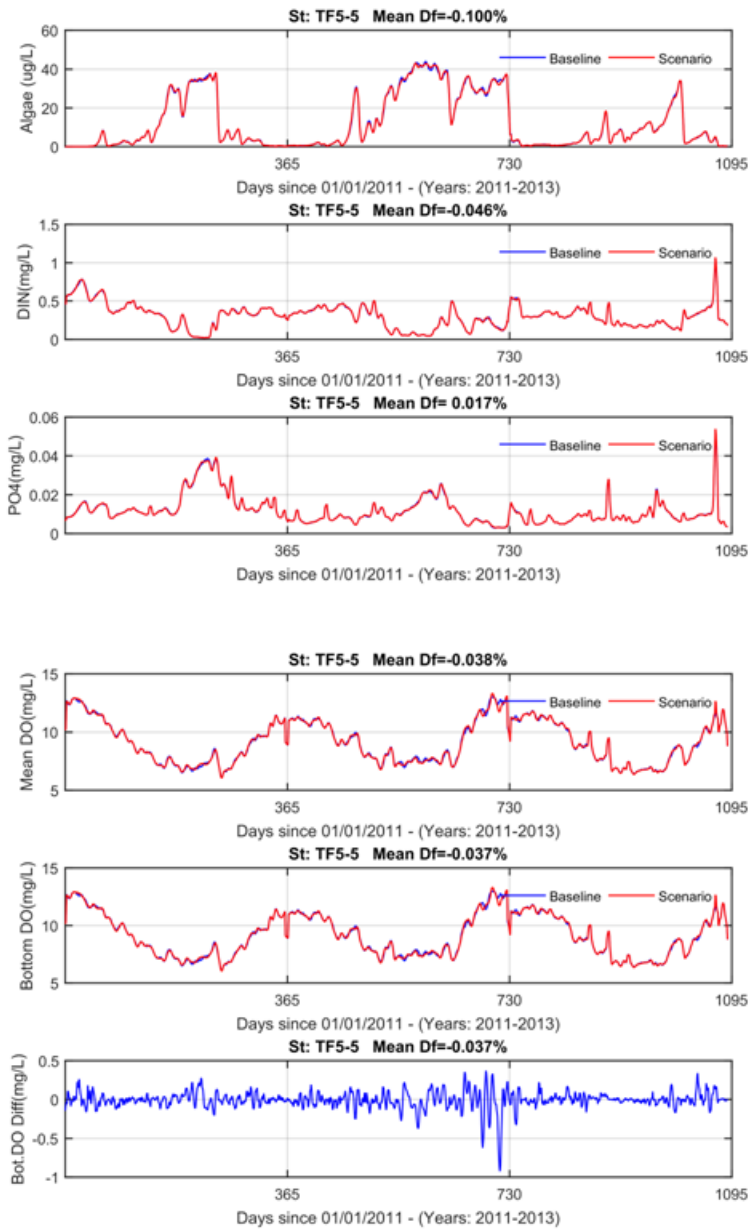
In the following plots. The Baseline is the results of baseline2 and Scenario is Scenario of 3-2.

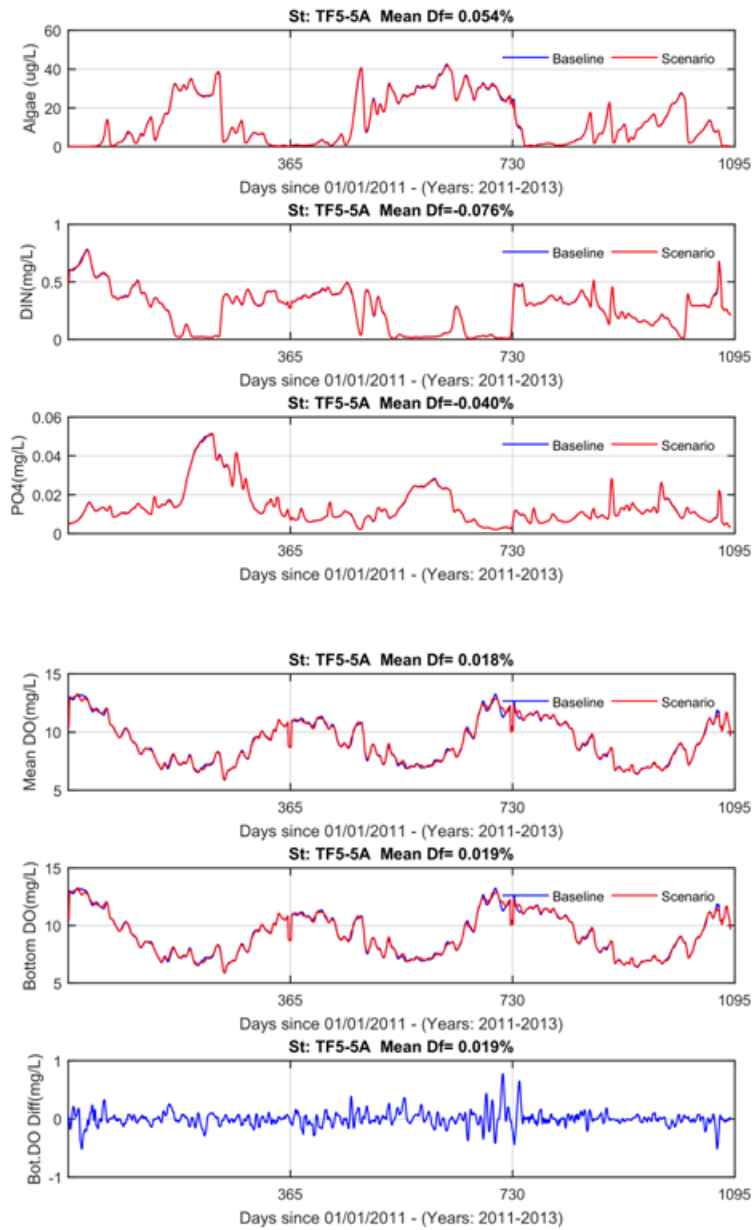


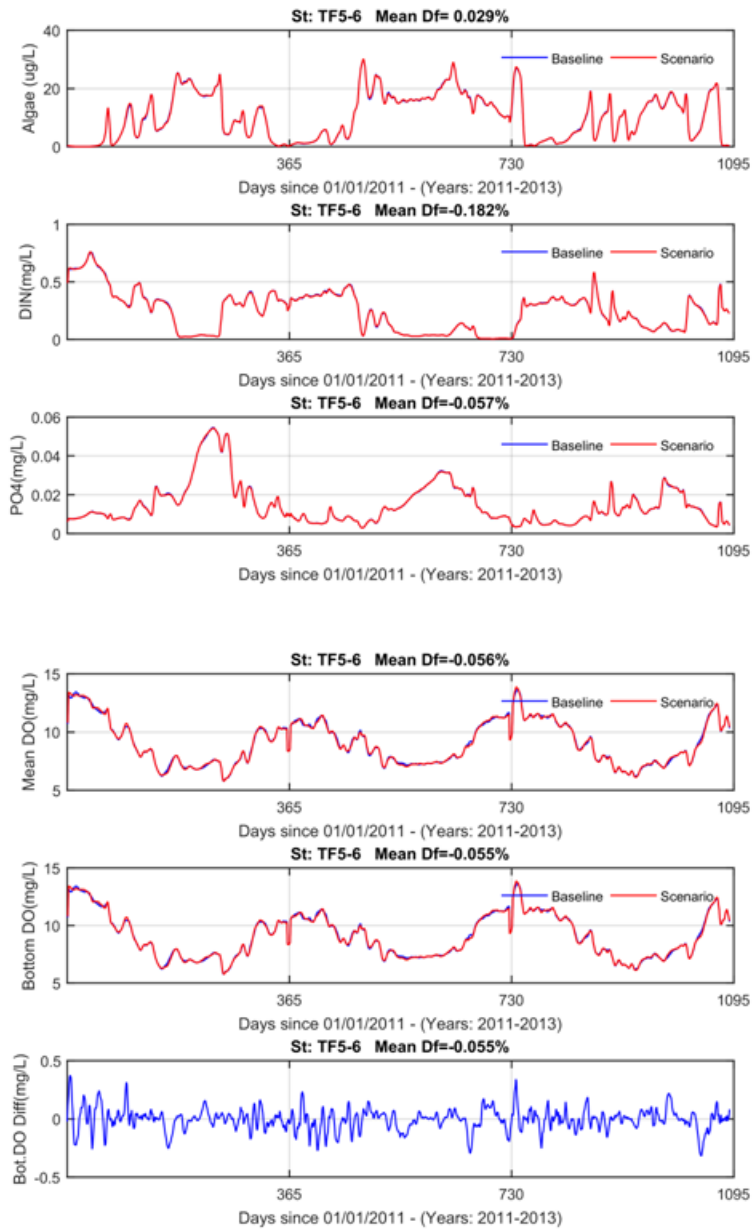


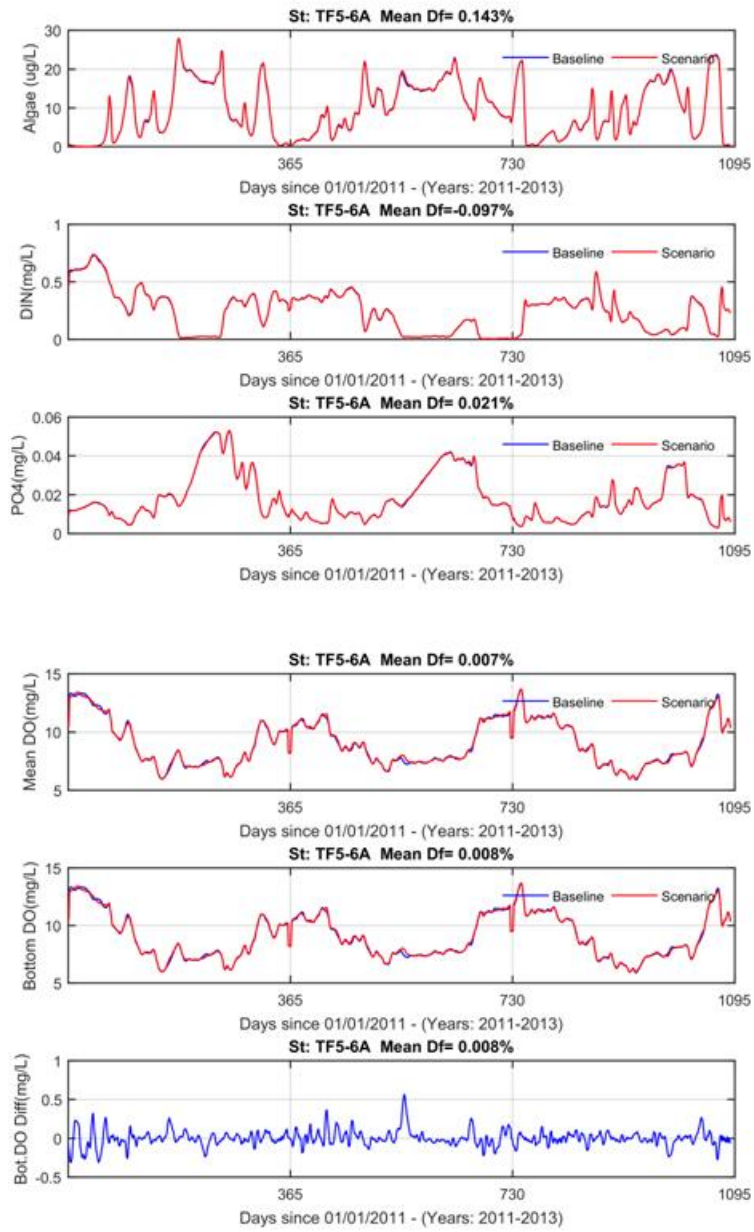


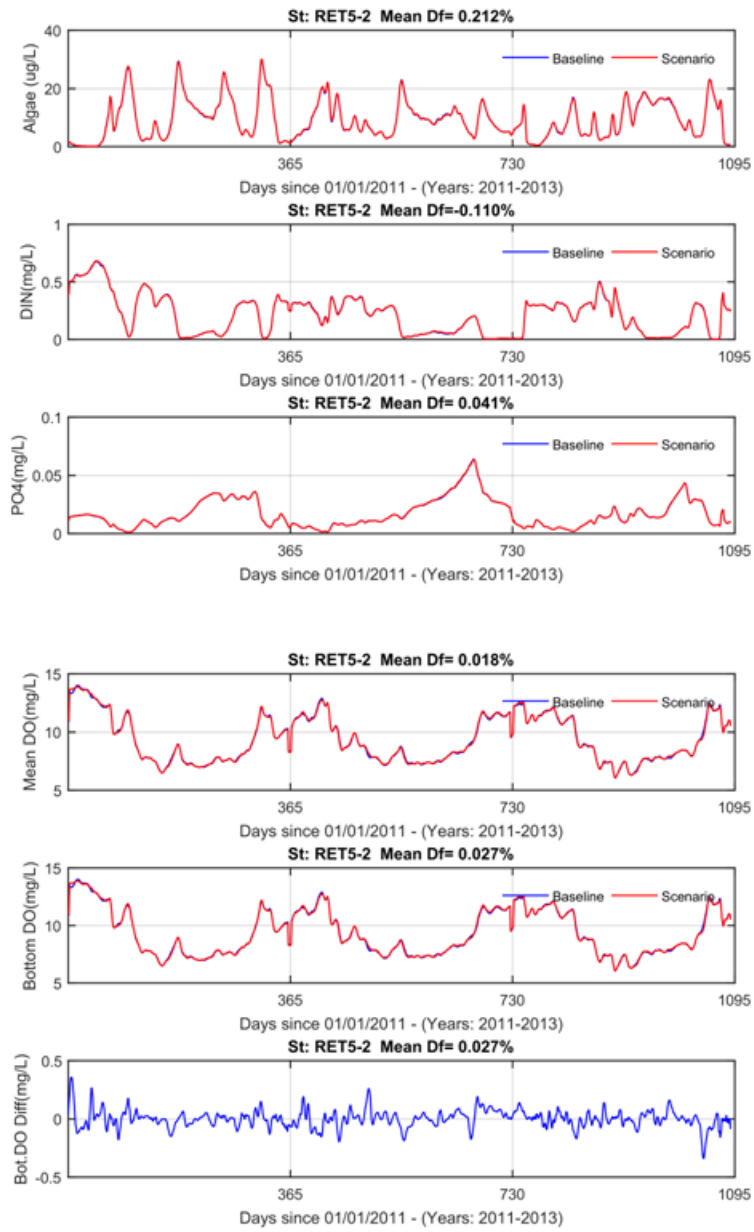


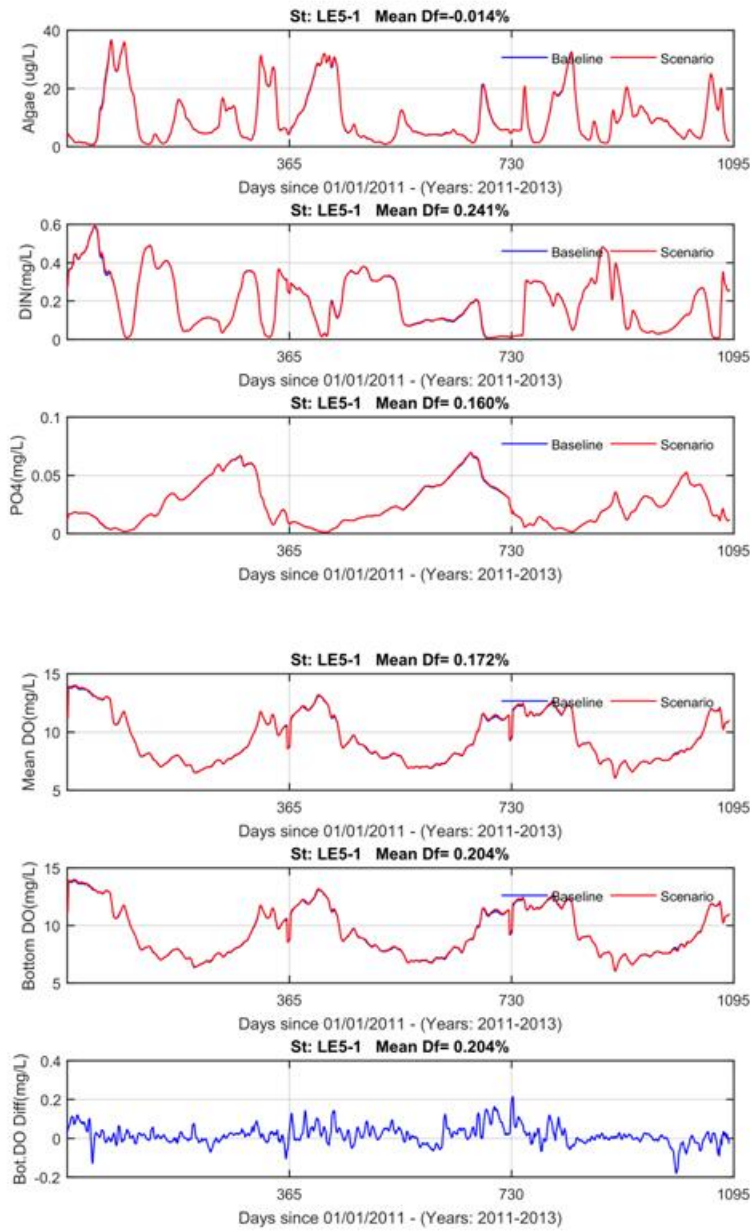


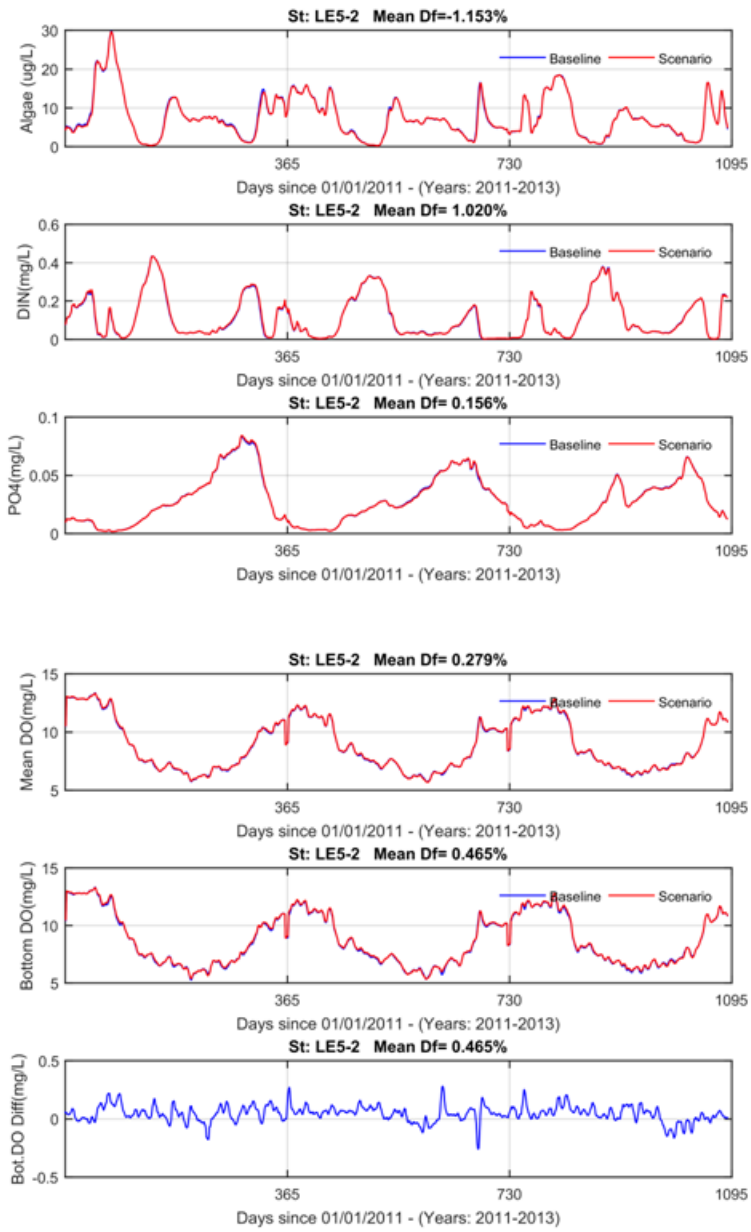


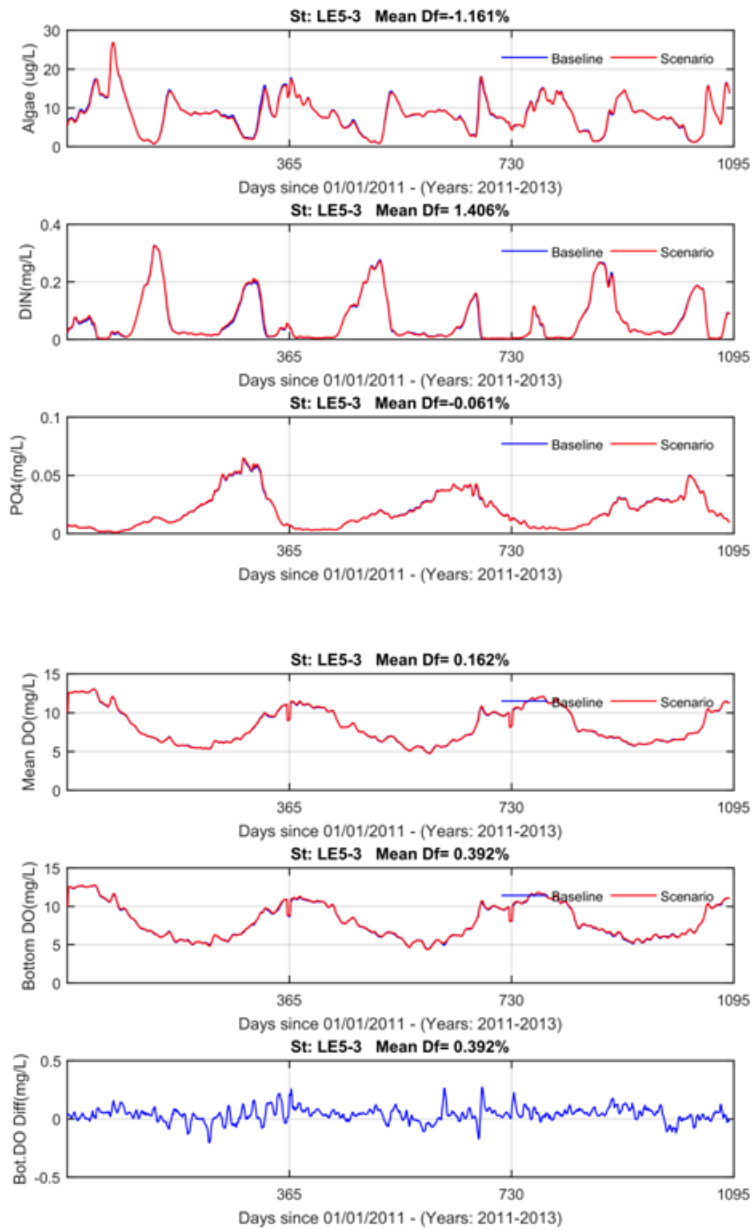


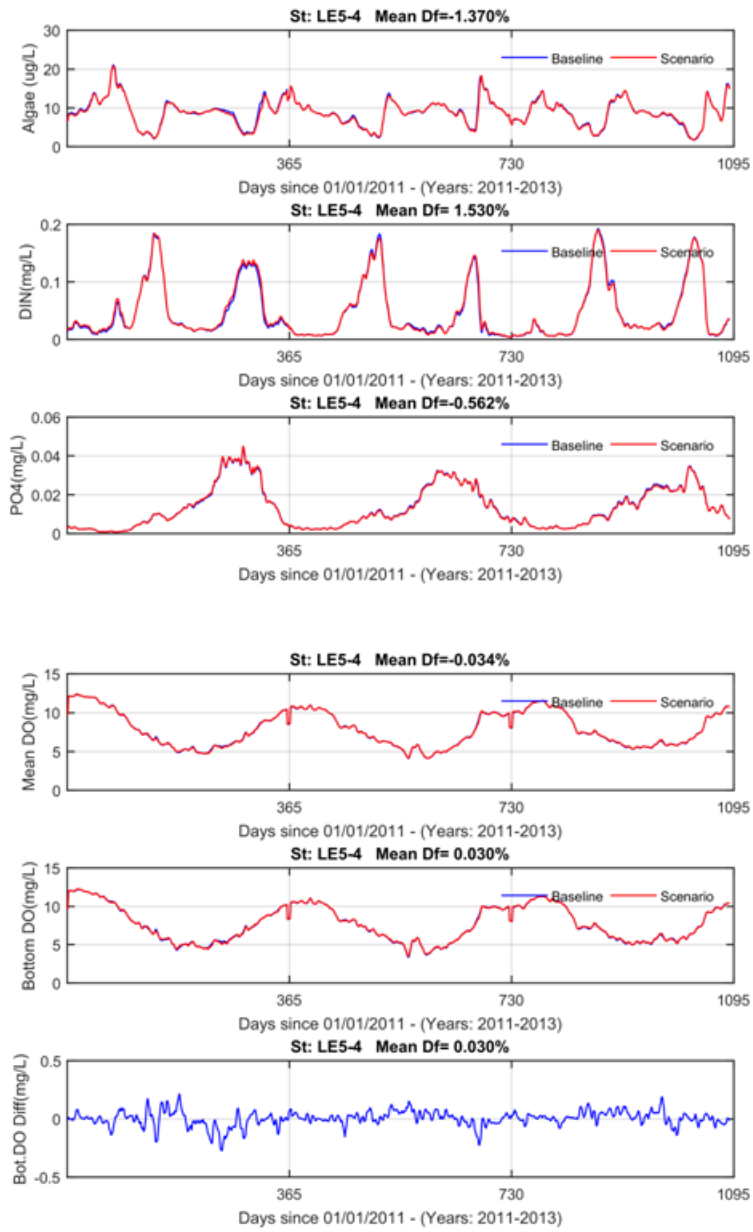


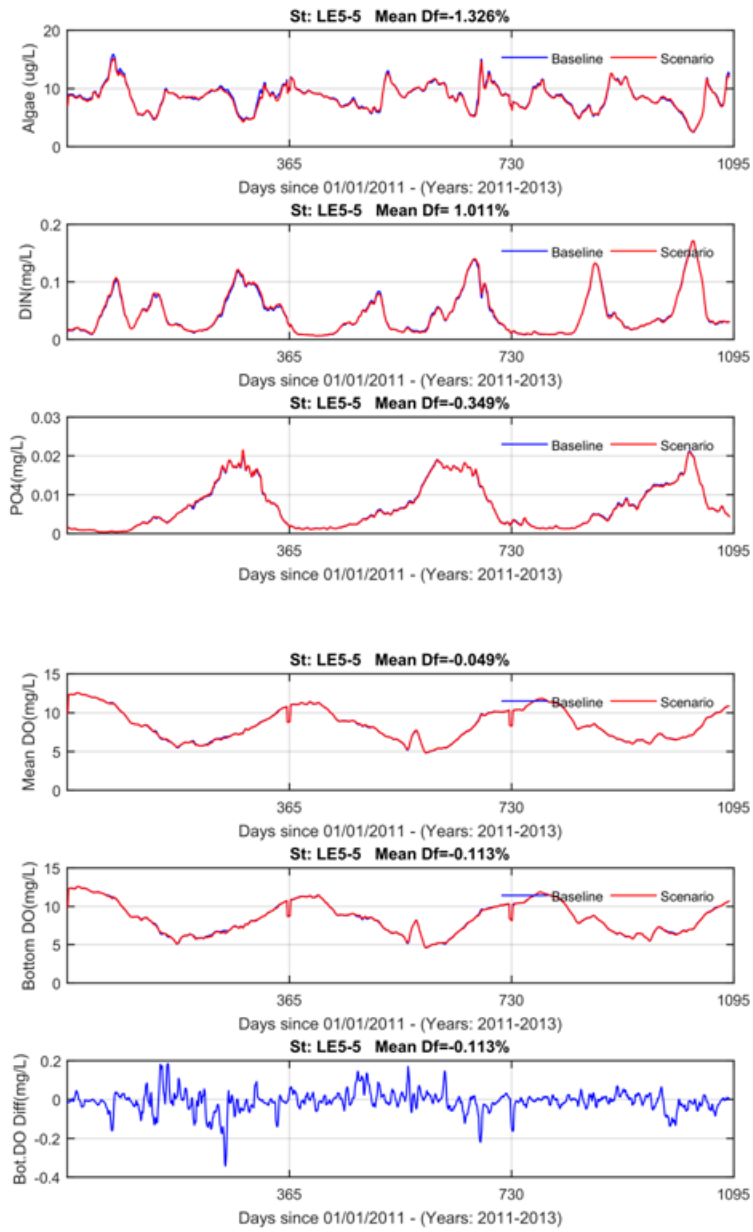


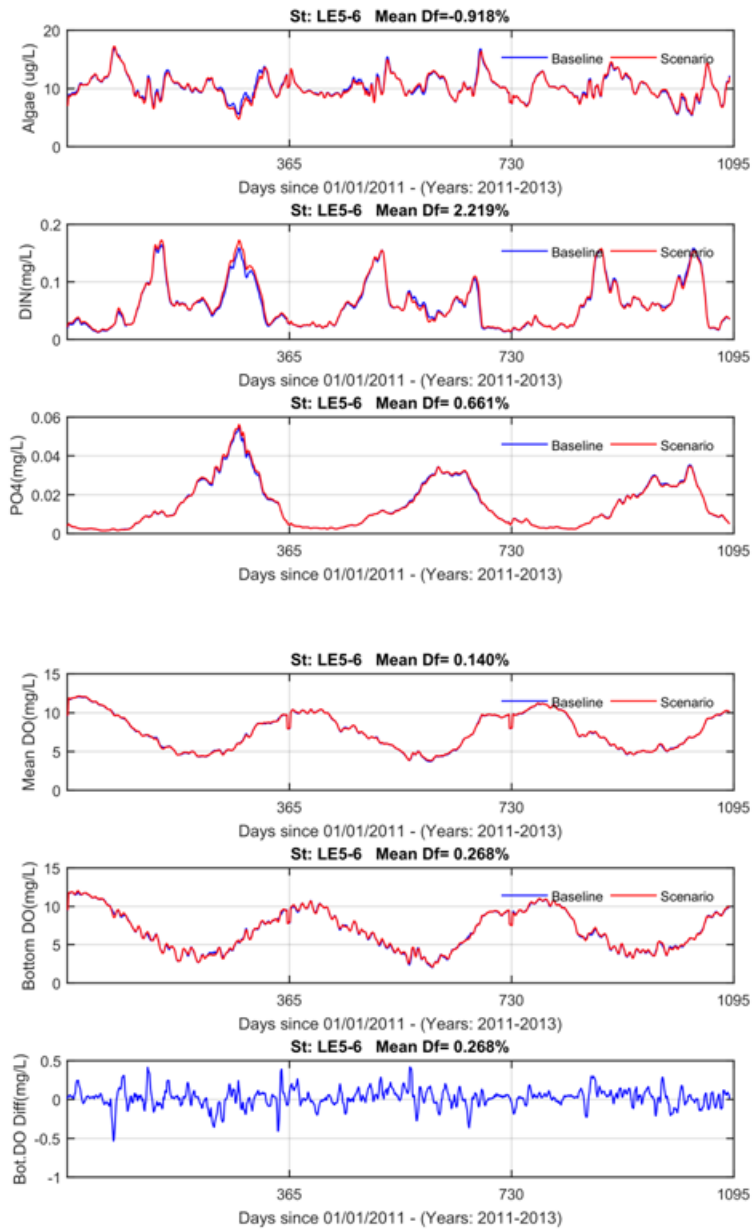


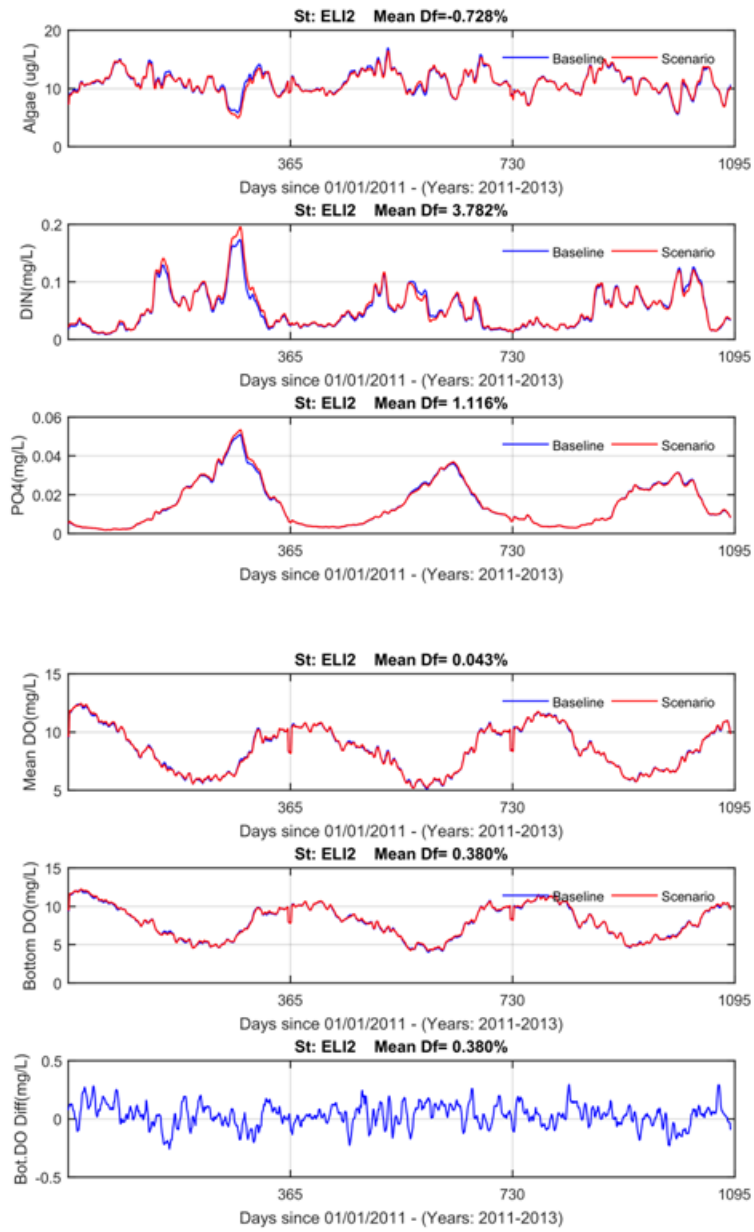


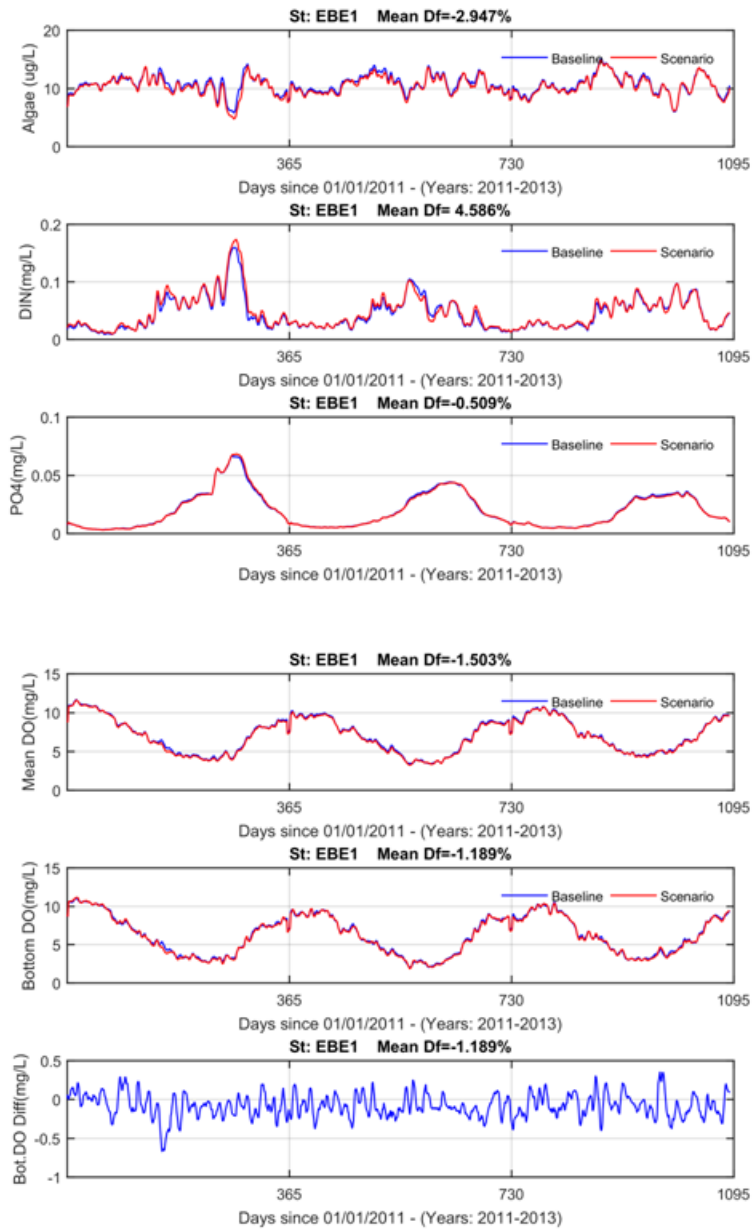


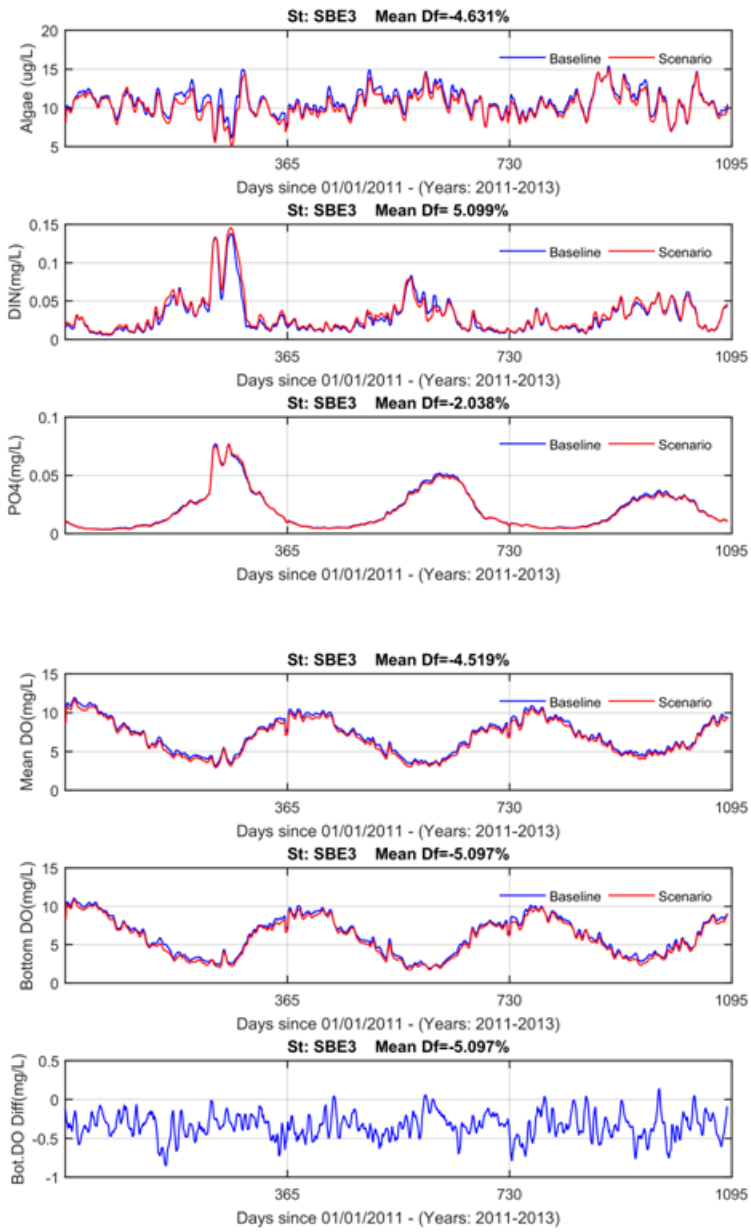


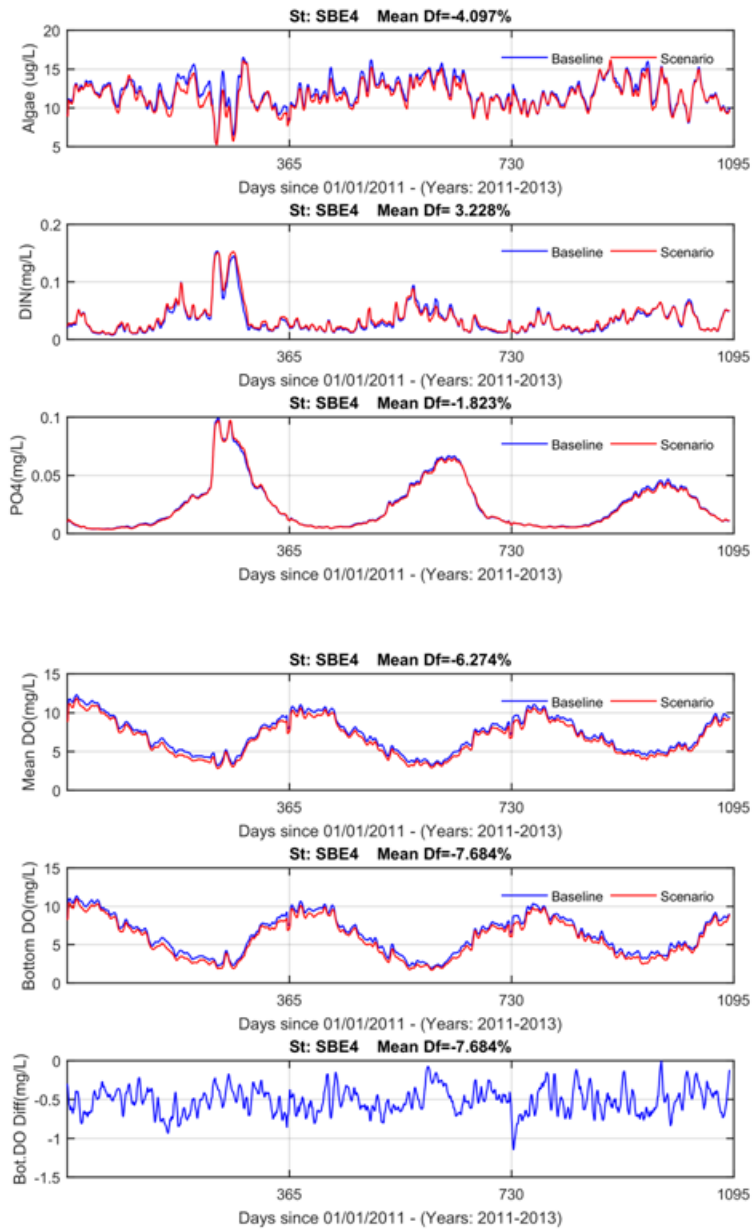


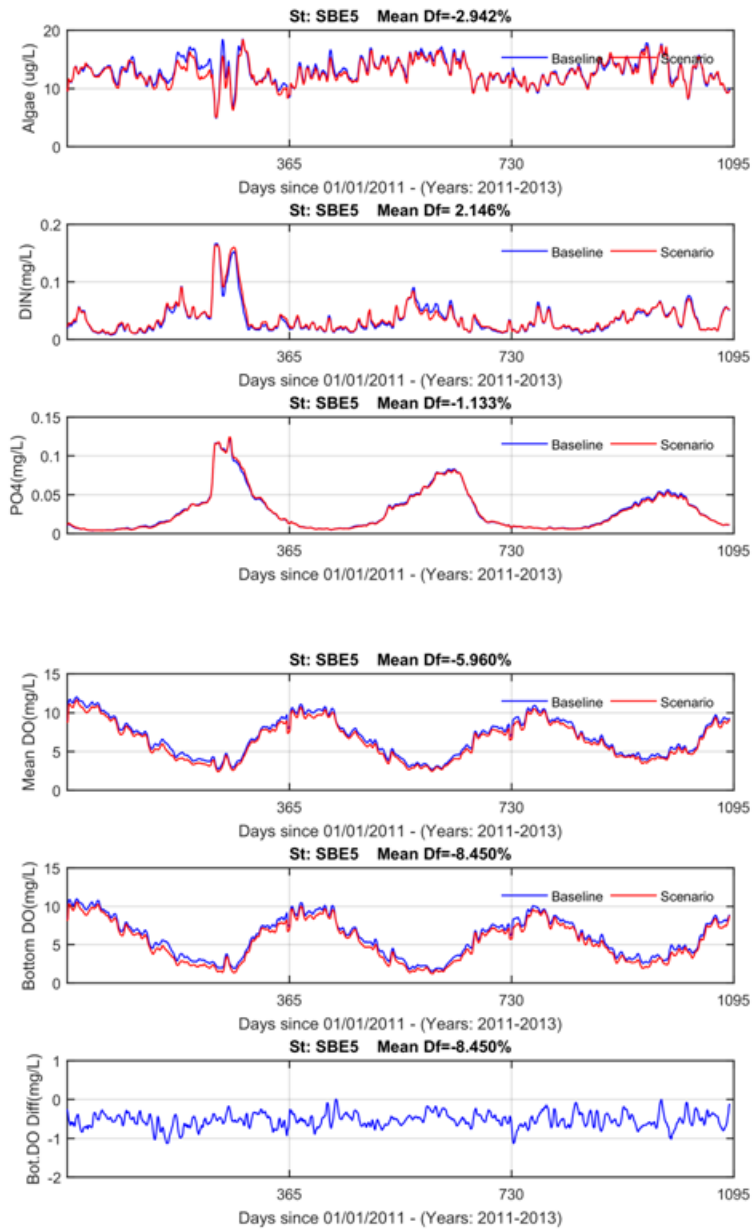


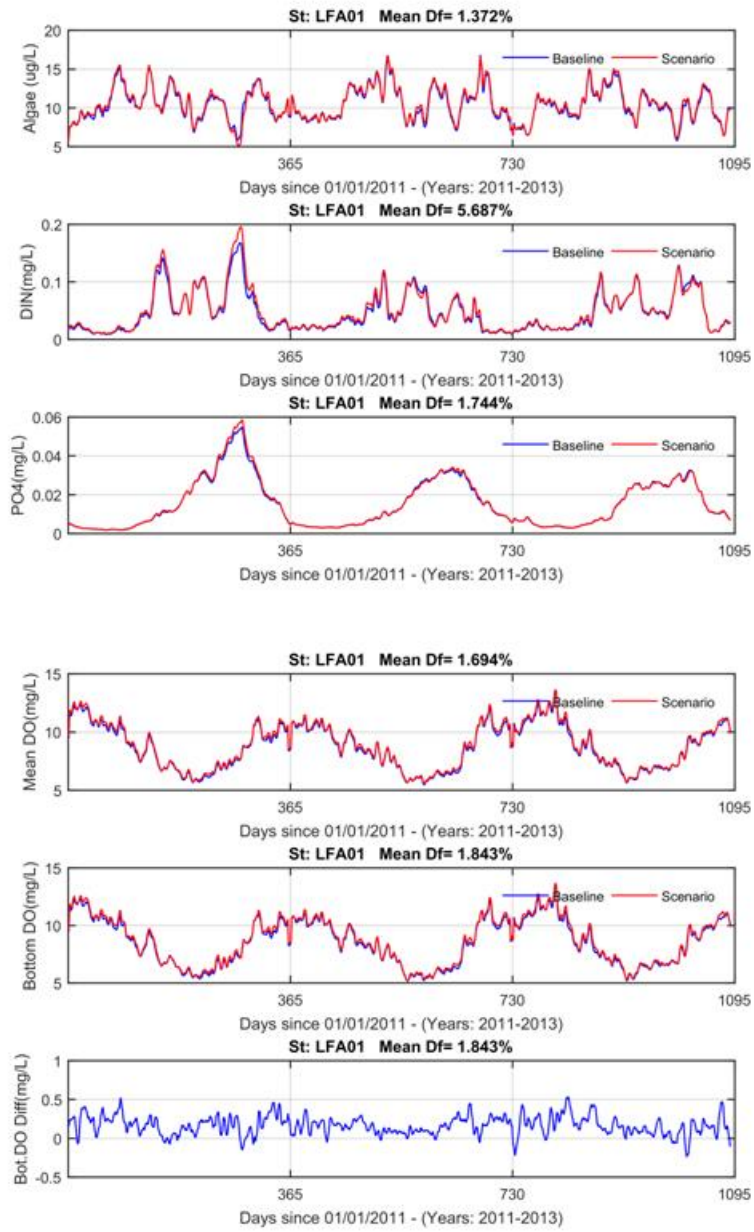


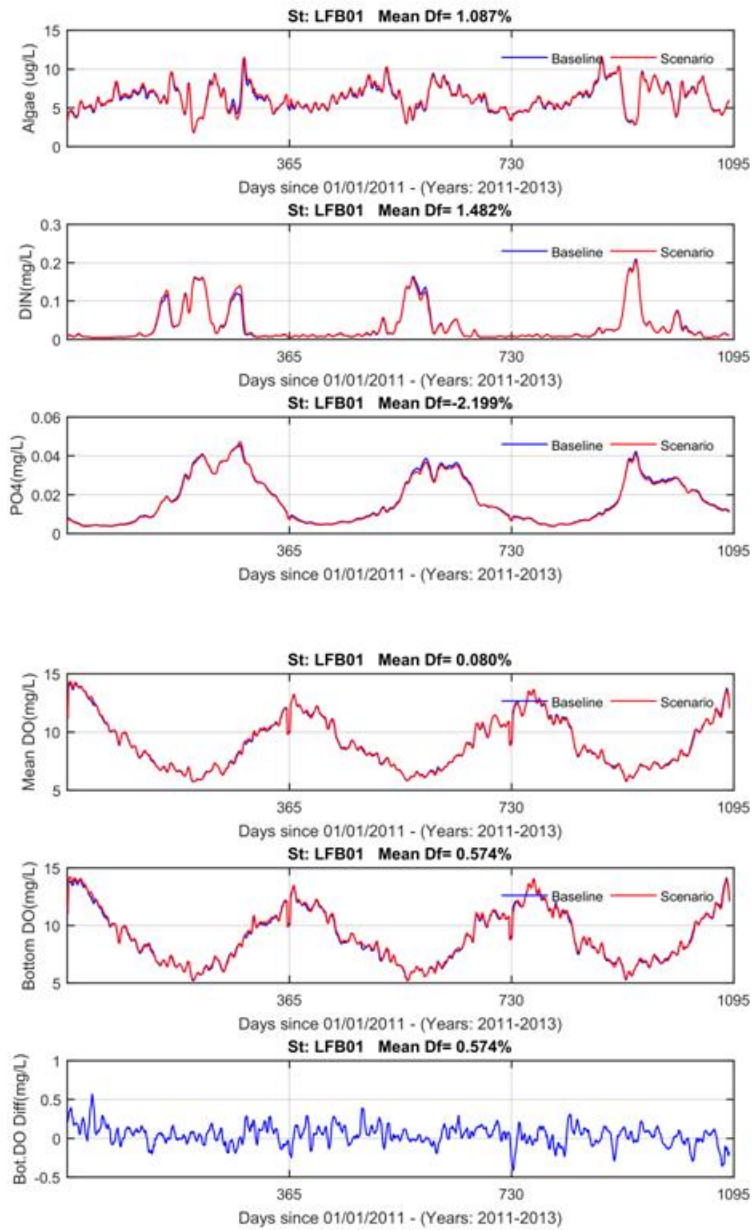


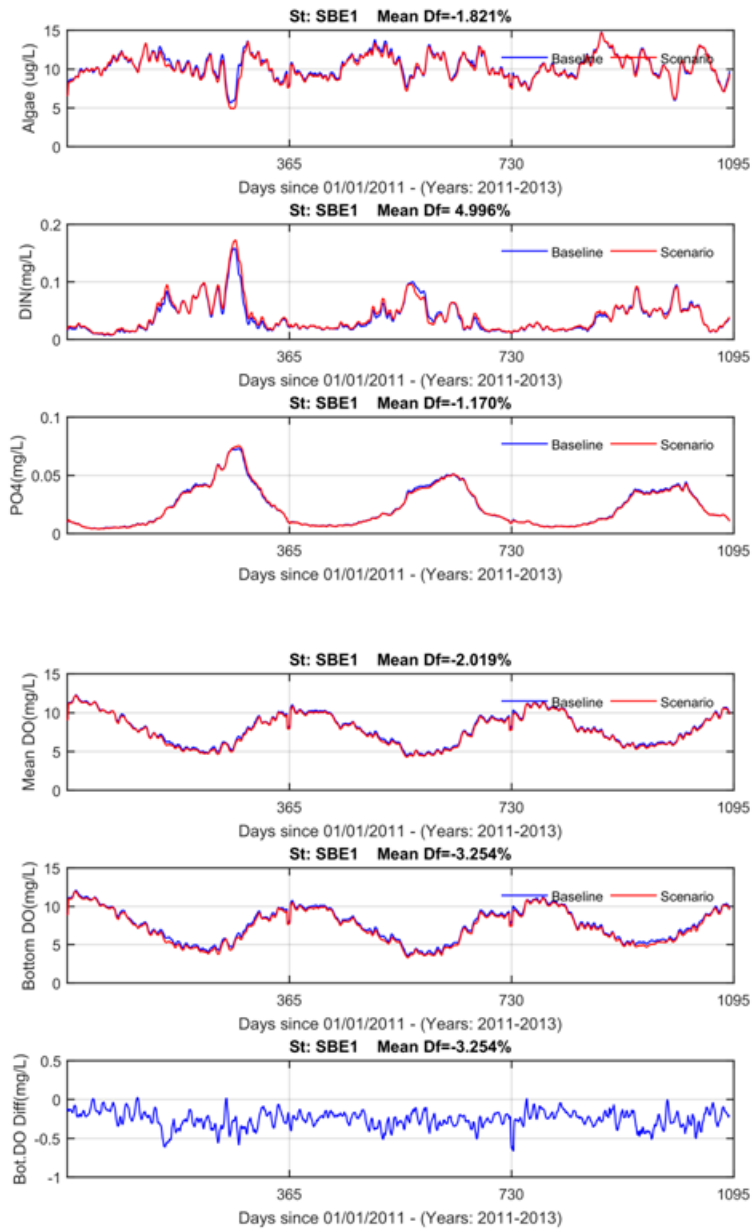


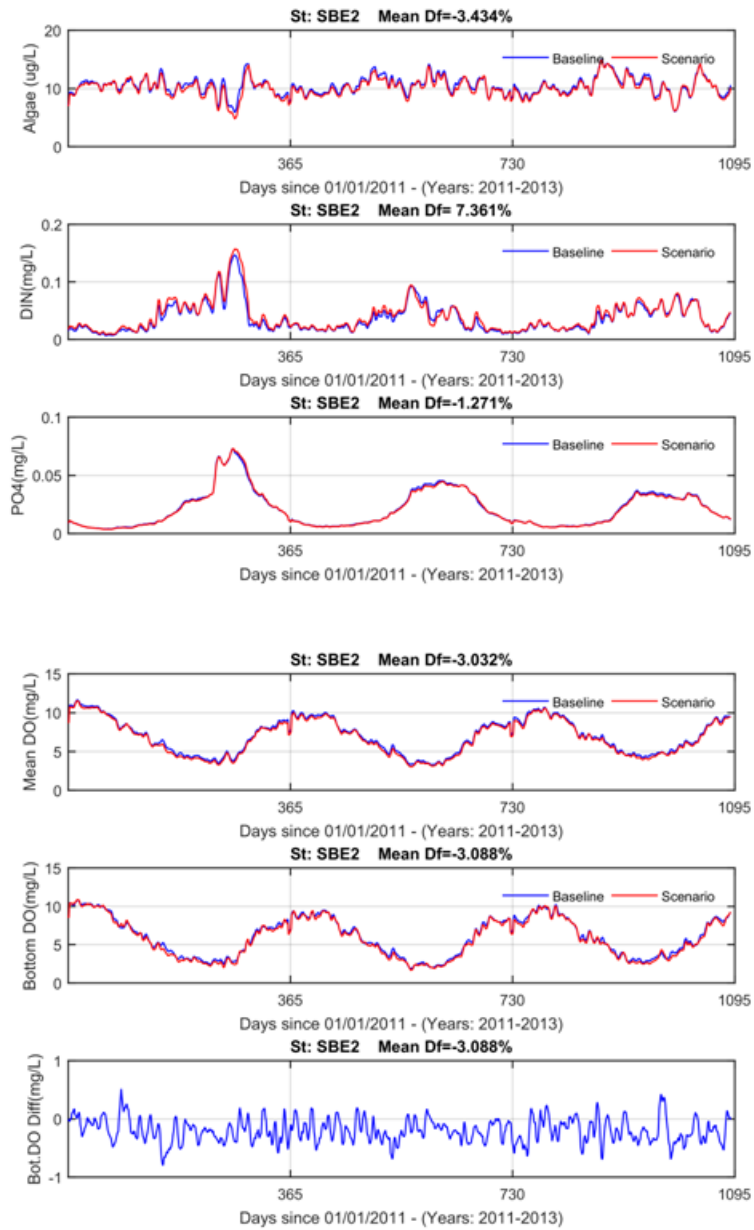


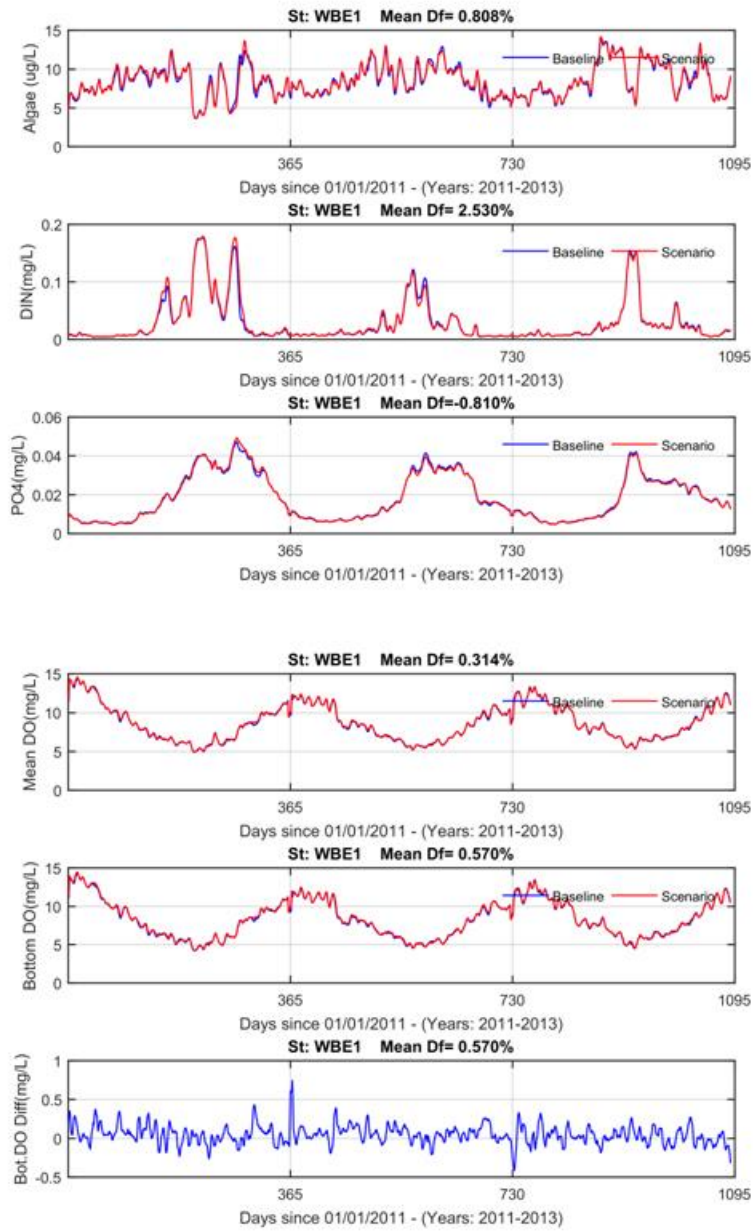






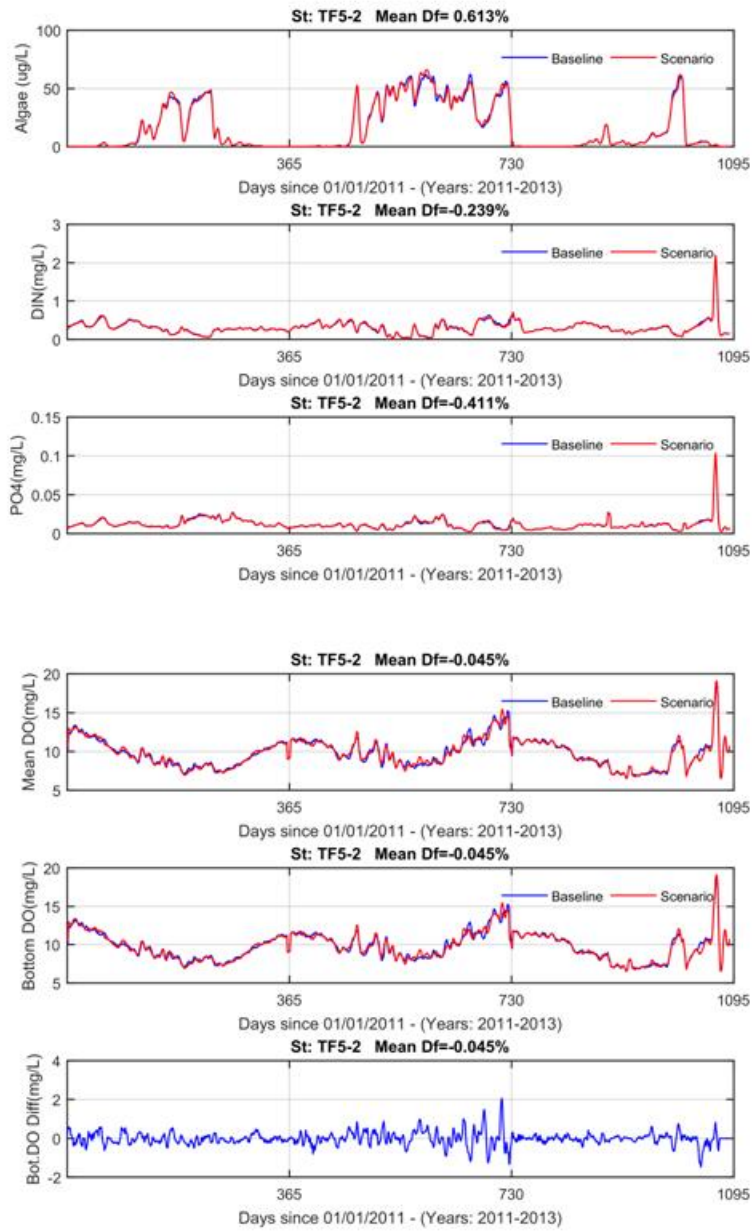


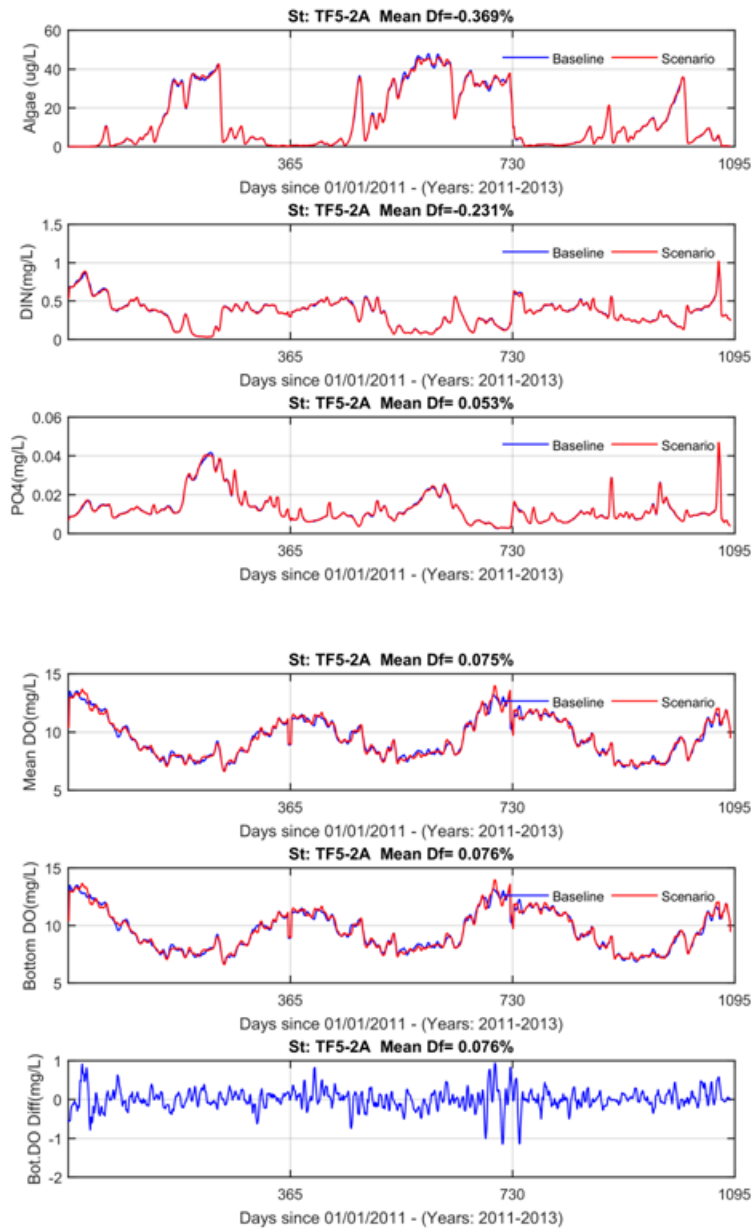


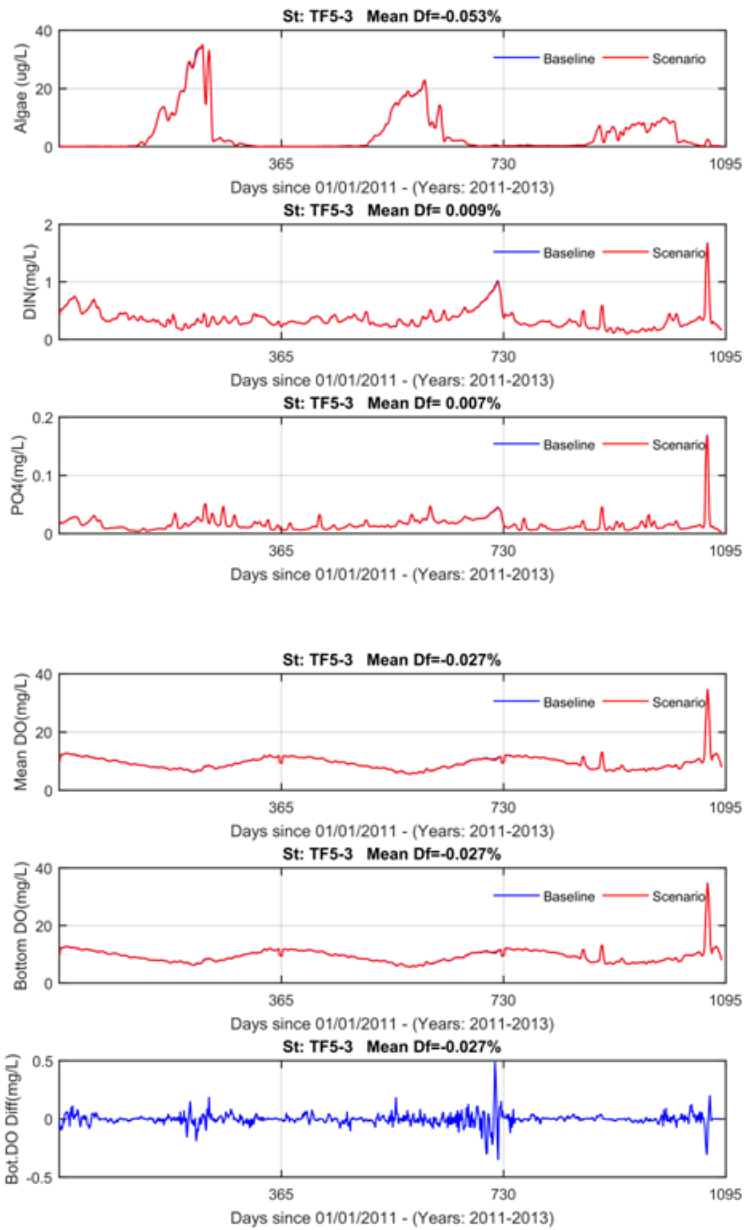


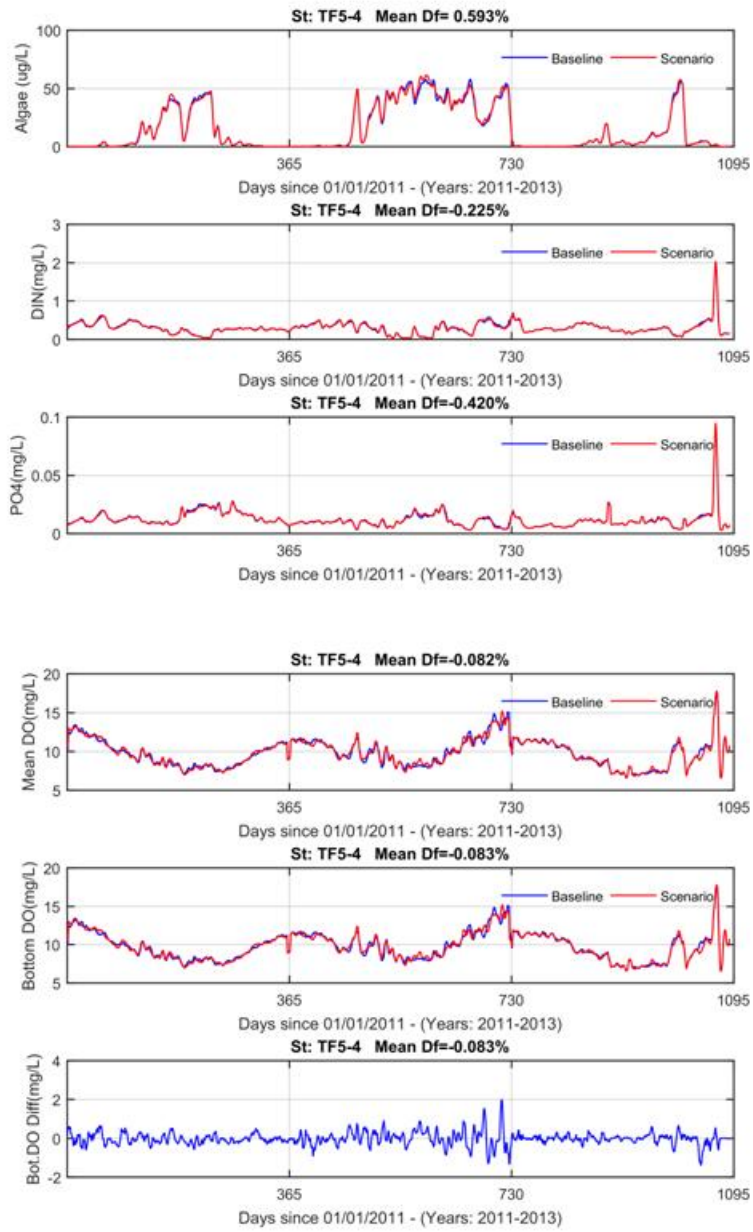
Model Simulation Baseline2 and Scenario 4-2

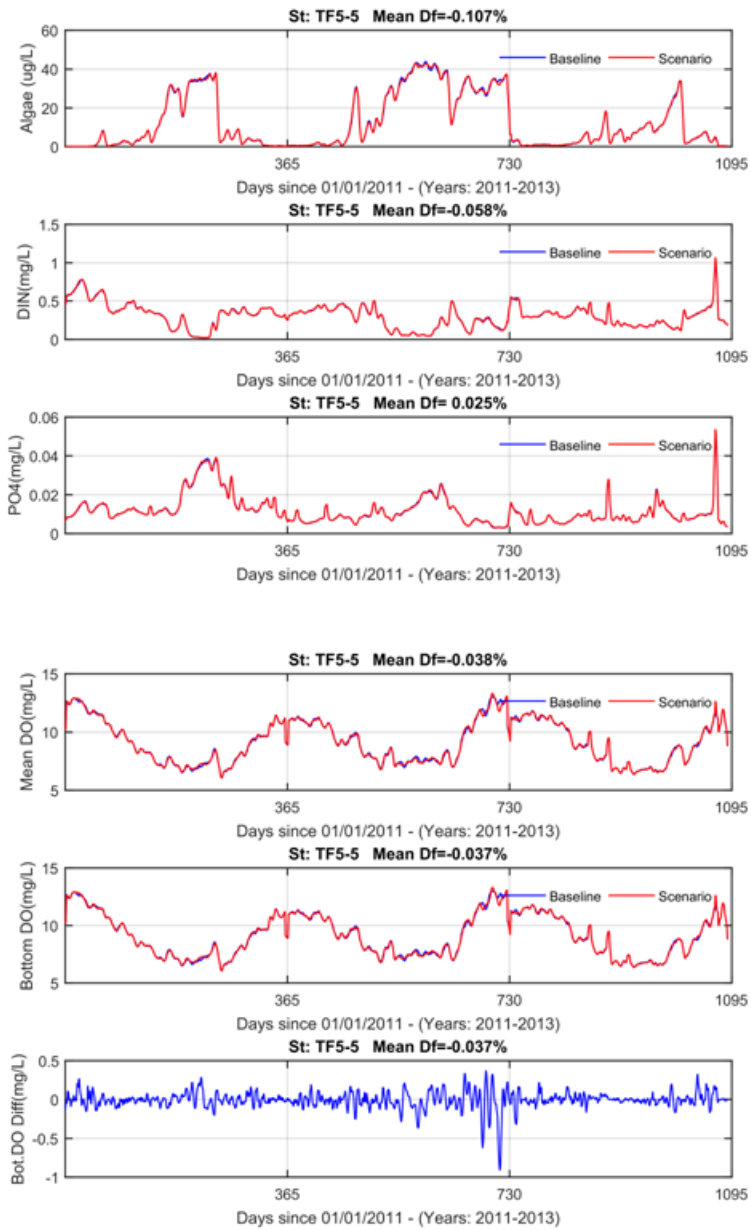
In the following plots. The Baseline is the results of baseline2 and Scenario is Scenario of 4-2.

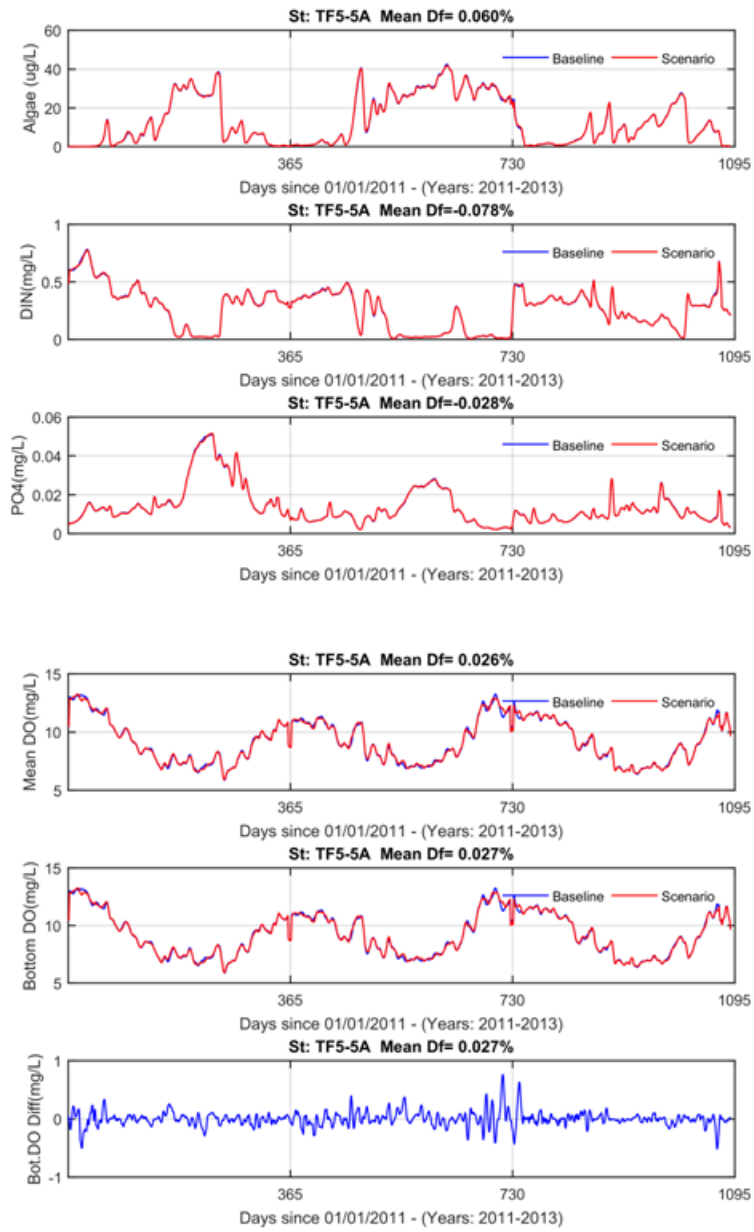


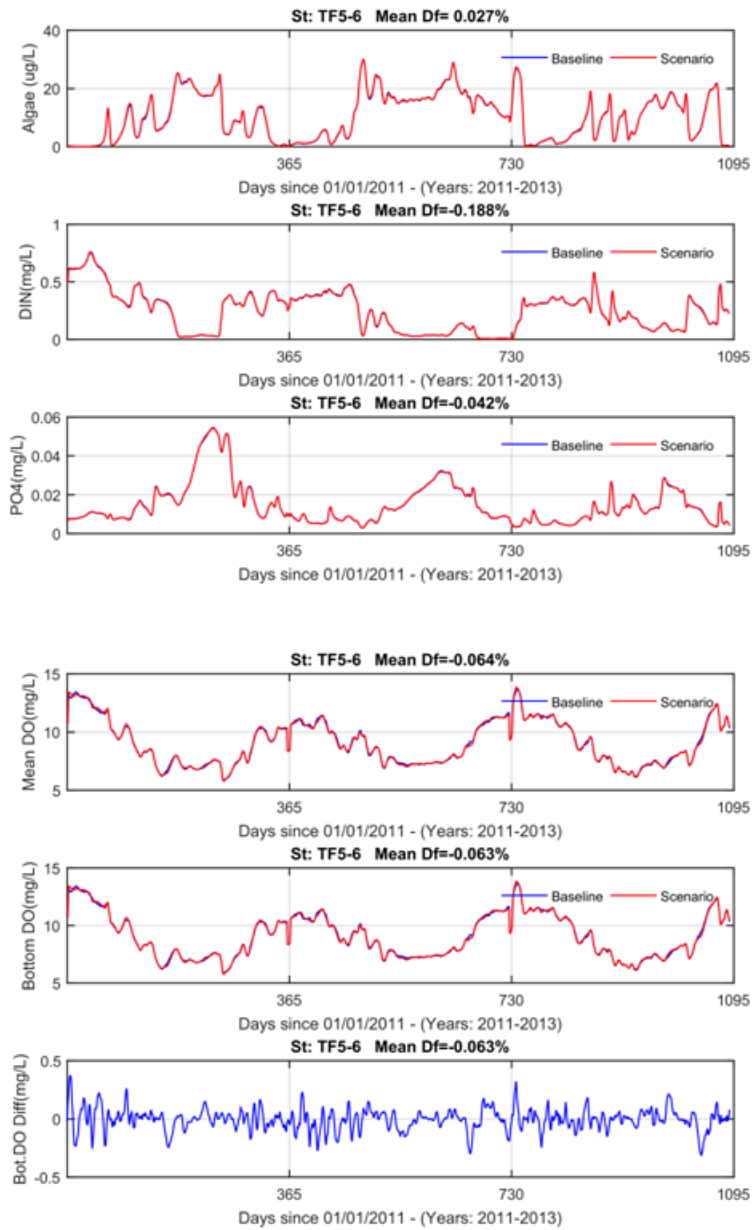


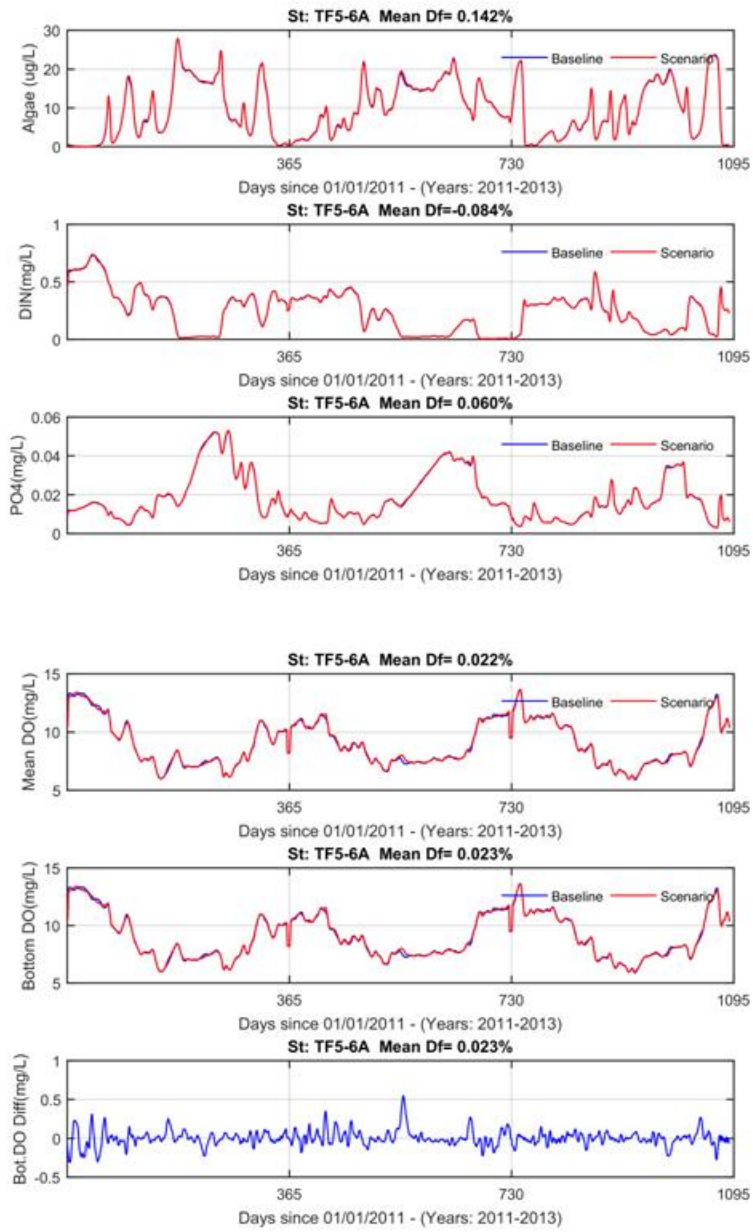


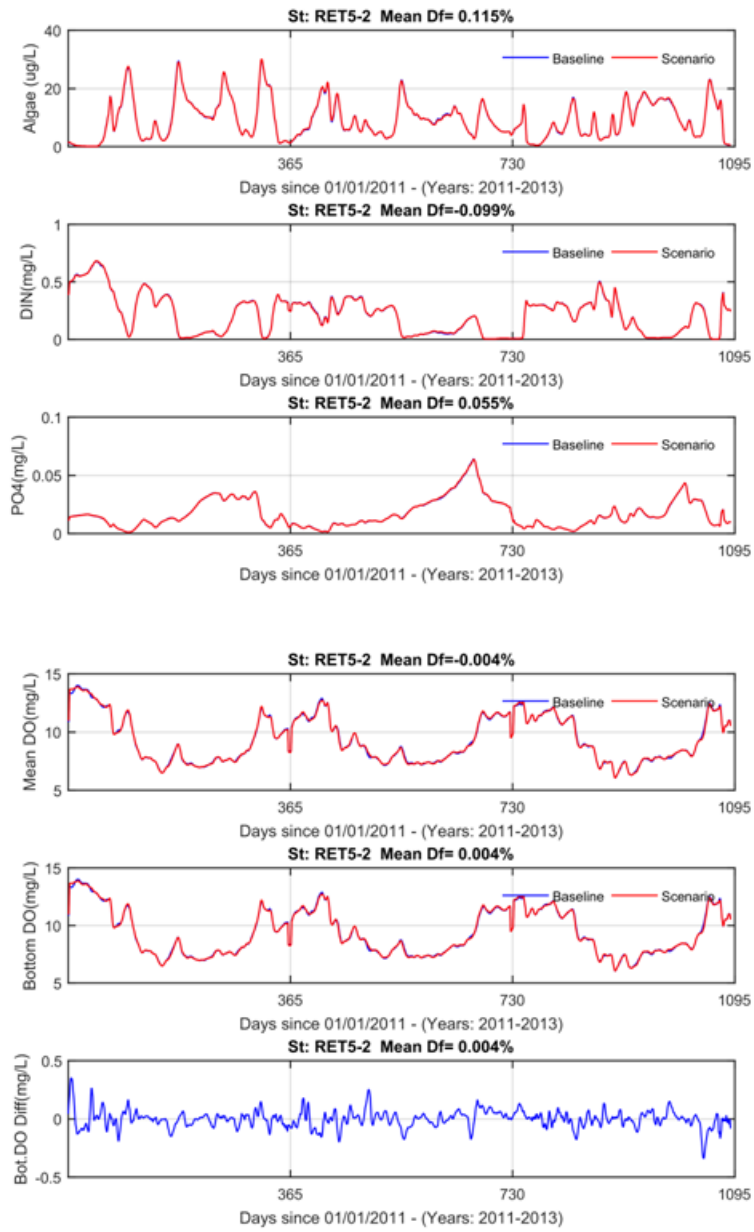


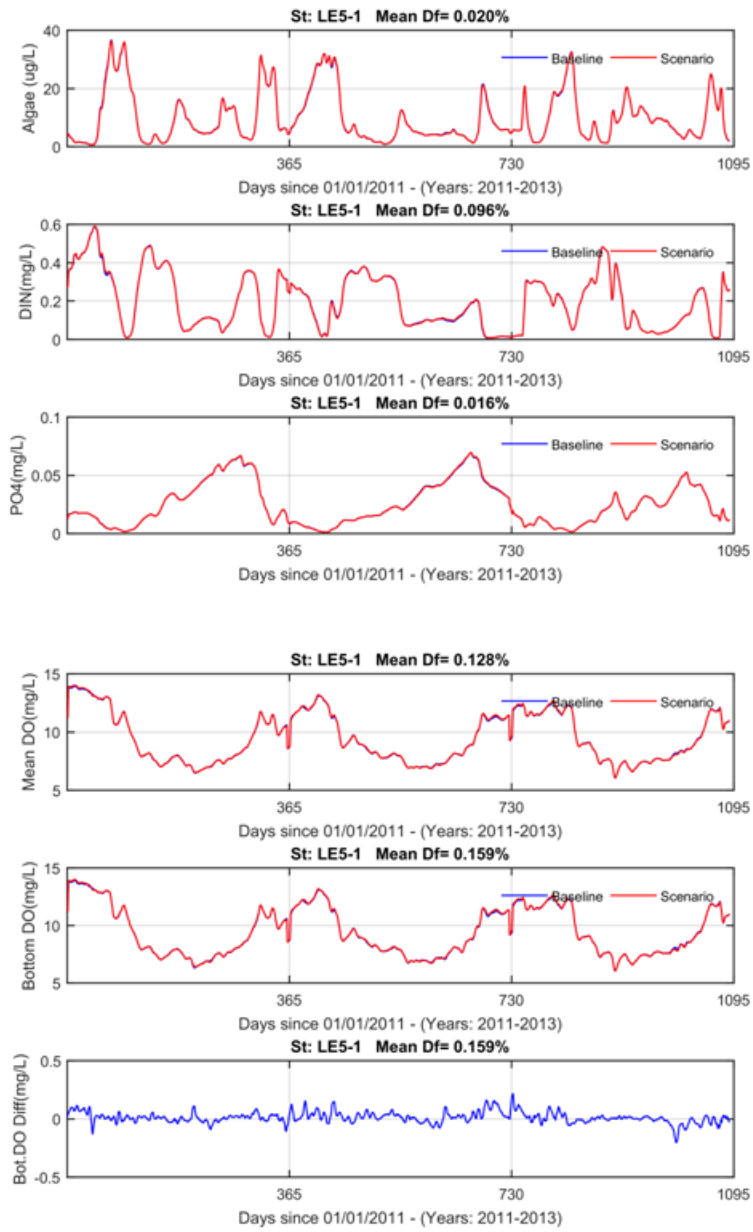


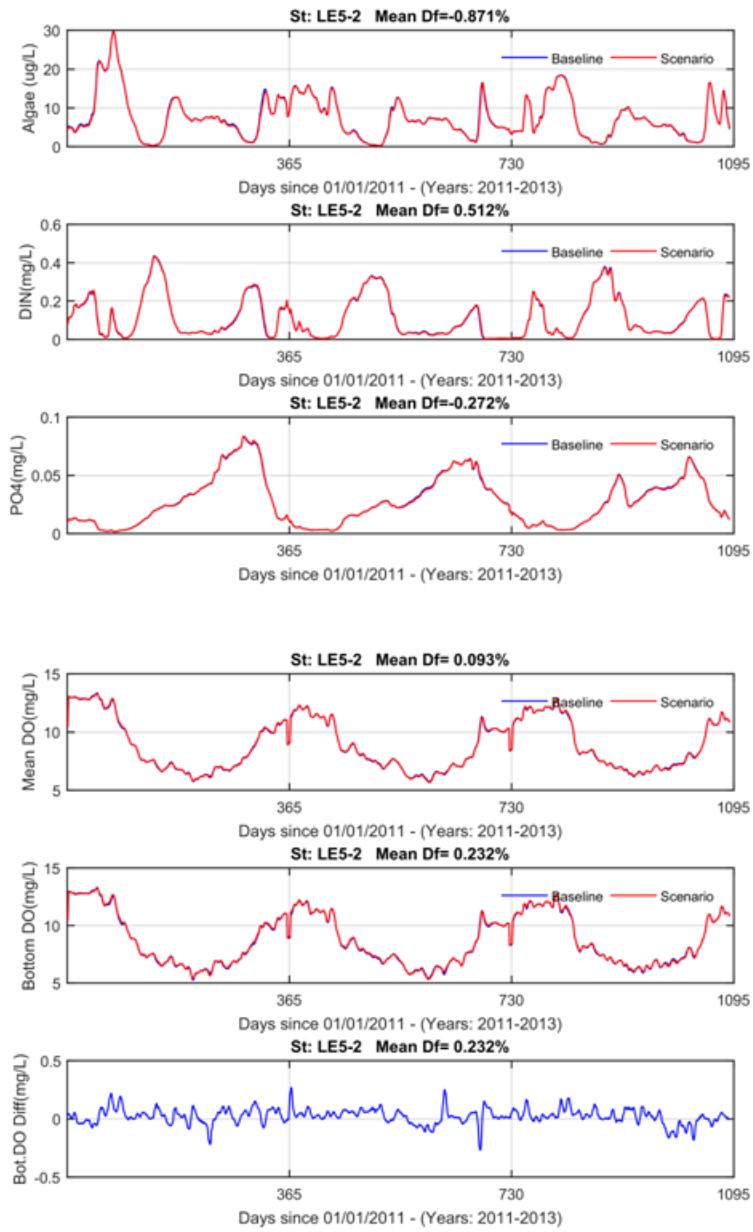


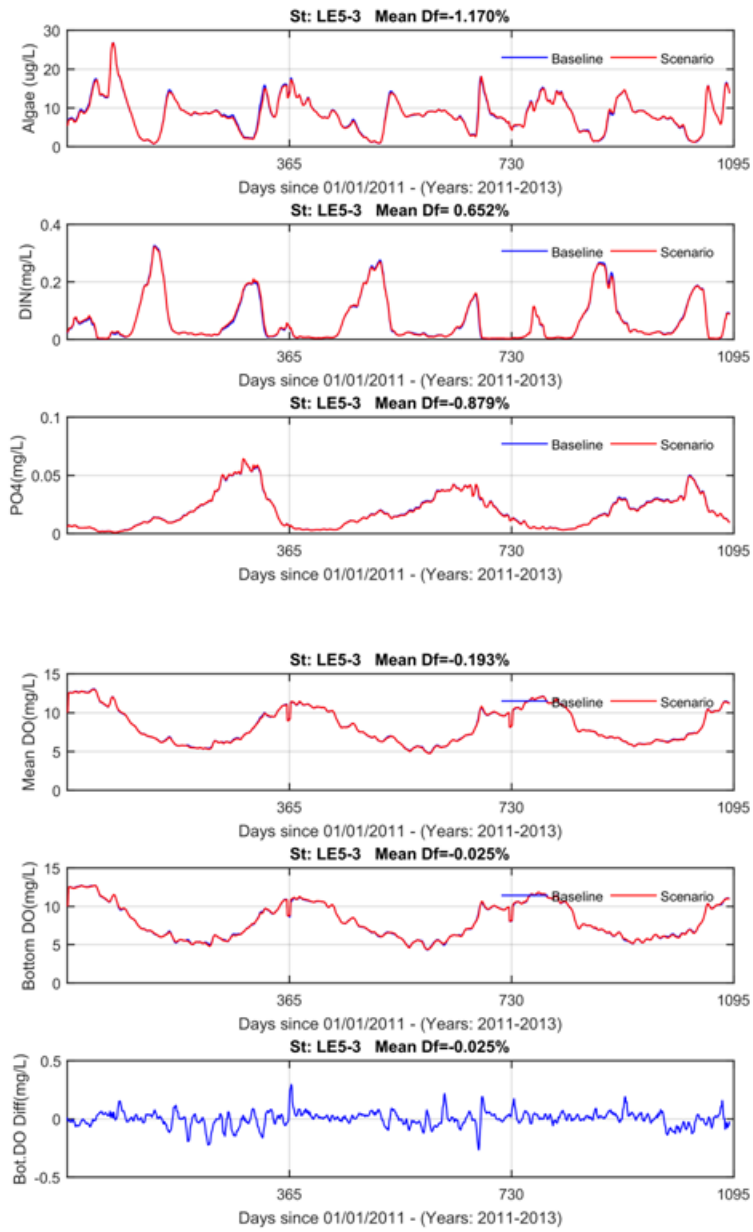


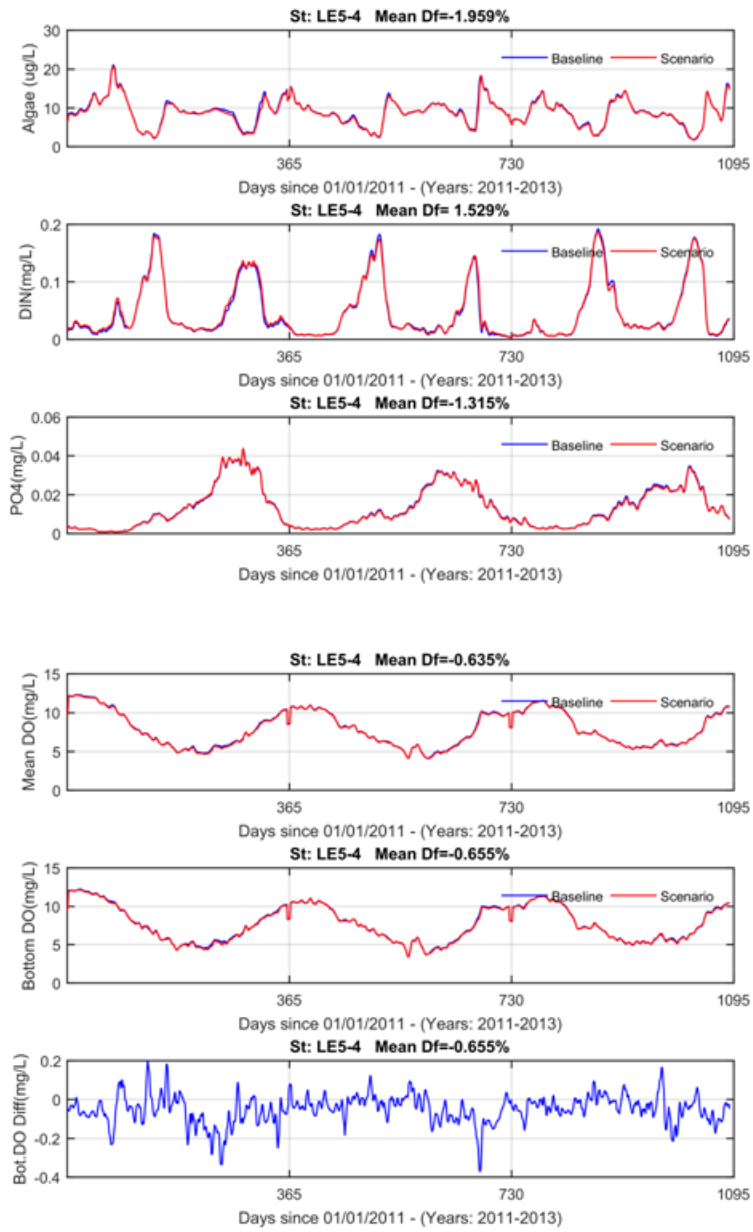


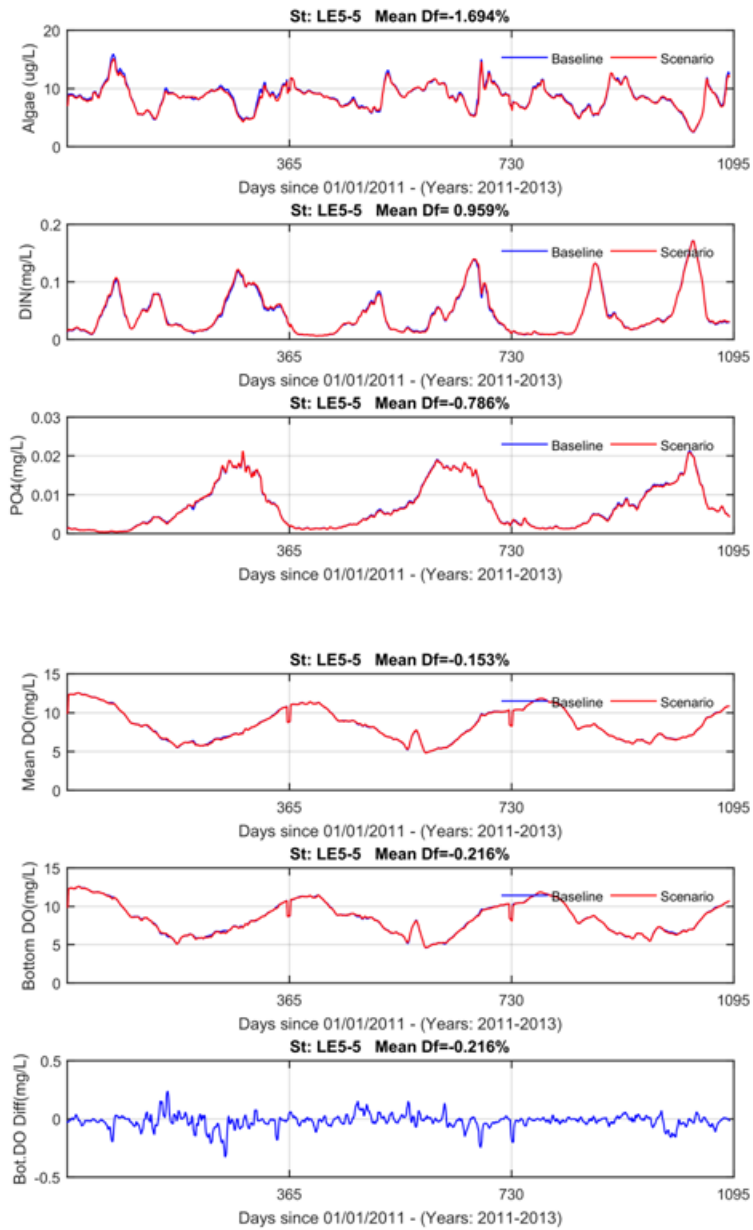


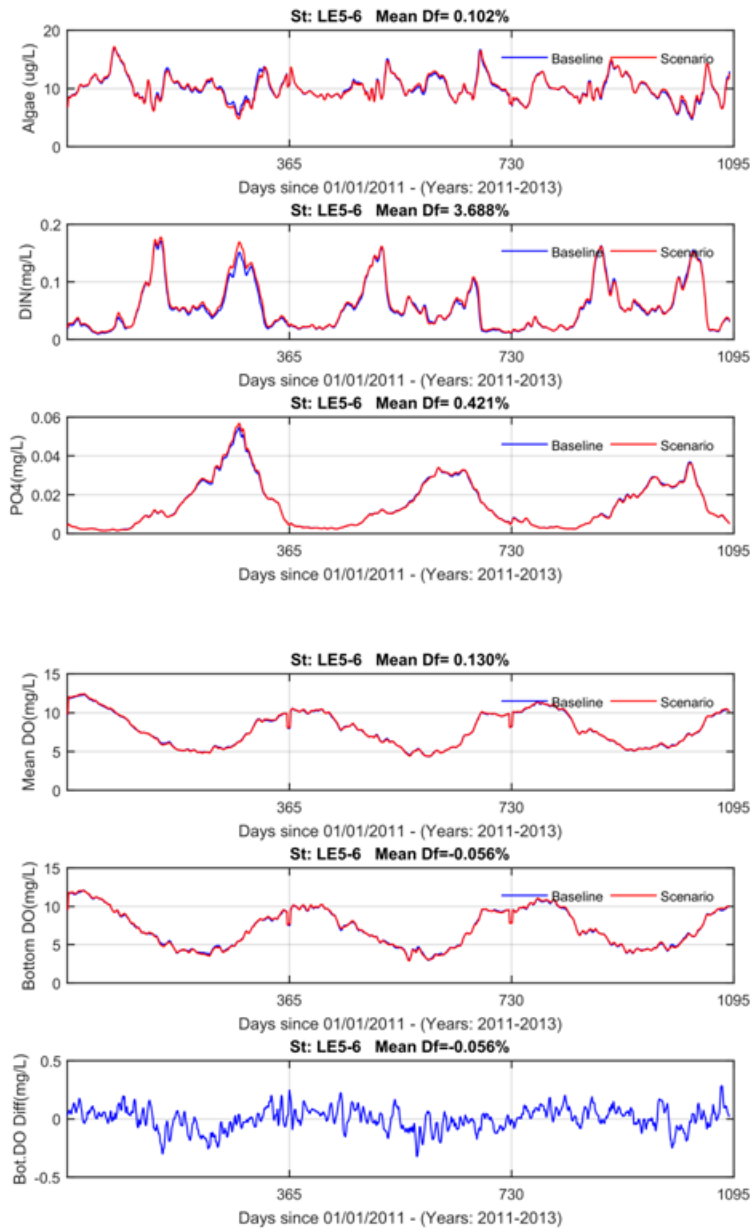


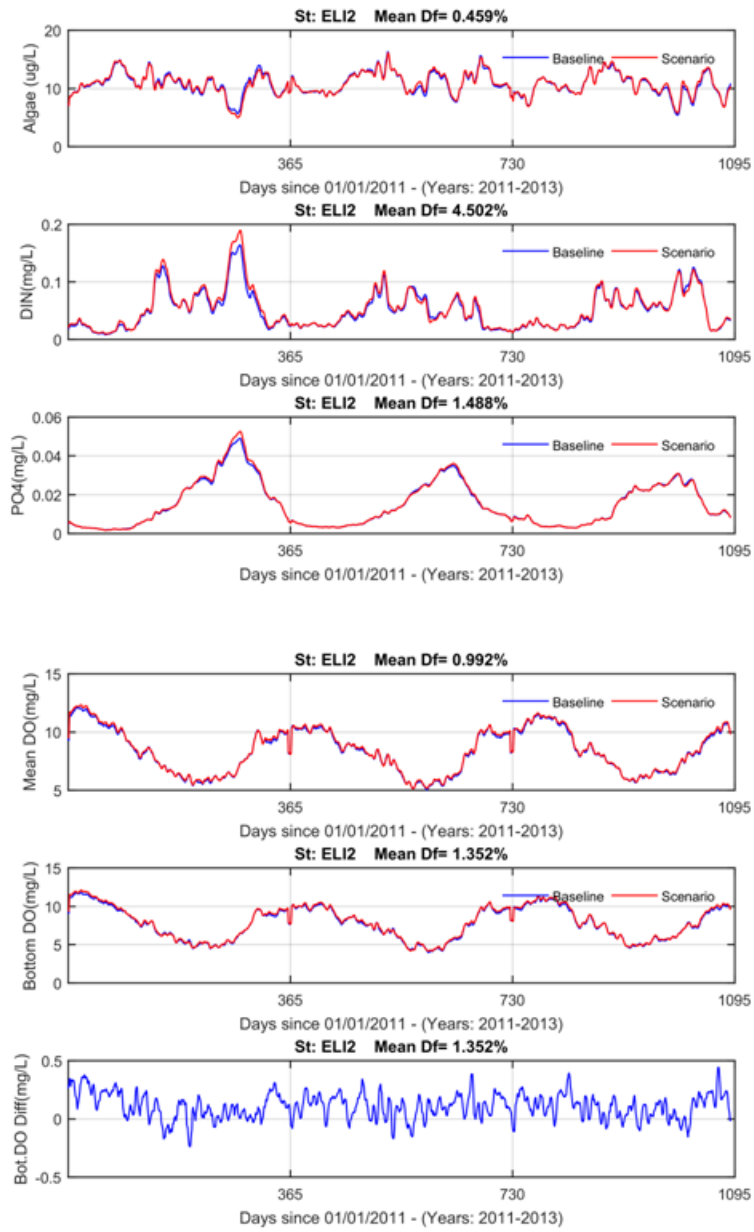


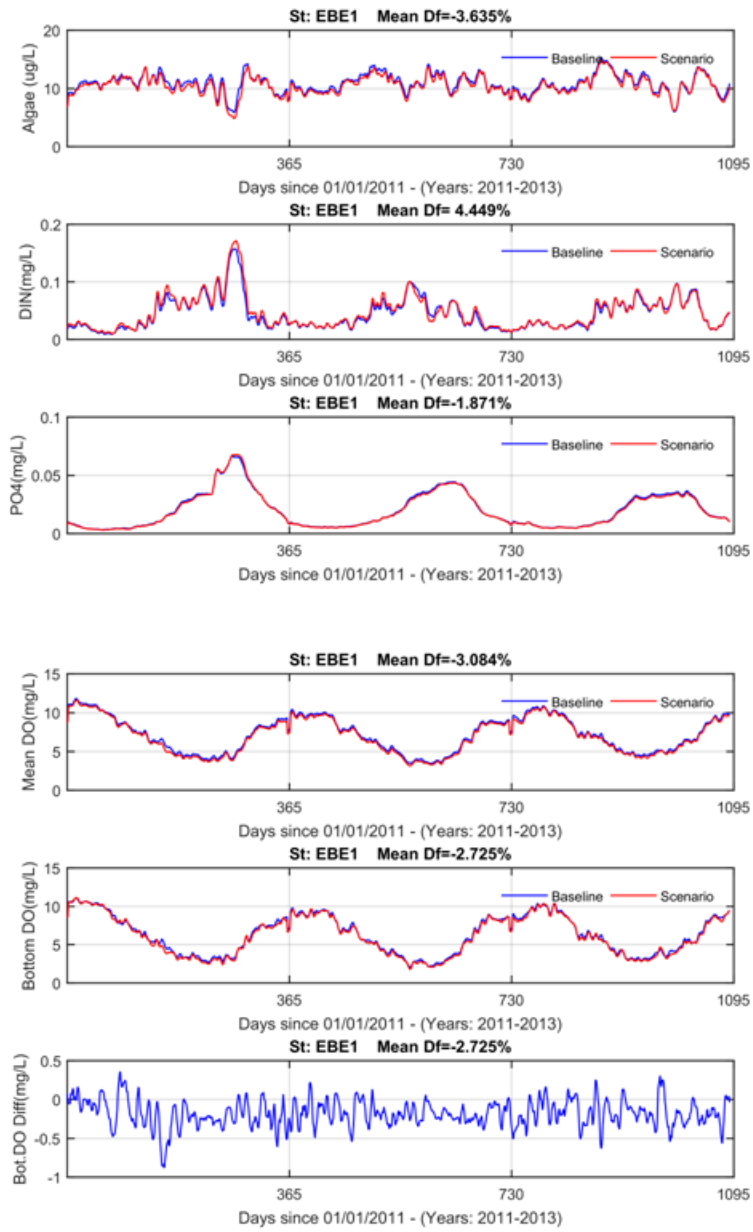


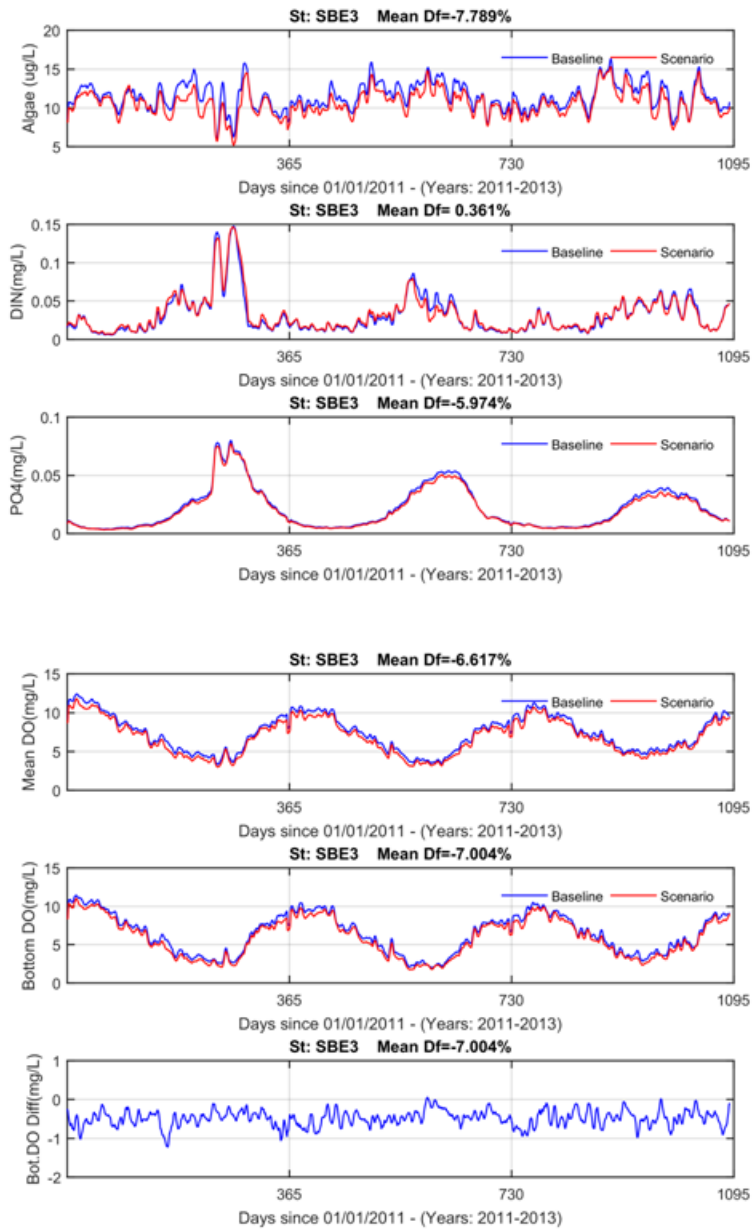


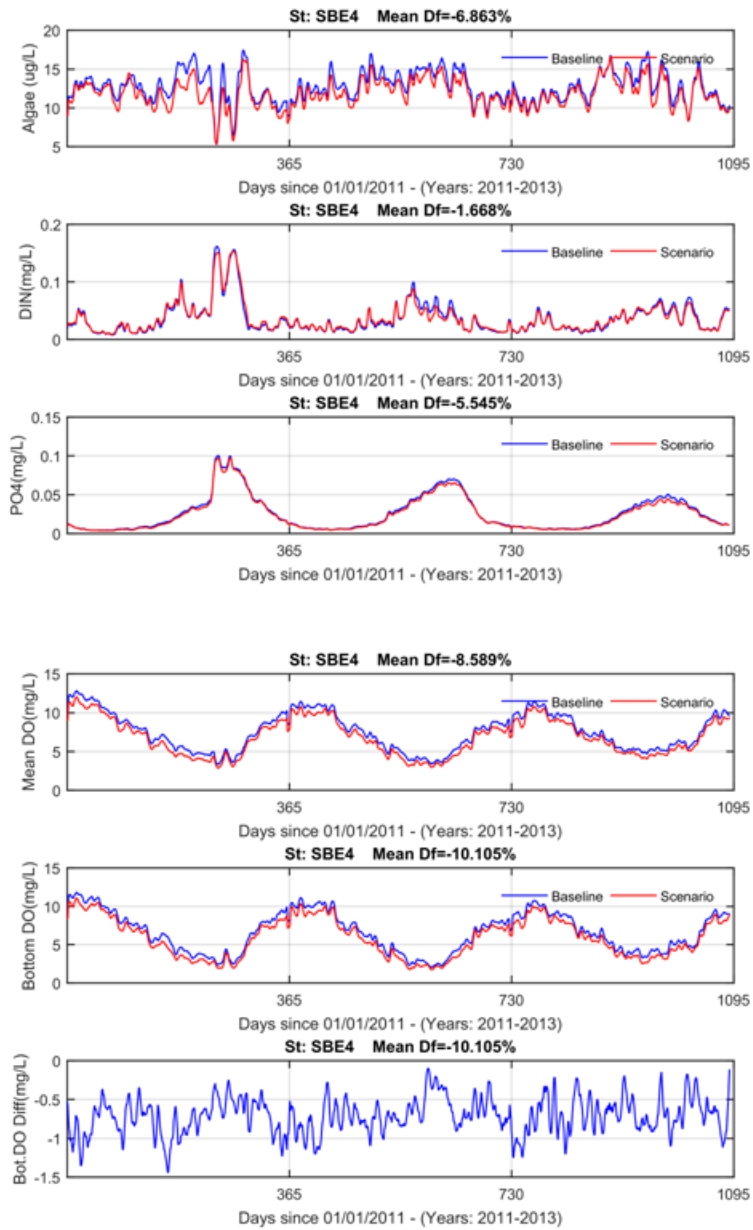


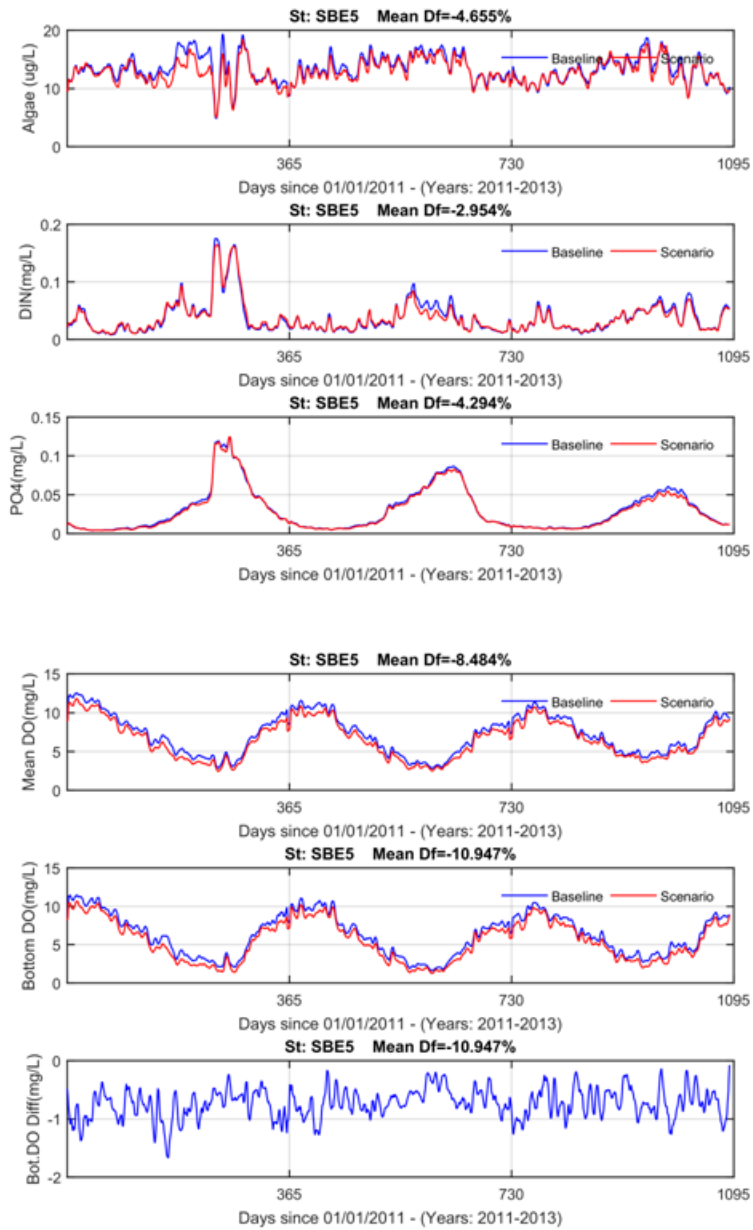


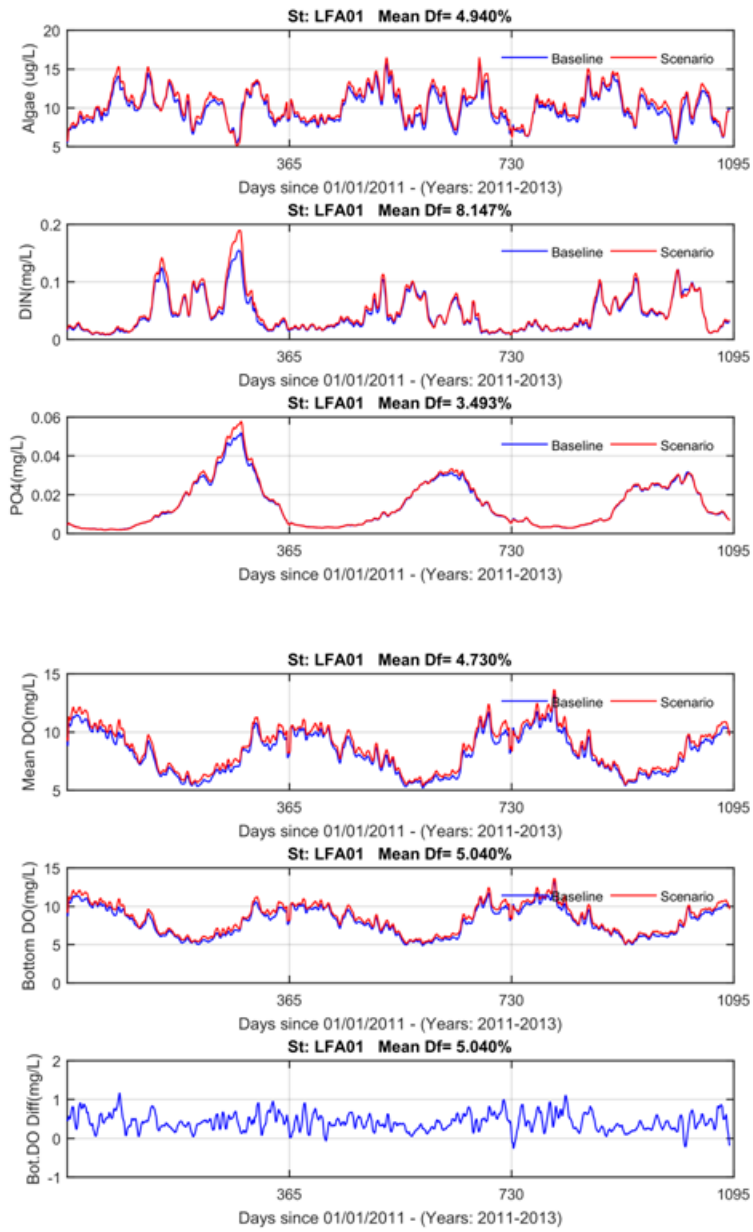


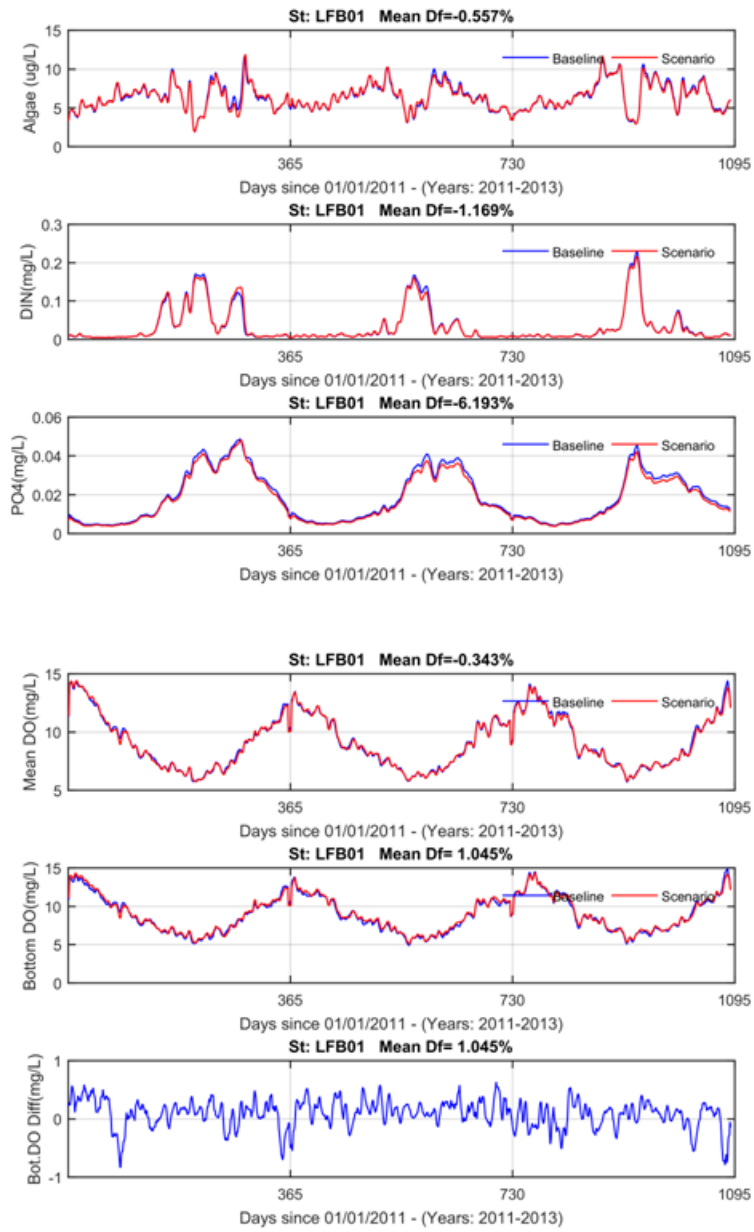


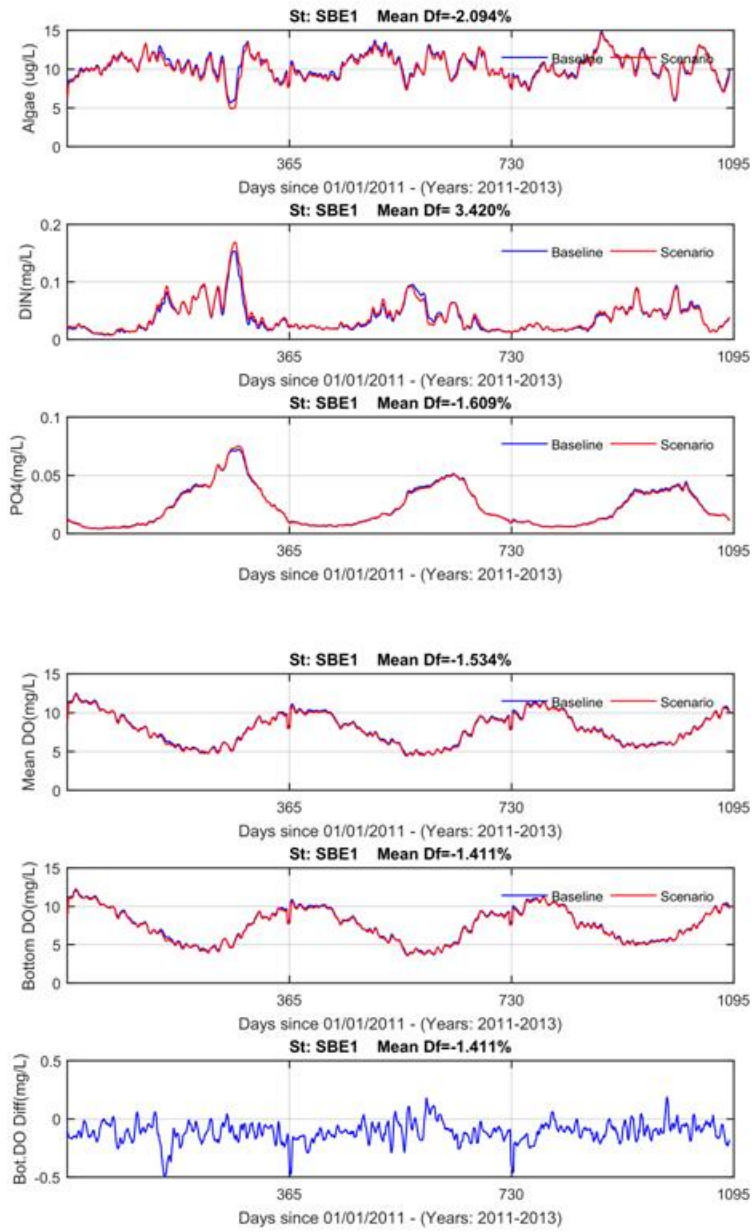


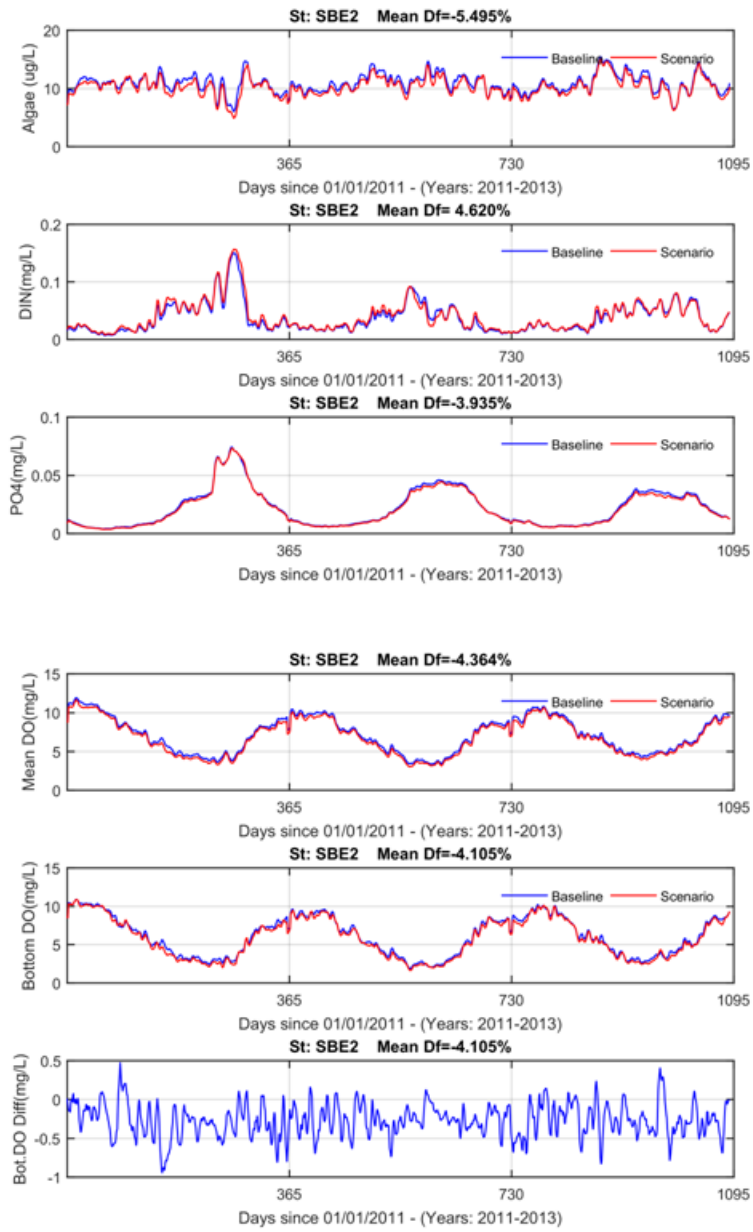


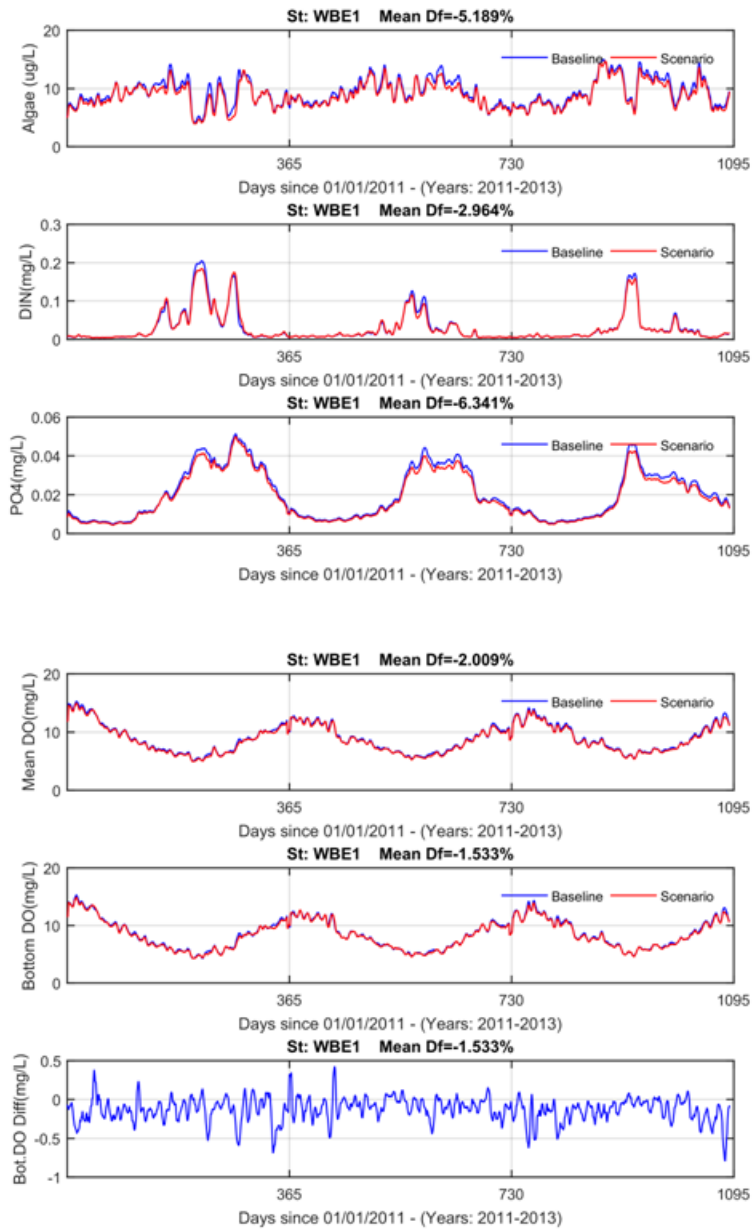












Model Simulation Baseline2 and Scenario 5-2

In the following plots. The Baseline is the results of baseline2 and Scenario is Scenario of 5-2.

